26th International QUENCH Workshop

6-9 December 2021
Virtual event organized by
Karlsruhe Institute of Technology
Karlsruhe, Germany

Editor: Martin Steinbrück

DOI: 10.5445/IR/1000141824

AGENDA

26^{th} International QUENCH Workshop

Organized by Karlsruhe Institute of Technology, Institute for Applied Materials, Germany
Virtual event via MS Teams, 06-09 December 2021

Daily starting time: 1 p.m. Karlsruhe (Paris, Berlin), 7 a.m. Washington, 9 p.m. Tokyo

Monday, 06 Dec 2021

0:00	Welcome	W. Tromm/M. Steinbrück, KIT
	QUENCH PROGRAM (Chair: M. Steinbrück)	
0:20	Update of the QUENCH program	M. Steinbrück, KIT
0:40	Results of metallographic analysis of the QUENCH-20 bundle with B_4C absorber	J. Stuckert, KIT
1:00	Analysis of QUENCH-20 Test with ASTEC V2.2.b	O. Murat, KIT
1:20	**Break/discussion**	
	EXPERIMENTS (Chair: J. Stuckert)	
1:40	Fuel rod / bundle behavior in the early stages of a severe accident in a nuclear reactor and spent fuel pool using the DEGREE facility	K. Nakamura, CRIEPI
2:00	Outline of the CLADS-MADE-03 test under steam-rich conditions and high heating rate	A. Pshenichnikov, JAEA
2:20	The CODEX-SBO experiment	R. Farkas, MTA
2:40	Refined relationship between through wall clad oxygen diffusion profiles and post-quenching impact properties of as-received and pre-hydrided Zircaloy-4, following High-Temperature (HT) steam oxidation	J.-C. Brachet, CEA

Tuesday, 07 Dec 2021

	MODELLING AND CODE APPLICATION II (Chair: F. Gabrielli)	
0:00	PSI-KIT Nitriding Model for Zirconium based Fuel Cladding Alloys	B. Jäckel, PSI
0:20	Development of New Model to Calculate High-Temperature Oxidation of ATF Chromium-Coated Zr-Based Cladding	A. Vasiliev, IBRAE
0:40	Implementation of LEI experience on modeling and uncertainty quantification of QUENCH tests for the development of QUENCH-20 numerical model	N. Elsalamouny, LEI

1:00	International Development and Assessment of a MATPRO-based Accident Tolerant Fuel Material Property Models and Correlation Library	S. Khalil, AU
1:20	**Break/discussion**	
	ATF CLADDING I (Chair: M. Steinbrück)	
1:40	ATF modelling in Severe Accident Codes	F. Gabrielli, KIT
2:00	Summary on IL TROVATORE WP 5 results	M.Grosse, KIT
2:20	Overview on the IAEA ATF-TS project	J. Stuckert, KIT
2:40	Experimental SiC coatings	B. Sartowska, INCT

Wednesday, 08 Dec 2021

	ATF CLADDING II (Chair: M. Grosse, KIT)	
0:00	The OECD-NEA project QUENCH-ATF	M. Steinbrück, KIT
0:20	The coating degradation mechanism during the isothermal steam oxidation of Cr-coated Zry-4 at 1200°C	J. Liu, KIT
0:40	Multilayer protective CrN/Cr coatings on E110 zirconium alloy	D. Sidelev, Tomsk PU
1:00	The results of high temperature single rod tests with chromium coated cladding	K. Vizelkova, KIT
1:20	**Break/discussion**	
	ATF CLADDING III (Chair: J. Stuckert, KIT)	
1:40	Magnetron-sputtered Cr-C-Al based coatings for enhanced accident tolerant fuel (ATF) zirconium-based alloy cladding	C. Tang, KIT
2:00	High-temperature oxidation of silicon carbide composites for nuclear applications	M. Steinbrück, KIT
2:20	Mechanical properties degradation of Cr-coated cladding under the loss-of-coolant accident conditions	P. Cervenka, CTU
2:40	Microstructural Analysis of Iron-Chromium-Aluminum Samples Exposed to LOCA-Type Conditions Followed by Quench	P. Doyle, ORNL

Thursday, 09 Dec 2021

	ZR-H SYSTEM I (Chair: M. Grosse, KIT)	
0:00	The SPIZWURZ Project – Bundle Experiment and Benchmark on Axial Hydrogen Diffusion	F. Boldt, GRS
0:20	KIT-INE contribution to the SPIZWURZ project	M. Marchetti, KIT
0:40	Neutron investigations of the hydrogen diffusion dynamics in different cladding tube materials	S. Weick, KIT
1:00	Elevated temperature hardness measurements of Zry-4 in the presence of hydrogen in solid solution	F. Fagnoni, PSI

1:20	**Break/discussion**	
	ZR-H SYSTEM II (Chair: M. Steinbrück, KIT)	
1:40	Hydrogen quantification in zirconium cladding materials using high-resolution neutron radiography imaging	L. Duarte, PSI
2:00	Hydrogen measurements and metallographic examination of high-burnup nuclear spent fuel claddings	M. Ayanoglu, ORNL
2:20	Fatigue Testing of High Burnup PWR Fuel Rods with Zircaloy-4 cladding with and without Heat Treatment to Simulate a Drying Cycle	P. Cantonewine, ORNL
2:40	Closure	M. Steinbrück, KIT

26th Int. QUENCH Workshop

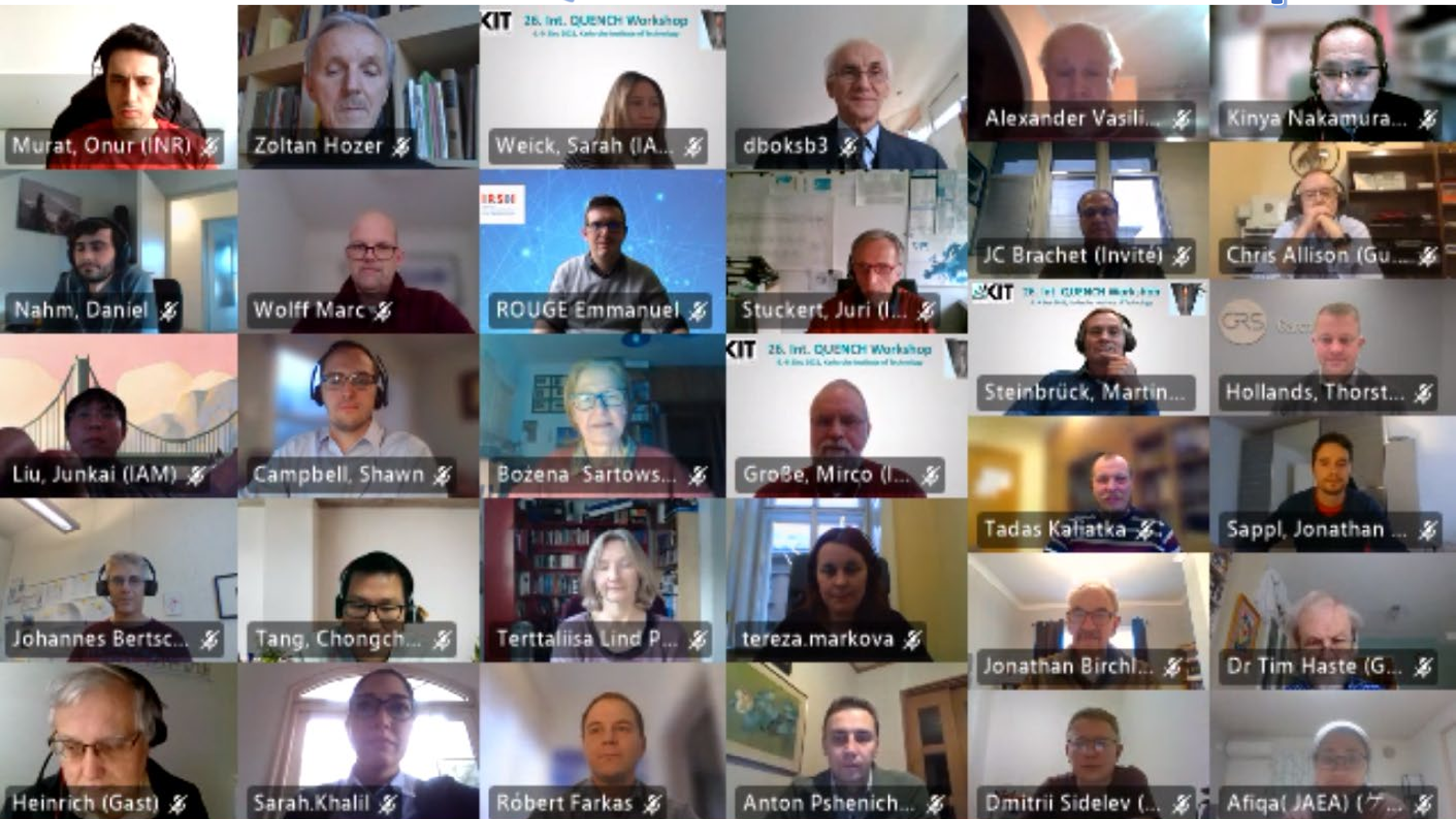

W. Tromm
KIT

Welcome address

The head of the nuclear safety program at KIT (NUSAFE) gave an overview on the program status and perspectives.

Karlsruhe Institute of Technology

Welcome Address: 26th QUENCH workshop at KIT

Outlook Programme NUSAFE at KIT and Helmholtz Association

Th. Walter Tromm, Programme Nuclear Waste Management, Safety and Radiation Research

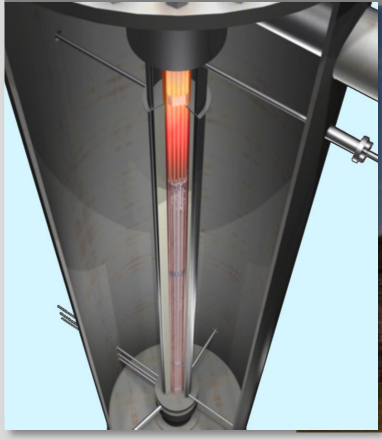

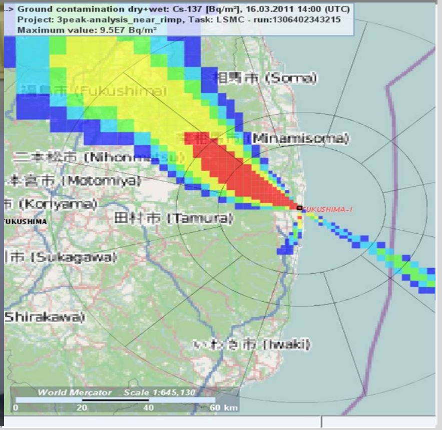

Reactor Safety Topic 2, Subtopic 1:

Design Basis Accidents and Materials Research

- Coupled reactor safety simulation tool for the complete calculation chain from the creation of input data over the conduction of core analyses to the analysis of design basis accidents as well as their validation
  - Multiphysics and multiscale approaches
  - Experiments at the high-pressure test facility COSMOS-H
- Safety investigations for liquid-metal-cooled innovative reactor systems and development of advanced corrosion-mitigation strategies
  - Test of devices under real operational and accidental conditions in the KALLA and KASOLA laboratory
  - Corrosion test facilities COSTA and CORRIDA for liquid lead coolant

COSMOS-H

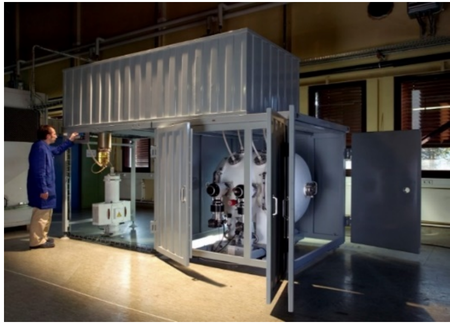

GESA
Pulsed Electron Beam Treatment

Topic 2, Subtopic 1: COSMOS - H

- Experiments in McSAFER (High-Performance Advanced Methods and Experimental Investigations for the Safety Evaluation of Generic Small Modular Reactors)
- Two series of experiments are planned to investigate the thermal hydraulics in different SMR concepts
  - Investigation of flow boiling up to the critical heat flux under reactor typical conditions

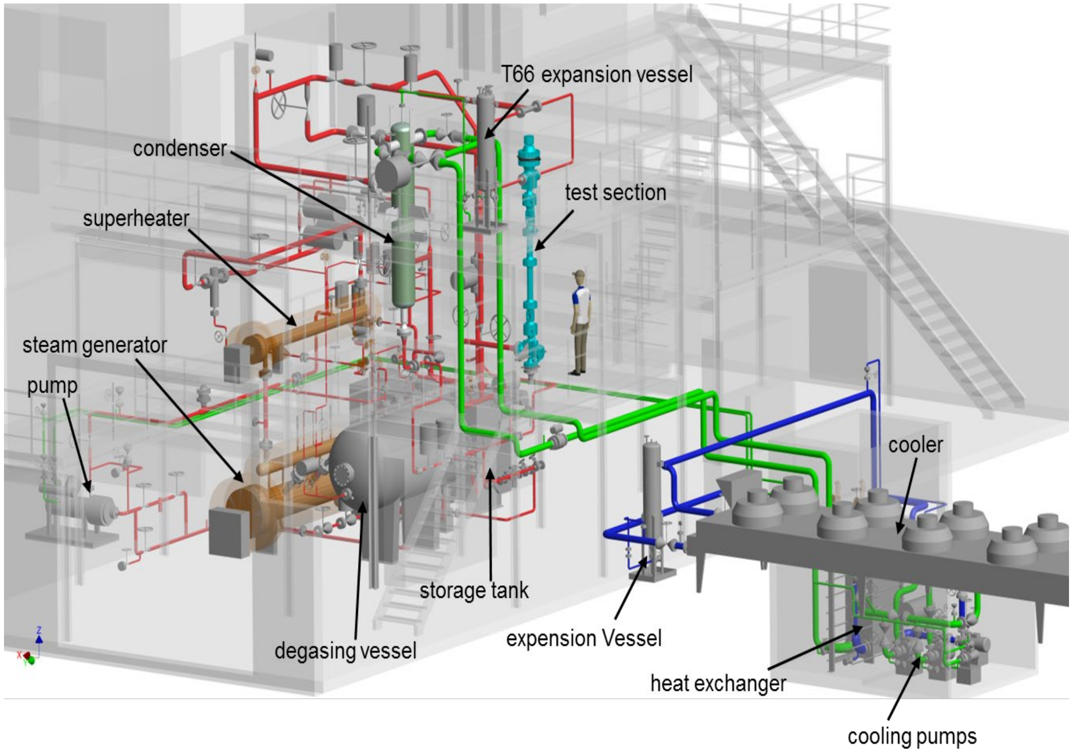

Objectives Topic 2, Subtopic 2:

- Beyond Design Basis Accidents
  - Development and validation of detailed physical models taking profit of the diverse KIT experimental facilities
  - Improvement of severe accident integral codes to support Severe Accident Management Guidelines
    MELCOR and ASTEC (Source Code)
- Emergency Management
  - Multi-criteria decision analysis (MCDA) as well as agent based modeling (ABM) to improve decision making under high uncertainties in all emergency situations with
    JRODOS real time online decision support system

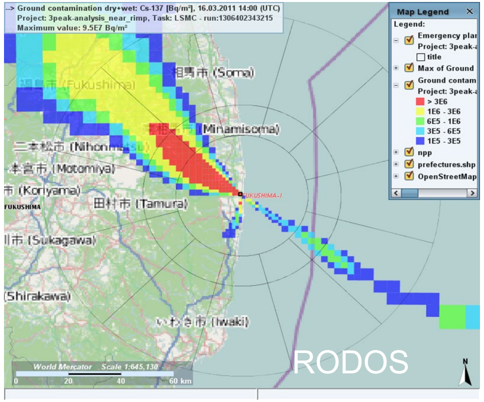

JRODOS Future

- JRODOS is used operational in many European countries and since more than 15 years in Germany
- It is installed – partly with the support the European Commission – in about 40 countries worldwide
- Ongoing installations are in the ASEAN countries, six Gulf states, six West-Balkan states, Armenia and Iran

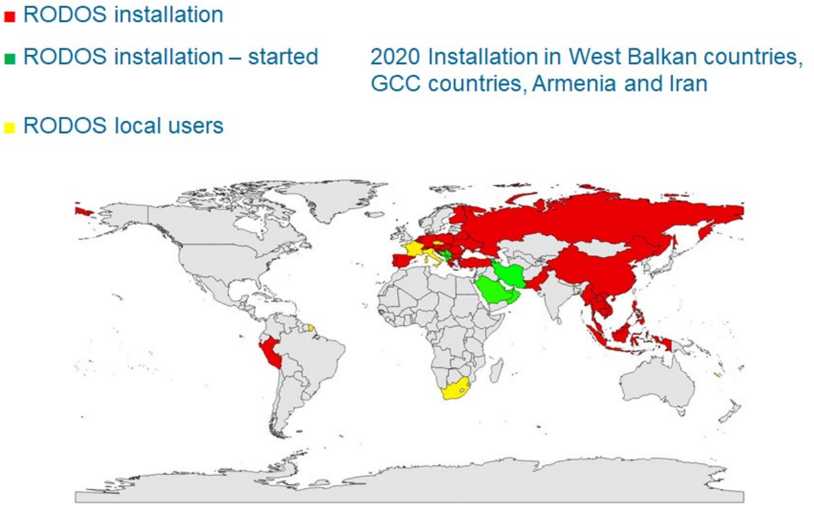

QUENCH-ATF Joint Undertaking

- Three bundle experiments with ATF cladding in the QUENCH facility (Cladding tubes provided by WEC (and others?))
- Time frame: 2021-2024
- Costs: 1.5 M€ (approx. 500 000 €/test) + NEA fee
  - 50% covered by KIT/Germany, 50% covered by collaborators

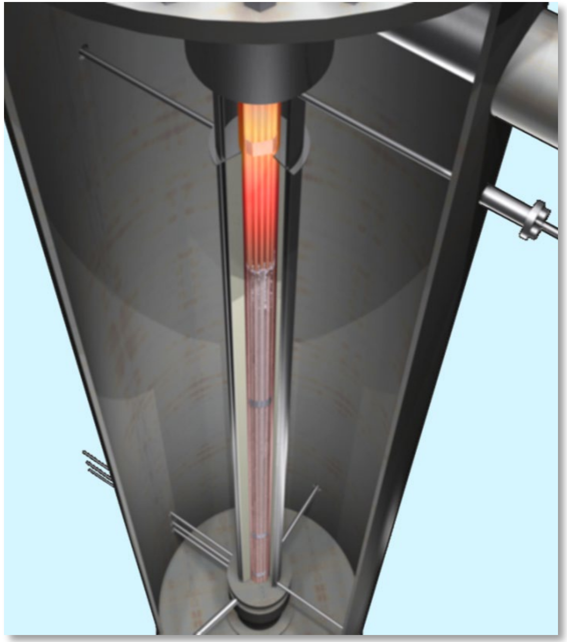

Status of the HOVER project
(Helmholtz Research and Technology Platform for the Decommissioning of Nuclear Facilities and for the Management of Radioactive Waste)

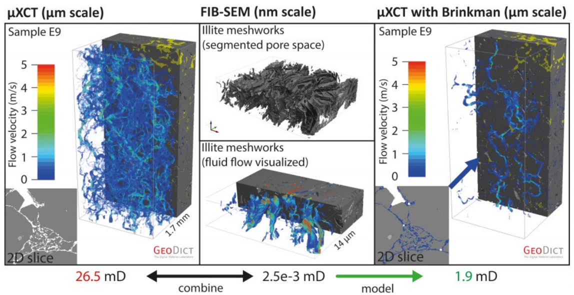

From A. Jacob et al. Solid Earth, 12, 2021

- **INE:** laboratory upgrade towards analysis of repository subsystems on various scales:
  - High speed video-rate AFM; dynamic processes at interfaces (nm scale)
  - µ-focus setup and hard X-ray sCMOS-camera at KARA
  - New capabilities for high-E X-ray scattering and tomography (µm scale)
  - Laboratory X-ray microscopy/µ-CT coupled to FIB-SEM
    In-situ flow-through µ-CT setup combined workflow to FIB-SEM (nm – mm scale)

  * Accelerator Mass spectrometry (AMS) for Ultra-trace RN analysis

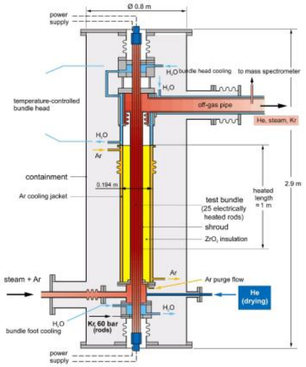

* **IAM:** LICAS Experiment: *L*ong-term *I*nvestigation of *C*l*A*ddings behaviour under *S*torage conditions

* **INR:** Virtual decommissioning laboratory

* **TMB:** Building Information Modelling (BIM)

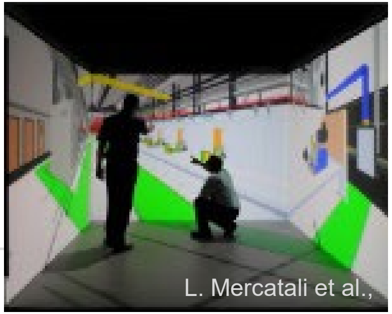

Research on extended interim storage of spent nuclear fuel

Karlsruhe Institute of Technology

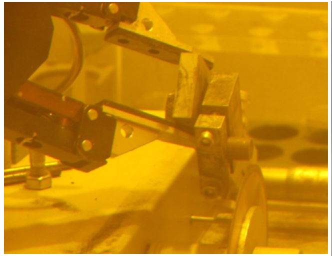

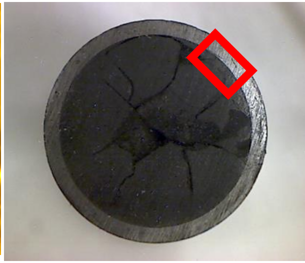

- Studying pellet / cladding interaction and cladding properties of spent UO_2 fuel and spent MOX fuel

- Cs-U-O-Zr-Cl-I and Cs-Cl/I bearing compounds found in the interaction layer of irradiated nuclear fuel → **for the 1st time utilising XAS based Cl K-edge and I K-edge measurements** → CsCl and CsI structures detected

- In future studies examining whether different compounds fuel-cladding interface have a potential impact on mechanical properties of the Zircaloy cladding

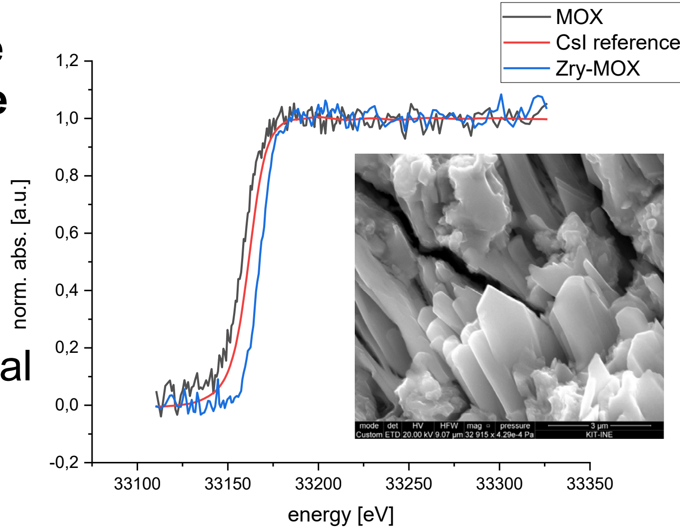

Recommendations of Strategic Advisory Board 2020
NUSAFE Topic 2 Reactor Safety

Karlsruhe Institute of Technology

- The NUSAFE programme on reactor safety with the major experimental projects Quench-ATF and KALLA as well as the multi-physics simulation, e.g project McSafer, is attractive and ensures highest-level reactor safety research. Hence, these projects are strongly supported by the SAB.
- The projects will help to attract young talents and by this contribute to know-how transfer and knowledge developing, strongly contributing to the programme of BMBF/BMWi/BMU on “Kompetenz- und Nachwuchsentwicklung für die nukleare Sicherheit”. The SAB recommends to foster competence keeping and development (especially of young scientists, also female).
- International cooperation with many countries is well developed by KIT. This also will help to keep competence in the relevant research fields and to contribute to specific questions pertaining to international nuclear safety.

Thank you for your attention
Karlsruhe Institute of Technology
Th. Walter Tromm
Karlsruhe Institute of Technology
Programme Nuclear Safety Research
walter.tromm@kit.edu
10

M. Steinbrück, J. Stuckert, M. Große
KIT

Update of the QUENCH program

The main objective of the QUENCH program at KIT is the investigation of the hydrogen source term and materials interactions during LOCA and the early phase of severe accidents including reflood. Bundle experiments as well as separate-effects tests are conducted to provide data for the development of models and the validation of severe fuel damage code systems.

The QUENCH bundle facility is a unique out-of-pile bundle facility with electrically heated fuel rod simulators and extensive instrumentation. So far, 20 experiments with various severe accident (SA) scenarios as well as a series of seven DBA LOCA experiments were conducted. The QUENCH-LOCA series was completed in 2016. One of the main results is the definition of the conditions for secondary hydriding around the burst position and its influence on the mechanical properties of the cladding rods.

The post-test examinations of the last two SA tests QUENCH-19 (FeCrAl cladding) and QUENCH-20 (BWR bundle) are almost finished, final reports will be published soon.

Separate-effects tests during 2020/21 were focused on the high-temperature behavior of various ATF cladding candidates as well as on the behavior of hydrogen in Zr alloys under long-term dry storage conditions.

QUENCH bundle tests are part of the validation matrices of most SFD code systems, which was also reflected during the session “Modelling and code validation”.

The next QUENCH bundle tests are planned with ATF cladding tubes in the framework of the OECD-NEA Joint Undertaking QUENCH-ATF. Furthermore, a long-duration test (8 month) is planned in the framework of the German SPIZWURZ project on long-term dry intermediate storage of used fuel elements.

Most activities of the QUENCH group are embedded in international cooperation in the framework of the EC, OECD-NEA and IAEA.

Finally, the status of reporting and publishing as well as the numerous national and international cooperations were briefly described and acknowledged.

Update of the QUENCH Program

M. Steinbrück, J. Stuckert, M. Große et al.

26th International QUENCH Workshop, MS Teams, 6-9 December 2021

Institute for Applied Materials, Programme NUSAFE

Outlook

- Motivation
- Experimental facilities
- ATF activities
- Long-term dry intermediate storage activities
- Modelling / Code validation
- Reporting
- Future planning
- Cooperation

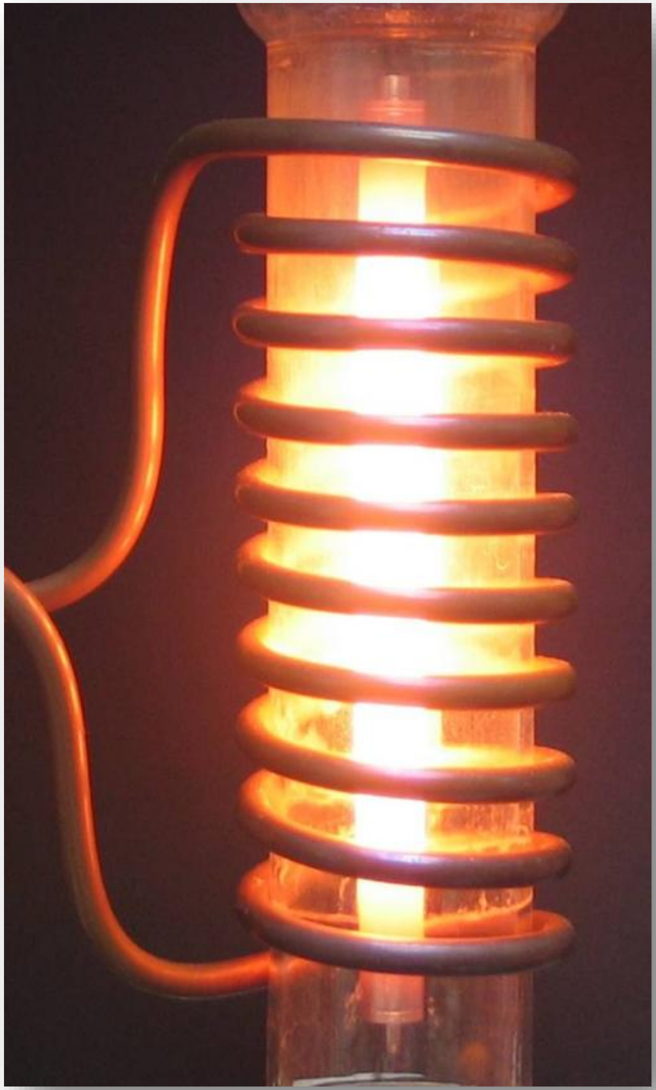

Motivation (LOCA, severe accidents)

- Reflood is a prime accident management measure to terminate a nuclear accident
- Reflood may cause temperature excursion connected with increased hydrogen and FP release (severe accidents) and embrittlement of cladding and secondary hydriding (LOCA)
- Coolability of a degraded core is a matter of high priority (Fukushima)

➡ QUENCH experiments (bundle+SET) provide data for development of models and validation of SFD code systems

New topics

- Accident tolerant fuel (ATF) cladding
  - Characterization of promising ATF cladding concepts at (very) high temperatures
  - Degradation mechanisms and kinetic data
  - Max. temperature and coping time for AMMs
- Long-term dry intermediate storage
  - Hydrogen/hydride behaviour in Zr cladding during 100 years storage e.g. in CASTOR casks
  - Hydride reorientation and its effect on mechanical properties

QUENCH Programme

Investigation of hydrogen source term and materials interactions during LOCA and early phase of severe accidents including reflood

Separate-effects tests

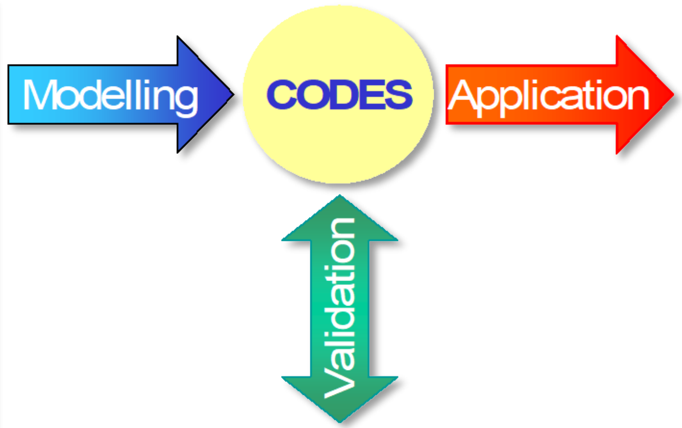

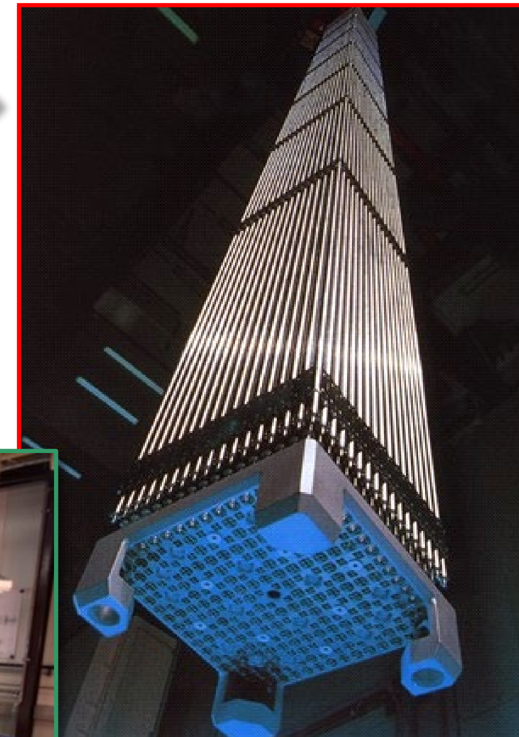

PWR fuel element

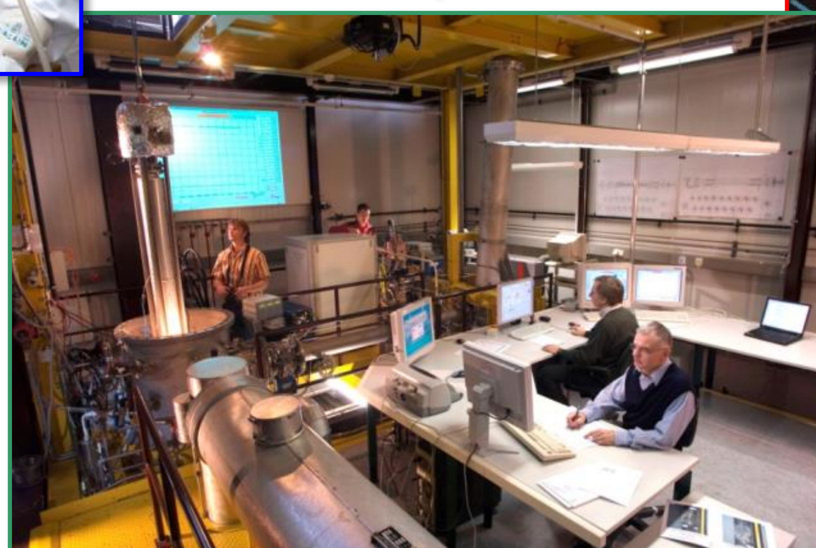

Bundle experiments

QUENCH/LICAS facility

- Unique out-of-pile bundle facility to investigate reflood of an overheated reactor core
- 21-31 electrically heated fuel rod simulators; T up to >2000°C
- Extensive instrumentation for T, p, flow rates, level, etc. + MS
- So far, 20 experiments on SA performed (1996-today)
  - Influence of pre-oxidation, initial temperature, flooding rate
  - B_4C, Ag-In-Cd control rods
  - Air ingress; debris formation
  - Advanced cladding alloys
- 7 DBA LOCA experiments with separately pressurized fuel rods

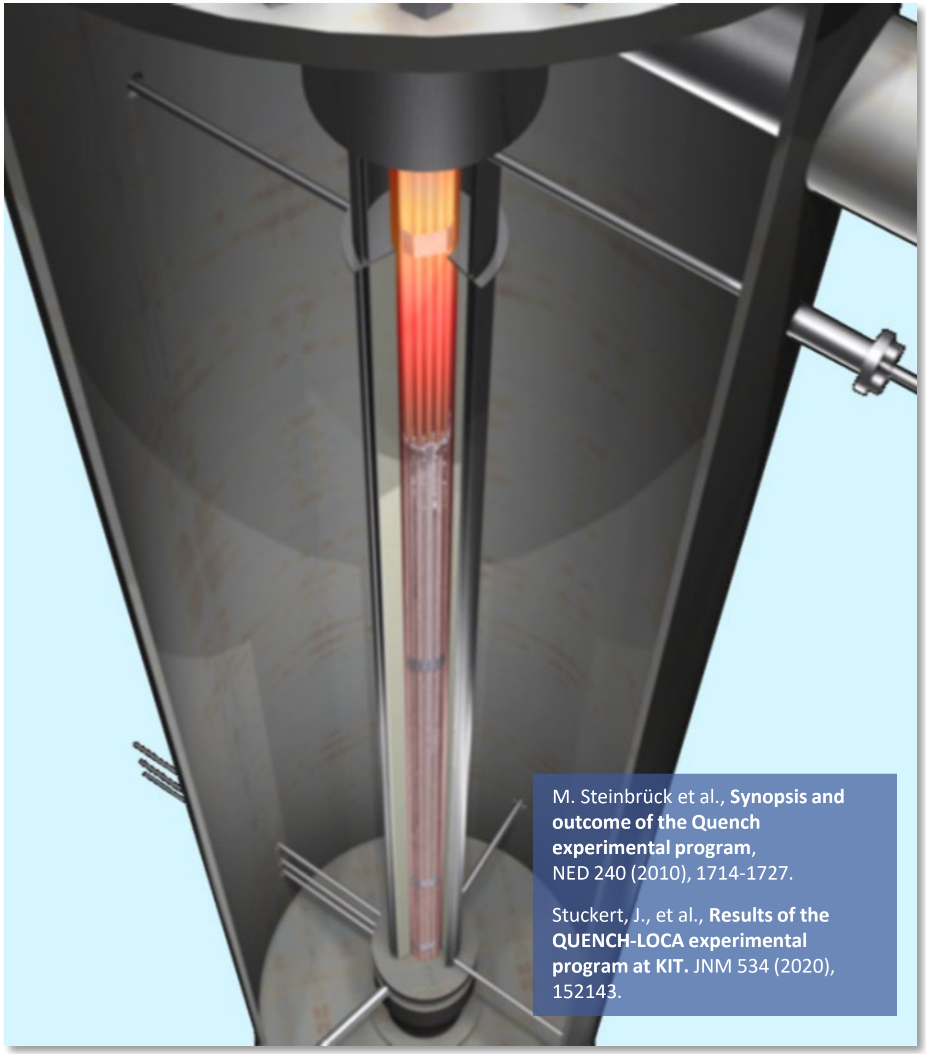

M. Steinbrück et al., **Synopsis and outcome of the Quench experimental program**, NED 240 (2010), 1714-1727.

Stuckert, J., et al., **Results of the QUENCH-LOCA experimental program at KIT.** JNM 534 (2020), 152143.

QUENCH Separate-effects tests: Main setups

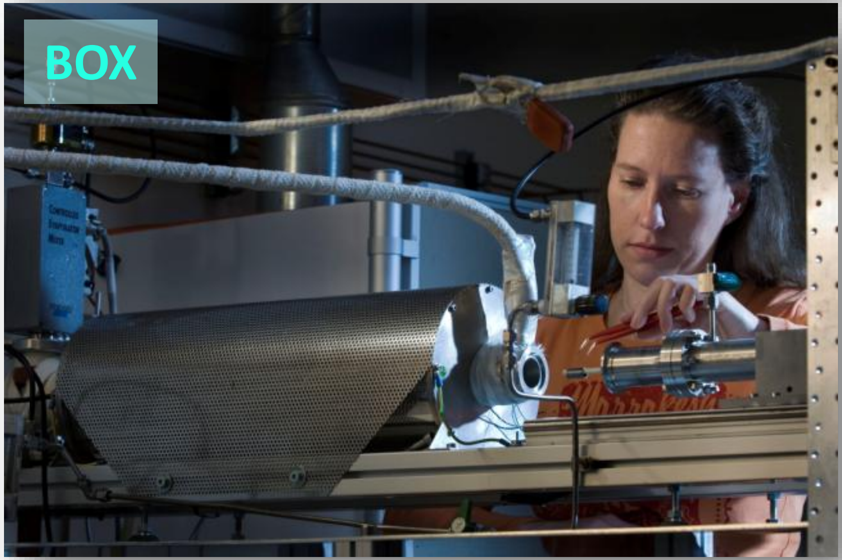

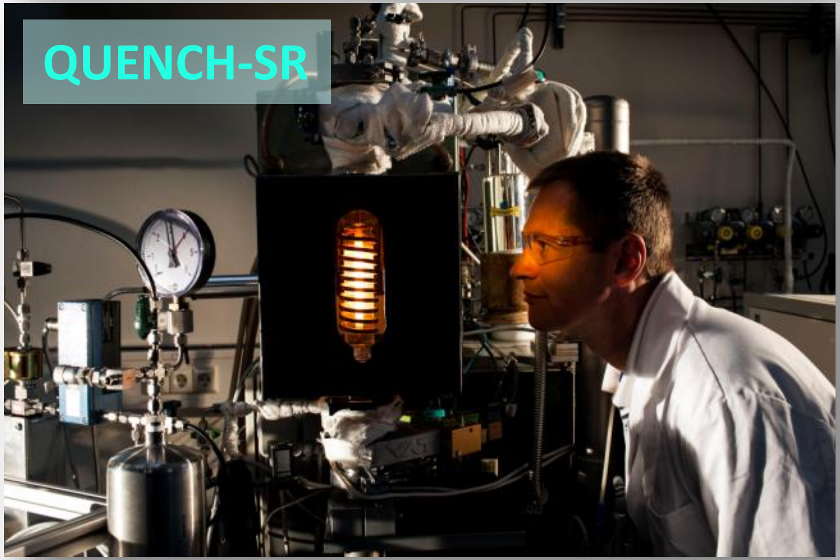

Review of tests QUENCH-19/-20

- QUENCH-19 (2018)
  - Worldwide first bundle test with FeCrAl ATF cladding
  - Strongly reduced hydrogen release compared to reference test QUENCH-15 with ZIRLO cladding
  - Some issues with FeCrAl oxide interaction with ZrO_2 pellets and mechanical behavior of bundle during reflood due to high CTE
- QUENCH-20 (2019)
  - Quadratic BWR bundle with boron carbide absorber blades and water channels
  - Strong degradation of absorber blades with intense melt formation
  - Only moderate hydrogen release compared to PWR tests Q-7/-9 with PWR geometry
- Post-test examinations and reporting for both experiments are at an advanced stage

QUENCH activities for Accident Tolerant Fuel Claddings

- Single-rod oxidation and quench tests with Cr-coated Zr alloy
- Ultra-high temperature oxidation tests with SiC_f-SiC
- Oxidation kinetics of various FeCrAl alloys
- Development of MAX phase coatings for Zr alloys

Recent results presented at TOPFUEL 2021

- Participation in various international collaborations on ATF
  - EC IL TROVATORE (Coordinator of WP “Coolant-cladding-fuel interaction”)
  - IAEA ATF-TS (Coordinator of Benchmark QU-19 and exp. program)
  - OECD NEA QUENCH-ATF (KIT is Operating Agent)
  - Various bilateral collaborations with Westinghouse, CEA, CTU Prague, Tomsk Polytechnic University, KONICOF, …

Long-term intermediate storage activities

- Work embedded in the German project SPIZWURZ (GRS, KIT) and the HGF HOVER infrastructure program
  - 8 month lasting bundle test
  - Various SETs on the system Zr-H
- Construction and commissioning of a Sieverts type chamber for hydrogen loading of small samples
- Investigation of the hydrogen uptake at temperatures relevant for dry storage of spent fuel
- Developing of a loading procedure for large tubes
- Investigation of a defined hydrogen loading with ZrH_2 powder
- Construction of an apparatus for in-situ neutron radiography experiments under defined mechanical load and temperature

Modelling and code validation

- QUENCH bundle tests are part of validation matrices of most SFD code systems
- Post-test calculations of QUENCH-19 in the framework of the IAEA ATF-TS project
- Post-test calculations for QUENCH-20 by KIT-INR
- Pre-test calculation of QUENCH-ATF-1 and LICAS-01 by GRS
- Separate-effects test data are used by PSI, RUB, EdF, ISS and others for model development

Reporting

- Papers and conference contributions (>20 Scopus references) in 2020/21
- Three chapters in Elsevier books
- QUENCH-18 report published
- 3 TV teams at QUENCH facility in 2021


thermo MDPI

Review

Steam Oxidation of Silicon Carbide at High Temperatures for the Application as Accident Tolerant Fuel Cladding, an Overview

Hai V. Pham [1,*], Masaki Kurata [1] and Martin Steinbrueck [2]

Journal of Alloys and Compounds 895 (2021) 162450

Contents lists available at ScienceDirect

Journal of Alloys and Compounds

journal homepage: www.elsevier.com/locate/jalcom

Review on chromium coated zirconium alloy accident tolerant fuel cladding

Jianqiao Yang [a,b,*], Martin Steinbrück [b], Chongchong Tang [b], Mirco Große [b], Junkai Liu [a,b], Jinming Zhang [a], Di Yun [a], Shuzhong Wang [a]

Nuclear Engineering and Design 379 (2021) 111267

Contents lists available at ScienceDirect

Nuclear Engineering and Design

journal homepage: www.elsevier.com/locate/nucengdes

Experimental and modelling results of the QUENCH-18 bundle experiment on air ingress, cladding melting and aerosol release

Juri Stuckert [a,*], Martin Steinbrueck [a], Jarmo Kalilainen [b], Terttaliisa Lind [b], Jona

M. Grosse et al.: Investigation of the 3D hydrogen distribution in zirconium alloys by means of neutron tomography

M. Grosse [a], B. Schillinger [b], P. Trtik [c], N. Kardjilov [d], M. Steinbrück [a]

[a] Karlsruhe Institute of Technology, Institute for Applied Materials/Applied Material Physics, Eggenstein-Leopoldshafen, Germany
[b] Technical University Munich, Physics Department, Garching, Germany
[c] Paul Scherrer Institut, Neutron Imaging and Activation Group, Villigen, Switzerland
[d] Helmholtz Zentrum Berlin, Institute for Applied Materials, Berlin, Germany

Investigation of the 3D hydrogen distribution in zirconium alloys by means of neutron tomography

Paper presented at the Symposium "Tomographic and Radiographic Imaging with Synchrotron X-rays and Neutrons" of the MSE 2018, 26–28 September 2018, Darmstadt, Germany

Outlook 2022

- QUENCH-ATF-01 experiment
  - Slightly extended DBA LOCA test with Cr-coated Optimized ZIRLO cladding
  - All bundle components, except cladding tubes, are available
- SPIZWURZ bundle experiment
  - Long-term intermediate storage test
  - 250 days, starting from 400°C with 1 K/d cooling rate
  - Three cladding types, two hydrogen concentrations, two pressures
  - Hydrogen pre-loading is next step before bundle assembly
- Final post-test examinations of QUENCH-19/-20
- SETs on various topics mainly on ATF cladding and Zry/H

Co-operations

Programs
- NUGENIA
- HORIZON 2020
- IAEA
- OECD-NEA

Bilateral
- PSI
- MTA EK
- IRSN, CEA, EdF
- RUB-LEE
- GRS
- Westinghouse
- USNRC
- KONICOF
- NECSA, BAM, HMI
- NRA, JAEA
- ISS
- ORNL
- Tomsk PTU
- Various Chinese Organizations

Acknowledgement

- Helmholtz Association for funding program NUSAFE at KIT
- Program NUSAFE and IAM institute’s management for broad support of our activities

- And last but not least the QUENCH team:
  J. Laier, J. Moch, H. Muscher, U. Peters, U. Stegmaier, C. Tang, K. Vizelkova, S. Weick

  guests: J. Yang, J. Liu (Xi’an Jiaotong University), C. Kim (KAIST)

J. Stuckert, U. Peters, U. Stegmaier
KIT

Results of metallographic analysis of the QUENCH-20 bundle with B_4C absorber

Experiment QUENCH-20 with BWR geometry simulation bundle was conducted at KIT on 9th October 2019. The test objective was the investigation of a BWR fuel assembly degradation including a B_4C control blade.

The test bundle mock-up represents one quarter of a BWR fuel assembly with absorber blades at two bundle sides. The 24 electrically heated fuel rod simulators were filled separately with krypton (overpressure of 4 bar). The bundle was firstly heated to maximum temperature of 1230 K at the cladding of the central rod at the hottest elevation of 950 mm. This pre-oxidation phase in steam lasted 4 hours. During the transient stage, the bundle was heated to a maximal temperature of 2000 K. The cladding ductile expansions and failures were observed at temperature about 1700 K and lasted about 200 s. Massive absorber melt relocation was observed 50 s before the end of transient stage. The test was terminated with the quench water injected with a flow rate of 50 g/s from the bundle bottom. Fast temperature escalation from 2000 to 2300 K during 20 s was observed. The mass spectrometer measured release of CO (12.6 g), CO_2 (9.7 g) and few CH_4 during the reflood as products of absorber oxidation. Hydrogen production during the reflood amounted to 32 g (57.4 g during the whole test) including 10 g from B_4C oxidation. These measurements allow estimate the reduction of the B_4C pins due to oxidation: only 4.6% of total B_4C mass reacted with steam.

The oxide layer thickness was measured on the corner rod, withdrawn on the end of the preoxidation stage, and showed the maximum value of 65 µm at the bundle elevation of 950 mm. The visual inspection of the bundle, freed from thermal insulation, showed a strong damage of shroud and channel box between elevations 600 and 950 mm at the angle positions with installed absorber blades. At these bundle elevations, the B_4C pins reacted eutectically with stainless steel blades. The formed melt has attacked the channel box and the shroud and partially relocated to lower elevations inside the gaps between the rods and the channel box as well as between the channel box and the shroud. Ductile shroud deformation (implosion) due to higher pressure outside shroud in comparison to system pressure was observed between the bundle elevations 350 and 1150 mm.

The bundle filled with epoxy resin was cut into cross slices with the axial step of 100 mm (corresponding to axial positions of thermocouples). The radial oxidation degree of claddings was not symmetrical: the claddings placed in the corner between the absorber blades were more oxidized in comparison to claddings placed in other three bundle corners. The greatest cladding oxidation in the axial direction was observed at 750 mm with the average ECR value here about 36% and oxide thicknesses between 100 and 480 µm, whereas the average ECR value at the elevation of 450 mm was about 14% with oxide thicknesses between 15 and 110 µm. The cladding melt was formed at the bundle elevations between 550 and 1050 mm and 1) released into the space between the rods with building of molten partially oxidized pools or relocated to the grid spacer at 550 mm, 2) moved down between pellet and outer cladding oxide layer to about 450 mm. The SEM/EDX analysis of the melt frozen near B_4C pins showed formation (Fe, Cr) borides and FeB_2 needles inside the Zr-steel eutectic melt. The relocation of the B_4C material was not very significant: some of the rods dissolved due to interaction with stainless steel and Zr and partially moved down with the melt, but most parts of absorber pin remained in their original positions.

Results of metallographic analysis of the QUENCH-20 bundle with B_4C absorber

J. Stuckert, U. Peters, U. Stegmaier

QWS-26, Karlsruhe

Institute for Applied Materials; Program NUSAFE

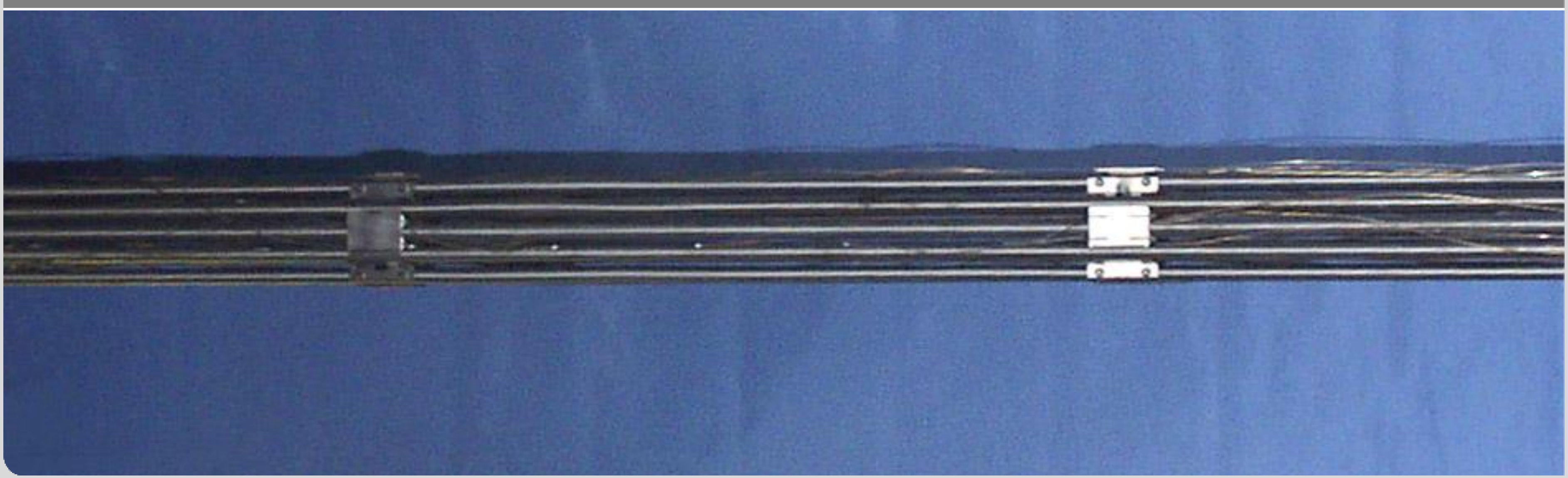

QUENCH-20 (SAFEST): Choice of BWR elements, which should be simulated during QUENCH-SAFEST

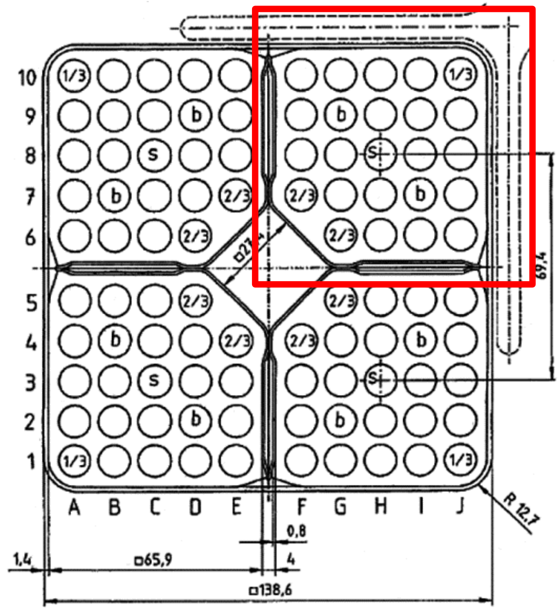

assembly cross section

SSM proposal: study of high temperature degradation of BWR assembly mock-up in QUENCH facility (melt formation due to eutectic material interaction inside absorber cross)

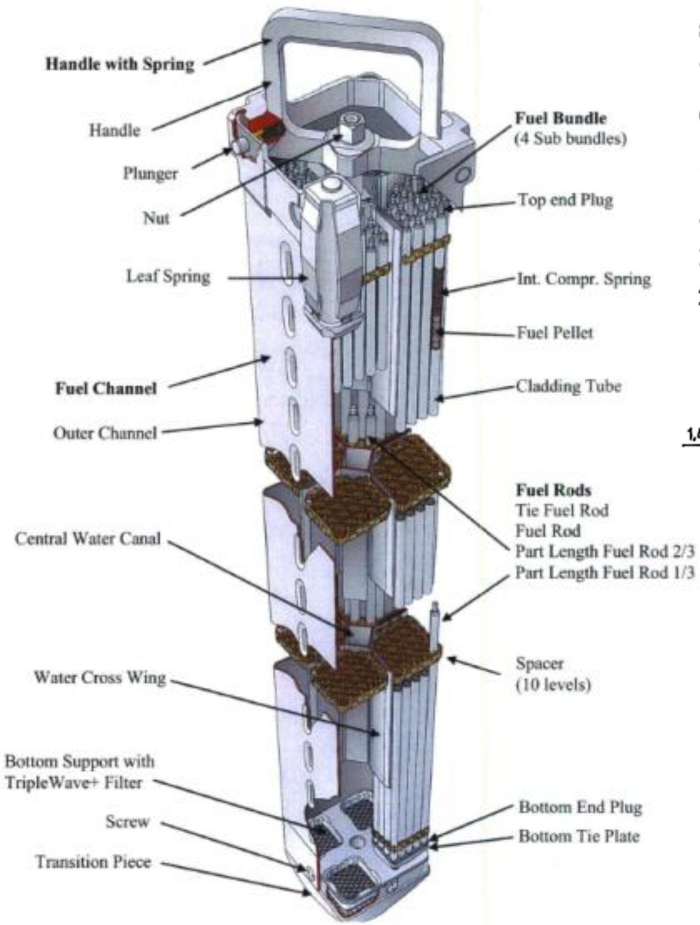

assembly SVEA-96 Optima

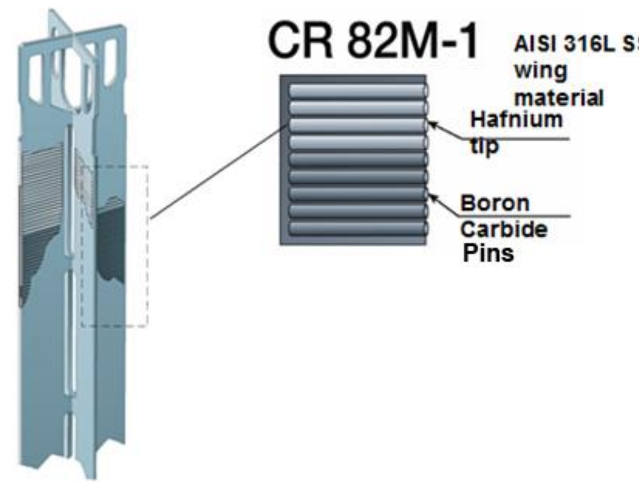

absorber cross

QUENCH-20: suggested test bundle composition (¼ SVEA-96 OPTIMA2 assembly)

Karlsruhe Institute of Technology

absorber steel blades with B_4C pins,
side length 67 mm;
mass ratio B_4C:steel=0.9:3.6=0.25

Inconel cooling jacket,
inner tube ID=158.3 mm

corner rod (Zry-4, OD 6 mm)

heated rods (24):
cladding Zy-2 with inner ZrSn-liner (10% of clad),

ZrO_2 pellet OD 8.48±0.05
ID 5.45±0.1 mm,
length 11 mm,

W heater
OD 5.25±0.025 mm

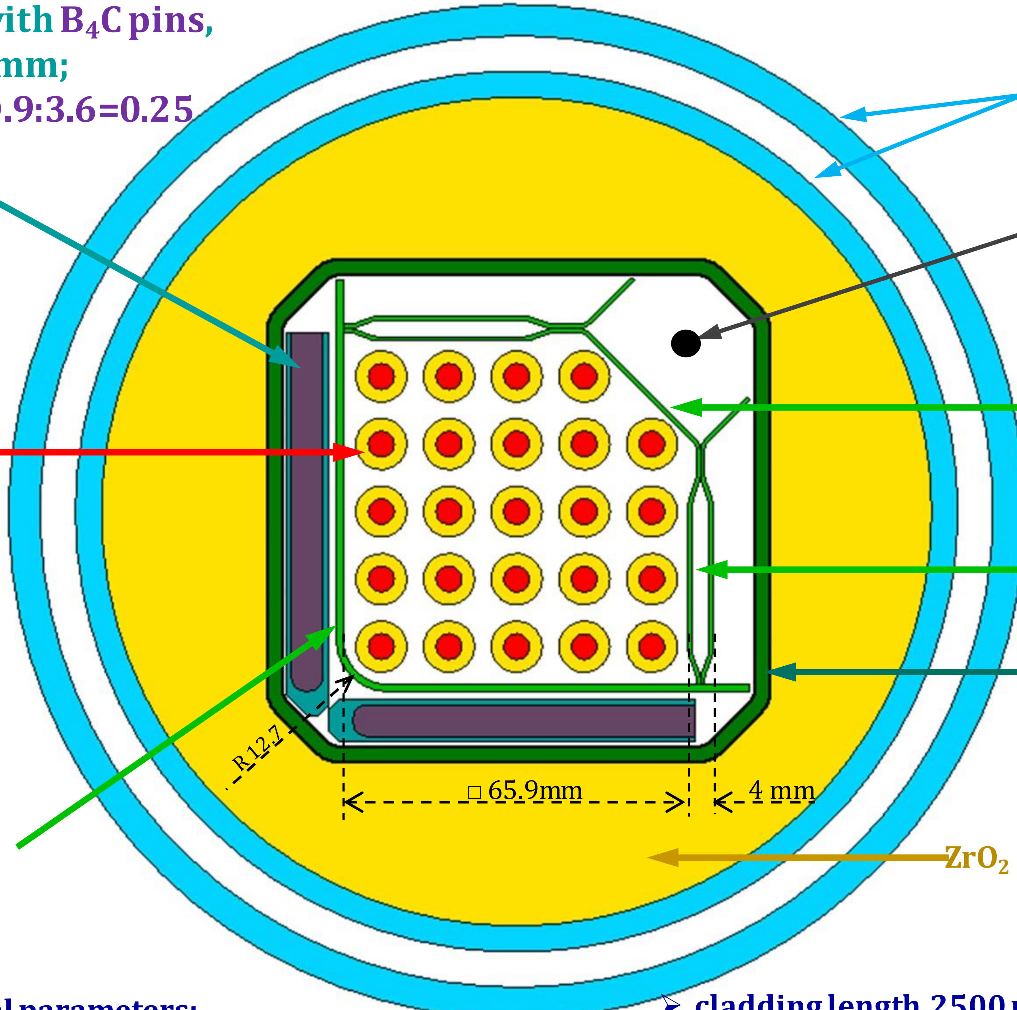

water channel box (ZIRLO),
side length 27.4 mm

water cross wing (ZIRLO),
wall thickness 0.8 mm

Zr shroud 90 mm x 114 mm
(inner clearance dimensions),
wall thickness 3 mm

advanced low tin ZIRLO
fuel channel box,
wall thickness 1.4 mm

ZrO_2 porous thermal insulation

Geometrical parameters:

- bundle pitch 12.898 mm;
- outer diameter of claddings 9.84 mm;
- thickness of claddings 0.605 mm;
- absorber blades: thickness 8.05 mm
- cladding length 2500 mm
- absorber and cannel box lengths 1600 mm
- water gap between channel box and absorber blade 2.5 mm (nominal inter-assembly gap in BWR-PROTEUS core is 13.8 mm -> water gap 2.875 mm)

QUENCH-20: test progress

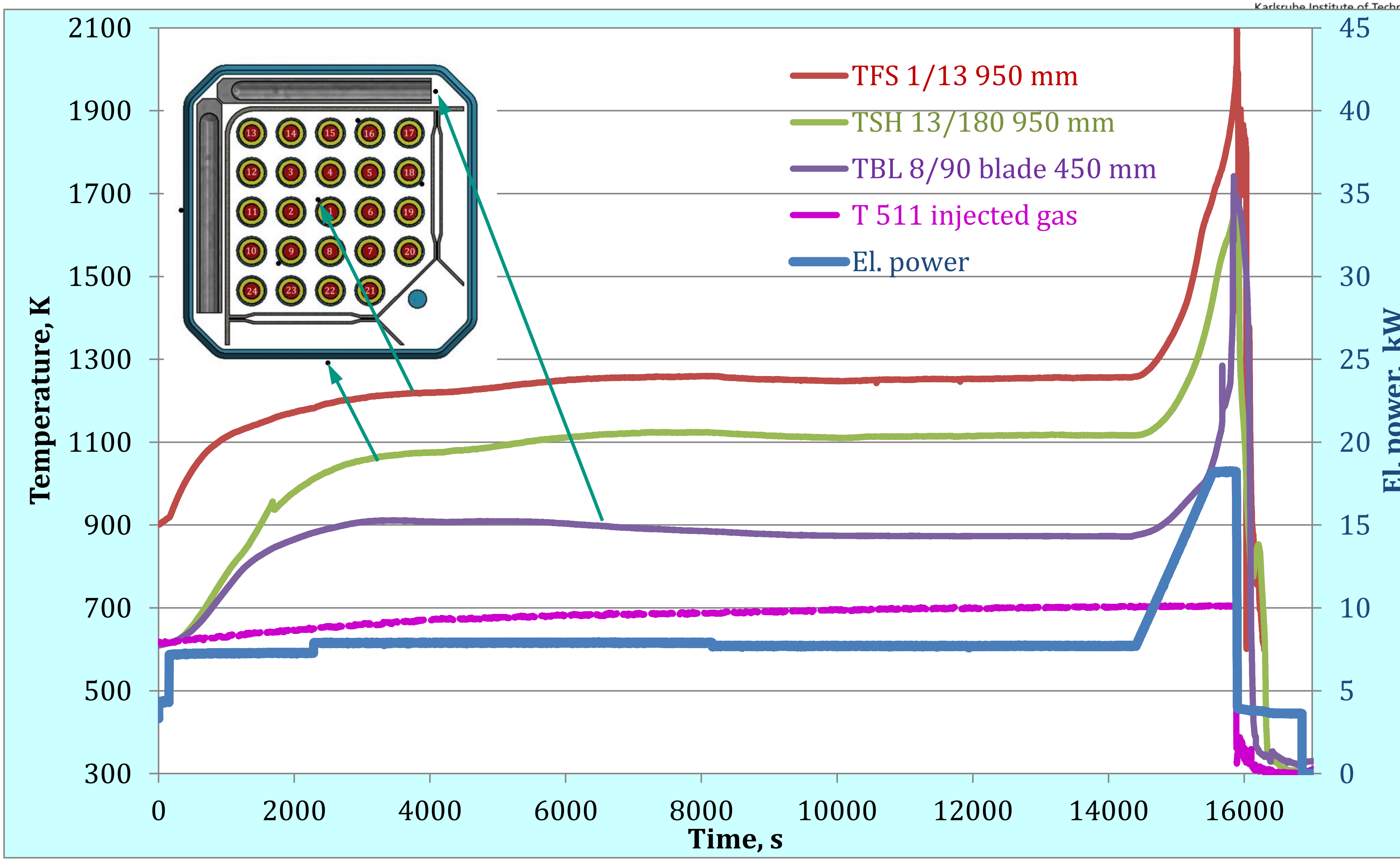

gas injection: Ar 3g/s during the whole test; superheated steam 3 g/s until the quench initiation

QUENCH-20: axial temperature profiles of outer cladding surfaces and outer shroud surface (temperatures averaged through the cross-section for each elevation)

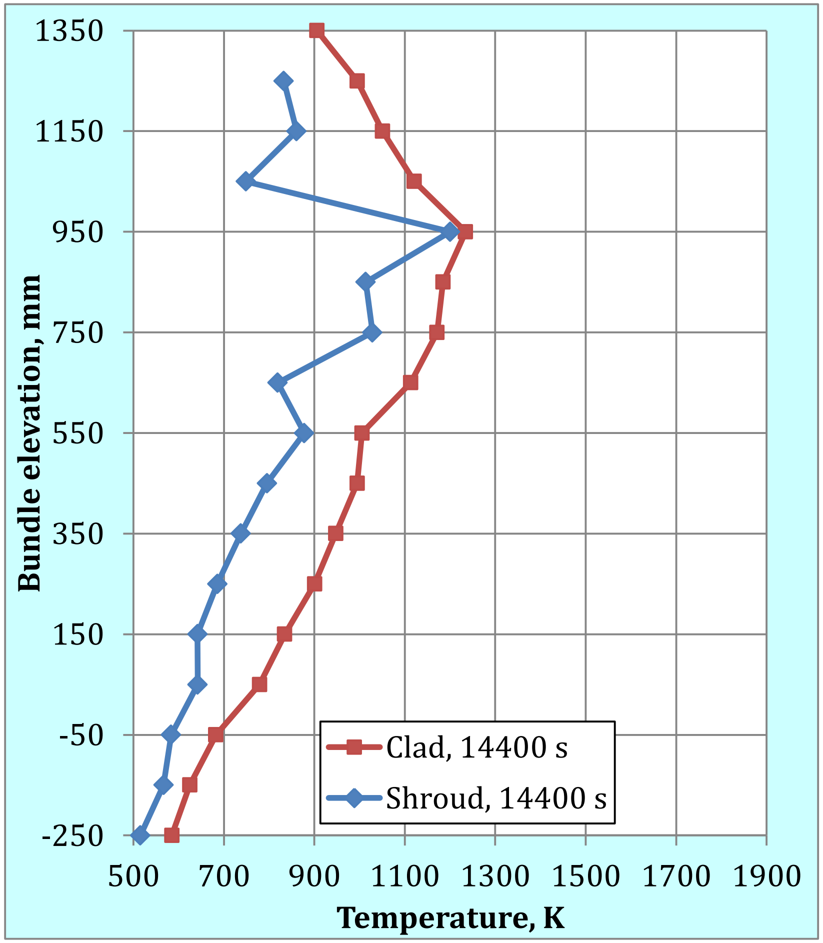

on the end of pre-oxidation (14400 s)

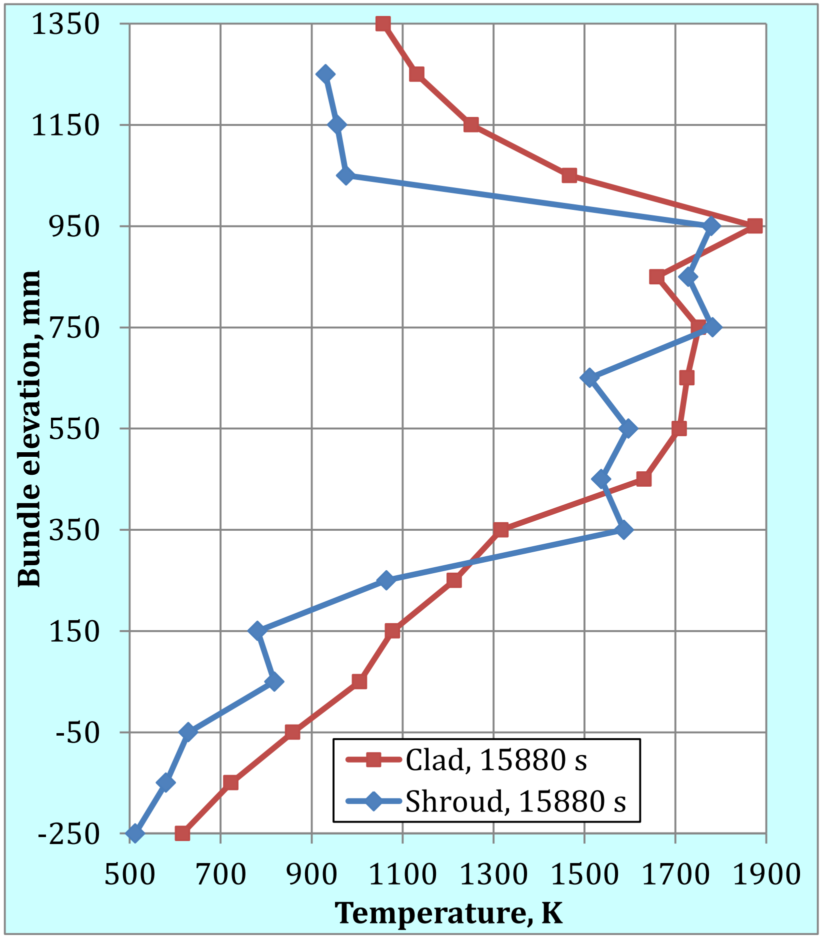

on the end of transient (15880 s)

QUENCH-20: oxidation of Zry-4 corner rod withdrawn on the end of pre-oxidation

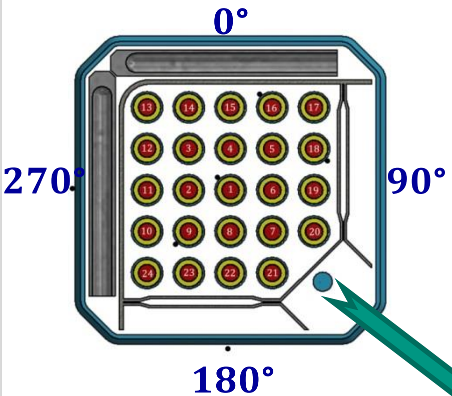

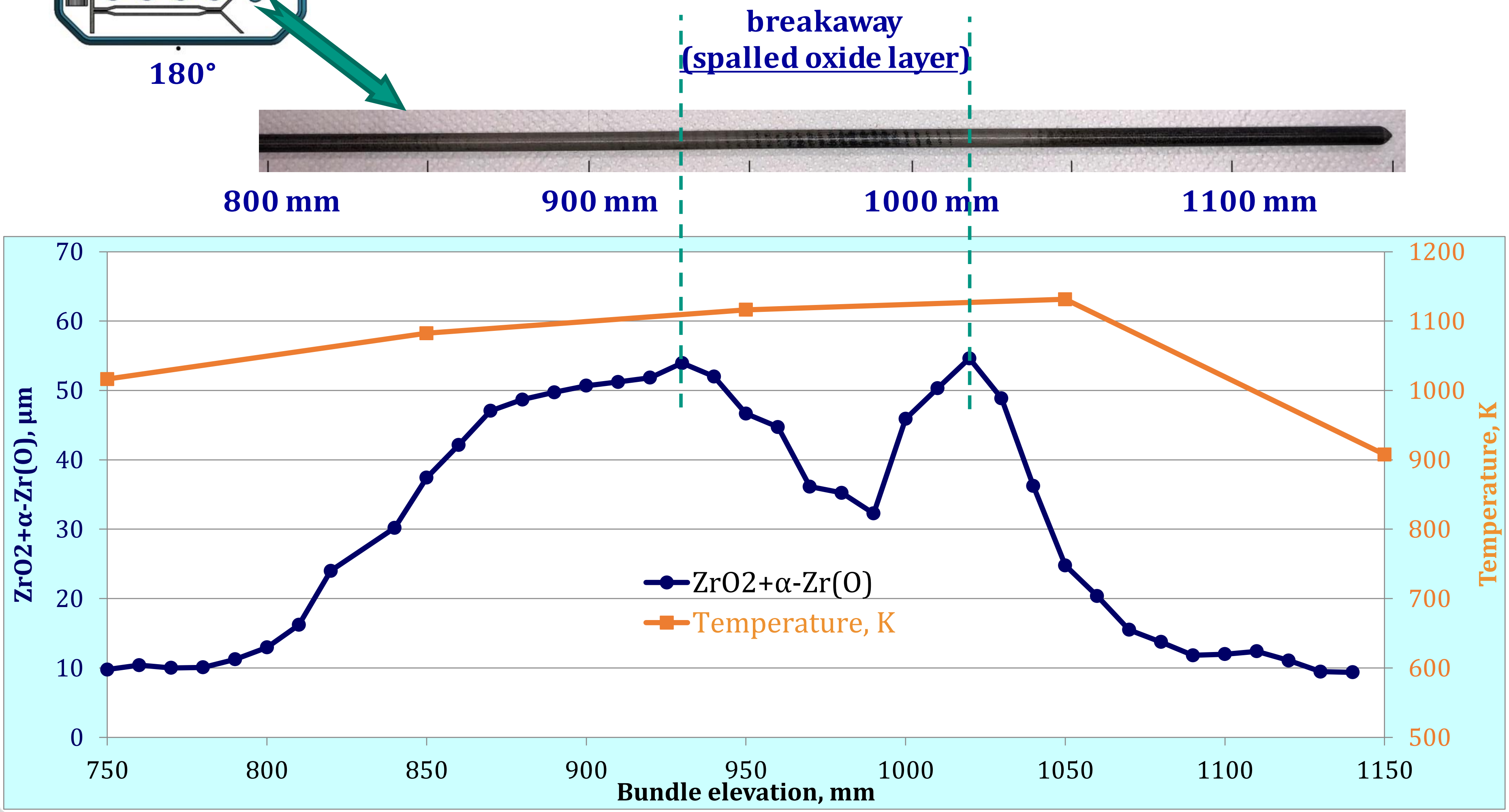

QUENCH-20 bundle surrounded by shroud: post-test view

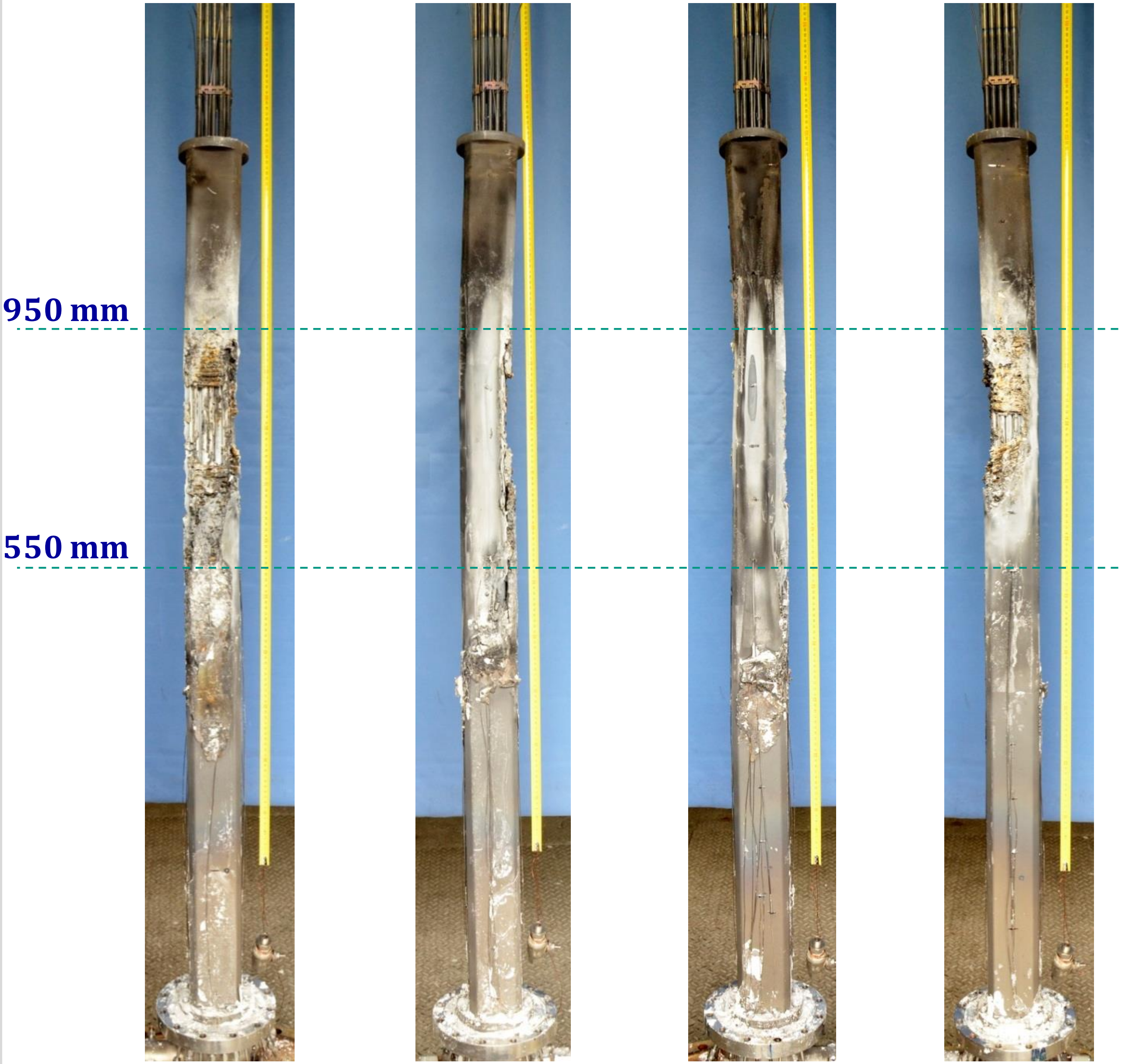

0° 90° 180° 270°

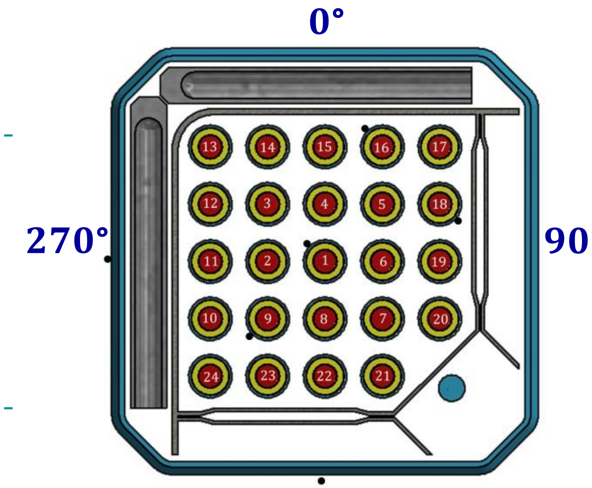

bundle cross-section, top view

QUENCH-20 bundle surrounded by shroud: post-test view

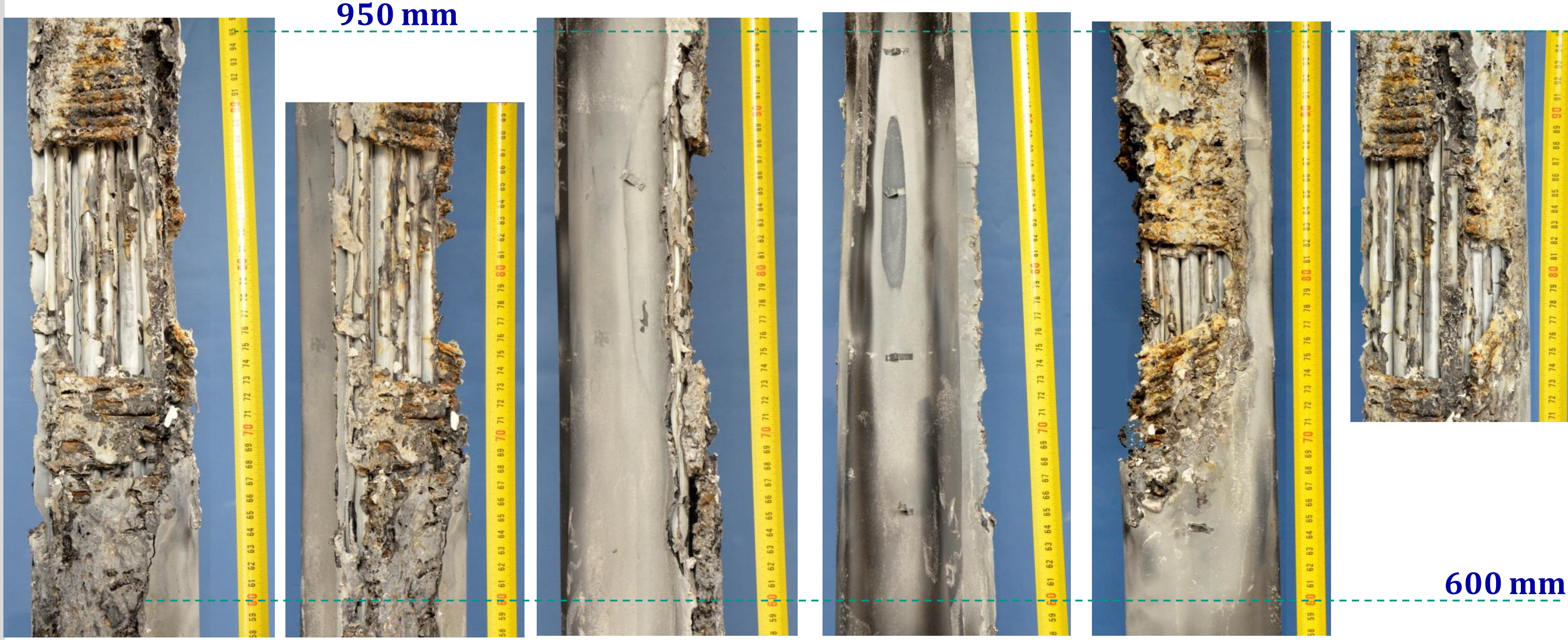

0° 45° 90° 180° 270° 315°

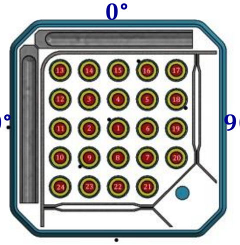

Strong degradation of absorber blades, channel box and shroud between elevations 650 and 950 mm at angle positions 0° and 270°

Overview of polished cross sections:
formation of <u>eutectic absorber melt</u> at elevations 450…950 mm; <u>deformation of Zr shroud</u> and ZIRLO channel box at ≈900 °C due to outer overpressure of 1 bar

	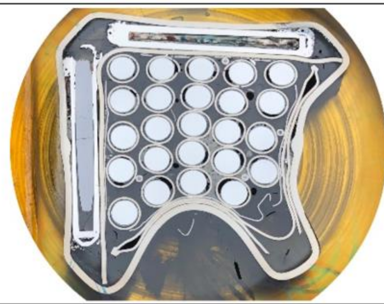		
1150 mm	1050 mm, bottom of 4th spacer	950 mm	850 mm
	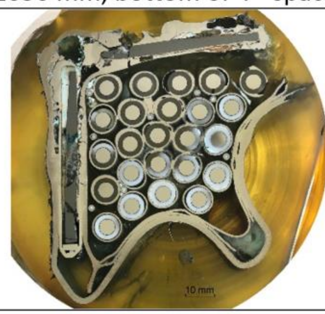	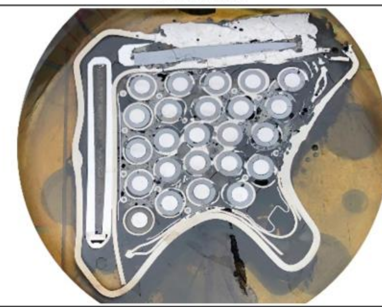	
750 mm	650 mm	555 mm, middle of 3rd spacer	450 mm
	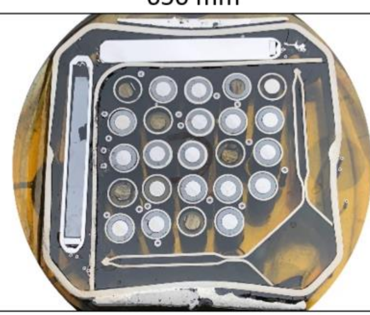		
350 mm	250 mm	50 mm, bottom of 2nd spacer	

Average thicknesses of outer ZrO_2 for each cladding at the bundle elevations 450…950 mm; *not symmetrical distribution of oxidation degree across the bundle due to influence of absorber blades*

Karlsruhe Institute of Technology

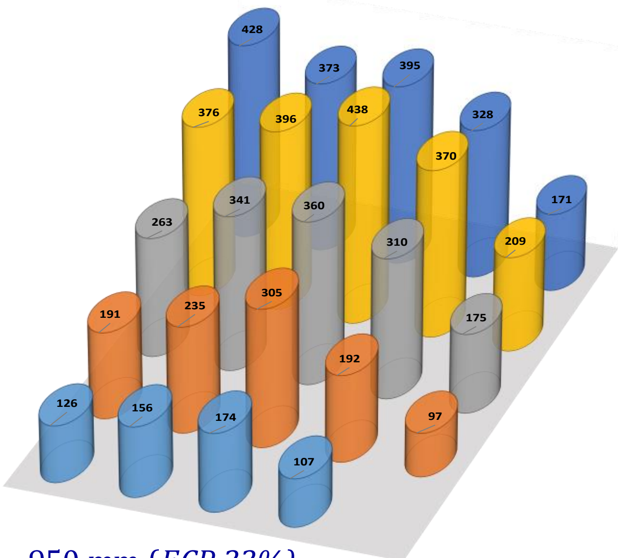

950 mm (*ECR 33%)*

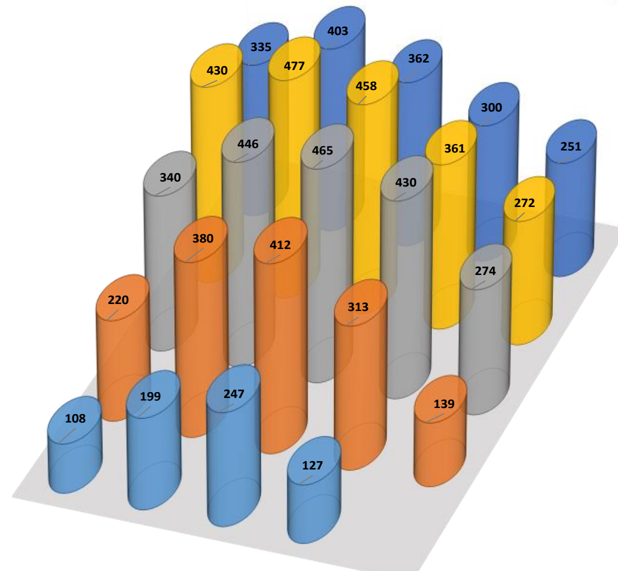

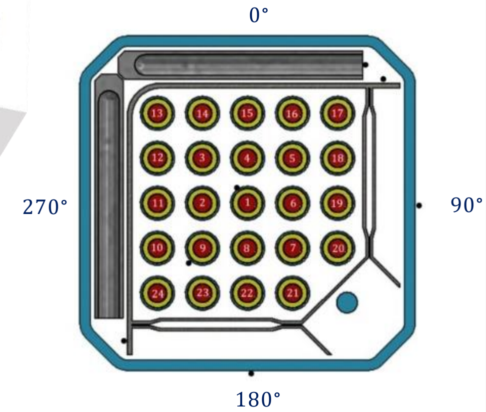

750 mm (*ECR 36%*): mostly oxidized (2nd oxidation degree of peripheral rods in comparison to 850 mm, cladding of inner rods at 850 mm were mostly melted)

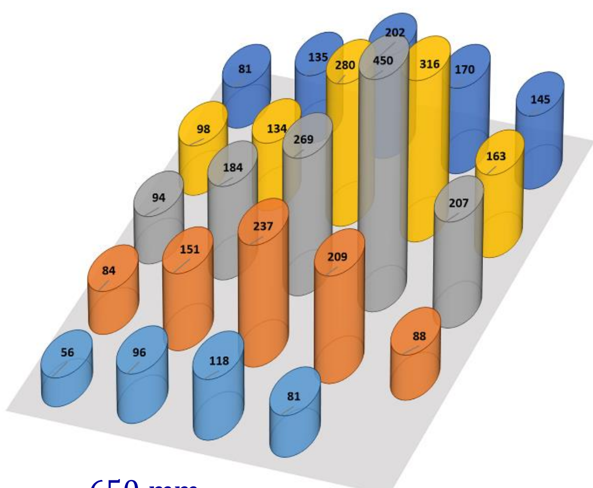

650 mm

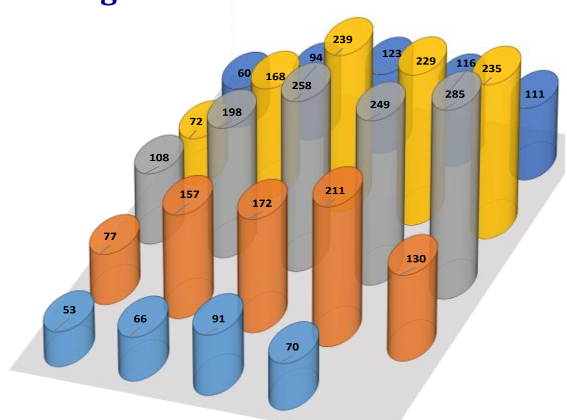

555 mm (grid spacer) (*ECR 21%*)

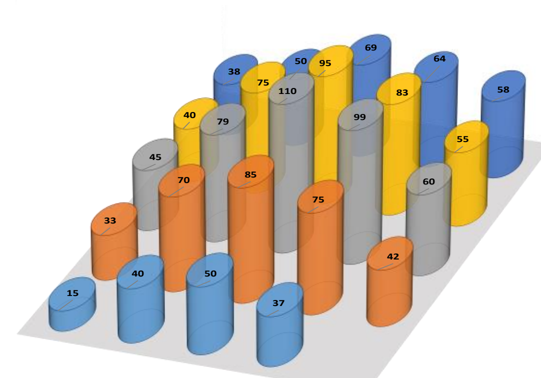

450 mm (*ECR 14%*)

Cladding behavior of relatively hot inner rods at 950 mm

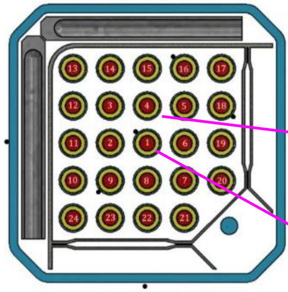

central rod (#1)

inner rod (#4)

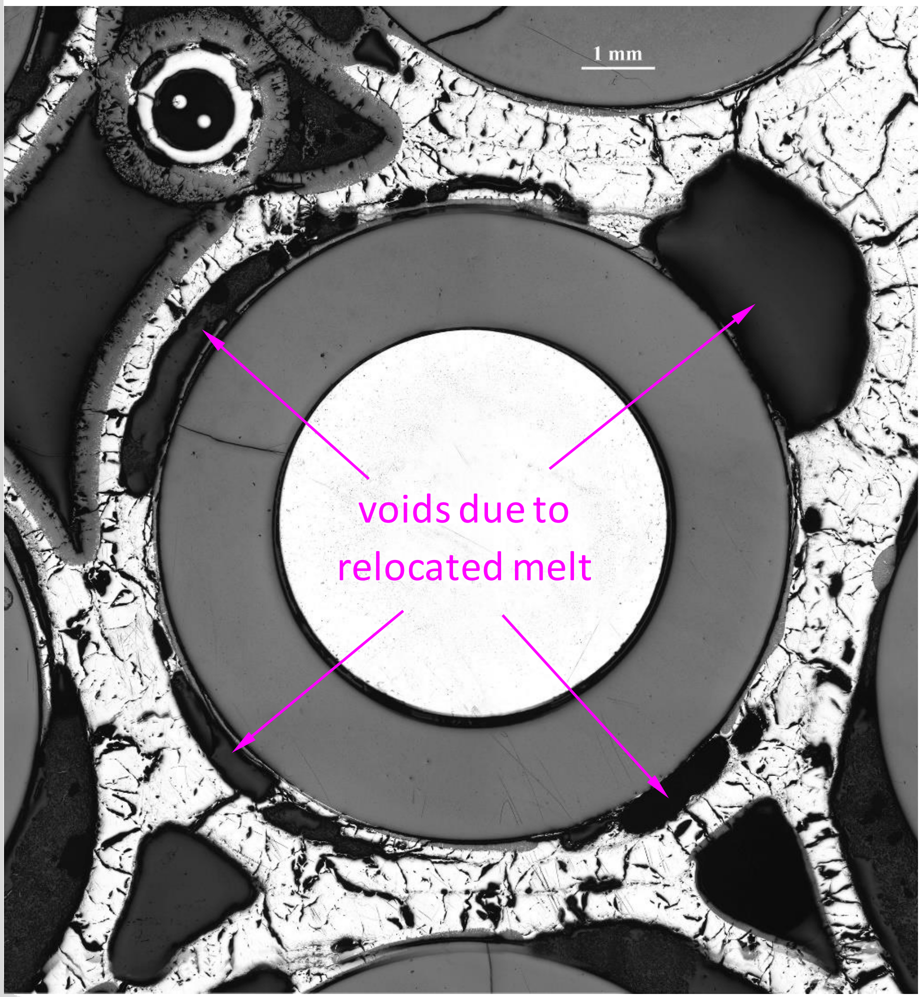

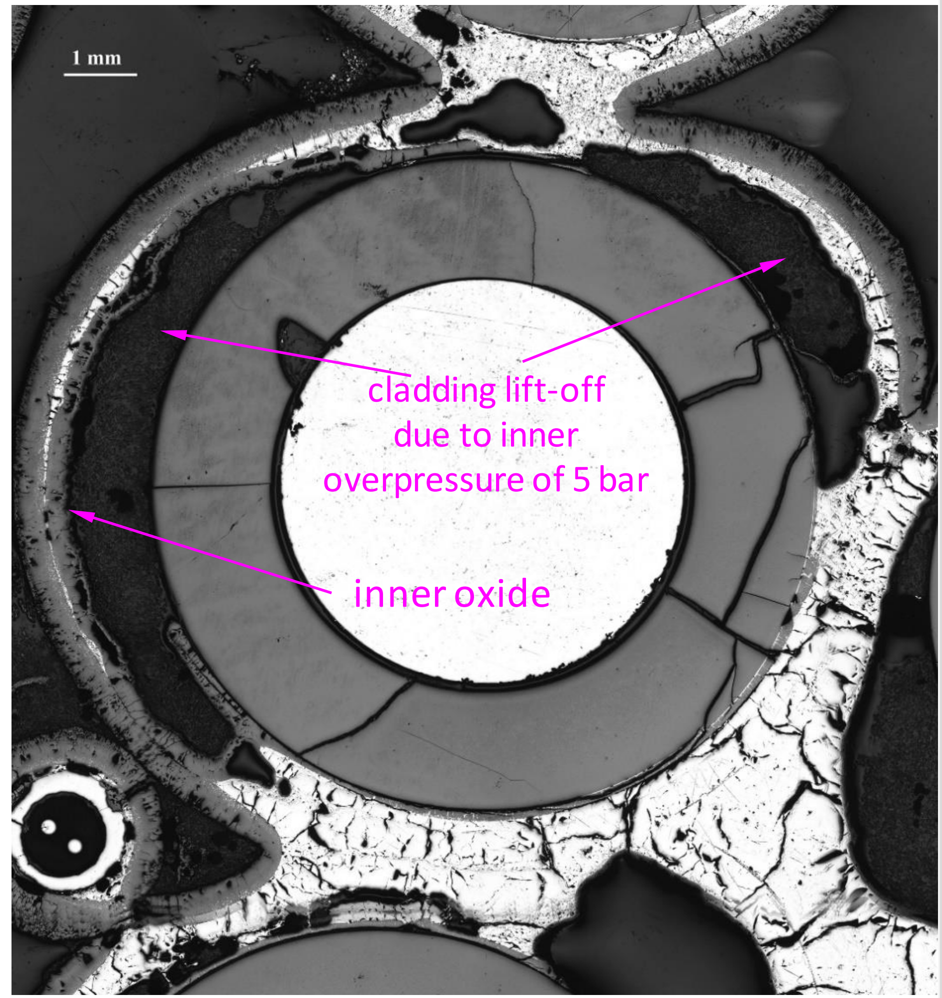

Karlsruhe Institute of Technology

Layer composition for peripheral road #12 at 950 mm: *not melted and melted β-Zr depend on the angle position*

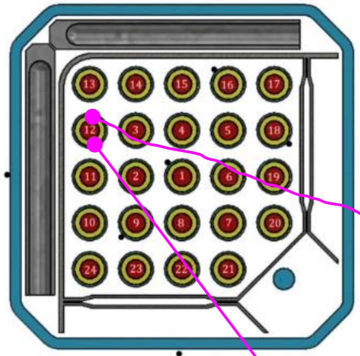

"cold" at 180°

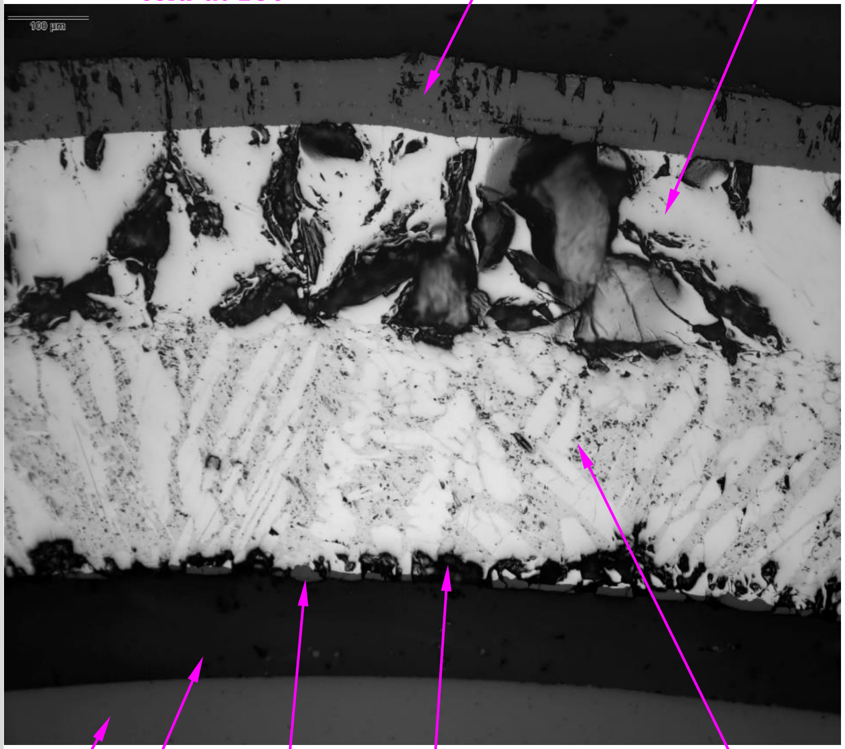

outer tetragonal ZrO_2

outer α-Zr(O) with parts deleted during polishing

ZrO_2 pellet

gap

inner thin tetragonal ZrO_2

inner thin α-Zr(O)

Widmanstätten pattern of β-Zr layer with segregated α lamellas

"hot" at 0°

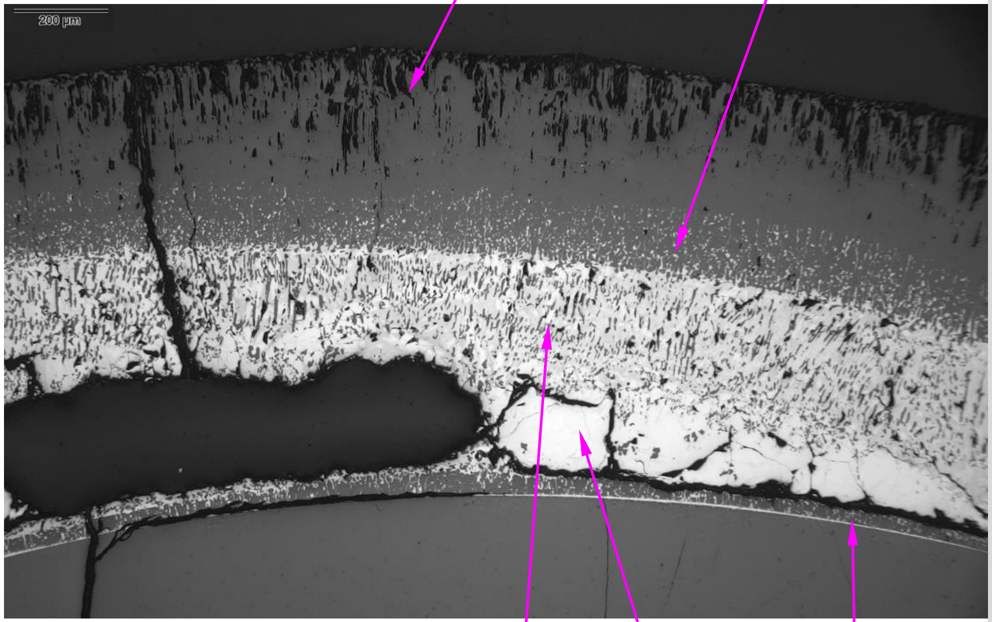

outer tetragonal ZrO_2

ZrO_2 sub-layer with reduced oxygen concentration (diffusion of oxygen to melt)

inner α-Zr(O)

ceramic precipitates formed due to oxygen transport from oxide to molten metal

inner ZrO_{2-x}

850 mm: formation of molten pools and gas channels

KIT Karlsruhe Institute of Technology

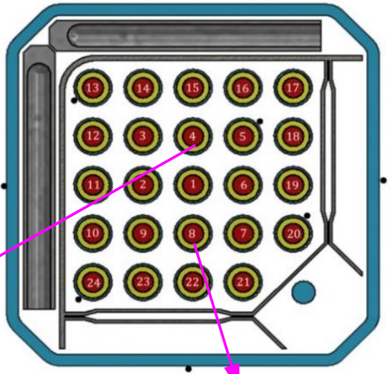

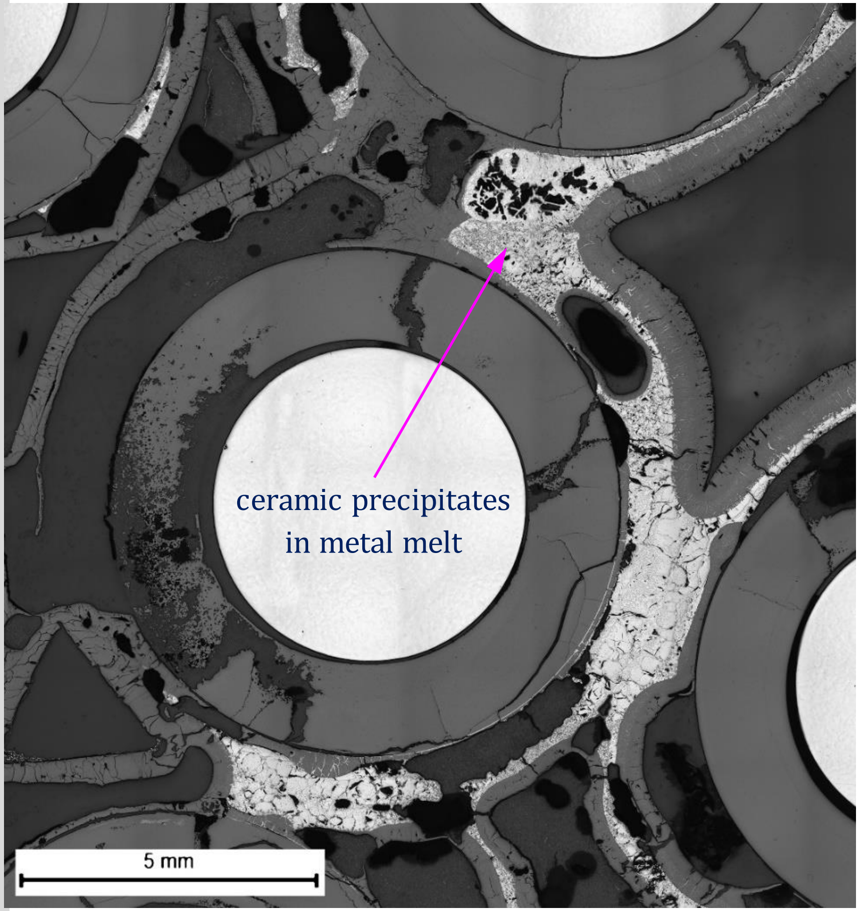

rod #4

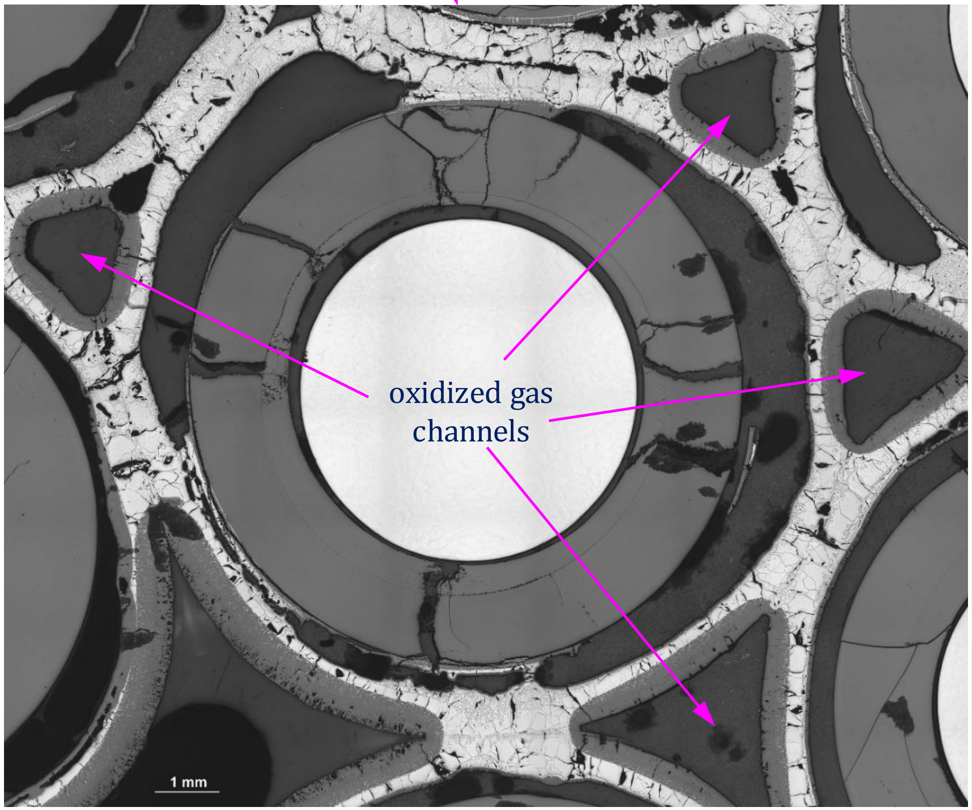

rod #8

IAM Institute for Applied Materials

750 mm: oxidation and melting of claddings, oxidation of ZIRLO water cross-wings

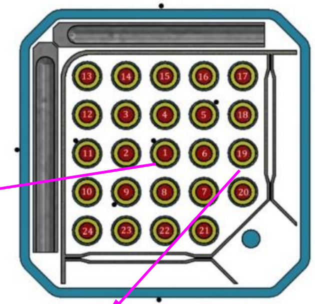

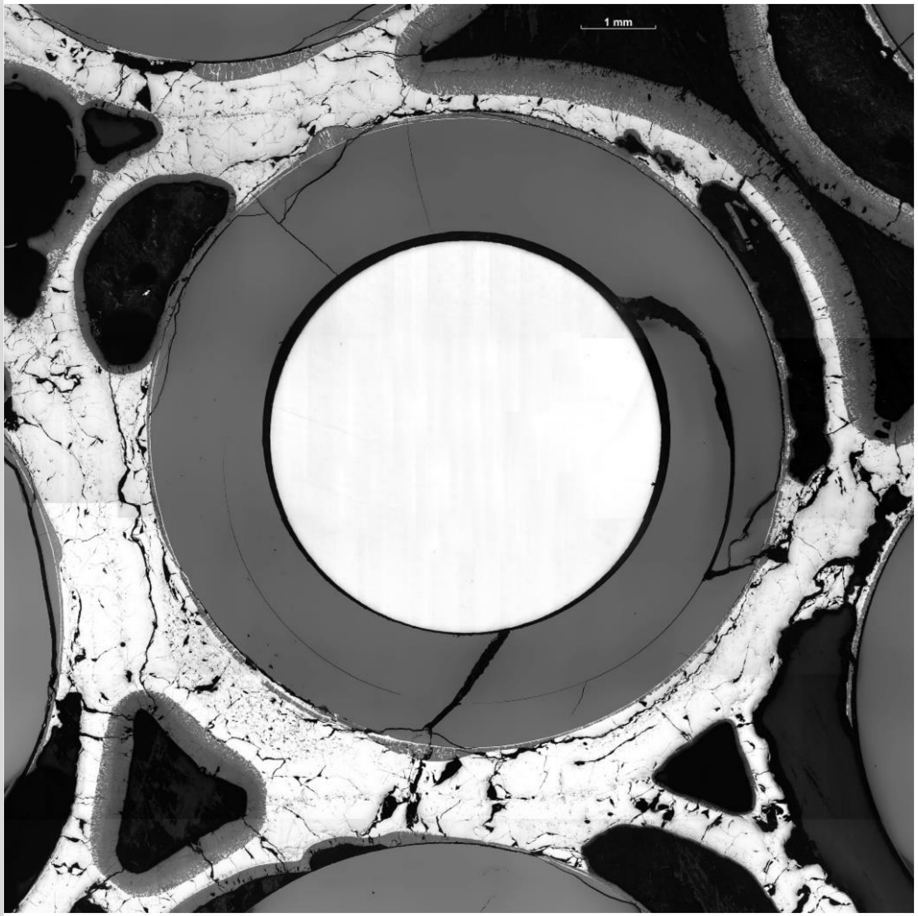

central rod (#1)

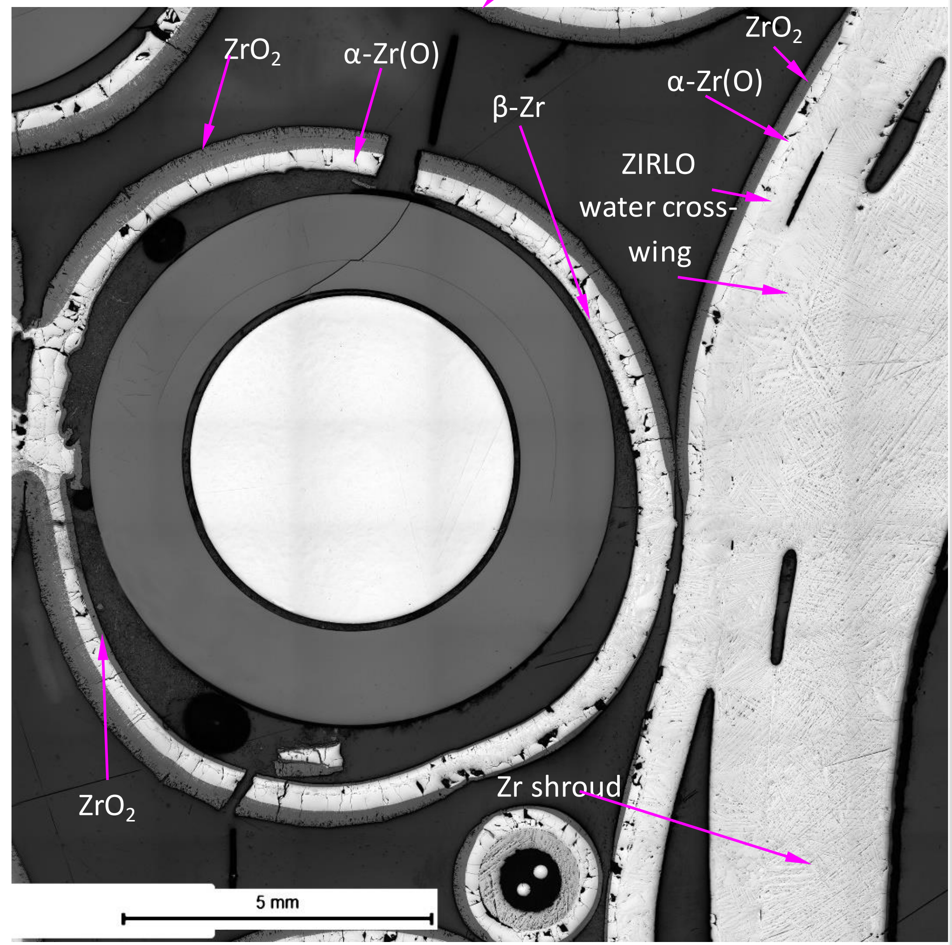

peripheral rod #19, ZIRLO water cross-wing and Zr shroud

750 mm: micro structure of claddings

internal rod #2 at 315°: melted and frozen β-Zr between outer α-Zr(O) and inner ZrO_{2-x}

peripheral rod #12 at 0°: partially oxidized metal melt between outer and inner ZrO_2

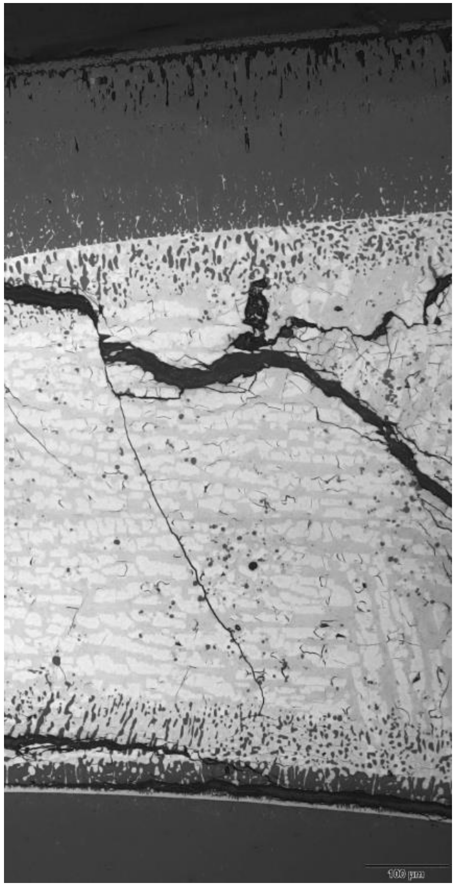

peripheral rod #17 at 45°: partially oxidized metal melt between outer and inner ZrO_2

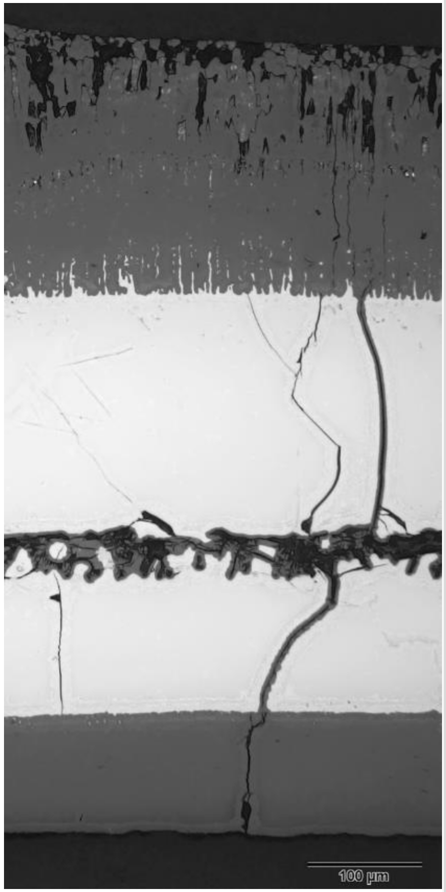

peripheral rod #21 at 315°: not melted metal, oxidation of cracks

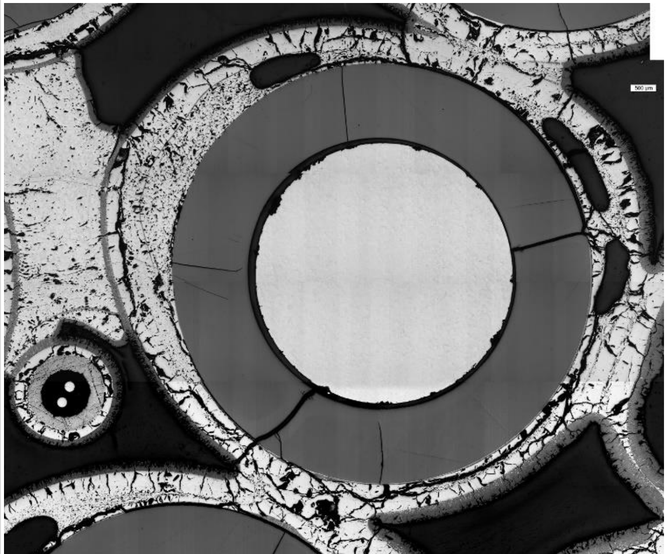

internal rod #4: melt
between outer α-Zr(O) and pellet

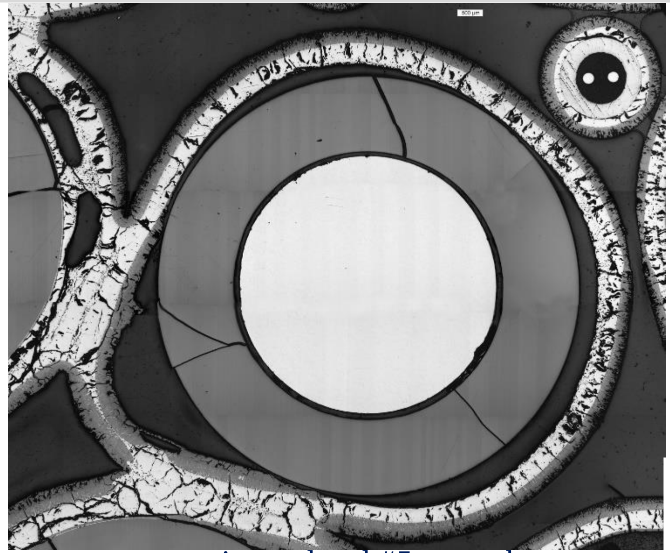

internal rod #5: no melt;
partial inner oxidation of cladding

peripheral rod #13: melt
between outer α-Zr(O) and pellet

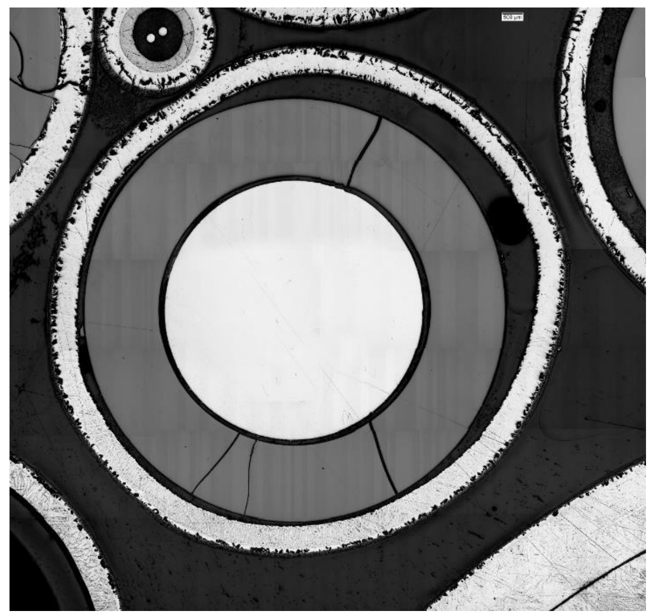

peripheral rod #23: no melt

650 mm: melt formed here and relocated from above

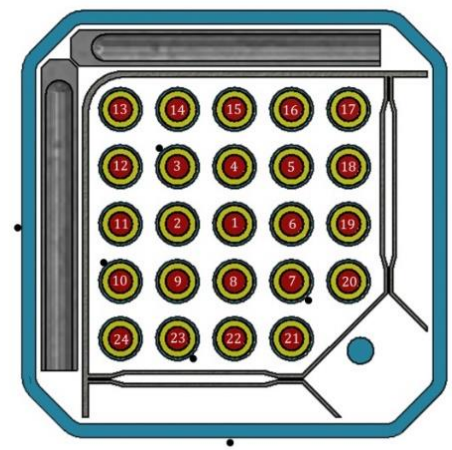

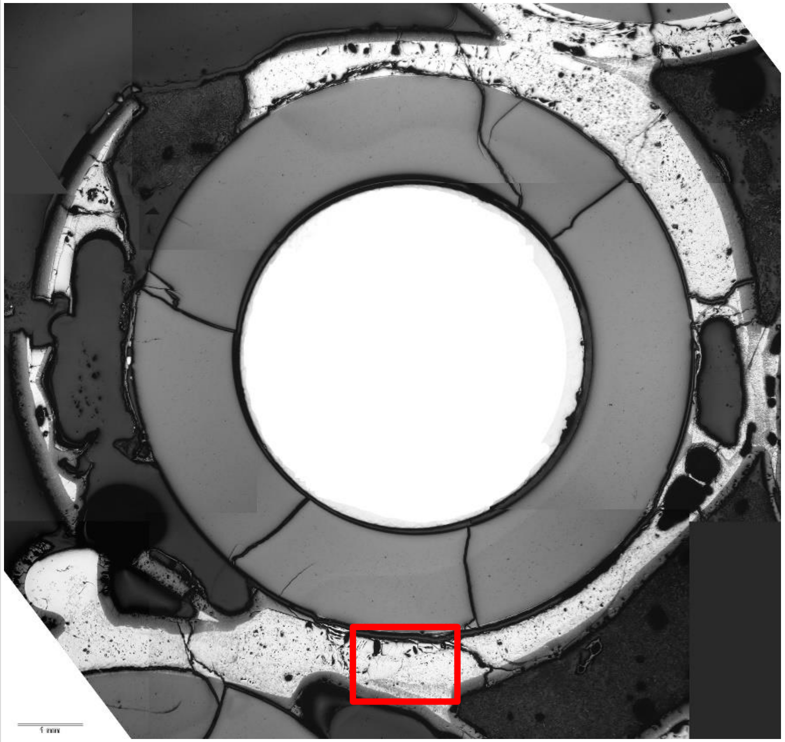

internal rod #4: melt (relocated from above) between outer α-Zr(O) and pellet

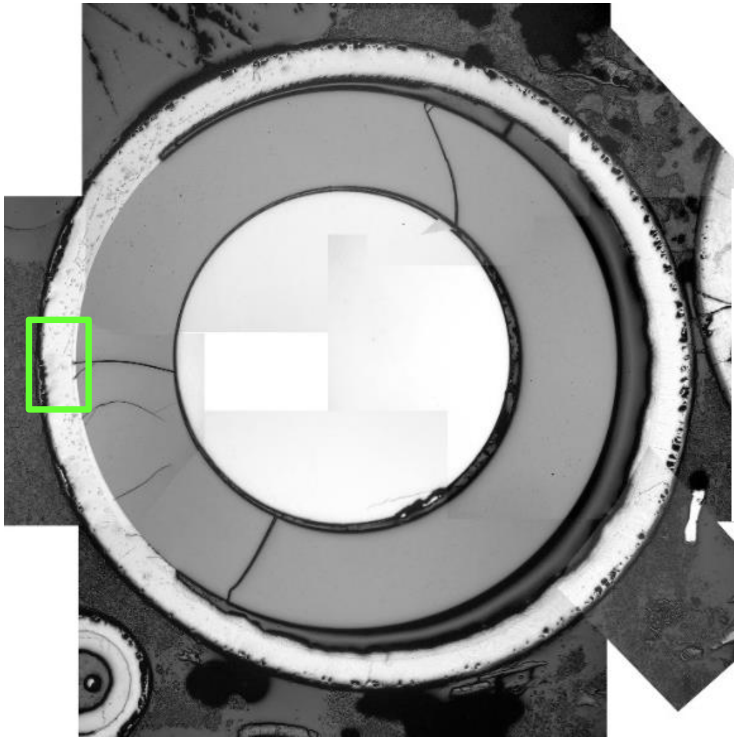

peripheral rod #12: melt relocated from above inside gap between cladding and pellet

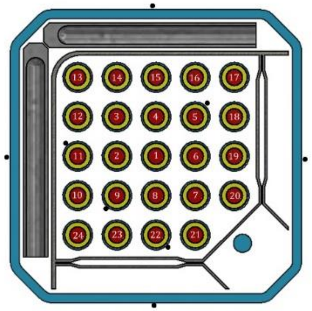

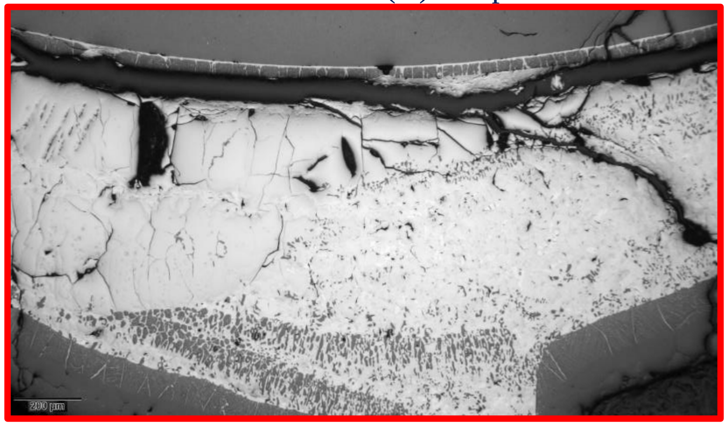

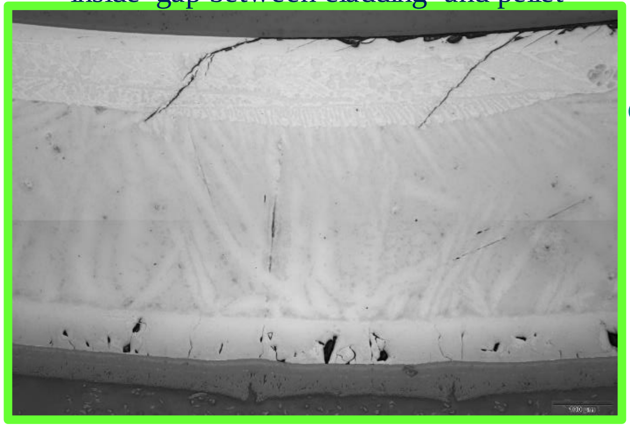

555 mm: melt formed here and relocated from above

450 mm: frozen melt relocated from above

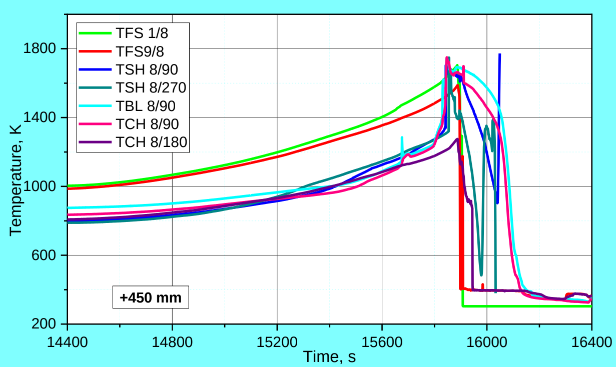

eutectic of Zr and steel

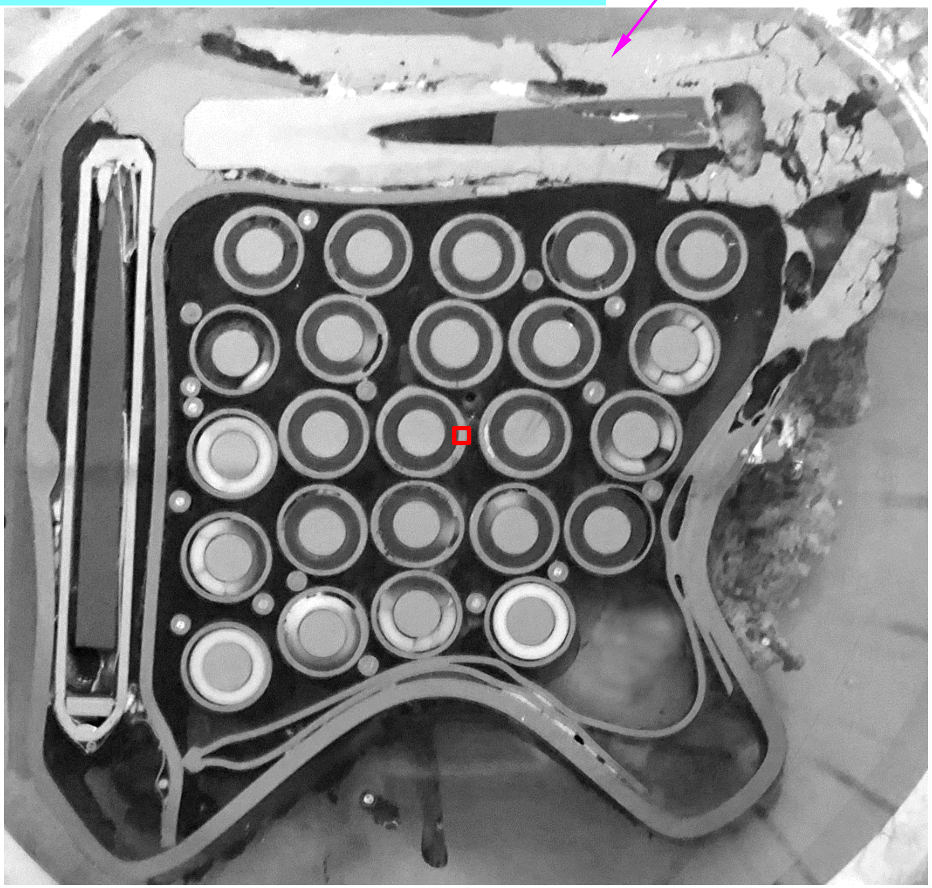

cladding of central rod #1,
original thickness 605 µm

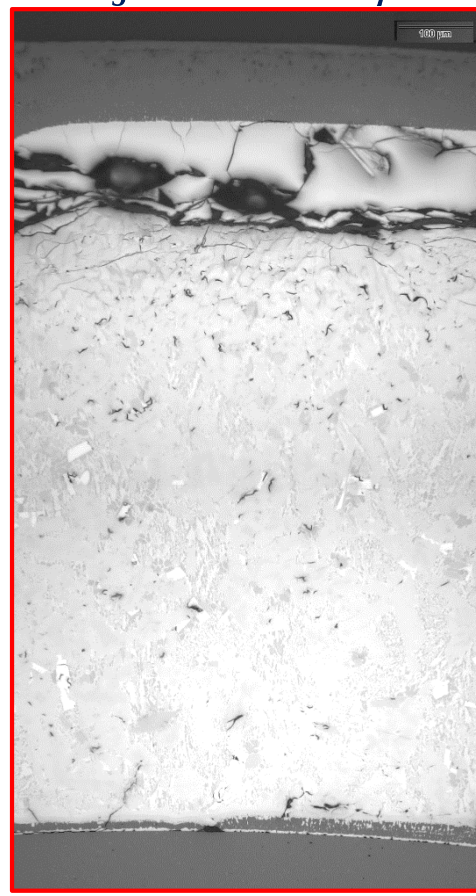

outer ZrO_2 , ***110 µm***

α-Zr(O) , ***120 µm***

β-Zr reacted with **metal melt** relocated from above; ***805 µm***

inner ZrO_{2-x} , ***25 µm***

pellet $ZrO_{2(-x)}$

Elevations without and with grid spacer

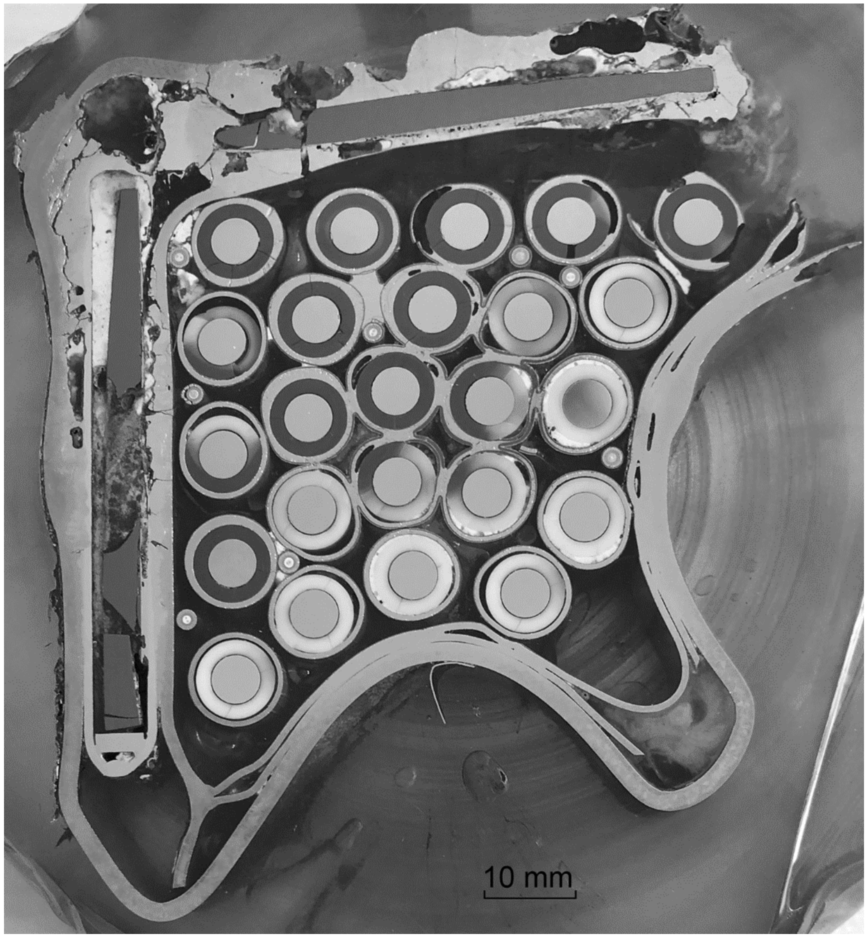

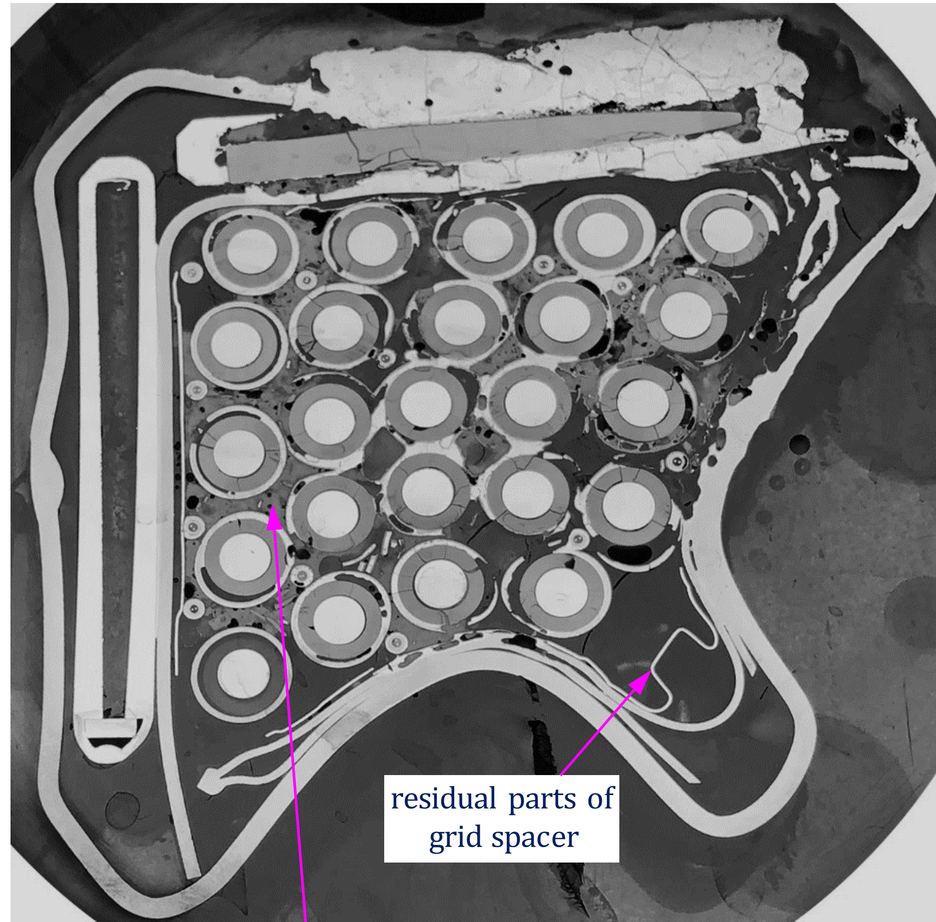

650 mm:
1) local blockages between several rods,
2) dark pellets contacted with inner melt: oxygen transport to melt
(white pellets had no contact with melt)

550 mm:
strong bundle blockage by melt collected inside grid spacer

QUENCH-20: absorber melt relocation from hottest bundle elevations to elevations 250-450 mm

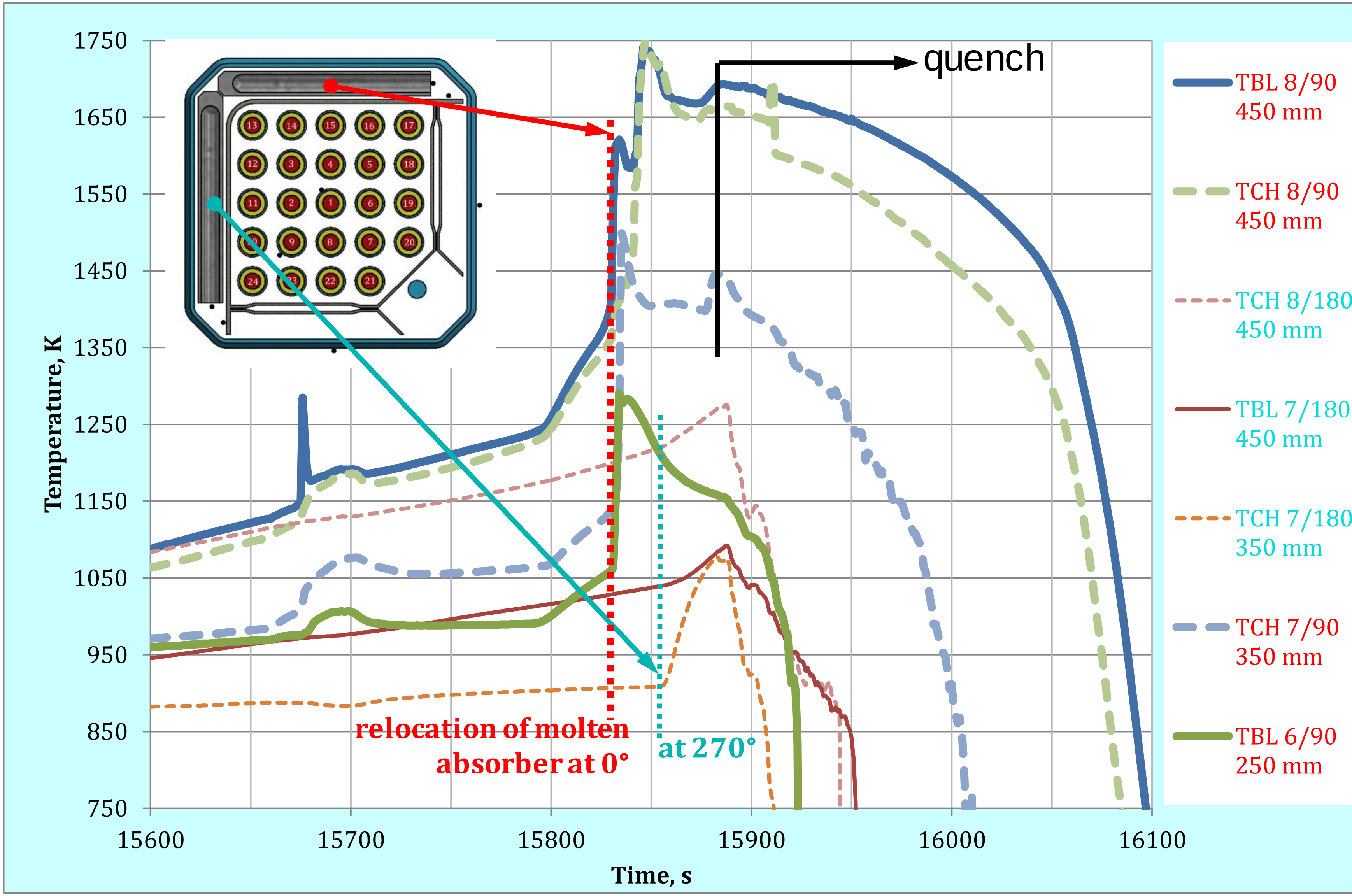

QUENCH-20: reaction of B_4C with steam

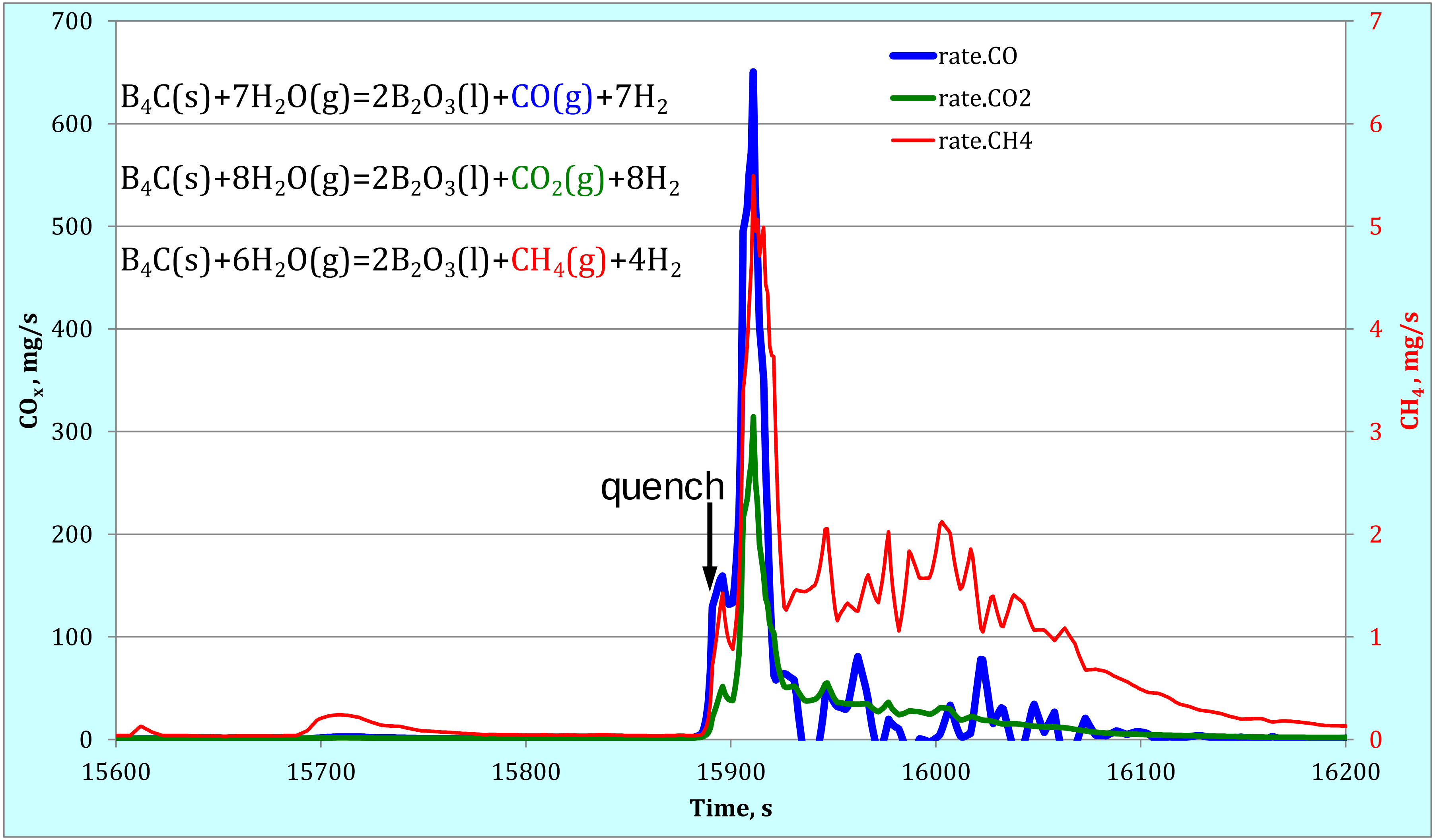

only small release of CH_4 before quench; CO and CO_2 formation firstly in the quench stage

QUENCH-20: reaction of B_4C with steam, integral gas release

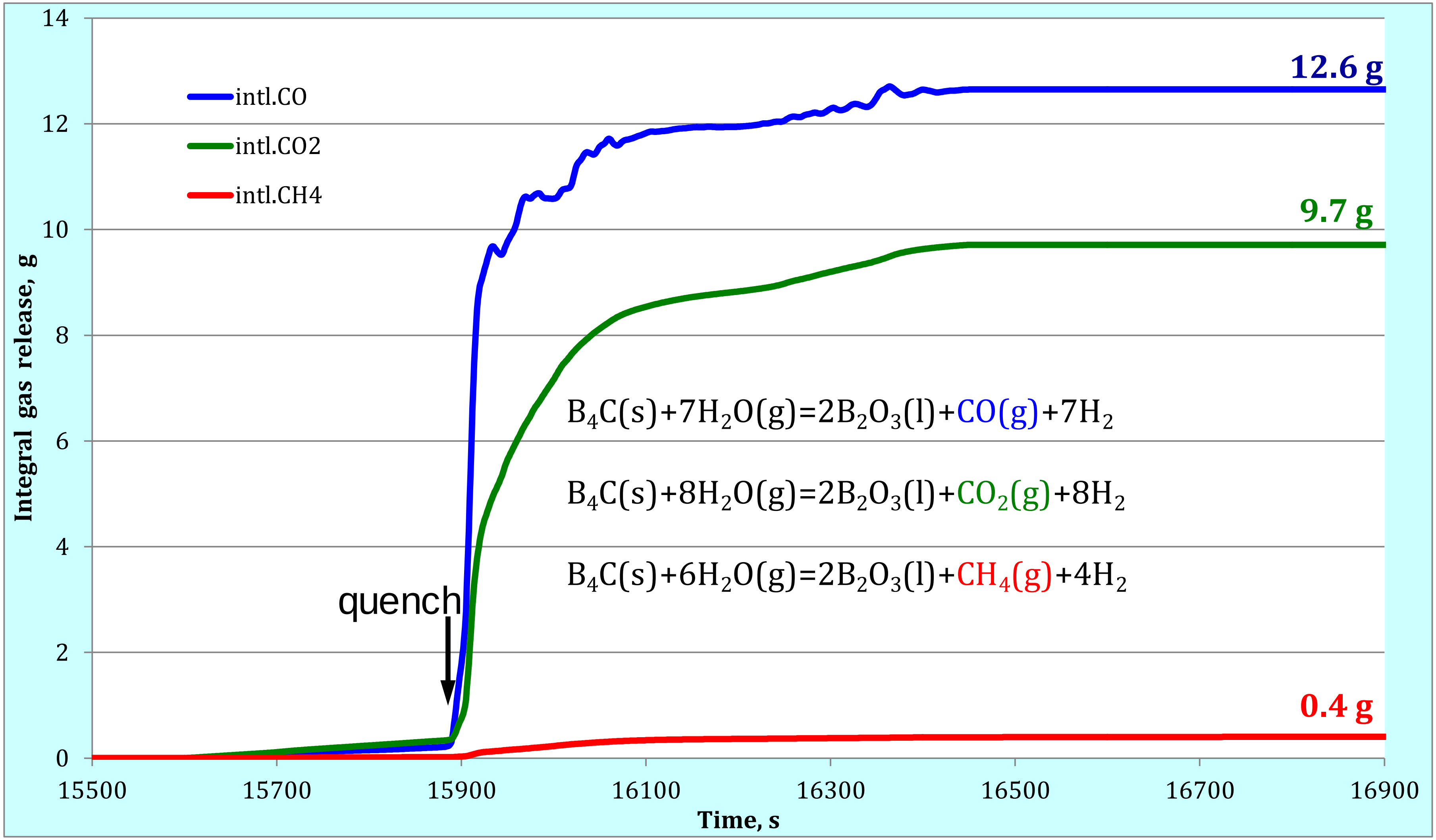

According to CO_x and CH_4 release: corresponding mass of B_2O_3 is 96.8 g; H_2 is 10.0 g; reacted B_4C 41 g, i.e. 4.6% of total B_4C mass (900 g)

QUENCH-20: hydrogen release

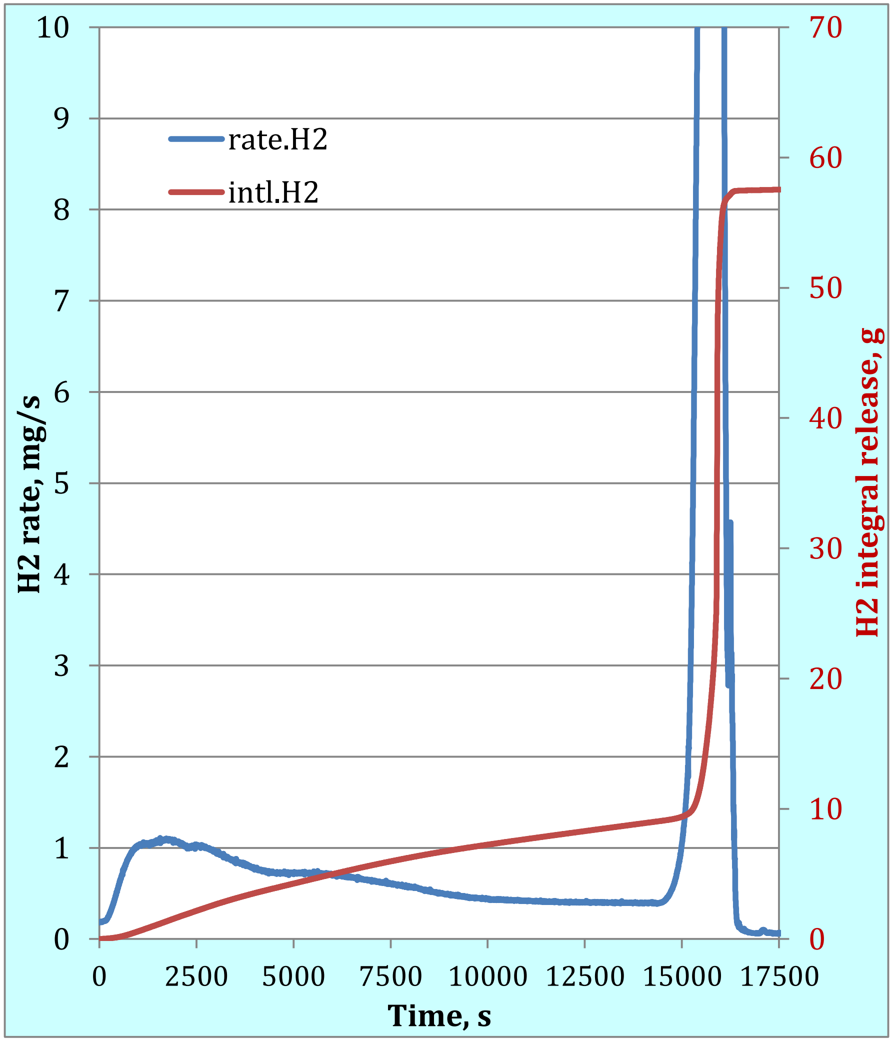

H_2 release during the whole test: 57.4 g;
before quench – interaction of steam with Zry,
during quench – steam interaction with Zry and absorber

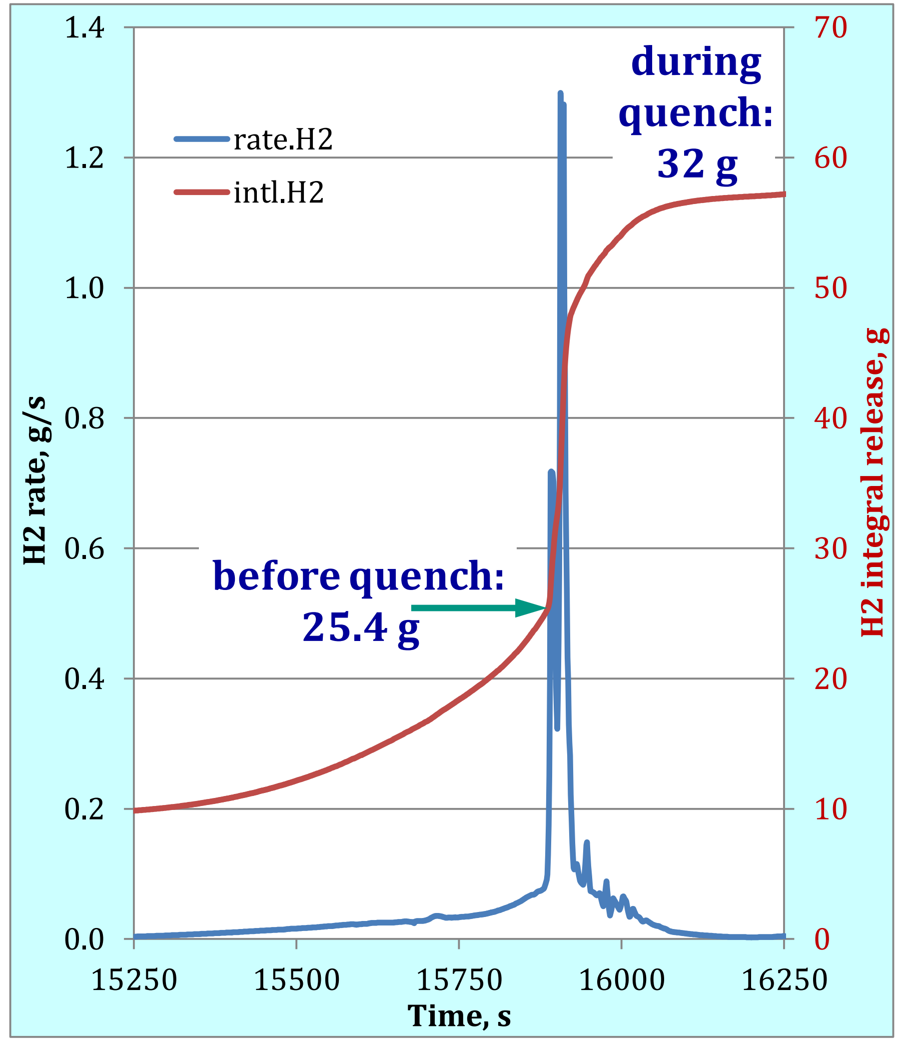

H_2 release during quench:
22 g (from Zry and molten steel) +
+ 10 g (from B_4C)

750 mm: interaction of stainless steel blade with B_4C and ZIRLO channel box

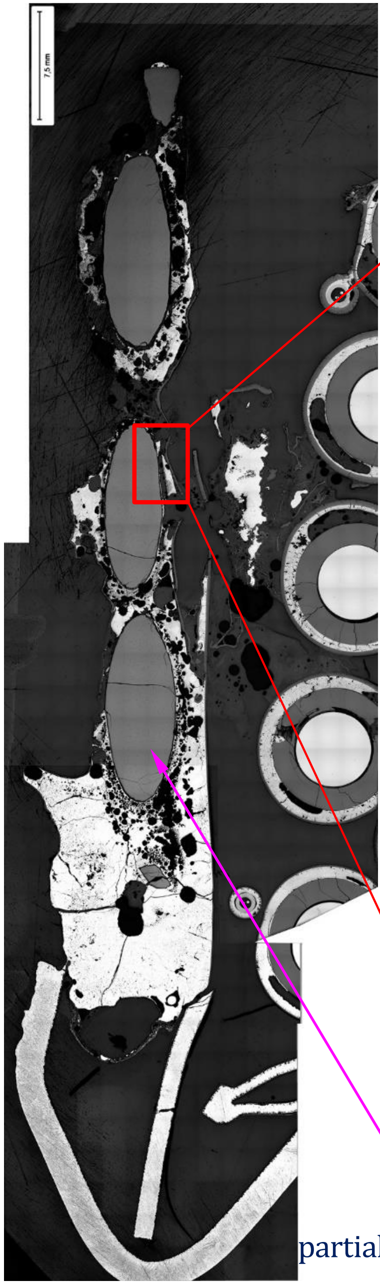

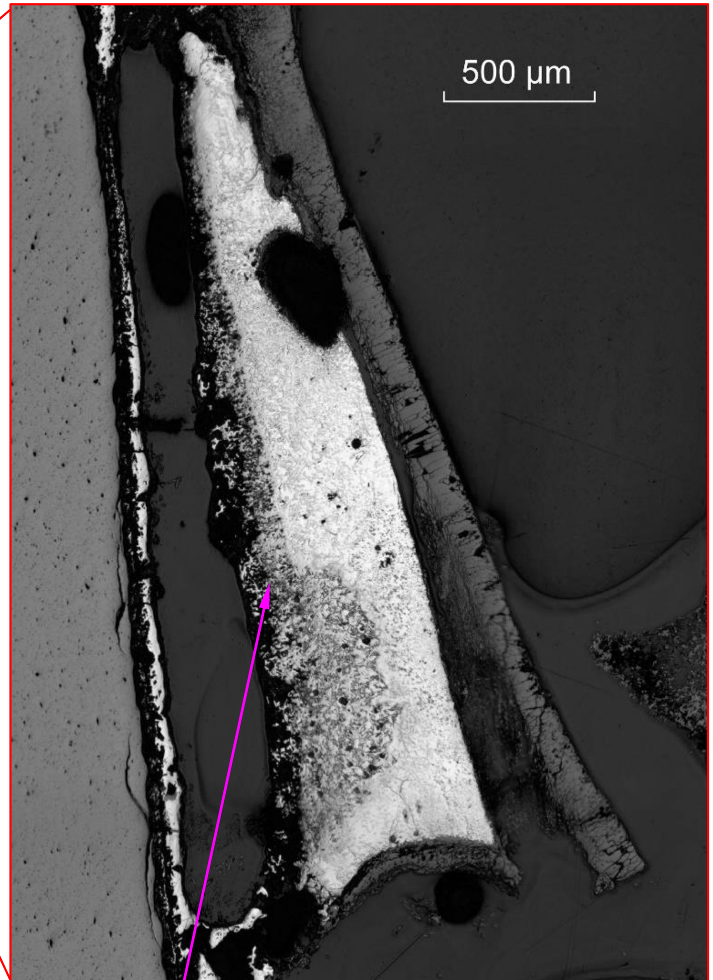

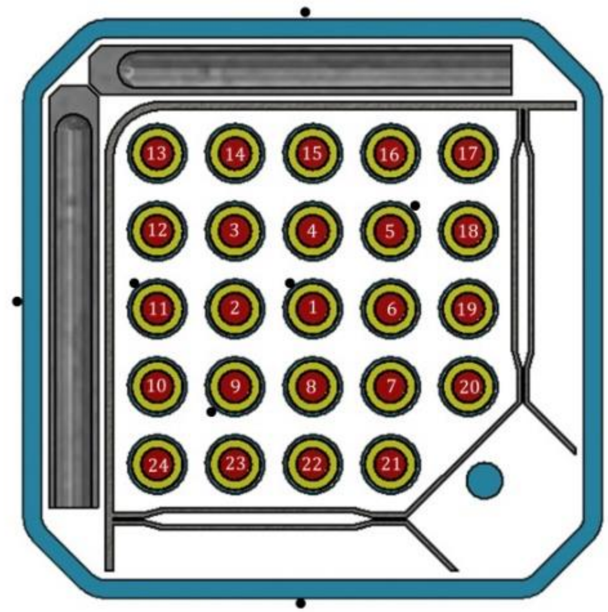

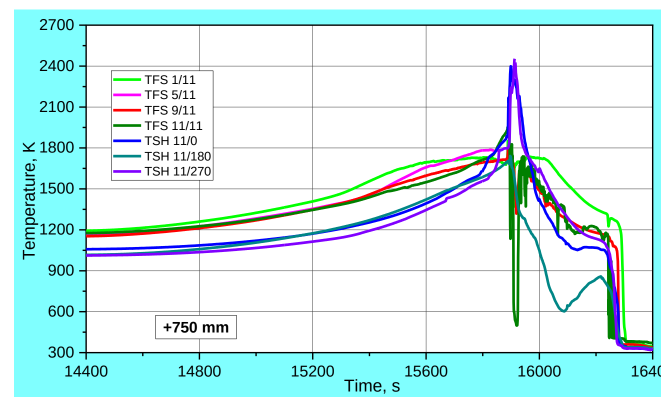

eutectic interaction B_4C pin ↔ blade at T>1500 K;

partially dissolved B_4C pin

750 mm: SEM/EDX investigation of interaction of B_4C with steel blade and ZIRLO channel box

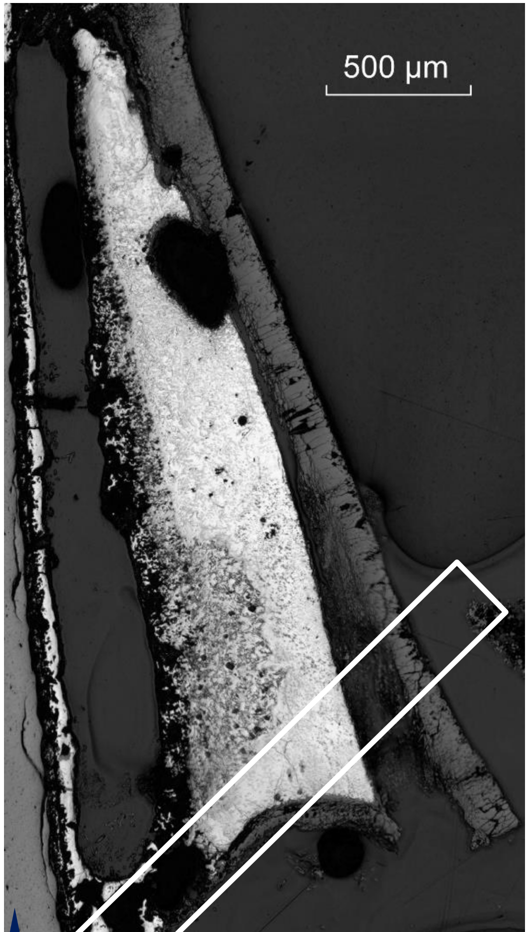

B_4C pin

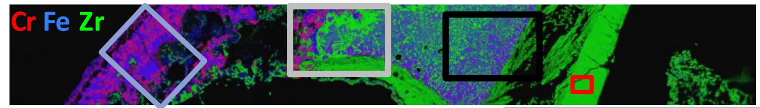

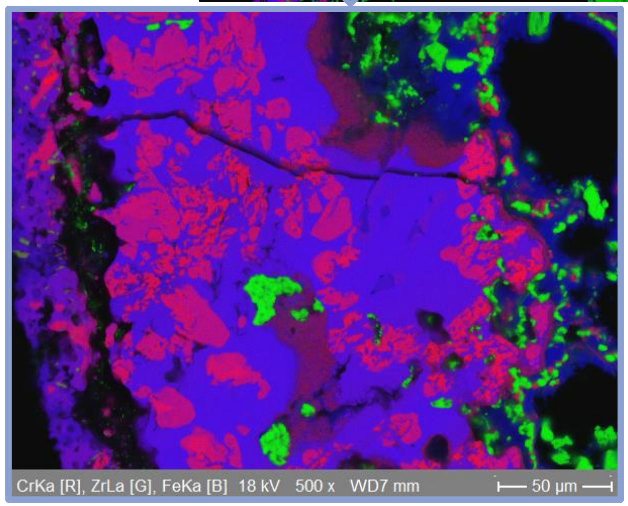

stainless steel blade: (Fe, Cr) boride (red) in steel melt (blue)

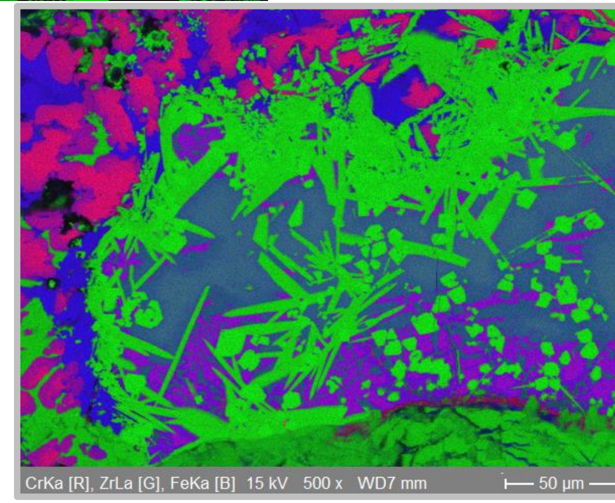

ZrB_2 needle precipitates in Zr-steel eutectic melt

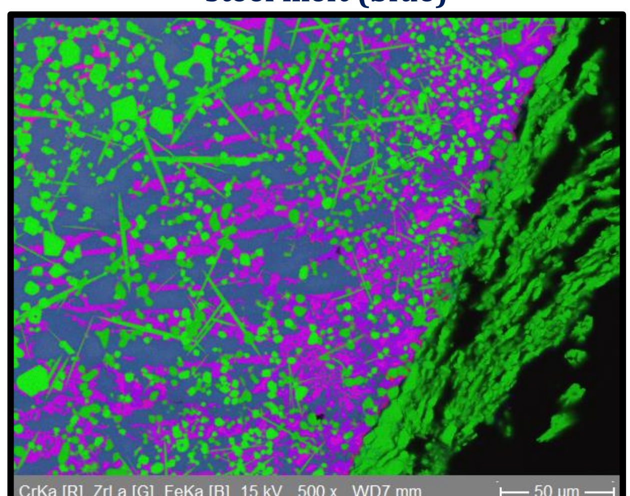

ZrB_2 needle precipitates in Zr-steel eutectic melt

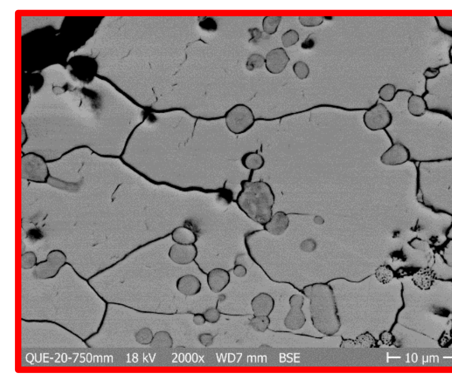

ZrO_2 layer

750 mm: SEM/EDX investigation of interaction of B_4C with steel blade and ZIRLO channel box

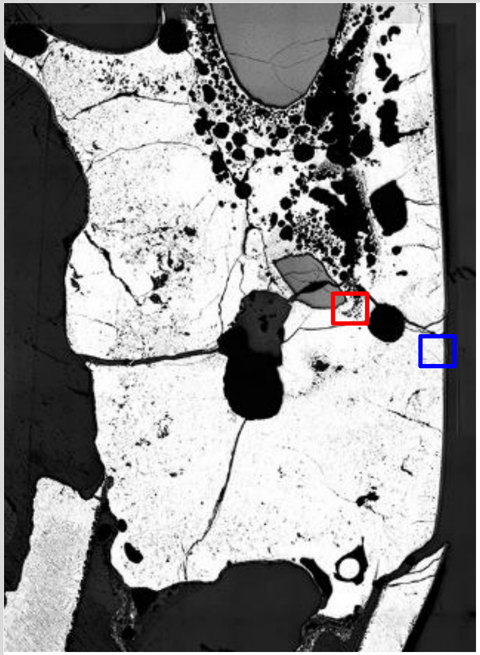

B_4C

(Fe, Cr) precipitates
(partially borides)
in Fe melt

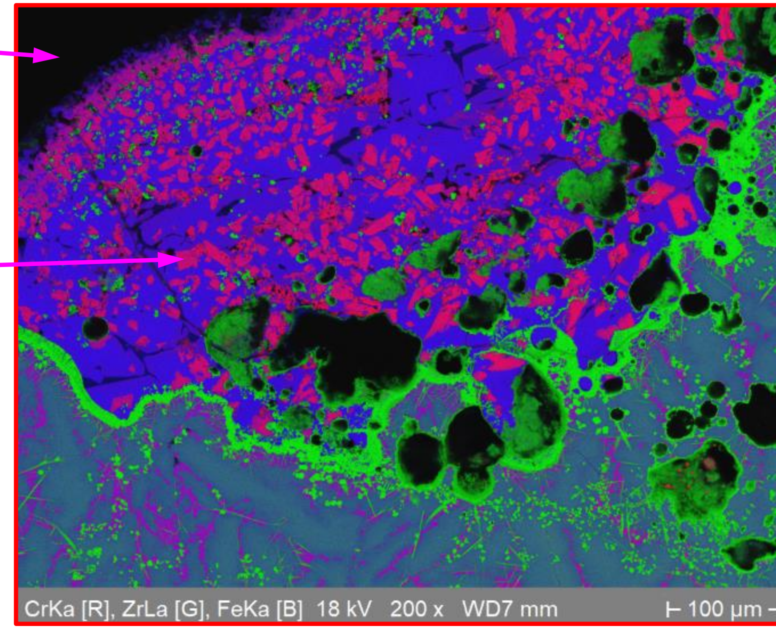

contact B_4C with steel blade

contact steel blade with ZIRLO channel box

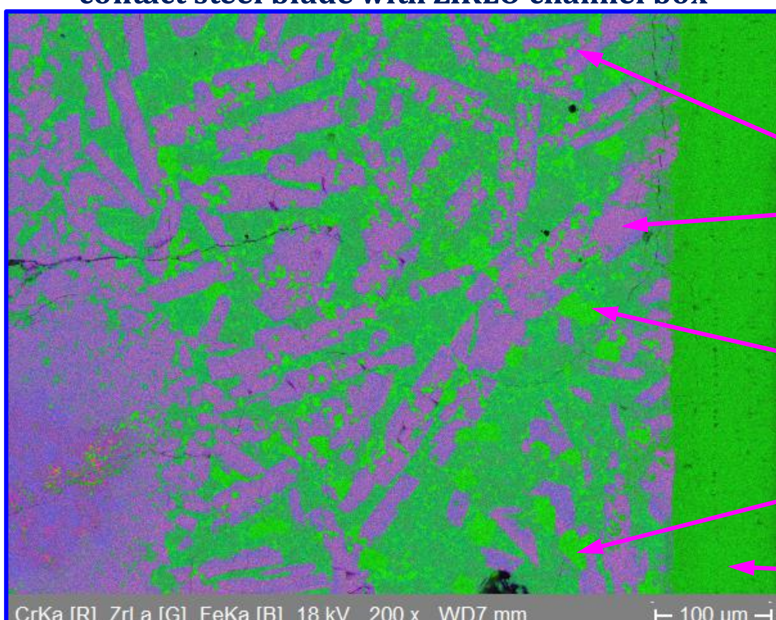

(Fe, Cr) precipitates
in (Ni, Fe, Zr) melt

ZrB_2 precipitates in
(Ni, Fe, Zr) melt

ZrO_2

Summary and conclusions

- The QUENCH-20 test bundle mock-up represented one quarter of a BWR fuel assembly with 24 electrically heated fuel rod simulators and B_4C control blade. The pre-oxidation stage lasted 4 hours at the peak cladding temperature of 1250 K. The Zry-4 corner rod, withdrawn at the end of this stage, showed the maximal oxidation with ZrO_2 thickness >55 µm at elevations between 930 and 1020 mm with signs of breakaway.
- During the transient stage, the bundle was heated to a maximal temperature of **2000 K**. *Massive absorber melt relocation was observed 50 s before the end of transient stage*.
- The test was terminated with the quench water injected with a flow rate of 50 g/s from the bundle bottom. Fast *temperature escalation* from 2000 to **2300 K** during 20 s was observed. The mass spectrometer measured *release of CO (12.6 g), CO_2 (9.7 g) and CH_4 (0.4 g) during the reflood as products of absorber oxidation; corresponding B_4C reacted mass was 41 g or 4.6% of total B_4C.*
- Hydrogen production during the reflood amounted to **32 g** (57.4 g during the whole test) including 10 g from B_4C oxidation.

Summary and conclusions (cont.)

- All claddings were failed during the transient with penetration of the steam into the gap between cladding and pellet. The average oxidation rate of the inner cladding surface is about 20% in comparison to the outer cladding oxidation.
- The distribution of the oxidation rate within each bundle cross section is very inhomogeneous: whereas the average outer ZrO_2 layer thickness for the central rod (#1) at the elevation of 750 mm is 465 µm, the same parameter for the peripheral rod #24 is only 108 µm.
- The bundle elevation 750 mm is mostly oxidized with ECR 36% due to 1) downwards shift of the temperature maximum from 950 mm (ECR 33%) during transient and quench, 2) due to cladding melt relocation inside and outside the rods from 800…1000 mm to lower bundle elevations.
- The oxidation of the melt relocated inside rods was observed at elevations 550…950 mm.
- The oxidation of B_4C pins was relatively low: only 4.6% of total B_4C mass has reacted with steam (mostly during the quench stage).
- The interaction of B_4C with steel blade and ZIRLO channel box was observed at elevations 650…950 mm with formation of eutectic melt relocated partially to lower positions. The typical components of this melt are (Fe, Cr) borides and ZrB2 precipitated in steel or in Zr-steel eutectic melt.

Acknowledgment

The QUENCH-20 experiment was performed in the framework of the SAFEST project in cooperation with Swedish Radiation Safety Authority (SSM), Westinghouse Sweden, GRS and KTH and supported by the KIT program NUSAFE. Personal thanks to Mr. Isaksson (SSM), Mr. Bechta (KTH), Mr. Hollands (GRS), Ms. Korske (Westinghouse) for their help and fruitful cooperation. The bundle materials and absorbers were provided by Westinghouse Sweden.

The authors would like to thank all colleagues involved in the post-test investigations.

Thank you for your attention

http://www.iam.kit.edu/awp/666.php
http://quench.forschung.kit.edu/

O. Murat, V.H. Sanchez Espinoza, R.
Stieglitz
KIT

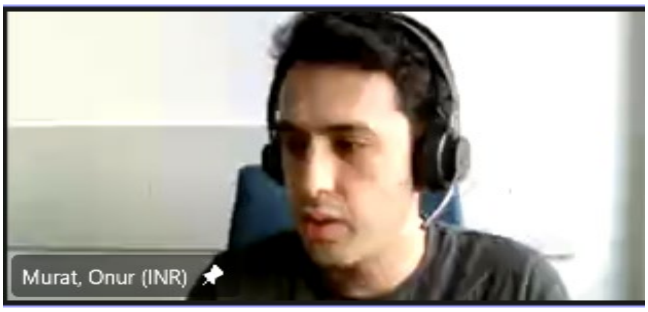

Analysis of QUENCH-20 Test with ASTEC V2.2.b

Latest recorded severe accident in the Fukushima Daiichi arose the importance of the safety evaluations of the plants and systems. In order to fulfill the necessity of the safety assessments, accident simulations are performed using by severe accident codes. European reference integral severe accident code ASTEC mainly developed for PWR type reactors in order to simulate from accident initiating event to radiological release. Since the BWR type reactors have typical structures in the core such as canisters, absorber cross, etc. simulations needs to be performed with consideration of these peculiarities. Comparison of the performed simulations with experiments are key point to ensure validity of the code and employed models.

In order to expand the database of degradation of the fuel bundles in case of severe accident situation, QUENCH-20 experiment, includes one quarter of SVEA-96 Optima-2 fuel assembly, was performed in KIT. Temperature of the fuel rods, hydrogen production and quench front parameters were followed up with simulation results and comparison was performed for validation purposes. Model of the QUENCH facility and the bundle was developed using by information of geometry, material and boundary conditions, which was mass flow rate, pressure and electrical power for heated rods. Prediction of temperature of the structures in ASTEC fairly follows up the test measurements during the transient. Hydrogen generation evaluated by the ASTEC in good agreement with test results. Total measured 57 g of hydrogen generation was predicted by ASTEC 53 g. Besides, oxidation of the boron carbide material reproduced by the ASTEC with resulting 15% of the total produced hydrogen, which is in good agreement with QUENCH-20 measurements.

Karlsruhe Institute of Technology

Analysis of QUENCH-20 Test with ASTEC V2.2.b

Name: Onur Murat
Supervisor(s): Dr. Victor Hugo Sanchez Espinoza, Prof. Robert Stieglitz

INSTITUTE for NEUTRON PHYSICS and REACTOR TECHNOLOGY (INR)

Outline

- Introduction
- Motivation
- QUENCH-20 Test
  - Test Facility
  - Selected Fuel Bundle (SVEA-96 OPTIMA2)
  - Test Transient
- Numerical Tool: ASTEC
  - ASTEC Model of QUENCH-20 Test Section
  - ASTEC Model of QUENCH-20 Heated Rod
  - Boundary Conditions
  - ASTEC Predictions of QUENCH-20 Test
- Conclusion

Introduction

- In case of long term LOCA in severe accident scenarios core uncovery occurs.
- Without heat removal capacity:
  - Heat-up in the core
  - Oxidation of metals by steam (more heat-up)
  - Hydrogen release by oxidation
  - Cladding deformation and loss of geometry
  - Fission product release
- Produced heat and degraded core leads corium and melt material corium threats:

IN VESSEL and EX-VESSEL

- Released H2+Non-condensable gasses threats:

EX-VESSEL

Prediction of in vessel phenomena is important for SAFETY

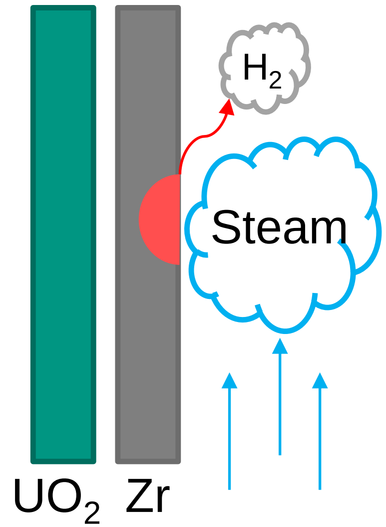

Introduction

- Not only oxidation process but also eutectic interactions are crucial for severe accident in vessel progression.

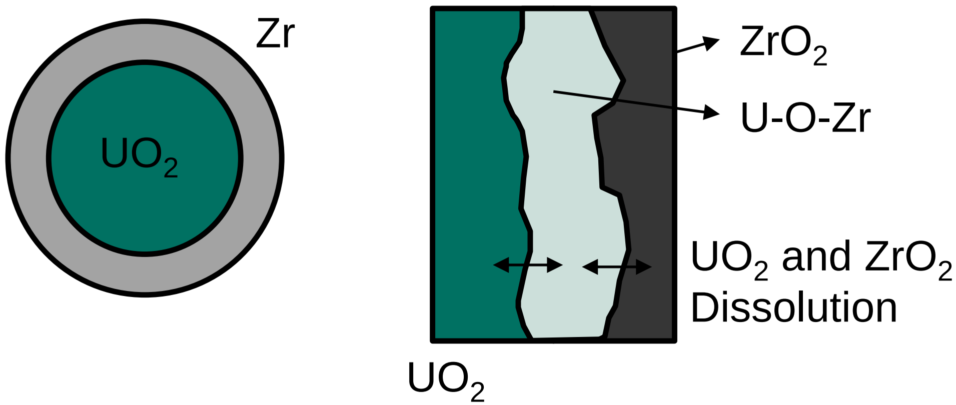

UO_2 liqufied 1000 K below its melting point

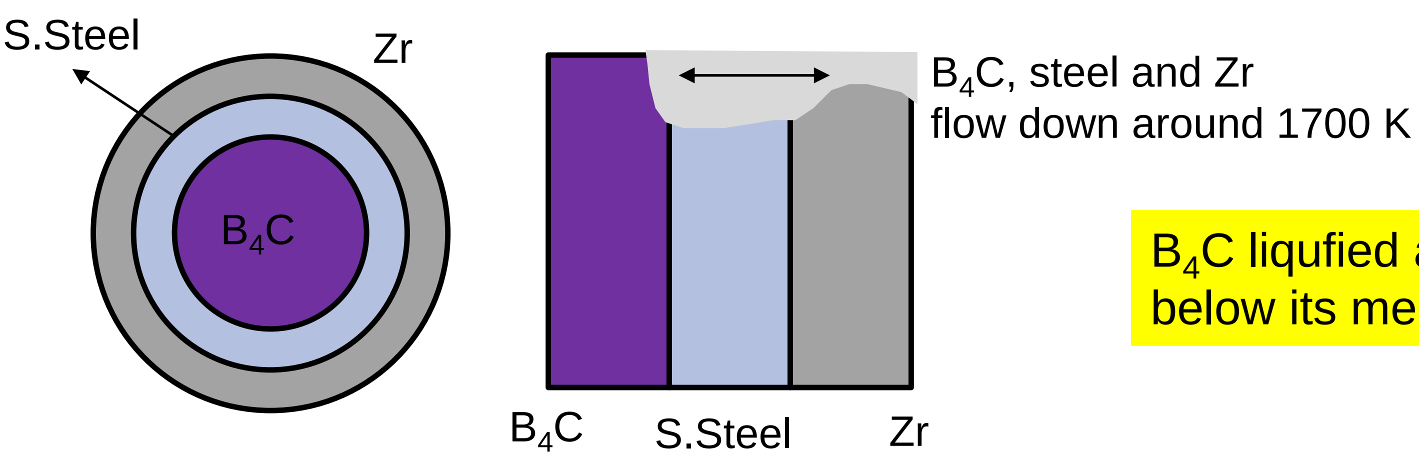

B_4C liqufied around 700 K below its melting point

Karlsruhe Institute of Technology
Institute for Neutron Physics and Reactor Technology

Motivation

Karlsruhe Institute of Technology

Are BWR type reactors different than PWRs?

BWRs contains: More Zr (water channel boxes)
More Fe (absorber blades)
B_4C (absorber blades)

Oxidation → more Heat, more H_2

Chemical reaction	Energy release
$Zr + 2\,H_2O \rightarrow ZrO_2 + 2\,H_2$	$\Delta H = 6.4$ MJ/kg $_{Zr}$
$2\,Fe + 3\,H_2O \rightarrow Fe_2O_3 + 3\,H_2$	Not significant
$B_4C + 8\,H_2O \rightarrow 2\,B_2O_3 + CO_2 + 8\,H_2$	$\Delta H = 15$ MJ/kg $_{B_4C}$

- Adequate models are necessary in order to predict the source terms during severe accident transients and improve severe accident management.
  - BWR Specific structures (Canister, absorber blades)
  - Eutectic interaction of BWR structures and their relocation models
  - Heat transfer models of BWR structures

QUENCH Test Facility

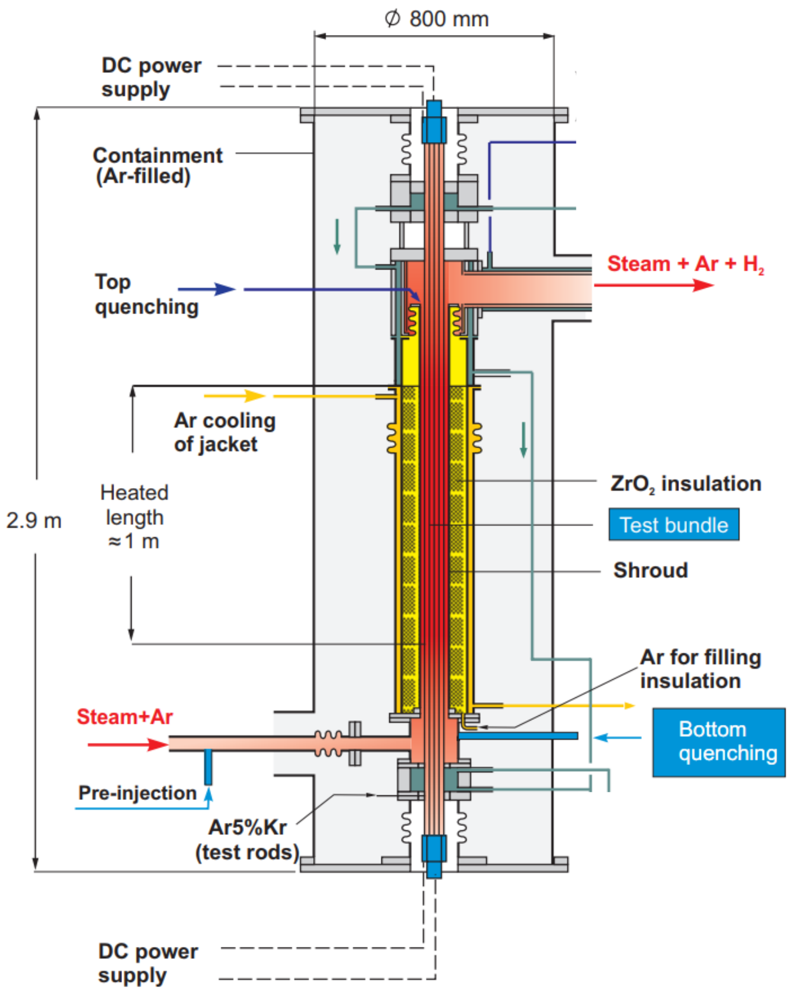

QUENCH Test Facility

In order to develop adequate models and validate severe accident codes for core degradation QUENCH experiments designed.

- Test facility enclosed and pressurized around 2 bar.
- Steam and Ar flow introduced from bottom and steam, Ar and hydrogen (produced from oxidation) flow upward outside of the bundle.

$$B_4C + 7H_2O(g) \leftrightarrow 2B_2O_3 + \boxed{CO(g)} + 7H_2(g)$$

$$B_4C + 8H_2O(g) \leftrightarrow 2B_2O_3 + \boxed{CO_2(g)} + 8H_2(g)$$

$$B_4C + 6H_2O(g) \leftrightarrow 2B_2O_3 + \boxed{CH_4(g)} + 4H_2(g)$$

B_4C oxidation

- Quench water supplied from the bottom of the section with constant flow rate and temperature.
- Temperature control provided for bundle head and off-gas pipe in order to mitigate condensation in test section.

Karlsruhe Institute of Technology
Institute for Neutron Physics and Reactor Technology

QUENCH-20 BWR Fuel Bundle (1/2)

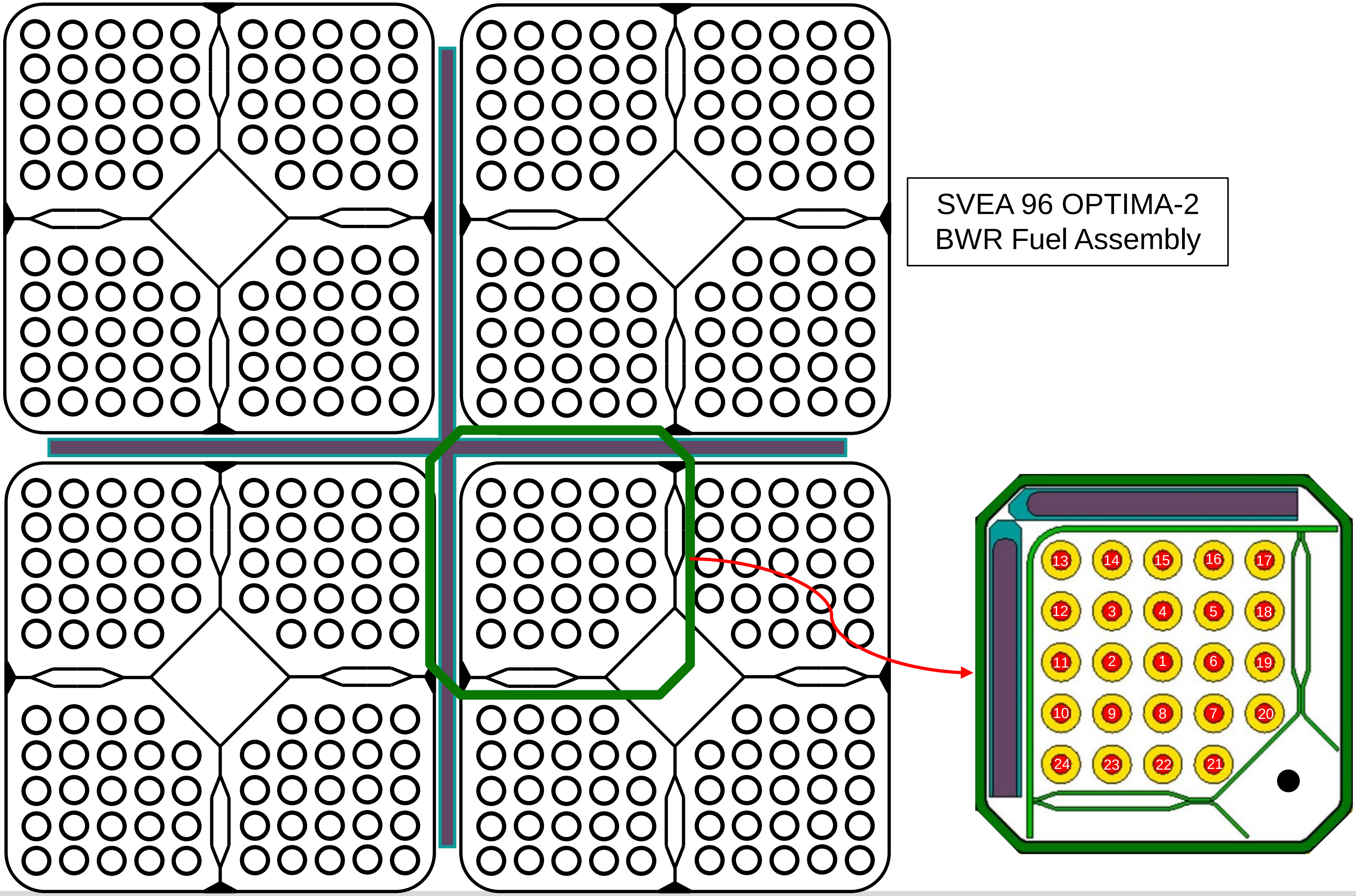

QUENCH-20 BWR Fuel Bundle (2/2)

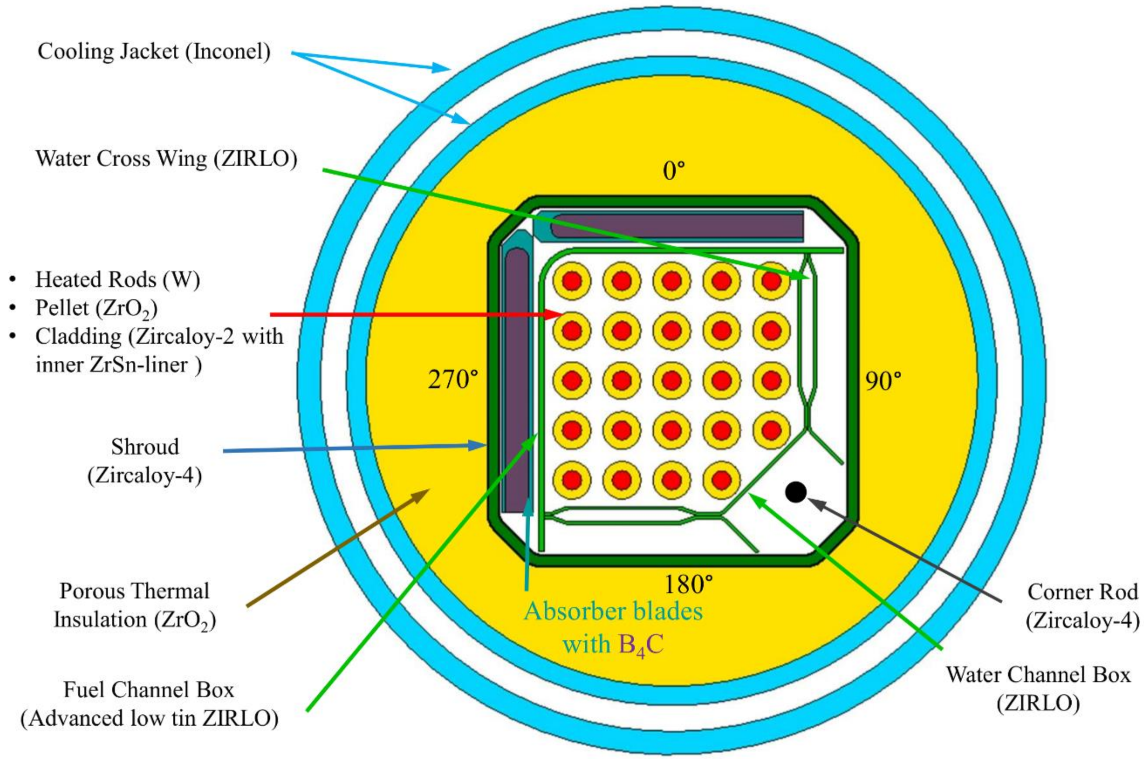

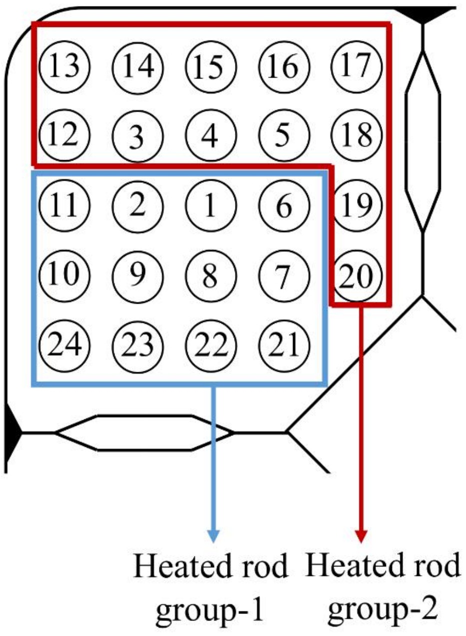

QUENCH-20 Test Bundle Cross Section (1/4 SVEA 96 OPTIMA-2)

QUENCH-20 Test Transient

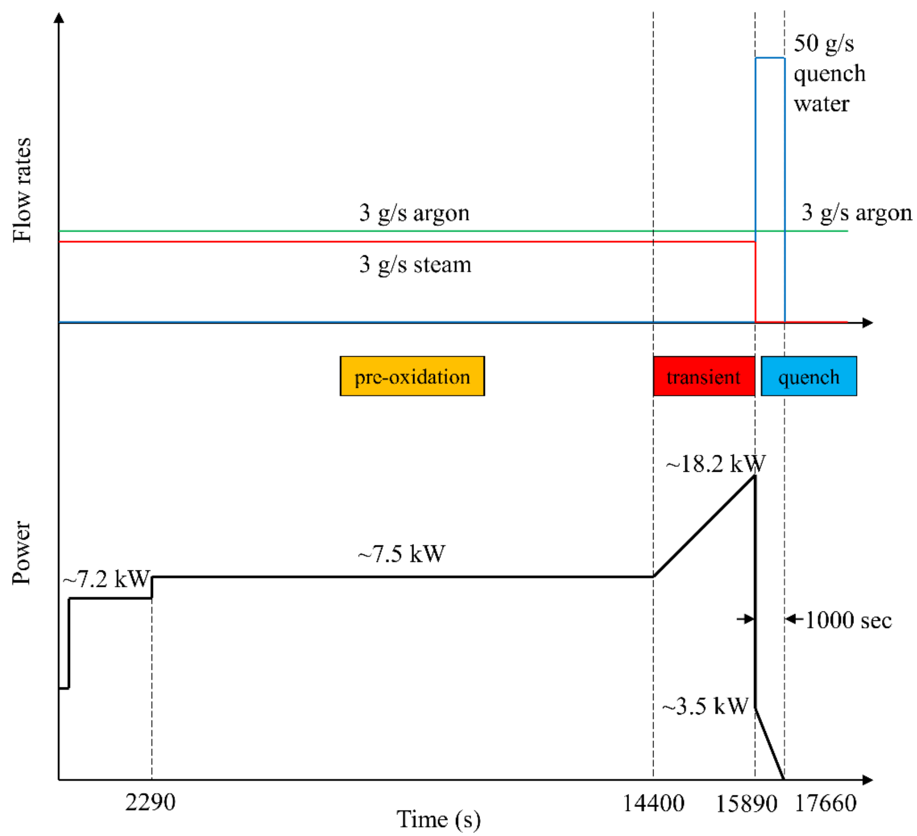

QUENCH-20 Test consist of three phases which are pre oxidation, transient and quench:

- **Pre-oxidation phase**: Superheated steam and Ar gasses (600-700 K) employed to the system from bottom. System pressure was 2 bar.
- **Transient phase**: Electric power increased. Steam and Ar flow maintained until quench phase.
- **Quench phase**: After transient case, 50 g/s quench water delivered to the bundle from bottom at room temperature.

Numerical Tool: ASTEC Code

Accident Source Term Evaluation Code

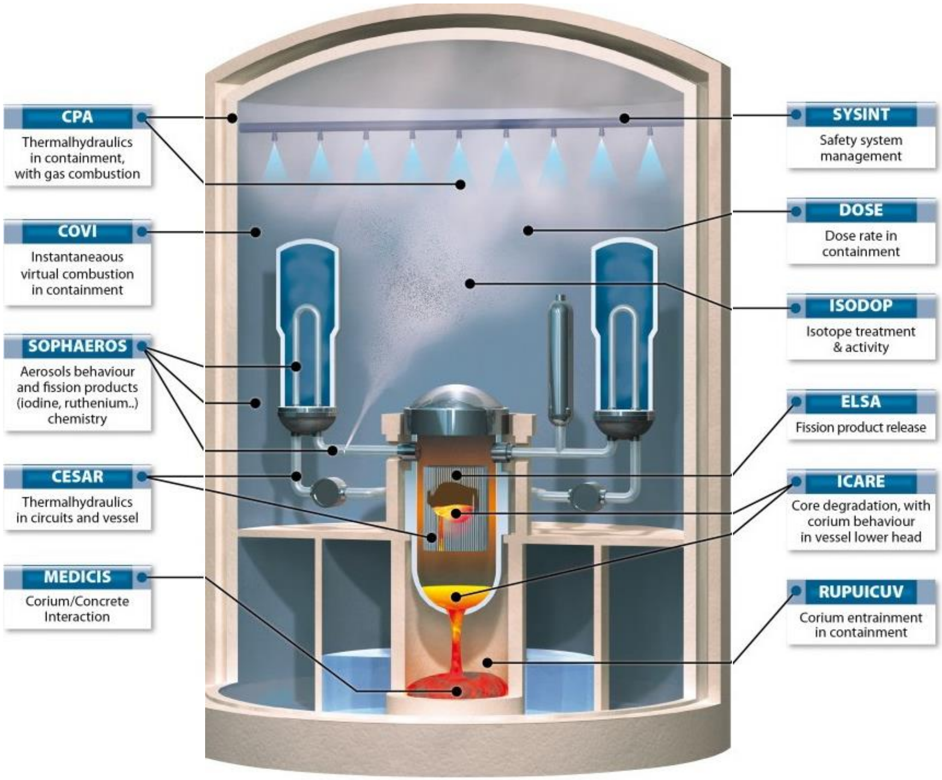

- European reference software for severe accidents.
- ASTEC simulates all sequences from initiating event to discharge of radioactive materials during core melt down accidents of LWRs.
- ASTEC has modular structure to implement physical models.
- Each module handles the part of the reactor and phenomena in there.

ASTEC Model of QUENCH-20 Fuel Bundle and Test Section

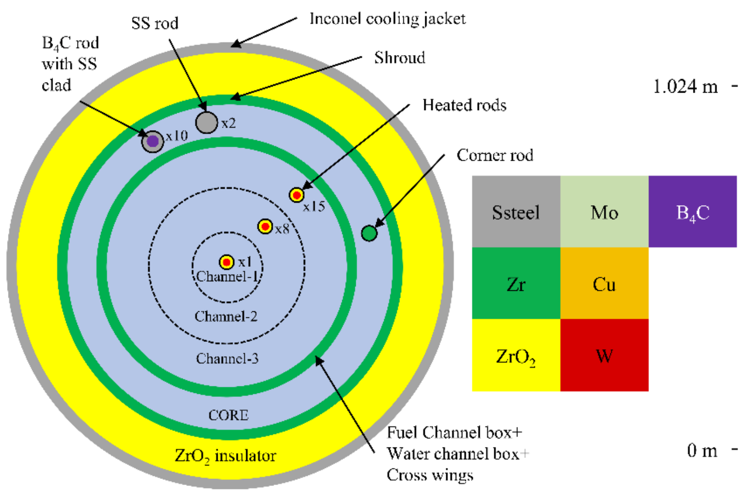

QUENCH-20 BWR bundle and test section ASTEC Model (Radial Representation)

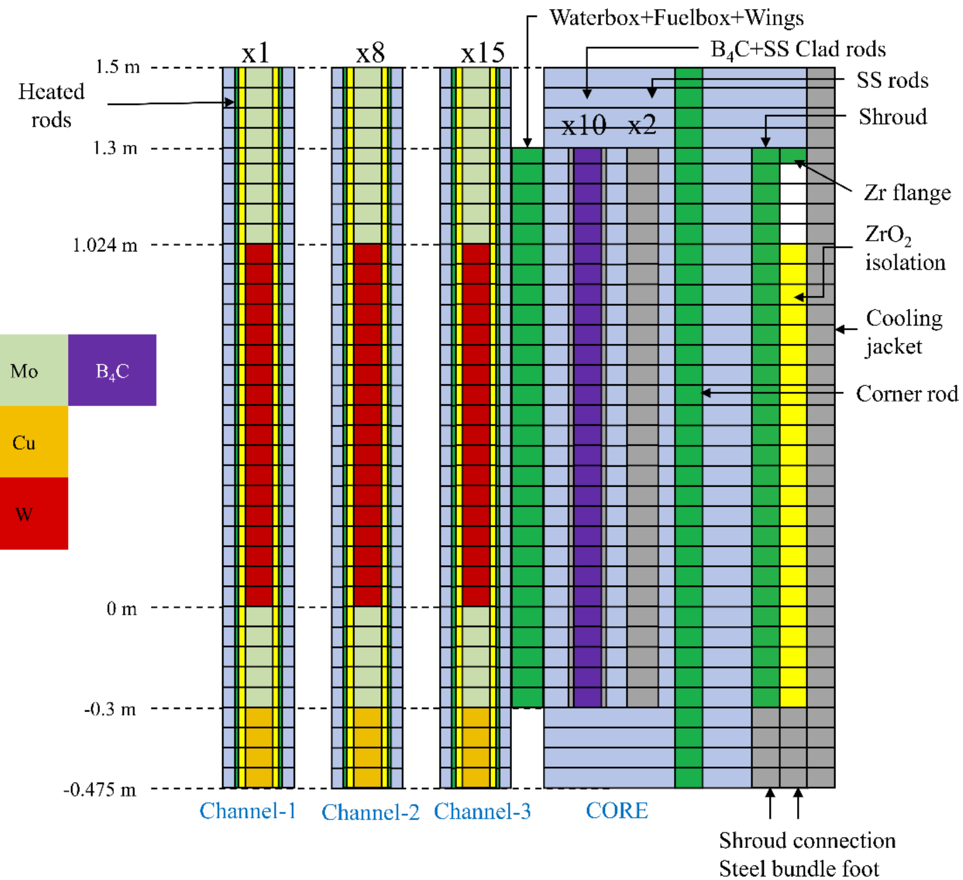

QUENCH-20 BWR bundle and test section ASTEC Model (Axial Representation)

ASTEC Model of QUENCH-20 Heated Rod

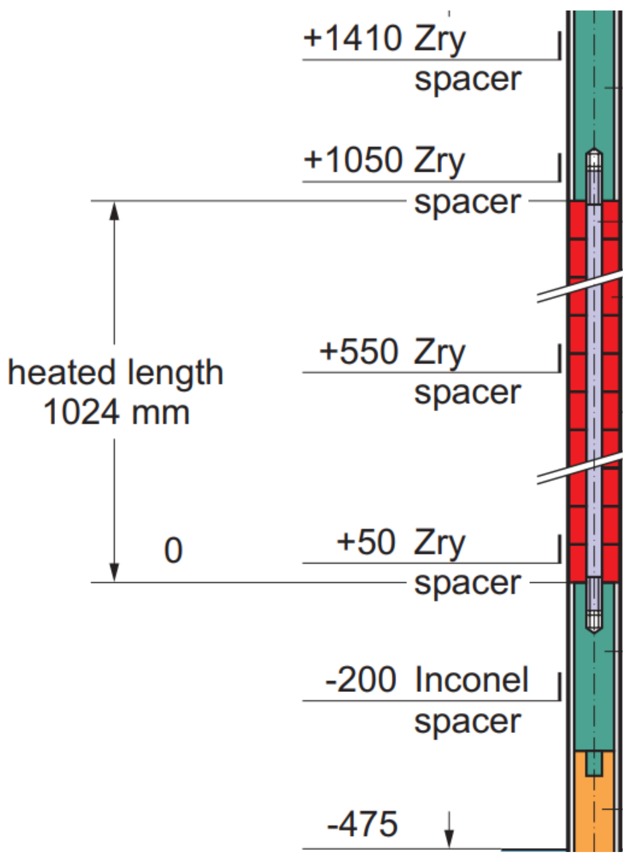

QUENCH-20 Heated Rod Composition

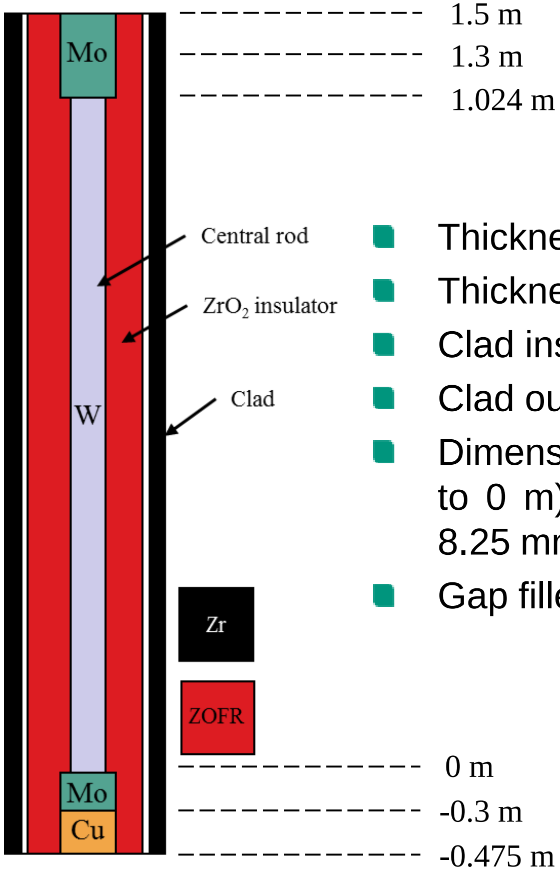

QUENCH-20 Heated Rod ASTEC Model

- Thickness of Mo and Cu = 7.85 mm
- Thickness of W = 5.25 mm
- Clad inside diameter = 8.63 mm
- Clad outside diameter = 9.84 mm
- Dimensions of ZrO2 = 8.25 mm (-0.475 to 0 m), 8.48 mm (0 to 1.024 m) and 8.25 mm (1.024 to 1.5 m)
- Gap filled with Kr (5 bar)

Boundary Conditions (1/2)

Described boundary conditions are employed according to QUENCH-20 test measurements:

- Electrical power generated for 24 heated rod one by one in the bundle by using test power output.

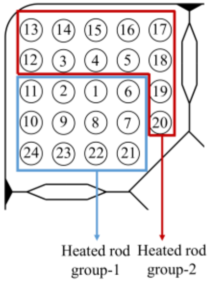

Electrical power is not same for Group-1 and Group-2 and rod distribution is not homogenous.

- Pressure boundary condition takes role at the top.
- Temperature and flow rate of steam and argon gasses at the inlet of the bundle introduced.
- Quench water temperature and flow rate takes action for quench phase.

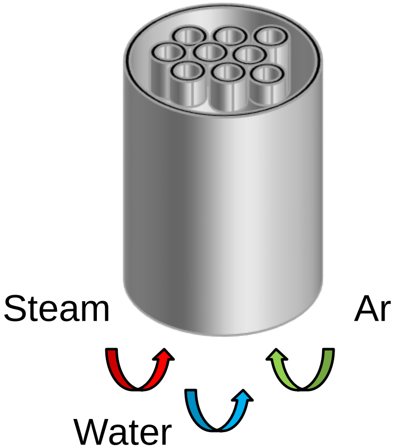

Boundary Conditions (2/2)

Described boundary conditions are employed according to QUENCH-20 test measurements:

- Temperature of cooling jacket along the its height defined.
- Cooling water was defined for the bottom face of cladding material of heated rods.

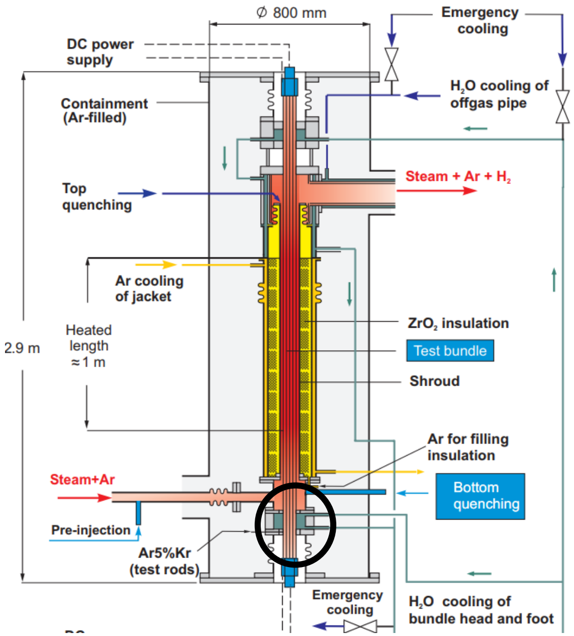

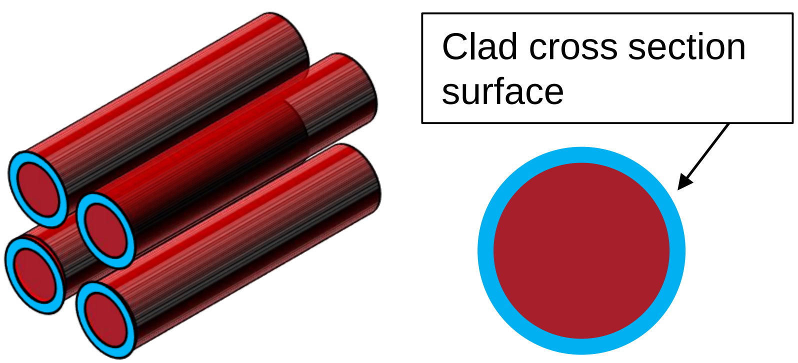

Karlsruhe Institute of Technology
Institute for Neutron Physics and Reactor Technology

ASTEC Predictions of QUENCH-20 Test (1/5)

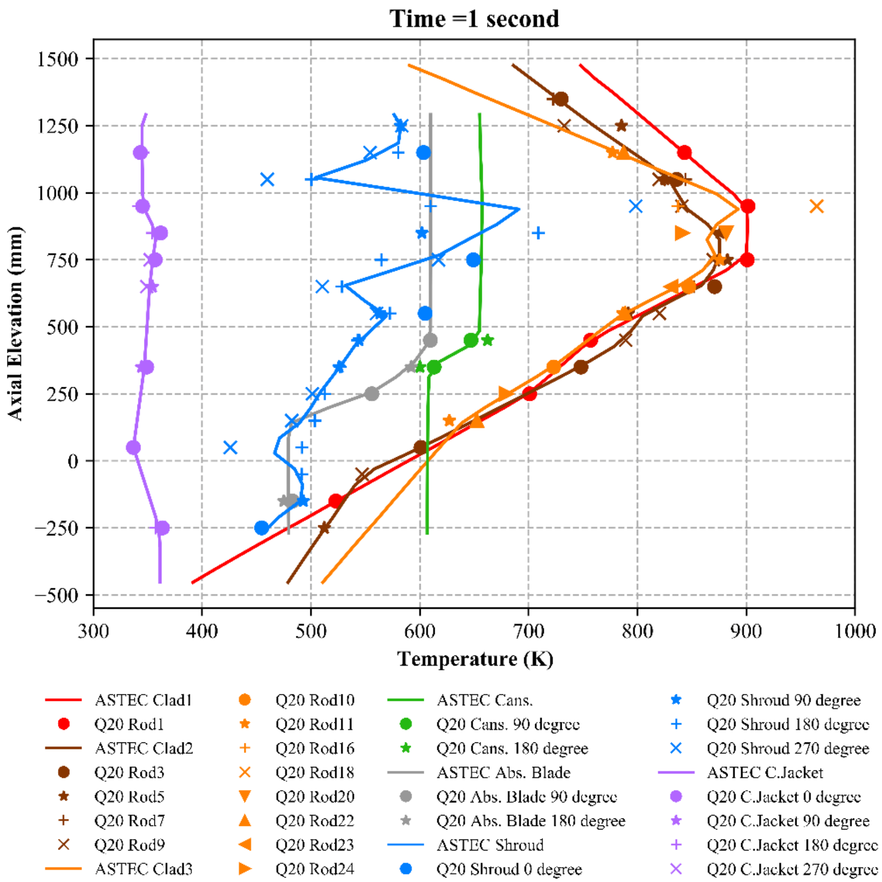

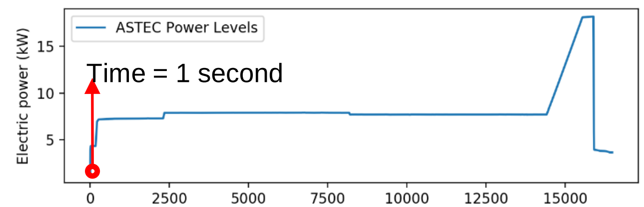

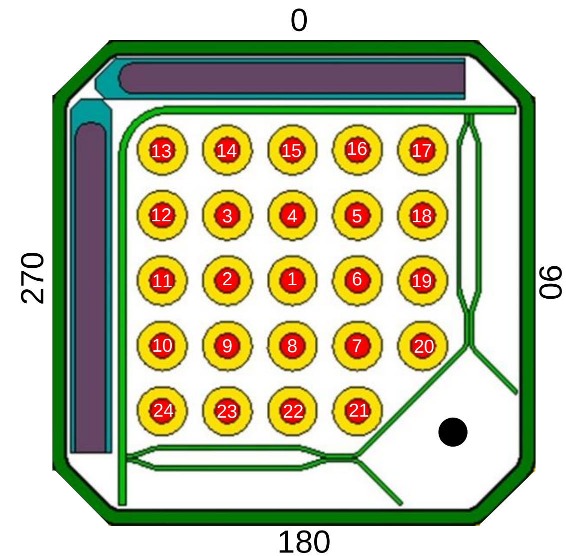

ASTEC Predictions of QUENCH-20 Test (2/5)

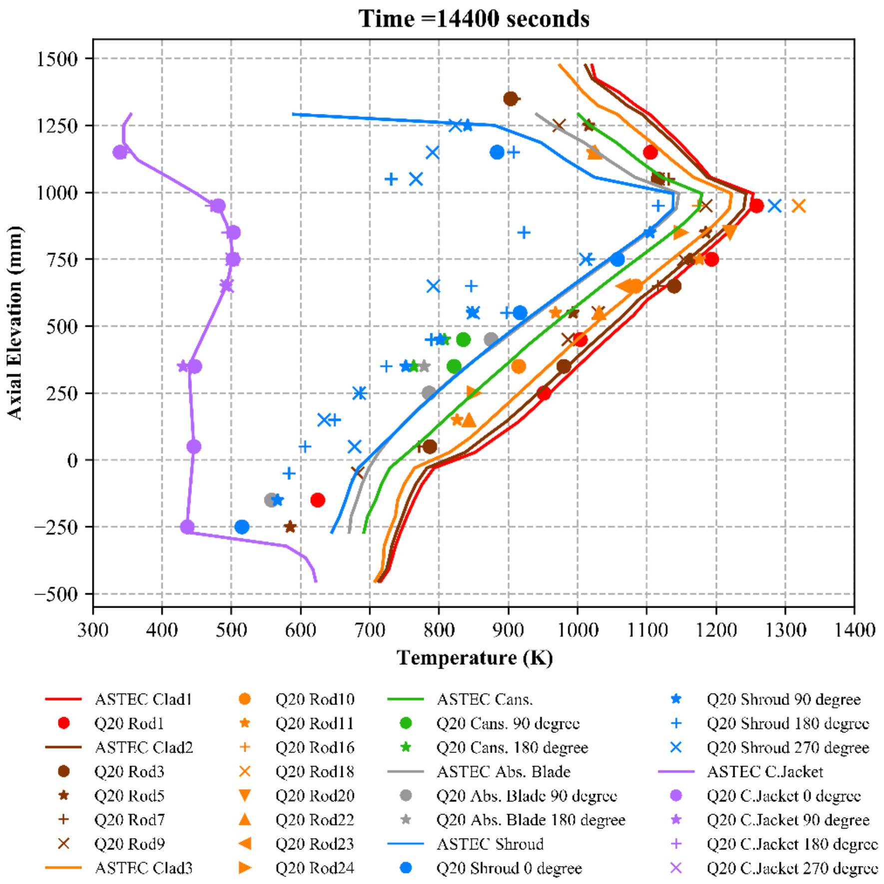

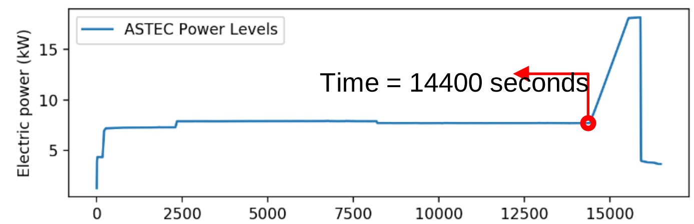

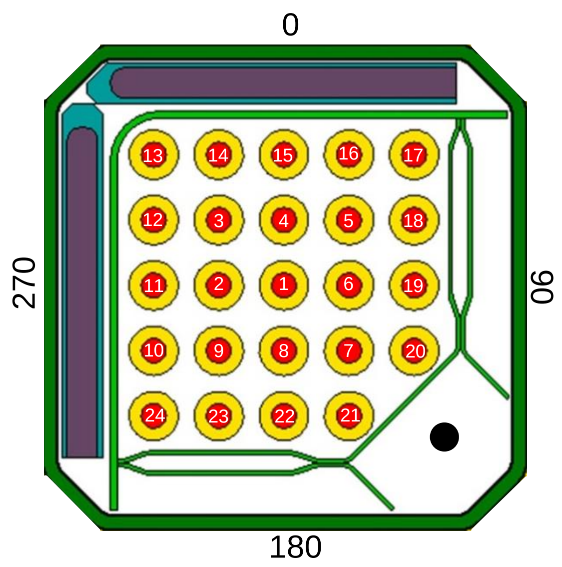

ASTEC Predictions of QUENCH-20 Test (3/5)

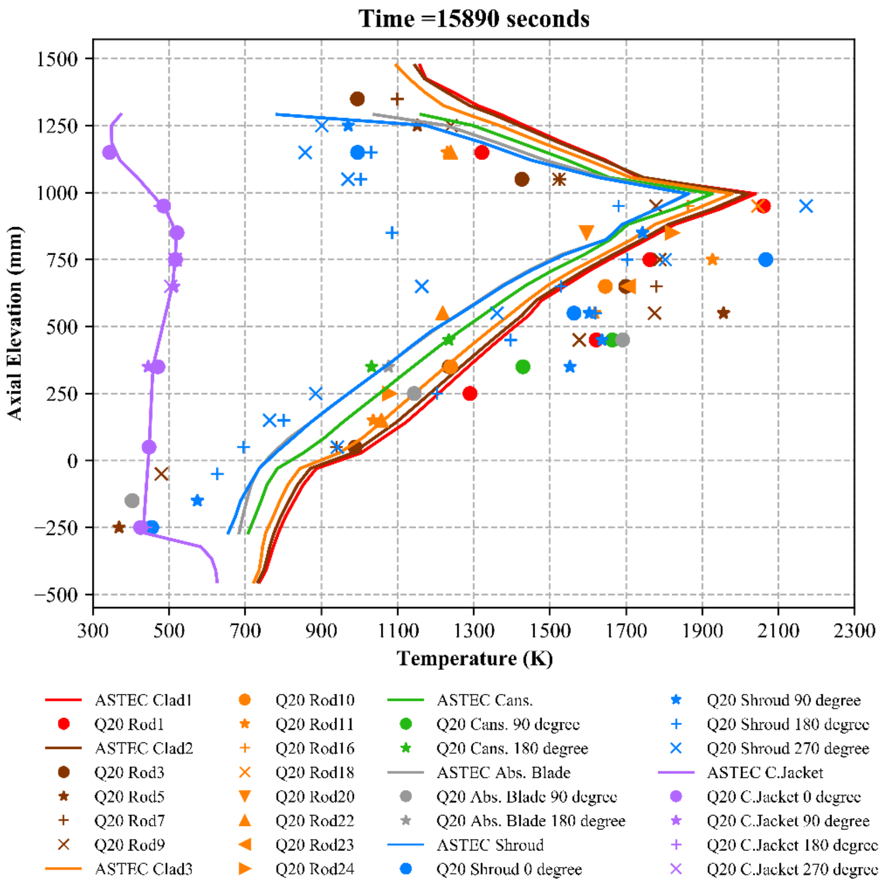

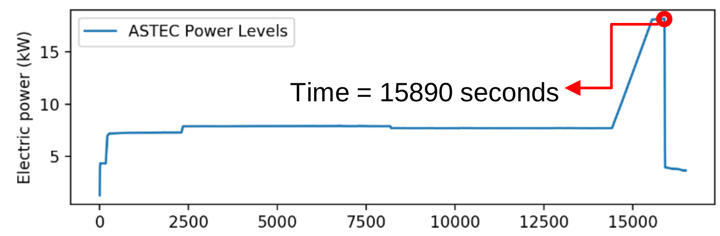

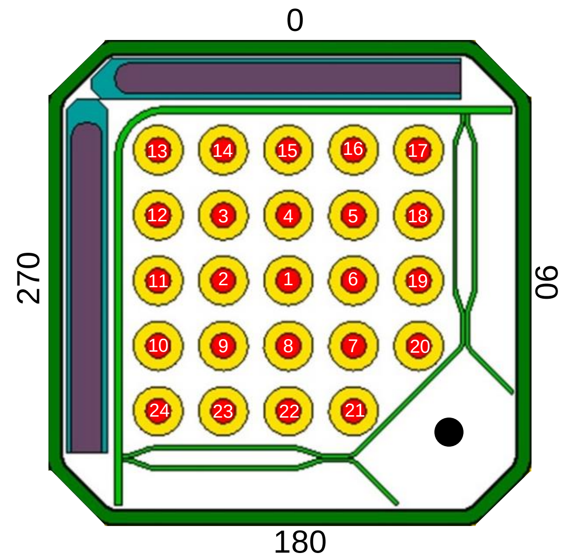

ASTEC Predictions of QUENCH-20 Test (4/5)

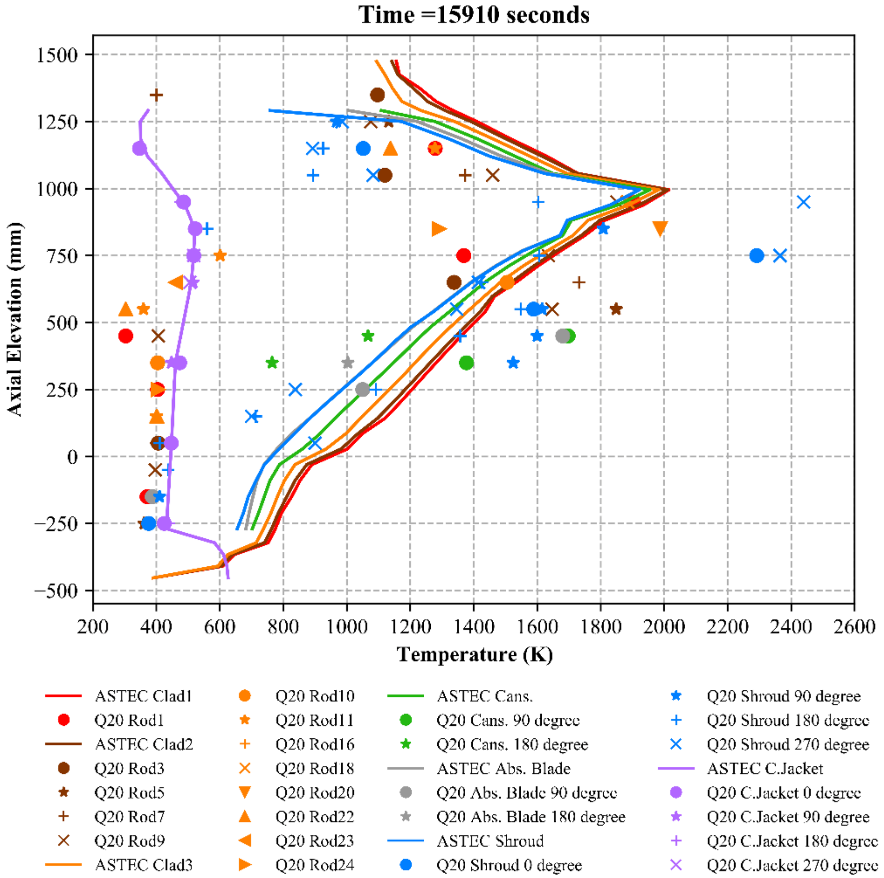

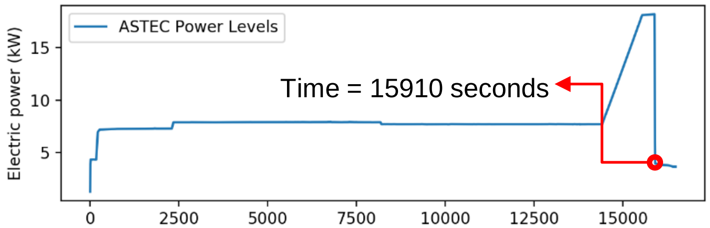

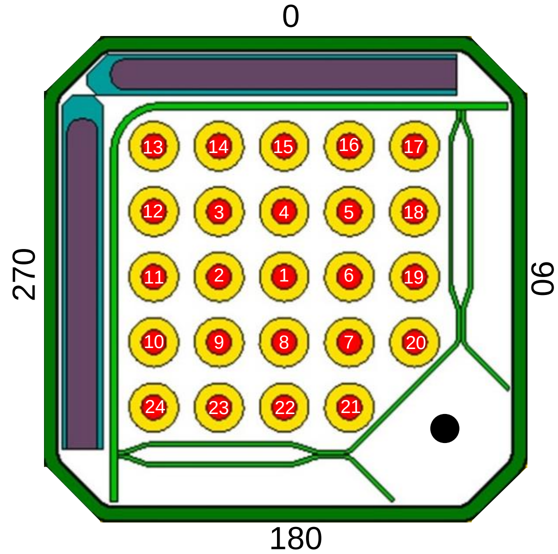

ASTEC Predictions of QUENCH-20 Test (5/5)

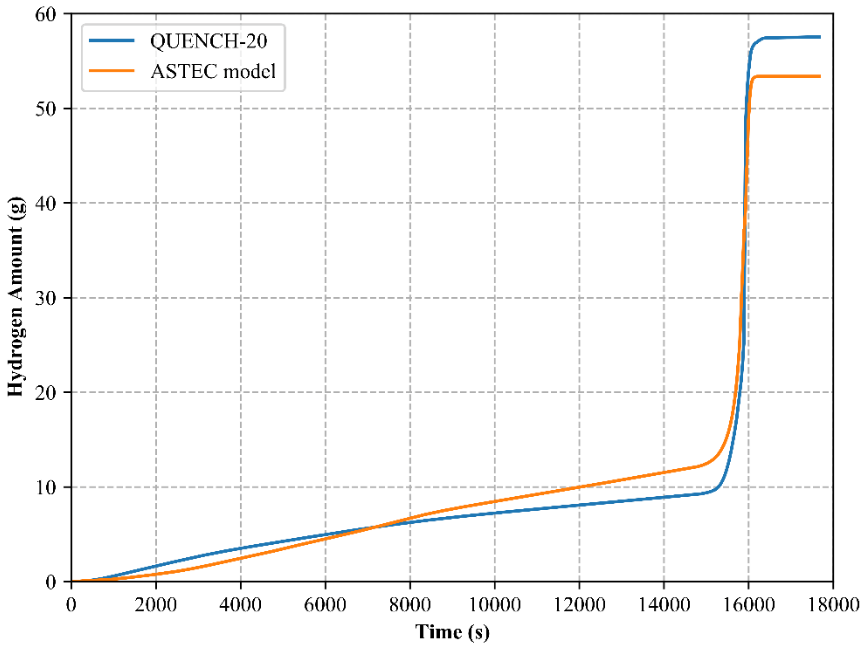

QUENCH-20 total H_2 amount = 57.4 g

B_4C oxidation contribution = 10 g

ASTEC prediction total H_2 amount = 53.4 g

B_4C oxidation contribution = 9.48 g

Further detailed informations: Onur Murat, Victor Sanchez Espinoza, Shisheng Wang, Juri Stuckert, *Preliminary validation of ASTEC V2.2.b with QUENCH-20 BWR bundle experiment*, Nuclear Engineering and Design 370 (2020)

QUENCH-20 Post Test Pictures

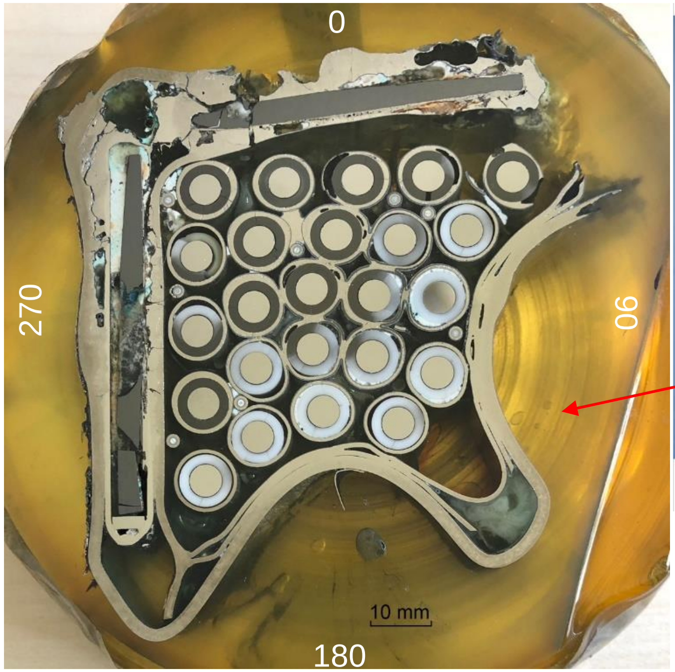

QUENCH-20 Bundle Post Test Cross Section (Height = 650 mm)

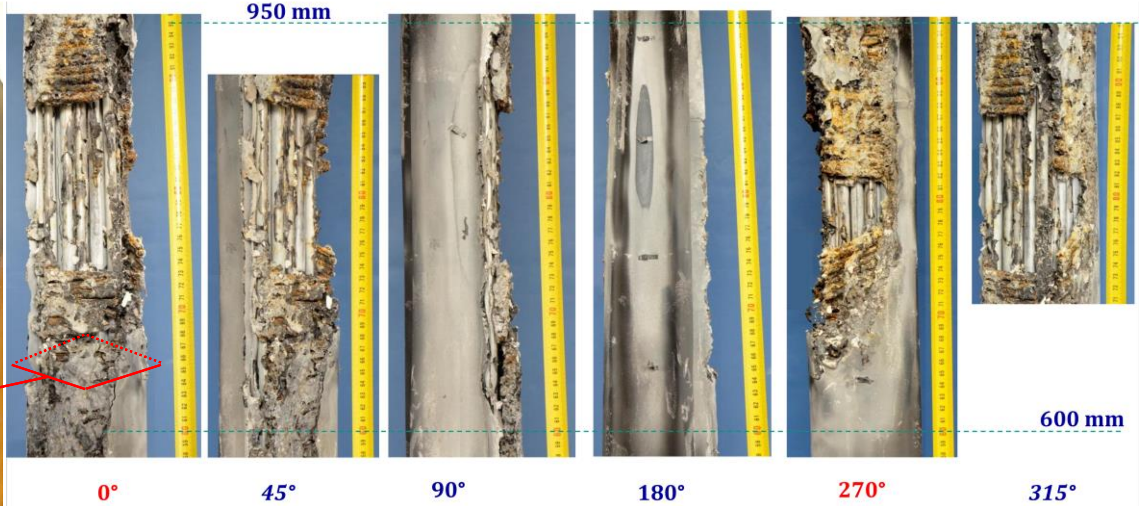

ASTEC did not predict strong degradation and failure of shroud

Conclusion

- Considering the geometrical modeling pecularities axial temperature of structures are in acceptable manner.
- Total amount of hydrogen generation, including B4C oxidation, are in good agreement with test readings.
- Shroud failure was not observed in the ASTEC model.
  - Inhomogenity of structural placement in the test section and eutectic interactions which based on the how close the metallic structures are reason for that.
- Correct geometrical representation and placement of Blades (Slab) and Fuel Channel Box (Rectangular) are necessary.
  - There was no radiative heat transfer model for reactangular fuel boxes for version V2.2.b.
  - Definition of absorber material inside slab blades are not possible, which means no eutectic interaction, no material relocation due to eutectic interactions.

K. Nakamura, K. Inagaki, T. Sonoda,
H. Ohta
CRIEPI

Fuel rod / bundle behavior in the early stages of a severe accident in a nuclear reactor and spent fuel pool using the DEGREE facility

To deepen understanding of the core degradation processes beyond design-basis events and to strengthen accident management measures for light water reactors, the out-of-pile integral test facility "DEGREE" was installed at CRIEPI in 2015.

For the early stages of a severe accident in a nuclear reactor, several degradation tests using a 3x3 bundle of Zircaloy-4 were conducted to heat the temperature up to 2000 ° C under a wide range of steam flow rates. These results revealed that under steam-rich conditions, the formation of a thick protective ZrO_2 layer on the outside surface of the cladding tubes prevents the test rods from severe degradation and the loss of geometric shape of the fuel bundle. Under the steam-starved conditions, however, the lack of the thick external oxide layer formation on the cladding tubes caused the exposed metallic melt (Zr,O) to relocate downward, resulting in the formation of massive blockage in the low temperature region.

Simulating a loss-of-cooling function and loss-of-coolant accident in a spent fuel pool, a ballooning and burst test of a single pre-hydrided fuel rod was performed with the parameters of heating rate, rod inner pressure, and steam-air mixing ratio. The post-test rod was analyzed by OM, EPMA, ToF-SIMS and hydrogen analyzer. The burst behavior of the test rods is discussed in relation to the initial hydrogen concentration, the growth of the nitrogen-containing precipitates produced along the microcracks formed at the ZrO_2/α-Zr(O) interface, and air ratio in a steam-air mixed atmosphere.

The DEGREE facility can contribute to the demonstration, elucidation, and validation of the processes of degradation behavior for fuel bundles, core structural materials, and advanced materials in reactors or SFPs under various prospected accident scenarios.

Fuel Rod / Bundle Behavior in the Early Stages of a Severe Accident in a Nuclear Reactor and Spent Fuel Pool using the DEGREE Facility

Kinya Nakamura, Kenta Inagaki, Takeshi Sonoda, Hirokazu Ohta

Central Research Institute of Electric Power Industry (CRIEPI)

The 26th International QUENCH Workshop

December 6-9, 2021

CRIEPI
Central Research Institute of Electric Power Industry

Outline

- The DEGREE facility
- Experience on
  - Bundle test in the early stages of a SA in a reactor
  - Ballooning & burst single rod test in the LOCA at SFP
- Conclusion & future work

The DEGREE facility

Background

- Good reproducibility of SA phenomena compared with the results of TMI-2 accident and plenty of in-pile and out-of-pile experiments conducted so far (ex. PHEBUS-FP, CORA, QUENCH, and CODEX)
  - ✓ However, large uncertainty in physico-chemical behavior of core materials at high temperature
    - Multi-component interaction between fuel rod, channel box, control rod and grid spacer
    - Physico-chemical interaction between molten materials and solid component
    - Competitive behavior of physical fuel failure and chemical dissolution of ZrO_2 by U-Zr-O melt

- As of 2012, there were few out-of-pile integral test facilities in Japan.

- The out-of-pile integral test facility “DEGREE” was built at CRIEPI in 2015

  in the framework of “Advanced Multi-scale Modeling and Experimental Test of Fuel Degradation in Severe Accident Conditions” supported by METI, Japan.

  - ➢ To deepen understanding of the core degradation processes beyond design-basis events,
  - ➢ To strengthen accident management measures for light water reactors

The DEGREE facility

Scope of Work

Performance tests has been conducted concerning

- The Zircaloy-4 fuel bundle in the early stages of a SA in a reactor
- Ballooning & burst of the sim. high BU single fuel rod under LOCA at SFP

The DEGREE facility

System diagram

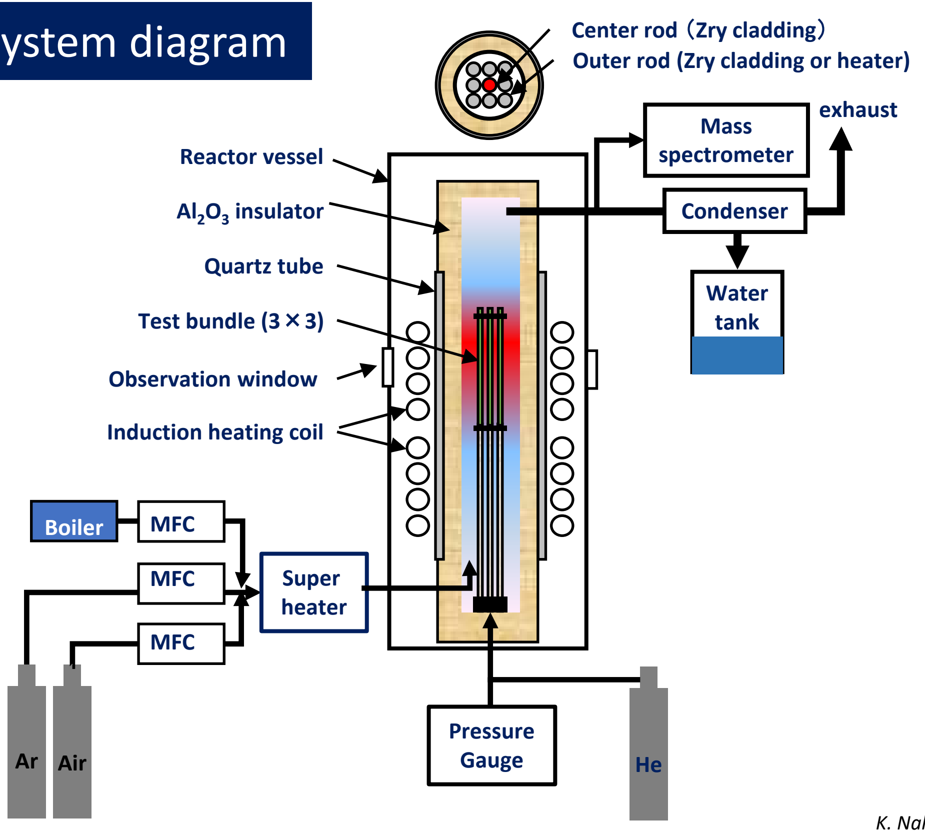

Major specification

Test Bundle	3×3 rods
Carrier gas	Steam, Ar, Air mixture
Heating rate	< 7 K/s
Cooling rate	> 3 K/s
Heating method	Induction (internal heating)
Max. temperature	2000℃
Heating region	200mm (upper), 300mm (lower)
System pressure	Atmospheric
Rod inner pressure	<12 MPa
Load cell	Not furnished
Quench medium	Argon gas
Nuclear material	Not available
Instrumentation	
Thermocouples, Pyrometers, Pressure gauges	
Gas chromatograph, QMS, Video recording system	

K. Nakamura et al., OECD/NEA WORKSHOP-TCOFF PROJECT, July 10-12, 2019, J-village, Fukushima, Japan.

Comparison with major out-of-pile core degradation facilities

Item	NIELS	CORA	CODEX	QUENCH	DEGREE
Institute	KfK	KfK	KFKI	KIT	CRIEPI
Period	1982-1986	1987-1993	1995-	1997-	2015-
Main target	Core degradation	Core degradation	Core degradation	Reflooding of damaged core	Core degradation
Fuel material	Non-irrad. UO_2	Non-irrad. UO_2	Non-irrad. UO_2	ZrO_2	ZrO_2
Fuel type	PWR	PWR, BWR, VVER	PWR, VVER	PWR, BWR, VVER	PWR, BWR,
Fuel length (m)	0.4	1.0	0.6	1.0	0.2-0.5
Number of rods	9	25-59	7-9	23	9
Heating rate (K/s)	0.3-4.0	0.2-1.0	0.5-0.6	0.45-6	0.0001 – 7
System pressure (MPa-abs)	0.1	0.2-1.0	0.2	0.2	0.1
Pressure in rods (MPa)	-	0.2-6.0	0.2	0.2-6.0	0-10
Max. Temp. (℃)	2250	2230	2030	2230	2000
Carrier gas	Steam, Ar, O_2	Steam, Ar	Steam, Ar, O_2, Air	Steam, Ar, Air	Steam, Ar, Air
Steam flow rate ($mg/cm^2/s$)	30	40-120	50	110	-38
Heating method	Electrical				**Induction**

K. Nakamura et al., OECD/NEA WORKSHOP-TCOFF PROJECT, July 10-12, 2019, J-village, Fukushima, Japan.

Bundle test in the early stages of a SA in a reactor

Bundle test in the early stages of a SA in a reactor

Test conditions

item	Test No				
	D-H27-01	D-H27-02	D-H27-04	D-H27-03	D-H26-01
Carrier gas	Ar	Steam+Ar	Steam+Ar	Steam+Ar	Steam+Ar
Steam flow rate (mg/s)	0	9	820	840	650
	Steam-starved		Steam-rich		
Heating rate* (K/s)	3.0	3.0	2.0	2.7	0.3
	LB-LOCA				SBO
Cooling gas	Ar				
Cooling rate at 1600℃ (K/s)	3	3	3	3	0.2

×100

×10

** Constant ramp rate of induction heating power to be regulated*

Non-pressurized Zircaloy-4 Test rod

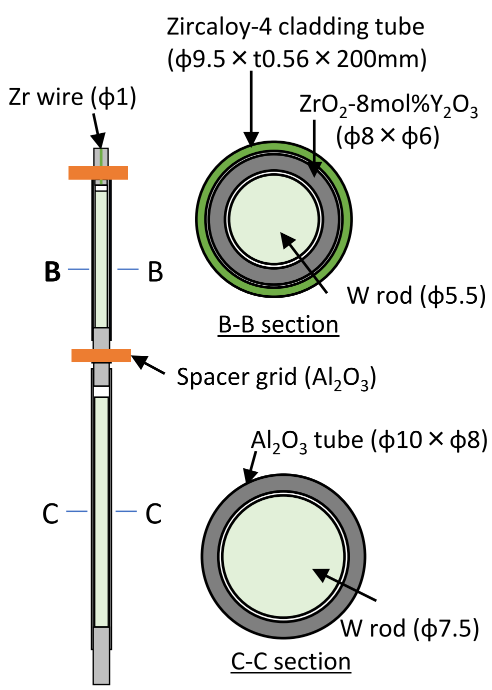

Cross-section of the bundle

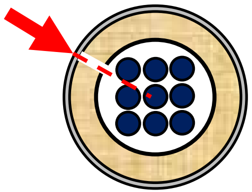

K. Nakamura et al., OECD/NEA WORKSHOP-TCOFF PROJECT, July 10-12, 2019, J-village, Fukushima, Japan.

Temperature history of central test rod

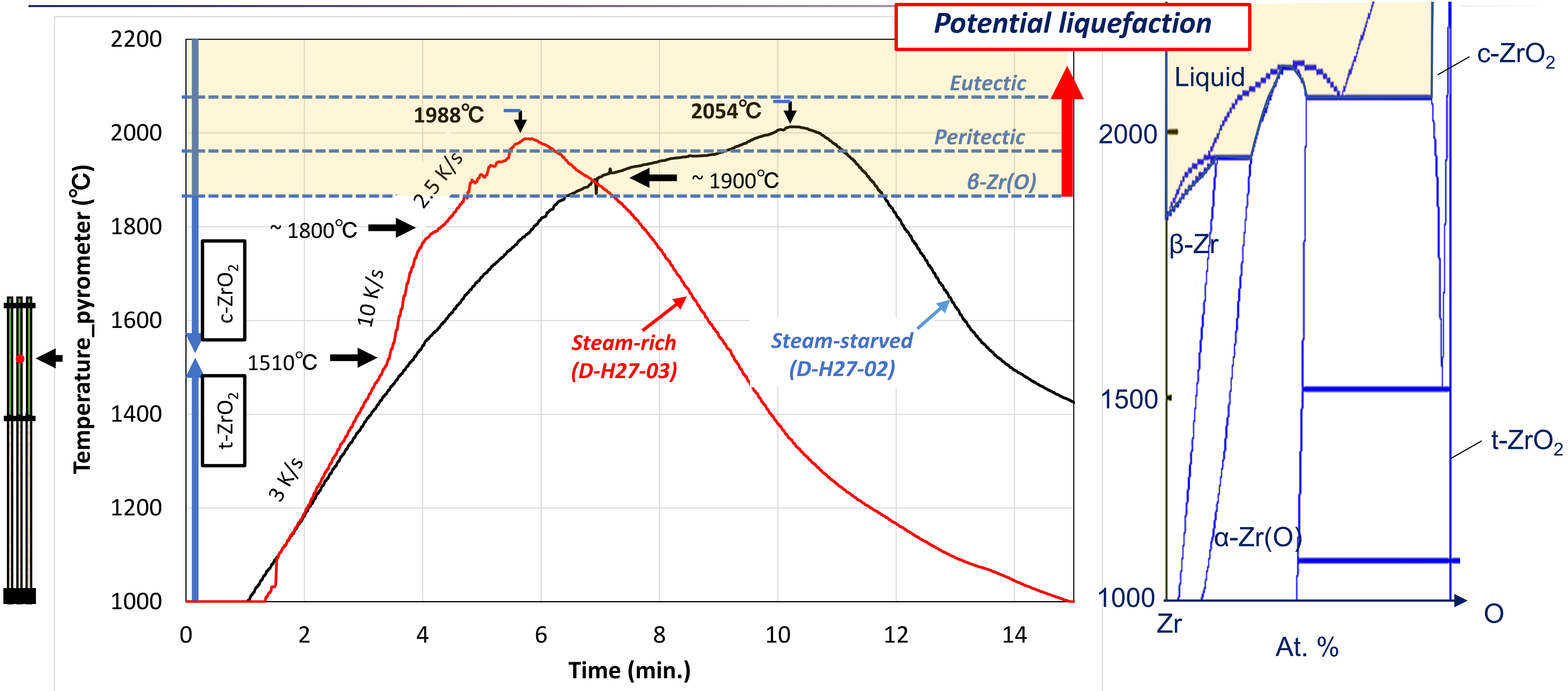

K. Nakamura et al., OECD/NEA WORKSHOP-TCOFF PROJECT, July 10-12, 2019, J-village, Fukushima, Japan.

Relocation of Zr-O melt at around 1900℃

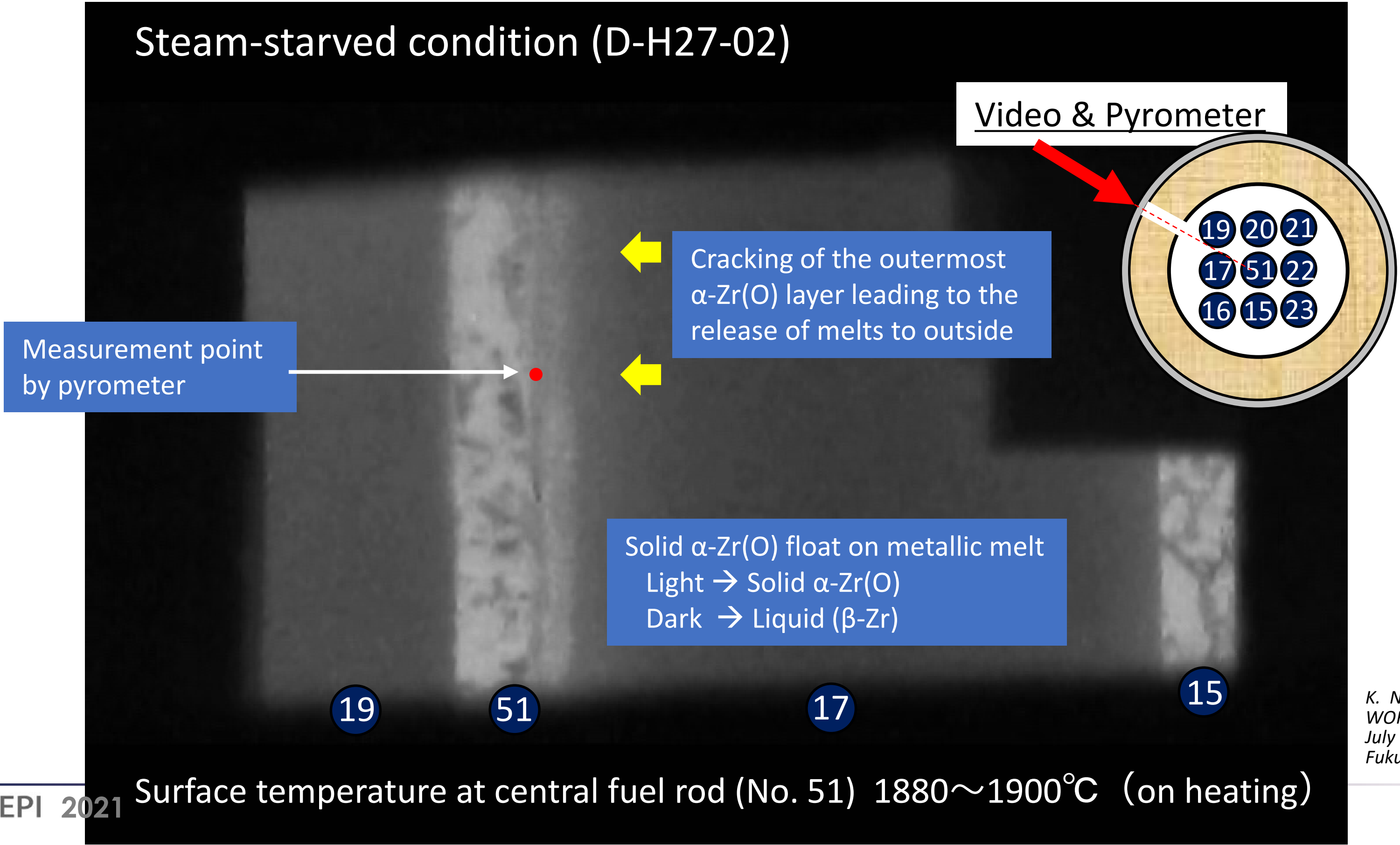

K. Nakamura et al., OECD/NEA WORKSHOP-TCOFF PROJECT, July 10-12, 2019, J-village, Fukushima, Japan.

Steam-starved condition

(Max. temp 2013℃, D-H27-02)

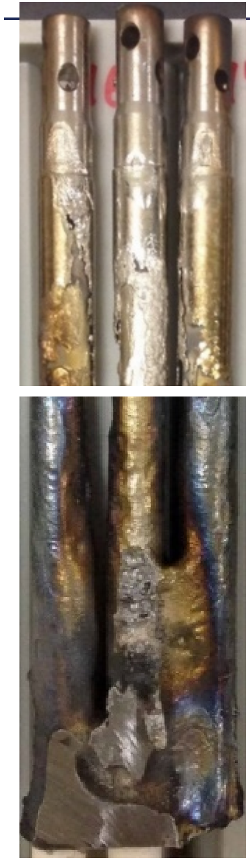

Top region

Relocation of metallic melt

Blockage at bottom region

Cross section at central height for the central test rod

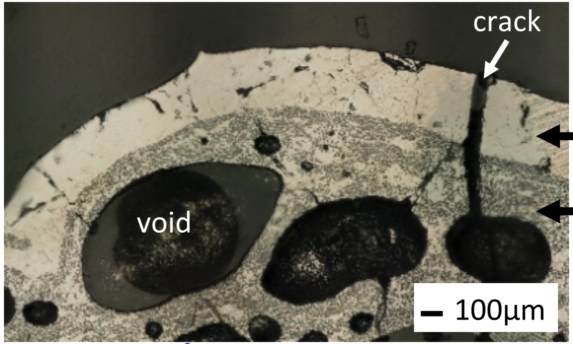

Solid α-Zr(O)

Solid-Liquid mixture of α-Zr(O)+β-Zr

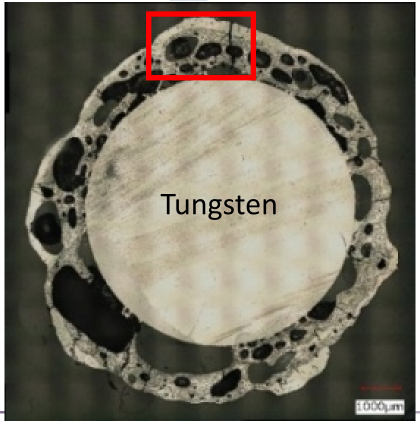

Phase diagram in the Zr-O system

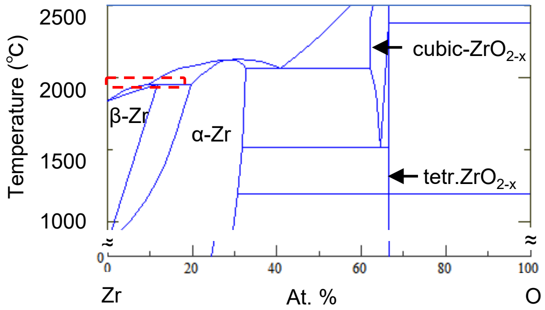

K. Nakamura et al., OECD/NEA WORKSHOP-TCOFF PROJECT, July 10-12, 2019, J-village, Fukushima, Japan.

Steam-rich condition

(Max. temp 1988℃, D-H27-03)

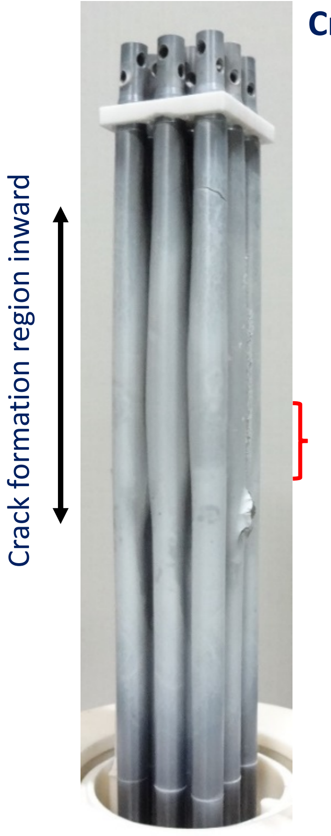

Cross section at central height for the central test rod

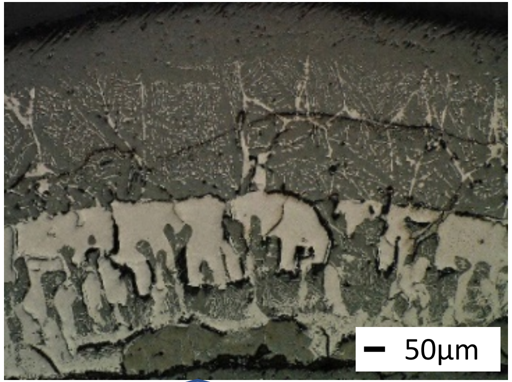

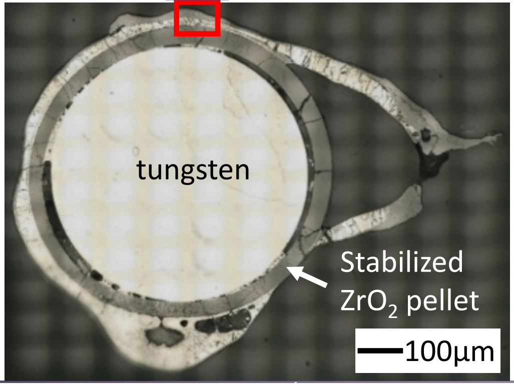

- No liquid phase formation, relocation and blockage
- Preservation of the coolable geometry up to ~2000℃

Cracking formation to central direction vertically along the ZrO_2/α-Zr(O) interface

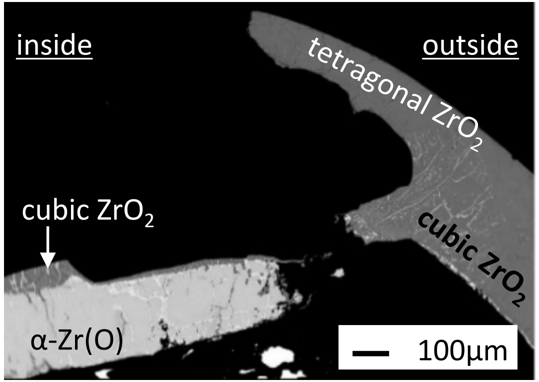

Phase diagram in the Zr-O system

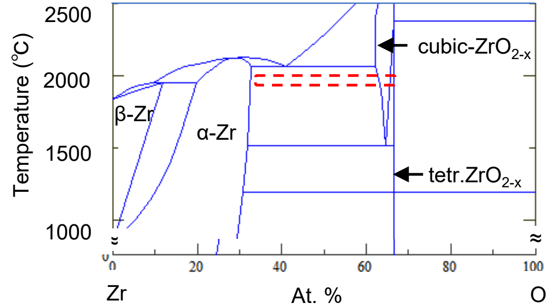

K. Nakamura et al., OECD/NEA WORKSHOP-TCOFF PROJECT, July 10-12, 2019, J-village, Fukushima, Japan.

Ballooning & burst single rod test in the LOCA at SFP

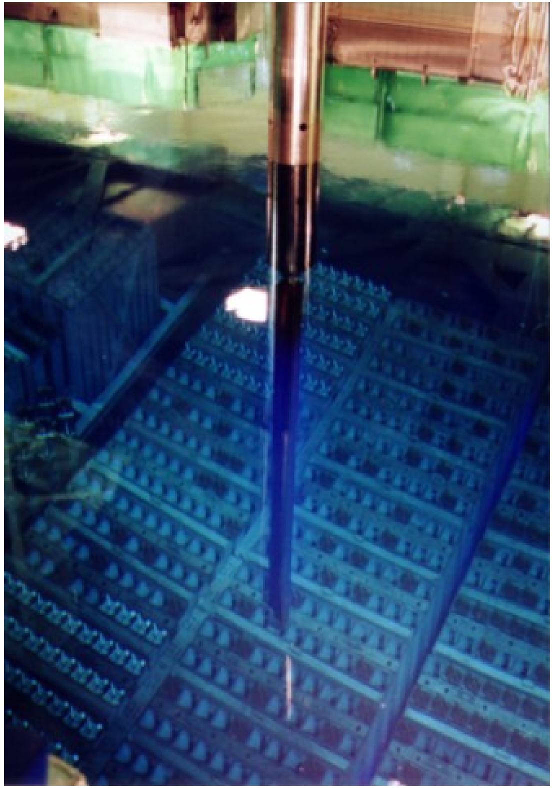

http://www.tepco.co.jp/fukushima1-np/b42307-j.html

Accident progression scenario at SFP

Occurrence of a causative event (Normal condition → Water level lowering)

Cladding burst resulting in FP release to RB (Fuel Uncovery → Collapse of Fuel rod)

	Normal condition	Water level lowering	Fuel Uncovery	Collapse of Fuel rod	Recovery
SFP water level and accident progression	**Main impact on Spent Fuel heat-up** ➢ Residual decay heat ➢ SF loading pattern ➢ Timing, location, and scale of coolant leaks from the SFP liner ➢ Reaction of spent fuel cladding with air/steam at high temperature	➢ Water temp. rise	➢ Zr-H_2O reaction ➢ H_2 production ➢ Enlargement of cladding strain	• Oxidation/Nitridation in air + steam • Severe H_2 production • Radioactive FP release in RB • Collapse of fuel rod	
Timing	Loss-of-cooling accident	1 day to weeks	Hours to days	hours	
	Loss-of-coolant accident	Hours to days			
AM measures ➢ Emergency power supply ➢ Alternative water injection system ➢ Mobile spray equipment ➢ Status monitoring function ➢ Recovery guidance ➢ Distributed arrangement of FA, etc.		• Mitigation of leakage • Alternative spray system (freshwater/ sea water) etc.	Accident progression in case of all AM countermeasures unavailable	• **Expansion of pollution in RB** • **Inhibiting the implementation of additional AM measures**	

Redrawn on the figure in OECD-NEA/CSNI/R(2015)2

Purpose of this study

To contribute evaluation of the effectiveness of AM measures and the implementation of PRAs with **sufficient knowledge and low uncertainty,**

- To present continuous dataset of the ballooning and burst behavior under a wide range of postulated LOCA conditions in SFPs based on the actual SFP system and the accident progression
- To propose a fuel cladding burst model in realistic LOCA conditions at SFPs

Experimental setup

Center rod

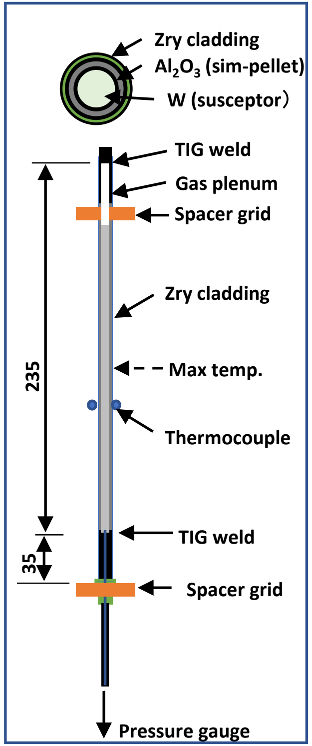

Outer heater rod

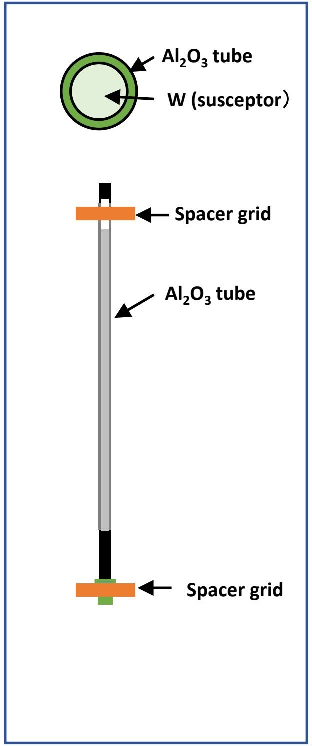

Cross-section of the bundle

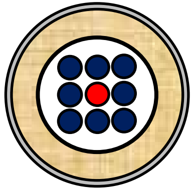

Typical Time History

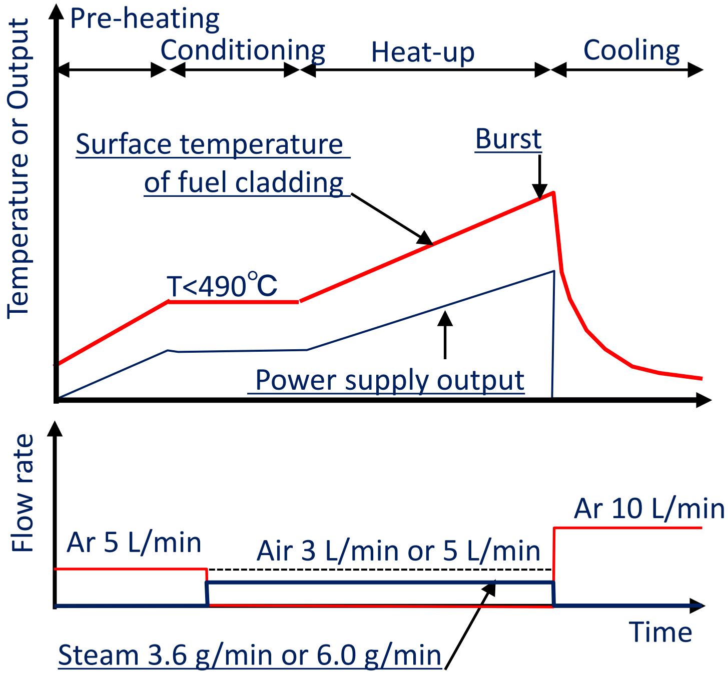

K. Nakamura et al., Proc. Global/TOP FUEL 2019, Seattle, WA, Sep. 22-26, 2019.
K. Nakamura, K. Inagaki, Proc. TOP FUEL 2021, Santander, Spain, Oct. 24-28, 2021.

Test conditions

Item	Unirradiated				Irradiated
Fuel cladding tube	Zircaloy-4 (SR)		Zircaloy-2 (RX)		on-going in NEA/SCIP-III/IV
	As-received	Pre-hydrided	As-received	Pre-hydrided	
Sim-fuel (mm)	Al_2O_3	Al_2O_3	Al_2O_3	Al_2O_3	
Susceptor (mm)	Tungsten	Tungsten	Tungsten	Tungsten	
Heating rate (℃/s) *1	10^{-4}, 10^{-3}, 10^{-2}	10^{-3}	10^{-4}, 10^{-3}, 10^{-2}	10^{-3}	
Rod inner pressure (MPa)	1, 4, 8, 12	4, 8	1, 2, 4	2, 4	
Air/(Air+Steam) ratio (%)	0, 40, 100	100	0, 40, 100	100	
Initial H_2 conc. (ppm)	<3	100-2400	<3	50-1290	
Internal volume (cc)	16	16	16	16	
Plenum temperature (℃)	20	20	20	20	
Circumferential temperature difference (℃)	<10	<10	<10	<10	
Fuel pitch (mm)	12.6	12.6	14.5	14.5	
Reference	Topfuel 2019 *2	Topfuel 2021 *3	Topfuel 2021 *3	In progress	

*1 *S. Nishimura, Consultancy Meeting on the Managing Decay Heat in Spent Fuel Storage, 9–12 Dec., Vienna, IAEA (2013).*
*2 *K. Nakamura et al., S. Nishimura, Proc. Global/TOP FUEL 2019, Seattle, WA, Sep. 22-26, 2019.*
*3 *K. Nakamura, K. Inagaki, Proc. TOP FUEL 2021, Santander, Spain, Oct.. 24-28, 2021.*

Ballooning and Burst behavior

As-received Zircaloy-4

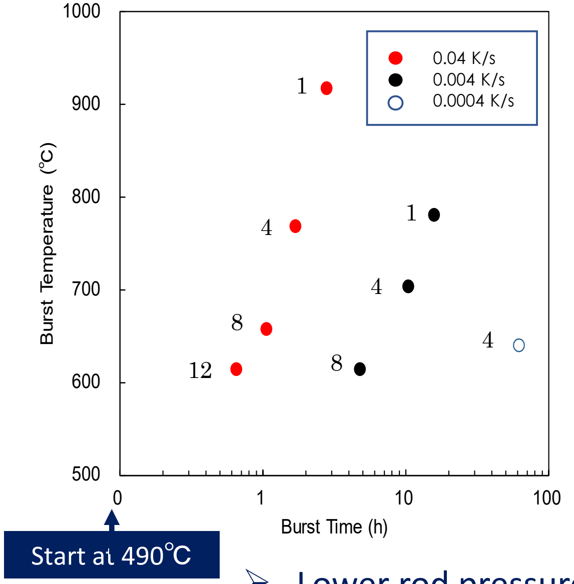

As-received Zircaloy-2

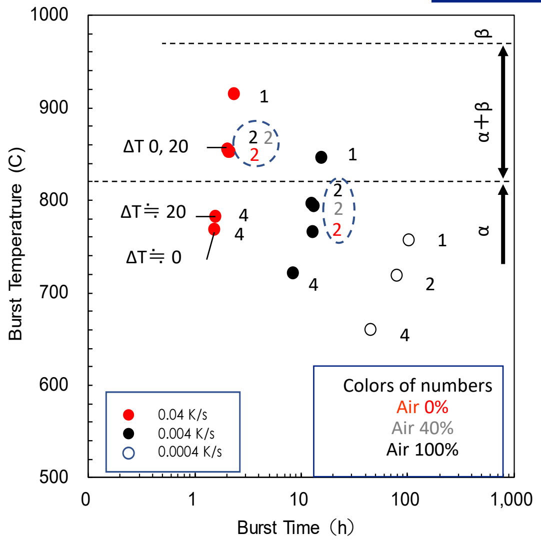

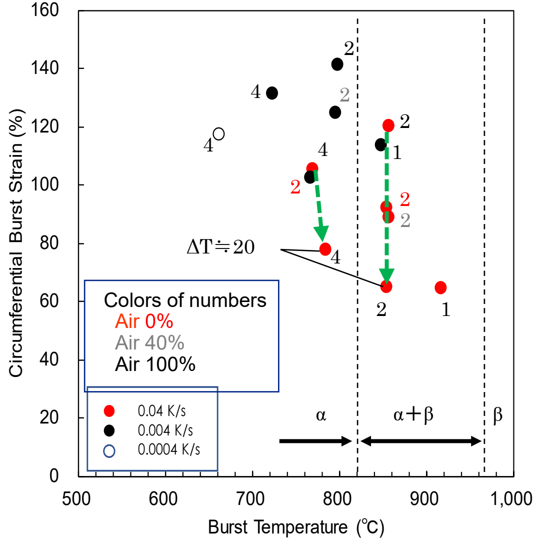

- Lower rod pressure and lower heating rate resulted in the extension of the time to burst.
- Less impact of the air ratio in the atmosphere on the burst condition
- Except for the strain behavior, the effects of thermodynamically stable phases on the ballooning and burst behavior of Zircaloy-2 were negligible.

K. Nakamura, et al., Proc. Global/TOP FUEL 2019, Seattle, WA, Sep. 22-26, 2019.
K. Nakamura, K. Inagaki, Proc. TOP FUEL 2021, Santander, Spain, Oct. 24-28, 2021.

Influence of pre-hydrogen concentration on ballooning and burst

Pre-hydrided Zircaloy-4
- Heating rate 0.004 ℃/s
- Air atmosphere

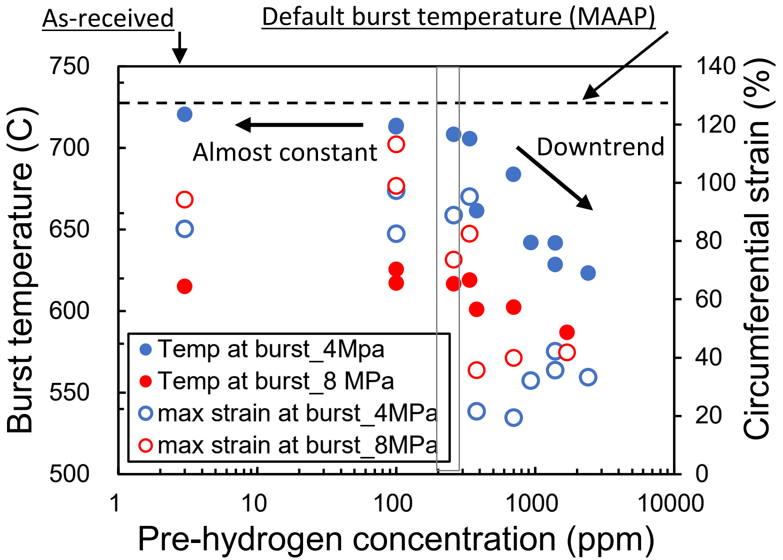

Pre-hydrided Zircaloy-4 (this

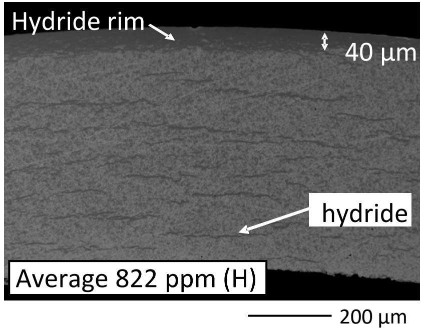

BWR fuel cladding after 5 cycles

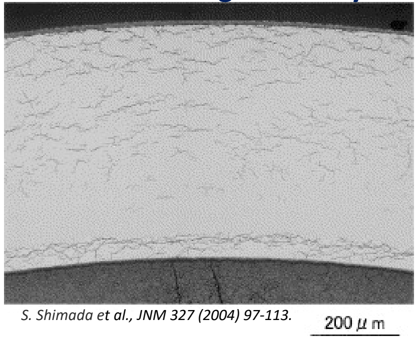

S. Shimada et al., JNM 327 (2004) 97-113.

Good similarity to hydride orientation found in high burnup fuel cladding

- ➢ The burst strain and the burst temperature
  - Below 200-300 ppm Remain unchanged
  - Above 300 ppm Decrease as the hydrogen concentration increases
- ➢ It is speculated that the observed changes are associated with the ductile-brittle transition of Zircaloy-4 cladding tube.

K. Nakamura, K. Inagaki, Proc. TOP FUEL 2021, Santander, Spain, Oct. 24-28, 2021.

Hydrogen concentration distribution

Pre-hydrided Zircaloy-4
- Heating rate 0.004 ℃/s
- Air atmosphere

Axial

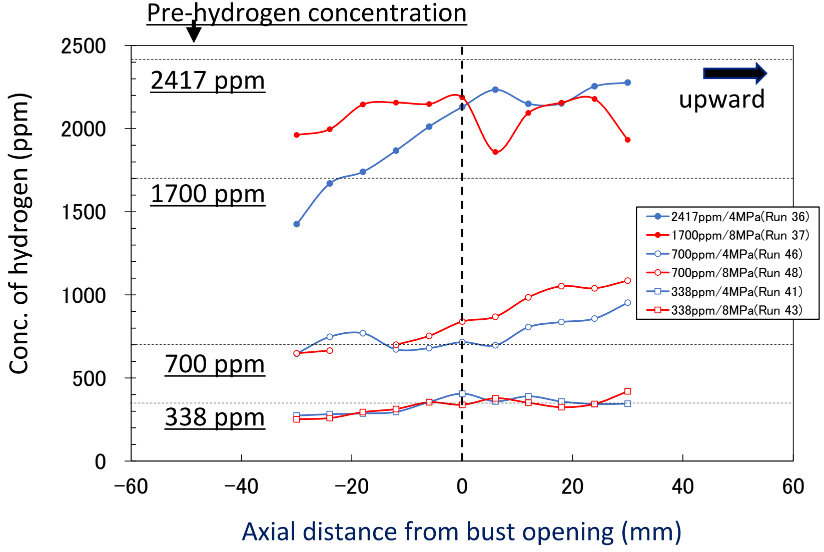

- Less change in the axial hydrogen concentration distribution during the accident progression in air atmosphere.

Radial

As-received Zircaloy-2
- Heating rate 0.004 ℃/s
- Steam atmosphere
- 603 ppm (H) at 24mm above the burst opening

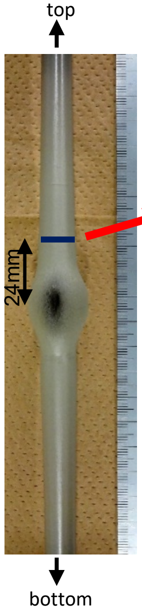

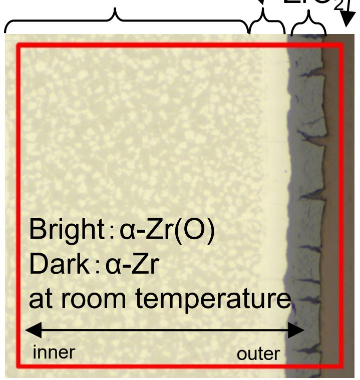

Optical microscopy image

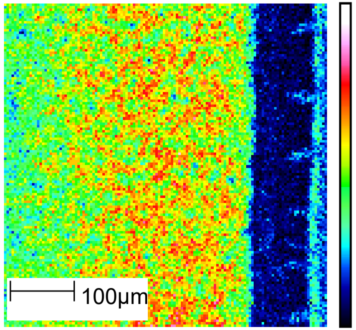

Ion image of hydrogen (ToF-SIMS)

- Hydrogen was concentrated in β-Zr phase of the α+β two-phase region at high temperature, similar to as-received Zircaloy-4.

K. Nakamura, K. Inagaki, Proc. TOP FUEL 2021, Santander, Spain, Oct. 24-28, 2021.

ZrN formation at the ZrO_2/α-Zr(O) interface

As-received Zircaloy-2

X-ray map of Nitrogen（EPMA）in cross section of burst opening region

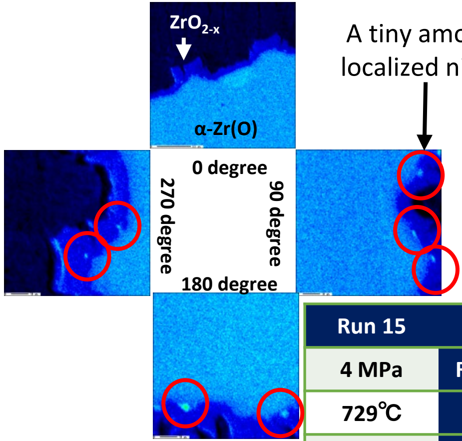

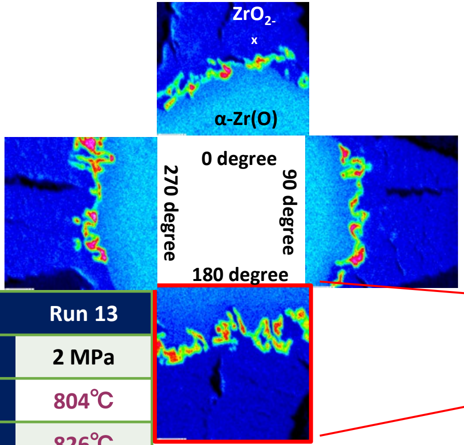

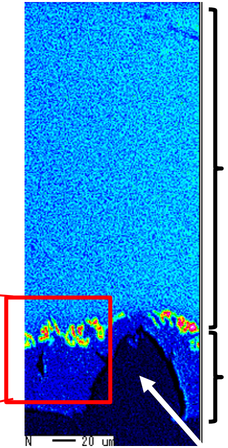

Run 15		Run 13
4 MPa	Rod inner pressure	2 MPa
729℃	Burst temp.	804℃
745℃	Max. temp	826℃
0.004℃/s	Heating rate	0.004℃/s
AIR	Atmosphere	AIR

- The formation of low-density ZrN, which make the corrosion rate increase lineally, was confirmed at the ZrO_2 / α-Zr (O) interface with cracking in the outer oxide ZrO_2 layer.
- The nitrogen maps suggest that the growth of the nitrogen-containing compound may proceed after the burst, thus supporting the finding that the impact of air ingress on burst behavior is small under LOCA conditions in an SFP.

K. Nakamura, K. Inagaki, Proc. TOP FUEL 2021, Santander, Spain, Oct. 24-28, 2021.

Conclusions

- With the DEGREE facility, a series of the bundle degradation tests in the early stages of a severe accident was performed in steam environments up to 2000 °C in CRIEPI.
  - In case of the steam-rich condition, the formation of a thick protective ZrO_2 on the outside surface of the cladding tubes prevented the test rods from severe degradation.
  - In the steam-starved condition, however, characteristic features such as formation of metallic melts throughout the bundle region, downward relocation of the melts, and formation of massive blockage were observed.
- Ballooning and burst tests for the simulated HB fuel cladding tube have also been studied focusing on the LOCA scenario at SFP.
- The DEGREE facility can contribute to the demonstration, elucidation, and validation of the processes of degradation behavior for fuel bundles, core structural materials, and advanced materials in reactors or SFPs under various prospected accident scenarios.

Future works

- The sim. high BU fuel rod under beyond DBA conditions
- The candidate ATF bundle tests under beyond DBA condition
  (ATF-TS in IAEA)
- The accident tolerant control rod (ATCR) tests under beyond DBA condition

Thank you for your attention!

A. Pshenichnikov, Y. Nagae, M. Kurata
JAEA-CLADS

Outline of the CLADS-MADE-03 test under steam-rich conditions and high heating rate

To investigate the real debris from the Fukushima Dai-Ichi (1F) Unit 1 is still a challenge because of a high dose rate due to melted fuel and fission products distributed in a damaged reactor pressure vessel (RPV) and a primary containment vessel (PCV). However, exact distribution, chemical composition and properties of the 1F units' debris remain uncertain.

After accidents at the 1F, JAEA/CLADS is constantly supporting TEPCO by making R&D to find proper solutions for current challenges. That is why we are developing a test approach for studying large-scale BWR bundles degradation under various conditions and study sim-debris to reduce the uncertainties [1]. This is a part of the big work with such ultimate goals as the understanding of BWR core degradation scenarios, debris formation mechanisms in BWRs, and possible properties of debris under 1F-like conditions.

This research was aimed at understanding of the features of melt progression and debris formation under postulated conditions, which mirror a beginning phase of an accident at the Unit 1. By using the available limited data and by comparison with the other Units' scenarios which were elaborated earlier [2], it was possible to grasp the 1F Unit 1 conditions. The CLADS-MADE-03 test allowed checking a materials' behaviour in high-temperature steam. The initial heating rate was 1 °C/s, reaching maximum temperature 1600 °C at the hottest top bundle point. The axial temperature gradient of 500 °C/m forced the metallic melt to solidify in between the channel boxes in the colder elevations and interact with bundle materials.

The result of this interactions was observed at the polished cross-sections and investigated using a complementary SEM, Raman imaging microscopy techniques and EPMA (WDS).

It was established, that there were lots of unreacted B_4C material encapsulated in the metallic melt under the temperature ≈ 1500 °C. The reacted traces of previous B_4C contained only pure graphite. Below this temperature a blockage consisted of solidified metallic Fe-based melt was found. Unlike previous tests, this time a partial formation of eutectic consisted of the Zr-SS-B_4C elements happened. A strongly localized character of Zr wall dissolution caused by the interaction was investigated metallographically. The degraded oxide layer was captured by Raman technique. The interaction of Zr-bearing eutectic melt with Zr oxide became a particular focus of the investigation.

After a comprehensive analysis of the available data it was possible to state the following:

- Ni effect on accident progression is low – it is always as admixture to Fe.
- Fe creates eutectics with B, which starts the degradation of the fuel control blade.
- If the oxide layer at the channel box is thin (approximately less than 10 µm), and such oxide is covered by Fe-B melt, oxide can be dissolved in channel box Zr bulk material and let Fe contact with metallic Zr.
- After formation of Zr-Fe eutectic the situation develops much more catastrophic, and melting continues eating out the walls of channel boxes and claddings sometimes with exothermic reaction – it is because we observed formation of $Zr(Fe,Cr)_2$ Laves phase.

Which causes release of free energy, which locally increases the temperature (according to preliminary data about 100-150 °C), which helps local destruction and dissolution of Zr oxide layer and supports the liquid state longer than for usual ferrous melt.

- Appearances of the Fe-rich melt and the Zr-rich melt during relocation are essentially different - a tiny oxide looked like a plastic bag at the surface of relocating Zr-rich melt can additionally decrease heat release to the outside and supports the liquid state.
- Cr is a phase stabilizing agent – in absence of Zr it preferentially stabilizes (Cr,Fe)B and other boride phases, but in case of Zr present in the melt, Zr accumulates all B from the melt and pushes all Cr to takes part in $Zr(Fe,Cr)_2$ formation. As a result, almost all Cr is concentrated in intermetallide Laves phase and all B in ZrB_2 borides.
- Formation of the two very stable phases from liquid releases much of energy to support longer high temperature enough for the relocation to colder areas, where oxide layer is thinner
- When oxide layer is covered by such Zr-bearing melt, it immediately dissolves the oxide layer in two directions into the bulk of base material and to the liquid melt. The latter process is much faster.
- Fe-Ni melt is still unable to penetrate the bulk of the channel box until the alpha layer exists.
- If penetration happens it happens very locally. At the same time, large amount of Zr-containing metallic melt can really dissolve large amount of oxide and completely liquefy the lower core region.

This knowledge provided new insights for understanding of the influence of an absorber blade melting on the overall bundle degradation under specific accident conditions close to 1F Unit 1. Post-test characterization of debris suggested need for the further investigation of the sim-debris properties because same kind of metallic debris with B are possible to find also in the PCV of the damaged 1F Unit 1.

A part of this study was performed in the framework of "Advanced Multi-Scale Modelling and Experimental Tests on Fuel Degradation in Severe Accident Conditions" supported by Ministry of Economy, Trade and Industry, Japan.

References

[1] A. Pshenichnikov, H. Shibata, T. Yamashita, Y. Nagae, M. Kurata Ten years of Fukushima Dai-Ichi post-accident research on the degradation phenomenology of the BWR core components, Journal of Nuclear Science and Technology, DOI: 10.1080/00223131.2021.1985647.

[2] A. Pshenichnikov, M. Kurata, D. Bottomley, I. Sato, Y. Nagae, S. Yamazaki New research programme of JAEA/CLADS to reduce the knowledge gaps revealed after an accident at Fukushima-1: introduction of boiling water reactor mock-up assembly degradation test programme (2019), Journal of Nuclear Science and Technology, 57:4, 370-379, DOI: 10.1080/00223131.2019.1691070

A. Pshenichnikov, Y. Nagae, M. Kurata
JAEA-CLADS

Outline of the CLADS-MADE-03 test under steam-rich conditions and high heating rate

Abstract

To investigate the real debris from the Fukushima Dai-Ichi (1F) Unit 1 is still a challenge because of a high dose rate due to melted fuel and fission products distributed in a damaged reactor pressure vessel (RPV) and a primary containment vessel (PCV). However, exact distribution, chemical composition and properties of the 1F units' debris remain uncertain.

After accidents at the 1F, JAEA/CLADS is constantly supporting TEPCO by making R&D to find proper solutions for current challenges. That is why we are developing a test approach for studying large-scale BWR bundles degradation under various conditions and study sim-debris to reduce the uncertainties [1]. This is a part of the big work with such ultimate goals as the understanding of BWR core degradation scenarios, debris formation mechanisms in BWRs, and possible properties of debris under 1F-like conditions.

This research was aimed at understanding of the features of melt progression and debris formation under postulated conditions, which mirror a beginning phase of an accident at the Unit 1. By using the available limited data and by comparison with the other Units' scenarios which were elaborated earlier [2], it was possible to grasp the 1F Unit 1 conditions. The CLADS-MADE-03 test allowed checking a materials' behaviour in high-temperature steam. The initial heating rate was 1 °C/s, reaching maximum temperature 1600 °C at the hottest top bundle point. The axial temperature gradient of 500 °C/m forced the metallic melt to solidify in between the channel boxes in the colder elevations and interact with bundle materials.

The result of this interactions was observed at the polished cross-sections and investigated using a complementary SEM, Raman imaging microscopy techniques and EPMA (WDS).

It was established, that there were lots of unreacted B_4C material encapsulated in the metallic melt under the temperature ≈ 1500 °C. The reacted traces of previous B_4C contained only pure graphite. Below this temperature a blockage consisted of solidified metallic Fe-based melt was found. Unlike previous tests, this time a partial formation of eutectic consisted of the Zr-SS-B_4C elements happened. A strongly localized character of Zr wall dissolution caused by the interaction was investigated metallographically. The degraded oxide layer was captured by Raman technique. The interaction of Zr-bearing eutectic melt with Zr oxide became a particular focus of the investigation.

After a comprehensive analysis of the available data it was possible to state the following:

- Ni effect on accident progression is low – it is always as admixture to Fe.
- Fe creates eutectics with B, which starts the degradation of the fuel control blade.
- If the oxide layer at the channel box is thin (approximately less than 10 µm), and such oxide is covered by Fe-B melt, oxide can be dissolved in channel box Zr bulk material and let Fe contact with metallic Zr.
- After formation of Zr-Fe eutectic the situation develops much more catastrophic, and melting continues eating out the walls of channel boxes and claddings sometimes with exothermic reaction – it is because we observed formation of $Zr(Fe,Cr)_2$ Laves phase. Which causes release of free energy, which locally increases the temperature (according to preliminary data about 100-150 °C), which helps local destruction and dissolution of Zr oxide layer and supports the liquid state longer than for usual ferrous melt.

- Appearances of the Fe-rich melt and the Zr-rich melt during relocation are essentially different - a tiny oxide looked like a plastic bag at the surface of relocating Zr-rich melt can additionally decrease heat release to the outside and supports the liquid state.
- Cr is a phase stabilizing agent – in absence of Zr it preferentially stabilizes (Cr,Fe)B and other boride phases, but in case of Zr present in the melt, Zr accumulates all B from the melt and pushes all Cr to takes part in $Zr(Fe,Cr)_2$ formation. As a result, almost all Cr is concentrated in intermetallide Laves phase and all B in ZrB_2 borides.
- Formation of the two very stable phases from liquid releases much of energy to support longer high temperature enough for the relocation to colder areas, where oxide layer is thinner
- When oxide layer is covered by such Zr-bearing melt, it immediately dissolves the oxide layer in two directions into the bulk of base material and to the liquid melt. The latter process is much faster.
- Fe-Ni melt is still unable to penetrate the bulk of the channel box until the alpha layer exists.
- If penetration happens it happens very locally. At the same time, large amount of Zr-containing metallic melt can really dissolve large amount of oxide and completely liquefy the lower core region.

This knowledge provided new insights for understanding of the influence of an absorber blade melting on the overall bundle degradation under specific accident conditions close to 1F Unit 1. Post-test characterization of debris suggested need for the further investigation of the sim-debris properties because same kind of metallic debris with B are possible to find also in the PCV of the damaged 1F Unit 1.

A part of this study was performed in the framework of "Advanced Multi-Scale Modelling and Experimental Tests on Fuel Degradation in Severe Accident Conditions" supported by Ministry of Economy, Trade and Industry, Japan.

References

[1] A. Pshenichnikov, H. Shibata, T. Yamashita, Y. Nagae, M. Kurata Ten years of Fukushima Dai-Ichi post-accident research on the degradation phenomenology of the BWR core components, Journal of Nuclear Science and Technology, DOI: 10.1080/00223131.2021.1985647.

[2] A. Pshenichnikov, M. Kurata, D. Bottomley, I. Sato, Y. Nagae, S. Yamazaki New research programme of JAEA/CLADS to reduce the knowledge gaps revealed after an accident at Fukushima-1: introduction of boiling water reactor mock-up assembly degradation test programme (2019), Journal of Nuclear Science and Technology, 57:4, 370-379, DOI: 10.1080/00223131.2019.1691070

R. Farkas, I. Nagy, N. Vér, Z. Hózer, P. Szabó,
G. Szabó, M. Horváth
CER Budapest

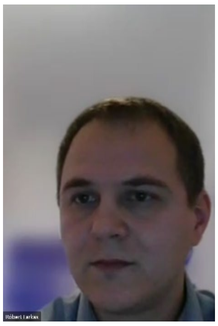

The CODEX-SBO experiment

A CODEX-SBO experiment was carried out at the Centre for Energy Research (EK) in order to simulate Station Black Out accident with injection of water from the hydroaccumulators during the event. The reference scenario was taken from safety analyses for the VVER-440 units of the Paks NPP.

Seven-rod electrically heated VVER type bundle was used with 600 mm heated length. The bundle was covered by Zr shroud. The composition of outlet gases was monitored with mass spectrometer. During the experiment, the maximum cladding temperature reached 1900 °C. The presence of steam in the atmosphere accelerated the oxidation of Zr components. The post-test examination confirmed that thick oxide layers were formed and part of the bundle suffered brittle failure.

Centre for Energy Research

The CODEX-SBO experiment

Róbert Farkas, Imre Nagy, Nóra Vér, Zoltán Hózer, Péter Szabó, Gergely Szabó, Márta Horváth

26th International QUENCH Workshop
2021

Objective

- The CODEX-SBO experiment was carried out at the Centre for Energy Research (EK) in order to simulate Station Black Out accident with electrically heated 7-rod bundle.

- The essential elements of the CODEX-SBO experiment are the following:
- 1. After loss of all power of the power plant, water injection starts from the hydroaccumulators to the bundle.
- 2. The bundle is successfully cool down, but without active cooling systems water boils and the zone dries out.

- Reference scenario was taken from safety analyses for the VVER-440 units of the Paks NPP.

- Pre-test calculations has been performed by NUBIKI.

- Cool-down of the bundle has been implemented by water quench.

Centre for
Energy Research

CODEX facility

- Water tank & gas inlet
- Steam generator & superheater
- Test section
- Condenser
- Condenser tank
- Pressurisation system

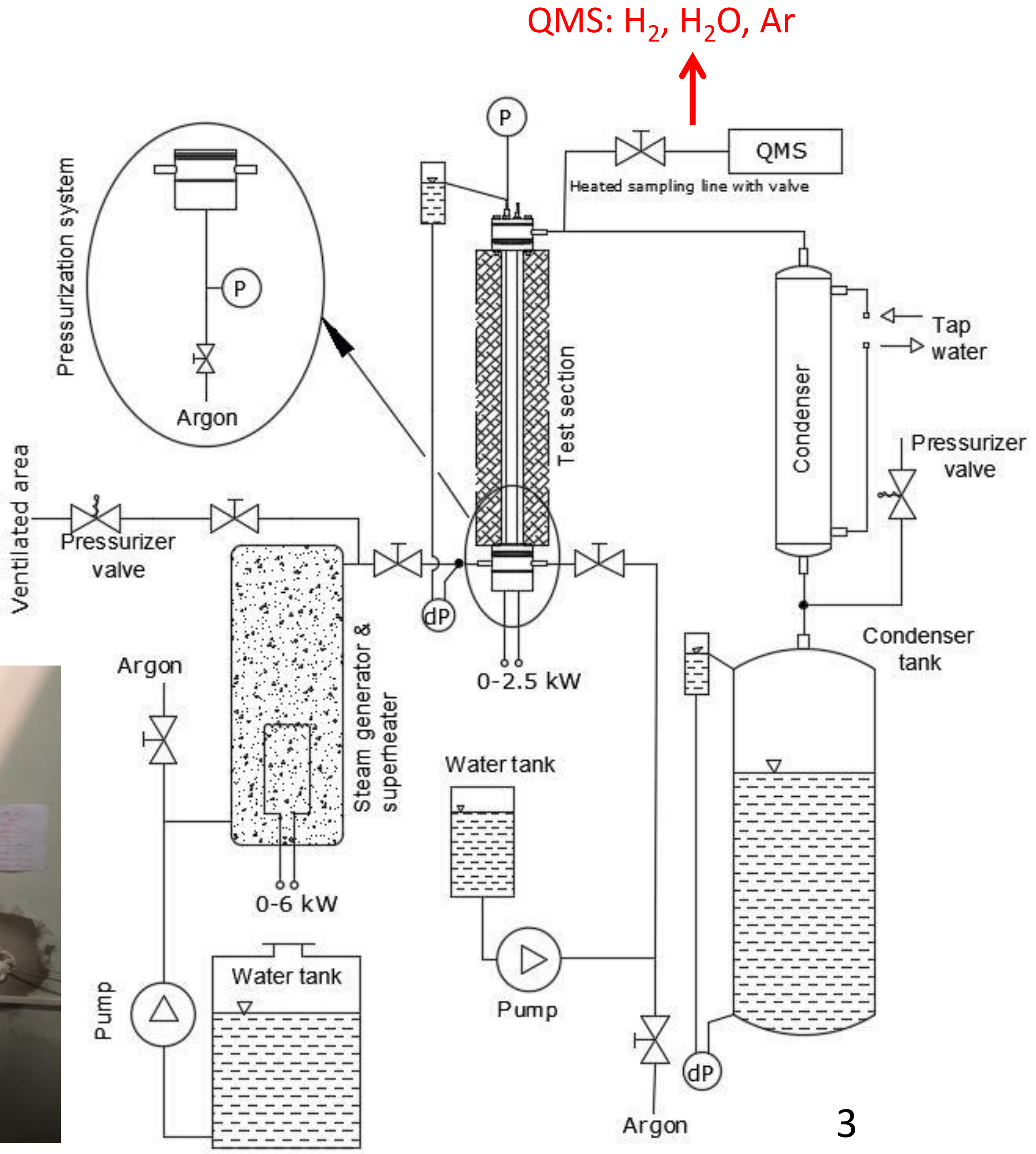

Bundle desing

- VVER bundle type:
  hexagonal arrangement of 7 rods
- Height of rods: 600 mm
  - 6 rods (periphery)
    electrically heated - no pressurized
  - 1 rod (in the center)
    unheated - pressurized
- Cladding material: E110 (3.,5.)
  E110G (1., 4., 7.)
  E110h.p. (2., 6.) alloy
- ZrO_2 ceramic pellets
- Tungsten heaters (580 mm)
- 2 spacer grids (Zr1%Nb alloy)
- Hexagonal shroud (Zr2.5%Nb alloy, 1000 mm)

Heated fuel rod

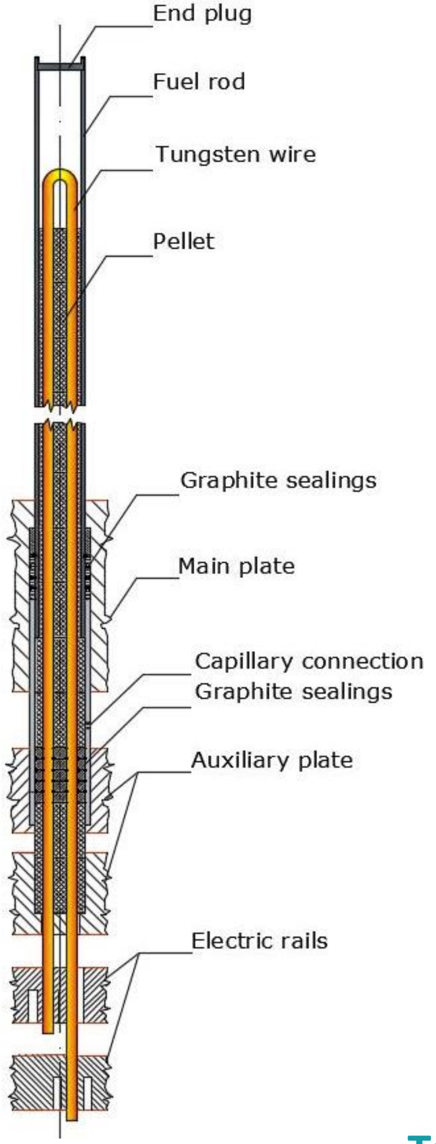

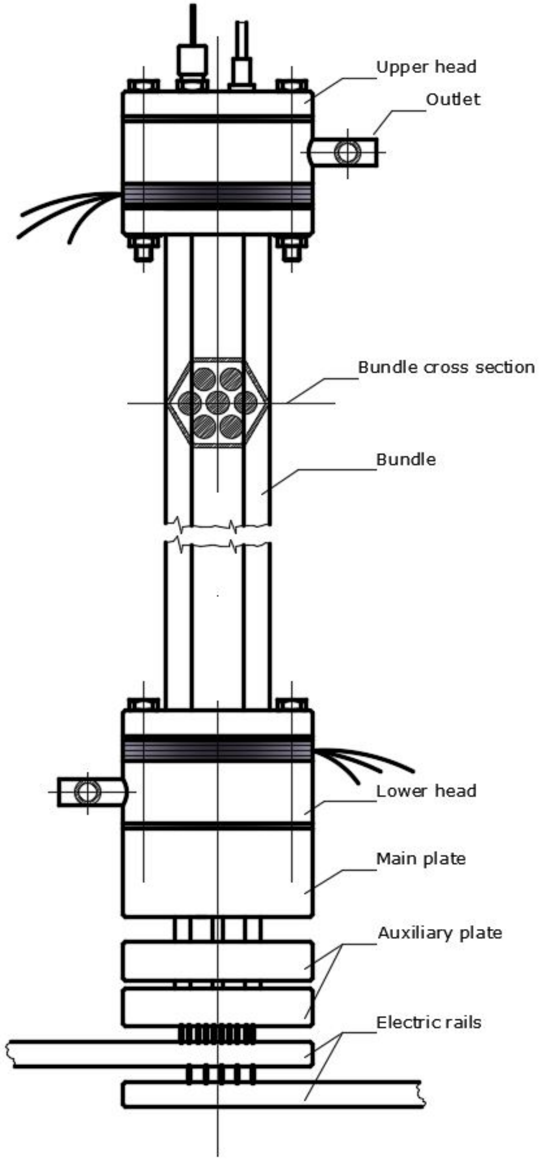

Test section with seven-rod bundle

Cross section of the test section with thermal insulations

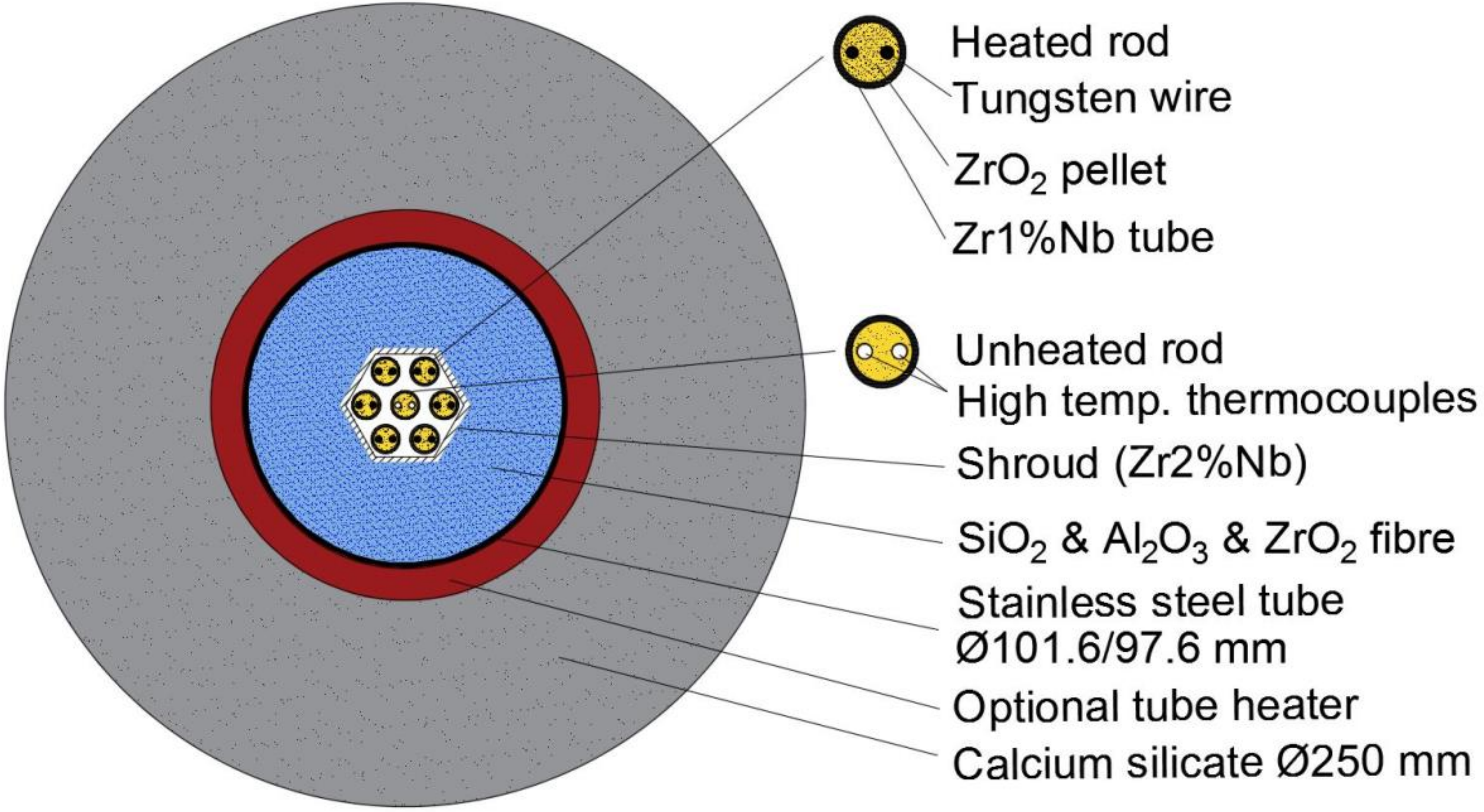

Centre for Energy Research

Measurement of parameters

Parameter	Device	Placement
Temperature	C-type- W5% Re/W26% Re in Zr shield tube	Rod surfaces and inner side
	K-type	Others (coolant , off-gas, stainless steel tube, …)
Argon flowrate	Calibrated flowmeter	Gas supply system
Steam flowrate	Calibrated pump	Pump
Gas composition	Mass spectrometer	Gas outlet
Power	DC power units	Rail of electric connections
System pressure	P transducer, 6 bar/4-20 mA	Test section upper head
Fuel rod pressure	P transducer, 100 bar/4-20 mA	Pressurization system
Water level	DP transducer device	Condenser tank

SPECIFIED SCENARIO

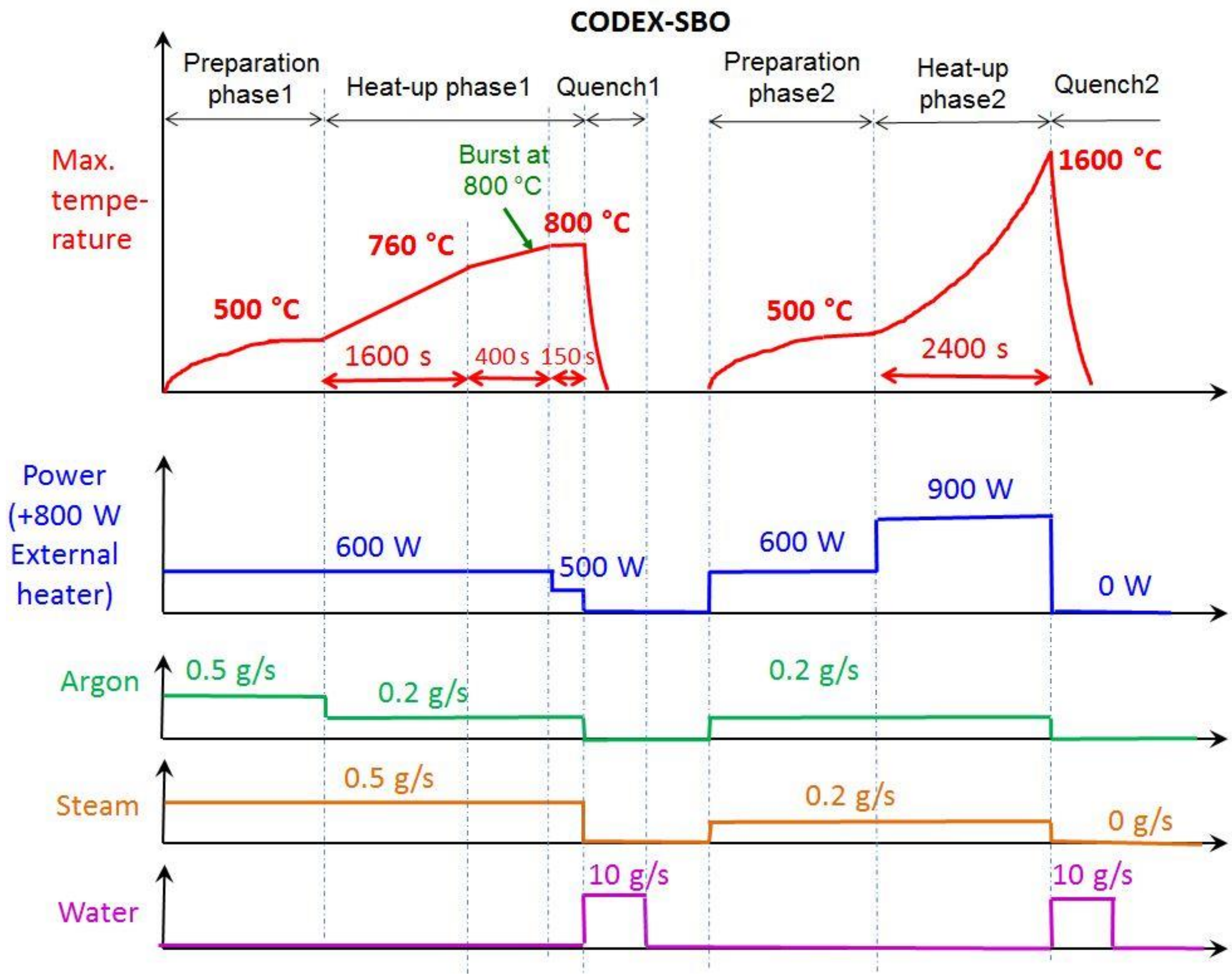

Targets in the pre-test calculations:

I. phase:

- T_{max} = 800 °C
- Cladding burst of the central rod

II. phase:

- Repeated heat-up in steam atmosphere
- t ≈ 40 min.
- T_{max} = 1600 °C

Centre for Energy Research

CODEX-SBO EXPERIMENT phase I.

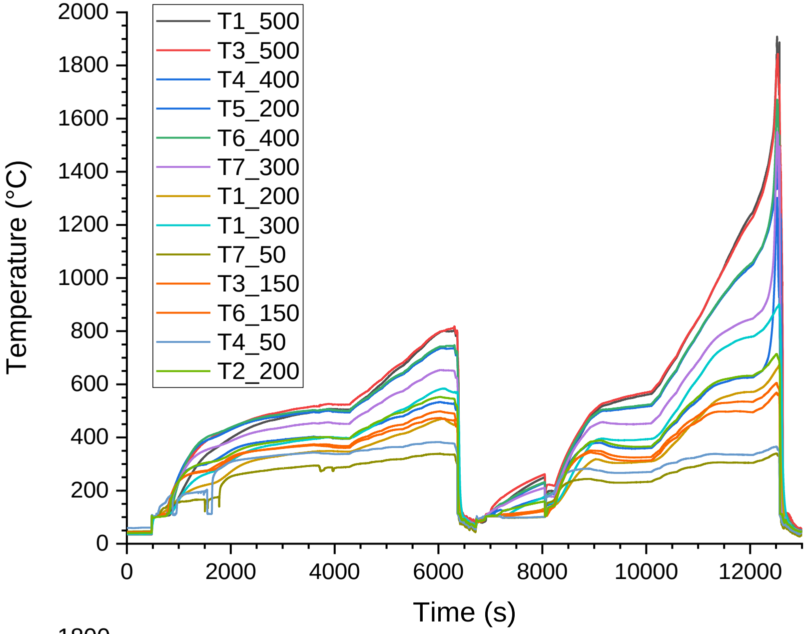

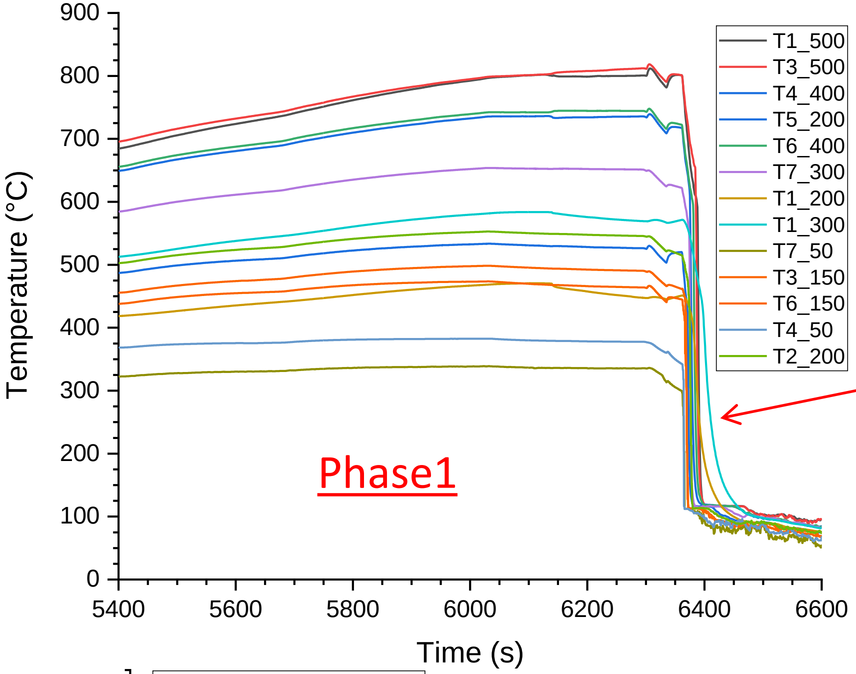

T_{max}=800 °C

Height: 500 mm

quench1

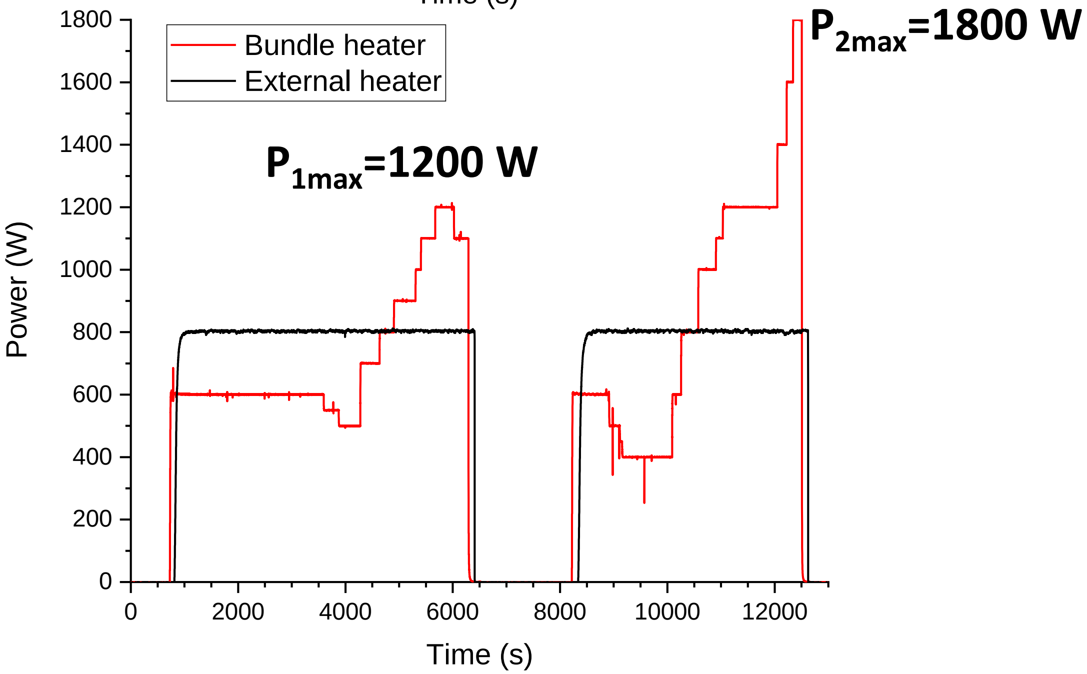

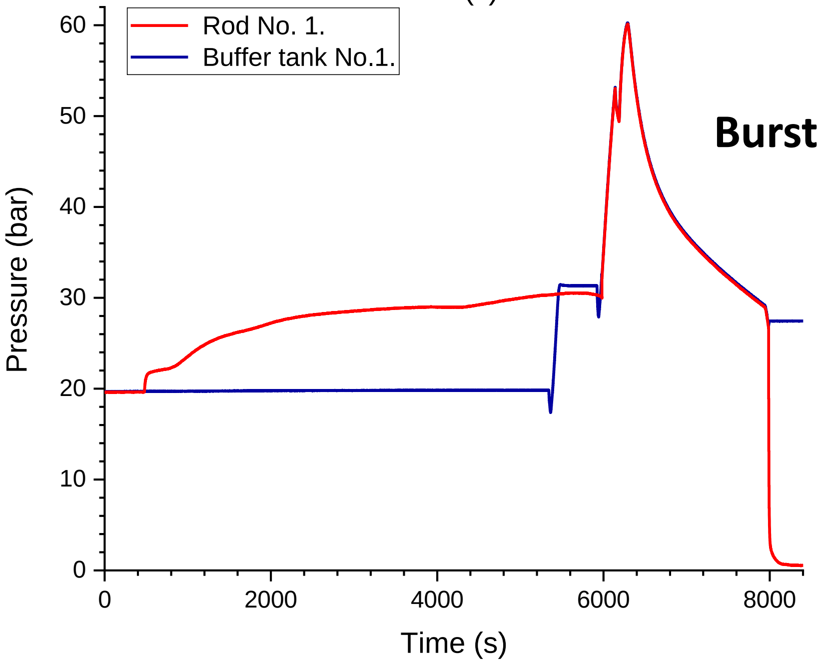

Burst at 60 bar (800 °C)

CODEX-SBO EXPERIMENT phase II.

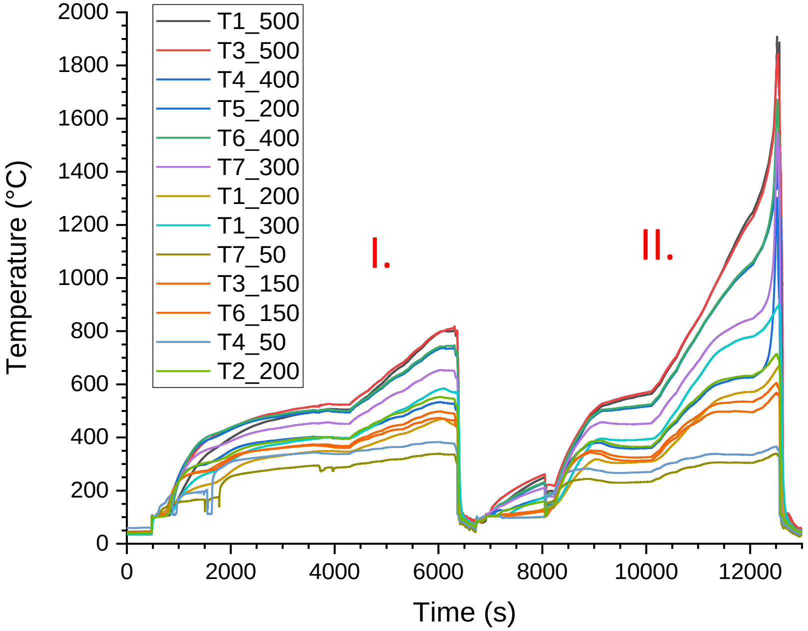

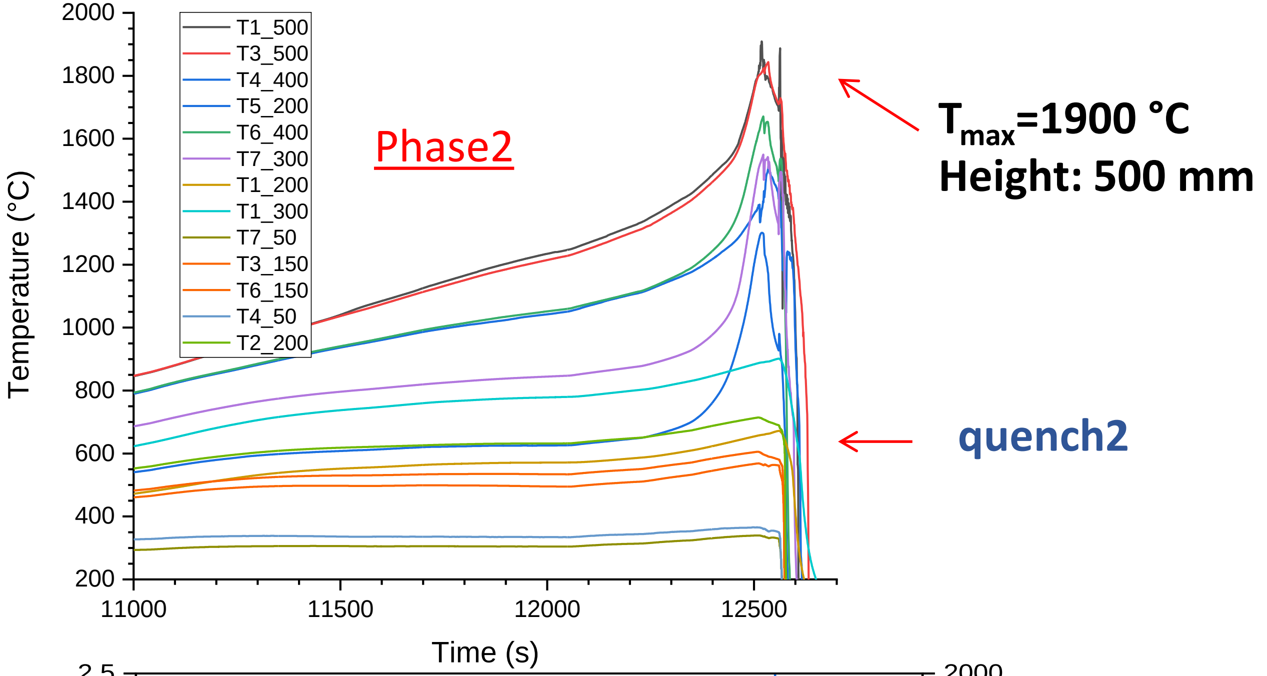

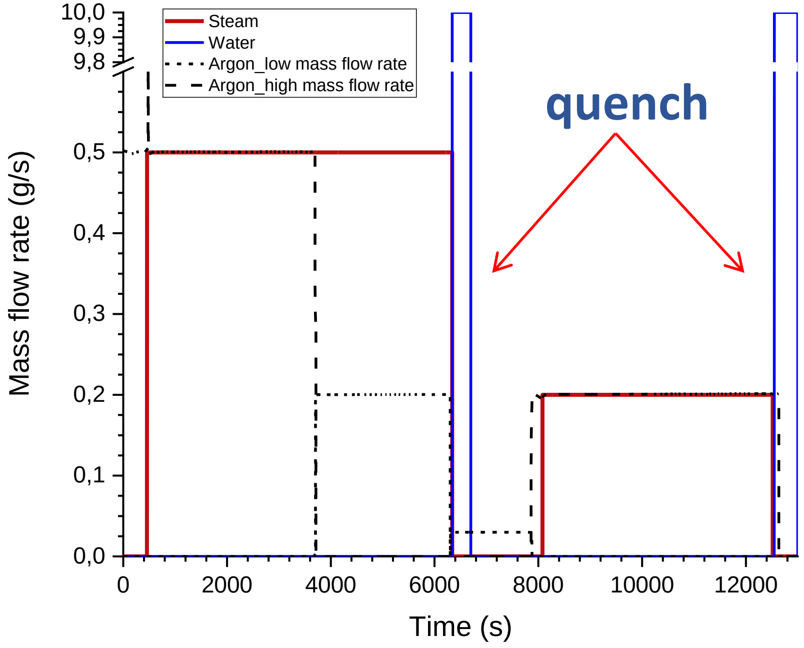

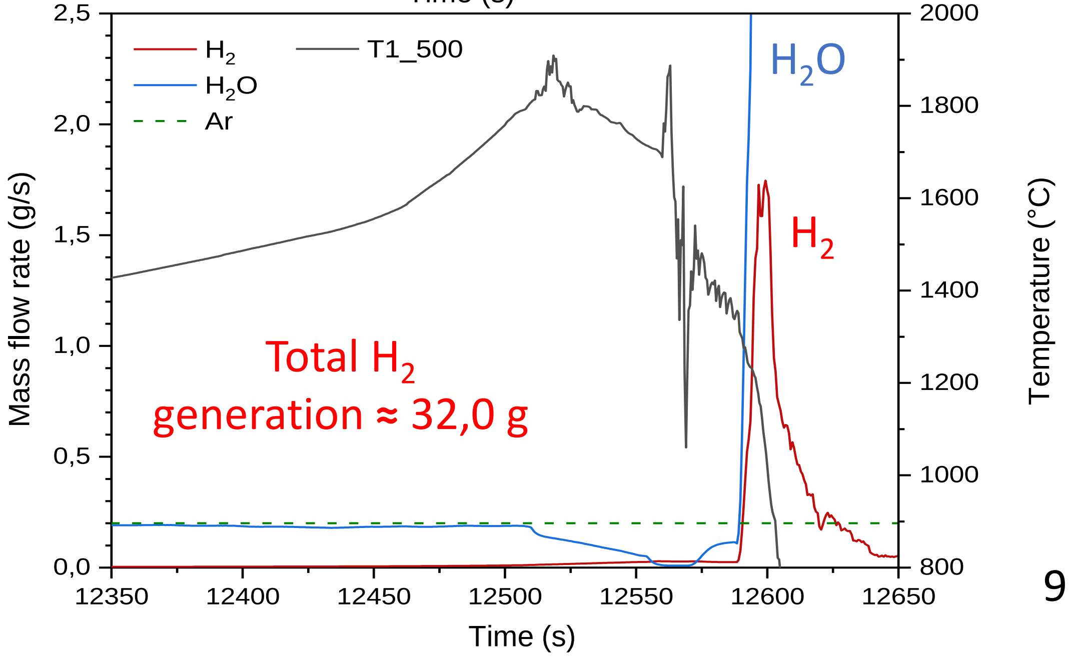

Images of the bundle (endoscopic)

- Debris was accumulated on the lower spacer grid

- Burst of the central rod

- Upper part of the 5th rod is broken down

- Thick oxide layers were formed on the upper part of the bundle and the shroud

Cross sections of bundle

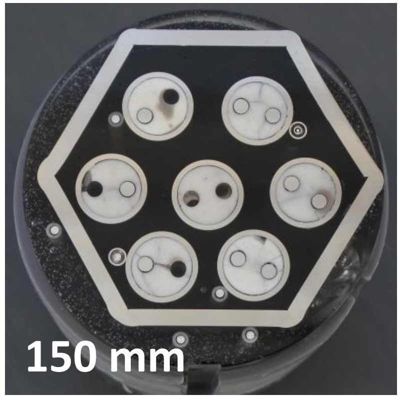

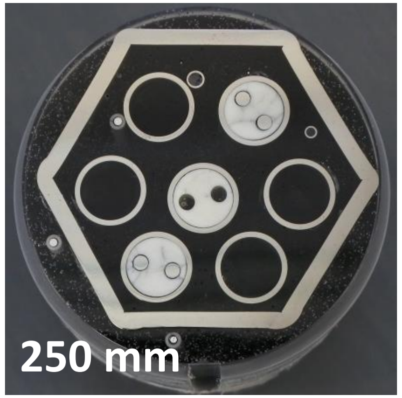

Oxide layer thickness

Outside oxide layer
Above 450 mm height: 400-500 μm
Under 450 mm height: 100 μm

Inside oxide layer only on central rod
Above 550 mm height: 40-80 μm

Cross sections of rods (Optical microscopy)

Centre for Energy Research

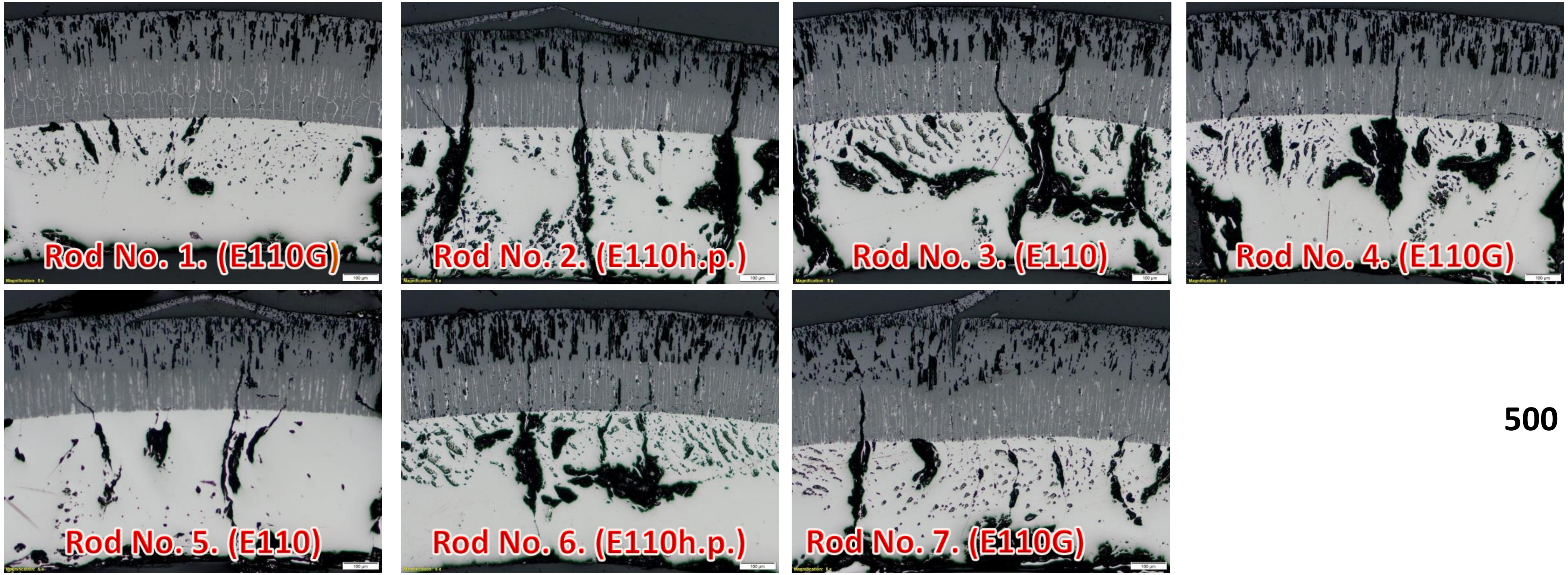

Compact oxide layer

metal

500 mm

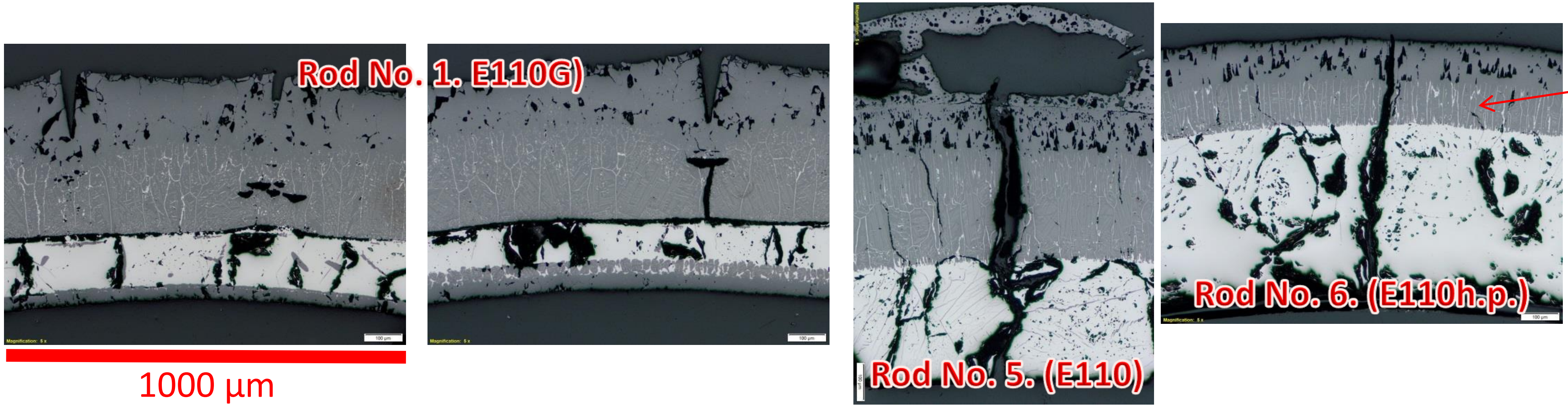

1000 µm

„metal in oxide layer”

550 mm

Scanning electron microscope images

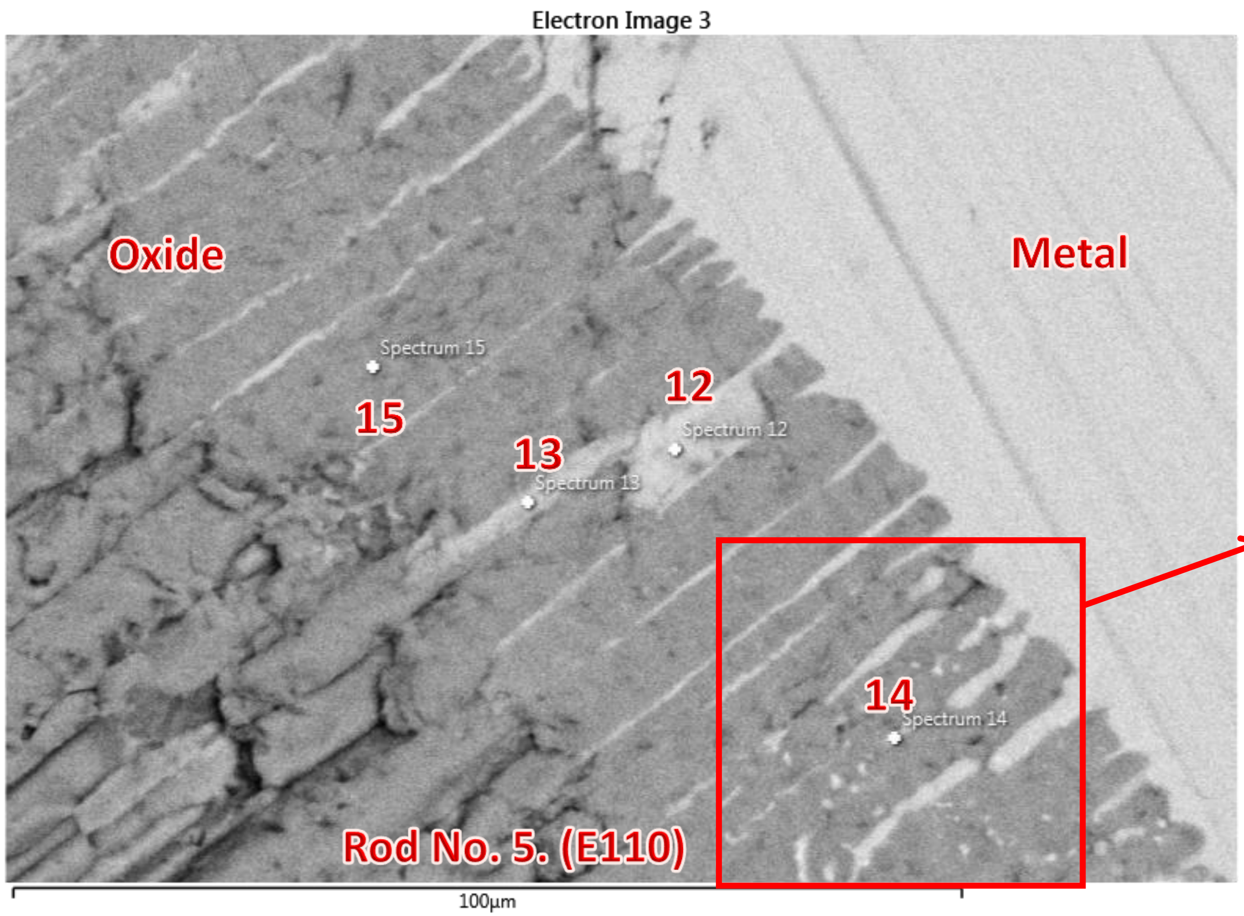

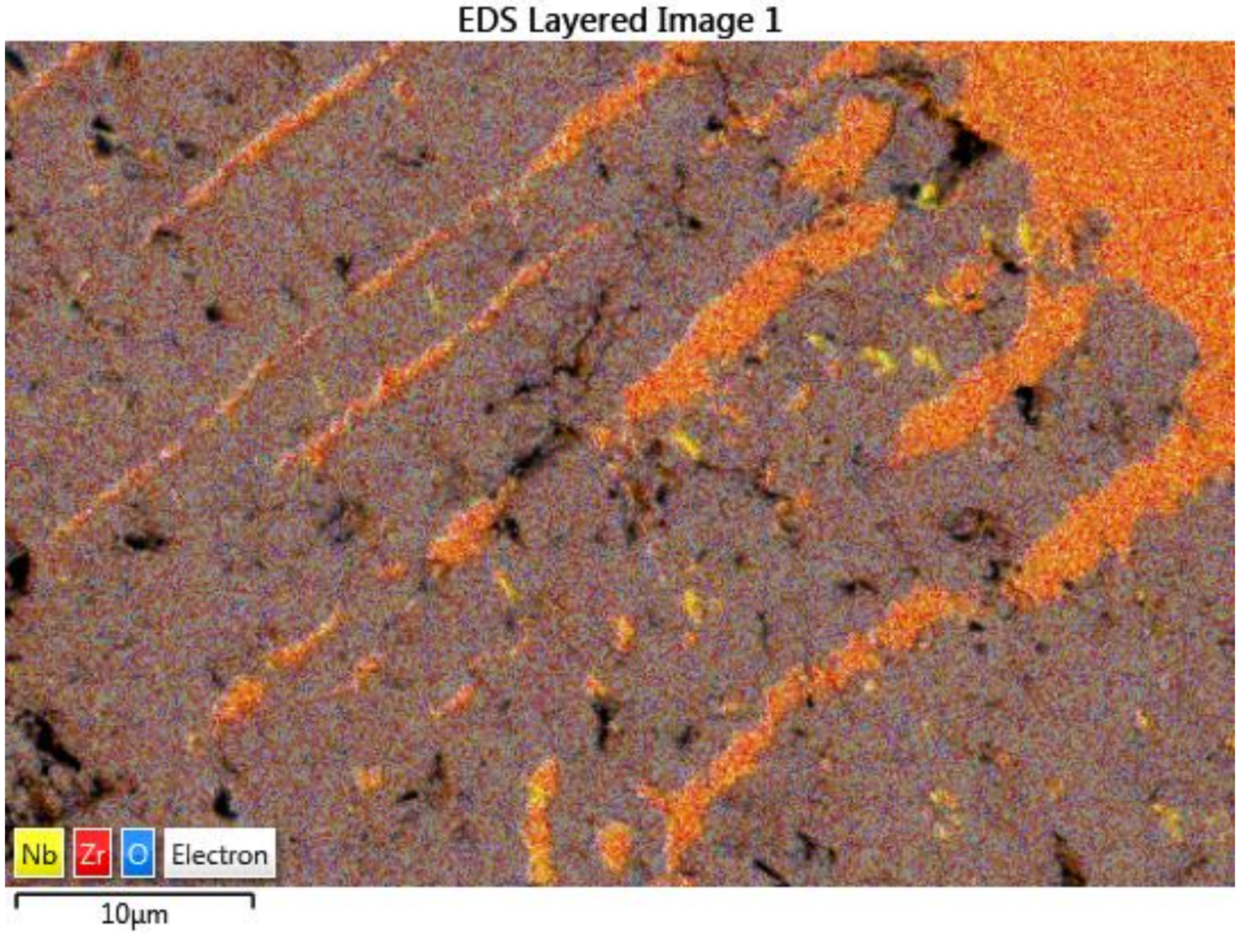

Spektrum	Spektrum12	Spektrum13	Spektrum14	Spektrum15.
O	11.88	15.32	27.19	30.75
Zr	86.42	82.96	71.11	67.80
Nb	1.69	1.72	1.70	1.46

Centre for Energy Research

Summary

- The CODEX-SBO test was successfully performed on the 11th October 2019.
- The experiment was carried out with temperature conditions which were close to the specified ones by pre-test calculations.
- Seven-rod electrically heated VVER type bundle with 600 mm heated length was used.
- The bundle was covered by Zr shroud.
- The composition of outlet gases was monitored with mass spectrometer.
- The presence of steam in the atmosphere accelerated the oxidation of Zr components.
- In the first phase the maximum temperature reached 800 °C. Cladding burst took place at the same temperature due to pressurization of the central rod. Consequence of the opening the coolant entered to the rod and started chemical reactions on both sides of the cladding.
- In the second phase the maximum cladding temperature reached 1900 °C.
- Total H_2 generation ≈ 32,0 g .
- Cool-down of the bundle was performed with water quench.
- The post-test examination was confirmed that thick oxide layers were formed and part of the bundle was suffered brittle failure.

Centre for
Energy Research

Acknowledgement

The CODEX-SBO experiment was supported by the National Research, Development and Innovation Fund of Hungary (contract number: NVKP_16-1-2016-0014).

NATIONAL
RESEARCH, DEVELOPMENT
AND INNOVATION OFFICE

Centre for Energy Research

Thank you for your attention!

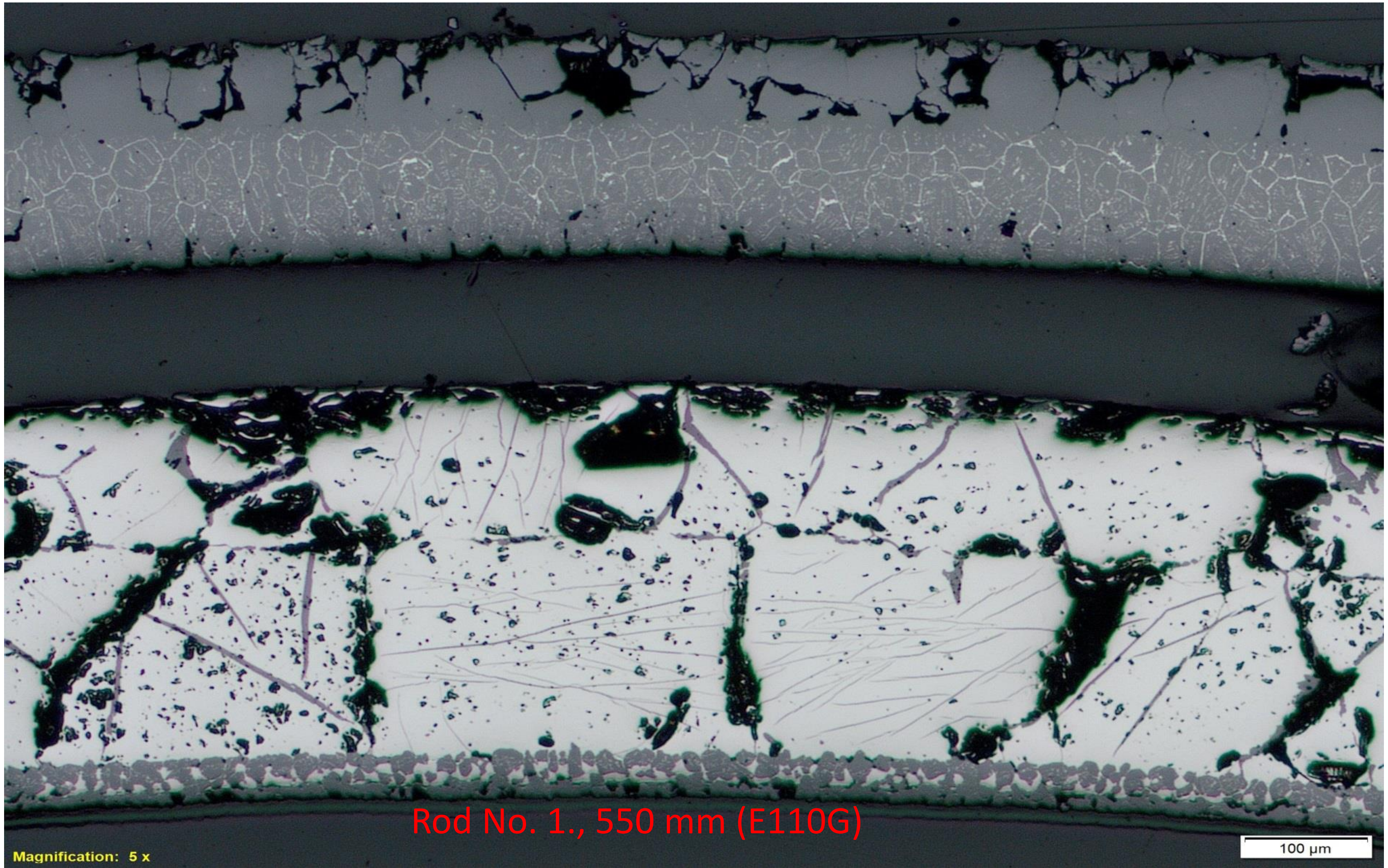

J.C- Brachet
CEA Paris-Saclay

Refined relationship between through wall clad oxygen diffusion profiles and post-quenching impact properties of as-received and pre-hydrided Zircaloy-4, following High-Temperature (HT) steam oxidation

The presentation will focus on impact properties of low-tin Zircaloy-4 claddings, pre-hydrided or not, after High Temperature oxidation followed by direct quenching. A "refined" relationship between these impact properties and the oxygen and hydrogen diffusion profiles & partitioning through the wall clad thickness will be presented and related to the local clad failure mode upon Room Temperature impact testing, using systematic Post-Quench fractographic examinations.

The presented "correlation refinement" is based on already published data [1], and, after updating, directly correlates the impact properties to the oxygen profiles measured by EPMA, with taking into account the additional effect of hydrogen, for pre-hydrided materials.

The presented work was performed at CEA in the framework of the “GAINES” project of the French Nuclear Institute I3P between CEA, Framatome and EDF.

Reference:

[1] JC. BRACHET, V. MAILLOT, L. PORTIER, D. GILBON, A. LESBROS, N. WAECKEL, J.-P. MARDON, “*Hydrogen Content, Pre Oxidation and Cooling Scenario Influences on Post-Quench Mechanical Properties of Zy-4 and M5TM Alloys in LOCA Conditions - Relationship with the Post-Quench Microstructure*”, ASTM 15th International Symposium on Zirconium in the Nuclear Industry, June 24- 28, 2007, Sunriver, Oregon, USA, Journal of ASTM International, Vol. 5, No. 4, Paper ID JAI101116, (2008)

Refined relationship between through wall clad oxygen diffusion profiles and post-quenching impact properties of as-received and pre-hydrided Zircaloy-4, following High-Temperature steam oxidation

JC. Brachet et al., ***CEA, Paris-Saclay Univ.***, *DES-ISAS/DMN/SRMA, France*
(jean-christophe.brachet@cea.fr)

26th International QUENCH Workshop
(virtual event), December 6-10, 2021

Associated references:

- *JC. Brachet et al., « Mechanical behavior at Room Temperature and Metallurgical study of Low-Tin Zy-4 and M5™ (Zr-NbO) alloys after oxidation at 1100°C and quenching”,, Proceedings of the Technical Committee Meeting on Fuel Behaviour Under Transient and LOCA Conditions,, Halden, Norway, (Sept 10–14,* ***2001****),* ***IAEA-TECDOC****,* ***1320****, pp. 139–158*
- *JP. Mardon et al., “Influence of hydrogen simulating burn-up effects on the metallurgical and thermal-mechanical behaviour of M5™ and Zircaloy-4 alloys under LOCA conditions”, 13th International Conference on Nuclear Engineering Beijing, China, May 16-20,* ***(2005)****,* ***ICONE13****-50457*
- *JC. Brachet et al., “Hydrogen Content, Pre Oxidation and Cooling Scenario Influences on Post-Quench Mechanical Properties of Zircaloy-4 and M5™ Alloys in LOCA Conditions - Relationship with the Post-Quench Microstructure”, ASTM 15th International Symposium on Zirconium in the Nuclear Industry, June 24-28, 2007, Sunriver, Oregon, USA,* ***Journal of ASTM International,*** *Vol. 5, No. 4, Paper ID JAI101116,* ***(2008)***

Overall objectives:

- To assess the residual Post-Quenching (PQ) mechanical properties (*strength, ductility, toughness…*) of Zr-based nuclear fuels claddings following High Temperature (HT) incursion in steam and a final water quenching – typical of some hypothetical accidental conditions (LOCA…)

- To take into account some potential « burn-up » effects (*i.e., hydriding due to in-service corrosion*)

***Several PQ mechanical testing methodologies*:**
- **Ring Compression Tests (RCT);**
- **3 or 4-Points Bending Tests (3-PBT or 4-PBT);**
- ***Axial or Ring Tensile Tests…***
- **<u>Impact Tests (*at Room Temperature, RT*)</u>**

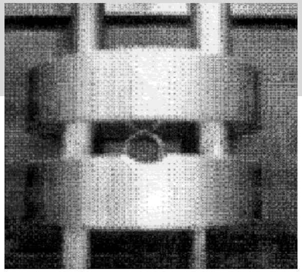

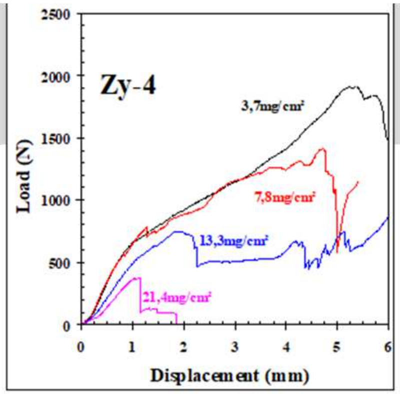

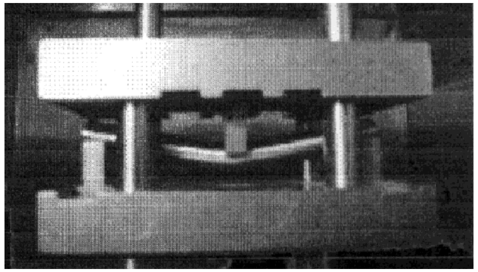

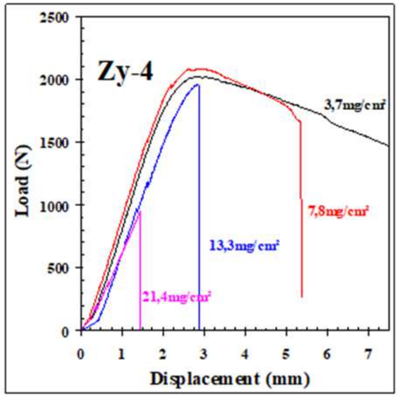

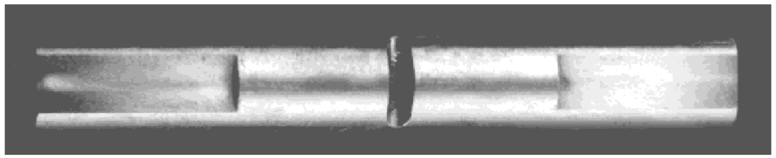

55 mm. length

(Pre-notch : radius=1mm, depth = 8mm.)

Impact pre-notched sample

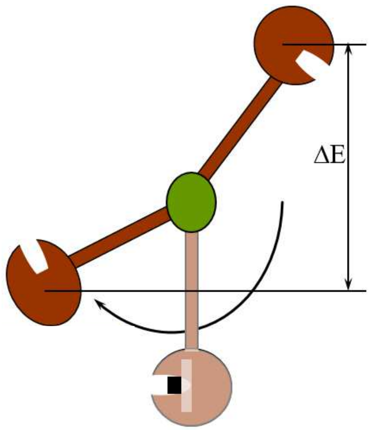

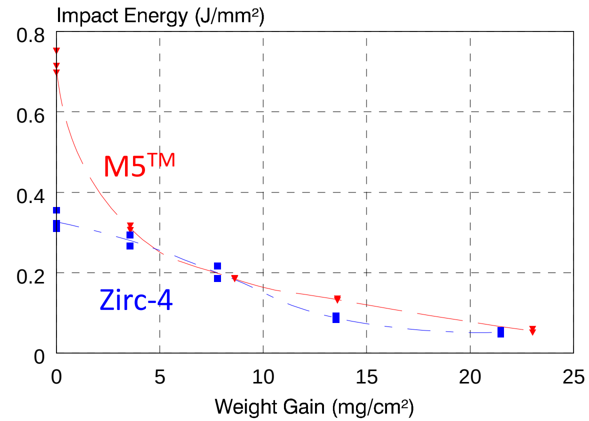

Correlation between PQ Mechanical properties vs. PQ clad µstructure + oxygen/hydrogen diffusion/partitioning, derived from previous studies carried out at CEA (1/4)

Compared to most usual PQ mechanical tests: RCT and/or 3 or 4P-BT carried out at 135°C, impact testing at RT after direct quenching from the HT β_{Zr} temperature range (>1000°C) should be viewed as:

- **a more demanding test,**
- **bringing additional informations on the residual toughness of oxidized cladding and the propagation mode of the crack**

⇒ **As recalled here-after, a quite simple correlation has been derived between PQ impact properties and microstructural-microchemical state of the HT oxidized and quenched claddings**

⇒ ***not so easy for RCT and 3-4P-BT due to heterogeneous stress/strain fields evolution inside the tested samples upon the mechanical testing*:**

FE calculations and experimental imaging + DIC of PQ RCT:

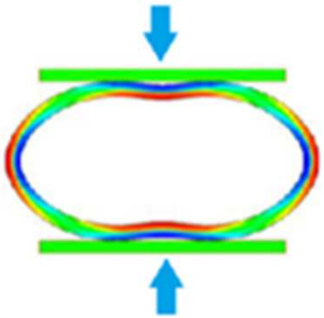

D. Leboulch et al., CEA

A. Charbal, G. Nony et al., CEA

Correlation between PQ Mechanical properties vs. PQ clad µstructure + oxygen/hydrogen diffusion/partitioning, derived from previous studies carried out at CEA (2/4)

Schematic of a LB-LOCA transient and of the associated microstructural -microchemical clad evolution

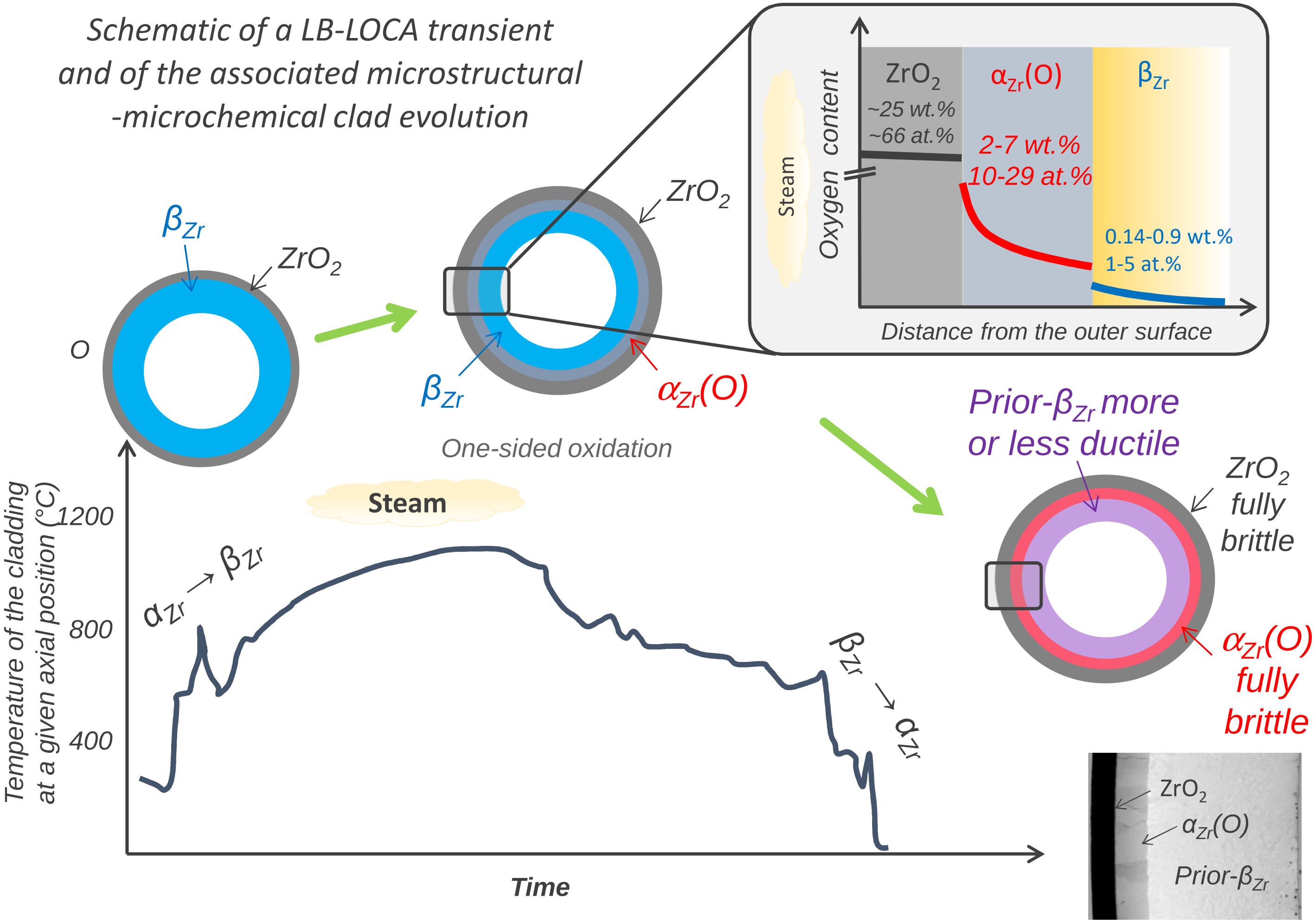

Optical Micrograph

⇒ « Critical » (water quenched) prior-β oxygen content value inducing Ductile-to-Brittle transition **at RT**:

$[O]_{prior-\beta}$ ~0.4-0.5wt.%

Remark: at 135°C, critical O content is slightly higher

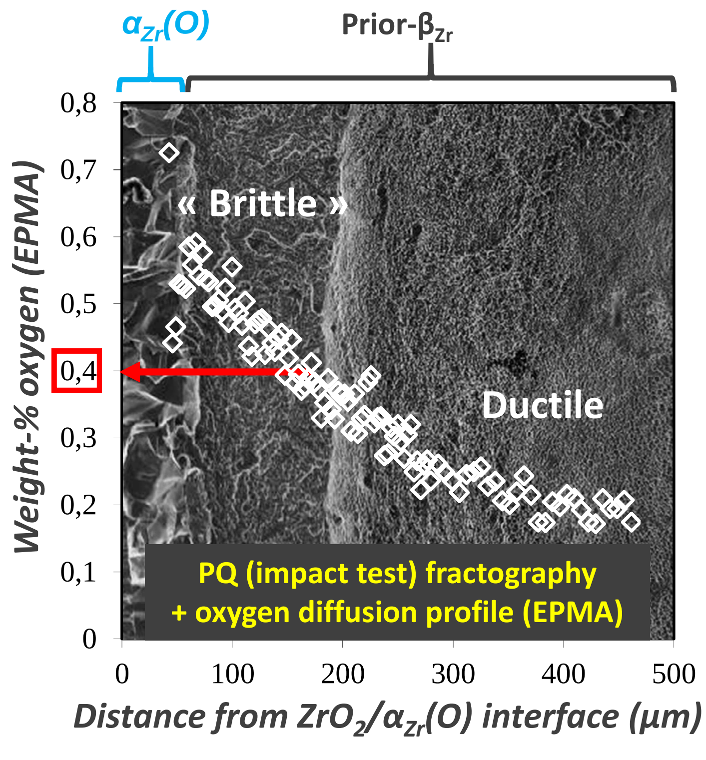

Study of pre-hydrided materials to simulate « Burn-Up » effects:

(1) « Intrinsic » hydrogen PQ embrittling effect
highlited by flash oxidation test (50s) at 1000°C followed by direct water quenching => ***ECR < 1%***

=> Impact Energy decrease vs. [H] content increase

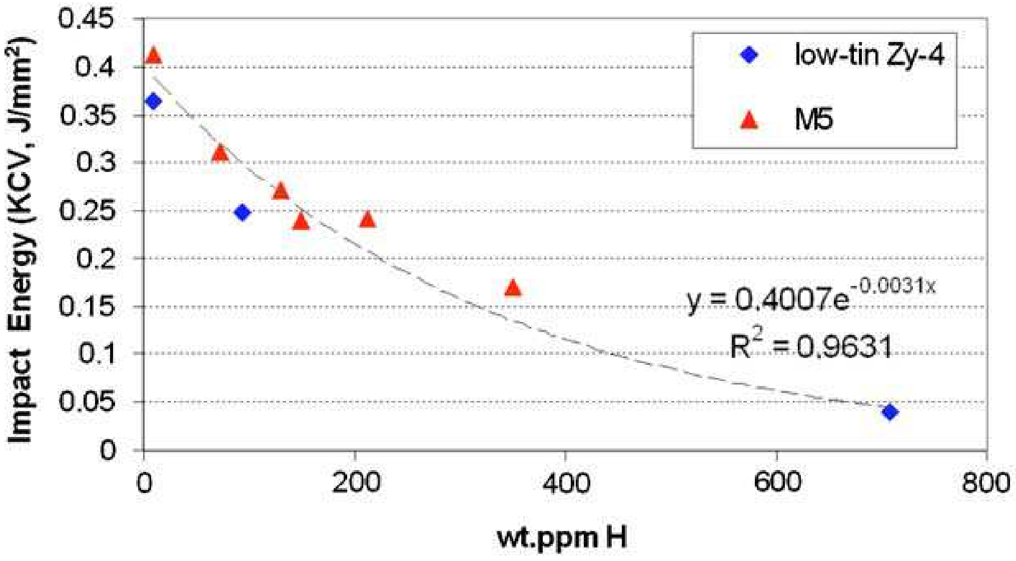

Journal of ASTM International (2008)

(2) « Indirect » hydrogen PQ embrittling effect
by increase of oxygen solubility within the β_{Zr} phase at HT (thus, increasing the overall oxygen quantity diffusing into residual prior-β_{Zr} layer)

As-received and prehydrided Zircaloy-4 ***one-sided oxidized for 180s at 1200°C:***

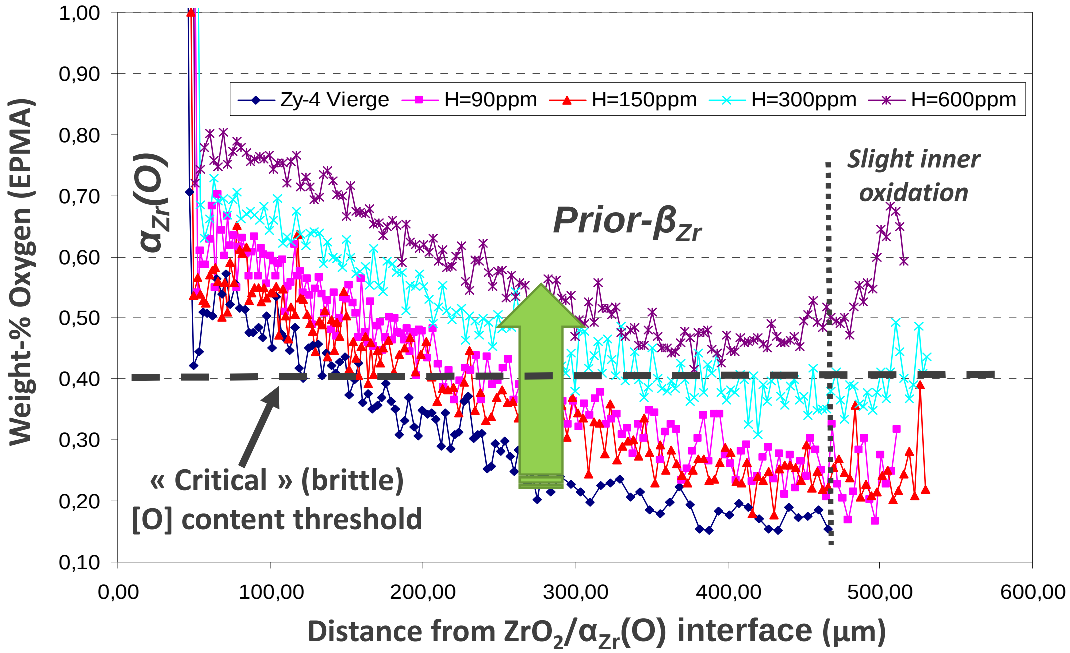

Correlation between PQ Mechanical properties vs. PQ clad µstructure + oxygen/hydrogen diffusion/partitioning, derived from previous studies carried out at CEA (4/4)

Based on previous results,
it was possible to **derive a preliminary relationship between**:

- Residual **prior-β_{Zr} layer thickness**;
- **Averaged prior-β_{Zr} oxygen and hydrogen(*)** respective **contents** *(assuming « additive » contributions of both O and H respective influences);*

and

the measured PQ **impact energy values**

Journal of ASTM International (2008)

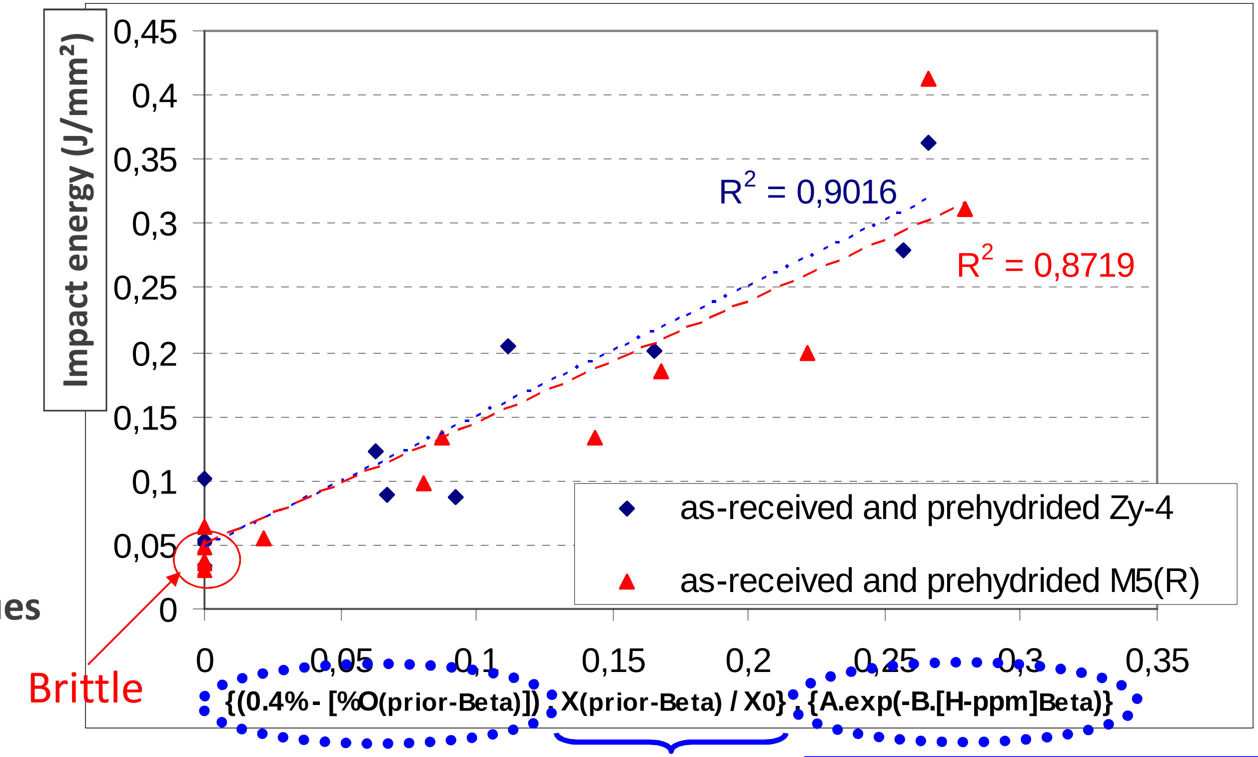

Effect of oxygen content assuming:
- a linear dependency of the PQ impact energy vs. prior-β_{Zr} O content
- [O] = 0.4 wt.% as a brittle threshold value

Prior-β_{Zr} relative thickness

Intrinsic H effect assuming an exponential relationship betweeen PQ impact energy and the actual(*) prior-β_{Zr} hydrogen content (*see left fig. of previous slide*)

(*) assuming that all the available hydrogen is concentrated within the residual prior-βZr layer (as highlighted by PQ µ-ERDA and/or µ-LIBS hydrogen quantitative mappings already done, (C. Raepsaet et al. - Nucl. Instr. & Meth. in Phys. Res. (2008), JC. Brachet et al. - JNM (2017)...)

Refinement of the correlation between through wall clad oxygen diffusion profiles and post-quenching impact properties of as-received and pre-hydrided Zircaloy-4 (1/5)

The « idea »: to **take benefit of the oxygen diffusion profiles measured by EPMA** on HT steam oxidized and quenched Zircaloy-4 clad samples (*pre-hydrided or not*), assuming that: the **residual prior-βZr layer can be considered as a multilayered structure, each sublayer having is own « toughness » (*i.e., impact energy*), depending on the local oxygen and hydrogen respective contents**

⇒ *Systematic comparison between prediction of the local failure mode and PQ fractograph examinations…*

Database used to assess the {PQ impact Energy vs. microstructural/microchemical parameters} correlation refinement:

- Materials: as-received and prehydrided low-tin Zircaloy-4 (H content ranging from <10 wt.ppm up to ~600 wt.ppm)
- One-sided steam oxidation at 1000, 1100°C and 1200°C + direct water quenching down to RT
- ECR_{BJ} ranging from ~5% up to ~27%
- Systematic PQ impact testing, fractography, accurate phase thicknesses measurements from OM and SEM, and EPMA

=> *see some illustrations on next slides*

Refinement of the correlation between through wall clad oxygen diffusion profiles and post-quenching impact properties of as-received and pre-hydrided Zircaloy-4 (2/5)

Typical through wall clad oxygen profiles measured by EPMA after one-sided steam oxidation at 1200°C:

=> Typical Oxygen absolute content measurement accuracy ~ 0.1 wt.% (as-received Zircaloy-4 oxygen content ~ 0,13 wt.%)

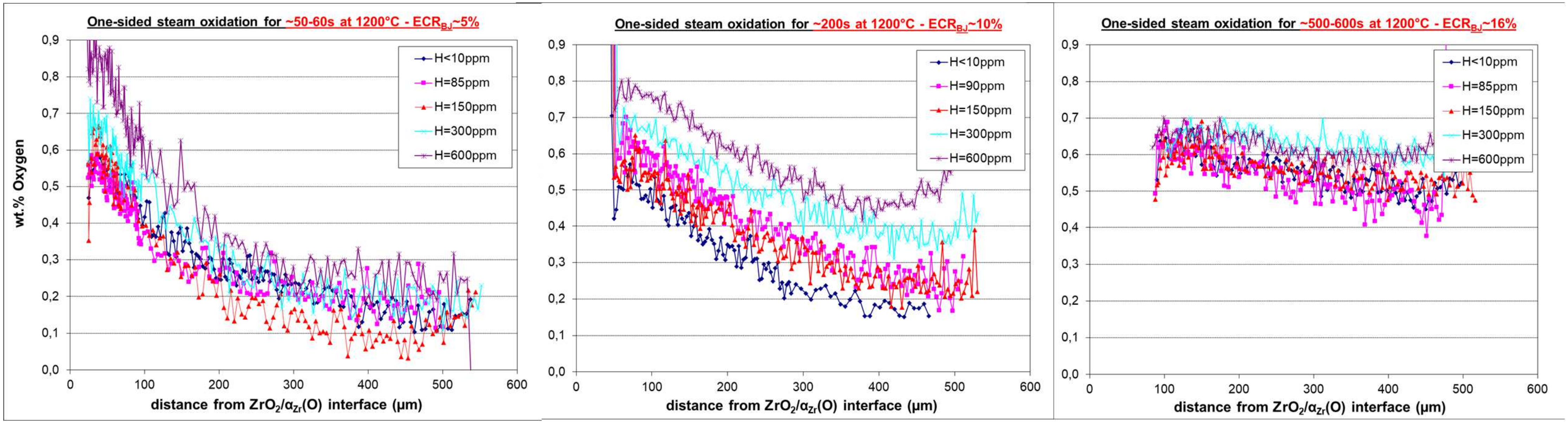

Refinement of the correlation between through wall clad oxygen diffusion profiles and post-quenching impact properties of as-received and pre-hydrided Zircaloy-4 (3/5)

Typical fractographs of PQ impact tested samples after one-sided steam oxidation at 1200°C for ~1 min:

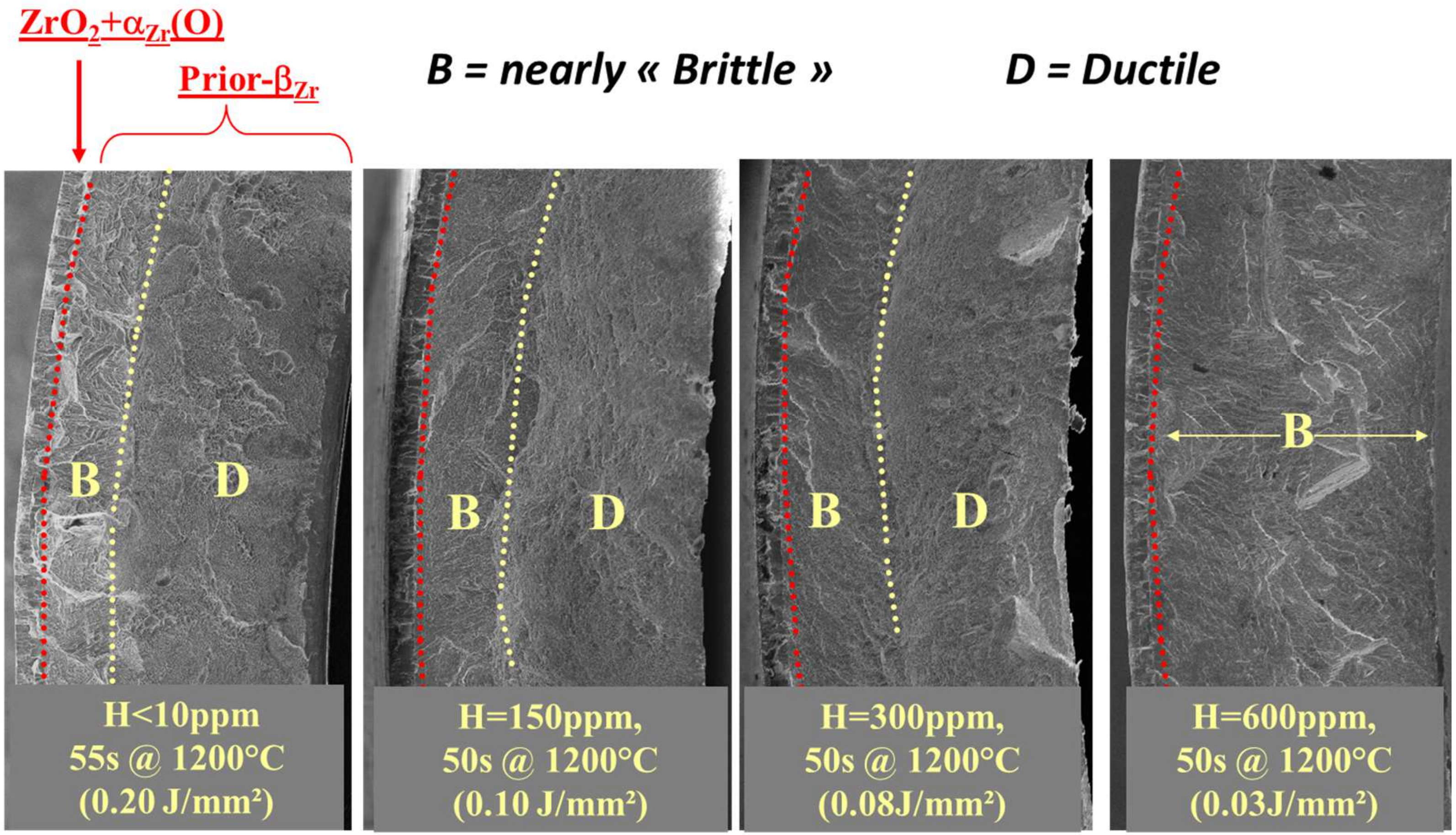

Refinement of the correlation between through wall clad oxygen diffusion profiles and post-quenching impact properties of as-received and pre-hydrided Zircaloy-4 (4/5)

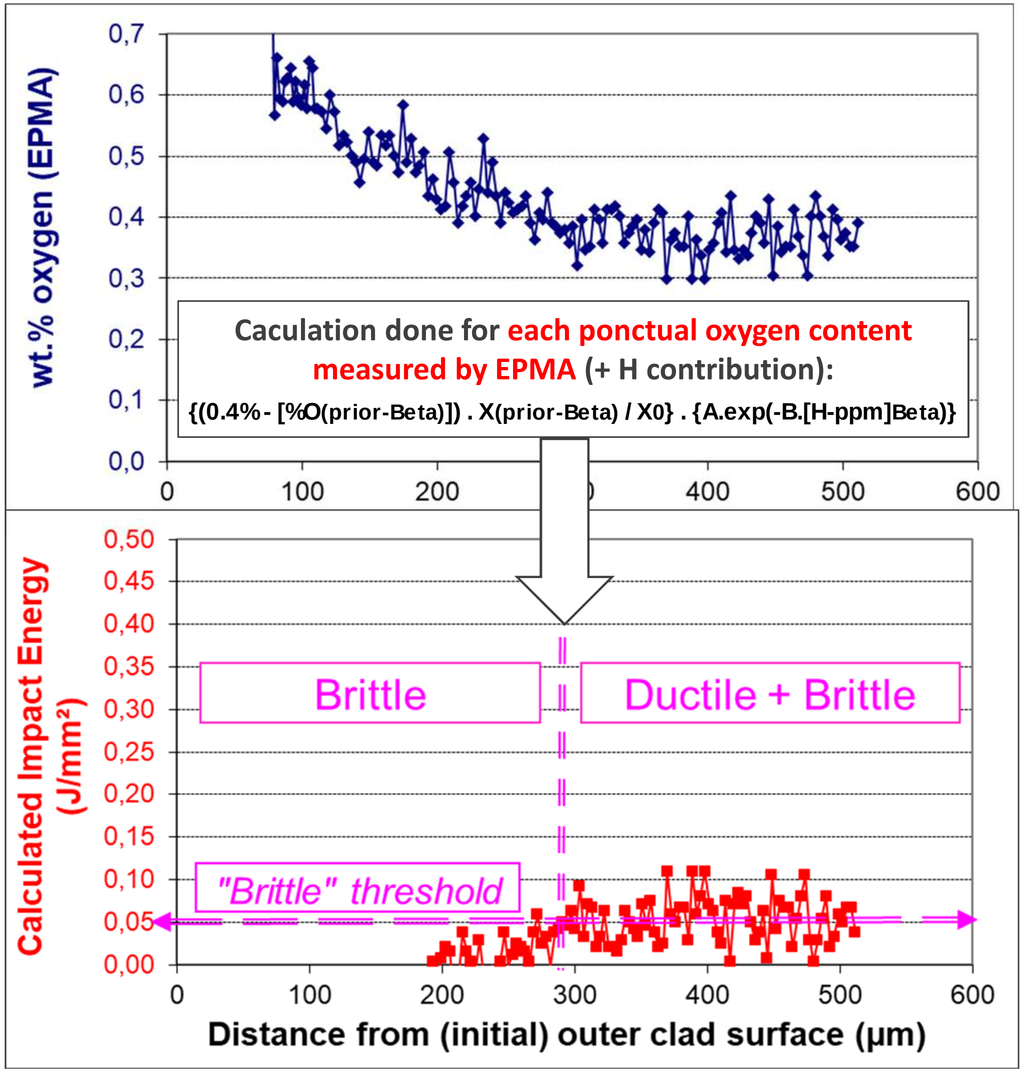

Ex.: Comparison betweeen <u>calculated</u> « local » impact energy from EPMA through wall clad oxygen profile and fractograph of a PQ impact tested sample

(*Zirc-4 + [H] ~100 wt.ppm, one-sided oxidized at 1100°C for ~500s*)

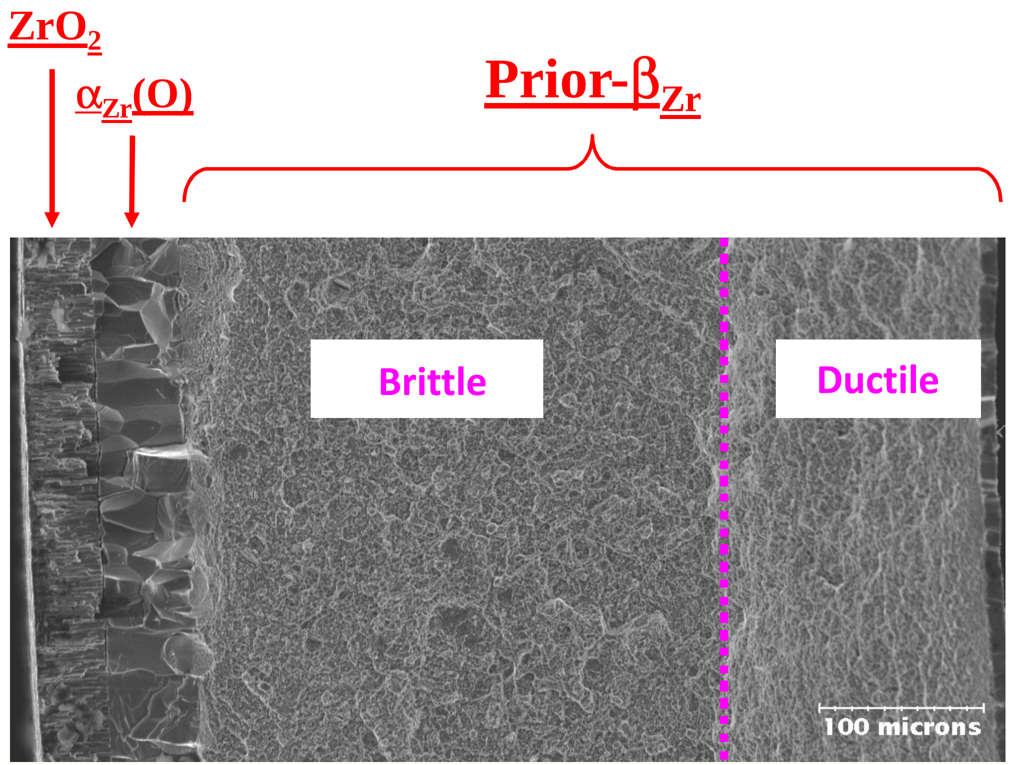

Refinement of the correlation between through wall clad oxygen diffusion profiles and post-quenching impact properties of as-received and pre-hydrided Zircaloy-4 (5/5)

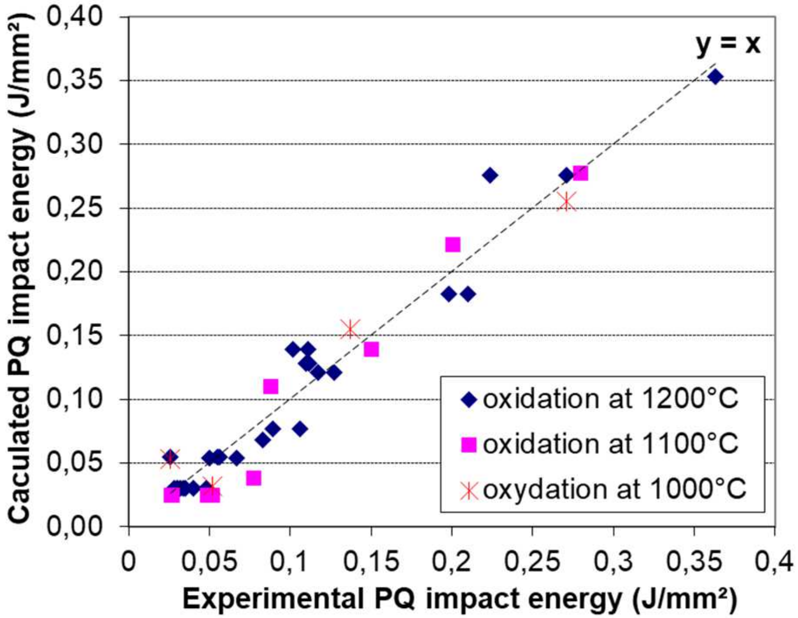

As-received + prehydrided low-tin Zircaloy-4 one-sided steam oxidized at 1000, 1100 and 1200°C + direct water quenching down to RT *(>30 samples PQ tested and analyzed)*	Overall prior-β_{Zr} failure mode from fractographic examinations (*PQ impact tests carried out at RT*)	Fraction of samples for which their failure mode is correctly predicted using the « refined correlation »
	100% DUCTILE	100%
	DUCTILE+BRITTLE	77%
	100% BRITTLE	64%
	Overall	**81%**

CONCLUSION: For Zr-based claddings that have experienced HT incursion in steam environment and quenching – *typical of hypothetical accidental transients such as LOCA* - the proposed (refined) correlation between through wall clad oxygen diffusion profiles and post-quenching impact properties (*taking into account the additional effect of hydrogen*) improves the prediction of post-quenching nuclear fuel claddings failure mode and associated impact energy.

It enables to capture the Ductile-to-Brittle failure mode transition that may occurs inside the residual prior-β_{Zr} layer (*not possible with the previous correlation based on « averaged » oxygen (& hydrogen) prior-β$_{Zr}$ contents…*).

On-going and further work

- **Extend the approach to other PQ mechanical tests using FE calculation (*RCT, 3 or 4P-BT, Tensile tests…*) and make the link with oxidation/diffusion numerical tools *(CEA – « Ekinox-Zr »…)* able to modelize/simulate the oxygen diffusion profiles upon HT oxidation (*taking into account also the H influence…*)**

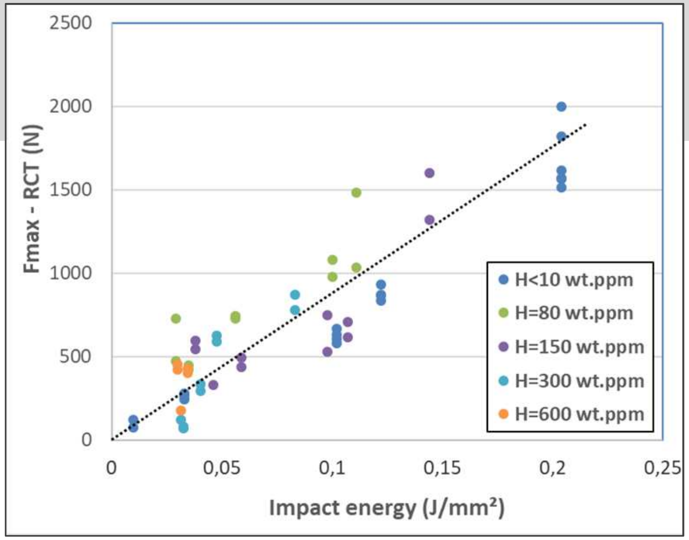

- **Extend the approach to Cr-coated (E-ATF) claddings:**

Prior-β$_{Zr}$ fractographs:

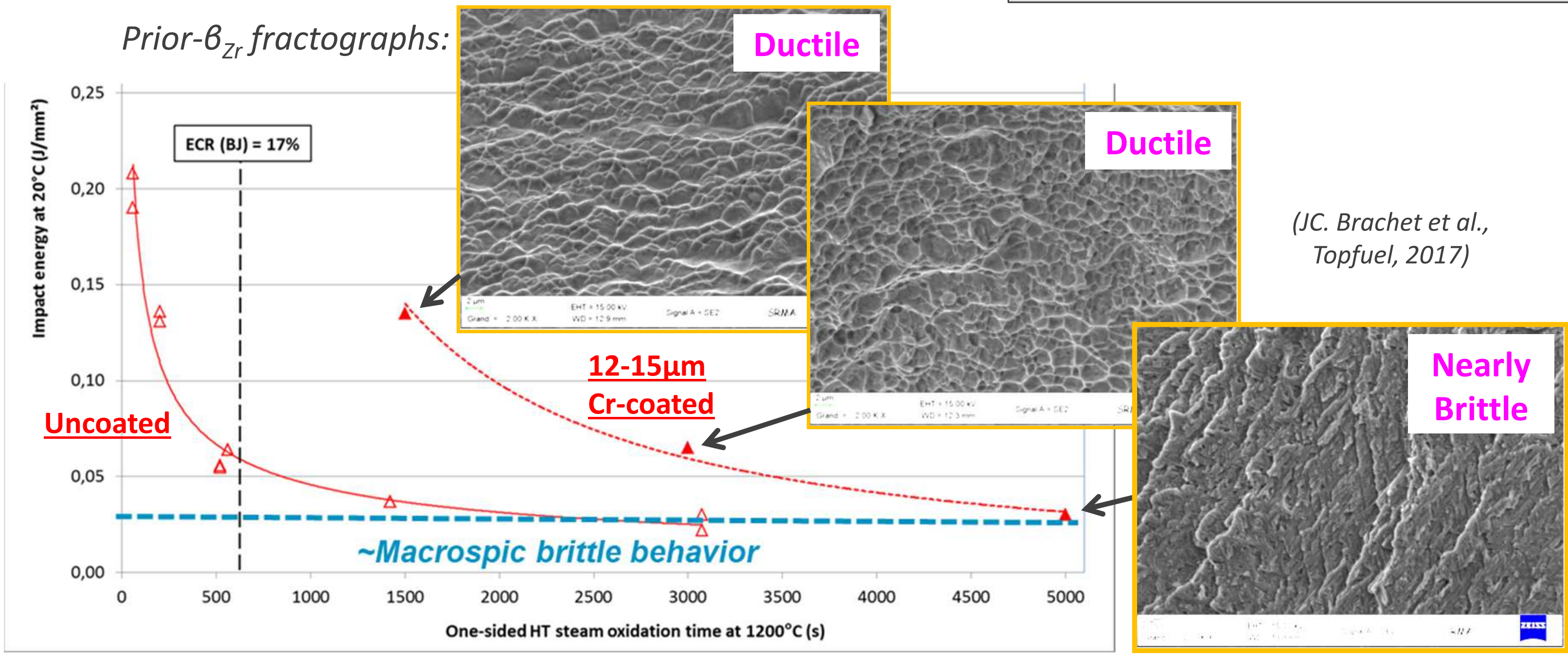

(JC. Brachet et al., Topfuel, 2017)

Thank you for your attention

Special thanks at CEA to:

- Didier Hamon, Thomas Guilbert and Thierry Vandenberghe for EPMA measurements;
- Annick Bougault, Stéphane Urvoy, Véronique Rabeau and Elodie Rouesne for OM and SEM / fractographic examinations;
- Roger Maury, Guillaume Nony, Marie Dumerval, Ali Charbal, Matthieu Le Saux and Valérie Vandenberghe for organizing & conducting HT oxidation and PQ mechanical tests;
- Caroline Toffolon-Masclet and Laure Martinelli for Thermodynamic and kinetics tools developements and calculations;
- Jean Henry, Jean-Luc Béchade, Laurence Portier, Philippe Bossis, Didier Gilbon and Thierry Forgeron for their encouragments and organizing support;
- And many others…

Work funded by the
CEA-Framatome-EDF
French Nuclear Institute

B.S. Jäckel[1], T.M. Lind[1], J.C. Birchley[1],
M. Steinbrück[2], S. Park[3]

[1]Paul Scherrer Institut, Switzerland
[2]Karlsruhe Institute of Technology, Germany
[3]Nuclear Energy Team, Lee & Ko, Rep. Korea

PSI-KIT Nitriding Model for Zirconium based Fuel Cladding Alloys

The QUENCH-16 and -18 experiments performed at KIT in Karlsruhe, Germany, with air oxidation under starvation of oxidant showed extensive formation of zirconium nitride followed by strongly enhanced hydrogen production during the quenching process with water. Separate-effect tests with air oxidation under oxygen starvation conditions also showed presence of zirconium nitride in the post-test examination. The Sandia Fuel experiments showed strong nitrogen uptake during the oxygen starvation stage of the experiments and nitrogen release during re-oxidation of the nitride zirconium later on. Not all those behaviours could be calculated with severe accident codes, because models for the nitrogen/nitride reactions were limited, e.g. ATHLET, or unavailable, e.g. MELCOR and SCDAP. PSI, Switzerland, and KIT, Germany, launched a project for the development of a computer model to describe the nitrogen as direct reaction partner in the oxidation of zirconium based cladding materials. The project comprises two steps.

The first step was to conduct separate-effect tests in the frame of a PhD thesis to produce a database for the kinetics of oxidation and nitriding reactions and for the oxidation of nitride. The second step was to construct and assess a computer model for the reactions, incorporate the kinetic parameters derived from the database, for inclusion in severe accident codes. The second step is in progress at this time.

This presentation describes the different model phases and its implementation in the severe accident code MELCOR. Beneath the standard oxidation correlations for metallic zirconium, the production of oxygen stabilized alpha zirconium (α-Zr(O)) by diffusion of oxygen from the oxide layer to the metal is included. The nitriding of α-Zr(O) and zirconium metal is included and the oxidation of α-Zr(O) and ZrN as well. Instead of one oxidation process, the new model includes five different chemical processes for the interaction of the atmosphere with zirconium based cladding materials. Due to the slower nitriding process compared with oxidation, the new model is most important when the temperature increases slowly, e.g. accidents where the nuclear heating is low enough that the escalation is largely driven by the chemical reactions. Those types of scenarios are most typical following an accident in spent fuel pools or wet storage pools, where the environment will include any or all of steam, oxygen and nitrogen. An accident in a spent fuel pool following total loss of coolant can lead to high temperatures and severe degradation of the fuel, opening ready pathways for major releases of volatile fission products. Moreover, reactions between oxygen and exposed overheated fuel can render some fission products in a more volatile state. The Sandia fuel experiments showed that once all the coolant is lost, the highly energetic zirconium-oxidation reaction and following sustained nitriding, can bring about such an escalation within half a day.

PAUL SCHERRER INSTITUT

B.S. Jäckel, T.M. Lind, J.C. Birchley, M. Steinbrück[1], S. Park[2] :: Paul Scherrer Institute

PSI-KIT Nitriding Model

26th QUENCH Workshop, December 6-10, 2021

[1] Karlsruhe Institute of Technology (KIT)
[2] Nuclear Energy Team, Lee & Ko, Seoul 04532, Korea

Laboratory for
Reactor Physics and Thermal-Hydraulics

Content

1. Motivation
2. Model
3. Implementation in MELCOR 1.8.6 (3084)
4. Summary

Motivation

- **QUENCH experiments with air oxidation under partial oxygen starvation conditions showed high hydrogen production and nitrogen release during the quench phase.**
- **Spent fuel pool experiments at Sandia showed nitrogen release in the late phase of the SFP experiments Phase I and Phase II.**
- **Seperate effect tests under oxygen starvation and presence of nitrogen showed ZrN presence in the post test examination.**
- **Non of the severe accident codes could calculate this behaviour.**
- **→ Nitrogen has to be used as direct reaction partner in the zirconium oxidation model**

Content

1. Motivation
2. Model
3. Implementation in MELCOR 1.8.6 (3084)
4. Summary

Model

New Materials:

- Oxygen stabilized alpha zirconium (α-Zr(O))
- Zirconium nitride (ZrN)

New Reactions:

- Diffusion of oxygen from ZrO_2 to Zr metal
- Nitriding of α-Zr(O) (fast nitriding), (no oxygen release)
- Nitriding of Zr metal (slow nitriding)
- Oxidation of α-Zr(O)
- Oxidation of ZrN (re-oxidation)

Model

Diffusion occurs when:

Zirconium oxide is in direct contact to zirconium metal

Diffusion is inhibited when:

Oxidation is running into break-away conditions (<1323K)
(Monoclinic oxide structure)

ZrN layer is produced between oxide and metal (>1323K)
(Tetragonal oxide structure)

Model

Fast nitriding occurs when:

α-Zr(O) is in direct contact to nitrogen in the atmosphere (break-away of oxide layer below 1323K)

Temperature of oxide layer is above 1323K (tetragonal structure)

1373 K, 1 h NT

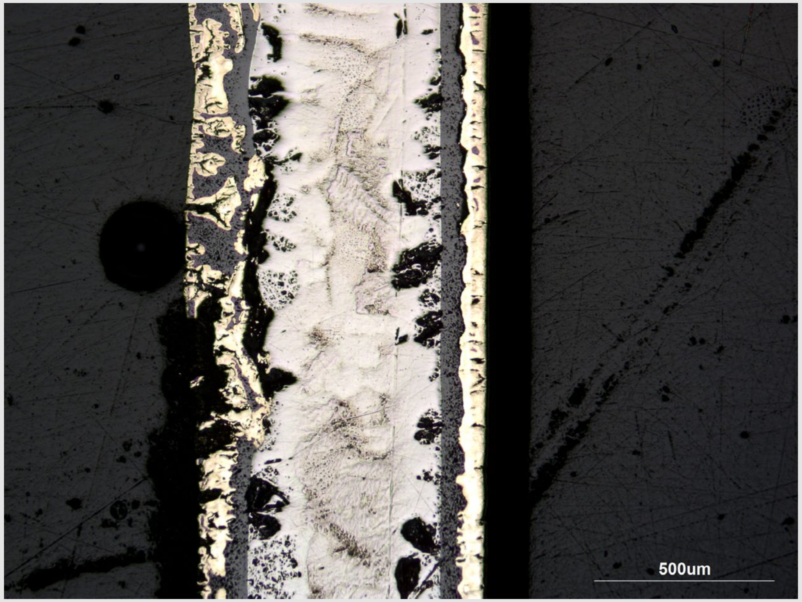

1273 K, 15 h NT, no break-away

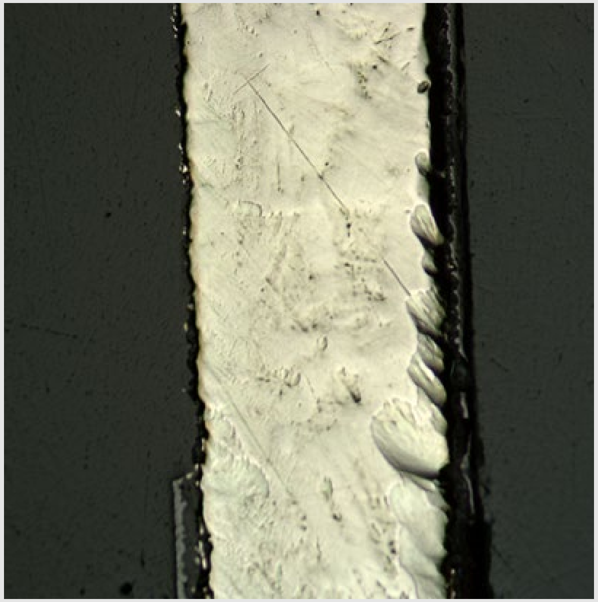

Model

Slow nitriding occurs when:

α-Zr(O) is not longer available

Nitrogen can directly contact zirconium metal

Oxidation of ZrN occurs when:

ZrN is available

Oxidation of α-Zr(O) occurs when:

ZrN is not present

Zirconium metal is not available

Content

1. Motivation
2. Model
3. Implementation in MELCOR 1.8.6 (3084)
4. Summary

Diffusion model

The weight gain of the alpha layer is based on the alpha layer thickness growth by Cathcart/Pawel – Prater/Courtright. It is not explicitly depending on the oxide layer thickness.

$WG_{Rate}(Temp) = 278.8 * \exp(-24227/Temp)$	Temp < 2073 K	Cathcart/Pawel
$WG_{Rate}(Temp) = 0.09422 * \exp(-10252/Temp)$	Temp > 2173 K	Prater/Courtright

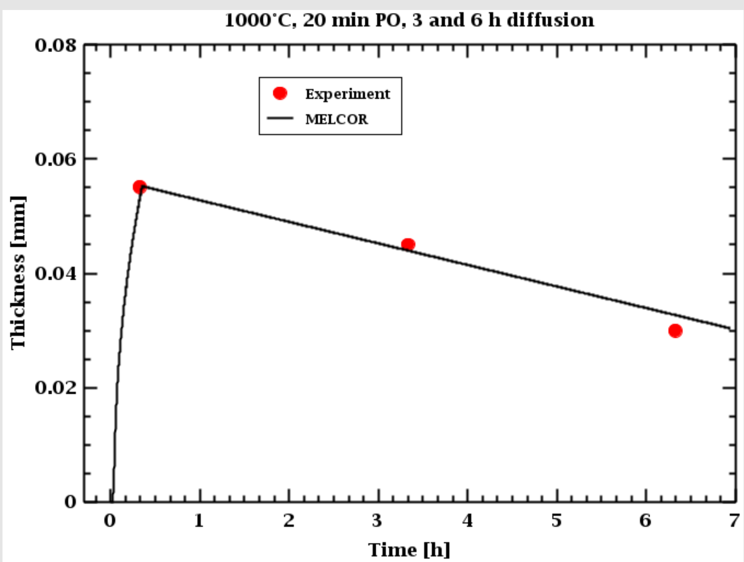

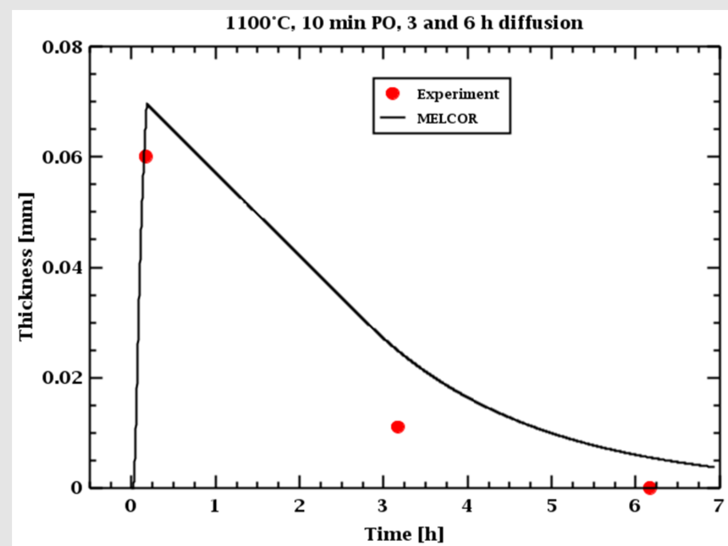

Nitriding

The weight gain of the fast nitriding reaction is based on separate effect tests performed at KIT.

It is only depending on the temperature (linear kinetic).

$$WG_{Rate}(Temp) = 213.88*exp(-22087.0/Temp)$$

The weight gain of the slow nitriding reaction is based on separate effect tests performed at KIT.

It is only depending on the temperature (linear kinetic).

$$WG_{Rate}(Temp) = 110.0*exp(-25000.0/Temp)$$

Oxidation

The weight gain of the oxidation of α-Zr(O) and the weight gain of zirconium metal oxidation are identical in the MELCOR model.

The weight gain of the oxidation of zirconium nitride is used as four times the weight gain of Cathcart/Pawel correlation.

In all three weight gain calculations the effective oxide thickness from the PSI air oxidation and break-away model is used to reach linear reaction kinetics after break-away of the oxide crust.

Example

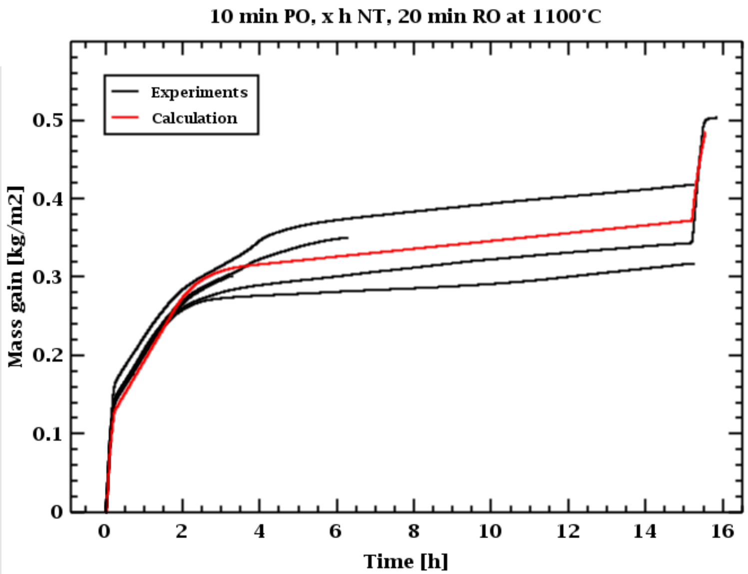

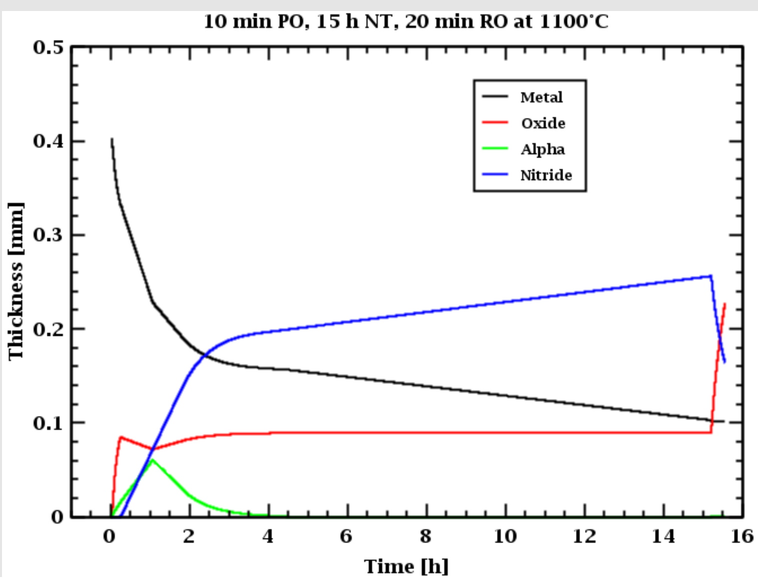

The upper graph shows the measured weight gain data of separate effect tests at 1100°C. After a pre-oxidation of 10 minutes different times for the nitriding reaction were selected. One experiment was conducted with 20 minutes of re-oxidation after 15 hours of nitriding.

The lower graph shows the development of the different layers of metal, oxide, alpha and nitride.

Content

1. Motivation
2. Model
3. Implementation in MELCOR 1.8.6 (3084)
4. Summary

Summary

The implementation of the nitriding model in the MELCOR 1.8.6 (3084) code version shows the ability of the model to recalculate the separate effect tests conducted at KIT, Germany.

The model includes the production of α-Zr(O) and ZrN and its reactions with nitrogen, steam and air (oxygen).

The diffusion of oxygen from the oxide layer to the zirconium metal can be calculated in a credible way.

This model will complete the steam and air-oxidation model implemented in MELCOR and will enable the code to calculate especially the spent fuel pool transients, which until now cannot be done in a credible way.

The implementation in MELCOR will allow the code to recalculate experiments with air under starvation conditions like some of the QUENCH experiments and the experiments of the Sandia Fuel Project, Phase I and Phase II.

Thank you for your attention !

Questions ?

Acknowledgement:
The project was financially supported by the Swiss Federal Nuclear Safety Inspectorate ENSI under contract CTR00321 (2017-2021).

A. Vasiliev

IBRAE

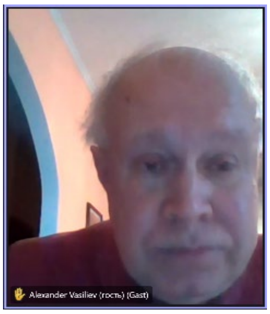

Development of New Model to Calculate High-Temperature Oxidation of ATF Chromium-Coated Zr-Based Cladding

Currently, the comprehension among the specialists and functionaries throughout the world is getting stronger that the nuclear industry can encounter serious difficulties in progress in the case of insufficiently decisive measures to enhance the safety level of nuclear objects and to ensure clean energy and green world. The keen competition with renewable energy sources like wind, solar or geothermal energy takes place presently and is expected to continue in future decades. One of main measures of nuclear safety enhancement could be a drastic renovation of materials used in nuclear industry.

The Zr-based cladding with protective chromium coating representing more evolutional way in nuclear energy progress is one of perspective advanced tolerant fuel (ATF) cladding candidates.

The analytical model of high-temperature oxidation of Zr/Cr cladding is developed based on oxygen diffusion consideration in the cladding. The model necessarily takes into account the initial oxidation of chromium layer with formation of chromium oxide, and, after the loss of its protective properties, the model considers the zirconium oxidation in two- or three-layers configuration.

The several consecutive phases of Zr/Cr high-temperature cladding oxidation are described: a) parabolic oxidation in a system Zr/Cr; b) transition phase; c) loss of chromium protective properties with transition to Zr oxidation.

The comparison of calculated results for Zr/Cr cladding high temperature oxidation with available experimental data is conducted. The reasonable agreement between calculated and experimental data is observed.

Development of New Model to Calculate High-Temperature Oxidation of ATF Chromium-Coated Zr-Based Cladding

Alexander Vasiliev
IBRAE, Moscow

Content

1. Introduction
2. New Analytical Model of Zr/Cr Clad Oxidation
3. Phase I. Oxidation in a System Zr/Cr
4. Phase II. Transition phase
5. Phases III-IV. Loss of Cr protective properties
6. Comparison with Experiments
7. Conclusions

Is Zr/Cr the best choice for ATF-cladding? Arguments for and against.

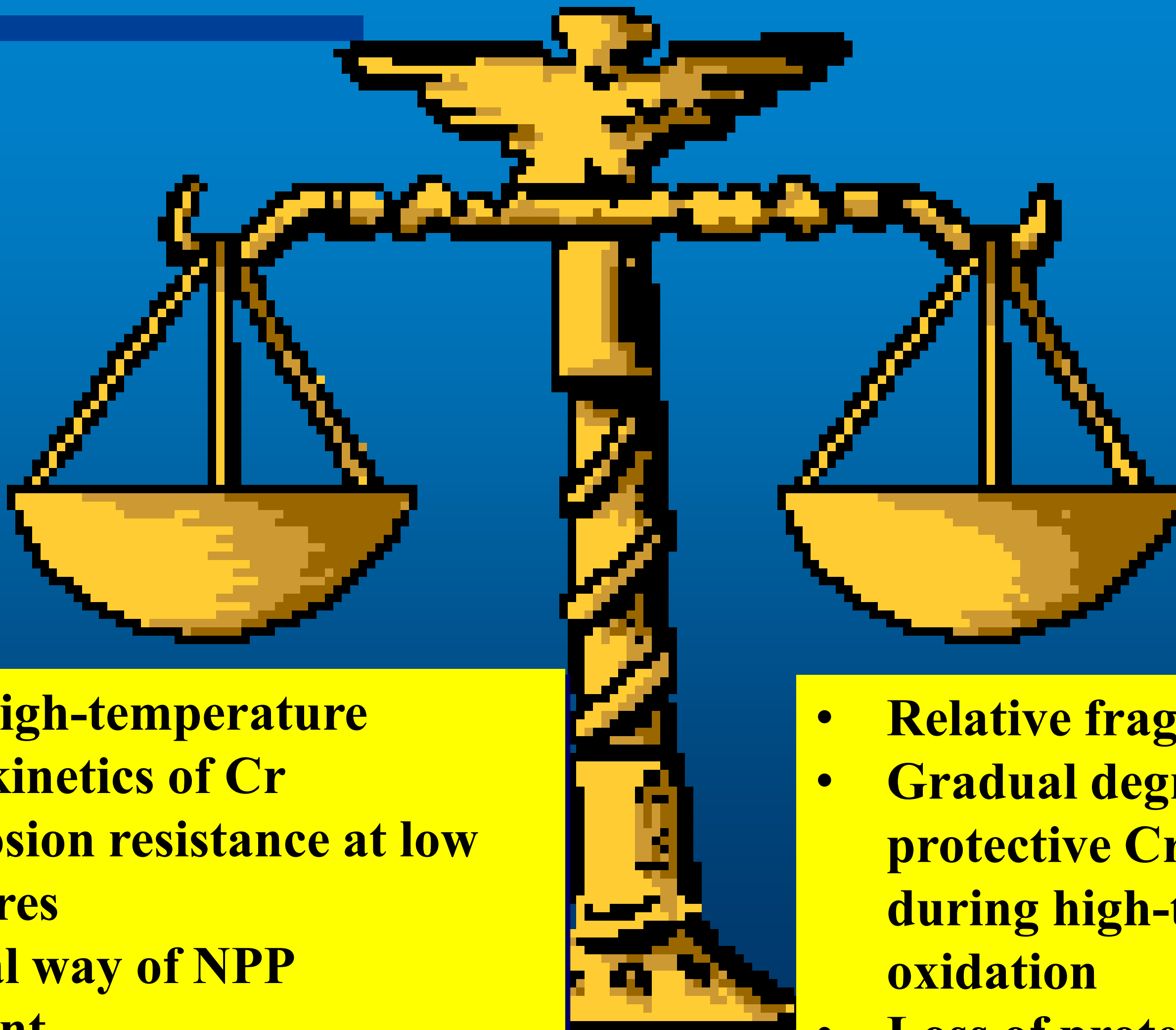

- Very low high-temperature oxidation kinetics of Cr
- High corrosion resistance at low temperatures
- Evolutional way of NPP development

- Relative fragility of Cr
- Gradual degradation of protective Cr_2O_3 layer during high-temperature oxidation
- Loss of protective properties

Short Review of Zr/Cr Oxidation

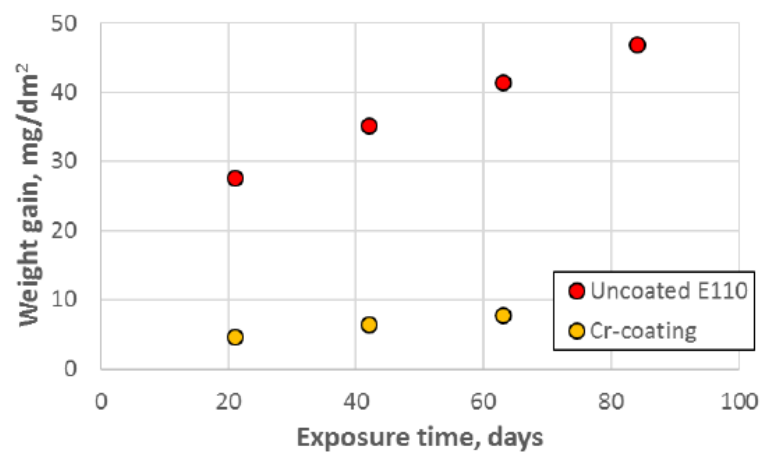

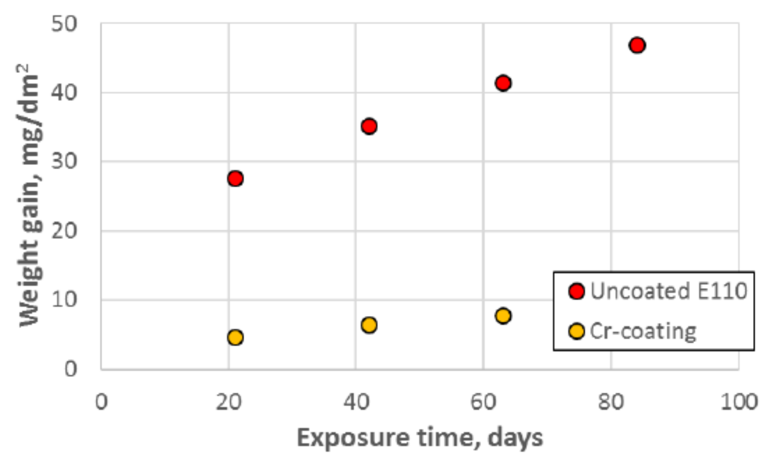

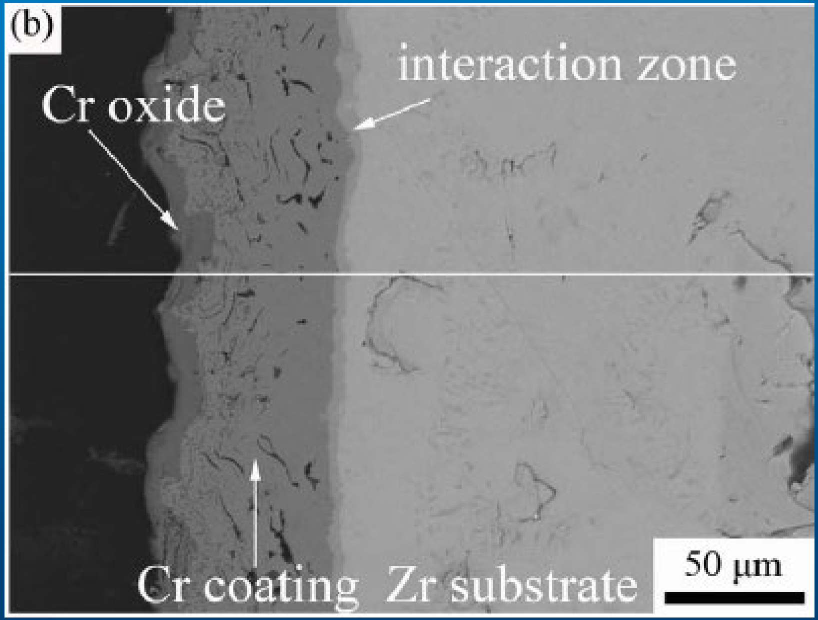

Krejci J., Sevecek M., Cvrcek L. et.al. Chromium and Chromium Nitride Coated Cladding for Nuclear Reactor Fuel. Proc. of QUENCH-23), Karlsruhe, Germany, October 17-19, 2017.

Wang Y., Zhou W., Wen Q. et. al. Behavior of Plasma Sprayed Cr Coatings and FeCrAl Coatings on Zr Fuel Cladding under Loss-of-Coolant Accident Conditions. Surface & Coatings Technology, 2018, V. 344, P. 141-148.

Cr-O Binary Phase Diagram

Kowalski M. and Spencer P.J. Thermodynamic Reevaluation of the Cr-O, Fe-O and Ni-O Systems: Remodelling of the Liquid, BCC and FCC Phases. Calphad, 1995, V. 19, N 3, pp. 229-243.

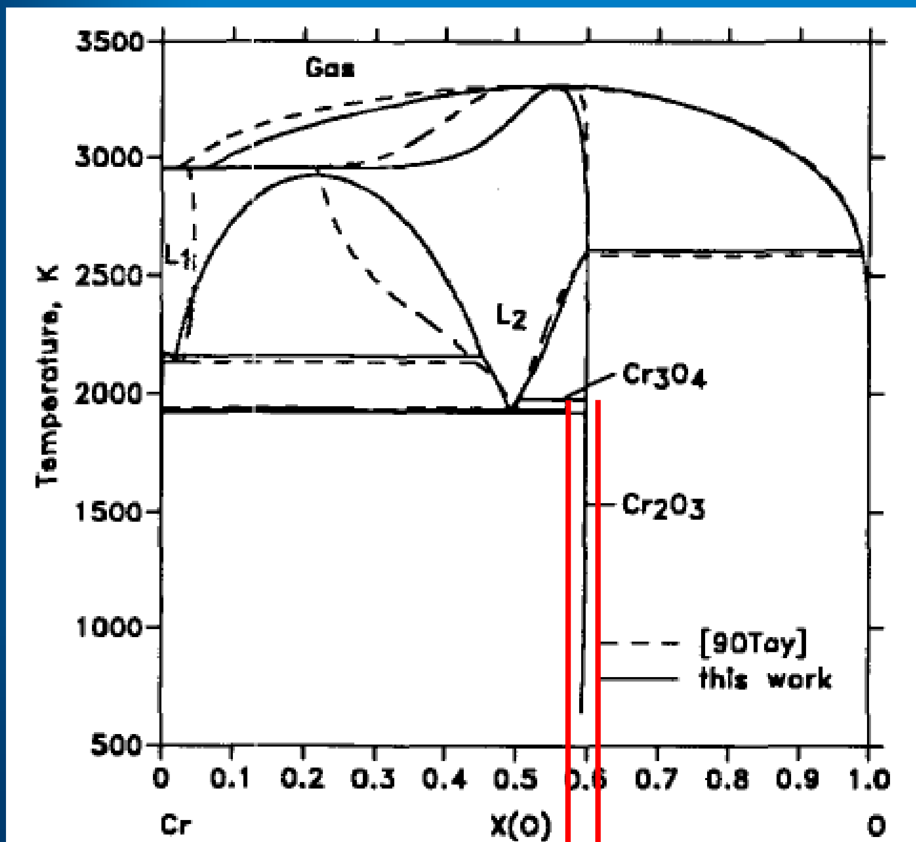

$c_{d/m}$ $c_{d/O}$

Oxygen Solubility in Chromium

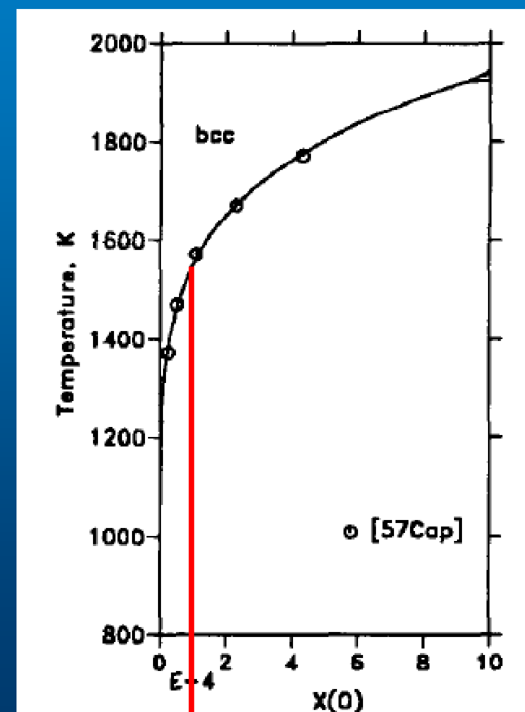

$c_{m/d}$

Interface Oxygen Concentrations

$c_{d/O}$

$c_{d/m}$

$c_{m/d}$

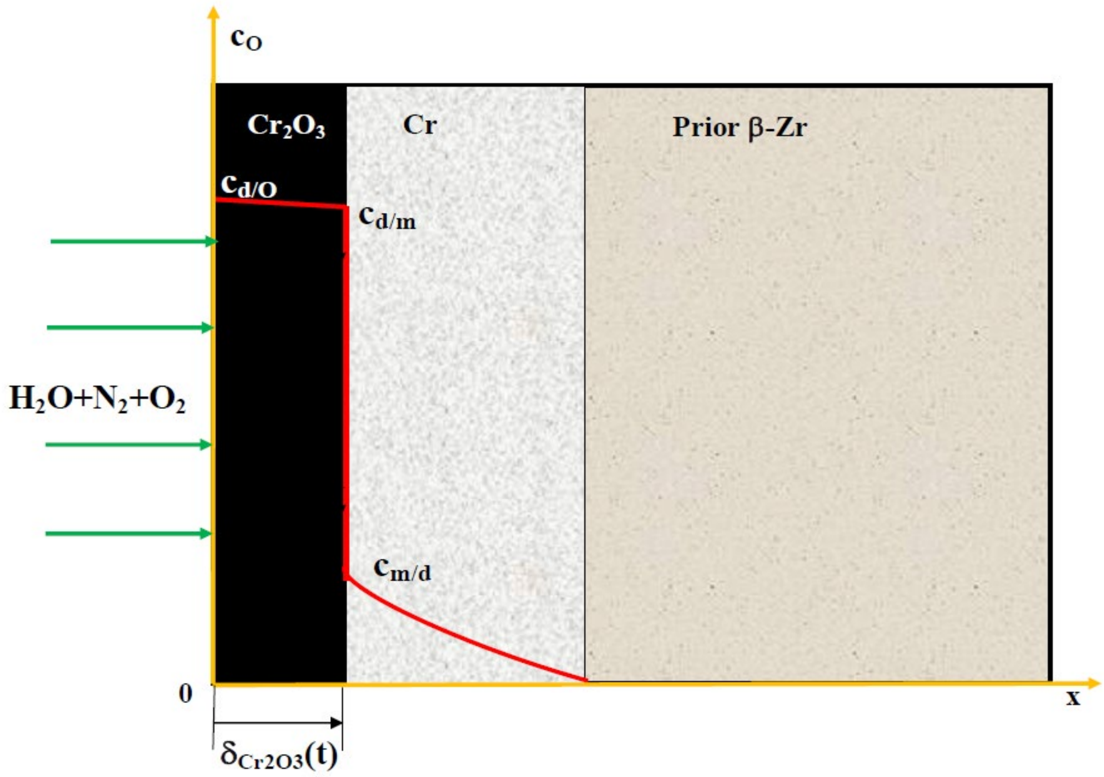

Consecutive Phases in the Course of Oxidation

I – Oxidation in a System Cr_2O_3/Cr

II – Transition phase

III – Enhancement of oxygen diffusion & formation of $\alpha - Zr(O)$ layer

IV – Loss of chromium protective properties & oxidation of zirconium

J.-Ch. Brachet, E. Rouesne, J. Ribis, T. Guilbert, S. Urvoy, G. Nony, C. Toffolon-Masclet, M. Le Saux, N. Chaabane, H. Palancher, A. David, J. Bischoff, J. Augereau, E. Pouillier, “High Temperature Steam Oxidation of Chromium-Coated Zirconium-Based Alloys: Kinetics and Process”, Corrosion Science, 167, 2020, 108537, 15 pp. Online version: https://doi.org/10.1016/j.corsci.2020.108537.

Oxygen concentration profile during phase I

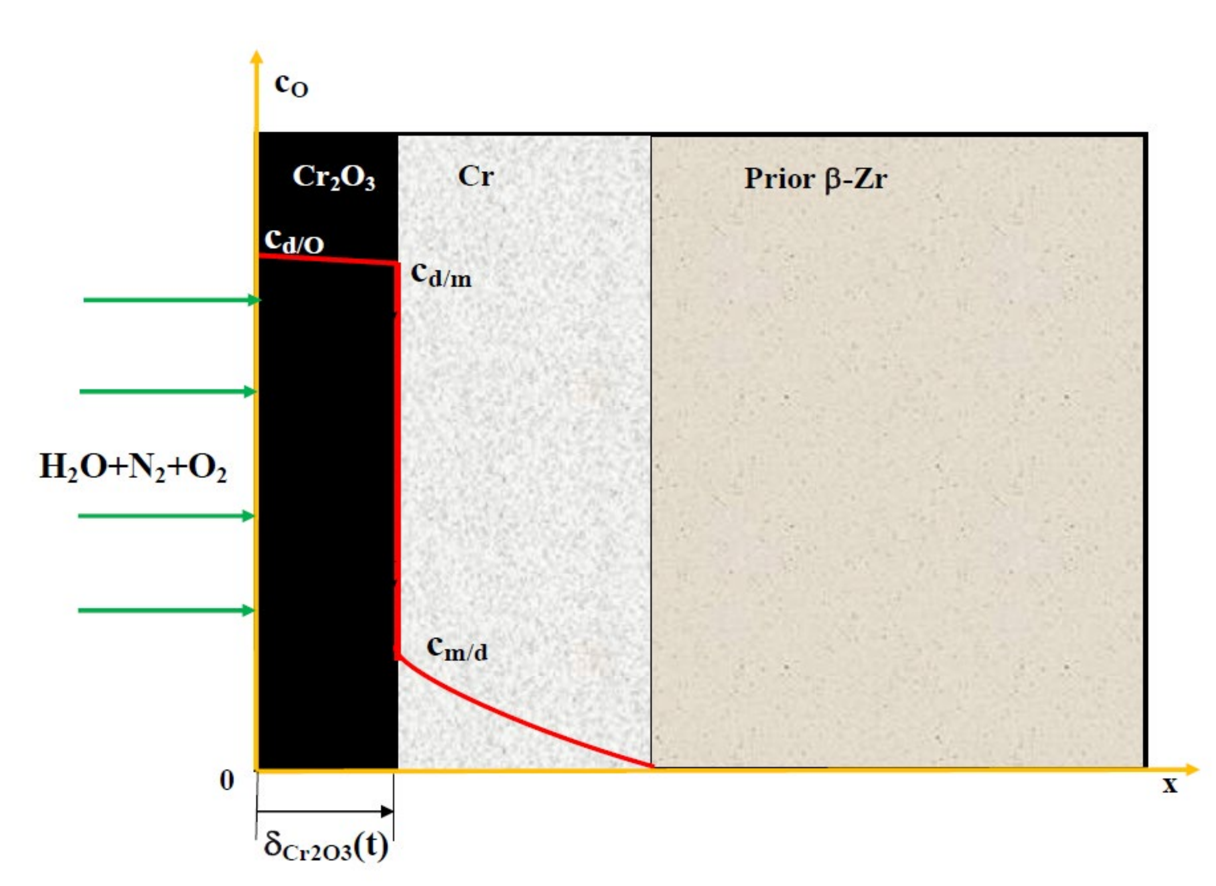

T=1473K $D_{d,Cr2O3} = 3.76\cdot10^{-12}$ m²/s $D_a = 7.14\cdot10^{-13}$ m²/s

$D_{d,ZrO2} = 8.50\cdot10^{-10}$ m²/s

Dd=6.06d-3*dexp(-31228.D0/T)

Da=1.15d-3*dexp(-31228.D0/T)

$c_{d/O} = 1645$ kg/m³ $c_{d/m} = 1633$ kg/m³ $c_{m/d} \approx 100\div500$ kg/m³

Parabolic Constant of Oxidation

$$r = \left(\rho_{Cr_2O_3}/\rho_{Cr}\right)\cdot\left(2\mu_{Cr}/\mu_{Cr_2O_3}\right)\approx 0.5$$

Bedworth-Pilling ratio

$$\delta_{Cr_2O_3} = \sqrt{k_p t} = K_d\sqrt{t}$$

$$\frac{K_d}{\sqrt{4D_d}} \cong \frac{\left[\sqrt{\frac{4c_{md}\cdot c_{md}}{\pi} + 8\frac{D_d}{D_m}\left(c_{d/m} - c_{m/d}\cdot r\right)\cdot\left[c_{d/O} - c_{d/m}\right]} - \frac{2c_{m/d}}{\sqrt{\pi}}\right]}{4\sqrt{\frac{D_d}{D_m}}\cdot\left(c_{d/m} - c_{m/d}\cdot r\right)}$$

$k_p = 4.83\cdot 10^{-5}\cdot e^{-\frac{31228}{T}}$ **m^2/s in accordance with work**

J.-Ch. Brachet, E. Rouesne, J. Ribis, T. Guilbert, S. Urvoy, G. Nony, C. Toffolon-Masclet, M. Le Saux, N. Chaabane, H. Palancher, A. David, J. Bischoff, J. Augereau, E. Pouillier, "High Temperature Steam Oxidation of Chromium-Coated Zirconium-Based Alloys: Kinetics and Process", Corrosion Science, 167, 2020, 108537, 15 pp. Online version: https://doi.org/10.1016/j.corsci.2020.108537.

Diffusion Equations to Solve

$$\frac{1}{D_d}\frac{\partial c}{\partial t} = \frac{\partial^2 c}{\partial z^2} \qquad Cr_2O_3$$

$$\frac{1}{D_m}\frac{\partial c}{\partial t} = \frac{\partial^2 c}{\partial z^2} \qquad Cr$$

Diffusion flux to Zr

$$q(t) = -D_m \left.\frac{\partial c}{\partial z}\right|_{z_{Cr/\alpha Zr}}$$

$$\Phi = \frac{1}{\sqrt{\pi D_{a,ZrO2}}}\int_0^t q\Big|_{t-\tau}\frac{e^{-\frac{z^2}{4\pi\tau}}}{\sqrt{\tau}} \qquad \alpha - Zr(O)$$

Kirchoff Transform of Oxygen Concentration on Diffusion Coefficient

$$\Re$$

$$\Re(c) = \int_0^c dc' \cdot \frac{D(c')}{D(0)}$$

$$\frac{\partial \Re}{\partial t} = \frac{D(\Re)}{r}\frac{\partial \Re}{\partial r} + D(\Re)\frac{\partial^2 \Re}{\partial r^2}$$

Using of Kirchoff transform makes solution of diffusion equation much easier !

Direct & Inverse Kirchoff Transforms

Direct Transform

$$\mathfrak{R}(c) = c, \qquad c \le c_{m/d}$$

$$\mathfrak{R}(c) = c_{m/d}, \qquad c_{m/d} < c \le c_{d/m}$$

$$\mathfrak{R}(c) = c_{m/d} + \left(c - c_{d/m}\right)\frac{D_d}{D_m}, \qquad c_{d/m} < c \le c_{d/O}$$

Inverse Transform

$$c = \mathfrak{R}, \qquad \mathfrak{R} \le c_{m/d}$$

$$c = \left(\mathfrak{R} - c_{m/d}\right)\frac{D_m}{D_d} + c_{d/m}, \qquad c_{m/d} < \mathfrak{R} \le c_{m/d} + \left(c_{d/O} - c_{d/m}\right)\frac{D_d}{D_m}$$

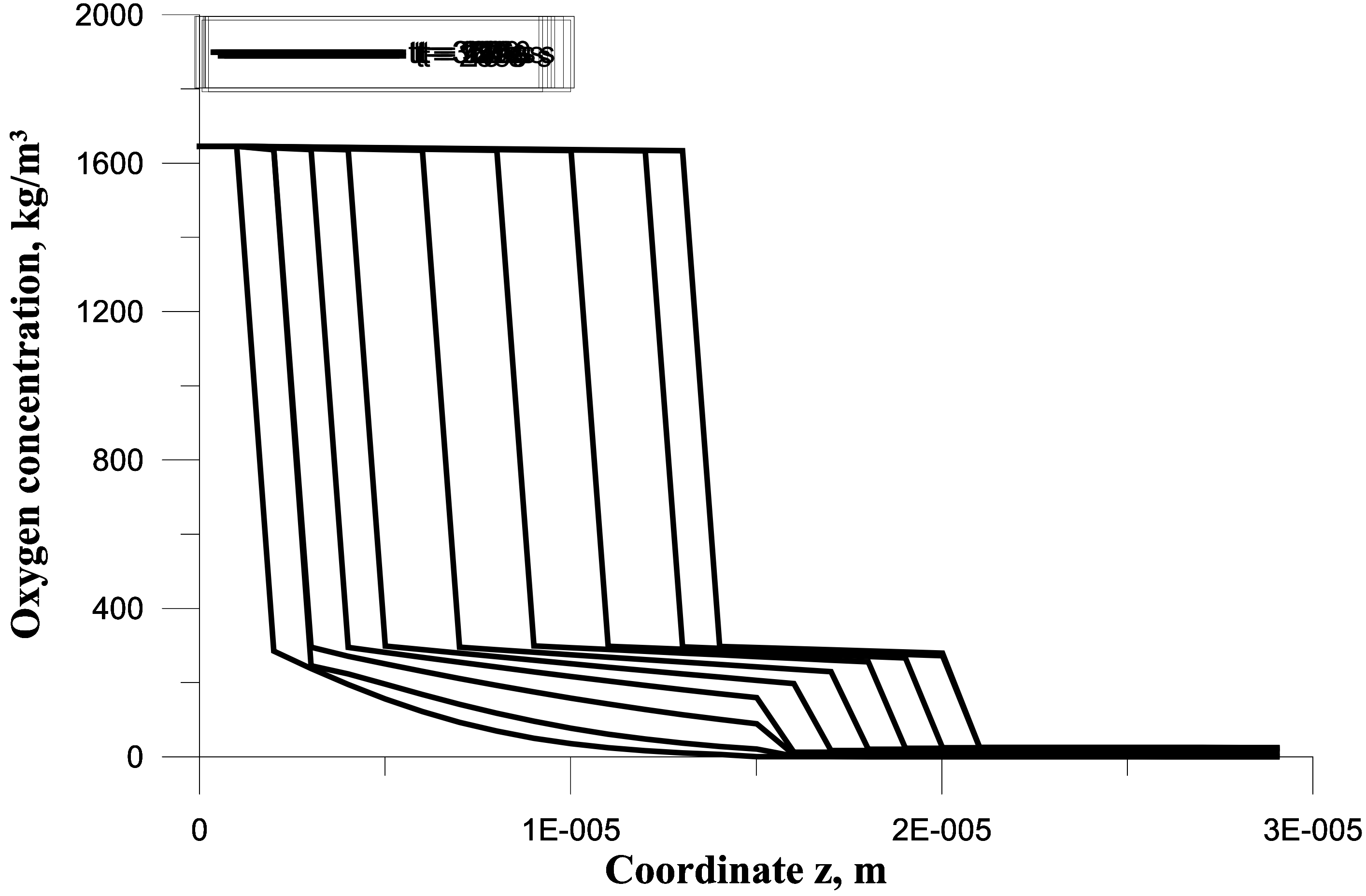

2000
1600
1200
800
400
0
Oxygen concentration, kg/m3
0
1E-005
2E-005
3E-005
Coordinate z, m

Temporal Dynamics of Oxygen Concentration Profile

J.-Ch. Brachet *et al*.

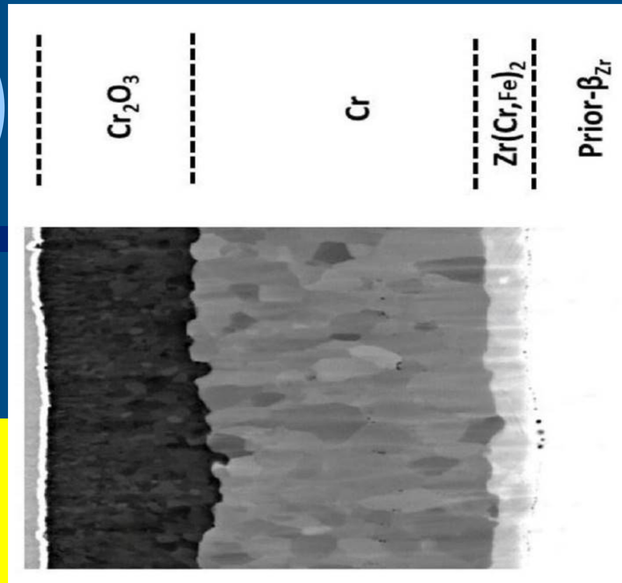

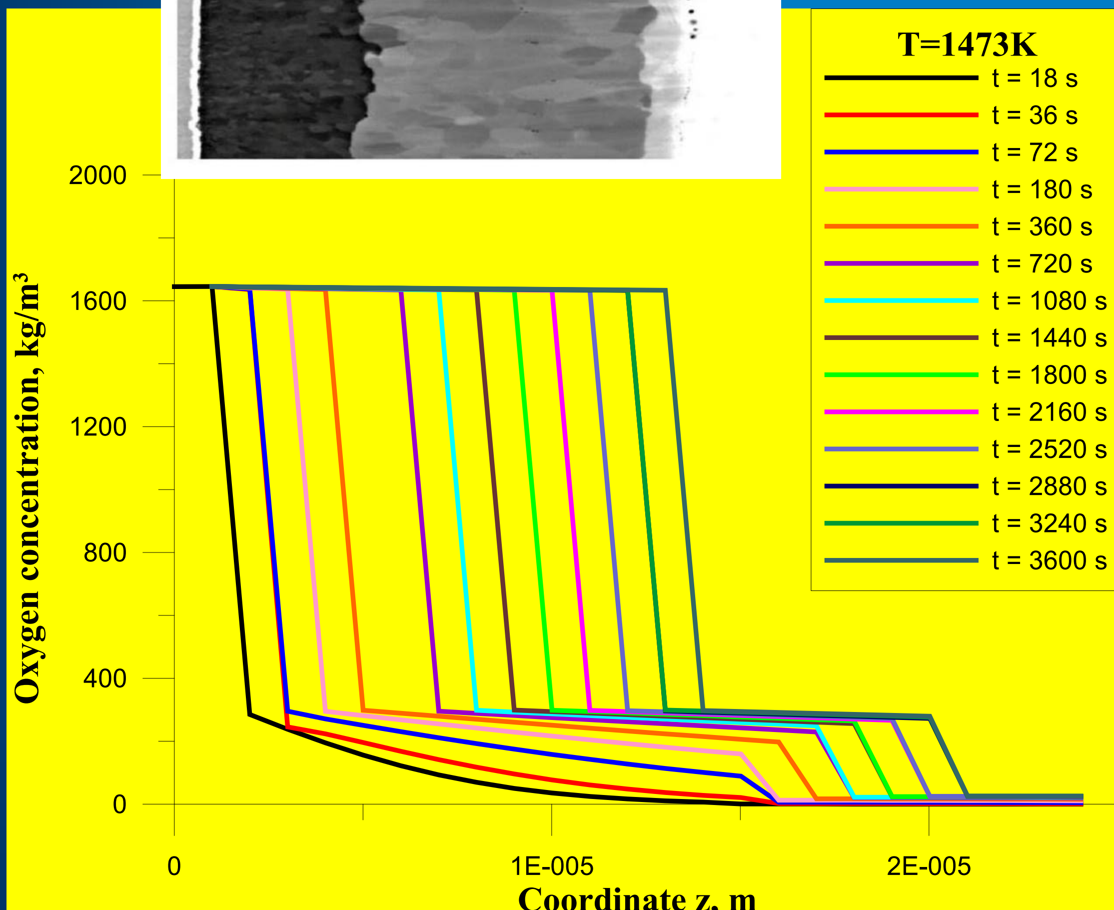

Oxygen concentration profile during phase II

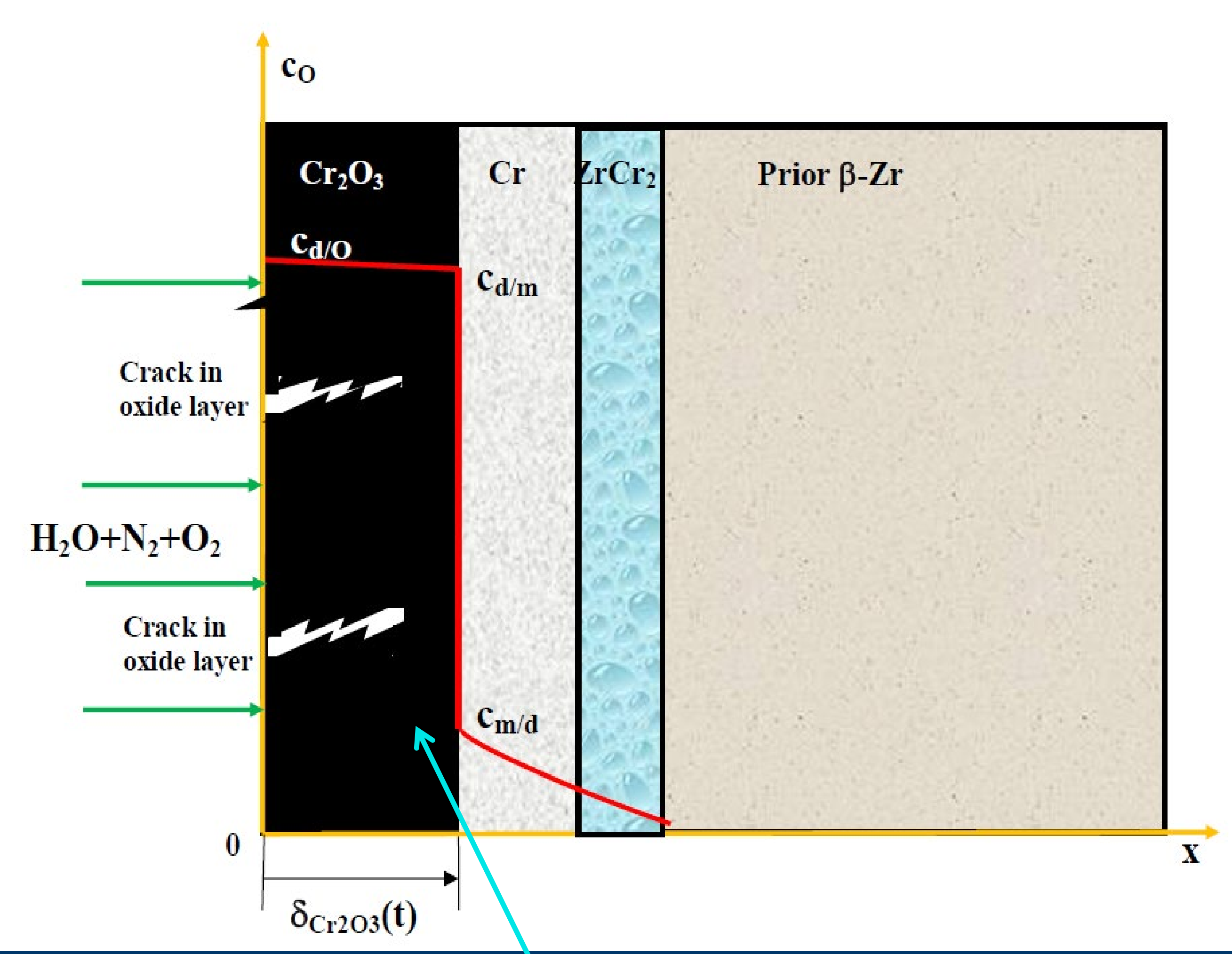

Formation of cracks in Cr oxide! It results in enhancement of oxygen diffusion in Cr_2O_3 !!

Influence of Oxygen Diffusion Coefficient Enhancement K_{diff} on Oxygen Concentration Profile

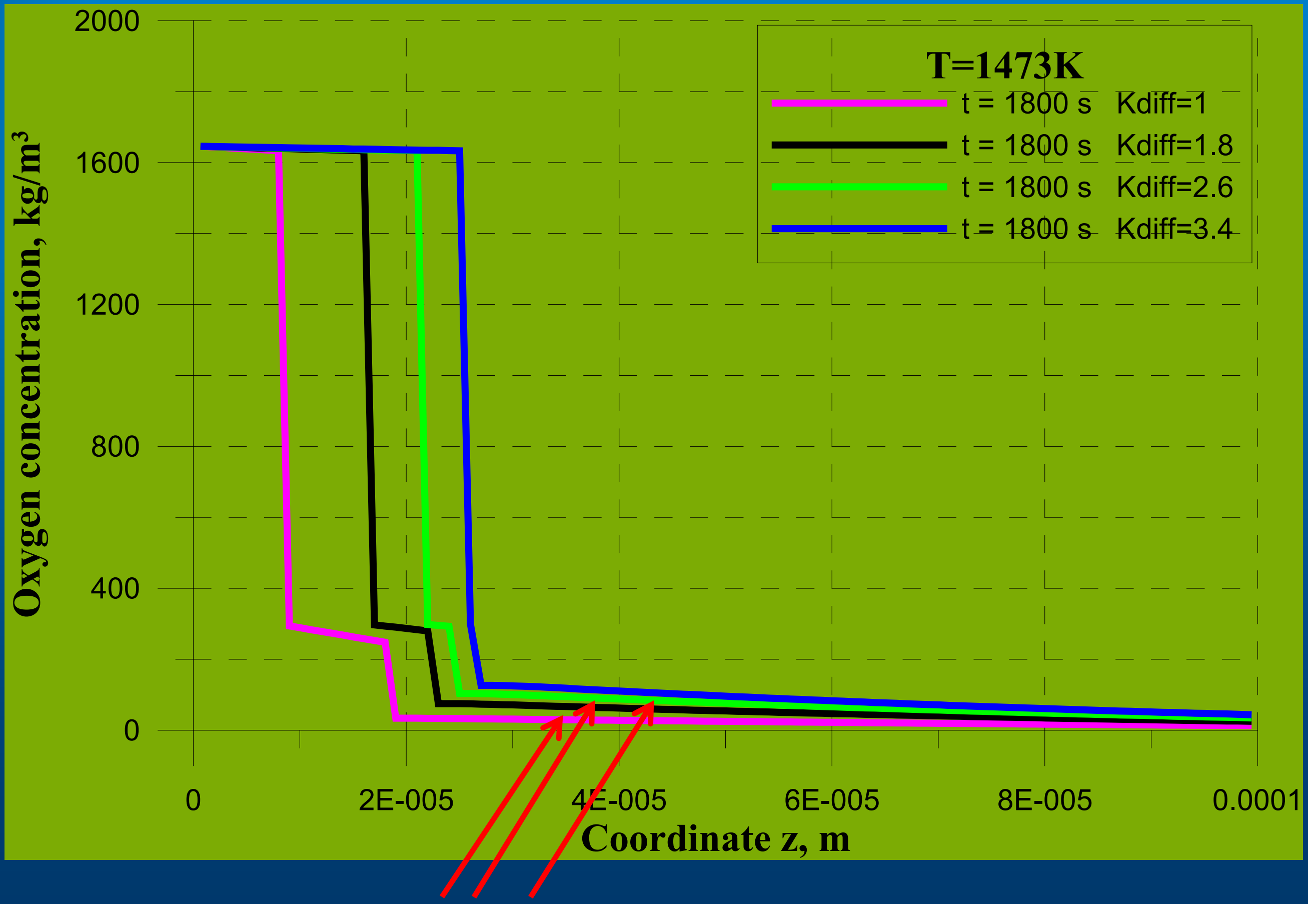

Growth of oxygen concentration in Zr metal – formation of α-Zr(O) phase !

Oxygen Concentration Profile during Phase III

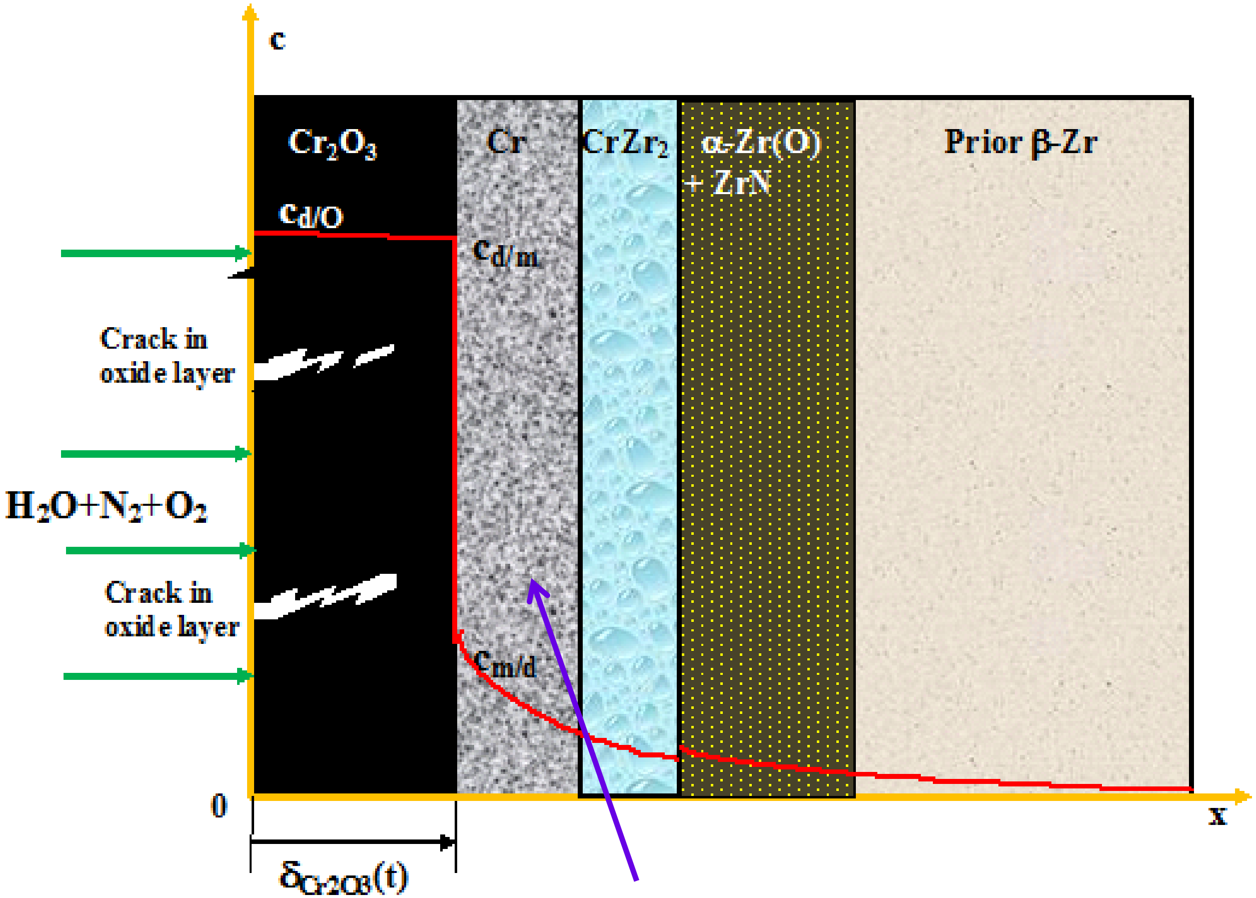

Formation of ZrO2 precipitates (grains) in metal Cr !
It results in enhancement of oxygen diffusion !

Dependence of Cr Oxide Thickness Dynamics on Factor of Oxygen Diffusion Coefficient Enhancement Kdiff

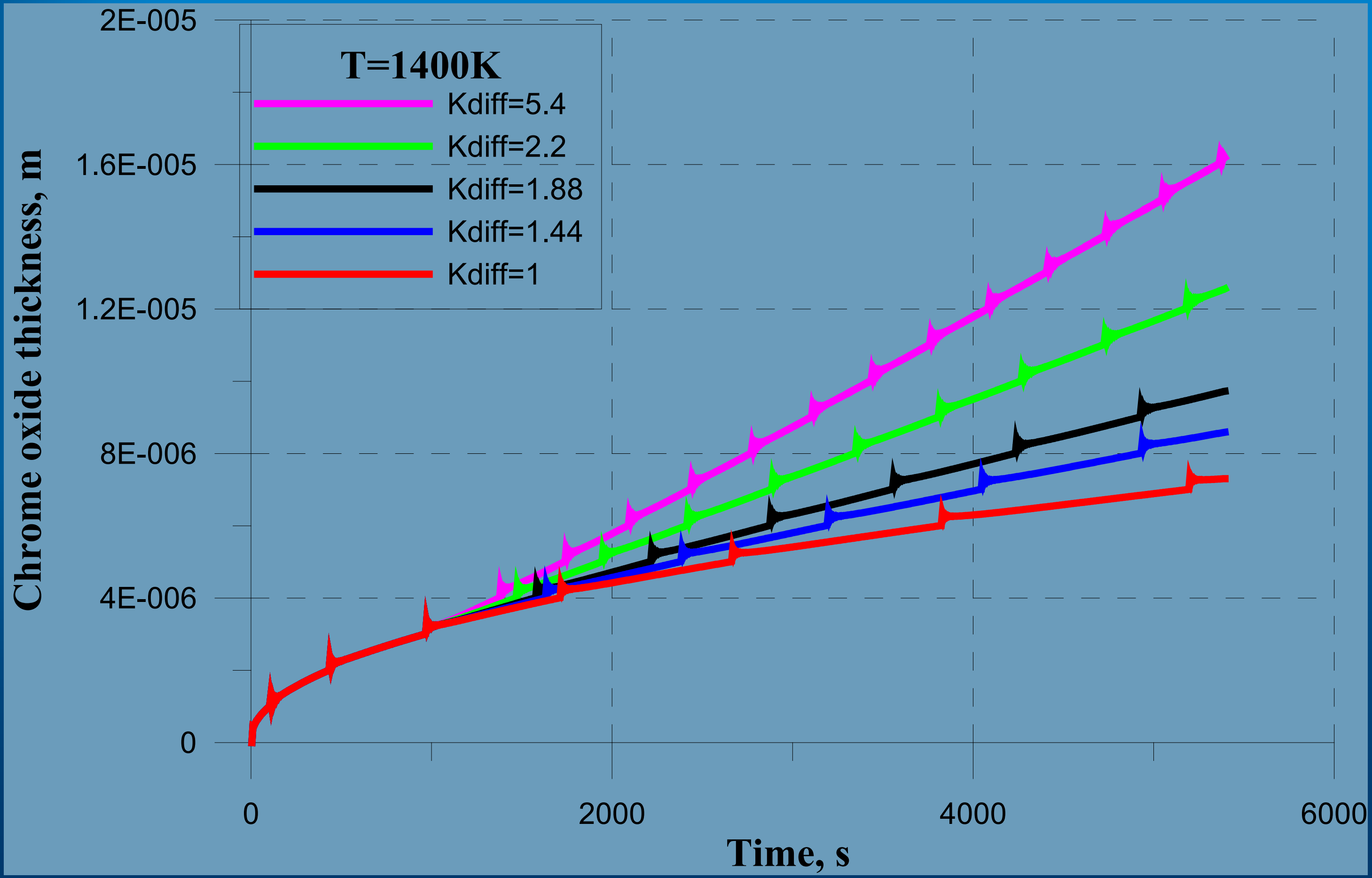

$D = D_{standard} \cdot Kdiff$

Key phenomenon is a loss of protective properties in temperature range $T \geq 1200°C$!

Oxygen concentration profile during phase IV

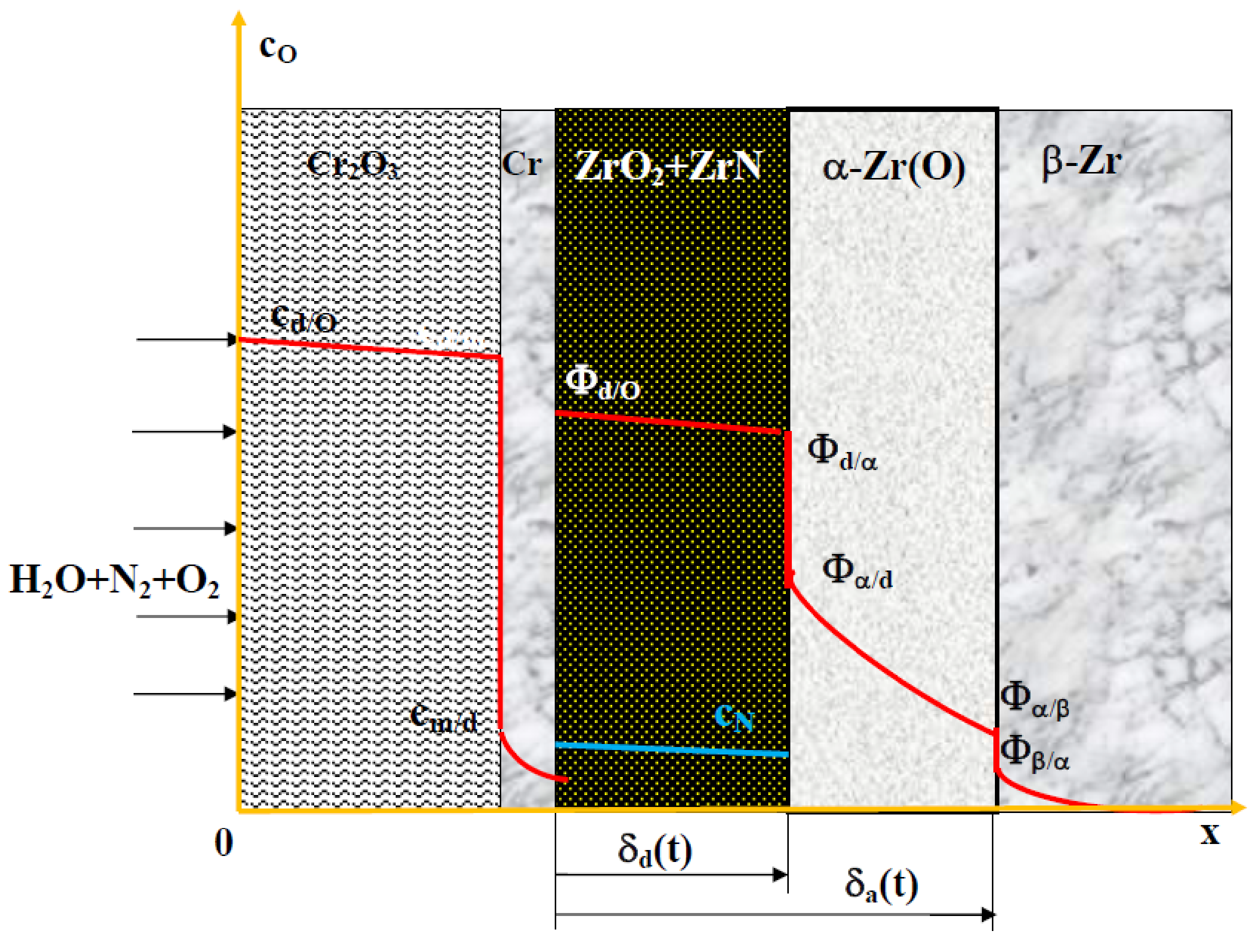

Chrome Oxide Thickness and Weight Gain at T=1200°C

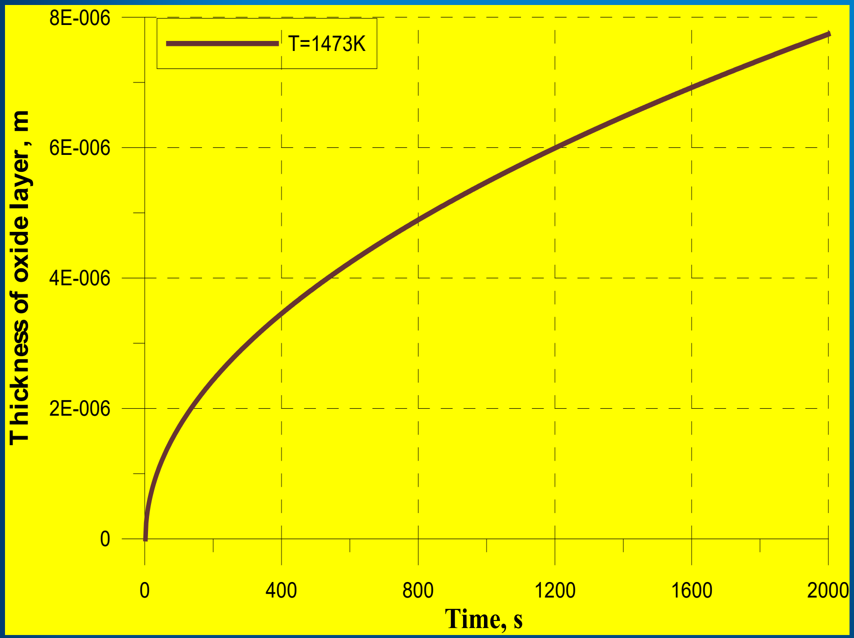

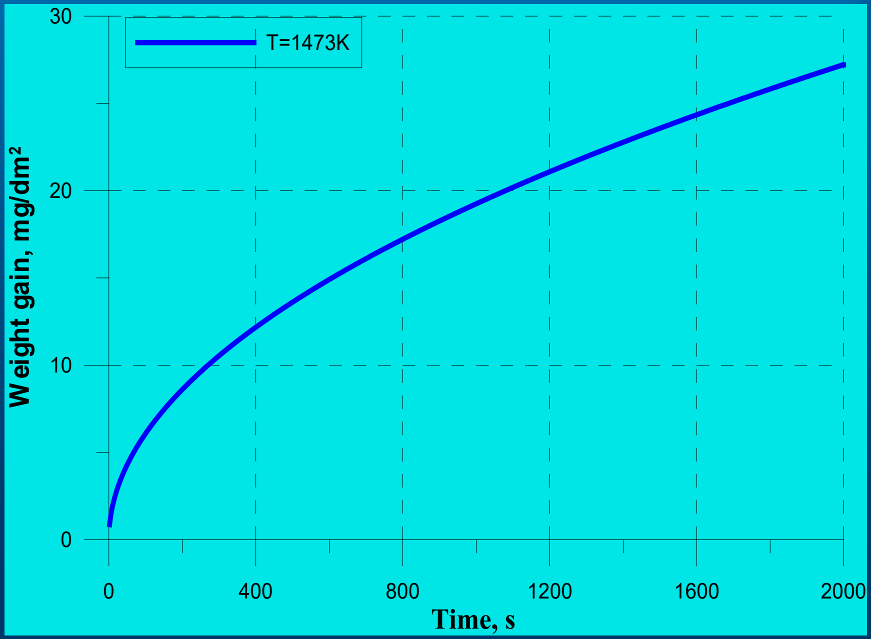

Dynamics of weight gain for uncoated (*ZrO_2*) and coated cladding (*Cr_2O_3*) at T=1473K

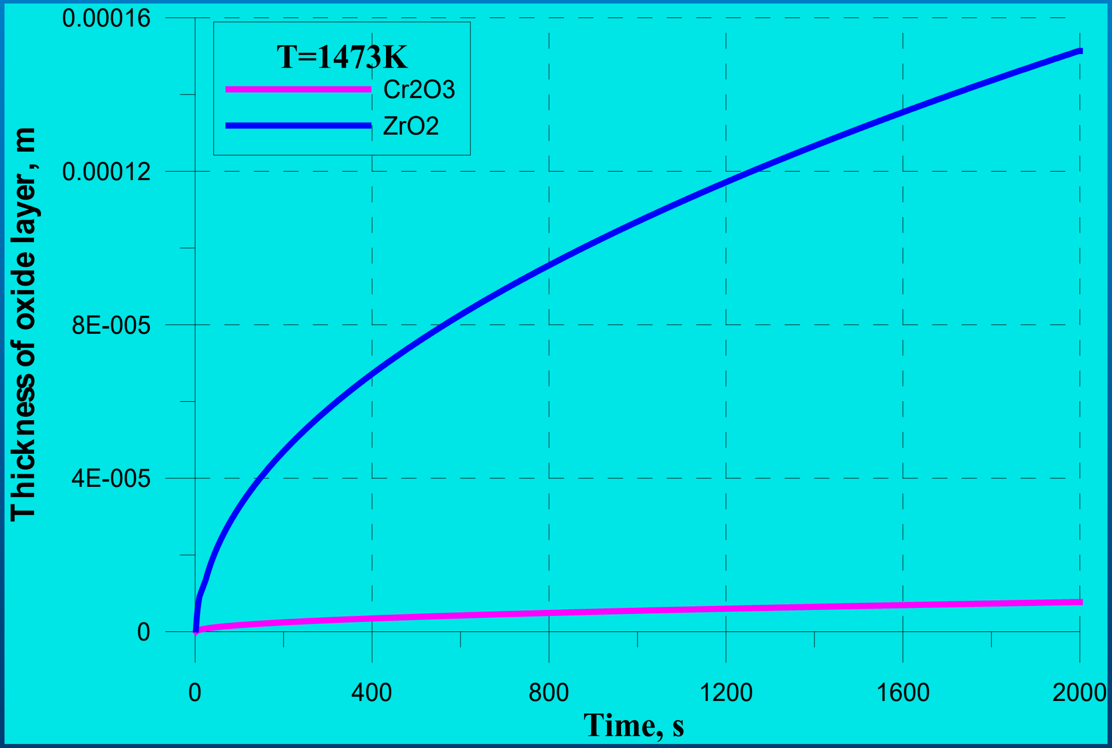

Oxide layer of Cr_2O_3 Should Be Dissappeared Like Zr Oxide in Case of Oxygen Starvation

Starvation points

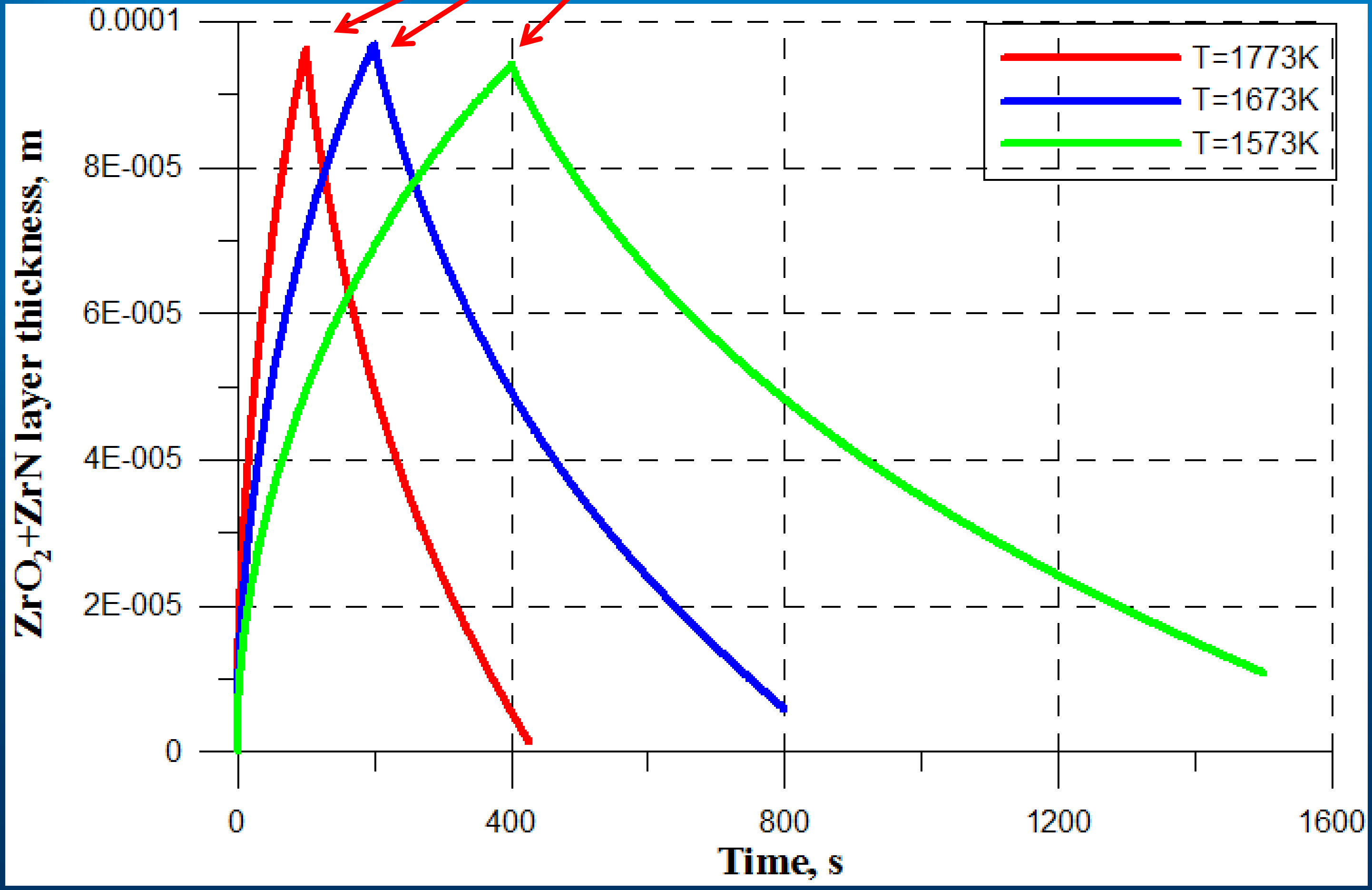

Comparison with Experiment (1)

Analytics

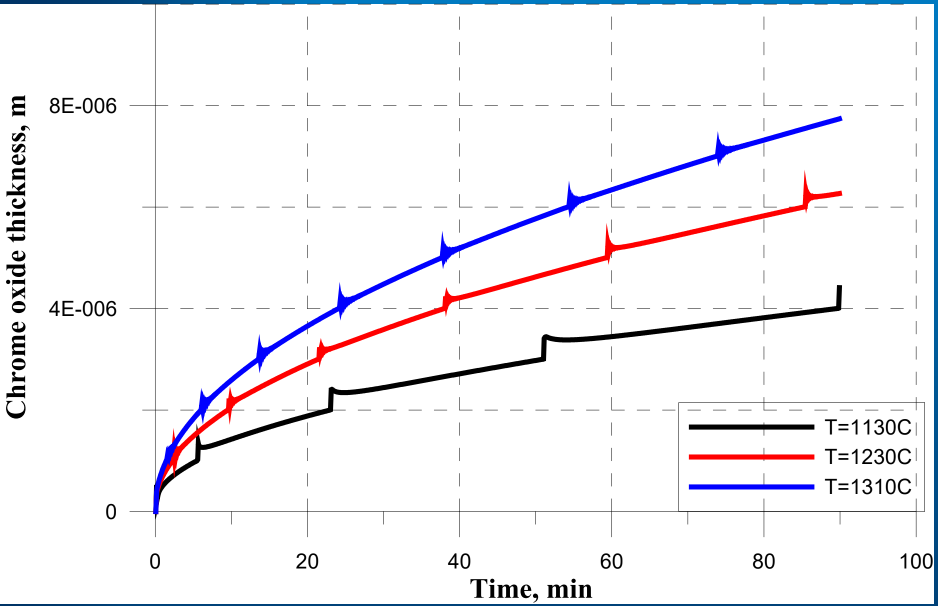

Experiment

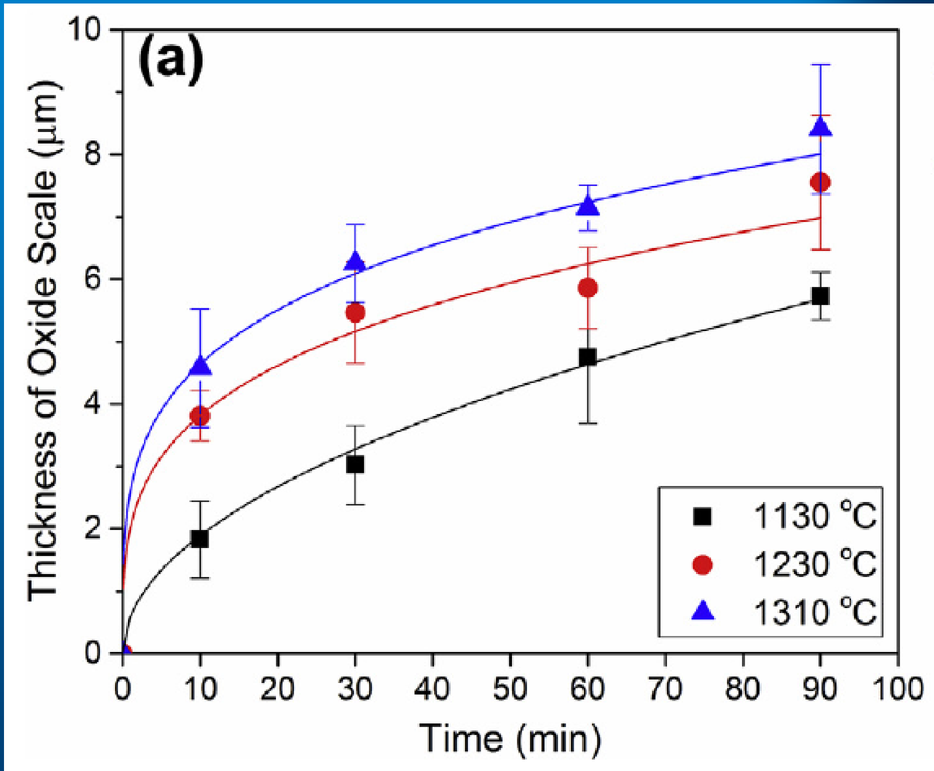

Experiment

Hwasung Yeom, Benjamin Maier, Greg Johnson, Tyler Dabney, Mia Lenling, Kumar Sridharan. High temperature oxidation and microstructural evolution of cold spray chromium coatings on Zircaloy-4 in steam environments. Journal of Nuclear Materials, V. 526, 2019, 151737. 10 pp.

Comparison with Experiment (2). Cr thickness is 10 μm

Calculation dynamics of cladding weight gain

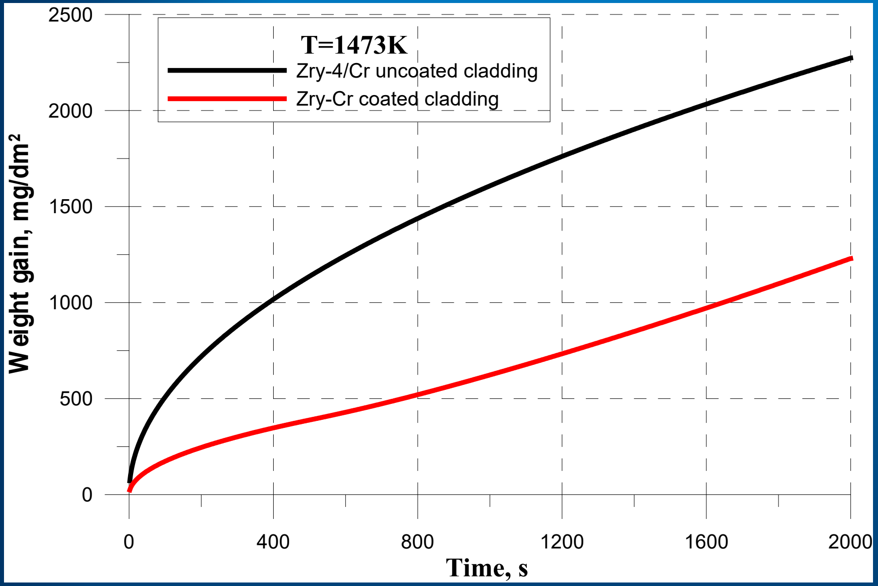

Experimental dynamics of cladding weight gain
J.-H. Park, H.-G. Kim, J.-Y. Park, Y.-I. Jung, D.-J. Park, Y.-H. Koo, High Temperature Steam-Oxidation Behavior of Arc Ion Plated Cr Coatings for Accident Tolerant Fuel Claddings", Surface & Coatings Technology, 280, 2015, pp. 256-259.

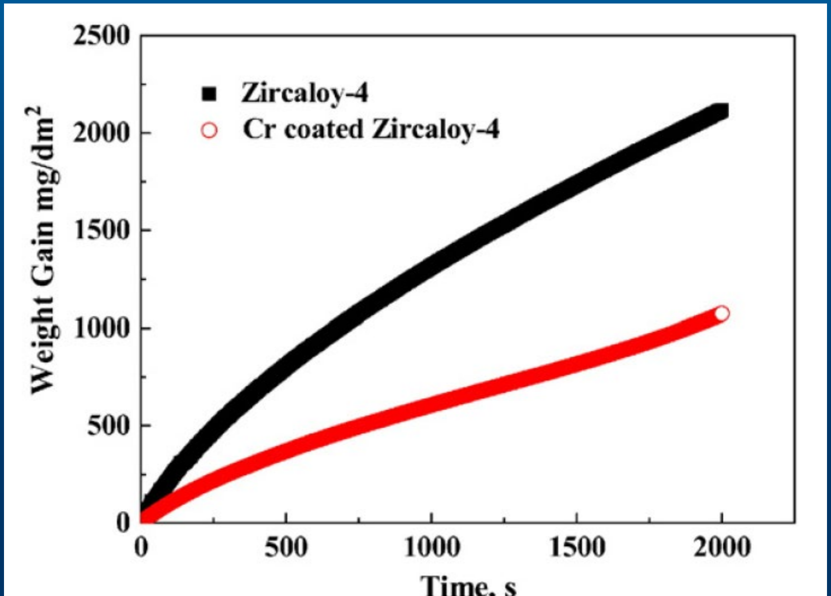

Oxygen diffusion coefficient D gradually enhances up to 16 times to time t=2000 s.

Conclusions (1)

The approaches to model the oxidation of perspective ATF zirconium-based cladding with chromium coating with the thickness up to 10-20 μm were described. The analysis of experimental and analytical results allows to state that *Zr*-based claddings with chromium coating possess low oxidation kinetics in temperature range *T*=700÷1300°C. However, four different phases are progressively developing during high temperature oxidation, which result in gradual worsening of oxidation characteristics in the course of oxidation.

Some illustrative results of analytical model developed are given in the presentation. They demonstrate the predictive ability of the model.

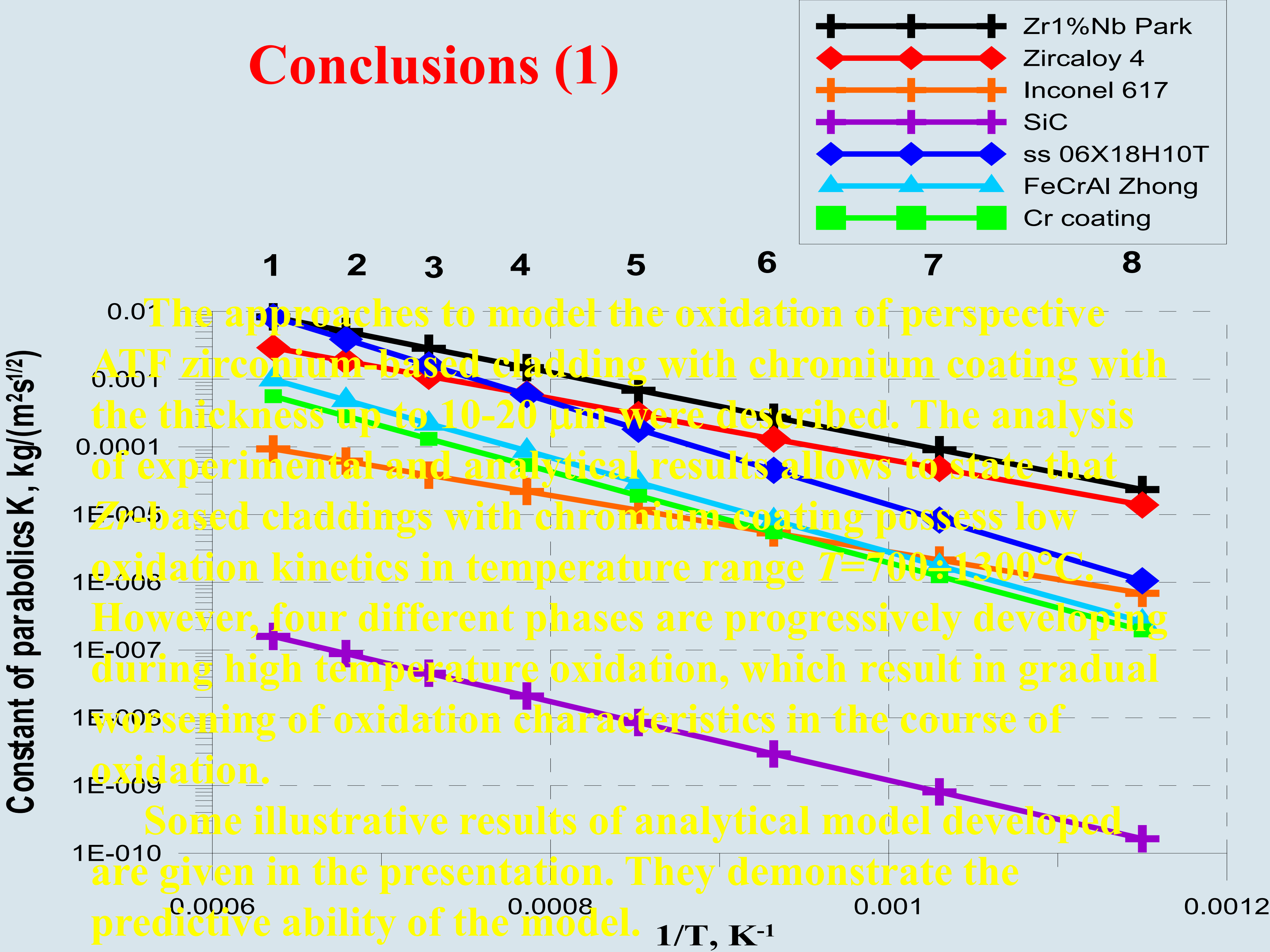

Conclusions (2)

On the whole, the application of ATF zirconium-based cladding with chromium coating in reactor claddings looks reasonable because of saving time and the possibility of exclusion of accident escalation in the course of severe accident mitigation strategy.

Thus, the most gain from use of *Zr*/*Cr* claddings is expected for scenarios with temperature range about 700°C-1300°C that is design-basis accident and respectively low hydrogen generation rate is expected. The difference in such parameters as chemical heat generation, hydrogen generation rate and cumulative hydrogen production may reach up to one order of magnitude in favour of chromium-coated claddings compared to standard Zr-based claddings.

N. Elsalamouny, T. Kaliatka

Lei

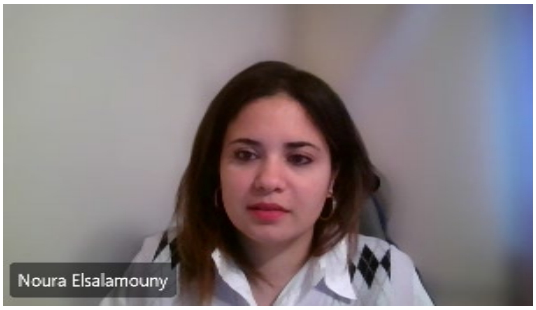

Implementation of LEI experience on modeling and uncertainty quantification of QUENCH tests for the development of QUENCH-20 numerical model

The Lithuanian Energy Institute (LEI) has experience in analyzing QUENCH tests (QUENCH-03, 06, 18), as it has performed the numerical analysis using severe accident codes ASTEC and RELAP/SCDAPSIM. For QUENCH-03 and 06 tests the uncertainty and sensitivity analysis were performed using uncertainty tools SUNSET and SUSA. LEI has publicized scientific articles for the modeling and uncertainty quantification of QUENCH tests and currently, is taking part in the QUENCH group of IAEA CRP I318. In this CRP uncertainty quantification for the QUENCH-06 test were provided by using RELAP/SCDAPSIM and SUSA tool.

LEI have interest to model QUENCH-20 experiment which corresponds to BWR type bundle. Comparing the boundary conditions of QUENCH 6 and 20 it was found many similarities. The main difference is the bundle structure. LEI experience in modelling of QUENCH facility and uncertainty quantification of the calculation results could be used for the developing QUENCH - 20 numerical model.

This presentation will observe the LEI provided modeling and results of uncertainty and sensitivity analysis of QUENCH experiments. Evaluating differences of QUENCH-06 and 20, will be discussed how to use gained experience in the development of the QUENCH – 20 numerical model.

LITHUANIAN ENERGY INSTITUTE
http://www.lei.lt

NATIONAL OPEN ACCESS SCIENTIFIC CENTRE FOR FUTURE ENERGY TECHNOLOGIES

OPEN R & D LITHUANIA

Implementation of LEI experience on modeling and uncertainty quantification of QUENCH tests for the development of QUENCH-20 numerical model

Noura Elsalamouny, Tadas Kaliatka

Content

- Lithuanian Energy Institute experience in modeling QUENCH tests
- Uncertainty Quantification for QUENCH-03 and QUENCH-06
- Participation in IAEA CRP I31033
- Development of QUENCH-20 numerical model using the previous experience

LEI experience in modeling QUENCH experiments

- Hollands, T, Bals, C. Tiborcz, L. Beuzet, E. Vasiliev, A. Kaliatka, T. Birchley, J. Steinbrück, M. *Pre-and Post-Test Simulation of the QUENCH-18 Bundle Experiment in the frame of the NUGENIA QUESA Project*,2019.
- Kaliatka A., Kaliatka T., Vileiniškis V., Ušpuras E. *Best estimate approach for the simulation of reactor core overheating and quenching experiments // Best Estimate Plus Uncertainty International Conference*. Multi-Physics Multi-Scale Simulations with Uncertainty (BEPU 2018) May 13-18, 2018, Lucca, Italija. 12 p.
- Kaliatka T., Ušpuras E., Allison CH. M. *Modeling of quench 10 experiment on air ingress using relap/scdapsim mod 3.5* // Proceedings of the 2017 25th International Conference on Nuclear Engineering ICONE25 July 2-6, 2017, Shanghai, China. p. 1-7
- Kaliatka T. *Implementation of QUENCH-10 experiment modelling experience for the modelling of severe accidents in spent fuel pools* // Proceedings 23rd International QUENCH Workshop Karlsruhe Institute of Technology, Germany (doi:10.5445/IR/1000076201) October 17-19, 2017. p. 366-395
- Vileiniškis V., Kaliatka T., Kaliatka A., Ušpuras E., Šutas A. *Uncertainty and sensitivity analysis of QUENCH experiments using ASTEC and RELAP/SCDAPSIM Codes* // The 10th International Topical Meeting on Nuclear Thermal-Hydraulics, Operation and Safety (NUTHOS-10) NUTHOS10-1206 Okinawa, Japan, December 14-18, 2014 p. 1-15
- Kaliatka T., Kaliatka A., Vileiniškis V. *Best estimate approach for QUENCH-03 and QUENCH-06 Experiments* // 20th International QUENCH Workshop Karlsruhe Institute of Technology, Campus North, November 11-13, 2014 p. 20
- Kaliatka T., Kaliatka A., Vileiniškis V., Ušpuras E. *Modelling of QUENCH-03 and QUENCH-06 Experiments Using RELAP/SCDAPSIM and ASTEC Codes* // Science and Technology of Nuclear Installations. dx.doi.org/10.1155/2014/849480 ISSN 1687-6075. 2014. Vol. 2014, Article ID 849480, p. 1-13.
- Kaliatka T., Ušpuras E., Kaliatka A. *Modelling of QUENCH 03 and QUENCH 06 experiments using RELAP/SCDAPSIM code* // Proceedings of the 2013 21th international conference on nuclear engineering (ICONE 21), Chengdu,China, July 29 - August 2, 2013. USA : ASME, 2013, p. 1-8.
- Kaliatka T. *Modelling of quench experiment using RELAP/SCDAPSIM code* // 9th annual conference of young scientists on energy issues CYSENI 2012: international conference, Kaunas, Lithuania, 24-25 May, 2012. Kaunas: LEI, 2012. ISSN 1822-7554, p. 668-677.

Uncertainty and Sensitivity analysis for QUENCH-03 and QUENCH-06

- 12 uncertain parameters were investigated.
- The results of uncertainty and sensitivity analysis provided using severe accident codes (ASTEC & RELAP/SCDAPSIM) and uncertainty tools (SUNSET & SUSA).
- Results of uncertainty analysis were in good agreement with experimental data.
- Results of sensitivity analysis indicated that significant influence on calculation results are:
  - The bundle cooling boundary conditions;
  - Thermal power (electrical resistance) of the electrical heaters;
  - Thermal properties of the shroud.

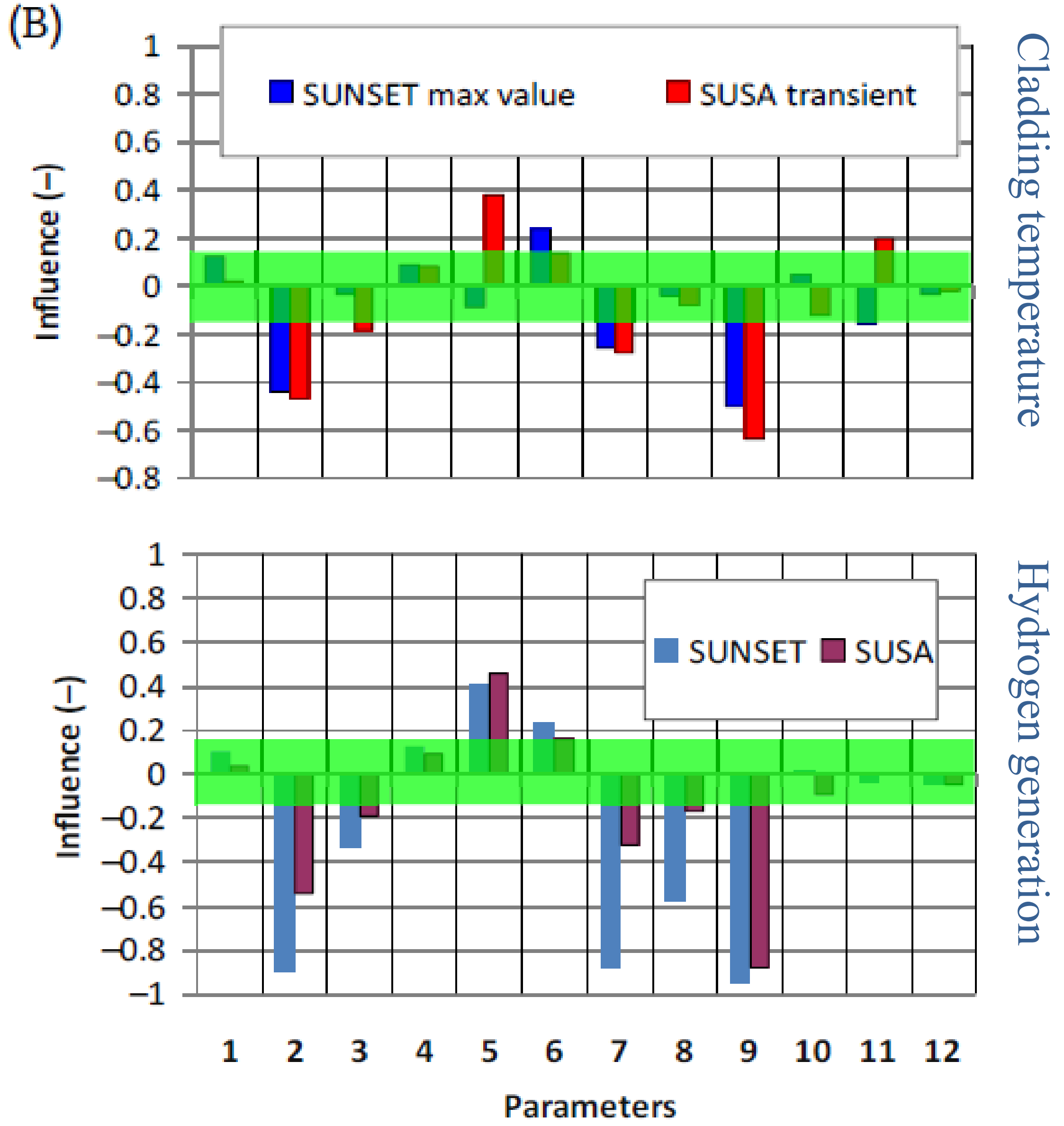

IAEA-CRP I31033

- In 2019 LEI took apart at IAEA-CRP I31033.
- LEI is a participant in the group working on uncertainty quantification of QUENCH-06 test.
- Group members agreed on the FOMs and the uncertain parameters to be analyzed.
- In this CRP LEI using RELAP/SCDAPSIM severe accident code and SUSA statistical tool.

LEI results of IAEA CRP

- In total 19 uncertain parameters (initial parameters (bundle geometry, cladding and shroud thermal properties), boundary conditions (electrical power, bundle cooling and quenching) and SCDAP modeling parameters) were used for the uncertainty quantification of QUENCH-06 test.

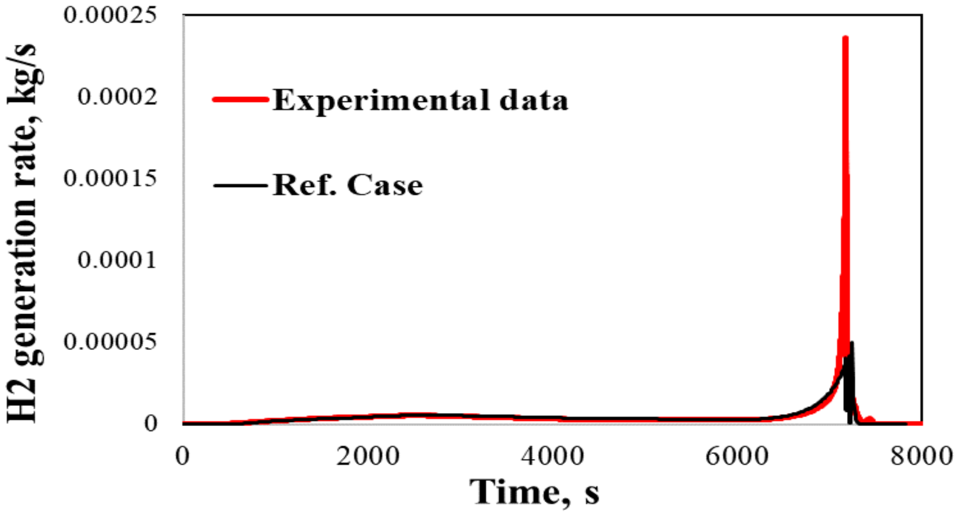

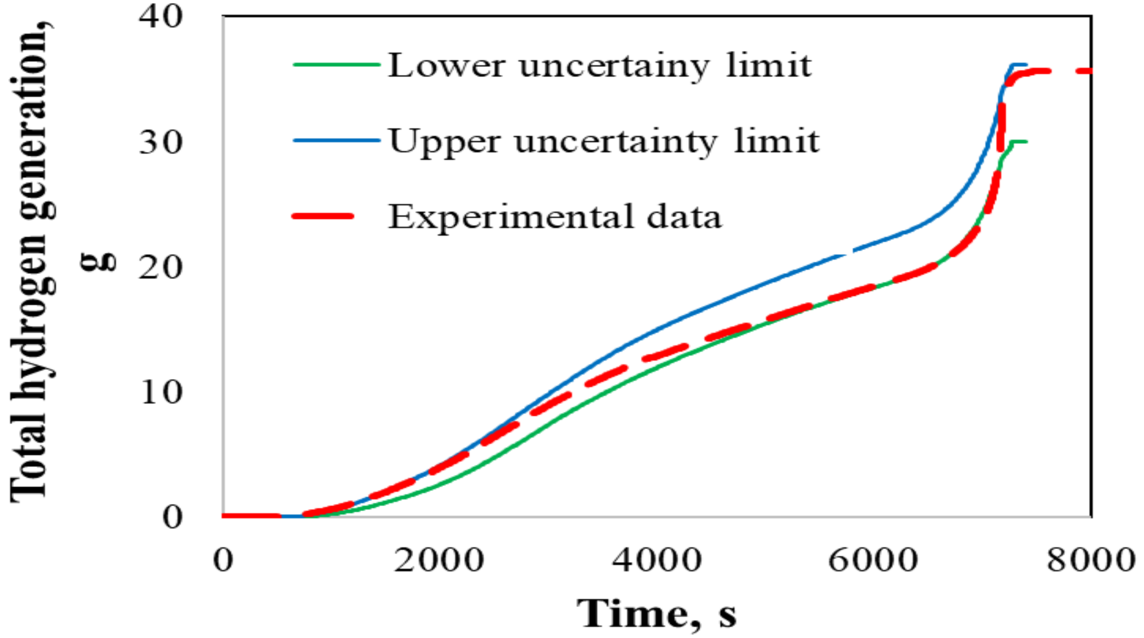

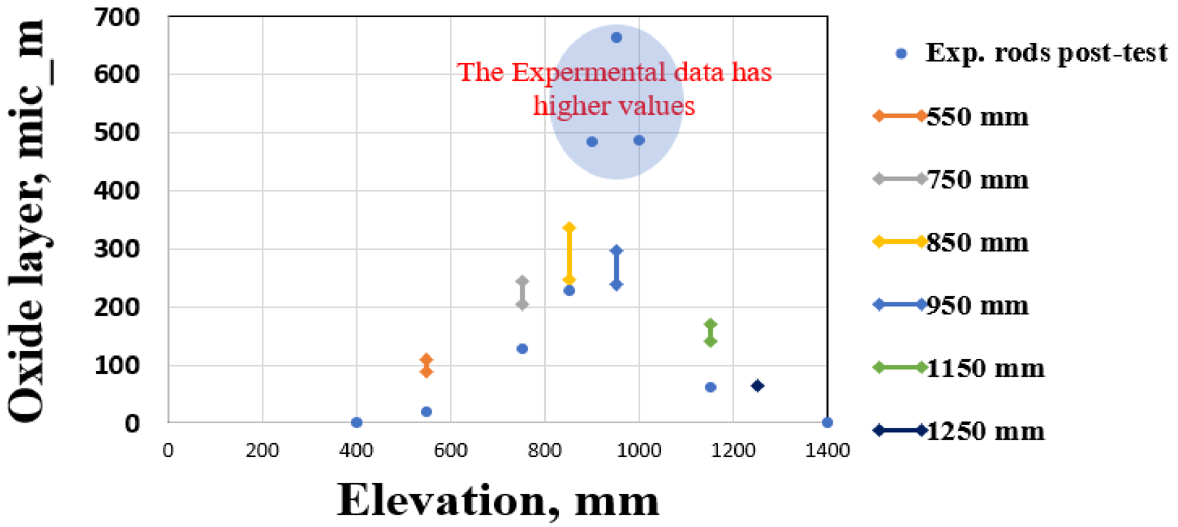

Sensitivity analysis

- For the biggest part of the uncertain parameters their influence could be neglected (≤±0.2).
- The parameters influence vary during test time. Decided to look at different phases.
- The most influenced parameters are cladding thickness, power, steam mass flow rate. Quench water injection influence appears only in the quench phase.

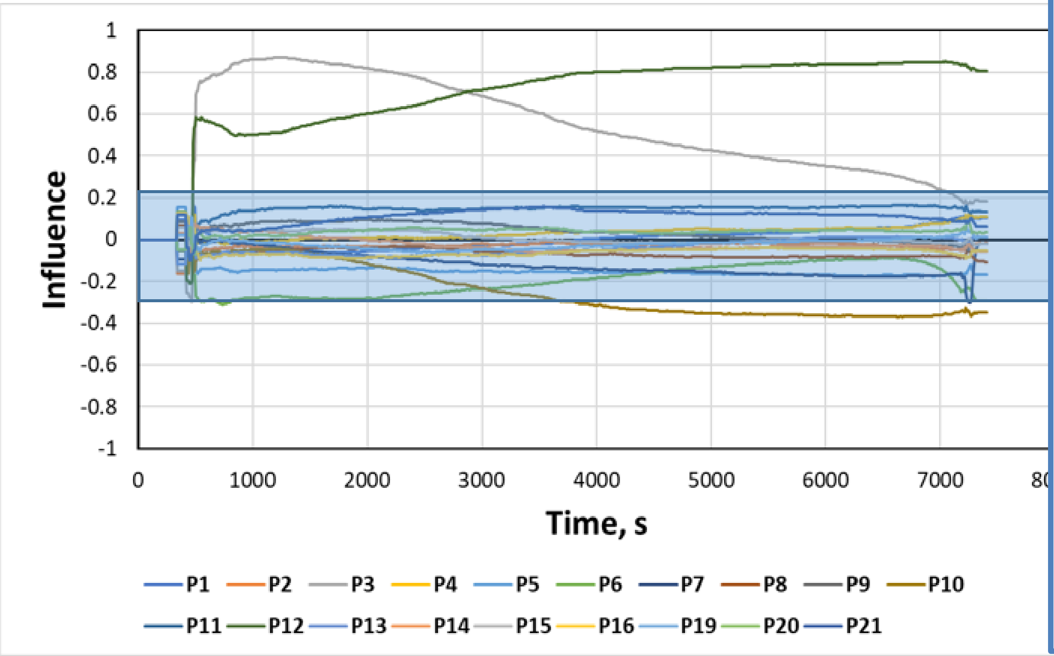

Hydrogen generation

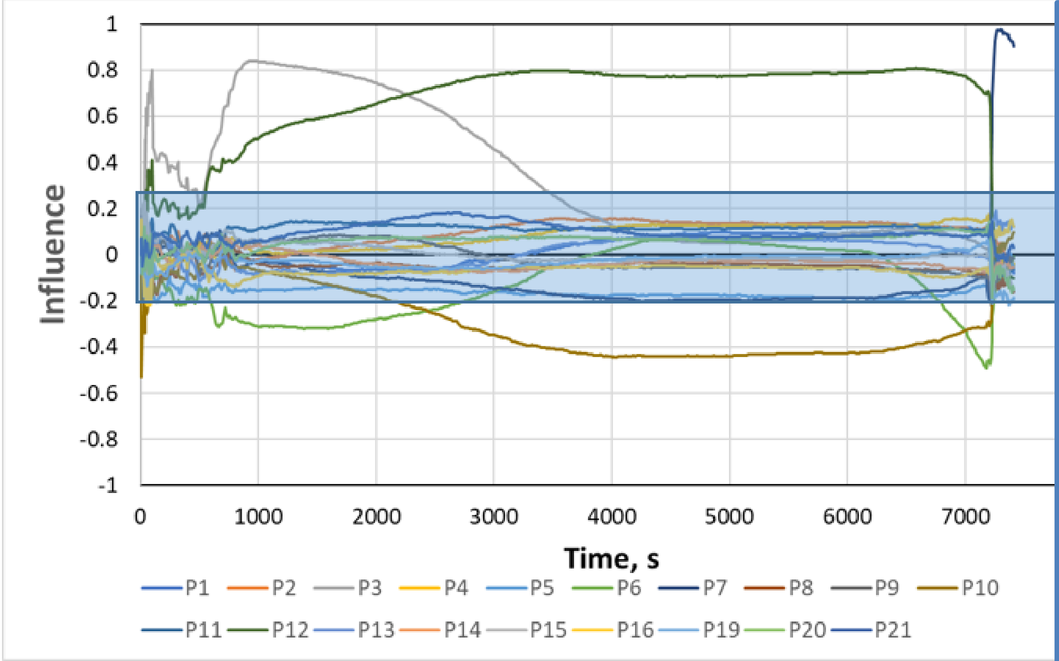

Cladding temperature

Modeling of QUENCH-10 & QUENCH-18

The specific for QUENCH-10 and QUENCH-18 was the Air injection.

- QUENCH-10: steam termination - air injection during bundle cooling
- QUENCH-18: a mixture of steam and air injection together during bundle cooling.
- For both experiments the formation of Zirconium nitride was an issue to be modeled.

- Parametric sensitivity analysis was done by using different oxidation models for steam and air ambient.

Summary of gained experience and its possible usage

- The previous analysis of QUENCH tests will enable us to have a better understanding of the computer code specifics and limitations.
- Uncertain parameters could be divided into different groups according their “nature” (initial parameters, boundary conditions, thermal properties of the shroud, modeling parameters, etc.) and their influence on calculation results at the specific test phases. Depending on the analyzed phase some group of parameters could have higher or lower influence on calculation results.
- Investigation of the QUENCH test is better provided by different phases, looking at the specific group of uncertain parameters.
- Influence on calculation results showed:
    - Parameters related to the bundle power and cooling;
    - Thermal properties of shroud;
    - The Zr oxidation models in steam/air ambient;
    - Smaller influence were given by SCDAP modeling parameters.
- Experience gained from previous analyses could be used for model development and calibration.

Development of QUENCH-20 numerical model using the previous experience

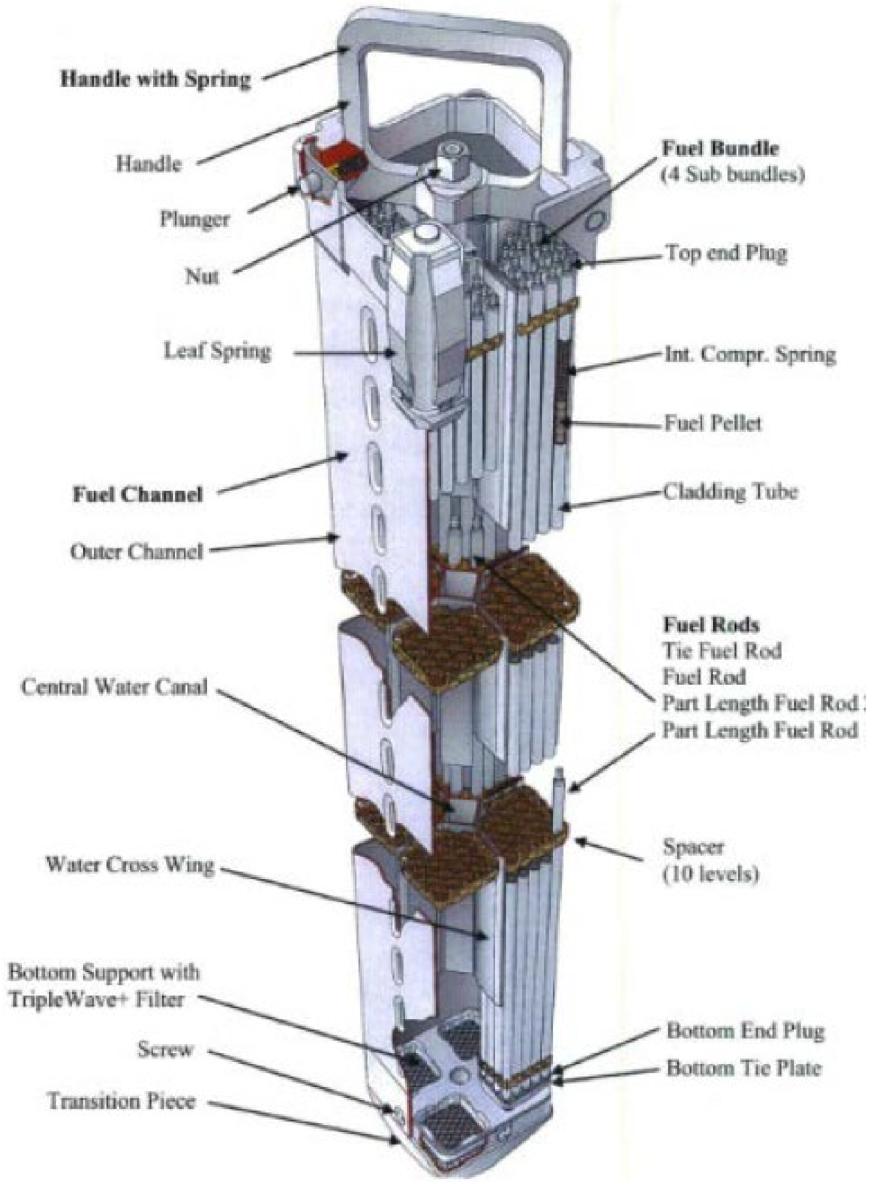

Power and steam flow rate

Parameter	QUENCH-06	QUENCH-20
Steam flow rate (g/s)	3 g/s	3 g/s
Argon flow rate (g/s)	3 g/s	3 g/s
Water injection (g/s)	40 g/s	50 g/s
Peak Power kW	18,2 kW	18,2 kW
Main phases	(pre-oxidation, transient, Quenching)	(pre-oxidation, transient, Quenching)

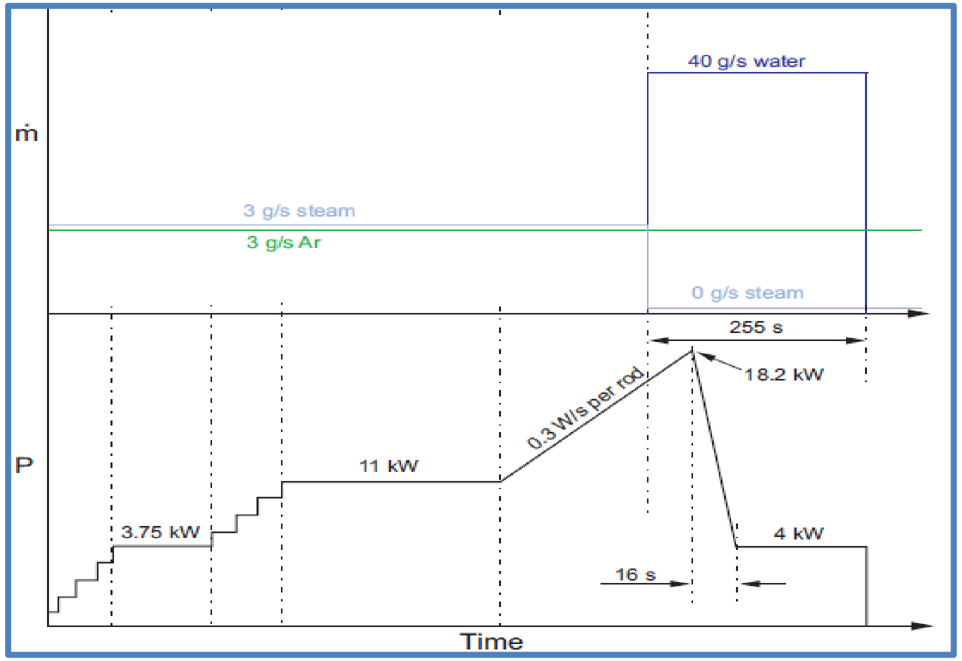

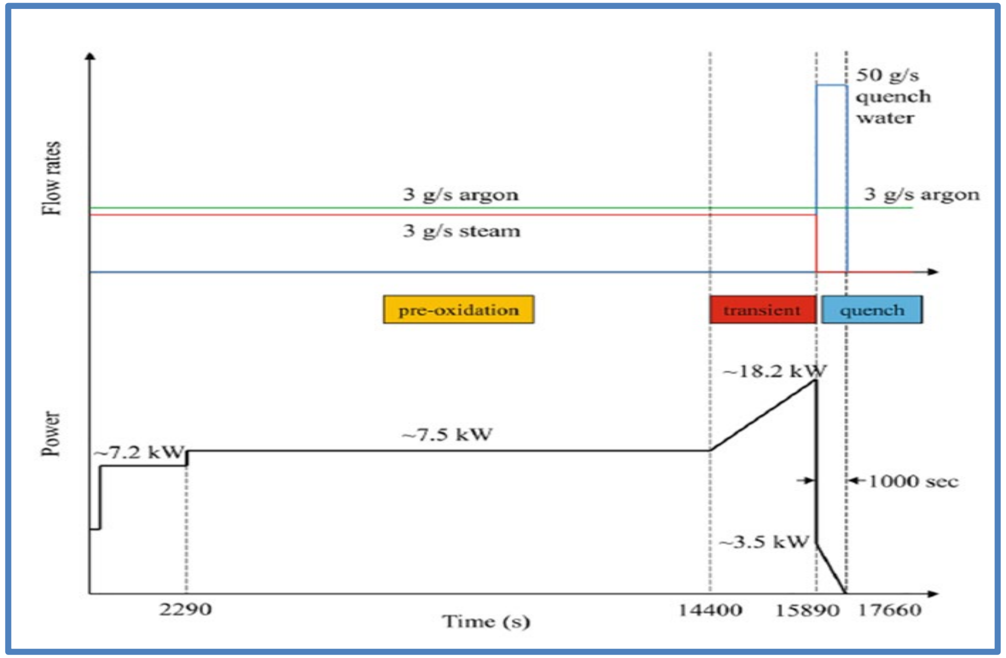

Test bundle

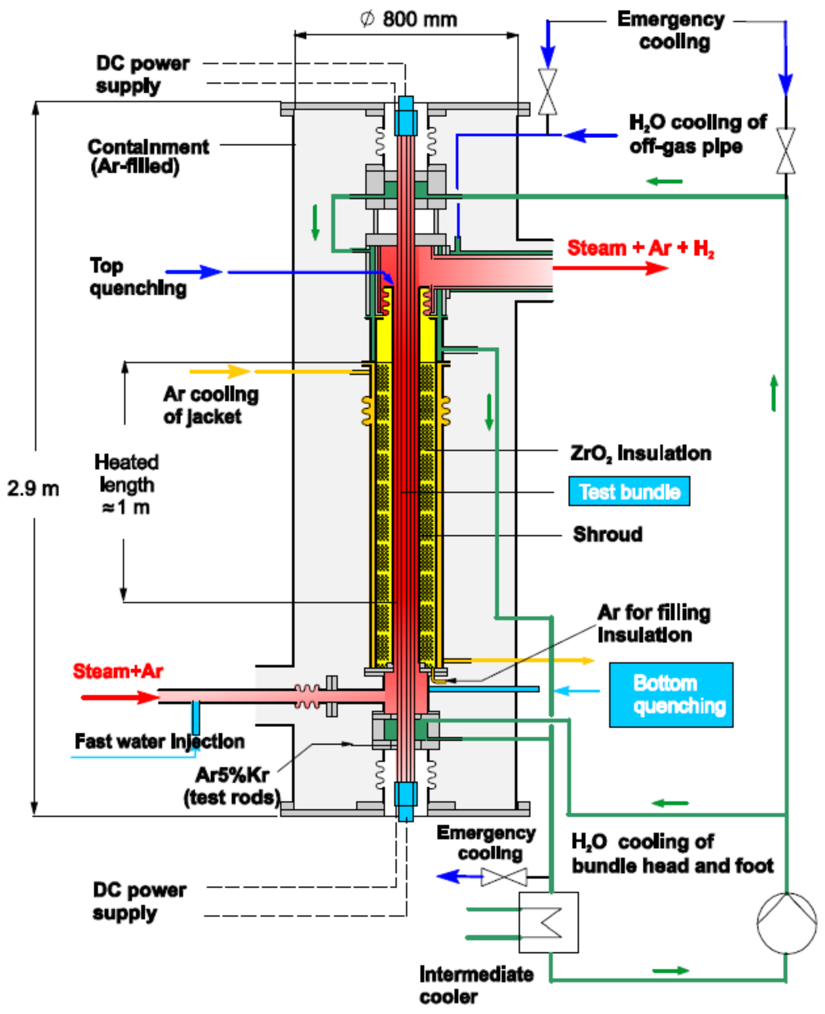

QUENCH-06

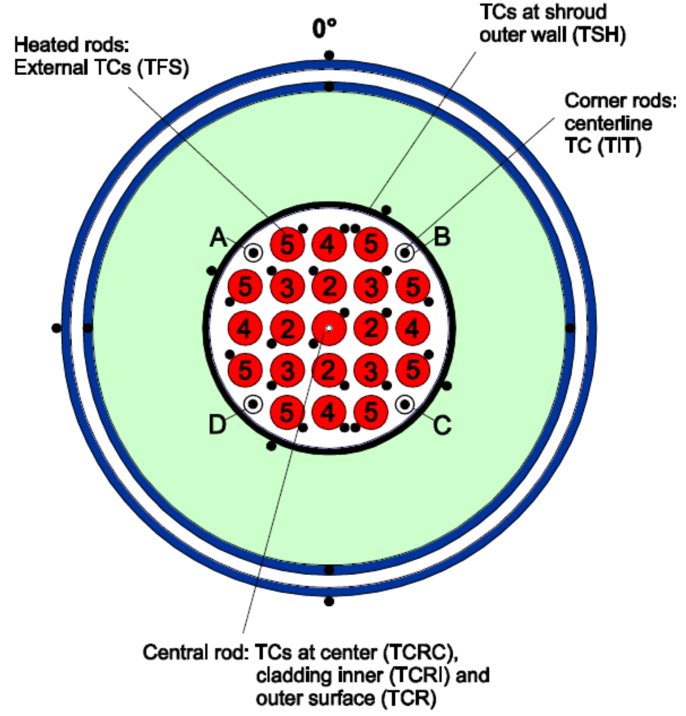

QUENCH-20

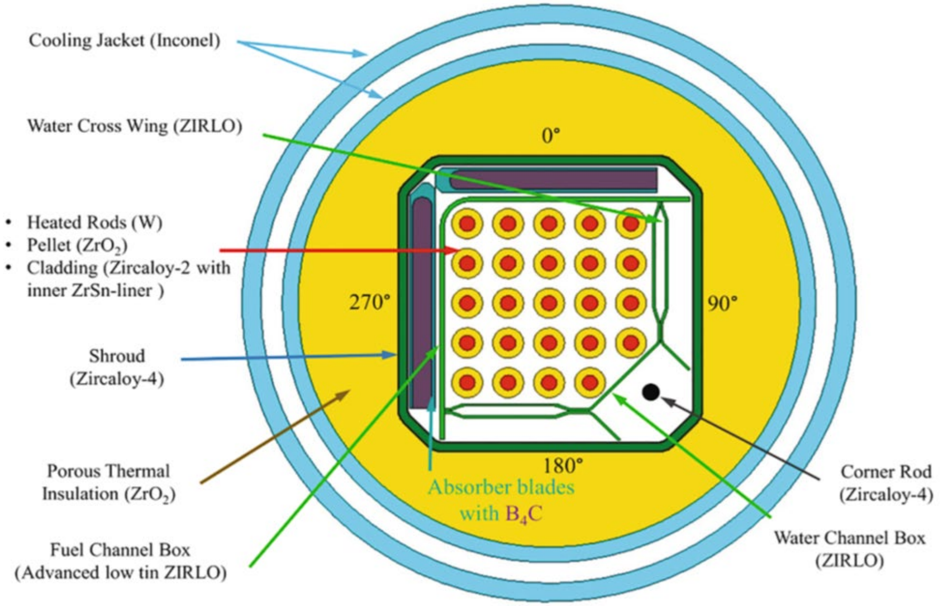

Axial profile of temperature

QUENCH-06

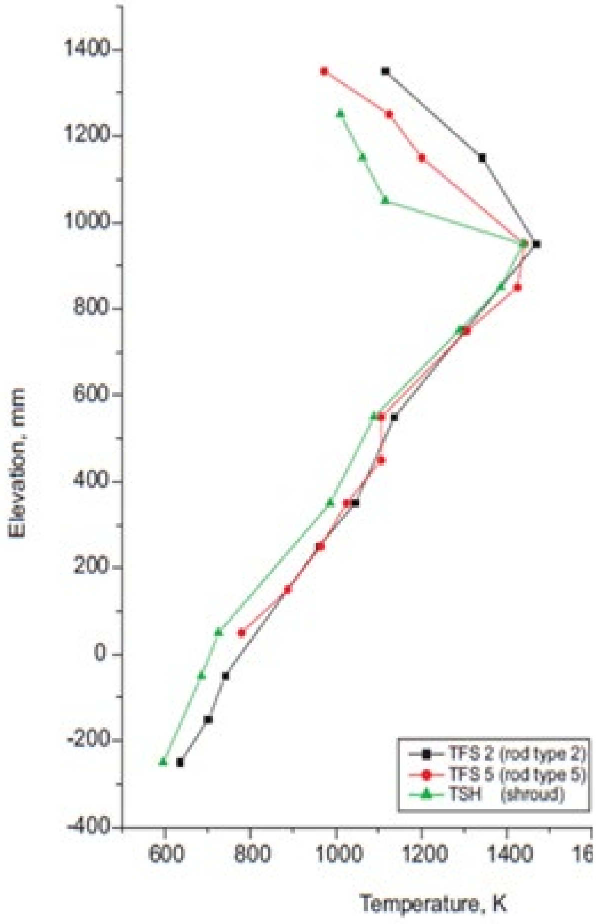

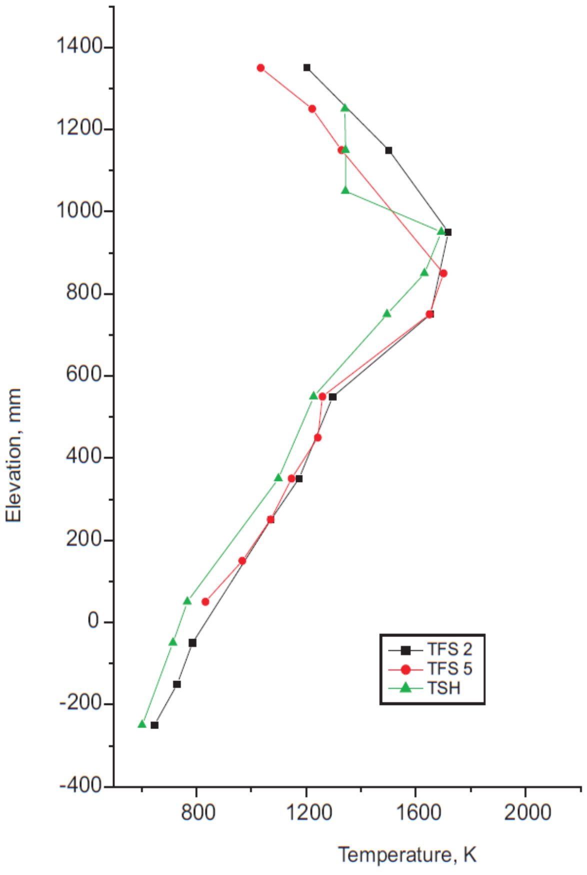

QUENCH-20

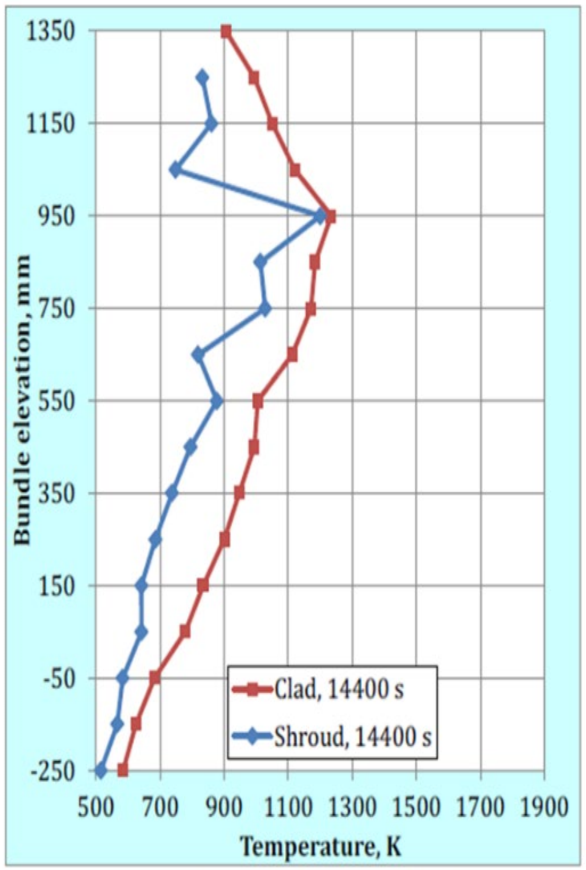

on the end of pre-oxidation (14400 s)

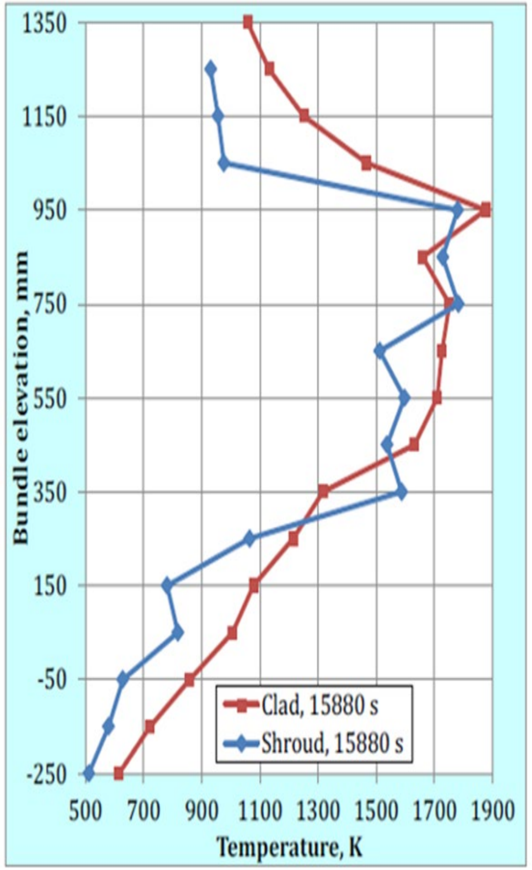

on the end of transient (15880 s)

Reactions of B_4C with steam (QUENCH-20)

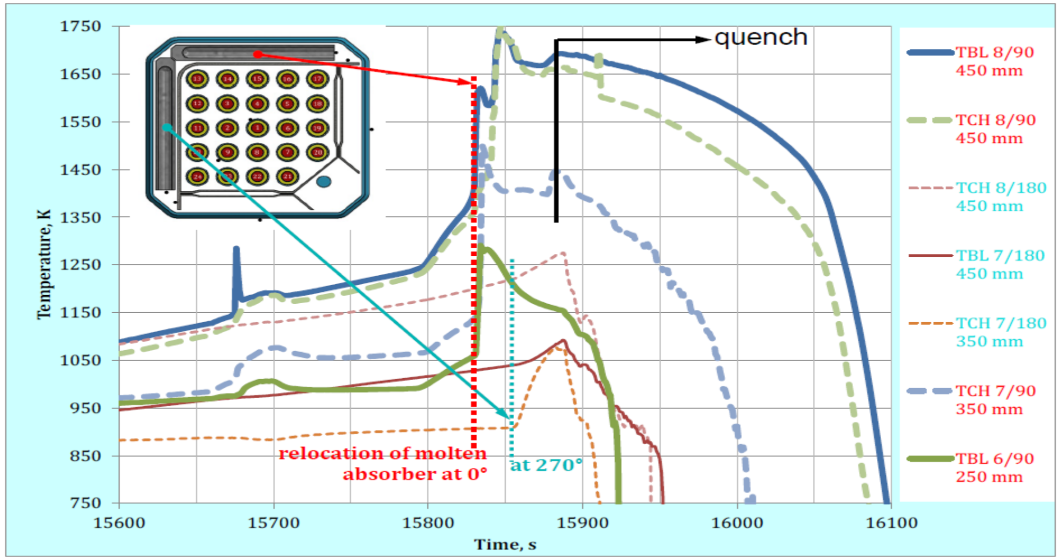

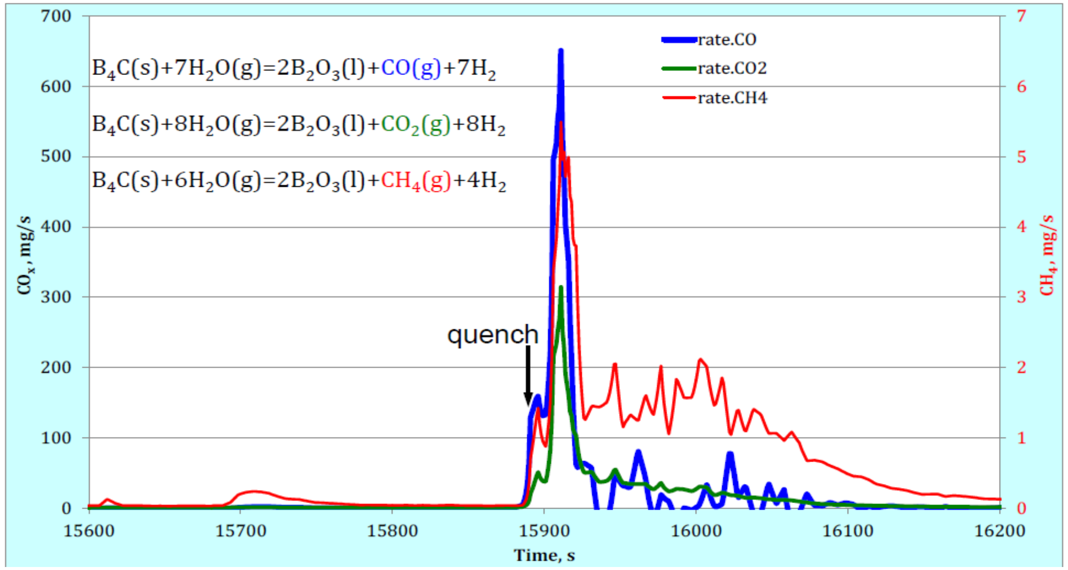

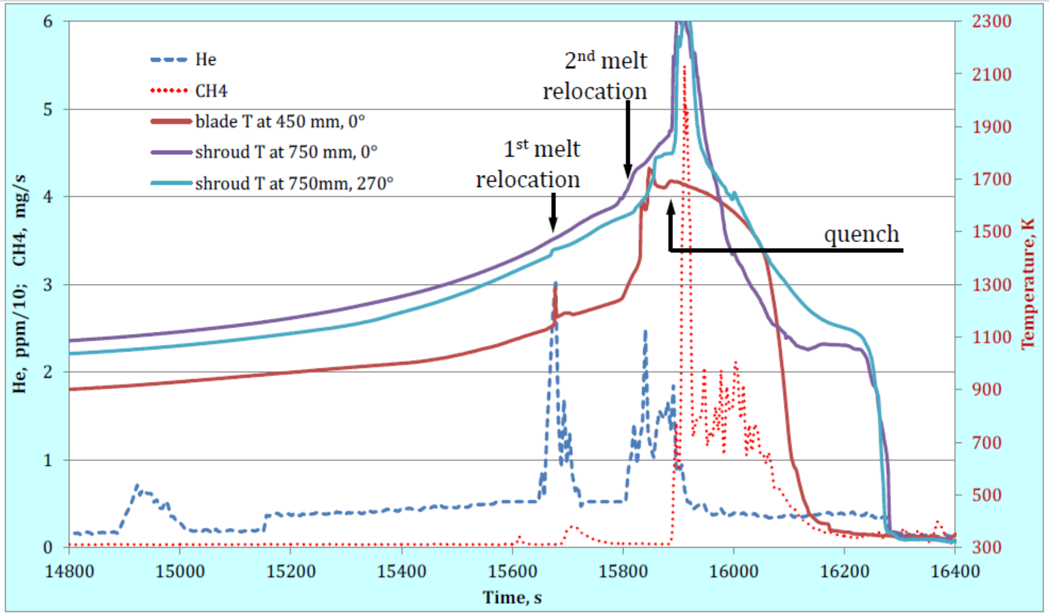

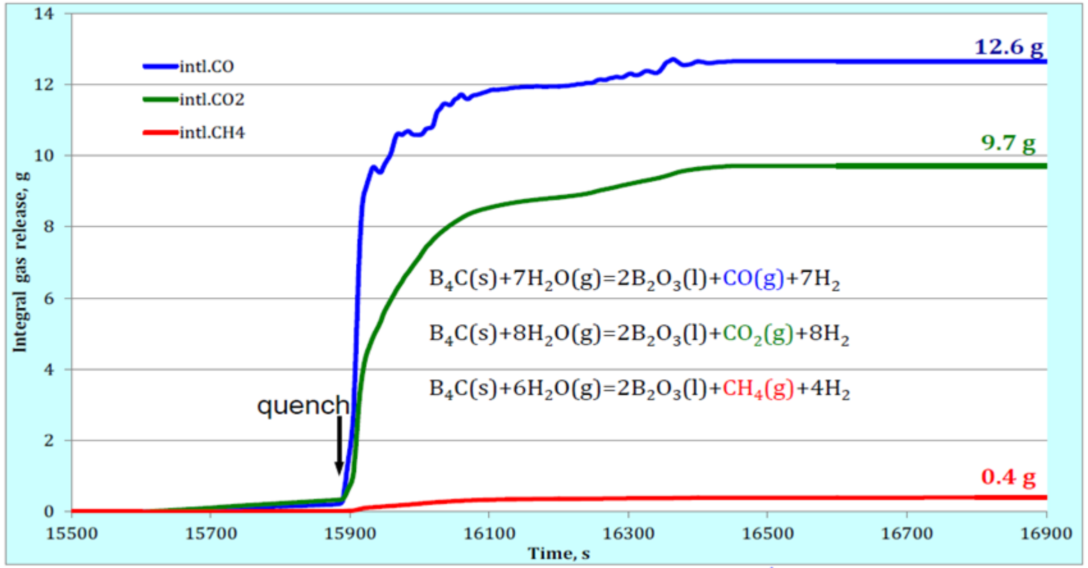

According to CO_x and CH_4 release: corresponding mass of B_2O_3 is 96.8 g; H_2 is 10.0 g

Shroud failure

QUENCH-06

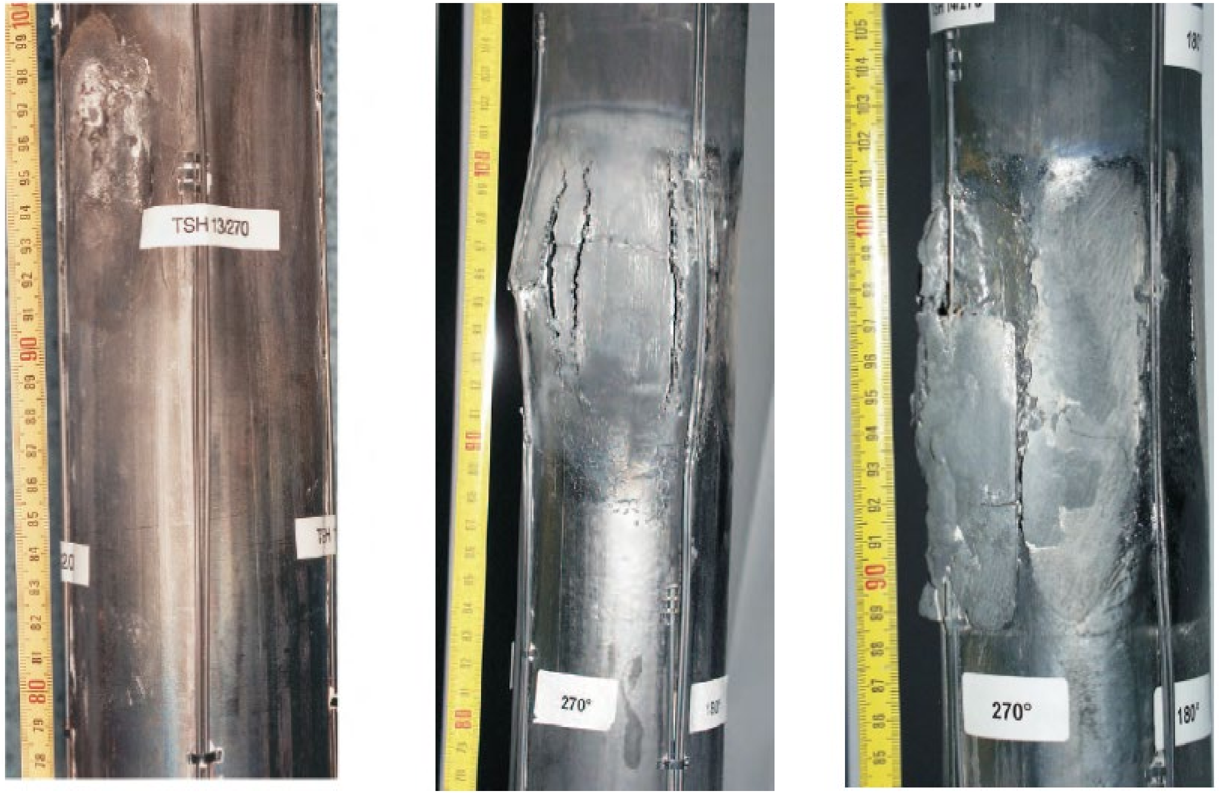

QUENCH-20

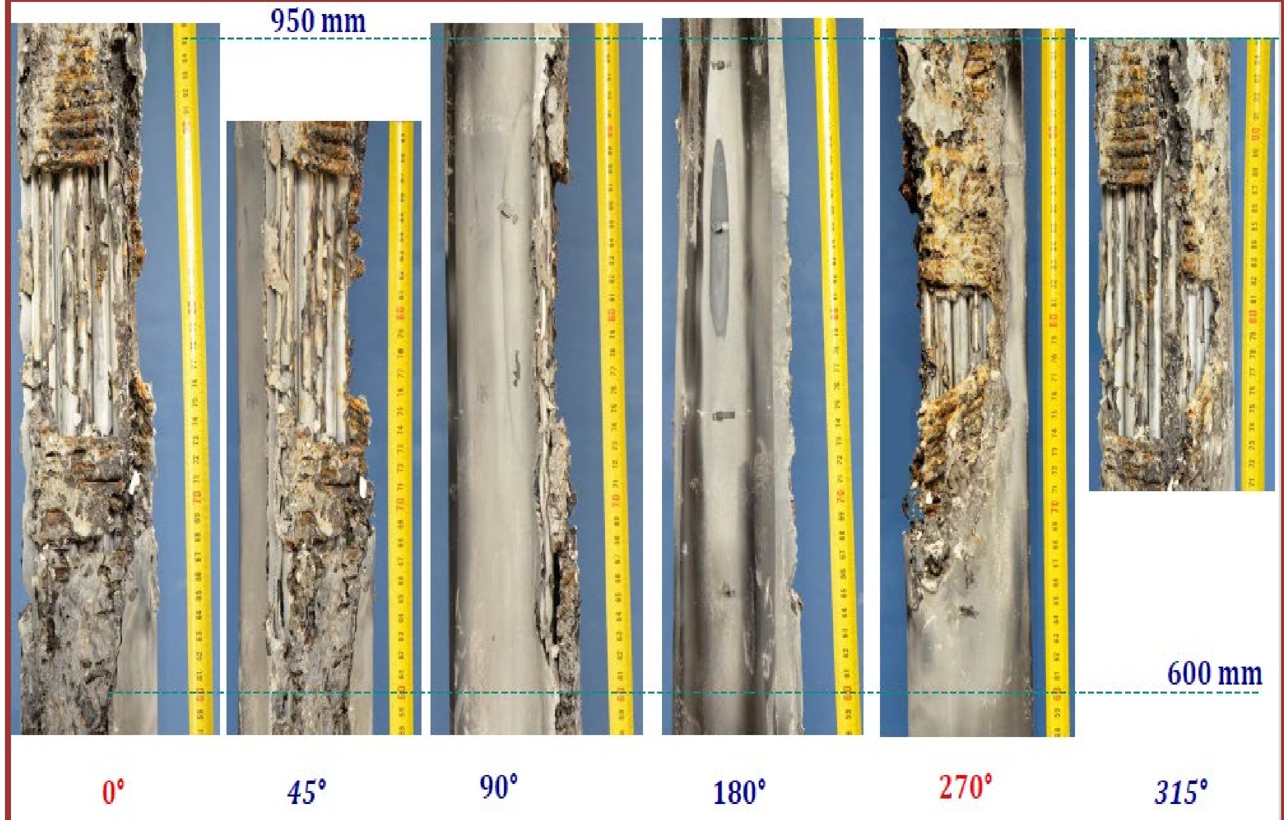

QUENCH-06 & QUENCH-20 Hydrogen generation

QUENCH-06

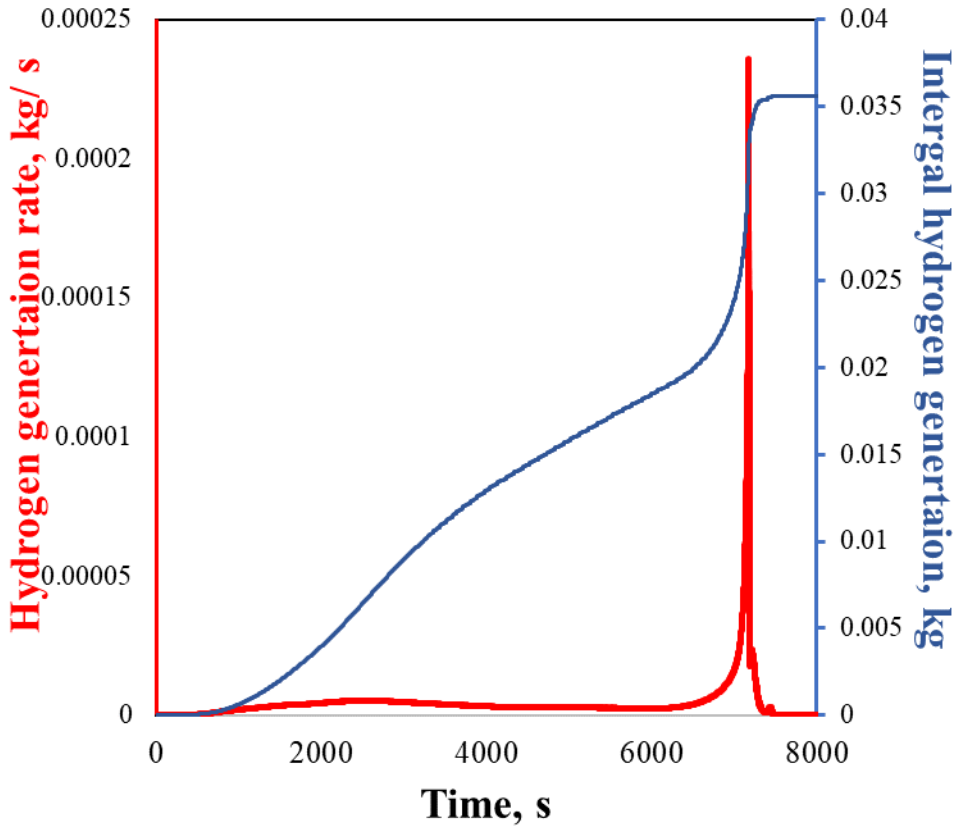

Before quenching – 32g;
After – 36g.

During quenching
4g

QUENCH-20

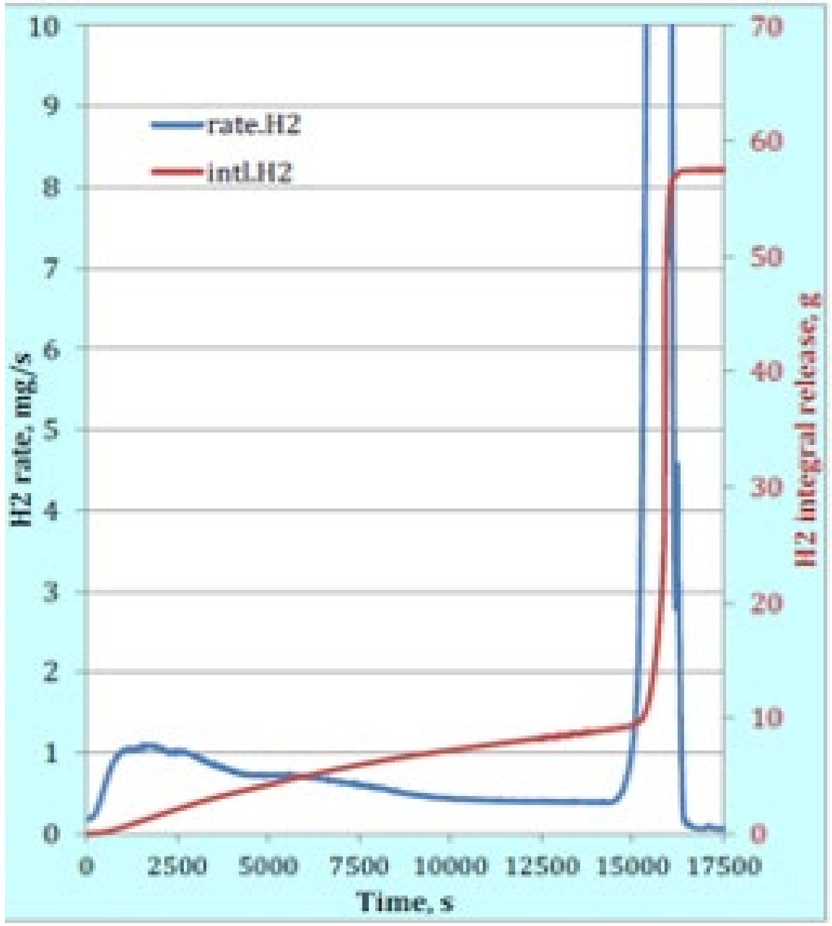

Before quenching – 25.4g;
After - 57.4g.

During quenching
32g

Conclusion

- The gained experience and knowledge form previous analysis could be used for new model development and calibration.
- The nodalization scheme of RELAP part from the previous analysis could be used the same for QUENCH-20 test.
- The bundle nodalization (SCDAP part) should be developed new in order to correctly respond physical phenomena during the test.
- The geometrical arrangement of the bundle test section of QUENCH-20 (BWR type) is very challenging:
  - o Severe accident codes uses modeling approach based on concentric rings in order to simulate fuel.
  - o Challenge in modeling control blades and B4C reactions with steam.
  - o Possible large uncertainties in calculation results.

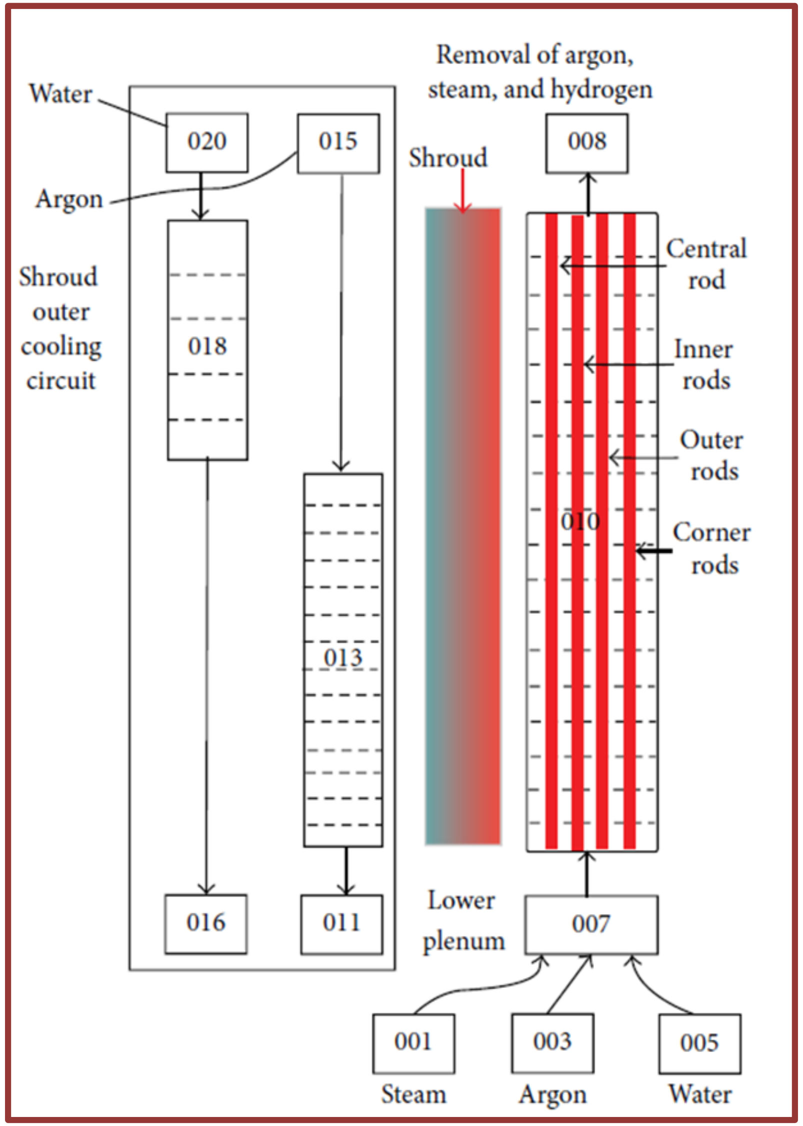

RELAP/SCDAPSIM Modelling of BWR and B4C

- RELAP/SCDAPSIM has the capability to model the absorber blades, channel box materials, B4C reaction and relocations.
- RELAP/SDCAPSIM mode 3.5 gave more realistic results in modeling the absorber blades relocations compared with experimental data than mode 3.4
- The relocation of control blade/channel box materials has a large deviation among code versions and has still large uncertainties.

- Madokoro, H. Sato.I, *Estimation of the core degradation and relocation at the Fukushima Daiichi Nuclear Power Station Unit 2 based on RELAP/SCDAPSIM analysis, Nuclear Engineering and Design*, 2020.
- Madokoro, H. Okamoto, K. Allison, C. Siefken, L. Hohorst, J. Hagen, S, *Assessment of RELAP/SCDAPSIM/MOD3.5 against the BWR core degradation experiment CORA-17,* Conference: The 10th International Topical Meeting on Nuclear Thermal-Hydraulics, Operation, and Safety (NUTHOS-10)At Okinawa, Japan 2014.
- Allison, C. Hohorst, J. Allison, B. Konjarek, D, Bajs. T, *Preliminary Assessment of the Possible BWR Core/Vessel Damage States for Fukushima Daiichi Station Blackout Scenarios Using RELAP/SCDAPSIM*, Hindawi Publishing Corporation Science and Technology of Nuclear Installations, 2012.

Currently, LEI have a license and using RELAP/SCDAPSIM version which is close to mod 3.4
ISS and LEI/KTU also were signed an agreement regarding RELAP/SCDAPSIM mod 3.6 (for Ph.D. student use only), however now the license is expired, and it is needed to ask for an extension.
Our plan is to use different versions of RELAP/SCDAPSIM for the QUENCH-20 analysis and to make comparisons and see possible improvements.

Nodilzation scheme of QUENCH developed for RELAP/SCDAP SA code

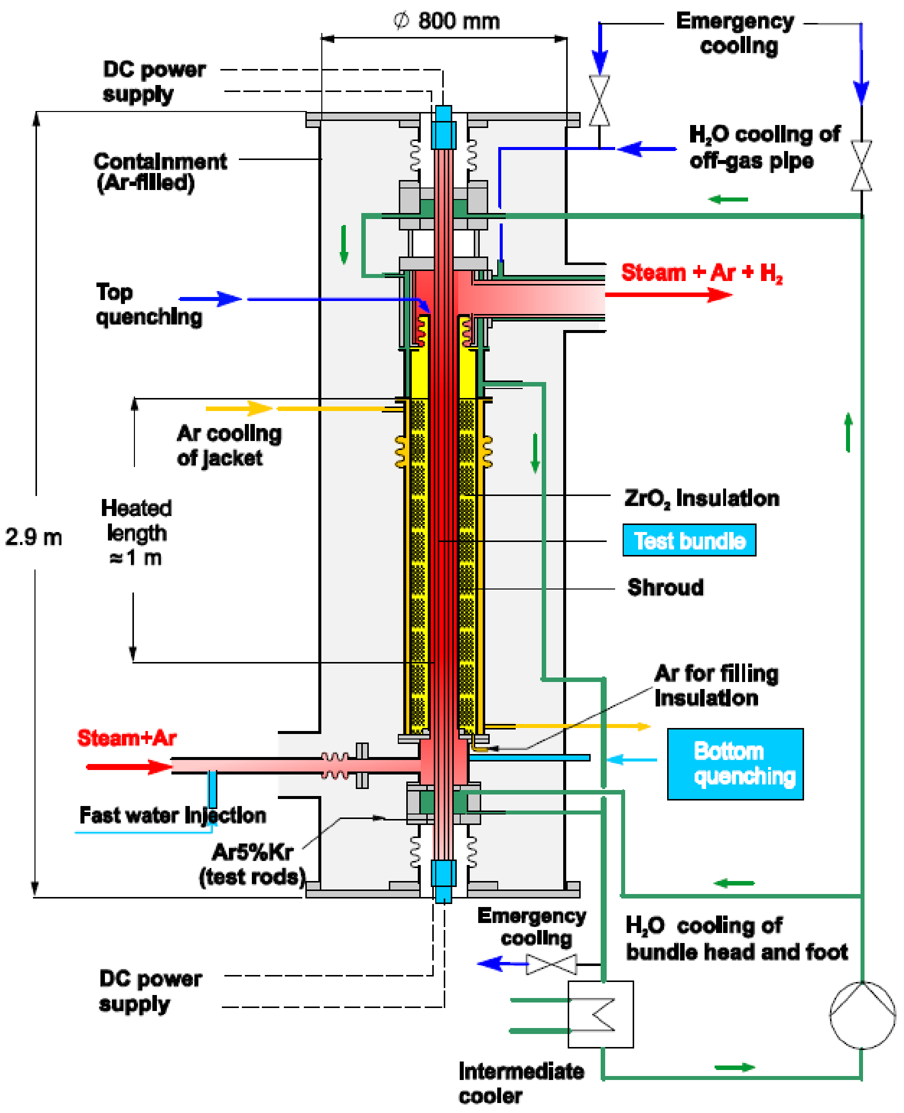

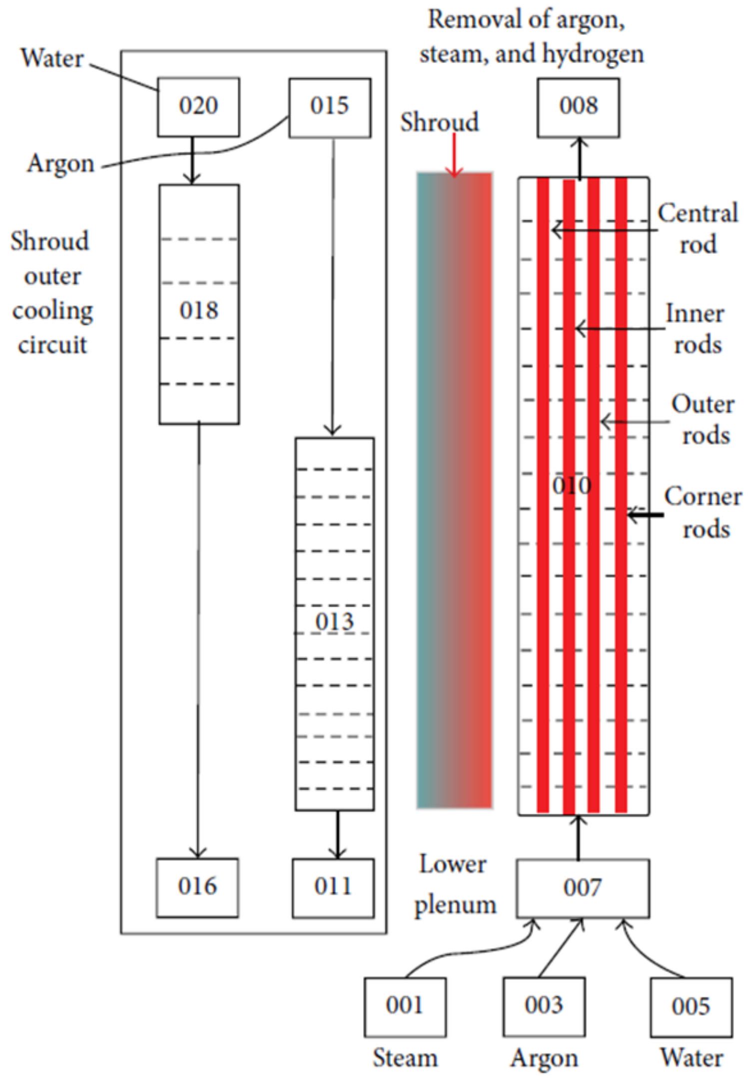

Thank you!

S. Khalil

Alexandria University

International Development and Assessment of a MATPRO-based Accident Tolerant Fuel Material Property Models and Correlation Library

As part of an on-going international IAEA cooperative research project on accident tolerant fuel (ATF) designs, the authors are leading an international team of university faculty members and graduate students, and other researchers to develop a publicly available material property library for accident tolerant fuel materials and designs. It will include the critical review and summary of relevant models and correlations described in the open literature, development of recommended modeling approaches and correlations for inclusion in fuel behavior models and codes, and assessment of the recommended approaches using publicly available integral and separate effects experiments. The recommended models and correlations will also implemented as an option for the MATPRO-based program library used in in a variety of steady state/transient fuel behavior codes including FUELSIM/SCDAPSIM (developed by Innovative Systems Software) and FRAPCON/FRAPTRAN (developed by the US NRC).

The material property library will, over time, expand to cover the wide range of materials and associated properties proposed for ATF designs for normal, design basis, and beyond design basis accident conditions for LWR and HPWR designs. The initial priorities for the project will be the definition of the properties for cladding materials including Fe and Zr alloys, coated Zr alloys, and SiC. The recommended models and correlations for these materials, as implemented in SCDAPSIM material property library, will be assessed using publicly available data from integral experiments such as the Quench-19 bundle experiment performed by the Karlsruhe Institute of Technology. Additional assessment will be performed over the coming 2-3 years using published data from separate effects and other integral experiments being performed as part of earlier and ongoing IAEA cooperative projects related to ATF. The assessment will also include the assessment of the impact of ATF materials on representative LWR/HPWR plant designs and transient conditions using such RELAP/SCDAPSIM and ASYST (an integral code used by the participants that includes SCDAPSIM).

International Development and Assessment of a MATPRO-based Accident Tolerant Fuel Material Property Models and Correlation Library

Presenter: Dr. Sarah Khalil

Nuclear and Radiation Engineering Department - Alexandria University

Content

- Introduction
- Motivation
- Collaborative effort
- Status of ATF M&C collaborative development
- Current work status at Alexandria University

Introduction

- RELAP/SCDAPSIM is a detailed RCS system analysis code with special options developed for user community

- RELAP/SCDAPSIM/ MOD3 and MOD4 used by general user community for production safety analysis
  - MOD3 recommended production version for combined coupled BE TH/fuel/severe accident analysis for LWR/HPWRs
  - MOD4.0 recommended production version for advanced BEPU TH and advanced fluid systems analysis

Introduction

- **RELAP/SCDAPSIM/MOD4 has the most advanced fluids modeling options for BEPU** (Best estimate plus uncertainty)
- Used for advanced model development and applications
- **Completely rewritten to FORTRAN 90/95/2000 standards** for easier model/code development and maintainability
- Includes **advanced system thermal hydraulics models and user options**
  - Integrated uncertainty analysis
  - Alternative fluids and correlations including Pb-Bi, Na, molten salts..
  - Advanced water property models and correlations
  - Links to 3D reactor kinetics
  - Advanced graphical user interfaces

Motivation

- IAEA CRP: Development and validation of ATF models and correlations
  - Material Property Summary Document
  - Associated Material Library

- Material property library developed for SCDAP/RELAP5 for LWR materials under DBA and BDBA no longer maintained by US NRC

ISS proposed "open source" material property library would be an extension of the widely used SCDAP/RELAP5 MATPRO library

Current Collaborative Effort

Current IAEA-CRP collaborators:

1. Nihon Onder - Chalk River National Laboratory
   - Support literature review and proposed models and correlations,
   - provide selected "open" material properties data and correlations for assessment
2. Alfredo Abe – IPEN – Brazil, Alejandro Soba – CNEA – Argentina
   - Support literature review and collection, perform model/correlation assessment
3. Bożena Sartowska – INCT – Poland
   - Support literature review and collection

Current Collaborative Effort

ISS and collaborative (non-CRP) team members backgrounds and proposed activities:

- Literature review, model development and assessment
- Preparation of reference RELAP/SCDAPSIM and ASYST integral
- Experiment and reference plant input models for DBA/BDBA Conditions

1. Rawan Mustafa (Materials/Quench integral experiment analysis) - Jordan Atomic Energy Commission
2. University of Alexandria –Sarah Khalil (materials) and Ayah Abou El- Naga (PWR TH analysis – DBA/BDBA), (4) PhD/MS students
   - Support literature review, review proposed models and correlations, perform small scale material properties experiments, analyze potential impact on plant behavior during DBA/BDBA conditions using RELAP/SCDAPSIM and ASYST
3. University of Mexico –Carlos Chavez (BWR TH analysis – DBA/BDBA)

Current Collaborative Effort

ISS and collaborative (non-CRP) team members backgrounds and proposed activities:

4. University Polytechnic Bucharest –Roxanna Mihaela Nistor-Vlad (CANDU TH analysis – DBA/BDBA)
5. University Polytechnic Catalunya/ENSO – Raimon Pericas (LWR TH and fuel behavior analysis (DBA/BDBA)

“Open source” material property library extension to MATPRO

Materials include uranium, uranium dioxide, mixed uranium-plutonium, dioxide fuel, zircaloy cladding, zirconium dioxide, stainless steel, stainless steel oxide, silver-indium-cadmium alloy, cadmium, boron carbide, Inconel 718, zirconium-uranium-oxygen melts, fill gas mixtures, carbon steel, tungsten, tantalum.

* Publicly available, peer-reviewed ATF correlations added to cover thermal and mechanical properties, chemical interactions, phase diagrams.

Status of ATF M&C Collaborative Development

- Literature review is underway for peer-reviewed, publicly available papers and documents

- ATF material property models and correlations would be documented in a form comparable to that used in the MATPRO NUREG *(Assessed BEPU)* (*and preferably published a publicly available IAEA document after standard IAEA peer review*

- ATF models and correlations would be initially incorporated into ISS maintained MATPRO library for distribution to interested CRP participants
  - Original SCDAP/RELAP5 MATPRO library updated by ISS for RELAP/SCDAPSIM and ASYST for latest FORTRAN standards

Current work status at AU

1. Research:
   - Neutronics and Thermal Hydraulic analysis of Fully Ceramic Microencapsulated (FCM) fuel with enhanced accident tolerance features in small integral pressurized water reactor with 330 MWth power (SMART reactor)

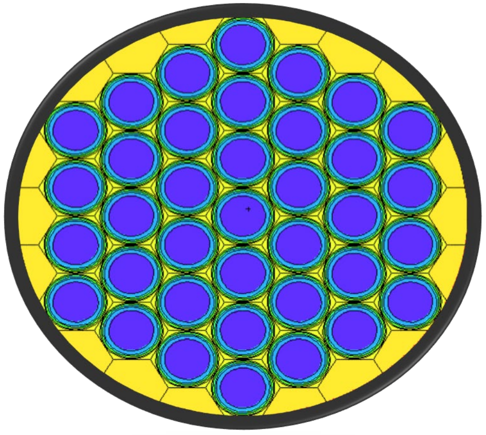

2. Materials Models and Correlations:
   - Mechanical Failure of FeCrAl Cladding in ATF
   - Oxidation of FeCrAl cladding during operation and on the onset of melting

Research

- <u>Objective:</u>

Investigating the use of UC with FeCrAl (as an ATF) to replace zirconium-UO_2 in SMR at normal operation conditions, by performing neutronic/thermal-hydraulic analysis for

- <u>Methodology:</u>

- Use of MCNPX 2.7.0 to obtain reactor physics parameters for FCM with FeCrAl cladding
- Calculating thermal-hydraulic parameters such as pressure drop in the core, surface heat flux, fuel centerline and coolant temperatures using RELAP code.

Research

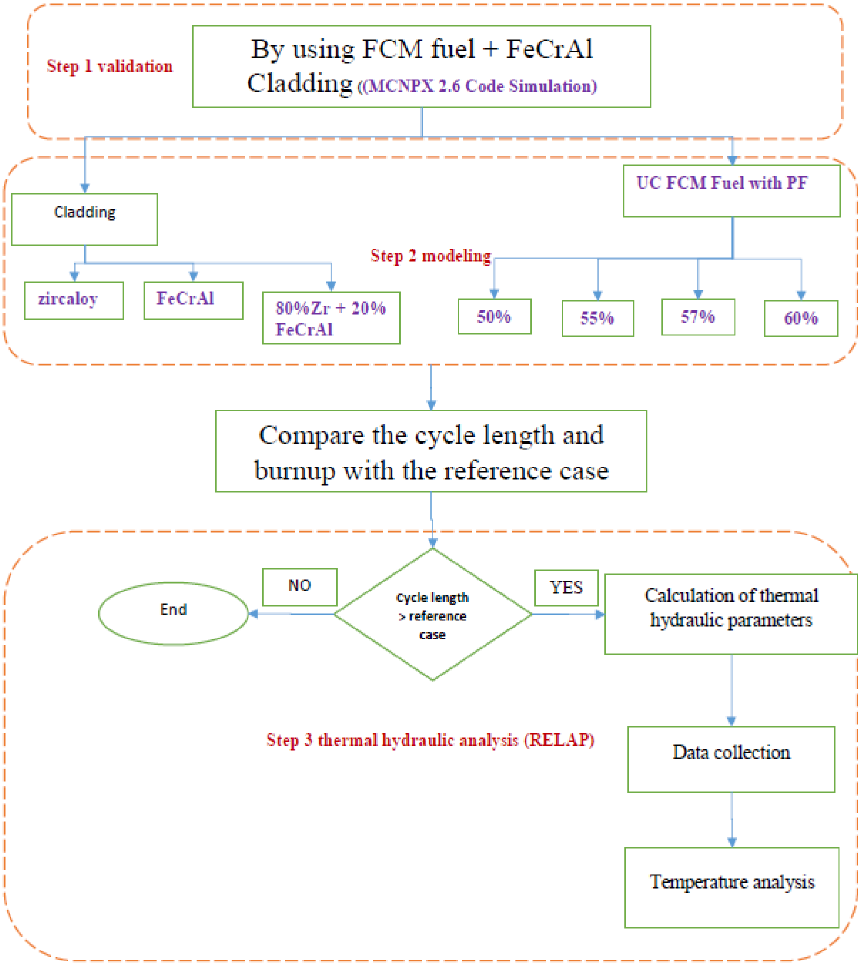

Step 1 validation
By using FCM fuel + FeCrAl Cladding ((MCNPX 2.6 Code Simulation)
Cladding
UC FCM Fuel with PF
Step 2 modeling
zircaloy
FeCrAl
80%Zr + 20% FeCrAl
50%
55%
57%
60%
Compare the cycle length and burnup with the reference case
End
NO
Cycle length > reference case
YES
Calculation of thermal hydraulic parameters
Step 3 thermal hydraulic analysis (RELAP)
Data collection
Temperature analysis

Research

Neutronics Calculations

Multiple cases are tested to determine the optimum fuel design from the reactivity point of view

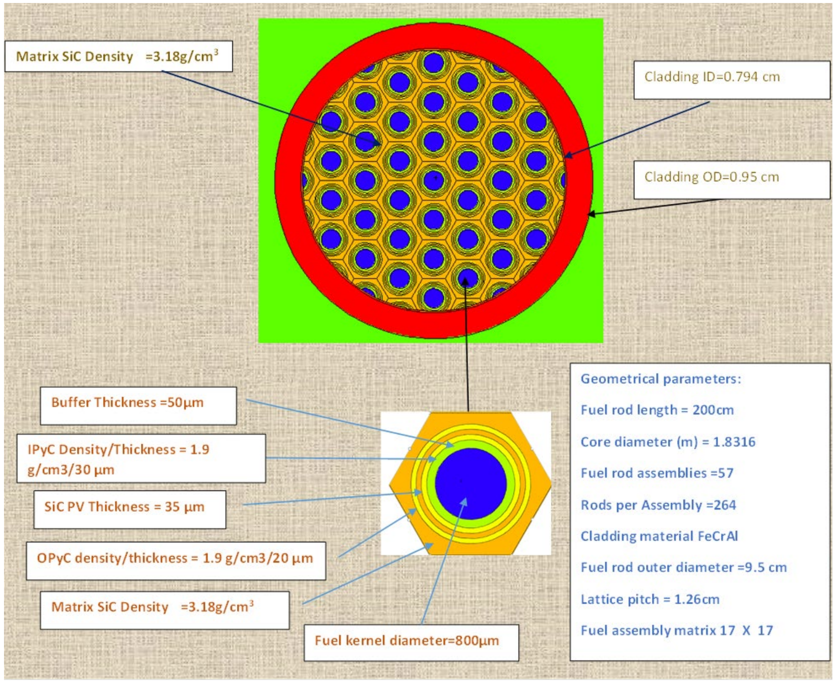

cases	1,2	3,4,5	6,7,8	9,10,11	12,13,14,15	16,17,18,19
Kernel diameter (µm)	870	880	890	900	900	920
Packing fraction	50,55	50,55,57	50,55,57	50,55,57	50,55,57,60	50,55,57,60

Research

Preliminary results

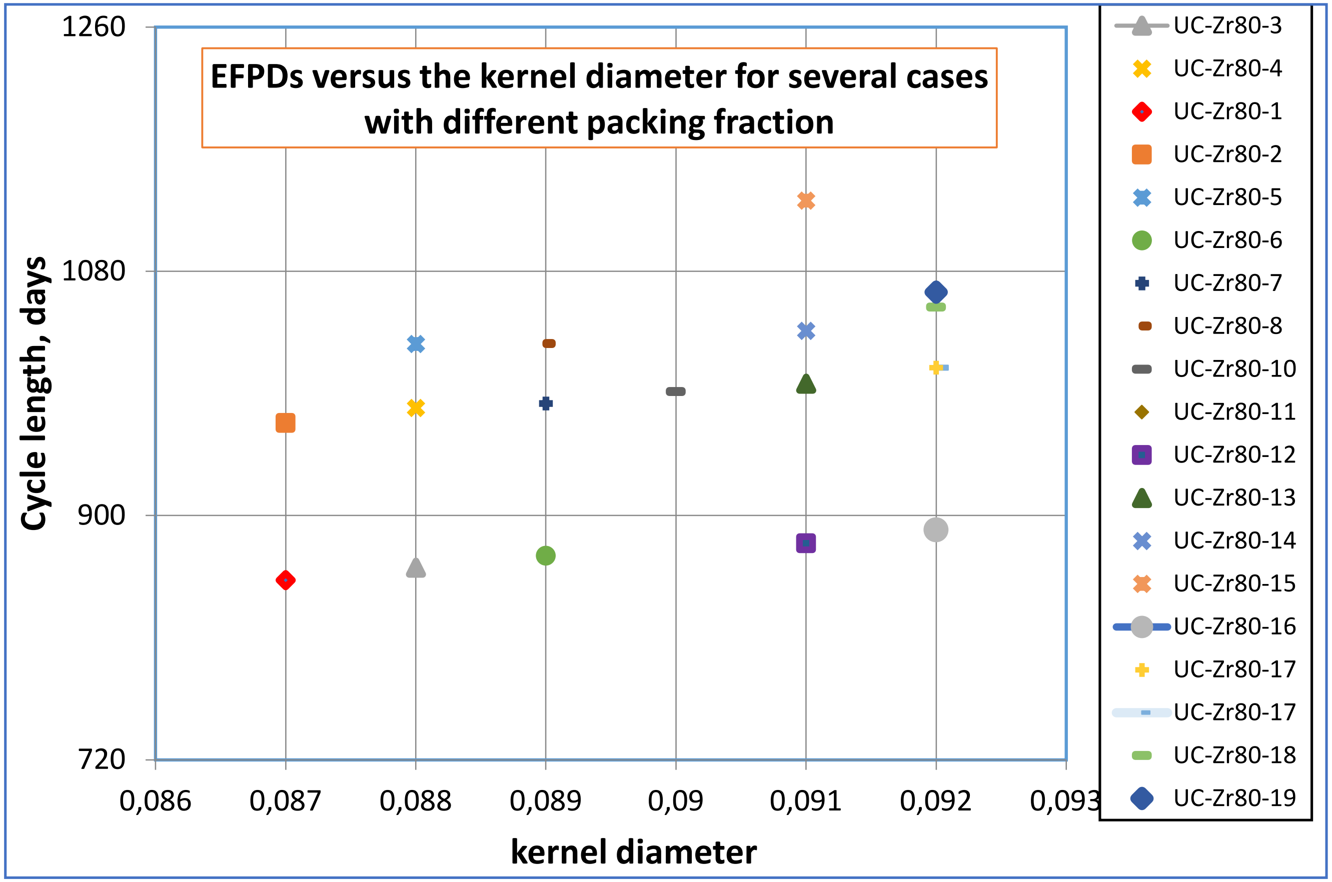

Oxidation Correlations
Gross Weight Gain

$$GWG = ae^{bx}$$

a	0.203456
b	1.017619

R2	0.9925
SD	24.413
RMSE	0.1203
RE	-0.211
AE	16.568

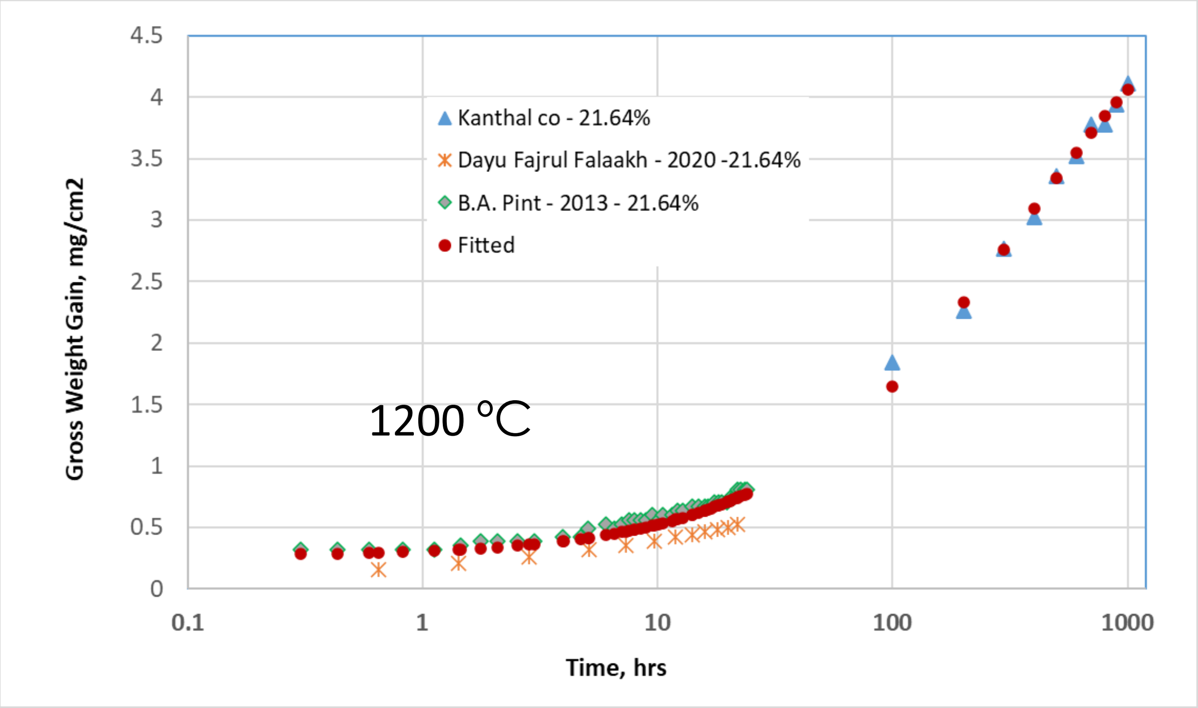

$$GWG = a + bt + ct^2 + dt^3 + e/t$$

a	1.267709
b	-0.000386
c	0.000003
d	-1.94E-09
e	-24.222905

R2	0.9963
SD	21.372
RMSE	0.0842
RE	-3.175
AE	13.859

Oxidation Correlations Gross Weight Gain

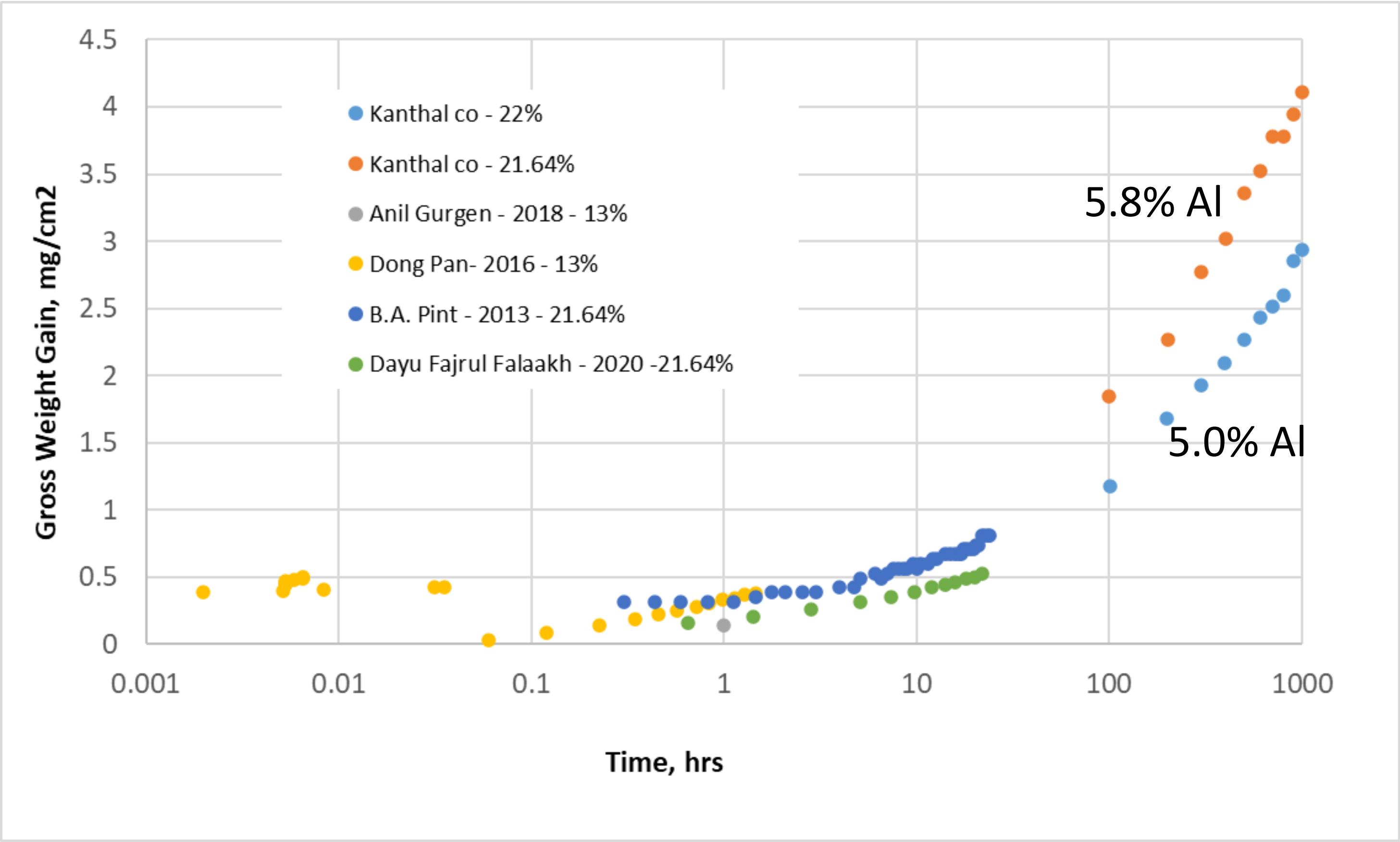

Oxidation Correlations
Gross Weight Gain

- Data Sensitivity

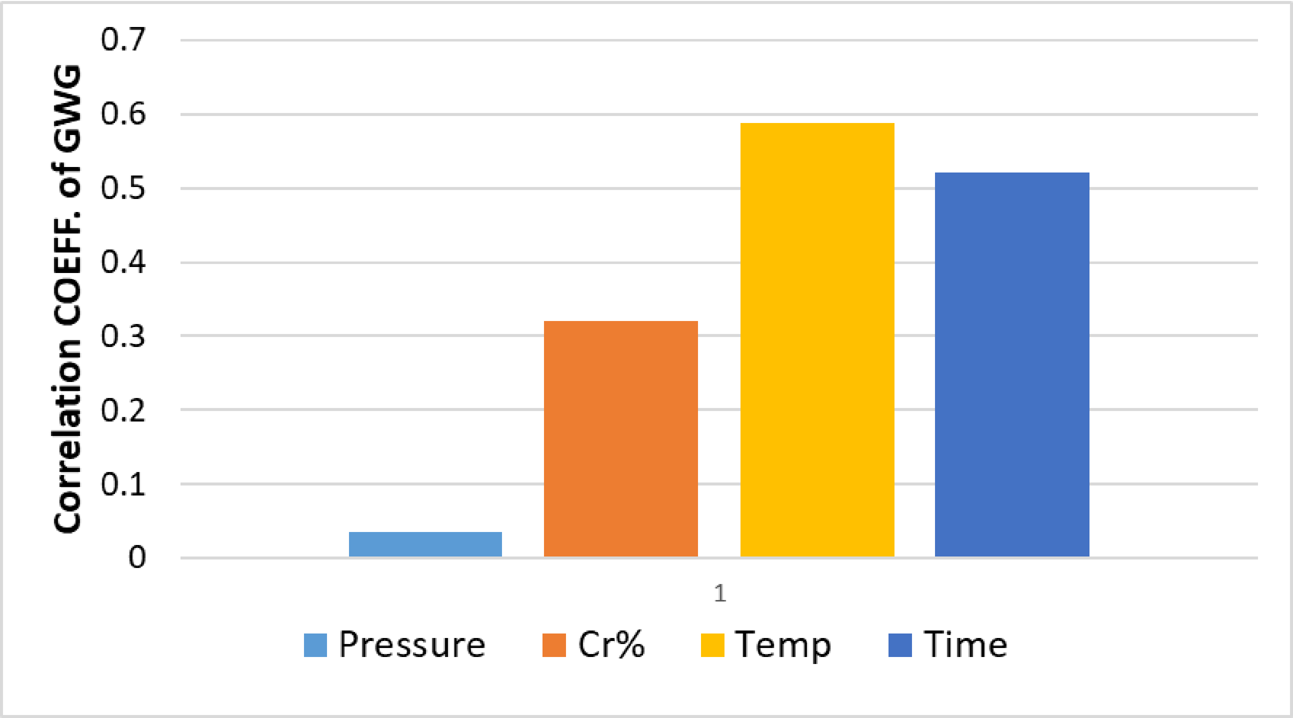

Concluding remarks

- Development and assessment of comprehensive material property library is a **long term project extending beyond CRP**
  - Implementation and assessment of ATF M/C for ISS and non- CRP collaborators will initially focus on Quench and other publicly available integral experiments

- **Assessment** of library accuracy and uncertainties and potential impact on DBA and BDBA behavior **depends on continued emphasis on integral and separate effects experiments**

F. Gabrielli[1], T. Hollands[2], L. Lovasz[2],
L. Carénini[3], D. Luxat[4], J. Phillips[4]

[1] KIT
[2] GRS
[3] IRSN
[4] SNL

International Development and Assessment of a MATPRO-based Accident Tolerant Fuel Material Property Models and Correlation Library

A range of Accident Tolerant Fuels (ATFs) are currently under study and testing worldwide to realize an alternative to Zirconium based claddings. This research is motivated by the potential for significant safety and performance improvements during normal operations, operational transients, and also accident events in Light Water Reactors. Such new materials are characterized by a much slower oxidation kinetics at high temperatures than the typical Zr-based alloy leading to lower in-vessel hydrogen build-up and energy generation as well as suppressing hydrogen explosions and Fission Product release. This results in extended times available to mitigate progression to a severe accident. This enhances the potential to activate or utilize accident management measures.

To enable safety assessment of nuclear systems employing ATFs, it is essential that code capabilities to model these novel fuel system material concepts be improved, with particular attention to the implementation and validation of representative oxidation kinetics models. Having this in mind, the current paper mainly aims at describing the status of the capabilities of the AC2/ATHLET-CD, ASTEC, and MELCOR severe accident codes to model the performance of materials in ATF systems under harsh accident conditions. The outcomes of preliminary studies on code validation of the QUENCH-19 (FeCrAl) experiment will also be shown and discussed. The results show that the code are able to reproduce with an acceptable level of confidence the experimental temperatures during the transient. Furthermore, hydrogen generation predictions may significantly vary due to the sensitivity of oxidation characteristics to FeCrAl composition.

ATF modelling in Severe Accident Codes

F. Gabrielli[1], T. Hollands[2], L. Lovasz[2], L. Carénini[3], D. Luxat[4] and J. Phillips[4]

[1] Karlsruhe Institute of Technology (KIT), [2] Gesellschaft für Anlagen- und Reaktorsicherheit (GRS) gGmbH

[3] Institut de Radioprotection et de Sûreté Nucléaire (IRSN), [4] Sandia National Laboratories (SNL)

Institute for Neutron Physics and Reactor Technology

Motivation

- ATFs have the potential for significant safety and performance improvements during normal/transient operations and severe accidents in Light Water Reactors.
- Much slower oxidation kinetics at high temperatures than the typical Zr-based alloy
  - → lower in-vessel H_2 build-up, lower energy generation, suppression of the H_2 explosions potential, Fission Product release reduction.

→ Enhancing the potential to activate/utilize accident management measures.

- Improvement of the severe accident codes capability to model ATFs is mandatory to enable the safety assessment of the innovative nuclear reactor concepts employing such materials.
- Extension of the modelling capabilities of AC^2/ATHLET-CD, ASTEC, and MELCOR is going on in the frame of the NEA QUENCH-ATF and IAEA CRP ATF-TS.
- In this phase, focus on FeCrAl and QUENCH-19 test.

Modeling New Materials in the SA Codes

- User usually employs the data stored in the available material database, i.e. for Zry/ZrO_2
  - Thermo-physical properties.
  - Oxidation models, i.e. Cathcart, Prater-Courtright, Urbanic, Best-fit,..
- The codes are flexible enough to introduce new materials either by adjusting the properties of a default material or to fully define behavior and properties by scratch.
- Current approach:
  - FeCrAl as a new material.
  - FeCrAl to be oxidizable.
  - FeCrAl/Oxide as the FeCrAl recipient oxide, whose properties defined based on the literature and on the feedback from the Quench experimental team.

MELCOR: Material Package (MP) Templating

- Material definition no longer requires a user to perform the two most common modification to materials.
  - Since core components only support certain material internally, users had to modify an existing material to alter properties, losing that material.
  - Create a wholly new material, which could only be used within the certain MELCOR packages such as the HS materials.
- It allows materials to assume a default material's behaviors and properties.
- Four core package user defined materials (UDMs) now available within the database for every core component → enhancement of the user flexibility.

```
MP_ID FeCrAl COR-USER-METAL UFCA
MP_BHVR ITSELF METAL OXIDATION-MODEL EJ-ZIRCALOY
MP_PRC   7100.0 1773.0  270000. .05223883683
MP_BETMU 3.1e-5 3313. 1.076e-3
MP_COREMIS linear - 0.0001 0.9999 0.042003702 0.0003474
MP_PRTF 4
     1 ENH FCA-IntEn
     2 CPS FCA-SpHeat
     3 THC FCA-Conduct TF
     4 RHO FCA-Density

MP_ID FeCrAl-Oxide COR-USER-OXIDE UFCAO
MP_BHVR ITSELF
MP_PRC 5180.0 1901.0 687463.0 0.08356138524
MP_COREMIS linear - 0.0 1.0 0.7 0.0
MP_BETMU 3.1e-5 3313. 1.076e-3
MP_PRTF 4
     1 ENH FCAO-IntEn
     2 CPS FCAO-SpHeat
     3 THC FCAO-Conduct TF
     4 RHO FCAO-Density
```

J. Phillips, D. Luxat, 2020. MELCOR Modeling of QUENCH-15/19, Experts' Meeting for the NEA joint undertaking QUENCH-ATF, OECD/NEA, Paris.
J. Phillips, 2020. Update on ATF Modeling: QUENCH-15/19, CSARP/MCAP Workshop.

ASTEC: Material Modeling

- User may define a new material in the input deck

```
STRU MDB
  STRU SET NAME 'Ar_cond'
    REF   "Properties of fictive material"
    TYPE  'MATERIAL'
    T_sol 5000.   T_liq 5001. M 1. ! always solid
    STRU PROPERTY NAME "rho_s(T)" LAW 'TABLE' VARIABLE 'T' SR1 VALUE  300.  2.0  2000.0 2.0  TERM END
    STRU PROPERTY NAME "lambda_s(T)" LAW 'TABLE'    VARIABLE 'T'
    SR1 VALUE  300.  0.2  800. 3.5  1060. 5. 1100 5. 1500. 10.0 2000. 20.0 TERM  END
    STRU PROPERTY NAME "h_s(T)" LAW 'TABLE' VARIABLE 'T'
    SR1 VALUE  300.  961.   900.  3.1D5 1500. 6.2D5  2000. 8.8D5 3000.  14.D5  4000. 19.D5  TERM END
    STRU PROPERTY NAME "em_s(T)" LAW 'TABLE' VARIABLE 'T' SR1 VALUE  300.  0.7 4000. 0.7  TERM END
  END
END
```

- or modifying the database

```
 HELP "m_O   (t+dt) = S ((m_O   (t)/S)**(1/model) + AGAIN EXP(-BGAIN/(R.T)) * dt )**model"
 HELP "e_O2Zr(t+dt) =   ((e_O2Zr(t))  **(1/model) + ATHIC EXP(-BTHIC/(R.T)) * dt )**model"
…..
STRUCTURE MODEL NAME 'BEST-FIT' LAW 'COEFF' VARIABLE 'T' VUNIT 'K' RUNLOW 0. RUNUPP 5000.
  SRG VALUE AGAIN 36.220D0 BGAIN 1.672D5 ATHIC 2.252D-6 BTHIC 1.502D5 MODEL 0.5 TERM
  X  1798.K
  SRG VALUE AGAIN 2.888D8 BGAIN 4.046D5 ATHIC 3.371D6 BTHIC 5.691D5 MODEL 0.5 TERM
  X  1900.K
  SRG VALUE AGAIN 2849.D0 BGAIN 2.23D5 ATHIC 0.008682D0 BTHIC 2.572D5 MODEL 0.5 TERM
 END
```

AC²/ATHLET-CD: FeCrAl Oxidation Model

- Assumption: Al oxidized only

$$Fe_xCr_yAl_z + z/2\cdot 3\ H2O \rightarrow Fe_xCr_yAl_{2z}O_{3z} + z/2\cdot 3\ H_2 + z\cdot\Delta h\ (\Delta h = 9.3\cdot 10^5\ J/mol)$$

- FeCrAl molar mass $M_{FeCrAl} = 99.3\cdot 10^{-3}$ kg/mol ($\Delta h = 9.36\cdot 10^6\ J/kg_{FeCrAl}$)

  $\rightarrow M_{Al2O3} = 102.0\cdot 10^{-3}$ kg/mol

- Oxidation Rate → Parabolic law derived from the analytical solution of the diffusion equation (as for Zr)

$$\mathbf{dW^2=K(T)\cdot dt}\ (W: m_{O2}/A\ [kg/m^2],\ K: \text{reaction rate } [kg^2/m^4s],\ t: \text{time } [s])$$

- Reaction rate from the Arrhenius formulation

$$K = A\cdot e^{-B/(RT)} g(p_s)$$

R=8.134 J/mol K, T: cladding Temperature [K], $g(p_s)$: reduction factor for steam starvation

A= 3.1 kg²/m⁴s, B= 2.78519 ·10⁵ J/mol (from KIT for one composition)

T. Hollands, 2020. Post-test analytical benchmarks–GRS simulation capabilities –, Experts' Meeting for the NEA joint undertaking QUENCH-ATF, OECD/NEA, Paris.

AC^2/ATHLET-CD: FeCrAl Oxidation Model

- FeCrAl/Al_2O_3 instead of Zry/ZrO_2 properties.
  - No temperature dependency considered
- Model 25 is based on a publication by Pint, et al., for KANTHAL APMT (69Fe+21.6Cr+4.9Al) and provided by KIT.
- Model 25 multiplied by 300 is derived from the ”State-of-the-Art Report on Light Water Reactor Accident-Tolerant Fuels“ of the OECD/NEA (NEA No. 7317).
- The new code version includes the possibility to implement additional correlations including enthalpy

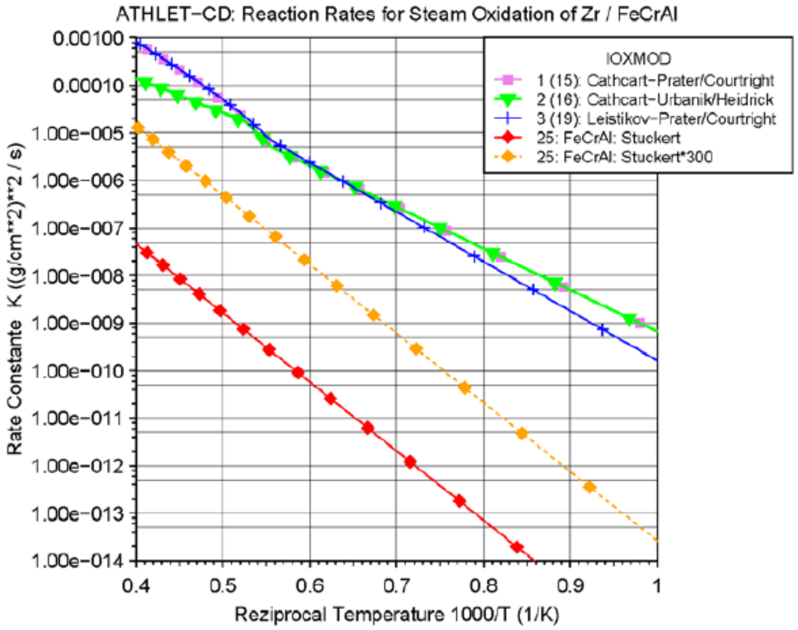

T. Hollands, 2020. Post-test analytical benchmarks–GRS simulation capabilities –, Experts’ Meeting for the NEA joint undertaking QUENCH-ATF, OECD/NEA, Paris.
Pint, B.A., et al., High Temperature Oxidation of Fuel Cladding Candidate Materials in Steam-Hydrogen Environments, Journal of Nuclear Materials 440, pp. 420-427, 2013.

MELCOR: FeCrAl Oxidation Model

- Based on prior work by INL/ORNL
- Reaction rates apply data from Pint, et.al., prior to breakaway.
  - Oxygen uptake data is converted to metal reacted and standard units.
  - Must assume prevailing oxides to convert from oxygen to metal reacted.

    $FE+4/3 \cdot H2O \rightarrow 1/3 \cdot Fe_3O_4+4/3 \cdot H2$
    $CR+3/2 \cdot H2O \rightarrow 1/2 \cdot Cr_2O_3+3/2 \cdot H2$
    $AL+3/2 \cdot H2O \rightarrow 1/2 \cdot AL_2O_3+3/2 \cdot H2$

  - **$K=4360 \cdot e^{-(41376/T)}$**

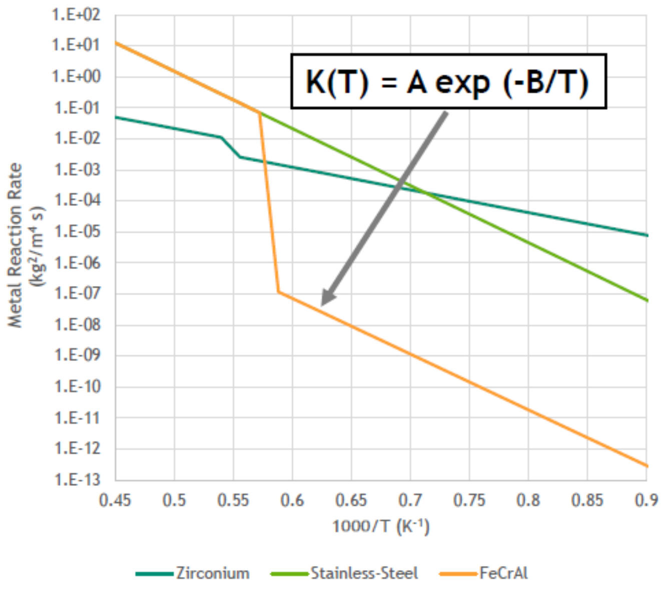

- New MELCOR modeling allows specifying all the reaction parameters

Merrill, B.J., Bragg-Sitton, S.M., Humrickhouse, P.W., Modification of MELCOR for Severe Accident Analysis of Candidate Accident Tolerant Cladding Materials, NED 315 170-178. 2017.
Robb, K.R., Howell, H., and Ott, L.J., Design and Analysis of Oxidation Tests to Inform FeCrAl ATF Severe Accident Models, Oak Ridge National Laboratory, ORNL/SPR-2018/893 (July 2018).
Pint, B.A., et al., High Temperature Oxidation of Fuel Cladding Candidate Materials in Steam-Hydrogen Environments, Journal of Nuclear Materials 440, pp. 420-427, 2013.
Phillips, J., Luxat, D., 2020. MELCOR Modeling of QUENCH-15/19, Experts' Meeting for the NEA joint undertaking QUENCH-ATF, OECD/NEA, Paris.
Phillips, J., 2020. Update on ATF Modeling: QUENCH-15/19, CSARP/MCAP Workshop.

ASTEC: FeCrAl Oxidation Model

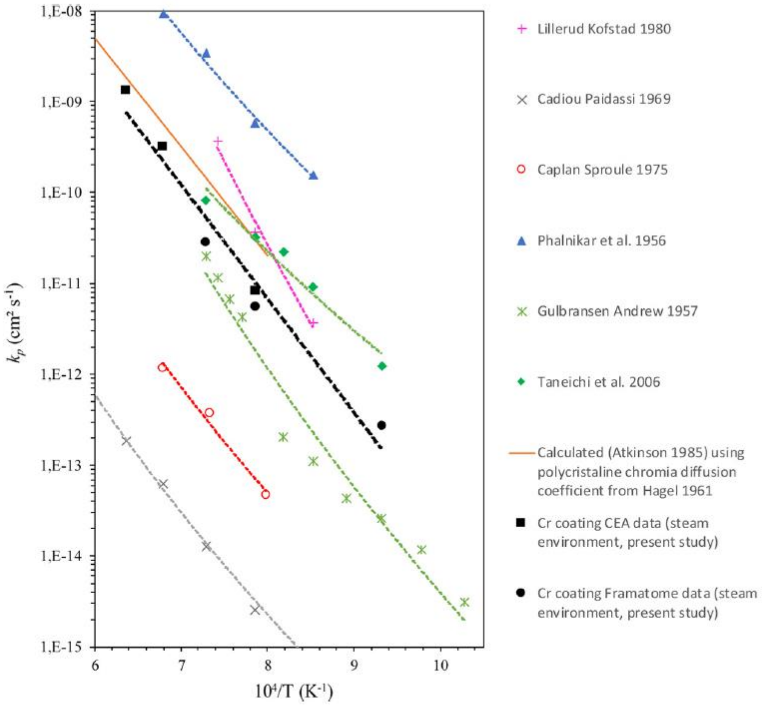

- **Brachet data considered.**
- **Fitting functions for weight gain and thickness grown of the oxide layer provided by J. Stuckert**

$$\boxed{\delta = 0.00377 \cdot e^{-\frac{123783}{R \cdot T}} \cdot \sqrt{t}}$$

$$\boxed{\Delta m = 19.62 \cdot e^{-\frac{123783}{R \cdot T}} \cdot \sqrt{t}}$$

Brachet, J.-C., et al., 2020. High temperature steam oxidation of chromium-coated zirconium-based alloys: Kinetics and process, Corrosion Science 167 (2020) 108537.
Gabrielli, F., Sanchez-Espinoza, V.H., Wang, S. 2020. ASTEC modelling capabilities for analyzing the QUENCH-ATF tests, Experts' Meeting for the NEA joint undertaking QUENCH-ATF, OECD/NEA, Paris.

ASTEC: FeCrAl Oxidation Model

- Modifying the laws for oxygen mass gain and oxide thickness growth in the database relevant to the cladding steam oxidation.
- **Assumptions: 1) No temperature dependency considered 2) Δh of Zr employed.**

$$m_o(t+dt) = S.\left(\left(\frac{m_o(t)}{S}\right)^{\frac{1}{model}} + AGAIN.e^{\frac{-BGAIN}{R.T}}dt\right)^{model}$$

$$e_{Zro2}(t+dt) = \left(\left(e_{Zro2}(t)\right)^{\frac{1}{model}} + ATHIC.e^{\frac{-BTHIC}{R.T}}dt\right)^{model}$$

```
…..
STRUCTURE MODEL NAME 'BEST-FIT' LAW 'COEFF' VARIABLE 'T' VUNIT 'K' RUNLOW 0. RUNUPP 5000.
  SRG VALUE AGAIN 384.944D0 BGAIN 2.47586D5 ATHIC 1.4213D-5 BTHIC 2.47586D5 MODEL 0.5 TERM
  X  1798.K
  SRG VALUE AGAIN 384.944D0 BGAIN 2.47586D5 ATHIC 1.4213D-5 BTHIC 2.47586D5 MODEL 0.5 TERM
  X  1900.K
  SRG VALUE AGAIN 384.944D0 BGAIN 2.47586D5 ATHIC 1.4213D-5 BTHIC 2.47586D5 MODEL 0.5 TERM
 END
```

Gabrielli, F., Sanchez-Espinoza, V.H., Wang, S. 2020. ASTEC modelling capabilities for analyzing the QUENCH-ATF tests, Experts' Meeting for the NEA joint undertaking QUENCH-ATF, OECD/NEA, Paris.

Summary of the Current FeCrAl Modeling

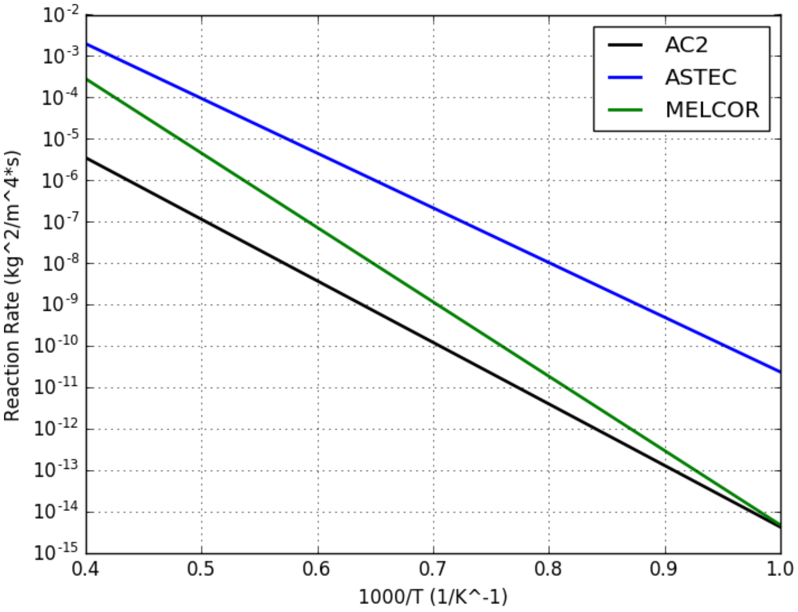

Code	Oxidation of	Enthalpy (J/kg)
AC2/ATHLET-CD	Al	$-9.36 \cdot 10^{6}$
ASTEC	Zr	$-8.93 \cdot 10^{6}$
MELCOR	Fe (74 wt.%)	$-2.495 \cdot 10^{5}$
	Cr (21 wt.%)	$-2.442 \cdot 10^{6}$
	Al (5 wt.%)	$-1.51 \cdot 10^{7}$

QUENCH-19 Test

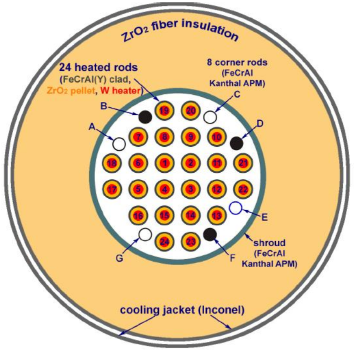

- Heated rods grouped in three radial rings:
  - Inner: 4 rods
  - Middle: 12 rods
  - Outer: 8 rods

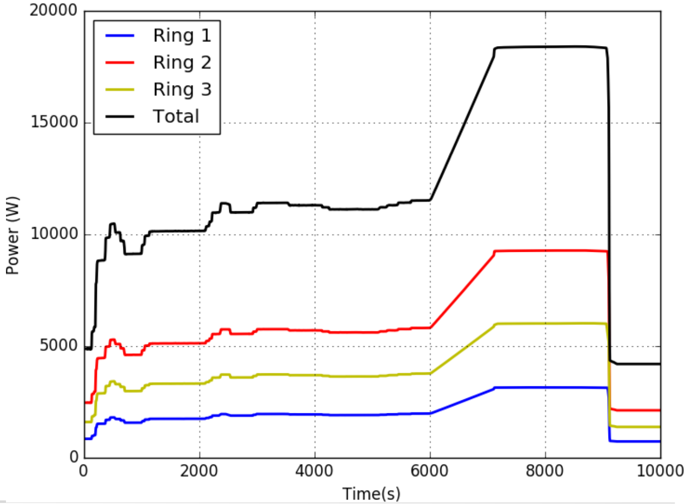

- Phase 1: heating up to ~600 °C (4 kW).
- Phase 2: power increase up to 11.5 kW (pre-oxidation).
- Phase 3: power increased up to 18.12 kW (5 W/s) (T_{pct}~1500 °C).
- Phase 4: power reduced to 4.1 kW.

- Atmosphere of Ar (3.45 g/s) and superheated steam (3.6 g/s).
- Reflooding at ~9100 s
  - Fast initial injection of 4 kg of water
  - Slow injection 48 ~ g/s of water

QUENCH-19 MELCOR and ASTEC Models

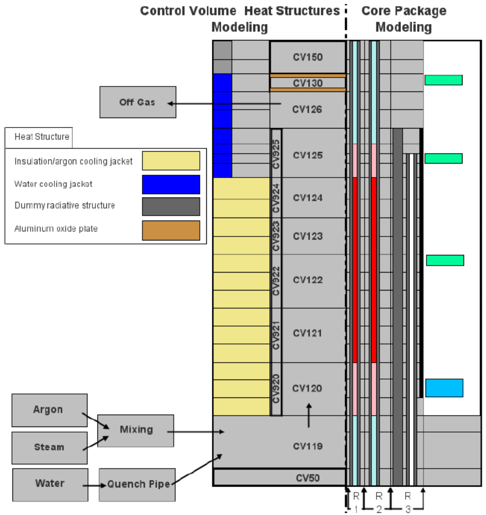

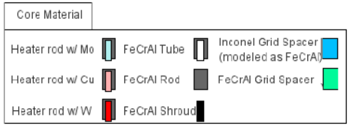

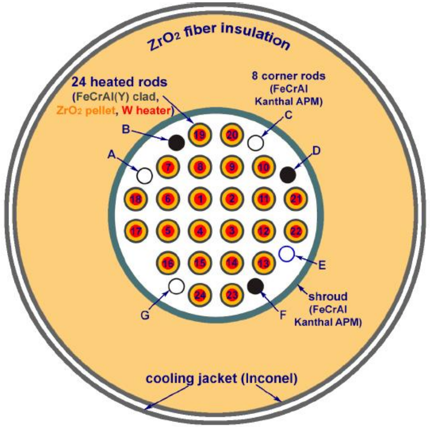

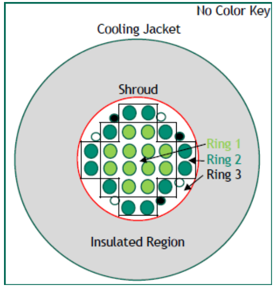

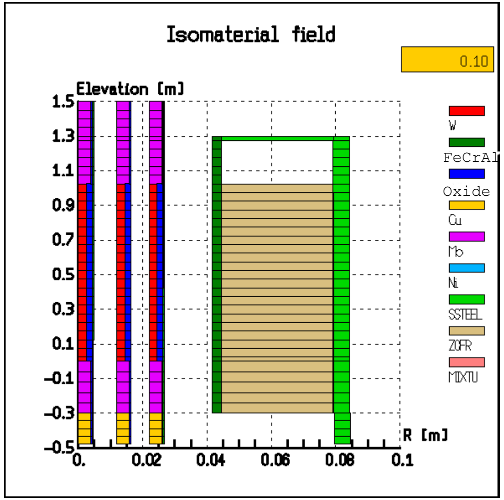

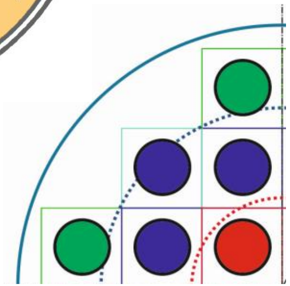

Ch. 3, 8 rods, r_{ext}= 41.5 cm

Ch. 2, 12 rods, r_{ext}= 28.4 cm

Ch. 1, 4 rods, r_{ext}=14.2 cm

Preliminary results: Clad Temp. @850 mm Height

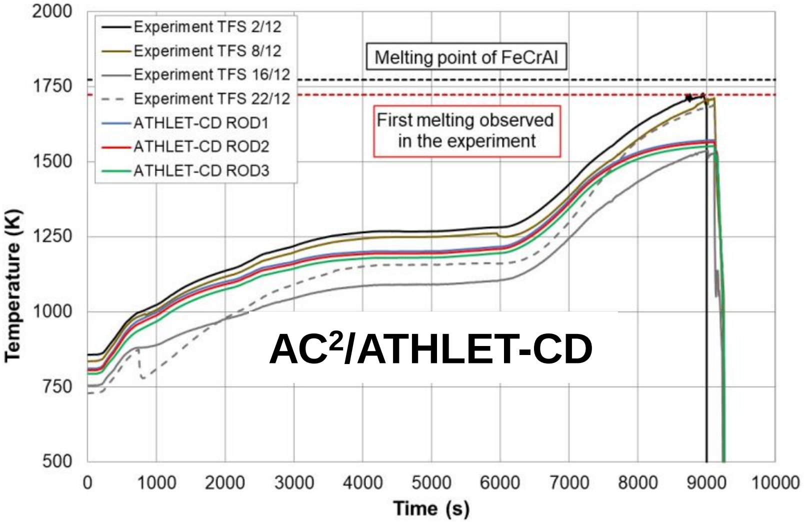

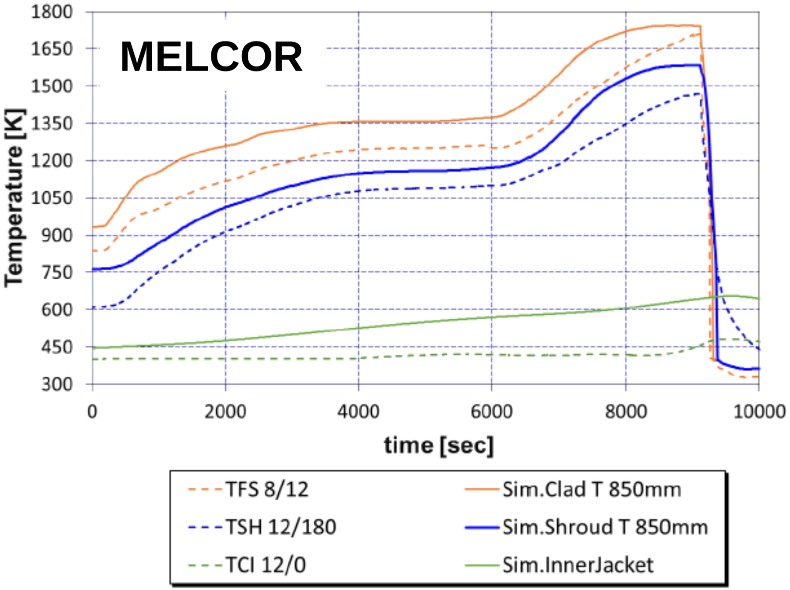

- Simulation of clad temperatures presently exceeds the experimental data.
- No temperature escalation is calculated as shown in the test.

Preliminary results: Clad Temp. @950 mm Height

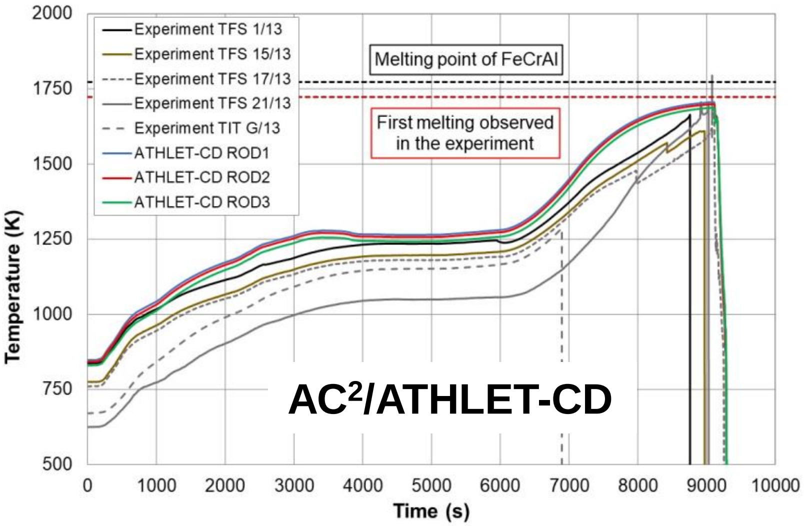

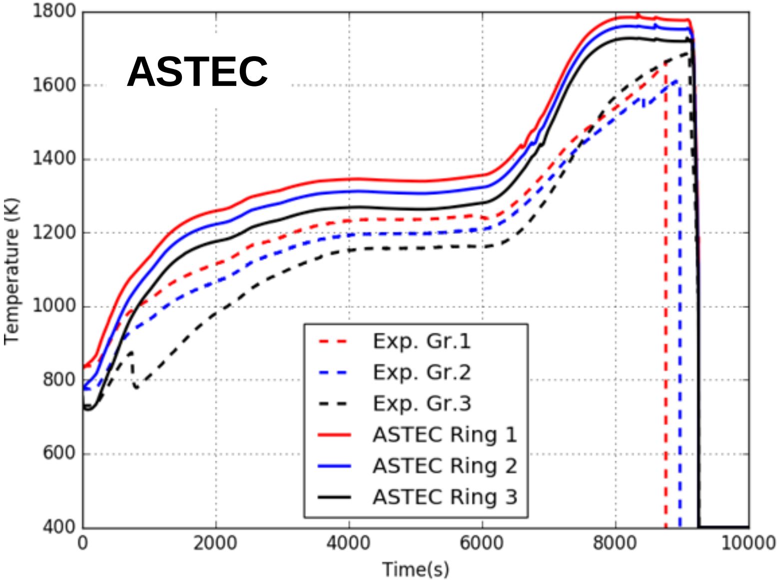

- No further temperature increase during quenching in agreement with the test.
- Good agreement of temperatures within heated length, but overestimation of temperatures above heated length observed.

Preliminary results: Hydrogen Production

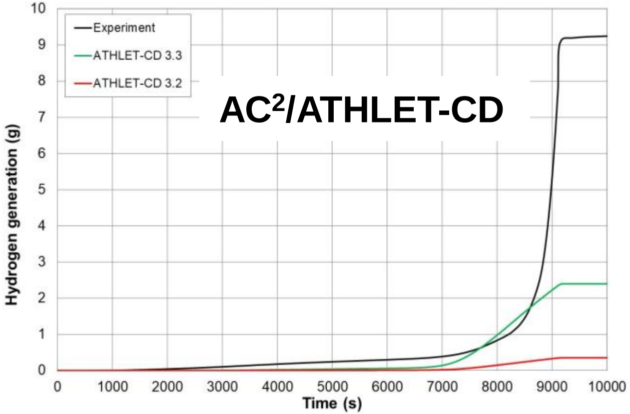

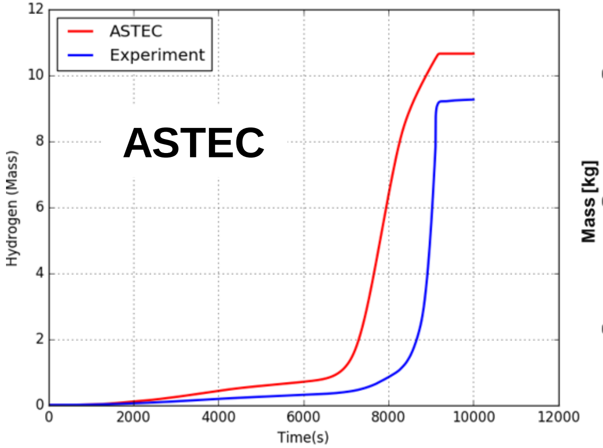

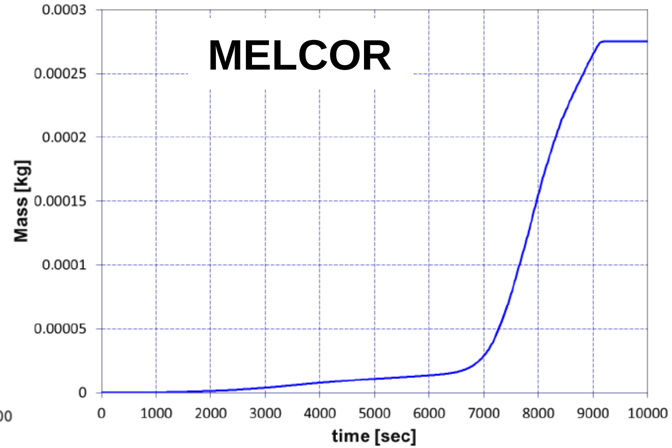

- MELCOR (0.27 g) predict a much lower H_2 production than the experiment (9 g).
- AC²/ATHLET-CD (2.4 g) still underpredicts the H_2 production. The new code version shows better results than first approaches.
- ASTEC results look reproducing the time-dependent behavior of the experiment (larger oxidation rate employed in the model).

Conclusions

- Efforts are going on to extend the capabilities of the AC^2/ATHLET-CD, ASTEC, and MELCOR codes to model the ATFs.
- A dedicated FeCrAl material has been implemented in the codes.
- The QUENCH-19 test has been employed for validating the new models.
- Preliminary results of the clad temperatures
  - Simulations exceed the experimental data
  - No escalation as well as no further temperature increase during quenching observed as in the test
- Preliminary results of the H_2 generation
  - MELCOR simulations significantly underestimates the experimental data
  - AC^2/ATHLET-CD simulations still underestimates the experimental data, but improved modelling
  - ASTEC predictions look qualitatively reproducing the experimental behavior
- Modeling and results still evolving.
- QUENCH-19 analysis a solid basis of understanding for further refinement of the models also in view of the activities in the OECD/NEA QUENCH-ATF project and IAEA CRP ATF-TS.

M. Grosse[a], K. Van Loo[b], F. Di Fonzo[c], K. Lambrinou[d], C. Tang[a], D. Freis[e]

[a]KIT
[b]Catholic University Leuven
[c]IIT
[d]SCK-CEN
[e]JRC Karlsruhe

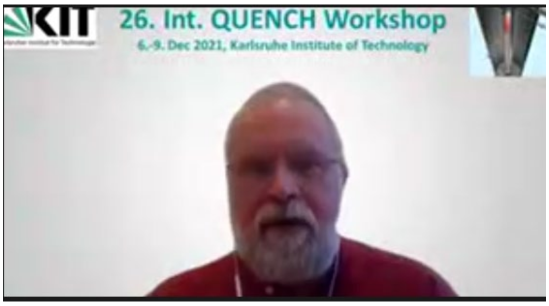

Update of the Results Obtained in the Framework of WP5 of the IL TROVATORE Project

In the framework of the Il Trovatore project sponsored by the EU research and innovation program HORIZON 2020 the interaction between promising ATF cladding materials and coolant is investigated. The materials produced by the project partners can be divided into four groups:

- MAX phases
- Oxides for coatings
- Advanced iron bases alloys (FeCrAl´s and HEA -High Entropy Alloys)
- SiC/SiC composites

The corrosion and oxidation performance under operation and accident conditions of the materials investigated is discussed in the paper. The tests under operational conditions were performed in static autoclaves at IIT and SCK·CEN as well as in a test loop at SCK·CEN. The coolant was pure water (IIT tests) or water with chemistry prototypical for light water reactors (tests at SCK·CEN). Additionally, oxidation tests in steam at high temperature up to 1200°C (design basis loss of coolant accident conditions) and at very high temperatures (severe accident conditions – above 1200°C) were performed. The paper gives an overview about the latest results obtained focused on the results obtained for SiC and Cr coatings with and without diffusion barrier.

At many of the systems both type of processes occur simultaneously:

- Processes reducing the mass (forming of volatile substances like carbon oxides or silicon mono oxide, dissolution in wet environment like Al_2O_3 or spallation of coating or oxide parts) and
- Processes resulting in mass gain like the formation of oxide scales or the inner oxidation.

Therefore, the description of the kinetics on basis of mass changes has to be handled carefully. It is very helpful to get additional information about the processes like for instance the hydrogen release or the consumption of coatings. For instance, the SiC/SiC_f sample show a low mass change but a very high hydrogen release during oxidation at 1200°C in steam. Obviously, mass gain and mass loss has a comparable value in this case.

Update of the Results Obtained in the Framework of WP5 of the IL TROVATORE Project

M. Grosse, K. Van Loo, F. Di Fonzo, K. Lambrinou, C. Tang, D. Freis

KIT / Institute for Applied Materials – Applied Material Physics / Program NUSAFE

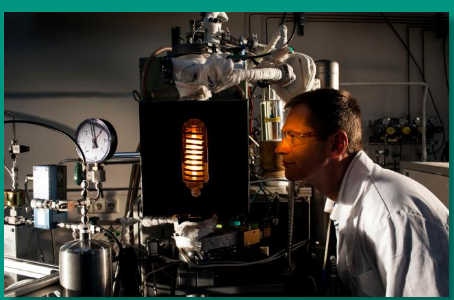

Content

- The IL TROVATORE project
- Materials
- Results
  - SiC
    - water corrosion
    - HT oxidation
  - Cr coated Zry
- Summary

The IL TROVATORE project

- **IL TROVATORE** = **I**nnovative C**l**adding Ma**t**e**r**ials f**o**r Ad**v**anced **A**ccident-**To**lerant Ene**r**gy Syst**e**ms
- Sponsored by the EU research and innovation program **Horizon 2020**
- Start in 2015; actual prolongation until end of next year because of COVID caused delay in the irradiation campaign in Mol (B)
- 31 partner organization (incl. associated) from Germany (8), UK (7), France (5), Sweden (4), Italy (2), USA (2), Japan (2) and Spain (1)

The IL TROVATORE Project

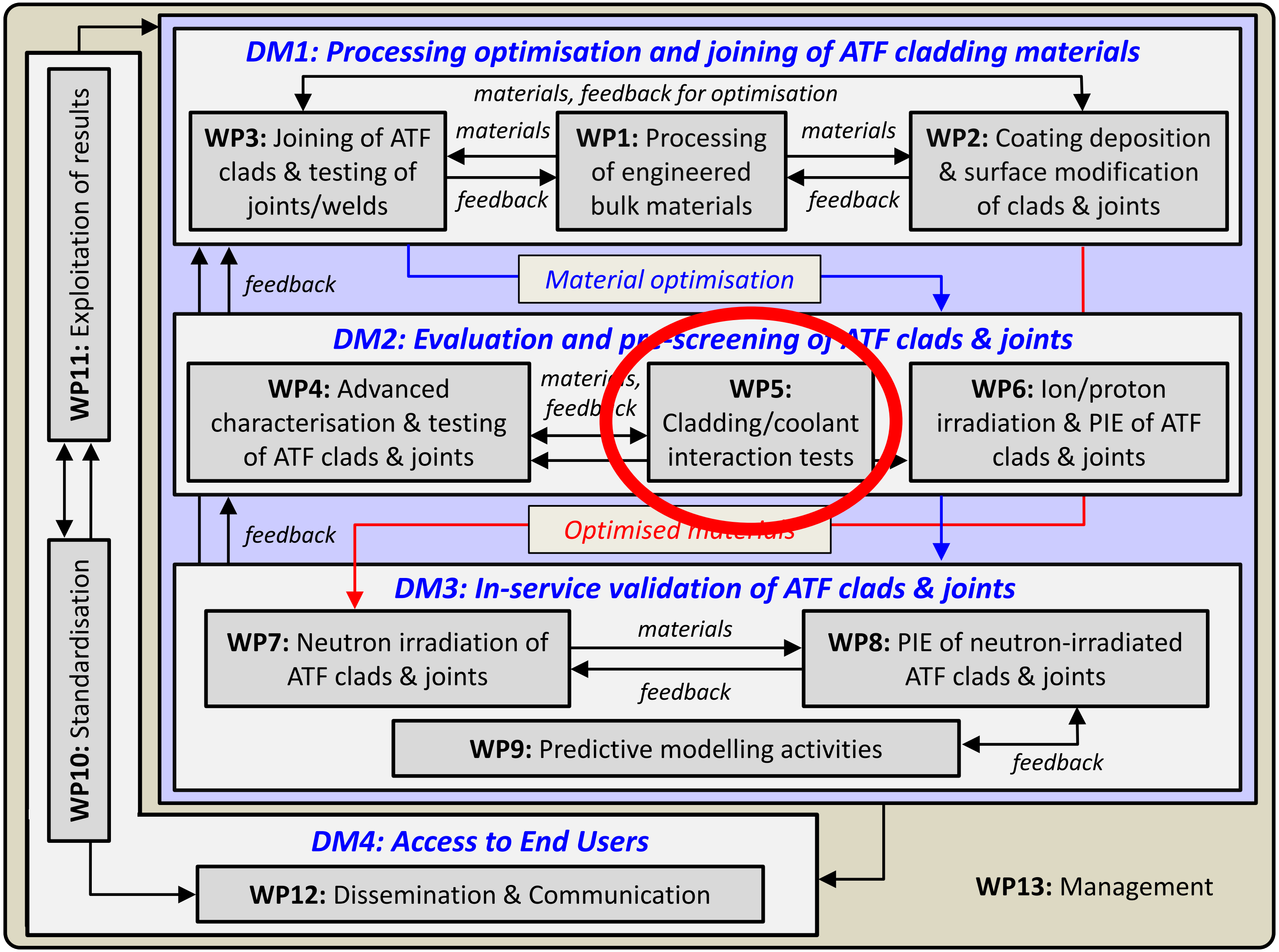

Institute for Applied Materials
Program NUSAFE

WP 5 coolant / cladding / fuel interaction

5.1 Definition of the test matix

5.2 Aqueous corrosion under nominal operation conditions

static autoclave and loop tests at 330 or 360°C in pure water or water with reactor chemistry under 50 .. 70 bar pressure

5.3 Steam oxidation under transient/accident conditions

go / bo go tests at 1200°C for 1 h
transient tests up to temperatures of 1500°C or 1830°C (SiC)
Isothermal tests at very high temperatures (<1200°C)

5.4 Fuel pellet / cladding interactions

SiC + UO_2
FeCrAl + UO_2

Institute for Applied Materials
Program NUSAFE

Materials

- Oxides (pure and doped alumina, titania, chromia and zirconia as well as yttrium silicates)
- SiC_f/SiC ceramics matrix compounds (CMC) inclusive coated SiC, joined SiC and SiC joining materials
- PVD Coatings (MAX phase, Cr_2O_3, Cr, Ti, multilayers)
- Bulk MAX phases
- FeCrAl alloys

Results - corrosion tests

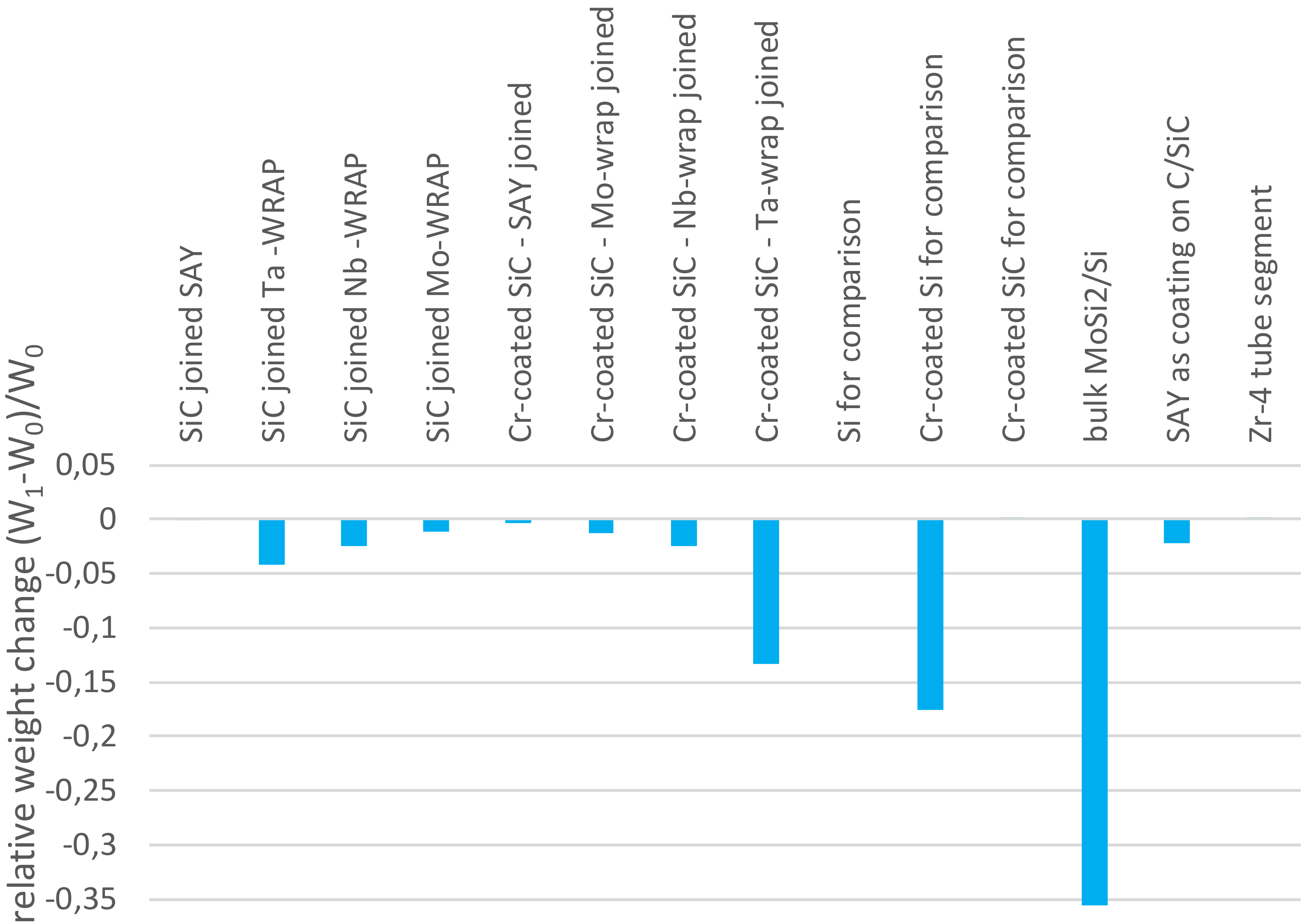

Relative mass change after static autoclave test at 330°C for 14 days

Results – HT oxidation

material	pre-test appearance	post-test appearance	mass change (mg/cm^2)	H_2 release (mg/cm^2)
SiC #C			0.017	0.254
SiC #J1			-0.45	271.6
SiC #J2			-0.12	71.6
Ti coated monolithic SiC			2.46	2.5

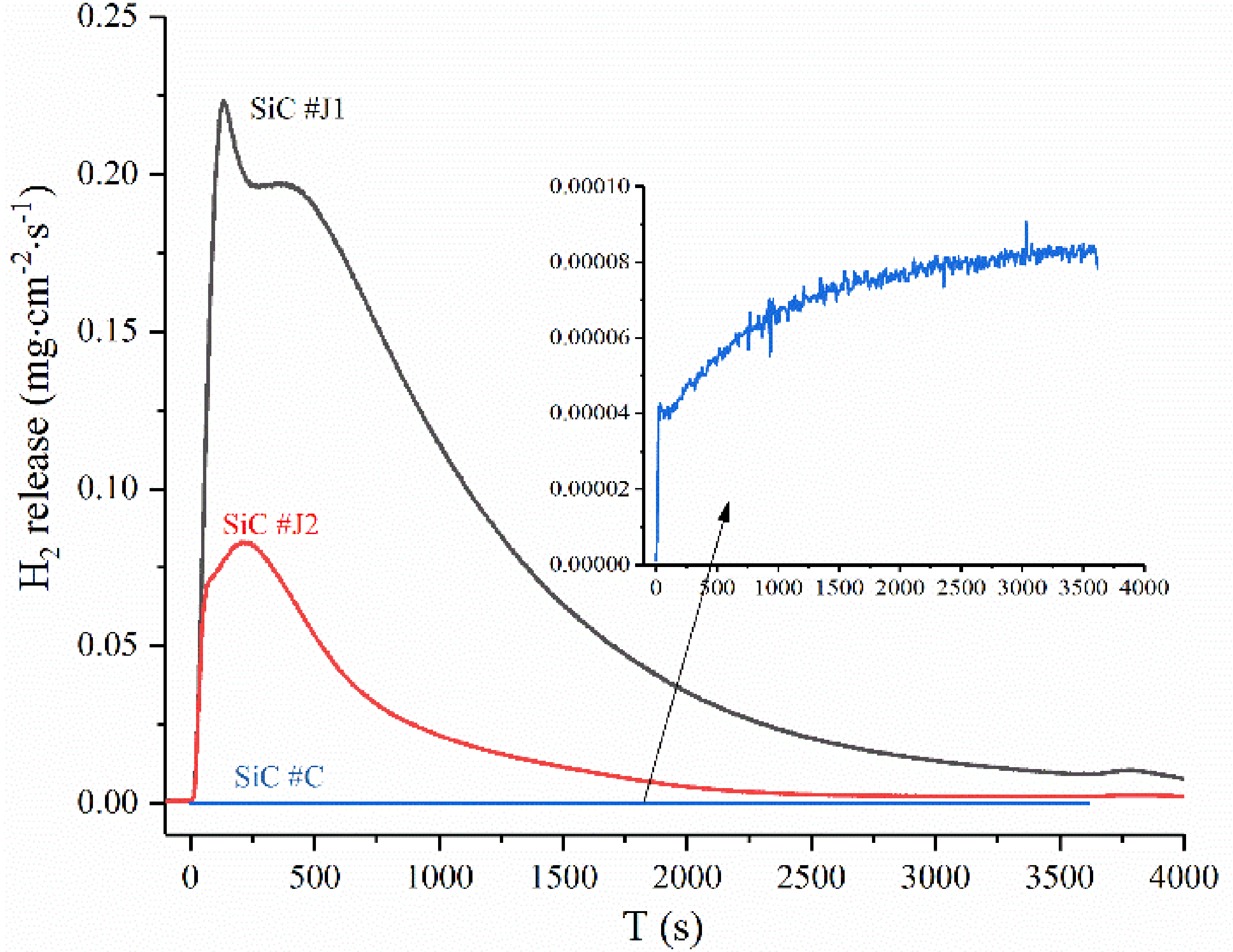
SiC #J1
SiC #J2
SiC #C
H_2 release (mg·cm^{-2}·s^{-1})
T (s)
0.25
0.20
0.15
0.10
0.05
0.00
0 500 1000 1500 2000 2500 3000 3500 4000
0,00010
0,00008
0,00006
0,00004
0,00002
0,00000
0 500 1000 1500 2000 2500 3000 3500 4000

Reason for the strong reaction is the absence of an inner monolithic SiC layer in combination with both side oxidation.

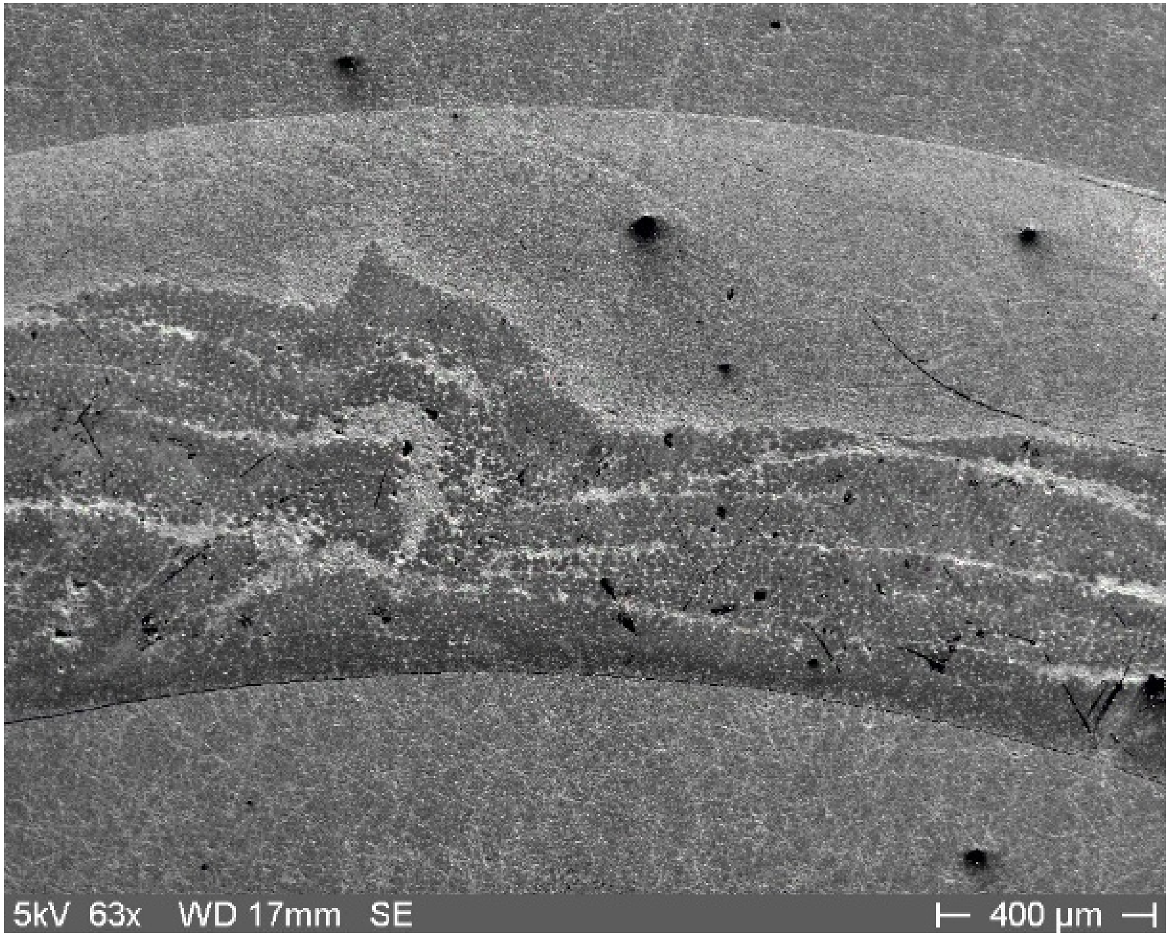

Results HT oxidation

Transient oxidation of Cr-coated Zry w/o and with diffusion barrier layer

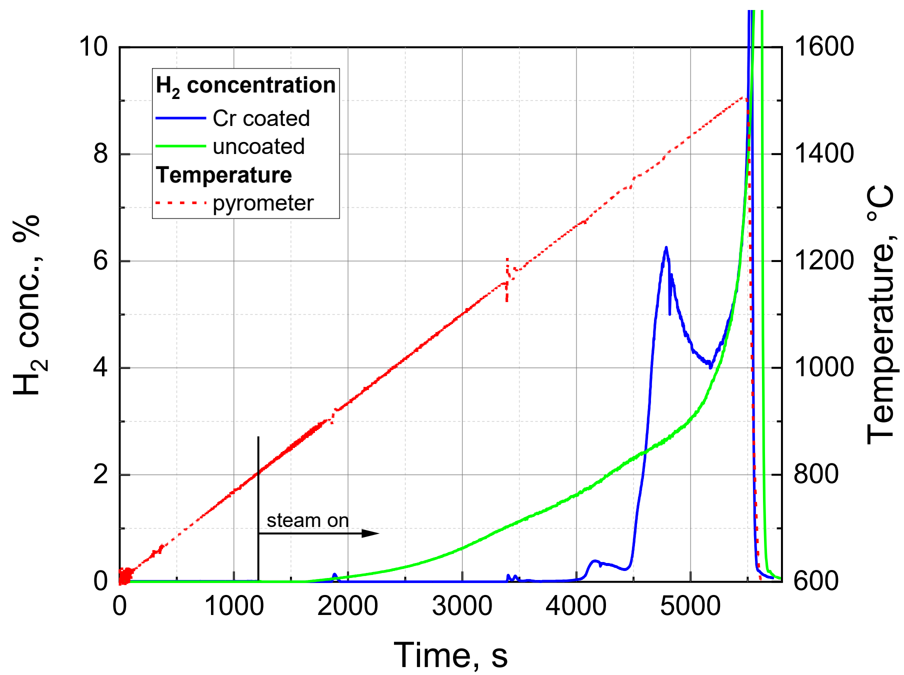

Cr coated Zry-4 without diffusion barrier

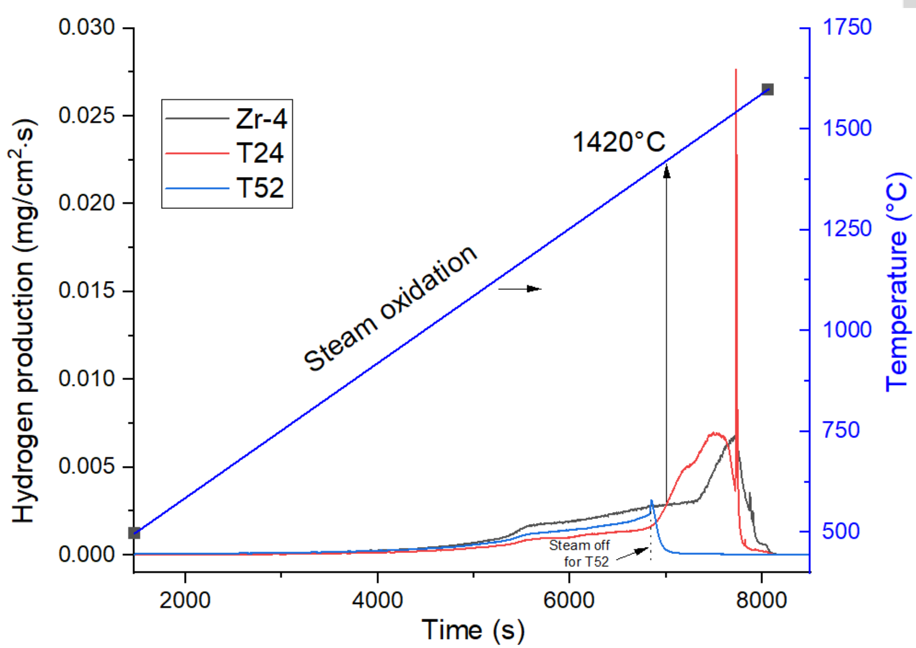

Cr coated Zry-4 with diffusion barrier

Results HT oxidation

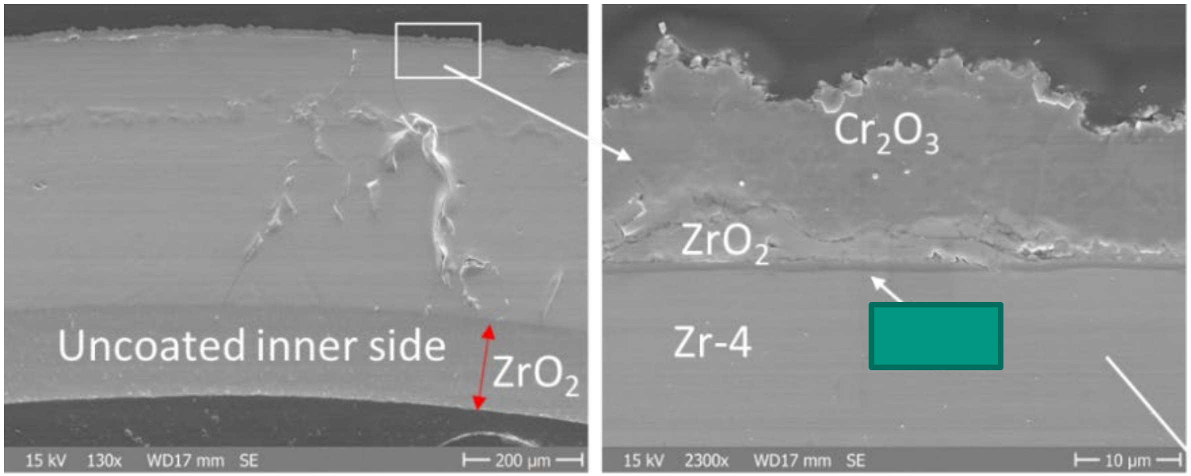

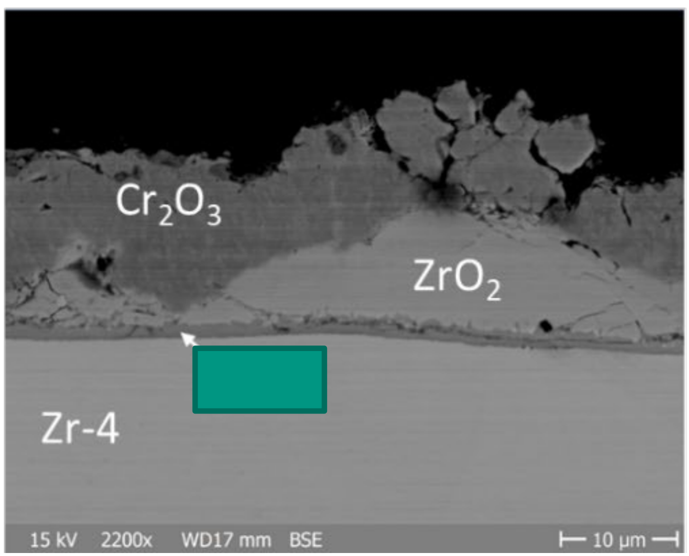

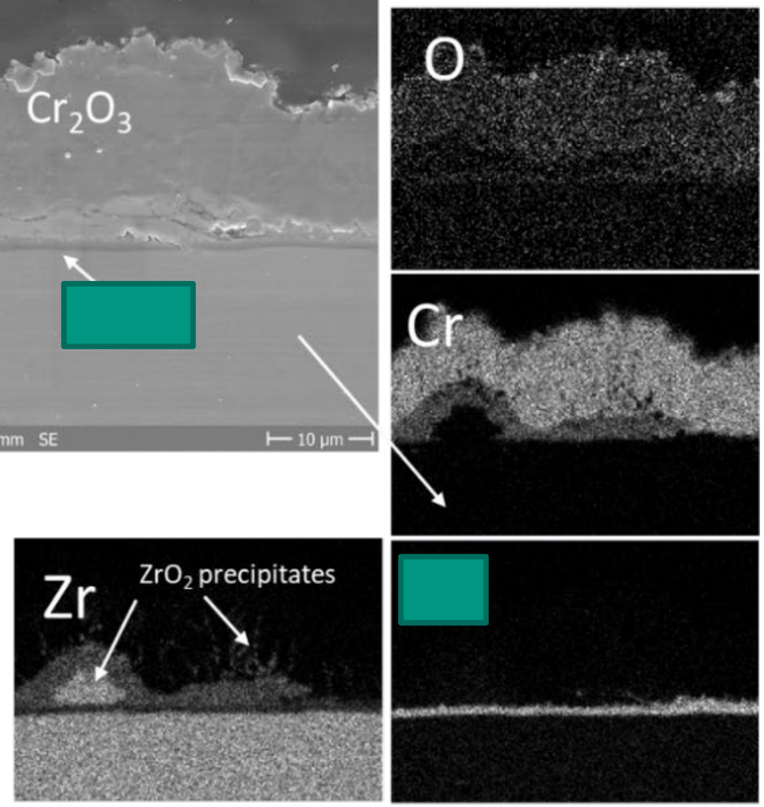

Element distribution at the cross section of the sample tested transient until 1420°C

Results Clad / Fuel Intera.

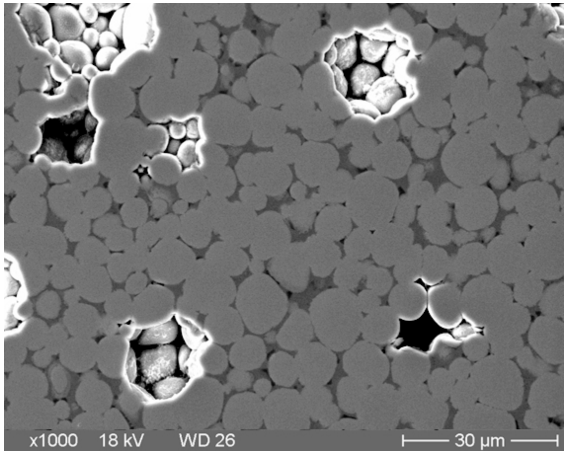

Finding from QUENCH-FeCrAl test: FeO melt attacks grain boundaries of ZrO_2 pellets. What happens with UO_2?

Test at JRC Karlsruhe:
FeCrAl C26M2 cladding (left) and UO_2 pellet after interaction test at 1400°C in O_2 (Test 1).

No interaction?

Summary and Conclusions

- The Coolant / Cladding / Fuel interaction tests are almost finished.
- A large number of different materials used as bulk or as coating material was investigated. The tests comprises oxides, SiC basis systems, MAX phases, Cr coated Zry and FeCrAl.
- View systems were satisfying under all test conditions.
- Chromium coated Zry is a really alternative to the currently used cladding alloys. The performance can be improved by diffusion barrier layers.
- SiC: Joining is still an issue. Joining with additional materials show not satisfying corrosion behavior.
- Strong reactions if steam can penetrate into the fiber range.
- A new proposal of a project dealing with the behavior of SiC_f/SiC CMC claddings (SCORPION) is submitted to EURATOM.

Acknowledgement

The work was sponsored by the HORICON2020 research program of the European Community.

Thanks to all colleagues from KIT, KU Leuven, SCK·CEN, IIT and JRC involved in the investigations.

Thank you for your attention

Karlsruhe Institute of Technology

Update of the Results Obtained in the Framework of WP5 of the IL TROVATORE Project

M. Grosse, K. Van Loo, F. Di Fonzo, K. Lambrinou, C. Tang, D. Freis

KIT / Institute for Applied Materials – Applied Material Physics / Program NUSAFE

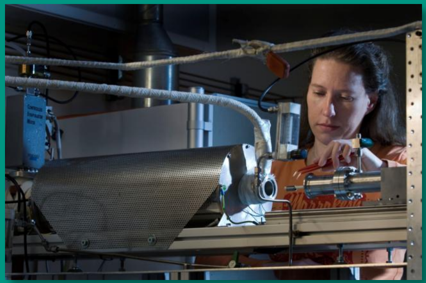
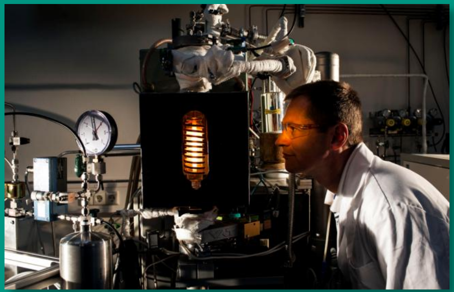
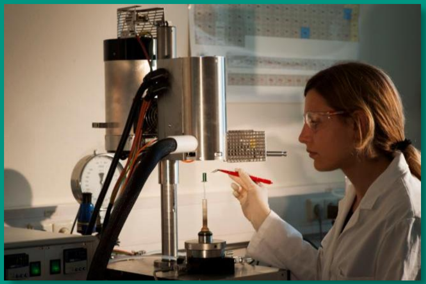


J. Stuckert

KIT

Overview on the IAEA ATF-TS project

The IAEA encourages and assists research on development and practical use of atomic energy and its applications for peaceful purposes throughout the world. It brings together research institutions from its developing and developed Member States to collaborate on research projects of common interest, so-called Coordinated Research Projects (CRPs).

Fuel modelling is a recurrent priority in the IAEA sub-program "Nuclear Power Reactor Fuel Engineering". Development and verification of computer codes are possible only based on good experimental data that requires long and expensive in-reactor and post-irradiation studies. That is why international cooperation in this area is highly desirable, and the IAEA traditionally supports interested Member States in their efforts to enhance the capacities of their computer codes to predict fuel behavior. Many Member States are considering new fuel types that range from using an oxidation resistant coating on zirconium-based cladding to alternate fuel and cladding materials. These new fuels/claddings under development must be licensed before being deployed industrially and therefore research is undertaken to assess their behaviors in reactor.

The respective CRP T12032 on “Testing and Simulation for Advanced Technology and Accident Tolerant Fuels” (ATF-TS) complements this effort by organization of round robin tests, collection of experimental data from single rod and bundle tests, coordination of benchmarks on modelling of these tests.

Overview on the IAEA ATF-TS project

J. Stuckert
in cooperation with IAEA

QWS 26

Institute for Applied Materials; Program NUSAFE

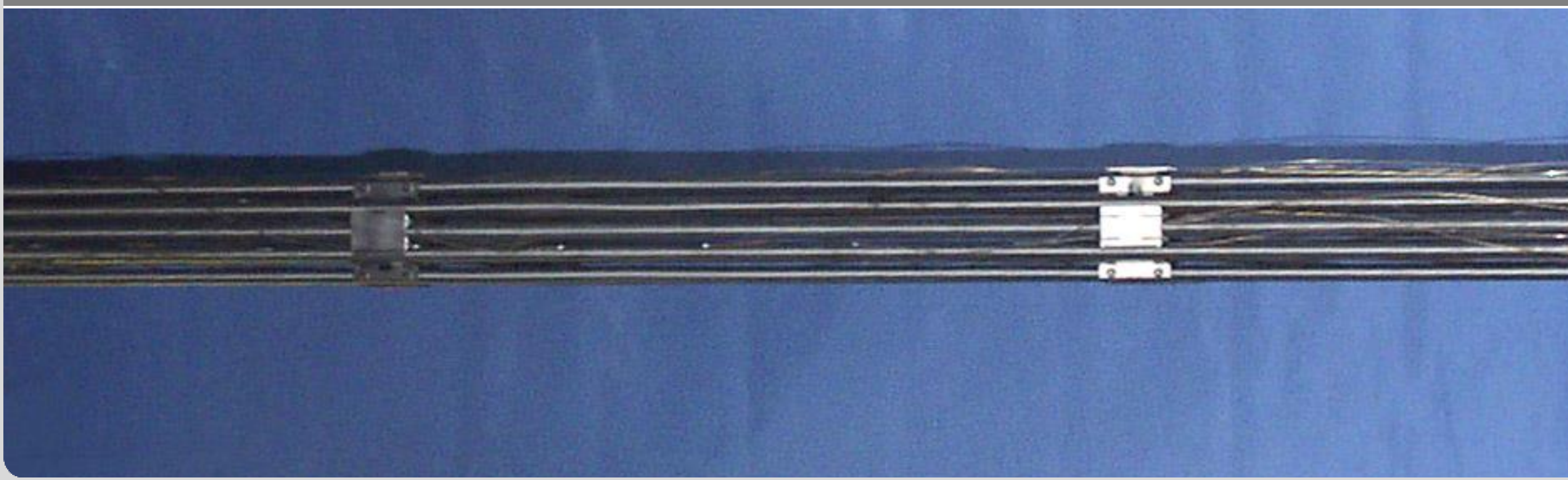

Fuel Engineering Programme at IAEA
Major tools of implementation

- Consultancy Meetings (Expert Reviews)
- Technical Meetings
- Coordinated Research Projects (CRP)

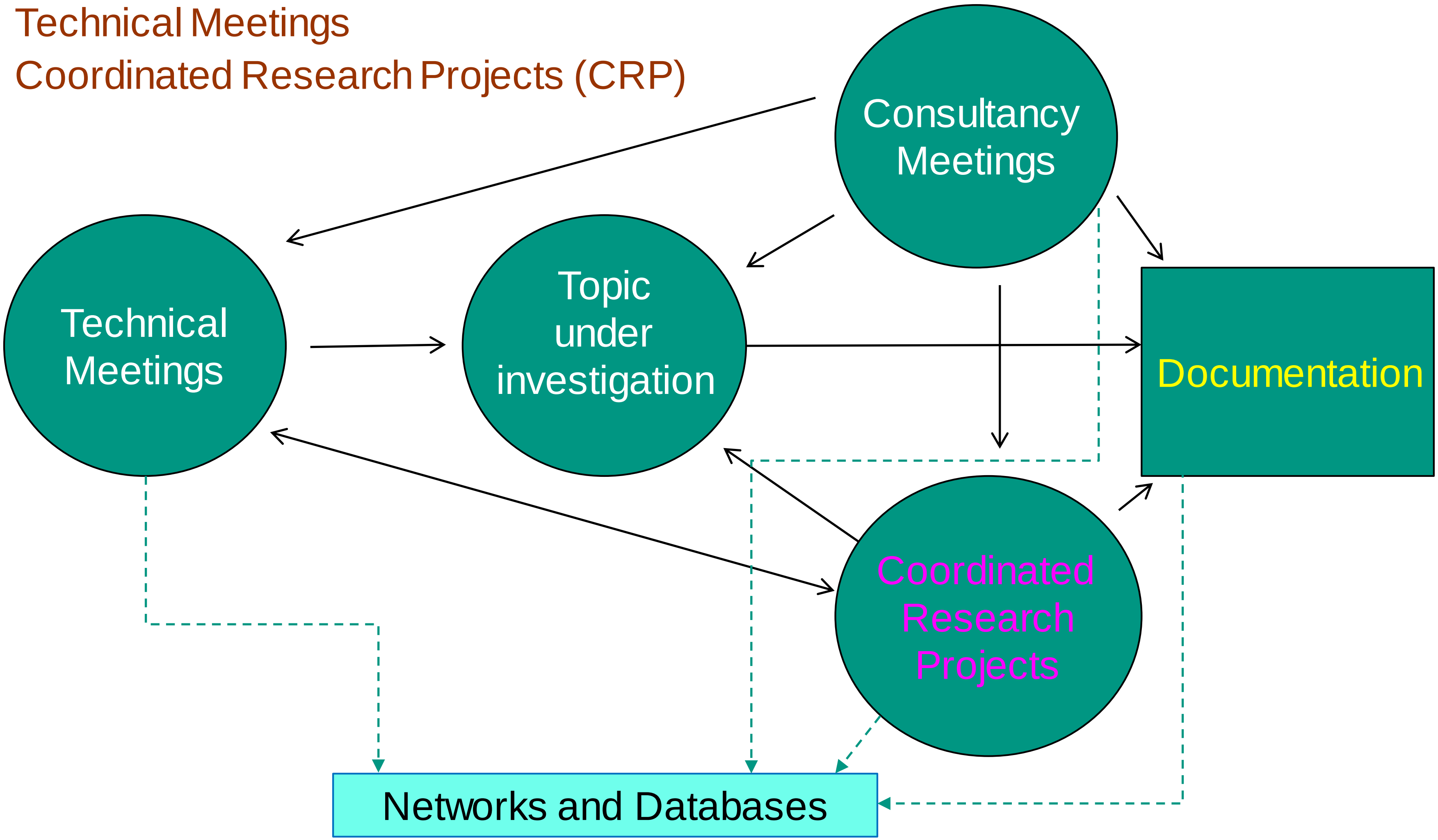

Coordinated Research Projects (CRPs)

- CRPs are a mechanism for coordinating international research within the IAEA programme of work
- A CRP theme is scoped in consultation with experts and authorized by the IAEA for proposals of work from Member States
- Typically ~4 years, organized around 3 Research Coordination Meetings (RCMs)
- A very good opportunity to work with many groups around the world
- CRP direction is largely defined in the first RCM by the CRP participants
- Research results finalized as an IAEA TECDOC
- Results are available, free of charge, to scientists, engineers and other users from all Member States

CRP on Testing and Simulation of Advanced Technology Fuels (ATF-TS) (2020-2023)

Specific Research Objectives

- To perform experimental tests including single rod and bundle tests on ATF performance under normal, DB and DE conditions
- To benchmark fuel codes against new test data obtained during the CRP as well as existing data relevant for advanced fuel and cladding concepts from other experimental Programmes
- To develop LOCA evaluation methodology for ATF performance with a view for NPP applications

Overall coordination of Work Tasks

CRP Chairman: P. Xu (INL)

Work Task 1: Experimental Program

Coordinators: M. Sevecek (CTU), J. Stuckert (KIT)

- **Round Robin tests**
  - coated claddings:
    - ballooning and burst isothermal
    - ballooning and burst transient and/or LOCA
  - FeCrAl:
    - high temperature oxidation tests
    - autoclave oxidation tests and mechanical tests, etc.
  - SiC (??)
- **Bundle tests**
  - DEGREE facility with ATF rods (Coated Zry-4) under SA and/or LOCA (CRIEPI, Japan)
- **Irradiation tests data**
  - Doped fuel pellets HALDEN tests: IFA 6771, IFA 7161

ATF concepts to be experimentally tested within ATF-TS (WT 1.1)

- 8-9 institutes to fabricate ATF **cladding** materials for testing
- Two reference uncoated samples (Zircaloy-4, Opt. ZIRLO)
- Coated Zr
  - Cr – KIT, CTU, AEOI, BSU, CNPRI
  - CrN – AEOI, CTU
  - TiAl - CNL
  - SiC – INCT
- SiC/SiC – CNPRI, Uni. Birmingham (?)
- FeCrAl – KIT (B136Y), CNPRI

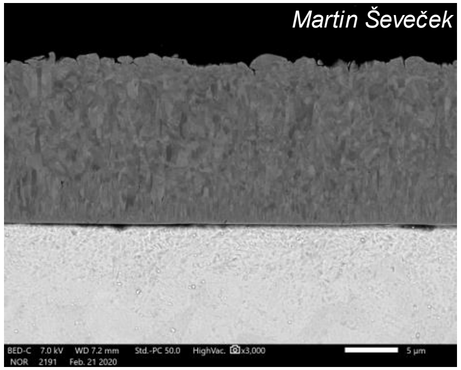

Result of SEM/EDX analysis: Cr-coated cladding microstructure immediately after LOCA transient from 600 to 1400 °C (*KIT, WT 1.1*)

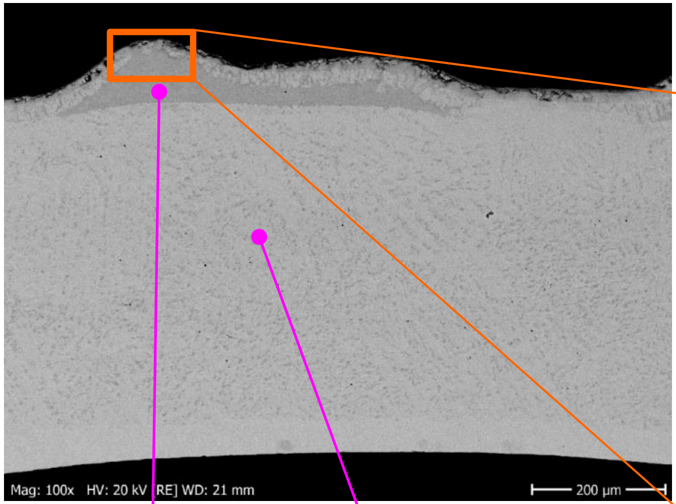

blister

prior β-Zr

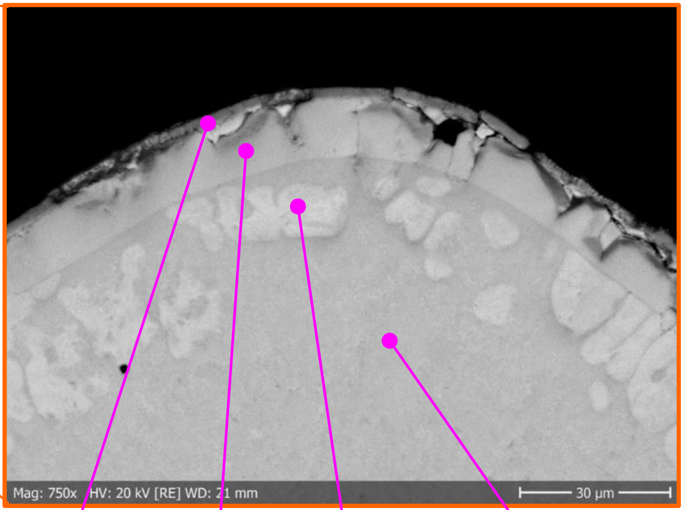

Cr_2O_3

α-Zr(O)

α-Zr(O) + Cr

α-Zr(O) + $ZrCr_2$

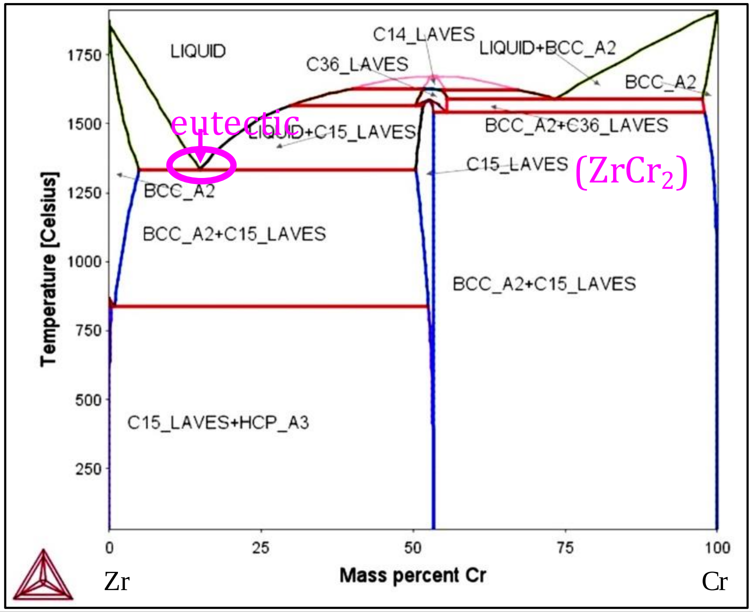

WT 1.2: DEGREE bundle tests at CRIEPI (WT 1.2)

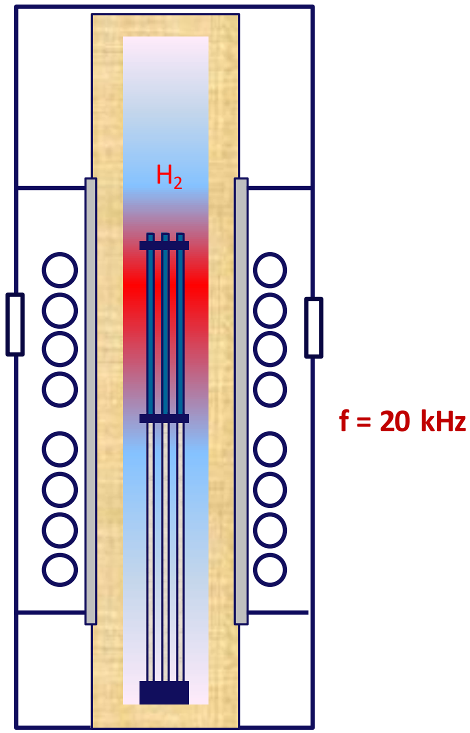

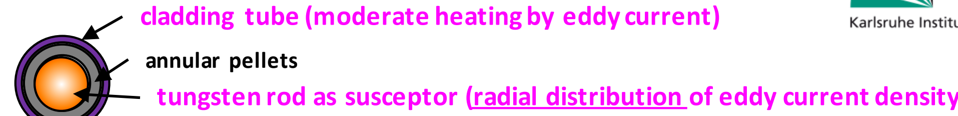

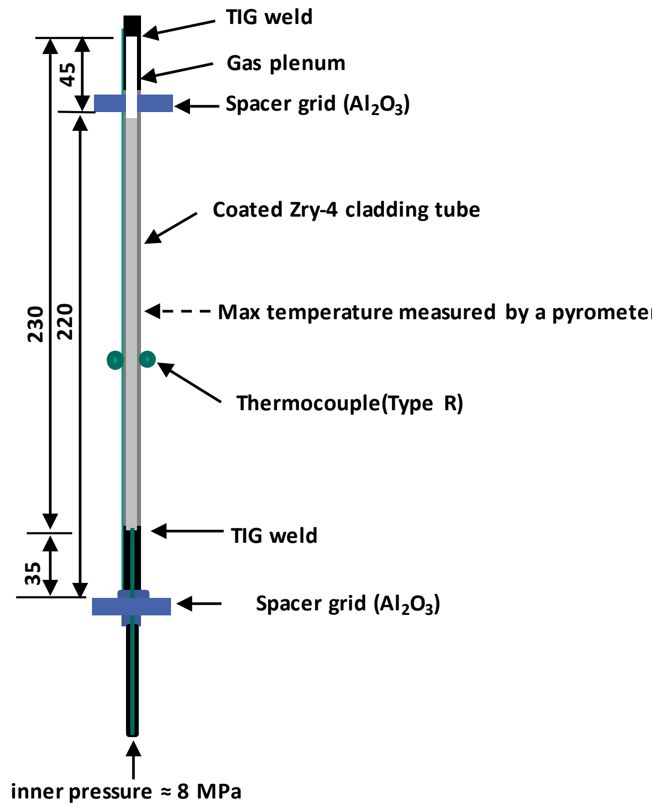

Eddy currents:

power distribution between tungsten heaters (≈70%) and claddings (20%?)

Test ID	B1	B2	B3	B4	B5	B6	B7
Accident scenario	DBA	BDBA					
Coating materials	20 µm Cr		*10 µm Cr*	*20 µm CrN/Cr*	*20 µm Cr*	*10 µm Cr*	-
Maximum temperature	1330°C	1500-1700°C			*1500-2000 °C*	*2000 °C*	*1500-1700 °C*

IAEA

CRP structure (cont.)

Work Task 2: Modelling

Coordinators: A. Boulore (CEA), G. Pastore (UTK)

- **Fuel performance codes benchmarks, including modeling improvements and uncertainty analysis (WT 2.1)**
  - FeCrAl / coated Zr cladding / uncoated Zr cladding against new RRT burst tests
  - Doped fuel pellets HALDEN tests – IFA 677.1 and IFA716.1
  - Power ramp test – SKIPP II ramp data
- **SA Modelling benchmark (WT 2.2)**

  Coordinator: J. Stuckert (KIT)
  - Database: Quench-19, DEGREE-B2
  - SA Codes: ASTEC, ASYST, ATHLET-CD, DIONSIO, FRAPTRAN, MELCOR, SOCRAT, RELAP/SCDAPSIM, TESPA-ROD

Work Task 2.1: benchmarks on bundle tests. Participants (9) and codes (9)

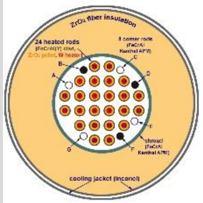

	CNEA Argentina	GRS Germany	CTU Czech Republic	KIT/INR Germany	NINE Italy	CRIEPI Japan	IBRAE Russia	UPM Spain	ISS USA
QUENCH-19 (FeCrAl)	DIONISIO	ATHLET-CD, TESPA-ROD	MELCOR, SCDAPSIM/ RELAP	ASTEC	MELCOR, ASTEC(?)		SOCRAT	MELCOR	RELAP/SCDAPSIM, ASYST
DEGREE-B2 (Cr-coated Zry-4)	DIONISIO	ATHLET-CD	FRAPTRAN	ASTEC	MELCOR	FRAPTRAN	SOCRAT	MELCOR	RELAP/SCDAPSIM, ASYST

Modelling output parameters for QUENCH-19:

1) temperature progress at the surface of claddings for the elevations 250, 550, 850, 950, 1050, and 1350 mm;
2) hydrogen release rate as indicator of cladding oxidation progress and integral hydrogen release.

Open questions for DEGREE:

1) code capabilities to correctly address the Cr coated cladding;
2) simulation of inductive heating: power distribution between tungsten heaters and direct heating of claddings by eddy currents.

CRP structure (cont.)

Work Task 3: : LOCA evaluation methodology development for NPP applications

Coordinator: J. Zhang (Tractebel)

- Qualification of Fuel rod codes for LOCA application based on IFA 650.10 with SOCRAT TH boundary conditions and uncertainty analysis, prediction for FeCrAl and/or coated Zr cladding
- Application to PWR prototypic fuel rod with TH boundary conditions (2 scenarios: LB and SB LOCA) and uncertainty analysis, prediction for FeCrAl and/or coated Zr cladding

Work Task 4: Material properties database for ATF

Coordinator: Ch. Allison (ISS)

- Development of “open source” material property models and correlations library
- Extension of widely distributed MATPRO library to include ATF specific M&C, as a publicly available IAEA document

Thank you for your attention

https://nucleus.iaea.org/sites/connect/NFEpublic/Pages/ATF-TS.aspx

http://www.iam.kit.edu/awp/163.php

http://quench.forschung.kit.edu/

B. Sartowska[1], W. Starosta[1], L. Waliś[1], D. Wawszczak[1], P. Sokołowski[2]

[1] Institute of Nuclear Chemistry and Technology, Warsaw, Poland
[2] Wroclaw University of Science and Technology, Wroclaw, Poland

Experimental SiC coatings

Thermal barrier coatings (TBC) are used in different industries as for example to protect blades of hot gases turbines. Silicon carbide (SiC) is well known material/compound with good thermal properties. It is used as component of TBC. It is also investigated as nuclear material as for example: SiC-SiC composite for claddings and for zirconium alloys coatings.

Zircaloys are used as cladding material for fuel elements due to very good water corrosion and radiation resistance at normal working conditions of nuclear reactors. But in the case of anomalous conditions, the fast oxidation at steam or/and air-steam mixture results in intense hydrogen generation.

The aim of INCT works is to develop protective SiC coating on zirconium alloy. The works consist of some stages. The first: production of silicon carbide composite (SiC+YAG garnet) using the sol-gel method. The second one: coating the zirconium alloy with (SiC+YAG) using the method of suspension plasma spraying (SPS). The third one: SiC coatings characterization.

The scientific background, proposed methodology and obtain results will be presented in this work.

EXPERIMENTAL SiC COATINGS

Sartowska Bożena *, Starosta Wojciech, Waliś Lech, Wawszczak Danuta
Institute of Nuclear Chemistry and Technology
Warsaw, Poland

Sokołowski Paweł
Wrocław University of Science and Technology
Wroclaw, Poland

THE AIM

- to propose and develop the protective coatings on zirconium alloy in the form of (SiC+YAG) composition
- Why:

- SiC coatings – promissing candidate for low corrosion applications
- YAG presence to avoid SiC degradation/drcomposition

- to evaluate their properties at accident scenario as well as in the reactor normal working conditions

WHAT WE KNOW

- Under extreme conditions, nuclear fuel will fail and the high temperature reaction between zirconium alloys and water will lead to generation of hydrogen with the potential for explosion – the case of severe nuclear accidents

- Development of the solution to minimize the risk related to unforseable situations is needed

- The concept of Accident Tolerant Fuels **(ATF)**

- it means materials and materials systems with increased accident tolerance -

has been developed and investigated recently for this purpose

WHAT WE KNOW

- Thermal barier coating (TBC) systems were developed to safeguard critical components under even the most demanding operating conditiona

- TBCs are multilayer coatings that protect a substrate from both heat and corrosion

- TBCs are used in - as for example- automotive, aerospace, power generation industries

Thermal barrier coatings (TBCs) are used - as for example - to protect turbine blades against extremely high temeperature in gas turbines

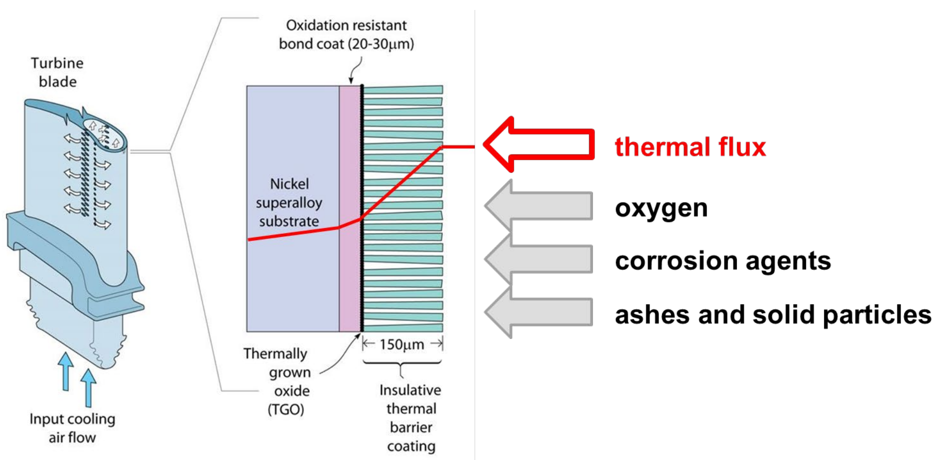

PLASMA SPRAY PROCESSES

* TBC can be produced using different fabrication technigues
* The most common methods for TBC fabrication are:

- Electron-Beam Physical Vapor Deposition (EB-PVD)
- **Plasma Spray Deposition**
- Electrophoretic Deposition
- Additive manufacturing

Mondal: Industrial and Engineering Chemistry Research, 2021, 60, 17, 6061

* Potential TBC materials (low thermal diffusivity): titania, zirconia, alumina, pocelain, porcelainite, pyrochlores, **garnets** (Y3AlxFe5-xO), monazite (LaPO4), perovskites (ABO3), lanthanum-magnesium hexa-aluminate, diamond

* **Y3AL5O12** garnet shows promise due to its good high temperature mechanical properties, low thermal conductivity, good phase stability, low oxygen diffusivity

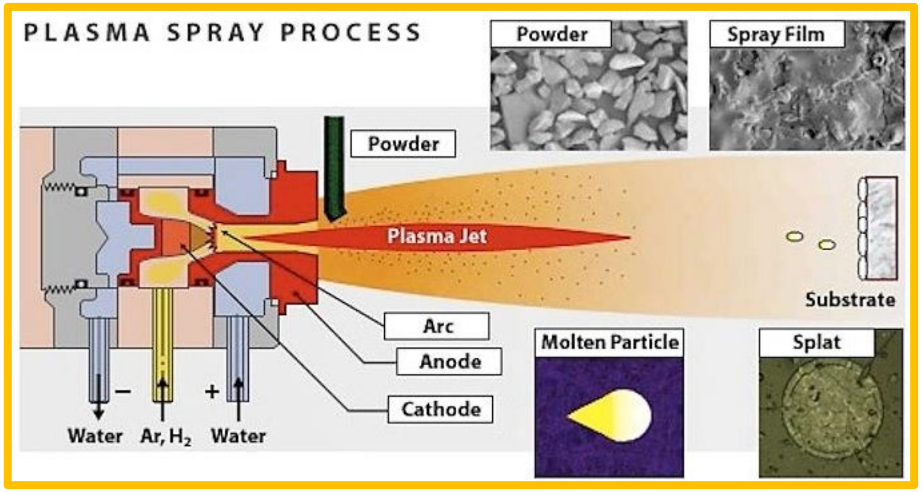

by TSET - Advanced Equipment Refurbishment Services

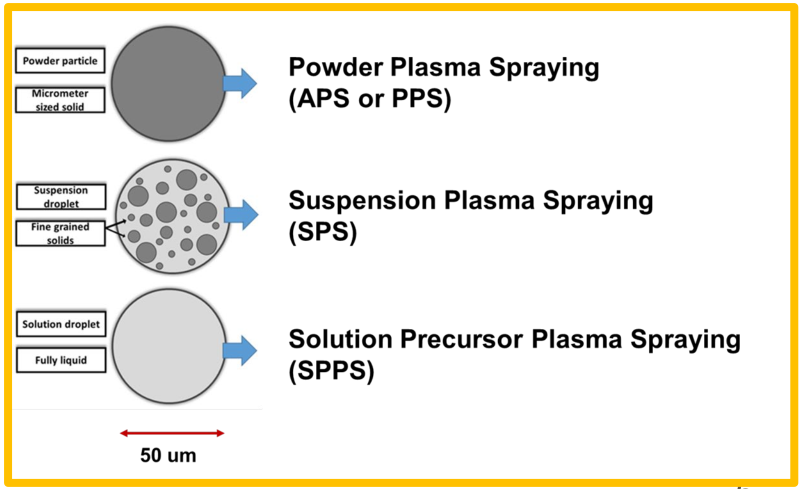

SUSPENSION PLASMA SPRYING (SPS)

SPS as an alternative
for
EB-PVD
electron-beam physical vapor deposition
APS
atmospheric plasma sprying

for TBCs
thermal barier coatings

(YSZ coatings)

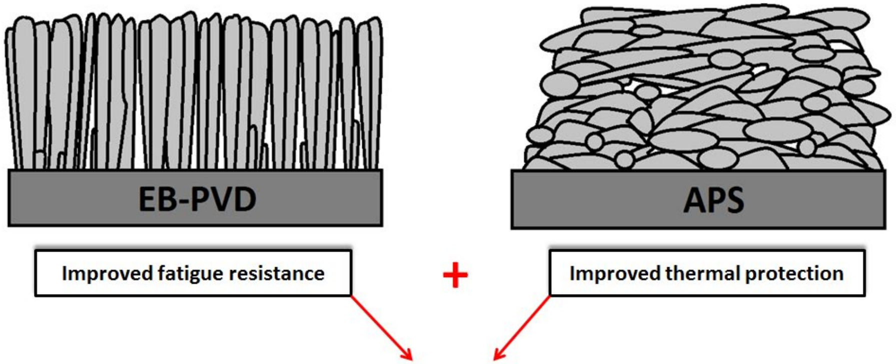

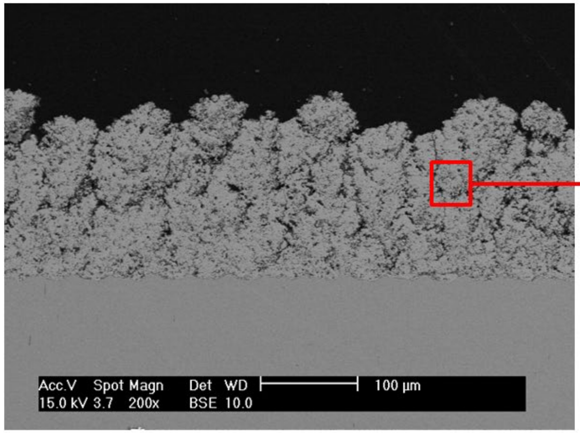

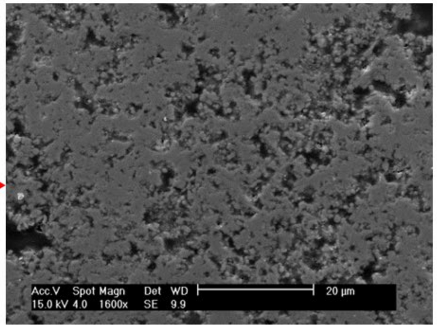

SUSPENSION PLASMA SPRYING (SPS)

What is the key point of using suspension (SPS) instead of coarse-grained powders (APS)?

Shifting from micrometer-sized to even nanometer-sized powders

Volume ratio:
$30/0.05\ \mu m \sim 2.16 \times 10^8$

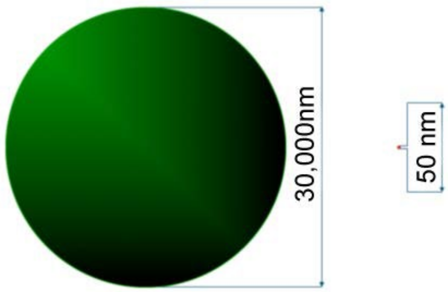

This means:

- Finely-grained coating structure
- Possibility of using complex (multi-material) suspensions
- Tailoring of coating microstructure (dense, porous, columnar, cracked, ….) due to greater proces complexity
- and many other advantages

EXPERIMENT & INVESTIGATIONS

Materials

Characterisation

Work stages (3 years)

(i) SPS coatings methodology

(ii) Si+YAG formation

(iii) coatings formation

(iv) coatings characterisation

SS AISI 304
ThussenKrupp Nirosta

Element	Concentration (wt.%)
Fe	70,801
Cr	18,60
Ni	8,08
Mo	0,25

Zircalloy Zr1Nb
AEOI, Iran

Element	Concentrati on (wt.%)
Zr	99
Nb	1,00

SiC commercial powder
grain size < 50 nm

1. Surface and cross-section observations: OM, SEM, HR SEMs
2. Elemental analysis: EDS with Quantax 400 (Bruker, Germany)
3. Phase analysis: X-ray diffractometer D8 Advanced (Bruker, Germany) with geometries Θ-2Θ, ω=5o, ω=10o
4. Oxidation tests :

4.1. different parameters (temperatures, time, atmosphere)

4.2. autoclave: 360°C/196/bar/water/in 21 days period, up to 1 year with each 3 month control testing/analyse

SUSPENSION PLASMA SPRYING (SPS)

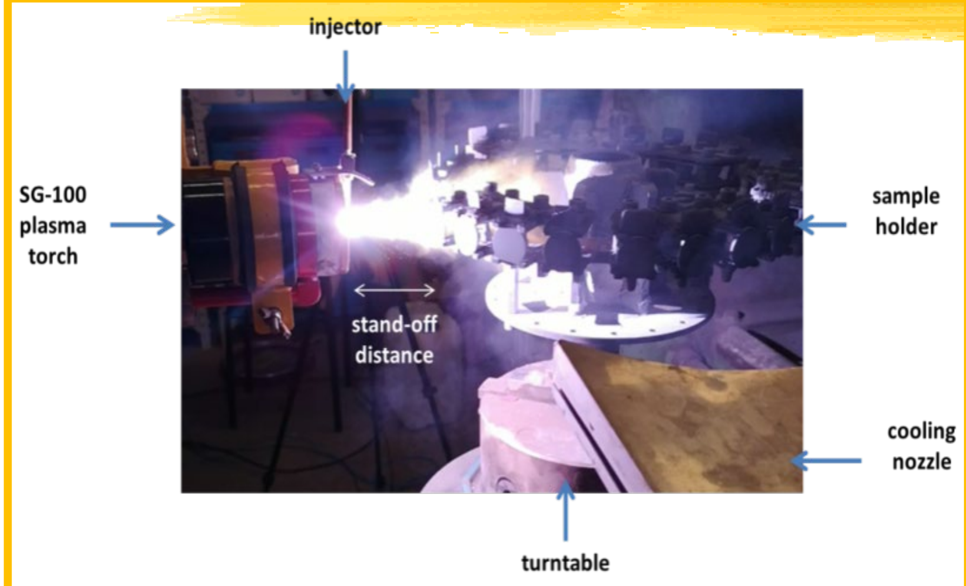

Plasma spraying processses
with spray system up to 100 kW of electric power
at
Wroclaw University of Science and Technology

Reference coatings – conventional YSZ TBCs doped with SiC

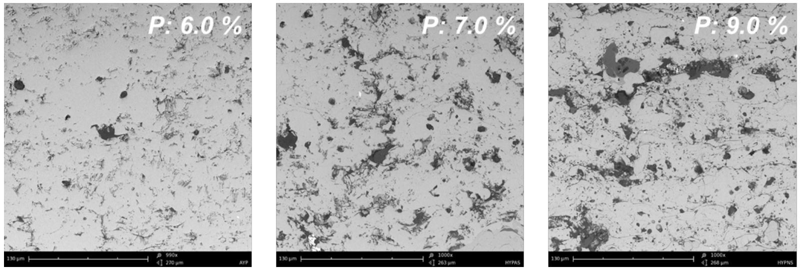

at higher magnification

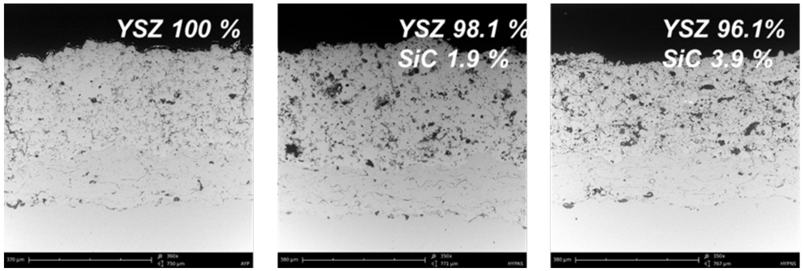

Coatings porosity and composition

YAG PRODUCTION using sol-gel method

powders with agglomerates in different shape and sizes

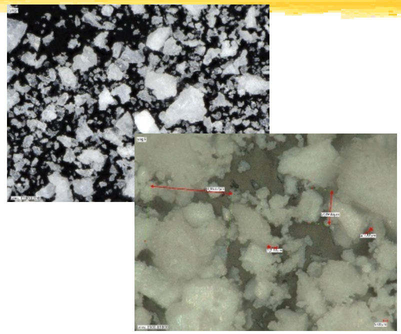

OM VHX-7000 Series (Kyence)

Procedure:
- zol production
- drying: 90C/3h/air
- calcination: 1200oC/3h/argon

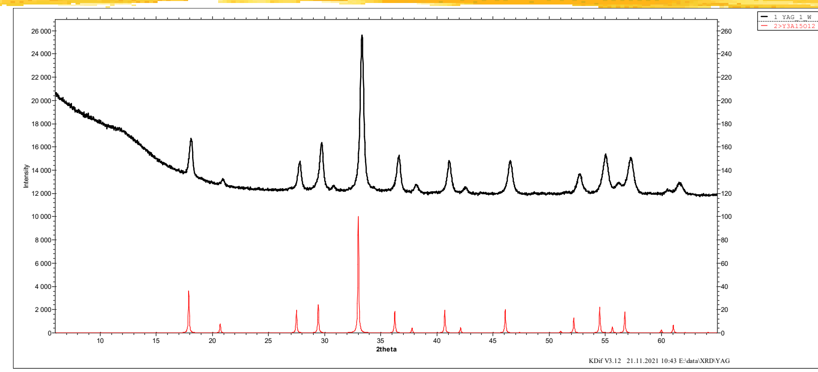

The XRD spectrum of powder sample after thermal treatment **(black)**
The spectrum calculated on the basis of cif file for Y3Al5O12 (mp-2050 structure from mateialsproject.org database, **red**)

EDS results

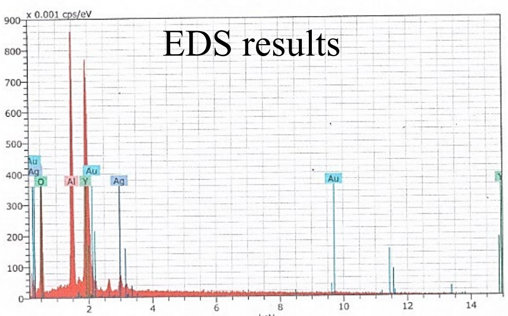

YAG 1 W		%wt				%at		
				średnia				średnia
Oxygen	32,03	32,78	33,4	32,73667	62,44	62,51	62,84	62,59667
Aluminium	17,73	18,76	19,15	18,54667	20,5	21,21	21,37	21,02667
Yttrium	44,75	46,63	46,01	45,79667	15,7	16	15,57	15,75667

Presence of Y, Al and O was confirmed

Recommendation

Y3Al5O12

element	atomic weight	wt%	at %
Y	88,90594	44,93053	15
Al	26,9815385	22,72617	25
O	15,99977	32,34331	60
	593,6227525		

On the base of mass proportion in INCT YAG is mostly close to the YAG in the form of $Y_3Al_5O_{12}$

SiC+YAG PRODUCTION using sol-gel method

Method used

- zol Al-Y, pH=3,5
- SiC in H2O
- mixing
- gelation proces
- calcination

1200oC/3h/argon

SEM

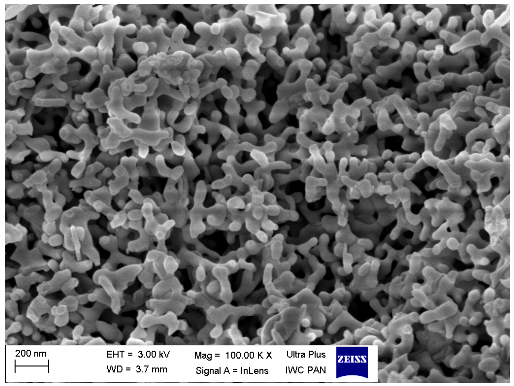

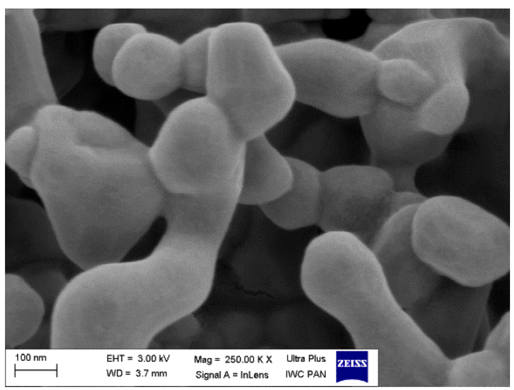

EDS

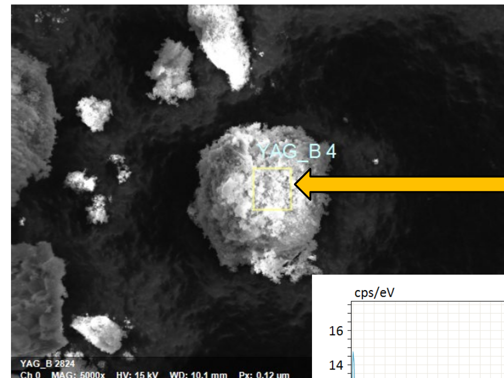

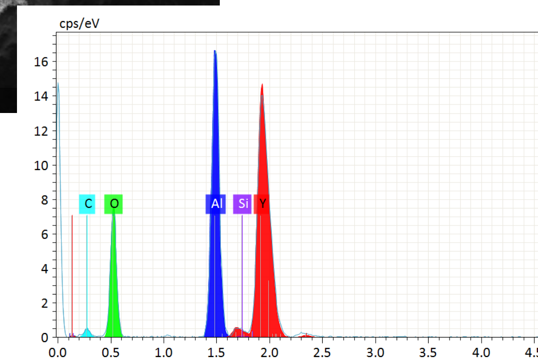

YAG_B 4

Element	At. No.	Netto	Mass [%]	Mass Norm. [%]	Atom [%]	abs. error [%] (1 sigma)	rel. error [%] (1 sigma)
Yttrium	39	76933	40.98	44.80	13.81	1.62	3.95
Oxygen	8	20221	29.67	32.43	55.56	3.86	13.03
Aluminium	13	57501	15.32	16.75	17.02	0.74	4.84
Carbon	6	1325	5.42	5.93	13.52	1.21	22.40
Silicon	14	279	0.08	0.09	0.09	0.05	58.24
		Sum	**91.48**	**100.00**	**100.00**		

Presence of Y, Al, Si, C, O was confirmed

FIELD ASSISTED SINTERING TECHNIQUES/ SPARK PLASMA SINTERING (FAST/SPS)

Spark plasma sintering (**SPS**), also known as **field assisted sintering technique** (**FAST**)

Guillon: Advanced Engineering Materials 2014,16, 7

* The field-assisted sintering technique/Spark plasma sintering (FAST/SPS) is a low voltage, direct current (DC) pulsed current activated, pressure-assisted sintering, and synthesis technique.

- This method can be used to synthesize new compounds and/or to densify materials in one step
- FAST/SPS is similar to hot pressing (HP), but the way the heat is produced and transmitted to the sintering material is different

Working schematic of a FAST apparatus.

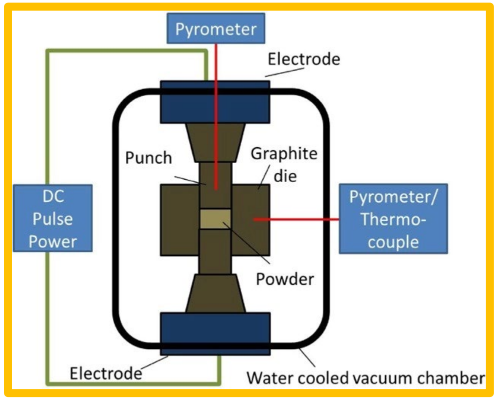

Institute of Electronic Materials Technology (Łukasiewicz - ITME), Warsaw, Poland

The Department of Ceramic-Metal Composites and Joints specializes in the fabrication of novel functional and structural composite materials, in the majority of cases based on metals and alloys reinforced with ceramic materials in different forms

ITME SPS facility

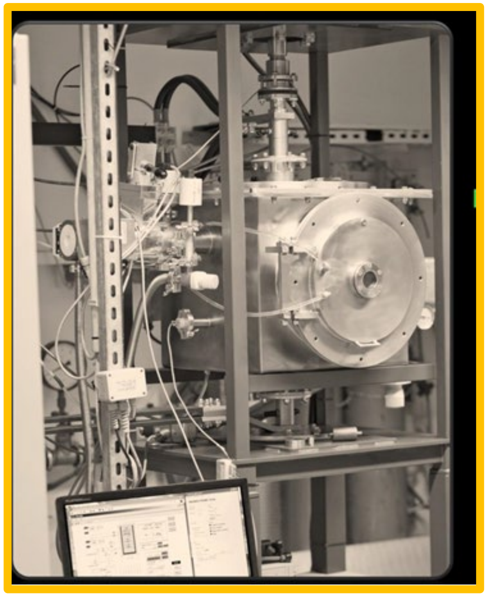

FIELD ASSISTED SINTERING PROCESS

To investigate behavior (SiC+YAG) composite

Substrates

SiC powder less 50 nm
+ 2.5% Al2O3
+ 2.5 % Y2O3

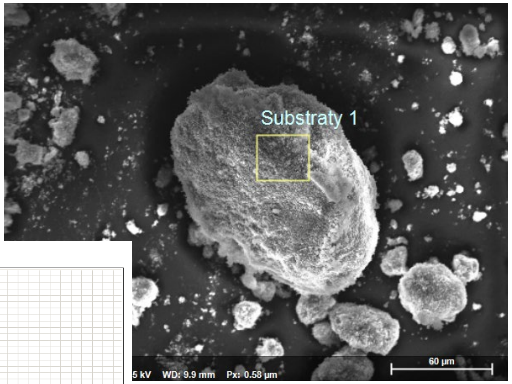

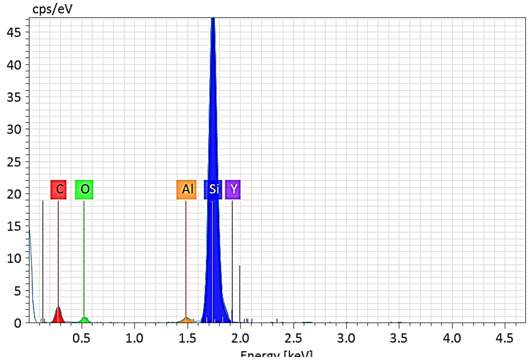

Substraty 1

Element	At. No.	Netto	Mass [%]	Mass Norm. [%]	Atom [%]	abs. error [%] (1 sigma)	rel. error [%] (1 sigma)
Carbon	6	3494	36.10	37.19	56.69	6.18	17.11
Oxygen	8	1272	4.81	4.96	5.67	1.09	22.70
Silicon	14	107175	55.16	56.84	37.05	2.33	4.22
Aluminium	13	1549	0.76	0.79	0.53	0.08	9.98
Yttrium	39	146	0.21	0.22	0.05	0.09	44.28
		Sum	97.05	100.00	100.00		

Presence of Si, C, Al, Y, O was confirmed

Sintering proces

- vacuum
- temperature 1900oC
- pressure 40 MPa
- time 5 min

FIELD ASSISTED SINTERING - FAST

Obtained bulk material

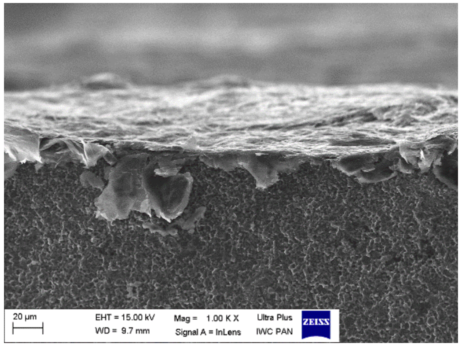

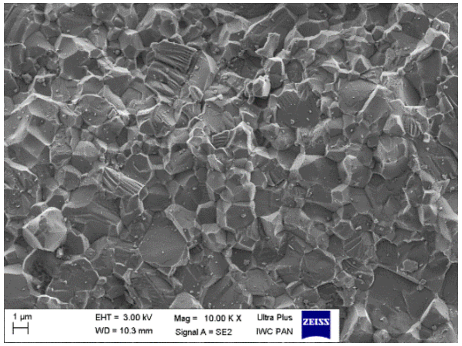

EDS (point analysis)

visible grain

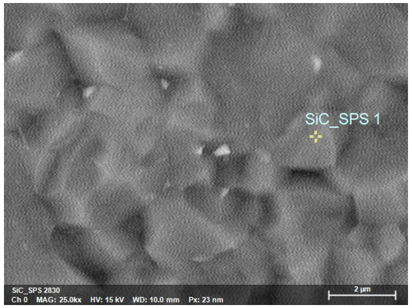

SiC_SPS 1

Element	At. No.	Netto	Mass [%]	Mass Norm. [%]	Atom [%]	abs. error [%] (1 sigma)	rel. error [%] (1 sigma)
Silicon	14	215952	67.19	67.37	47.21	2.82	4.20
Carbon	6	4291	31.81	31.89	52.26	5.23	16.44
Aluminium	13	2606	0.74	0.74	0.54	0.07	9.49
		Sum	99.73	100.00	100.00		

Confirmed presence: Si, C

between grains

SiC_SPS 1

Element	At. No.	Netto	Mass [%]	Mass Norm. [%]	Atom [%]	abs. error [%] (1 sigma)	rel. error [%] (1 sigma)
Silicon	14	188110	72.82	66.09	54.76	3.05	4.20
Carbon	6	1677	16.35	14.84	28.75	3.33	20.34
Oxygen	8	3731	9.23	8.38	12.18	1.59	17.19
Aluminium	13	7886	2.76	2.50	2.16	0.16	5.94
Yttrium	39	7662	9.03	8.19	2.14	0.42	4.66
		Sum	110.18	100.00	100.00		

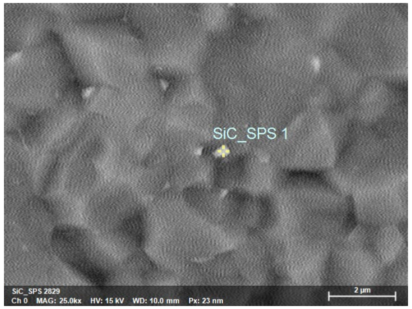

Confirmed presence: Y, Al, O and Si,C

SUMMARY

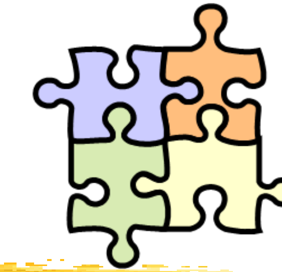

1. Proposed material: SiC+YAG can be considered as protective layer for Zry during normal work in PWR conditions

2. Protective mechanism is predicted to presence thermal barriers coating (TBC) formed with suspension Plasma Spraying (SPS)

3. Work realisation plan:
   3.1. ad. Suspension Plasma Spraying SPS: SiC+YAG coating formation
   3.2. ad. Field assisted sintering techniques FAST: optimisation of the sintering processes (different parameters as for example: substrates proportion, time and temperature)
   3.3. coatings characterisation:
- physicochemical properties
- useful properties including high temperature oxidation tests and long time autoclave experiments

EXPERIMENTAL SiC COATINGS

Thank you for your attention

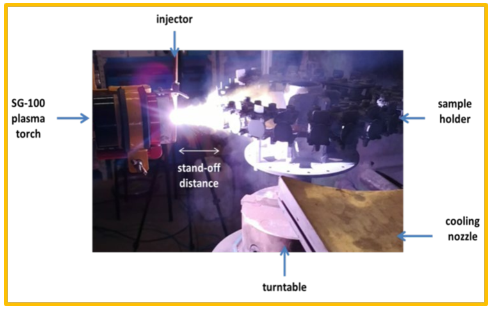

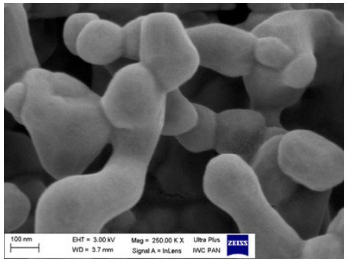

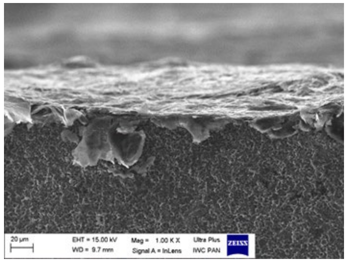

Acknowledgements

This work has been partially supported under IAEA Research Contract No. 24053/2020

The finanical support under the framework of joint JINR Dubna - Polish research groups programme 04-5-1131-2017/2021 is greatfully acknowledged

M. Steinbrück, J. Stuckert, M. Grosse

KIT

J.-F. Martin, D. Costa, D. Jacquemain

NEA

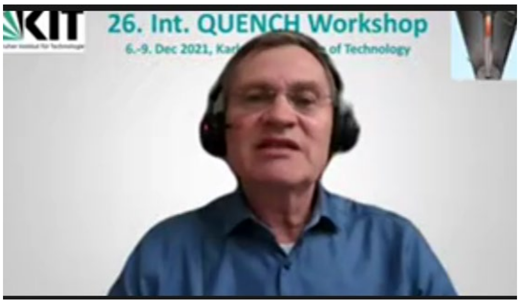

The OECD-NEA joint undertaking QUENCH-ATF

The purpose of the QUENCH-ATF project is to investigate the chemical, mechanical and thermal-hydraulics behavior of ATF claddings in Design Basis Accidents and Beyond Design Basis Accidents scenarios. This will be achieved through a series of three bundle tests at the QUENCH facility at the Karlsruhe Institute of Technology, Germany. Such ATF designs represent an alternative to the standard UO_2/Zry system, focusing on the reduction of hydrogen and heat release during severe accident scenarios, and thus increasing coping time for accident management measures, while maintaining or even improving the fuel assembly properties and performance during normal operation. Further requirements include reasonable costs, licensing as well as front end and back end performance. Prior commercial use, extensive testing of the new designs is paramount to demonstrate the advanced safety features; and the NEA QUENCH-ATF project contributes to this effort.

The project officially started with 18 partners in October 2021 and will last four years.

The focus of the first two tests will be on Cr-coated Zr alloys, a technology with a higher technology readiness level. The first test will be investigate conditions slightly beyond DBA LOCA. The scenario of the second test will be BDBA severe accident conditions T>1200 °C, above the Zr-Cr eutectic temperature). The decision about the third test will be made by the Management Board depending on the outcome of the first two tests and the availability of SiC CMC (ceramic matrix composite) rods with 2.3 m length. The third test may be another test with Cr-coated zirconium alloy (DBA or SA) or a test with SiCf-SiC cladding tubes under BDBA conditions.

The OECD-NEA joint undertaking QUENCH-ATF

M. Steinbrück, J. Stuckert, M. Grosse (KIT), J.-F. Martin, D. Costa, D. Jacquemain (NEA)

26th International QUENCH Workshop, MS Teams, 6-9 December 2021

Institute for Applied Materials IAM-AWP & Program NUSAFE

Zirconium alloys in nuclear reactors

- Zr alloys are used for fuel rod cladding worldwide for decades
- Advanced Zr alloys provide excellent properties during operation conditions with respect to neutronic and mechanical properties as well as corrosion resistance
- During accident scenarios, i.e. at higher temperatures, the exothermic reaction between Zr and steam results in degradation of mechanical properties as well as release of hydrogen and heat
- Strong effect of this reaction on accident progression as seen in Fukushima accidents
- Global research on more accident-tolerant fuel (ATF) materials after the Fukushima accidents
- ATF materials should reduce release of hydrogen and heat and increase coping time for accident management measures (AMM)

Materials selection for ATF cladding

<u>High temperature oxidation resistance</u> of metals, alloys and non-oxide ceramics is based on the selective formation of protective oxides, namely of <u>SiO_2, Al_2O_3 and Cr_2O_3</u>

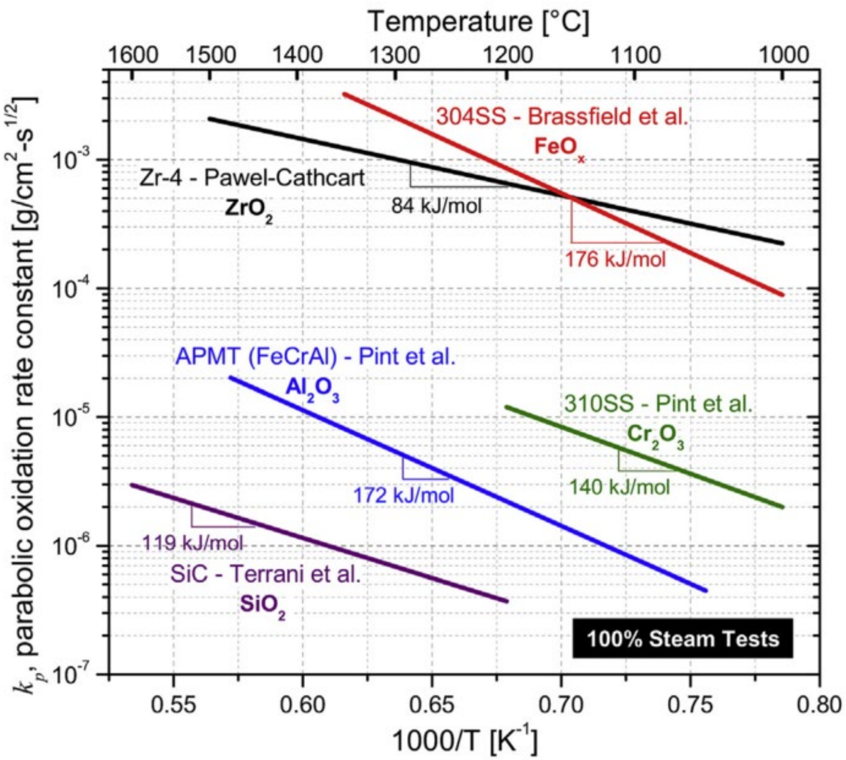

Parabolic oxidation rates of selected materials

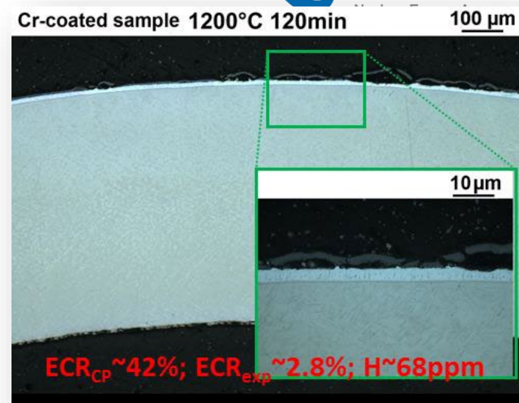

Cr-Zry
2 h 1200°C
steam
4 µm Cr_2O_3
ZrO_2: 250 µm

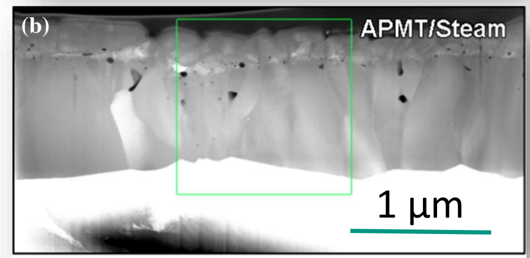

FeCrAl
4 h 1200°C
steam
1 µm Al_2O_3
ZrO_2: 350 µm

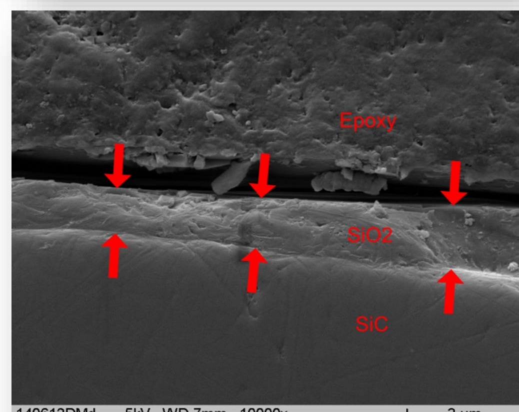

SiC
1 h 1700°C
steam
1 µm SiO_2
ZrO_2: 2400 µm

Terrani. JNM 501 (2018) 13-30
Krejci, TOPFUEL 2018
Unocic, OxMet 87 (2017) 431-441
Avincola, NED 295 (2015) 468-478

QUENCH-ATF

OECD-NEA joint undertaking

- on large-scale bundle tests
- at the QUENCH facility (KIT)
- with ATF cladding materials
- simulating design-basis and severe accident scenarios
- under the auspices of NEA/CSNI and NEA/NSC

Proposal for the Joint Undertaking

- Three bundle experiments with ATF cladding in the QUENCH facility
  - Cladding tubes provided by WEC (and others?)
- Supporting separate-effects tests
- Code support for test preparation and code benchmark exercises
  - GRS volunteered to coordinate benchmark activities
- Time frame: 2021-2025
- Costs: 1.6 M€ (approx. 500 000 €/test) + NEA fee
  - 50% covered by KIT/Germany
  - 50% covered by collaborators

Planned experiments

1. Cr-coated Zry: extended DBA LOCA conditions
2. Cr-coated Zry: BDBA conditions
   - above the Zr-Cr eutectic temperature
   - application of ATCR under discussion (CRIEPI proposal)
3. To be decided:
   - SiC: BDBA conditions   OR
   - Cr-coated Zry: scenario depending on outcome of previous tests
   - ➢ GO/NOGO on SiC in 2022/23

Reference tests with ZIRLO would be available for various scenarios

Participants from 8 countries (19 organizations + Third parties)

- **Czech Republic**
  - ÚJV Řež
- **France**
  - CEA
  - EDF
  - Framatome
  - IRSN
- **Germany**
  - GRS
  - KIT (Operating Agent)
- **Japan**
  - CRIEPI
  - JAEA
- **Russian Federation**
  - Bochvar Institute
  - Kurchatov Institute
  - TVEL
- **Switzerland**
  - PSI
  - ENSI
- **United Kingdom**
  - NNL
- **United States**
  - EPRI
  - GA
  - NRC
  - Westinghouse*

Project status and next steps

- Agreement signed by 18 of 19 partners (> 95 % of the budget)
- Official start Oct 25, 2021, duration 4 years
- First management board meeting took place on 2nd Dec 2021
- First test under preparation
- Technical meeting to be planned in advance of the first test for final discussion of test conduct

Main results of the 1st MB meeting

- Chair: Hossein Esmaili (US-NRC)
- Program Manager: Martin Steinbrück (KIT)
- SSM (Sweden) request to join the project
- Financial report and call for contributions 2021 are approved

- Time line for the 1st test
  - Dec 7: MTA signed
  - Dec 10: Ship samples
  - Sample arrival: 3-6 weeks after ship date
  - 6-8 working weeks for bundle assembly and testing
  - Test conduct: March 2022

QUENCH-ATF-1 bundle and scenario

- Reference test QUENCH-LOCA-3HT
- Test bundle with 24 heated rods, pitch 12.6 mm
- Heating-up rate during heating in superheated steam: 5 K/s
- Peak cladding temperature at the end of the heat-up stage: 1600K
- Duration of cool-down stage from 1600 K to 1200 K in steam: ≈ 200 s
- Rate of water flooding after cool-down stage: ≈ 4 g/s/rod

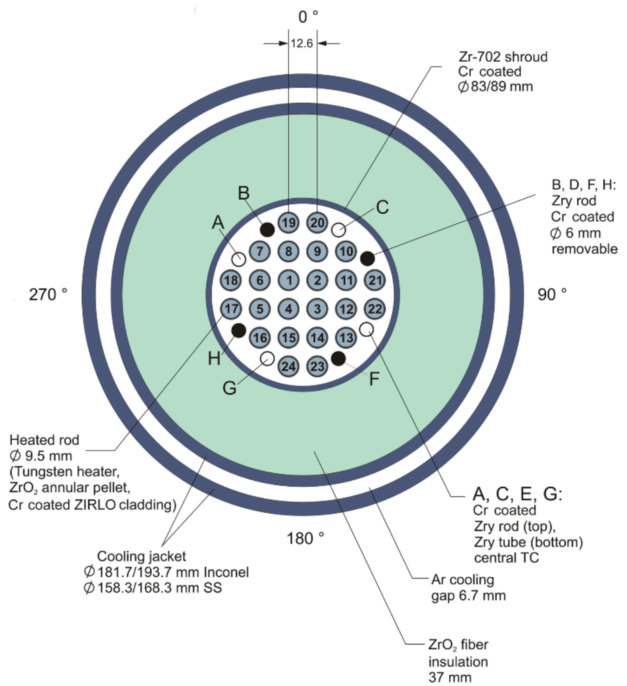

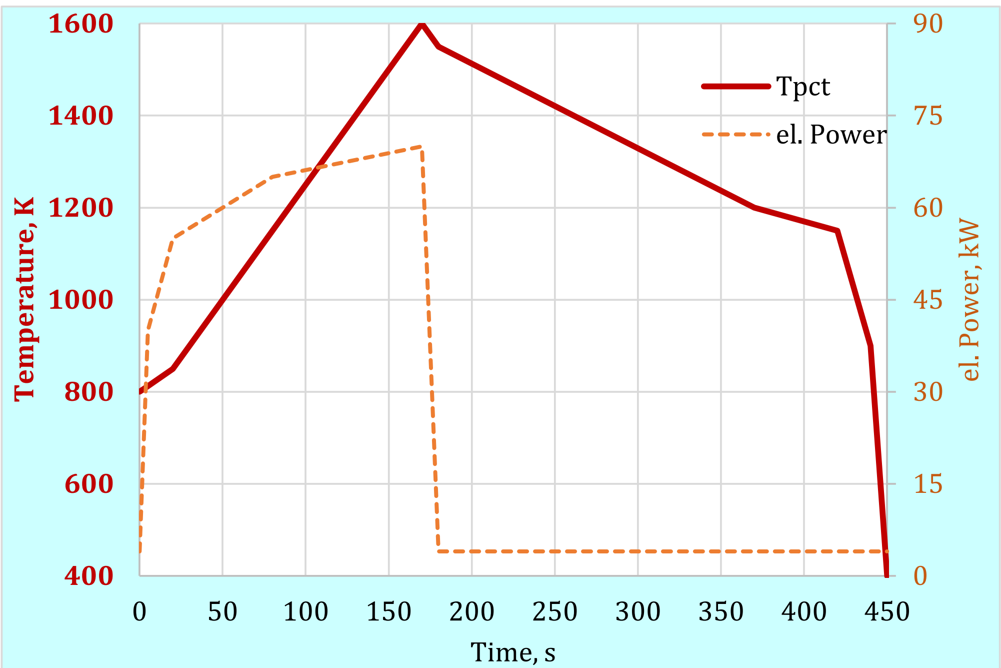

Heated rod parts: heaters, electrodes, pellets

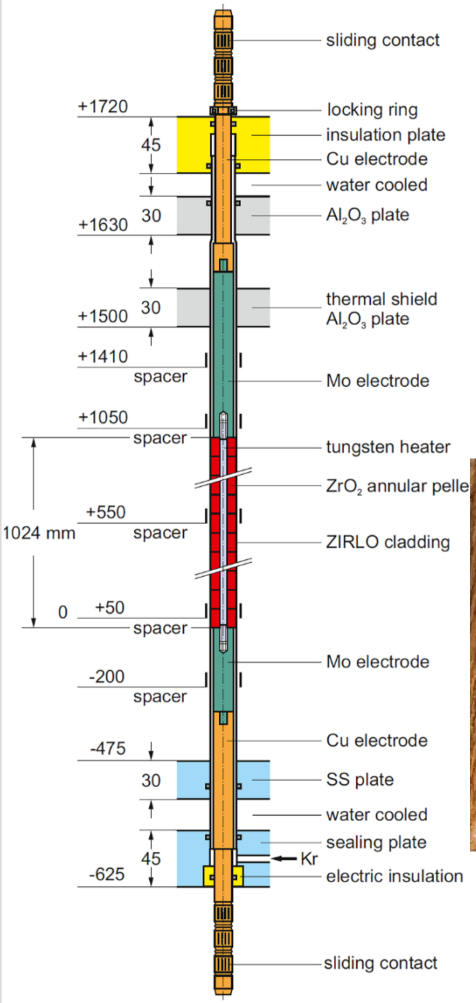

24 heated rods

2234 ZrO_2 pellets
OD=7.93 mm,
ID=4.75 mm

24 W heaters, OD 4.6 mm

24 Mo/Cu upper electrodes
partially coated by ZrO_2 (200 µm)
OD 7.75 mm in coated region

24 Mo/Cu lower electrodes
partially coated by ZrO_2 (200 µm)
OD 7.75 mm in coated region

Zr shroud coated with Cr on the inside

Zr sheet (thickness 3 mm)
PVD coated with Cr (10 µm, X-ray measured)
at one side

Tube bending

weld seam

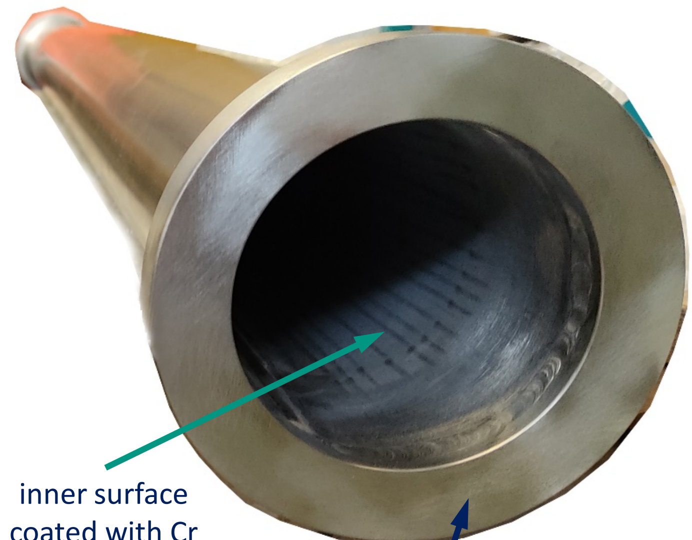

inner surface
coated with Cr

Zr flange

Bundle composition and instrumentation

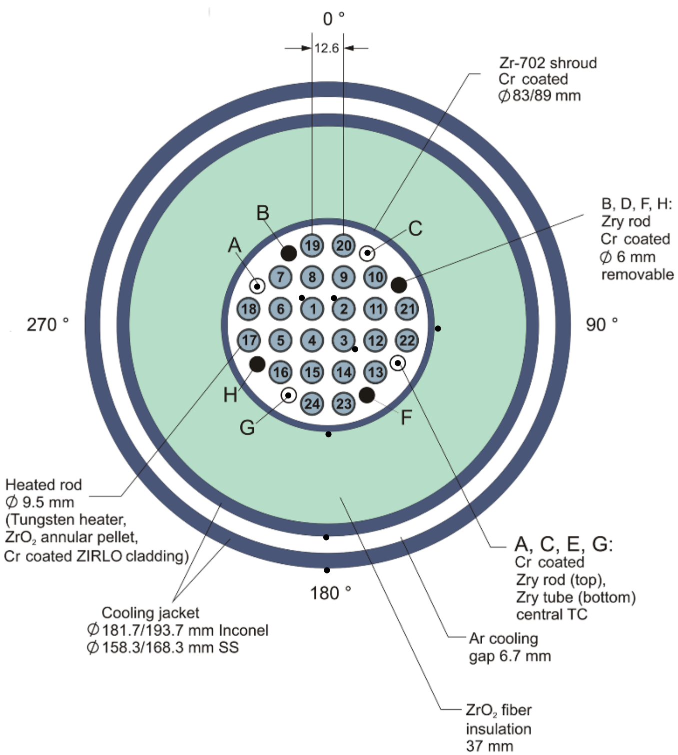

bundle cross section with 24 heated rods,
4 corner rods, 4 instrumented corner tubes
and surface thermocouples

corner rods and tubes (OD 6 mm)
PVD coated with Cr (10 µm)

75 NiCr/Ni thermocouples
sheathed with stainless steel

Thank you!

J. Liu, U. Stegmaier, C. Tang, M. Steinbrück,
M. Grosse

KIT

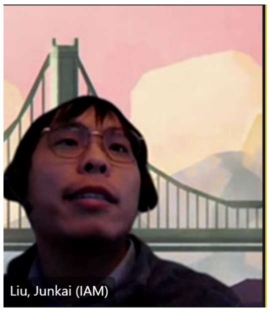

The coating degradation mechanism during the isothermal steam oxidation of Cr-coated Zry-4 at 1200°C

The isothermal steam oxidation behavior of Cr-coated Zry-4 at 1200°C was comprehensively studied at "BOX" rig in KIT. The temperature of all samples rose sharply from room temperature to 1200°C to avoid elemental inter-diffusion between the coating and the substrate during the heating-up stage.

The duration of the steam exposure varied from 5 min to 3 h. The hydrogen produced by the oxidation in furnace was in situ analyzed by a mass spectrometer. The microstructure of the samples after steam oxidation was investigated by XRD, OM, SEM, and TEM.

The results show that an oxidation kinetics transition occurs at ~30 min. The transition is mainly attributed to the reduction of the Cr_2O_3 scale thickness. The decrease in thickness is caused by the reaction between the Cr_2O_3 scale and the Zr, which diffuses from substrate to the Cr_2O_3/Cr interface along the Cr grain boundaries. This reaction will further lead to the formation of pores on the Cr_2O_3/Cr interface. When the thickness of Cr_2O_3 scale decreases to a certain value, with the formation of ZrO_2 diffusion channel inside the unoxidized Cr coating, a lot of oxygen diffuses into the Zry-4 substrate and results in the coating degradation.

The coating degradation mechanism during the isothermal steam oxidation of Cr-coated Zry-4 at 1200°C

Institute for Applied Materials (IAM-AWP)

Junkai Liu

Ulrike Stegmaier, Chongchong Tang, Martin Steinbrück, Mirco Große

The 26th International QUENCH Workshop

08.12.2021

1. Motivation

Q1 Why the thickness of Cr_2O_3 layer decreases?

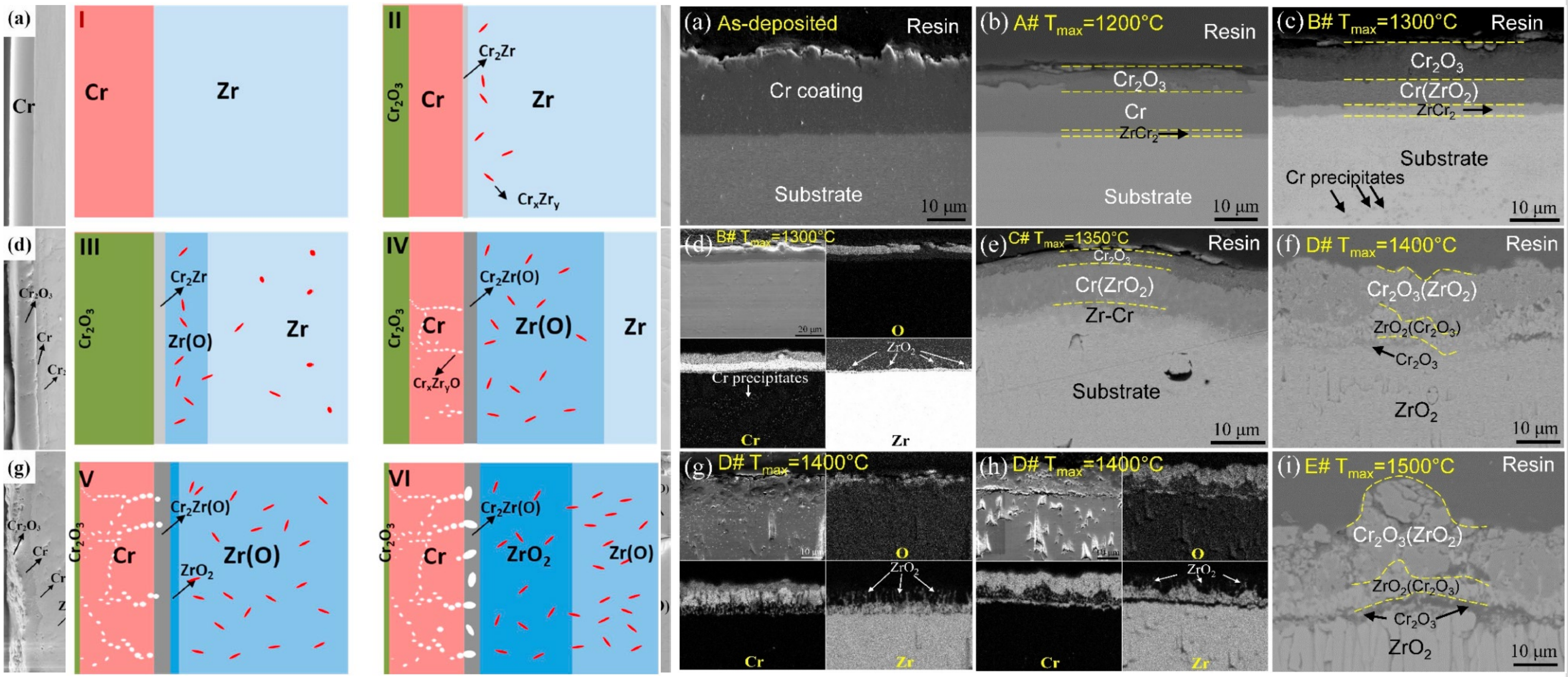

- The thickness of the Cr_2O_3 scale first increases by the reaction between Cr coating and steam
- When the thickness of oxide layer reaches its maximum value, the oxide layer will be reduced by the redox reaction between Cr_2O_3 and Zircaloy substrate
- ZrO_2 forms in Zircaloy substrate when the thickness of the Cr_2O_3 layer decreases

[1] X. Han et al. Corros. Sci. 174 (2020), 108826. [2] J. Liu et al. Corros. Sci. 192 (2021), 109805.

1. Motivation

Q2 The relationship between the reduction of Cr_2O_3 and the outward diffusion of Zr?

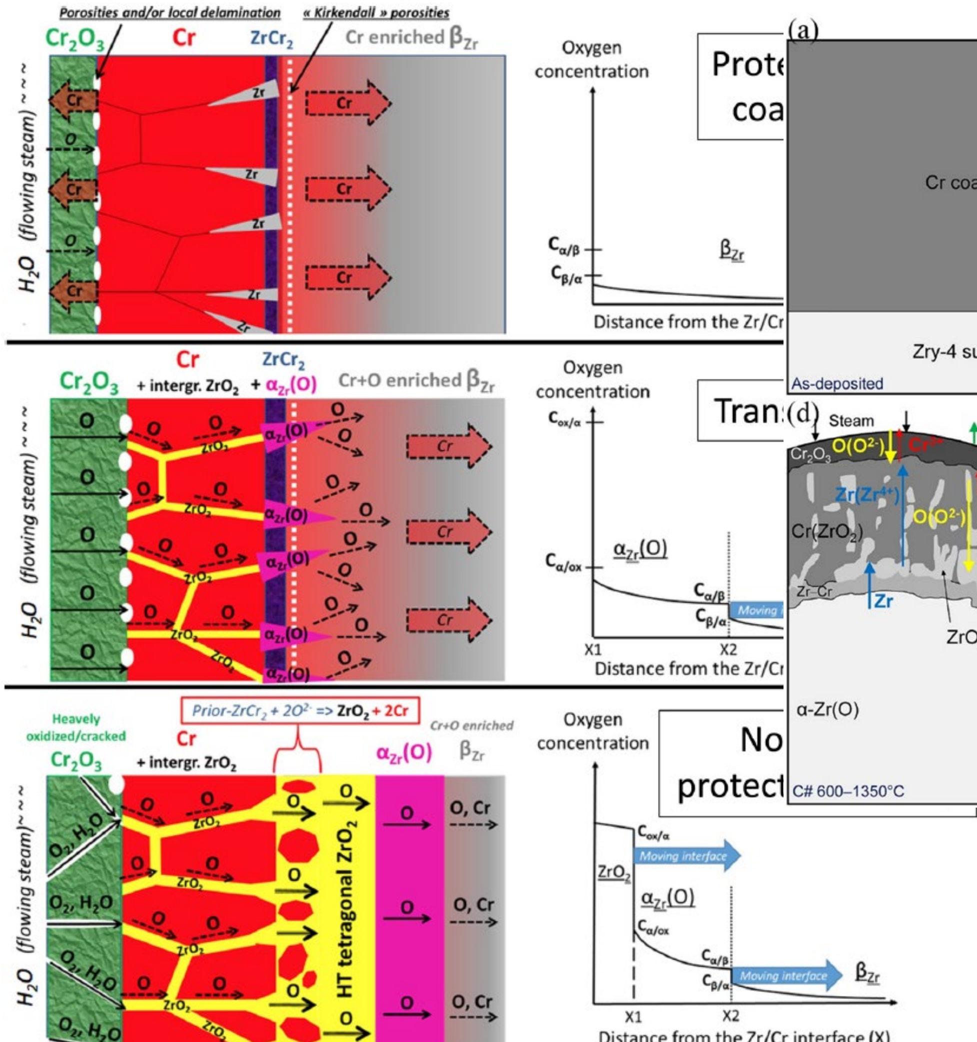

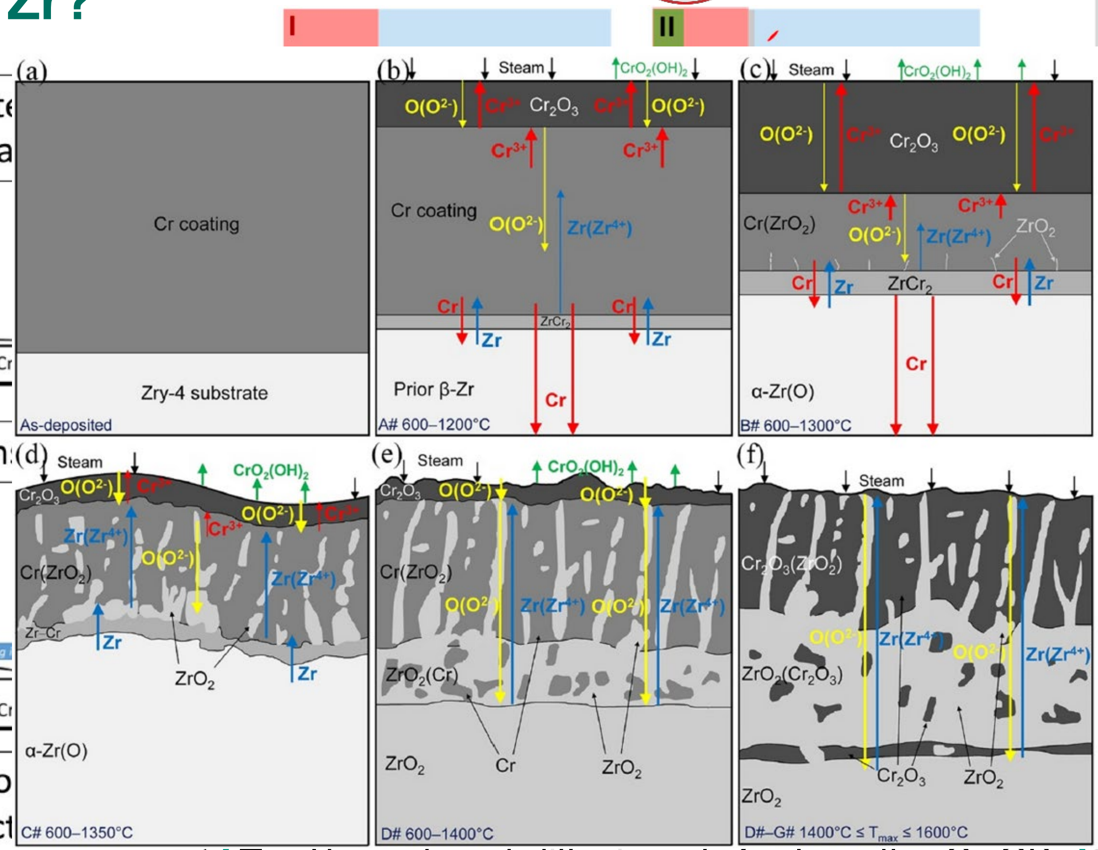

- The outward diffusion of Zr along the Cr GBs and the formation of ZrO_2 provide the diffusion paths for O
- Zr is oxidized by O diffused from the atmosphere

[1] J. Brachet e tal. Corros. Sci. 167 (2020), 108537. [2] X. Han et al. Corros. Sci. 174 (2020), 108826. [3] J. Liu et al. Corros. Sci. 192 (2021), 109805.

1. Motivation

Q3 The effect of the interfacial pores/voids?

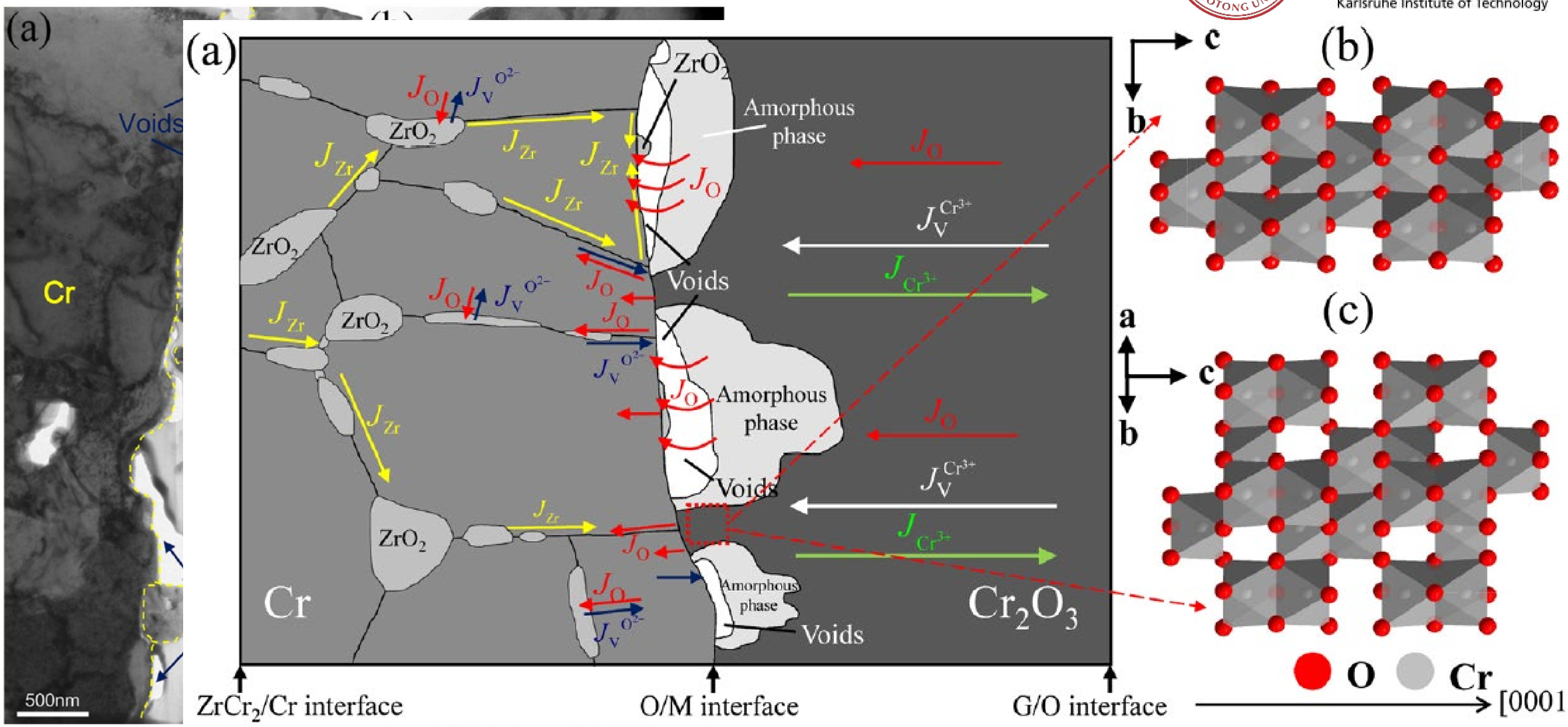

- Pores/voids form on the O/M interface due to the vacancy condensation
- Cr^{3+} vacancies diffuse from the G/OI to the O/MI, O^{2-} vacancies diffuse from ZrO_2 to the O/MI
- The formation of interfacial pores/voids affects the oxidation mechanism of Cr and leads to the decomposition of Cr_2O_3
- The incomplete decomposition of Cr_2O_3 produces the amorphous phase

[1] J. Liu et al. Corros. Sci. (2021), 109682.

2. Experimental

Test facility: BOX rig in KIT

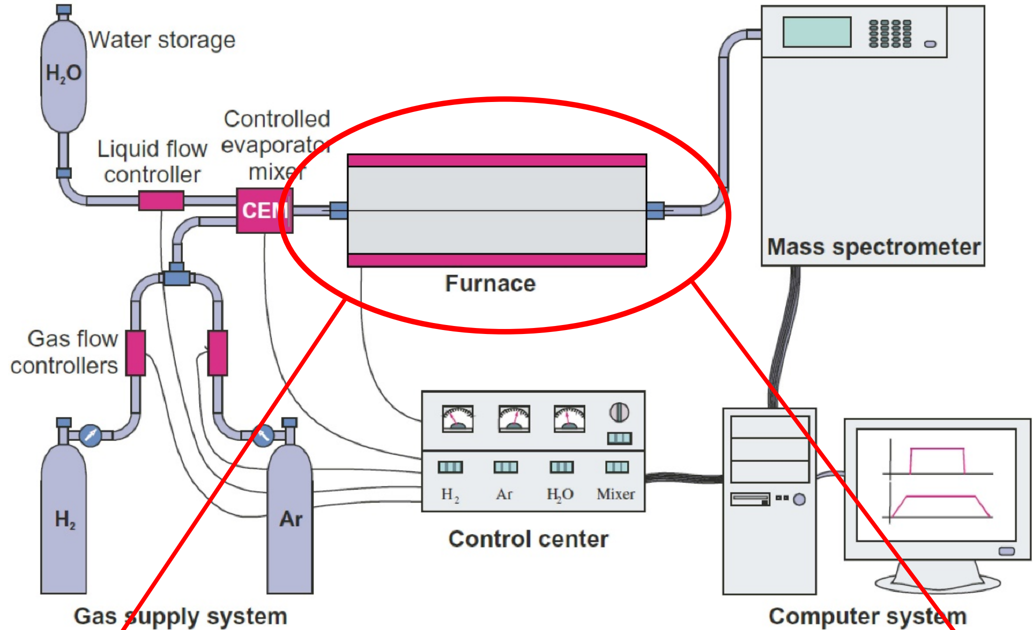

- *Before oxidation: Sudden heated up to 1200 °C*
- *After oxidation: Quench in argon*

Very important !!!

- Oxidation time(min): 5, 10, 20, 30, 45, 60, 90, 120, 180
- Steam flow: 20 g/h
- Argon flow: 20 L/h

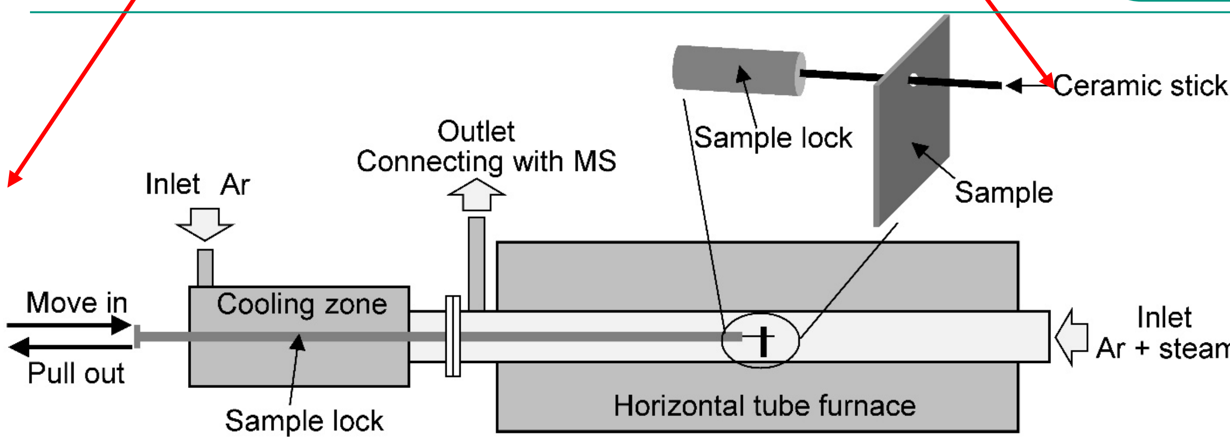

3. Results
3.1 Hydrogen release curves and weight gain curves

❖ Hydrogen release curves

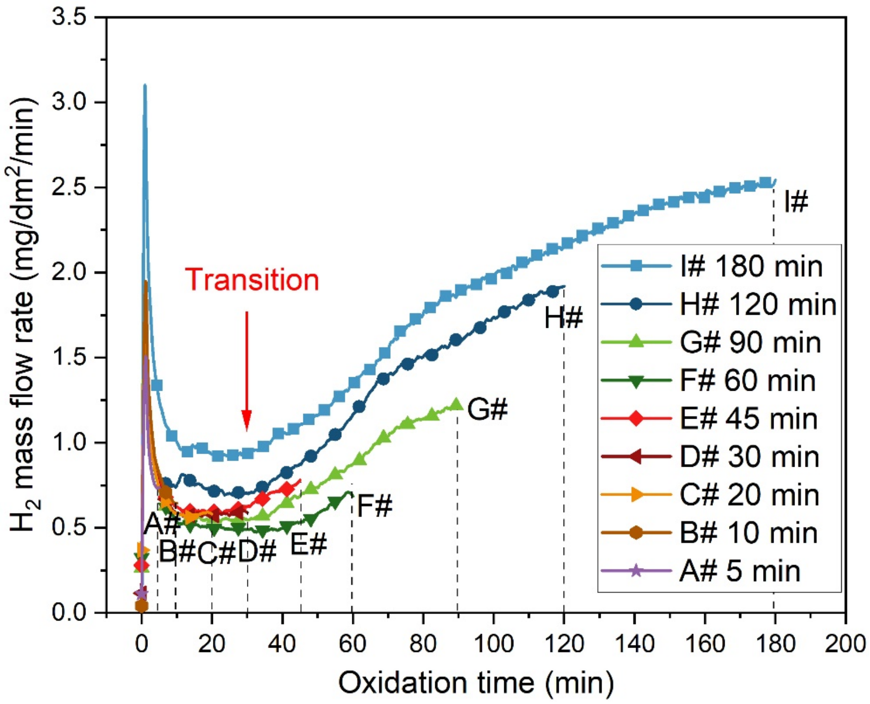

❖ Weight gain curves

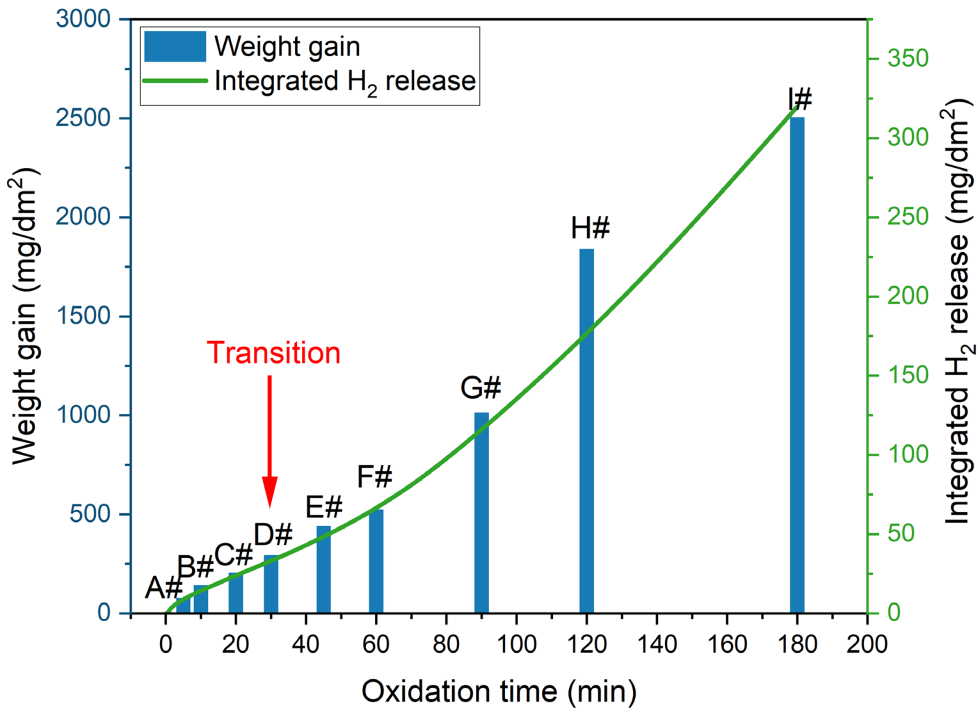

- Oxidation transition occurs at ~30 min
- Similiar trends of different curves

- Parabolic law before transition
- Linear law after transition

3. Results

3.2 Surface XRD

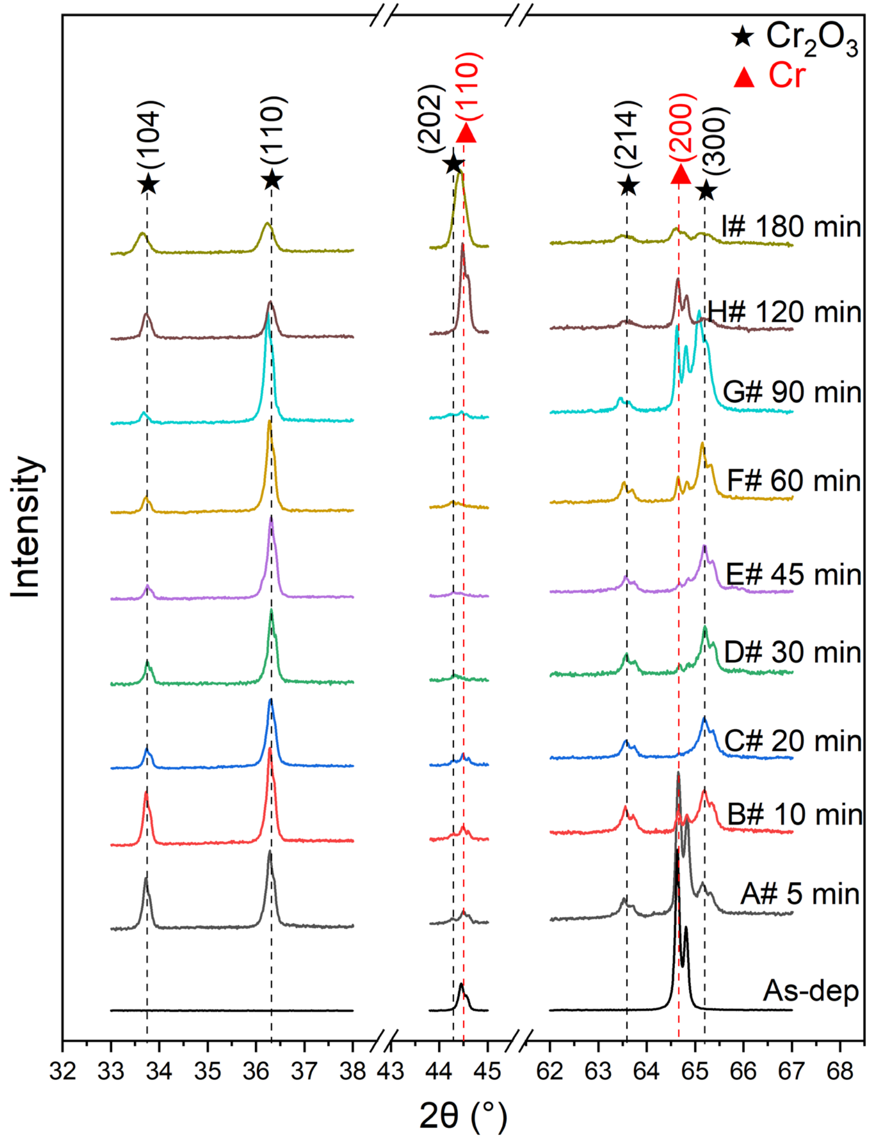

- The c-Cr peaks decrease and almost disappear after oxidation for 30min → the oxidation of Cr coating and the thickness increase of Cr_2O_3
- The c-Cr peaks appear again after oxidation for ~60min, then the intensity of the Cr (110) peak increases with oxidation time → the transformation of Cr_2O_3 to Cr
- The Cr_2O_3 peaks exist in every samples after oxidation

3. Results

3.3 Microstructures before transition: 5-30 min

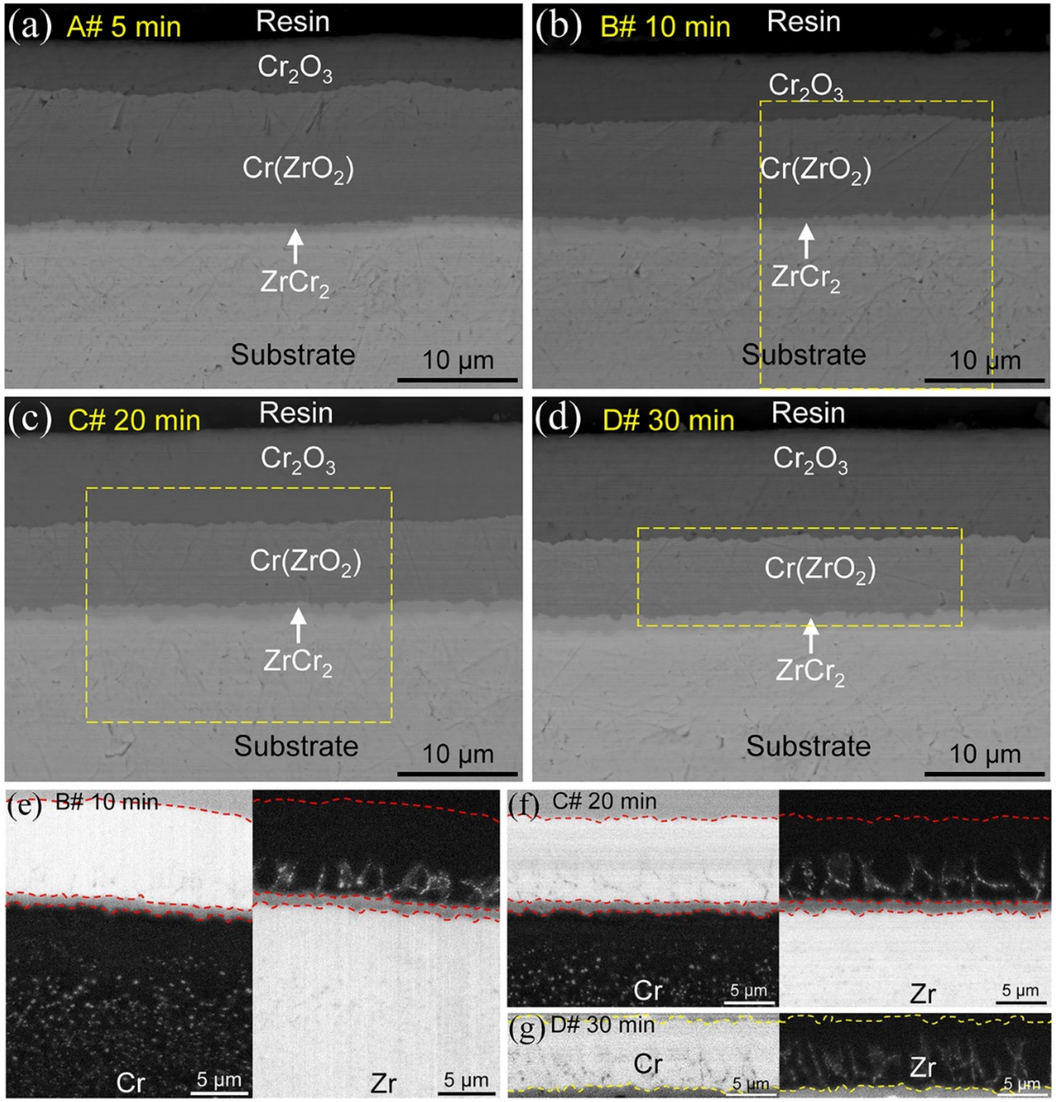

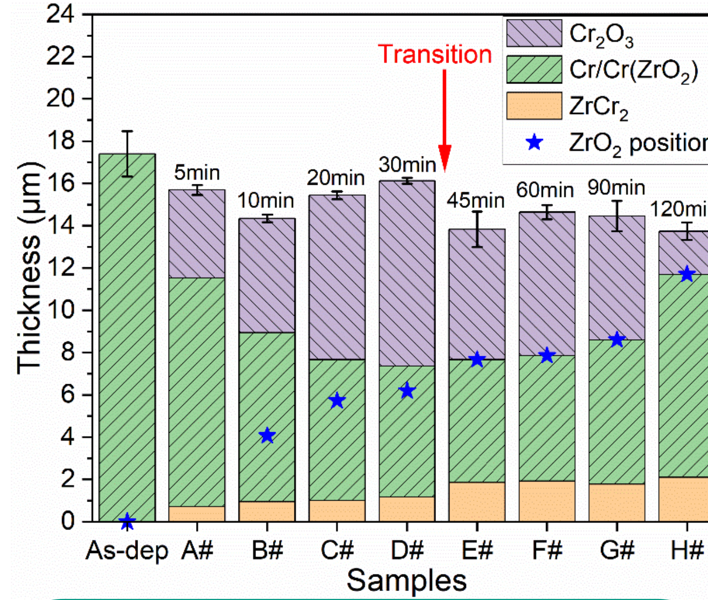

- Thickness evolution: Cr_2O_3↑, Cr↓, $ZrCr_2$↑
- Zr diffuses outward along the grain boundaries of Cr. The diffusion distance increases with oxidation time. The diffusion coefficient decreases with oxidation time
- *Before transition, Zr does not reach the Cr_2O_3/Cr interface*

3. Results
3.4 Microstructures after transition: 45-90 min

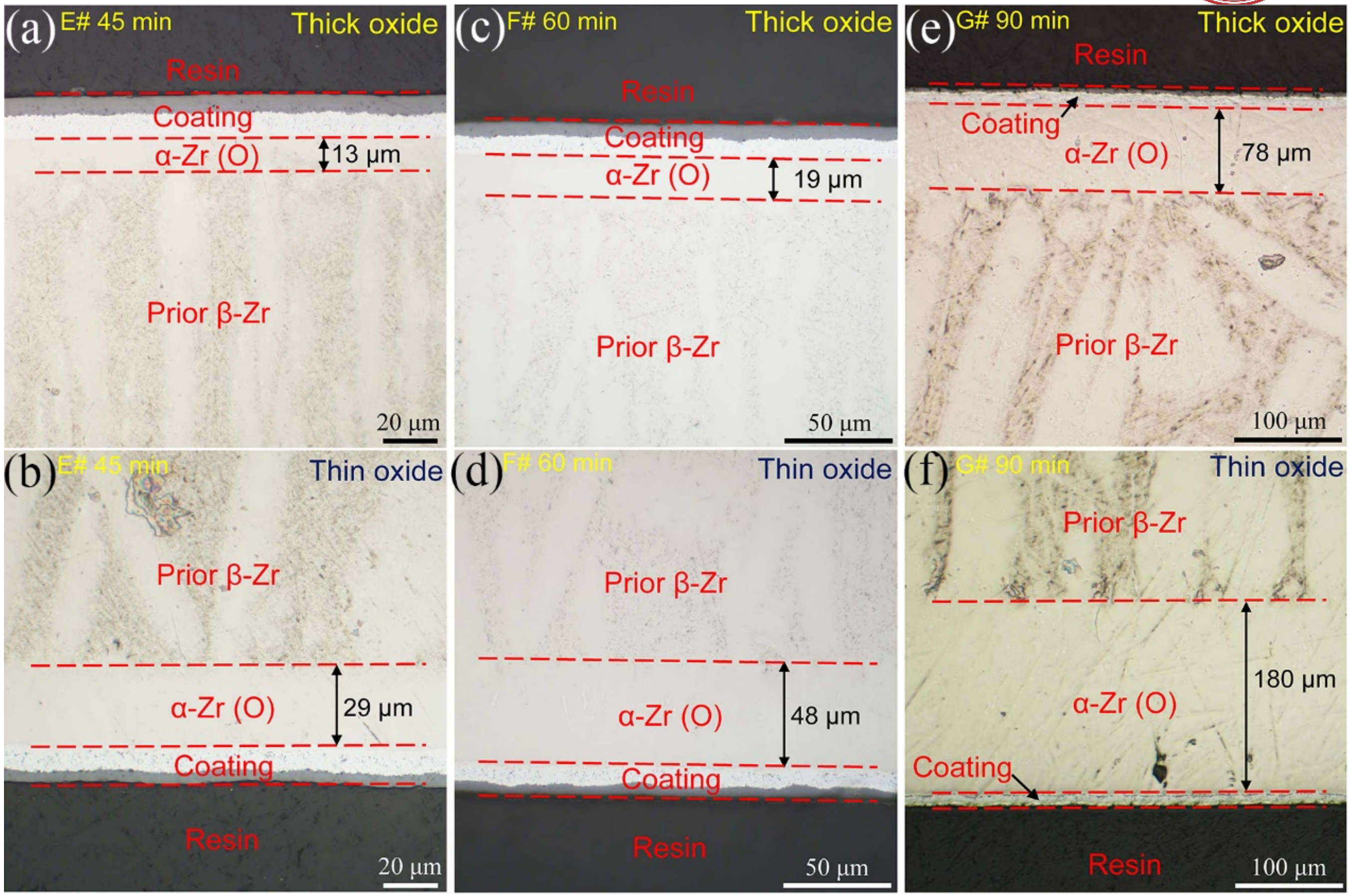

- The thickness of Cr_2O_3 is different on two surfaces, and is not related to the steam flow direction
- The formation of α-Zr(O) layer after transition
- The thickness of α-Zr(O) layer is related to the thickness of the Cr_2O_3 layer

3. Results

3.4 Microstructures after transition: 45-90 min

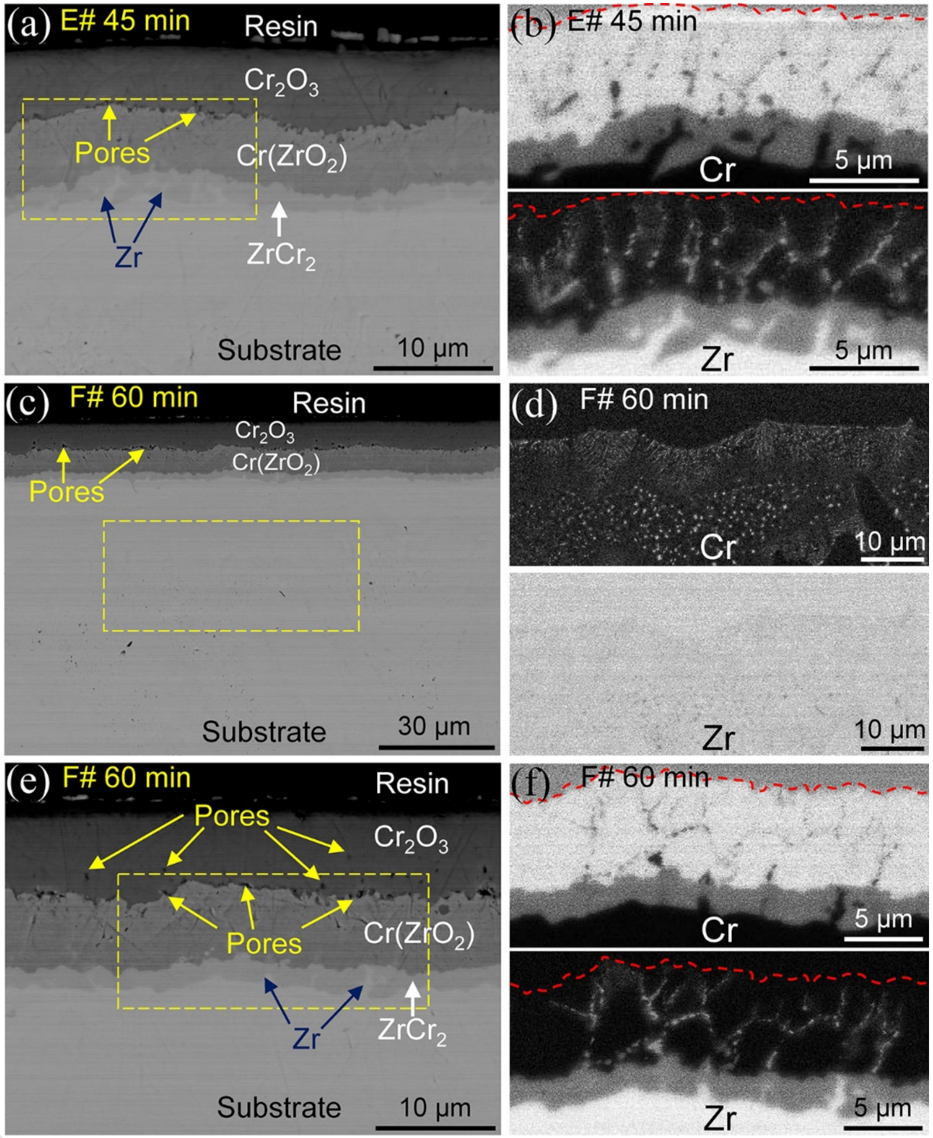

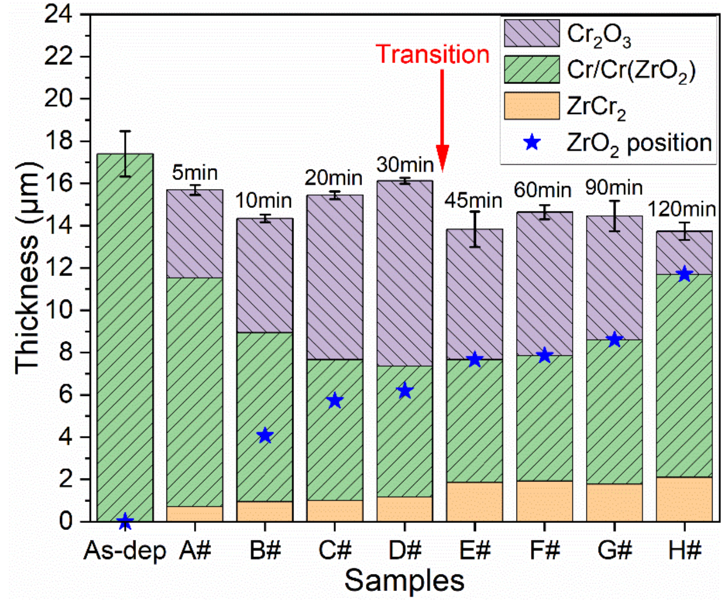

- From 30-45 min, the thickness of Cr_2O_3 ↓
- Zr reaches the Cr_2O_3/Cr interface after transition
- Pores form on Cr_2O_3/Cr interface
- The Cr_2O_3/Cr and Cr/$ZrCr_2$ interfaces transform from flat to flection
- The $ZrCr_2$ layer is not continuous
- Formation of Cr-rich particles in substrate
- From 45-90 min, the thickness of Cr_2O_3 does not change too much

3. Results
3.4 Microstructures after transition: 45-90 min

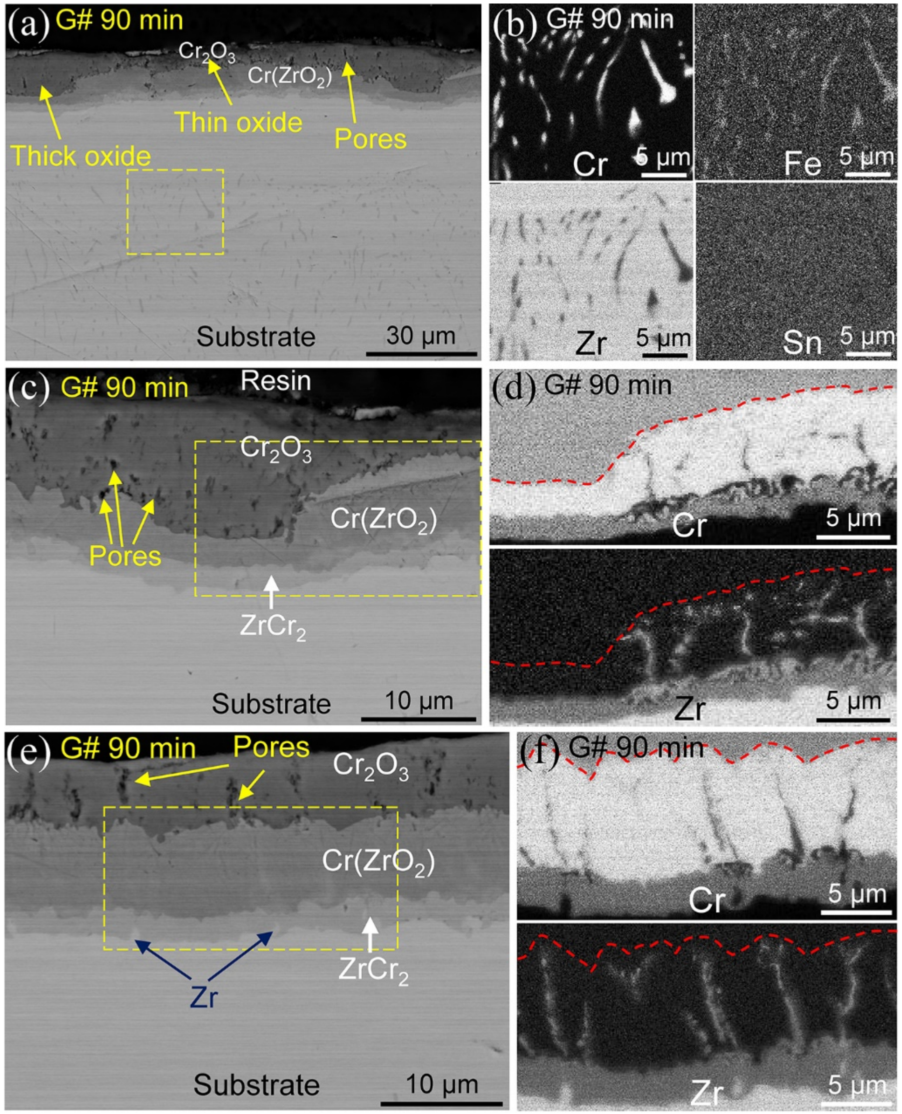

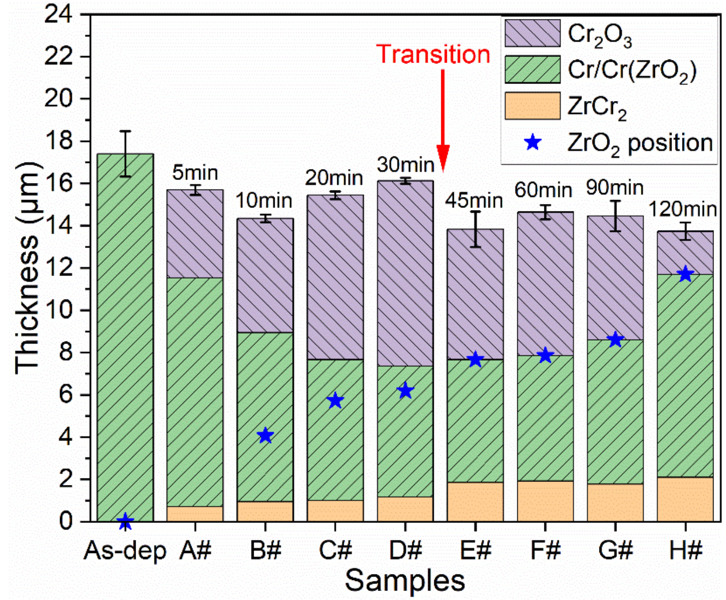

- The thickness of Cr_2O_3 is related to the outward diffusion of Zr
- Pores form on Cr_2O_3/Cr interface
- It is the outward diffusion of Zr causes the wave-like Cr_2O_3/Cr interface
- The formation of pores inside the Cr_2O_3 scale
- Slightly increase of the thickness of Cr layer
- Cr-rich precipitates transform to large clubbed shape, Fe segregates in these precipitates

Cr_2O_3 scale should be mainly reduced by the reaction between Cr_2O_3 and Zr diffused to the interface

3. Results

3.5 TEM results of the G# sample oxidation for 90 min

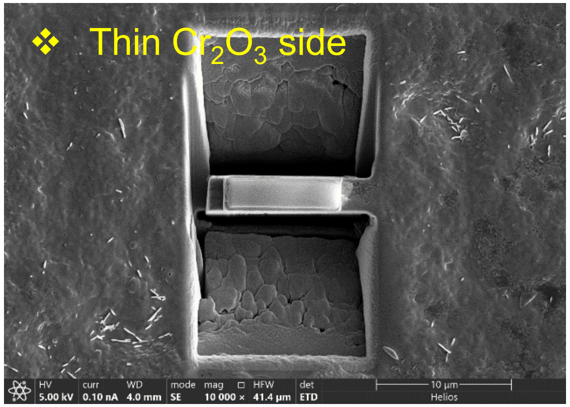

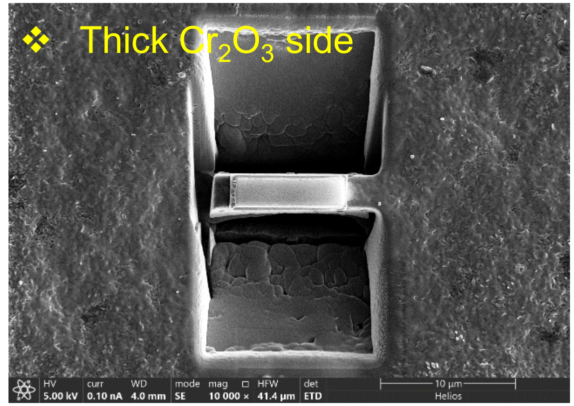

- TEM specimens are lifted by FIB on both two surfaces of the G# sample due to the *different thickness of Cr_2O_3 layer between two surfaces*

❖ Thick Cr_2O_3 side

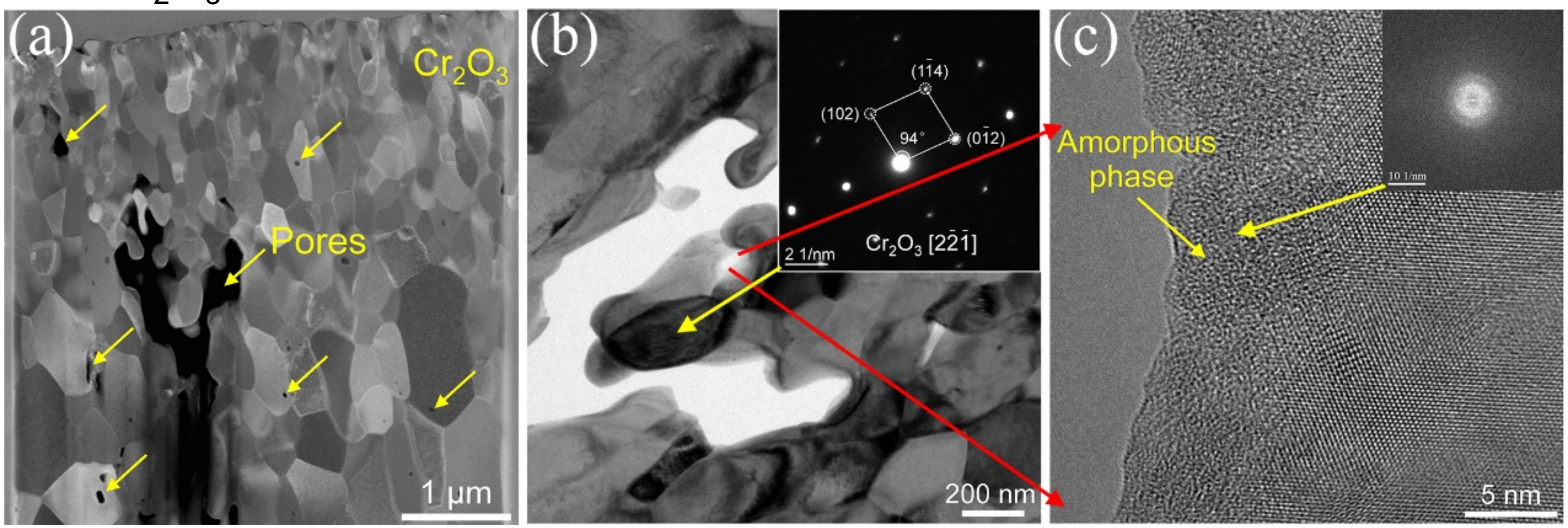

- The appearance of pores inside the Cr_2O_3
- The amorphization of Cr_2O_3 close to the pores

3. Results

3.5 TEM results of the G# sample oxidation for 90 min

❖ Thin Cr_2O_3 side

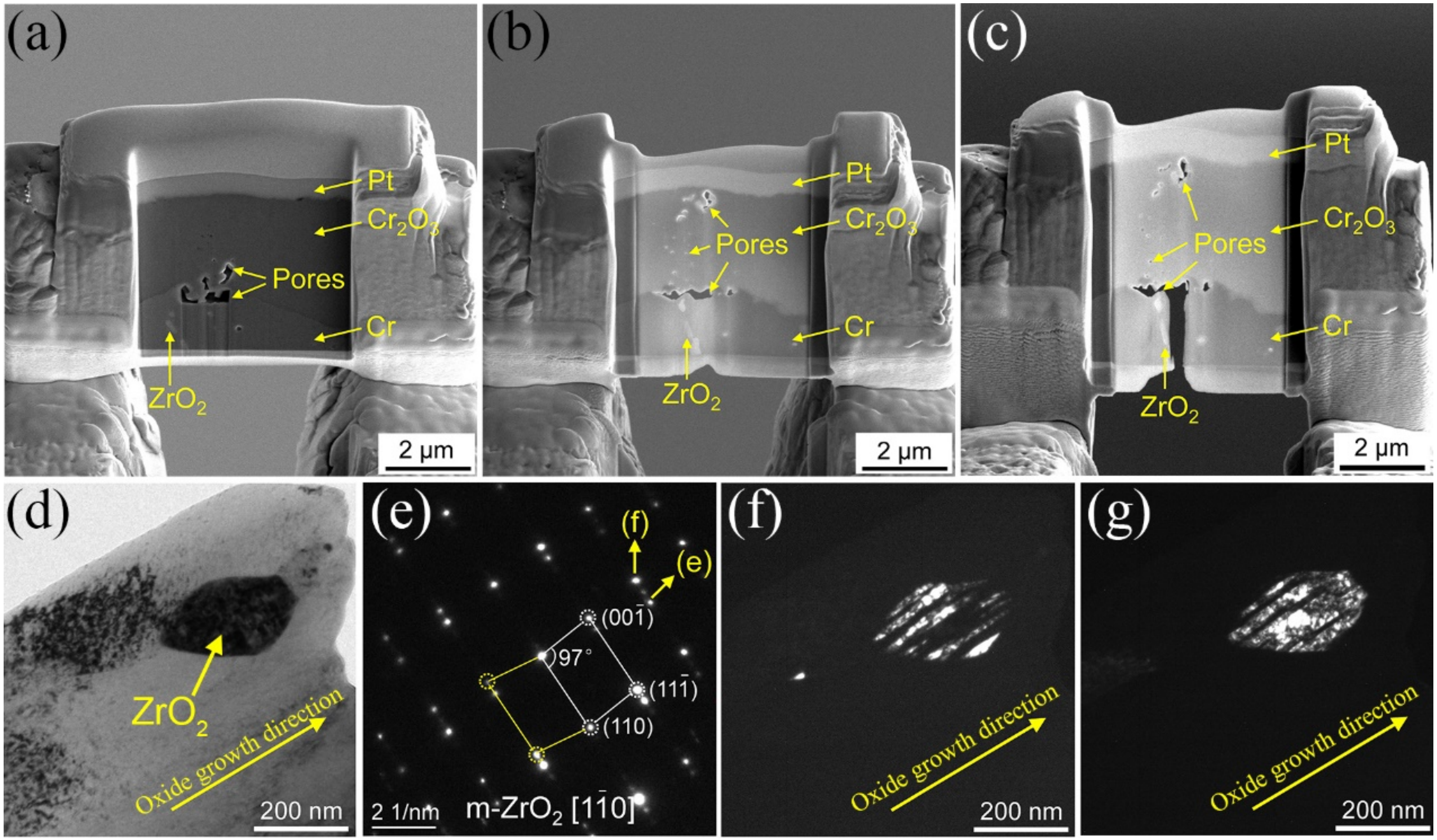

- The formation of pores on Cr_2O_3/Cr interface and inside the Cr_2O_3 is related to the outward diffusion of Zr
- The ZrO_2 precipitate on the Cr grain boundaries has the twins structures

The formation of interfacial pores is related to the reaction between Cr_2O_3 and Zr

The formation of interfacial pores inhibits the reaction between Cr_2O_3 and Zr

3. Results
3.6 Microstructures after transition: 120-180 min

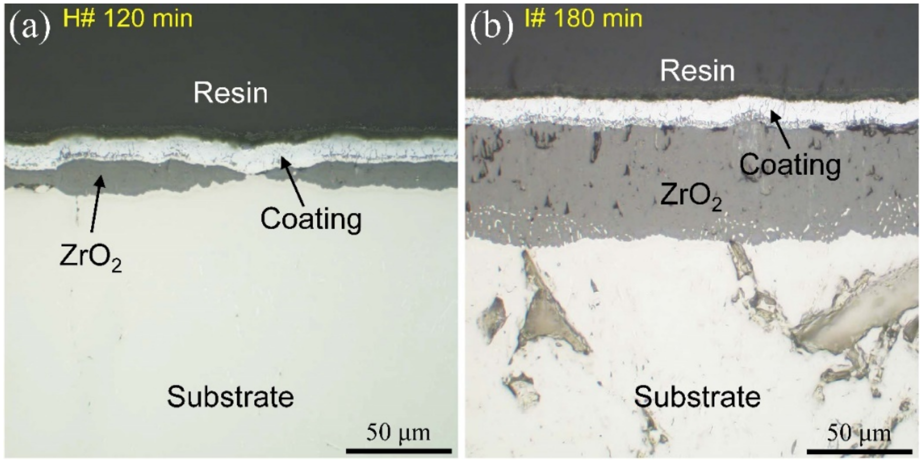

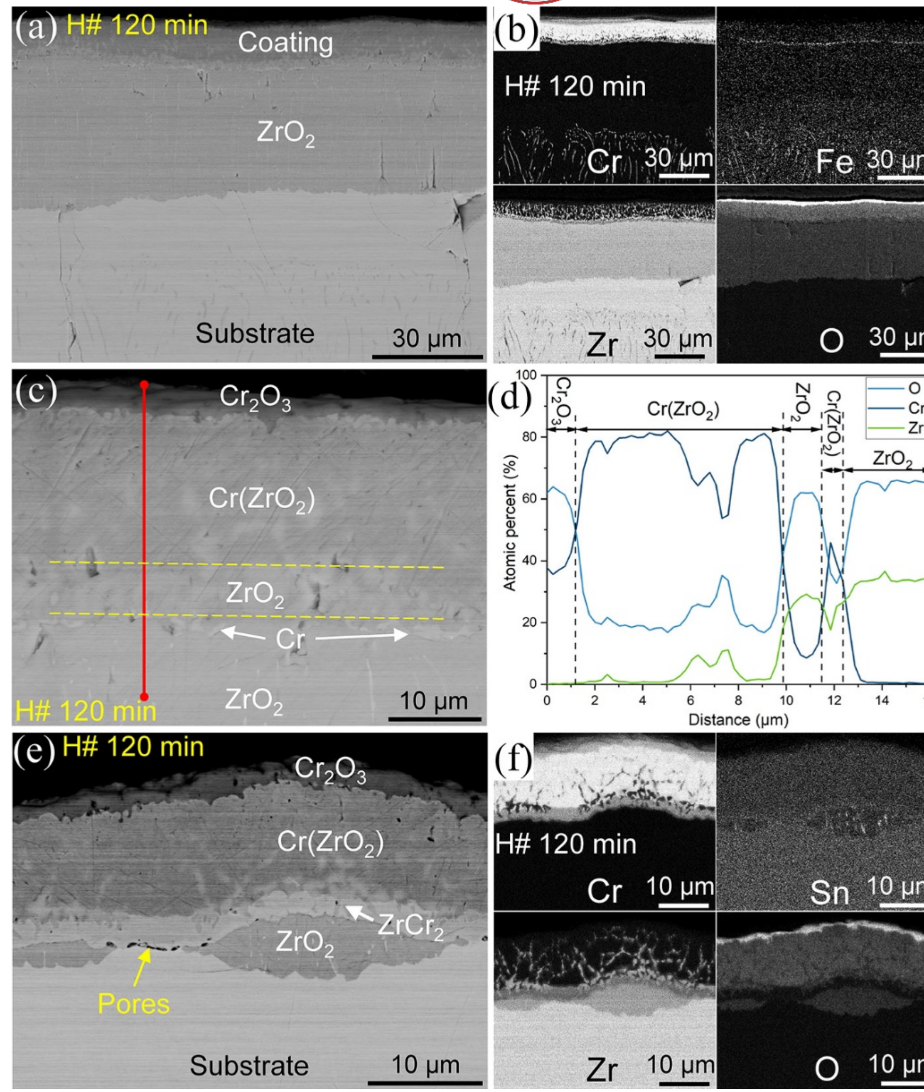

- Most regions of the substrate is oxidized in H#, all regions of the substrate is oxidized in I#
- The thickness of Cr_2O_3 is very thin
- $ZrCr_2$ is oxidized into ZrO_2 and Cr
- *The oxidation of substrate is related to the outward diffusion of Zr*
- The outward diffusion of Zr is related to the pores on $ZrCr_2$/substrate interface

4. Summary

- The oxidation kinetics transition of the Cr-coated Zircaloy should be directly related to the rapid inward diffusion of O to the substrate through the coating and the further formation of α-Zr(O) in the substrate. *The acceleration of the inward diffusion of O should be attributed to the combined effects of the thickness decrease of the Cr_2O_3 scale and the formation of ZrO_2 networks inside the unoxidized Cr coating*.
- It is the outward diffused *Zr on the Cr grain boundaries reacts with Cr_2O_3 scale when Zr reaches the Cr_2O_3/Cr interface, and this reaction further leads to the thickness decrease of the Cr_2O_3 scale*. The diffusion coefficient of Zr along the Cr grain boundaries decreases with the growth of the Cr_2O_3 scale before transition.
- When the thickness of the outer Cr_2O_3 scale decreases to a very small value, and combined with the formation of ZrO_2 diffusion paths in Cr coating, the coating degradation occurs and the substrate beneath the coating is oxidized.
- Pores form on the Cr_2O_3/Cr interface above the ZrO_2 precipitates in Cr coating after transition. *The formation of the interfacial pores should be due to the vacancy condensation on the interface and the reaction between Zr and Cr_2O_3*. These pores affect the oxidation mechanism of the Cr-coated Zry-4.
- Pores are also observed inside the Cr_2O_3 scale after transition. These pores just distribute above the interfacial pores. The amorphization of Cr_2O_3 grains occurs close to the pores. The formation of these pores should be attributed to the decomposition of Cr_2O_3 grains.
- The thickness of the $ZrCr_2$ layer increases gradually before transition, then after transition, the continuous $ZrCr_2$ layer transforms to a discontinuous one due to the increase of the diffusion coefficient of Zr from the substrate to the Cr coating. After coating degradation, the $ZrCr_2$ layer is finally oxidized into ZrO_2 and Cr.

Thanks!

Karlsruhe Institute of Technology

谢谢！

XI'AN JIAOTONG UNIVERSITY 1896

D.V. Sidelev, S.E. Ruchkin, M.S. Syrtanov,
E.B. Kashkarov

Tomsk Polytechnic University

Multilayer protective CrN/Cr coatings on E110 zirconium alloy

Multi-cathode magnetron sputtering was used to deposit single-layer Cr and multilayer CrN/Cr coatings on E110 zirconium alloy. The thickness of Cr and CrN multilayers was equal to 100, 250 and 750 nm, the total coating thickness ~10 µm. Three types of experiments were performed such as thermocycling (at 1000 °C, time of one cycle – 2 min, atmosphere - air), oxidation in water steam at 1200-1400 °C.

The short-term (4 cycles) thermocycling showed similar kinetics of weight gain was observed in the Cr and CrN/Cr coatings. The long-term tests (more than 75 cycles) presented that the single-layer Cr coating had the higher resistance to cracking and thermal shock compared to the multilayer CrN/Cr films.

High-temperature oxidation tests in water steam showed that the multilayer CrN/Cr coatings can be more resistant to oxidation due to the growth of a ZrN phase in the alloy because of CrN decomposition on Cr_2N and N at high temperatures (650 °C and more). It results in slowing down a Cr-Zr interdiffusion at the "coating-alloy" interface. However, such effect is significant only for a short period at 1200 °C and strongly decreased at the higher temperature (1330-1400 °C).

The reported study was funded by RFBR and ROSATOM, project number 20-21-00037.

Multilayer protective CrN/Cr coatings on E110 zirconium alloy

D.V. Sidelev[a,*], S.E. Ruchkin[a], M.S. Syrtanov[a], E.B. Kashkarov[a]

[a] Tomsk Polytechnic University, 30 Lenina av., Tomsk, 634050, Russian Federation

*Tel.: +7-3822-70-17-77-1-2518#; e-mail: sidelevdv@tpu.ru

TOMSK POLYTECHNIC UNIVERSITY
ТОМСКИЙ ПОЛИТЕХНИЧЕСКИЙ УНИВЕРСИТЕТ

Karlsruhe Institute of Technology

26th International QUENCH Workshop

ATF cladding based on Cr-coated Zr alloy

- **Chromium-based coatings** demonstrate excellent protective properties for nuclear fuel claddings produced from Zr alloys under normal operation and accidental condition.

- However, the maximum operation temperature of Cr-coated Zr alloys in water steam is limited by **~1200-1250 °C** as Cr and Zr have high diffusion coefficients at such temperatures. The **interdiffusion** leads to fast **consumption** of Cr coatings and formation of **eutectic Cr-Zr phase** (with the melting point of ~1305-1335 °C) at the coating/alloy interface resulting in non-protective scale at temperatures higher than ~1300 °C.

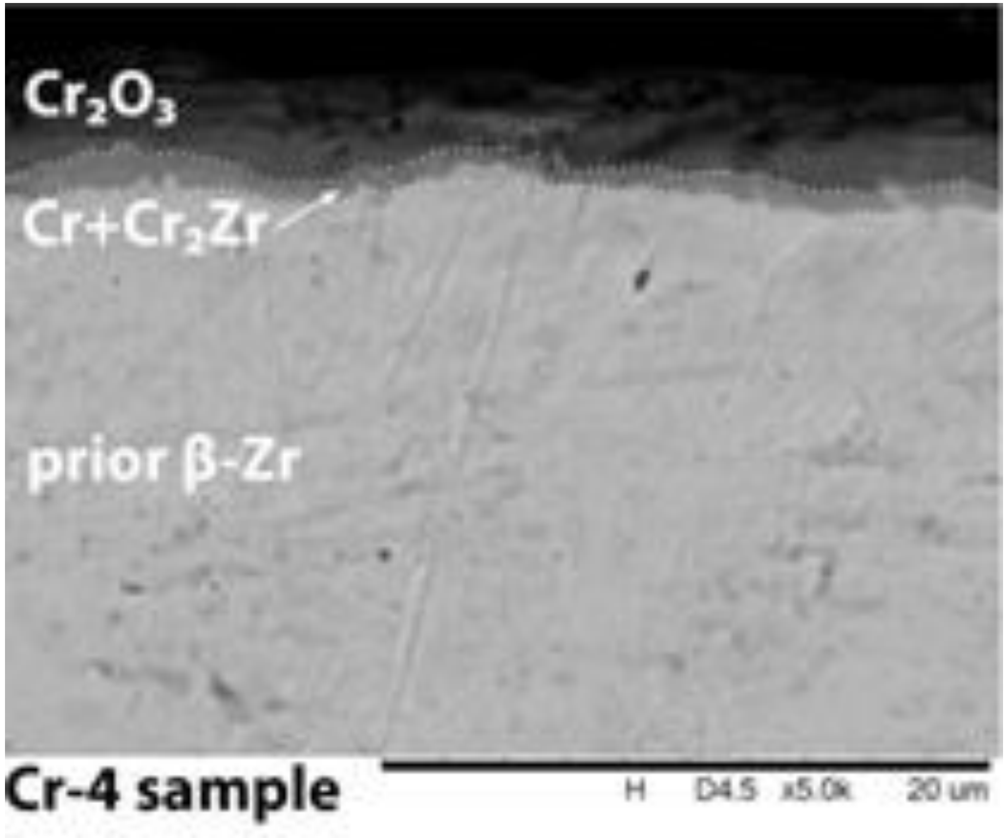

- Much attention - to find a material of **barrier sublayer** to slow down Cr-Zr interdiffusion.

Barrier layers for Cr coating

Metallic barrier layers (Mo, Ta, Nb and Re)

- Mo and Re can form a eutectic phase with Zr at ~1550-1600 °C, and even lower temperature for triple Cr-Mo-Zr and Cr-Re-Zr systems.
- Ta and Re have high thermal neutron cross-section of 20.6 and 89.7 barn.
- Nb has unlimited solubility in the β-Zr phase.

Ceramic compounds (CrN, ZrO_2)

- Krejci et al. [1]: barrier thick CrN.
- Wang et al. [2]: the suppression of inward O and outward Zr diffusion using ZrO_2.

Coating cracking due to difference in CTE between ceramic compounds and Zr alloy.

- To use of **multilayer coating approach** to improve cracking resistance of Cr-based coatings with ceramic barrier layer.

- **The goal of the study** – identify the oxidation behavior of the Cr coatings with barrier layer of CrN/Cr multilayers deposited on Zr alloy under thermal cycling and steam oxidation.

1. https://doi.org/10.1016/j.net.2019.08.015
2. https://doi.org/10.1016/j.corsci.2021.109494

Oxidation in air: preliminary test

Oxidation conditions.

- Temperature– 1100 °C.
- Oxidation atmosphere – ambient air.
- Oxidation time: 10-40 min.
- Heating/cooling rate – 25 °C/min.

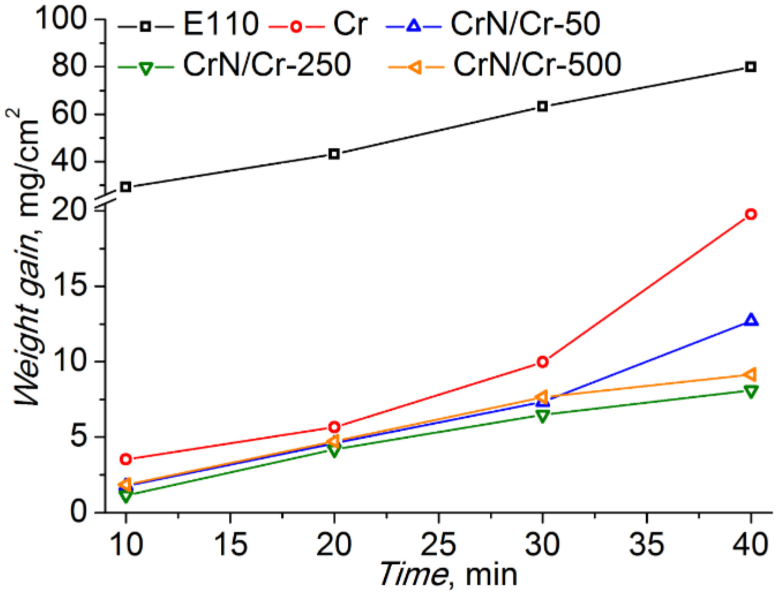

Fig. 1. Mass gain of the samples after oxidation in air [3].

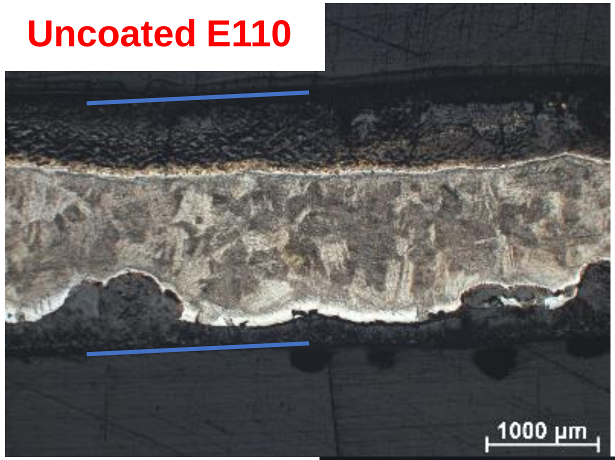

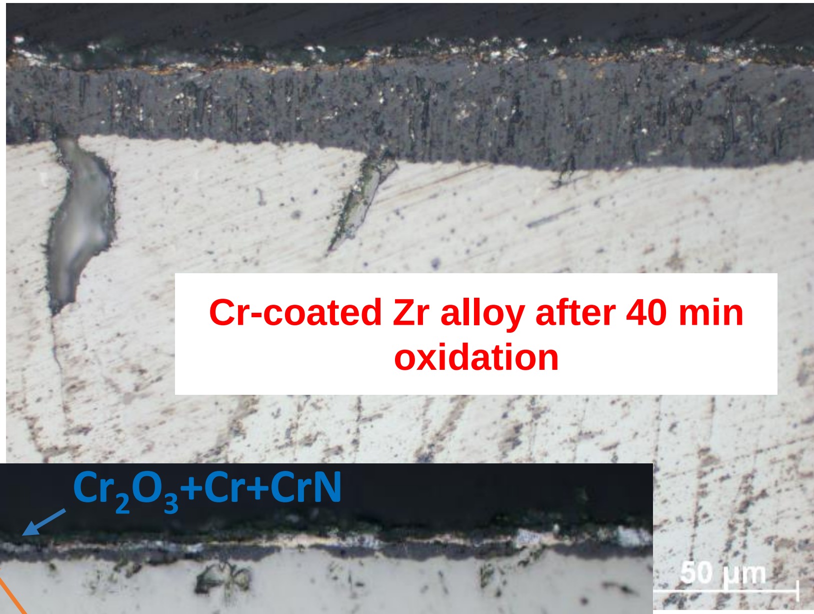

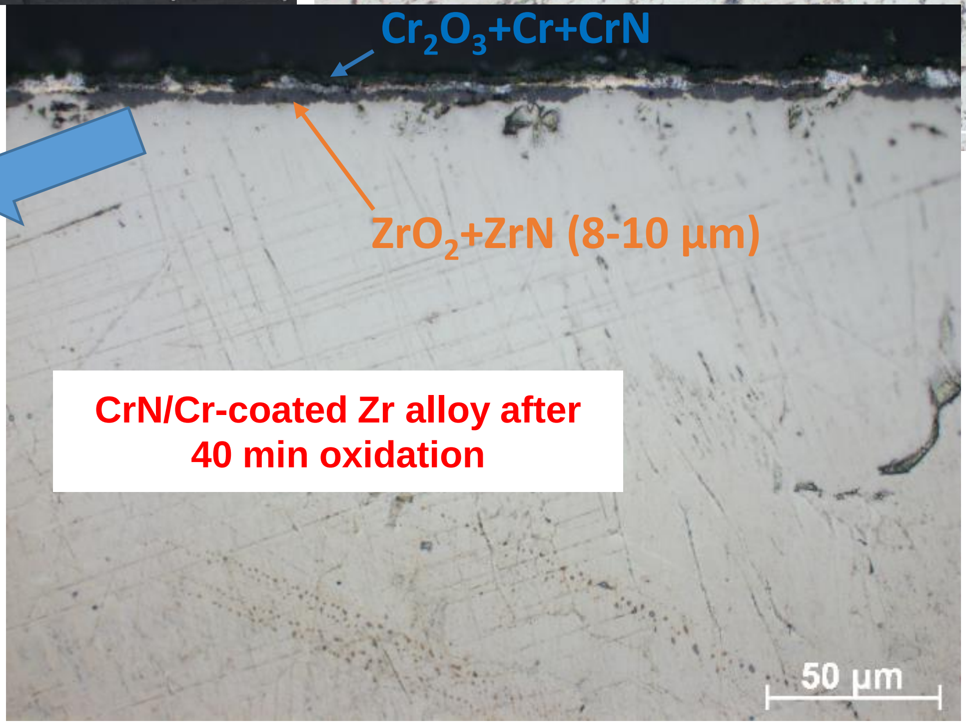

The preliminary test showed the higher oxidation resistance of CrN/Cr coated Zr alloy in comparison with Cr-coated one.

3. https://doi.org/10.3390/coatings11020227

In situ XRD diffraction of CrN/Cr-coated Zr alloy

Cr coating

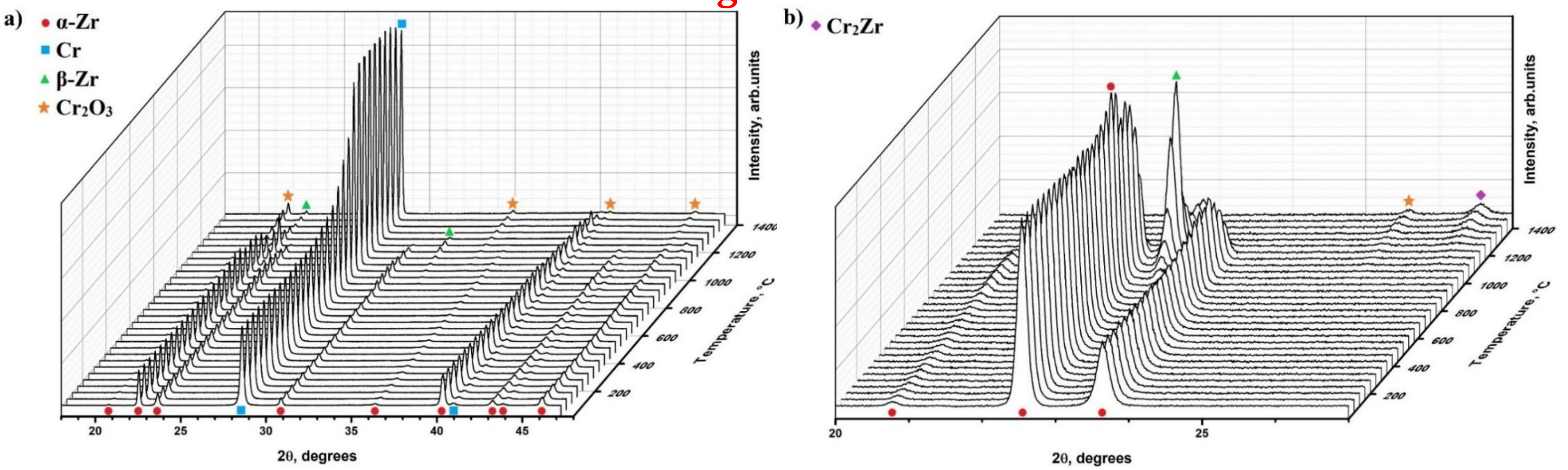

The intermetallic Cr_2Zr phase appears when the temperature reaches **1200 ° C.**

CrN/Cr-250 coating

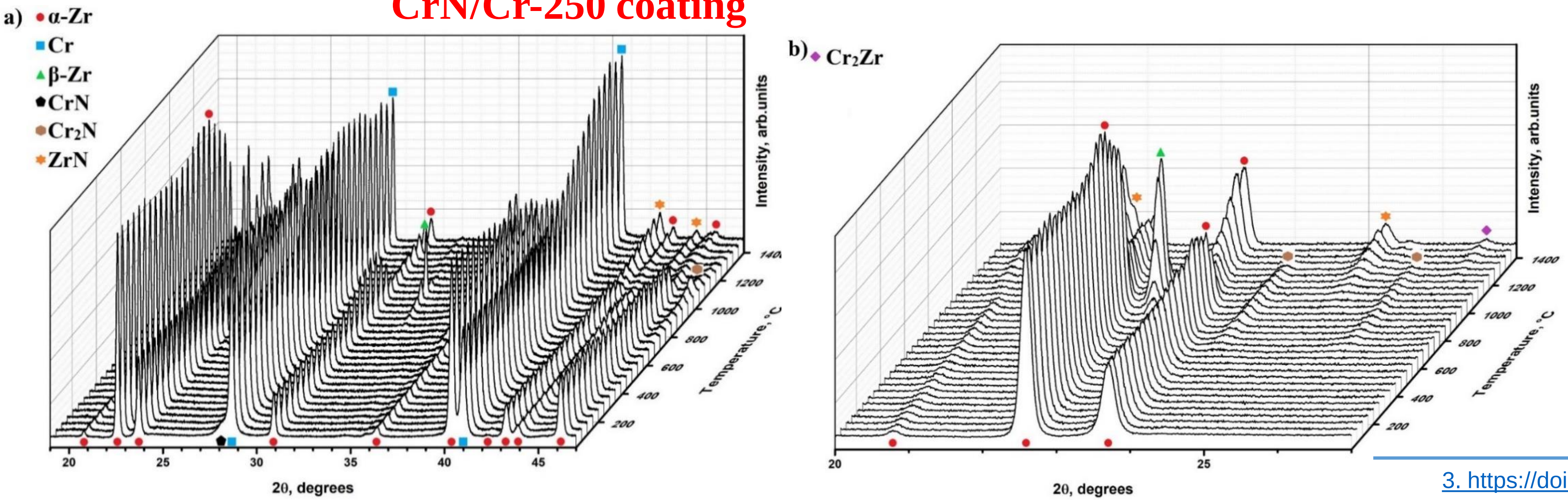

The intermetallic Cr_2Zr phase was observed only at the T above **1350 ° C.**

3. https://doi.org/10.3390/coatings11020227

In situ XRD diffraction of CrN/Cr-coated Zr alloy

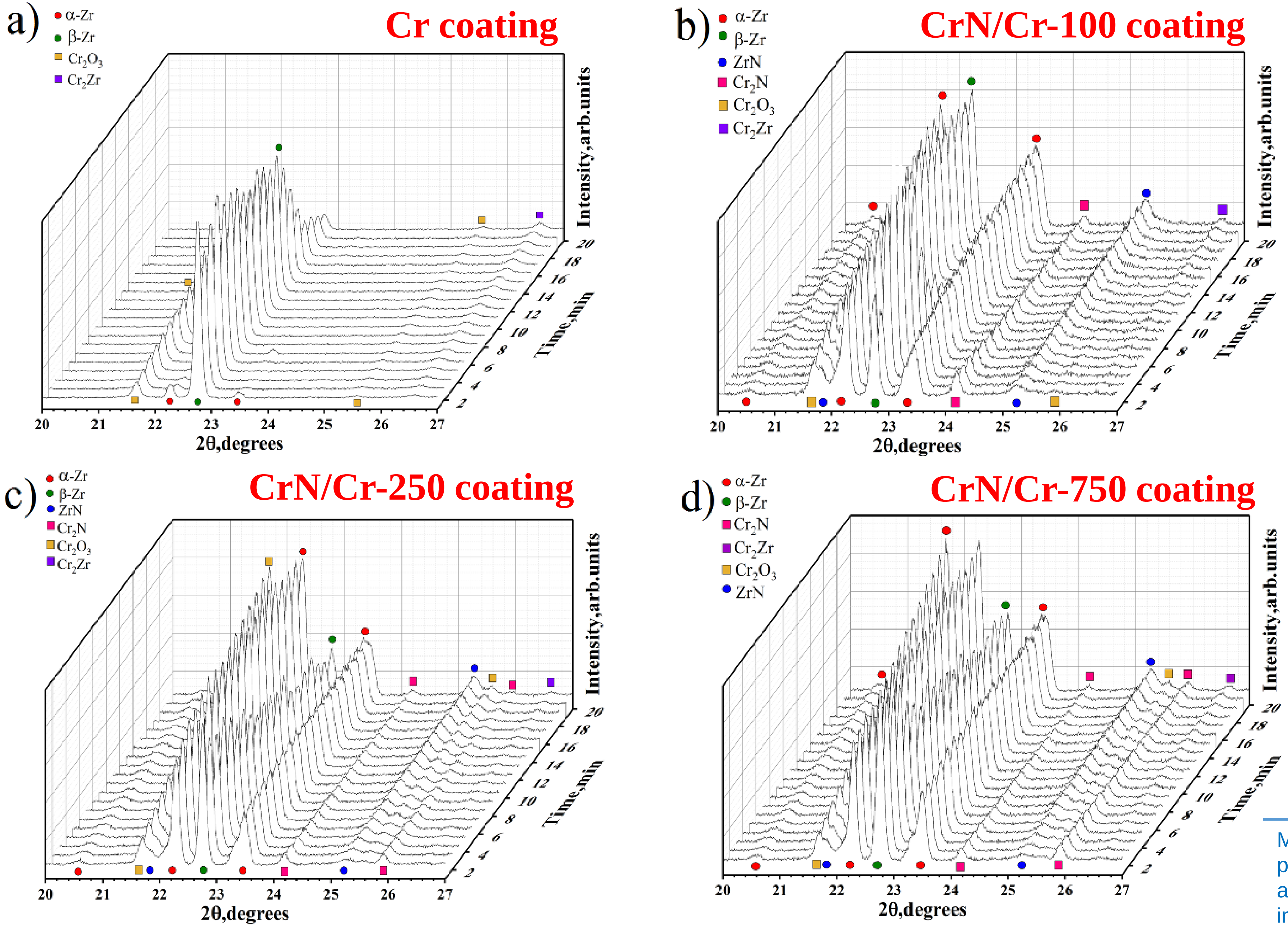

Test at 1200 ° C:

- 6 min – CrN/Cr-50;
- 12 min – CrN/Cr-250;
- 10 min – CrN/Cr-500.

M. Syrtanov, A. Pirozhkov, D. Sidelev, In-situ phase transformations in CrN/Cr-coated E110 alloy under high temperature, Mater. Sci. Forum, in print.

Thick (9-11 µm) Cr and CrN/Cr coatings

Four coating series were prepared by magnetron sputtering:

- **a – Cr coating: single-layer** – 11.2 µm;
- **b – CrN/Cr-100** coating: alternating Cr and CrN with a step of 100 nm (30 layers) – 9.2 µm;
- **c – CrN/Cr-250** coating: alternating Cr and CrN with a step of 250 nm (12 layers) – 9.4 µm;
- **d – CrN/Cr-750** coating: alternating Cr and CrN with a step of 750 nm (4 layers) – 9.6 µm.

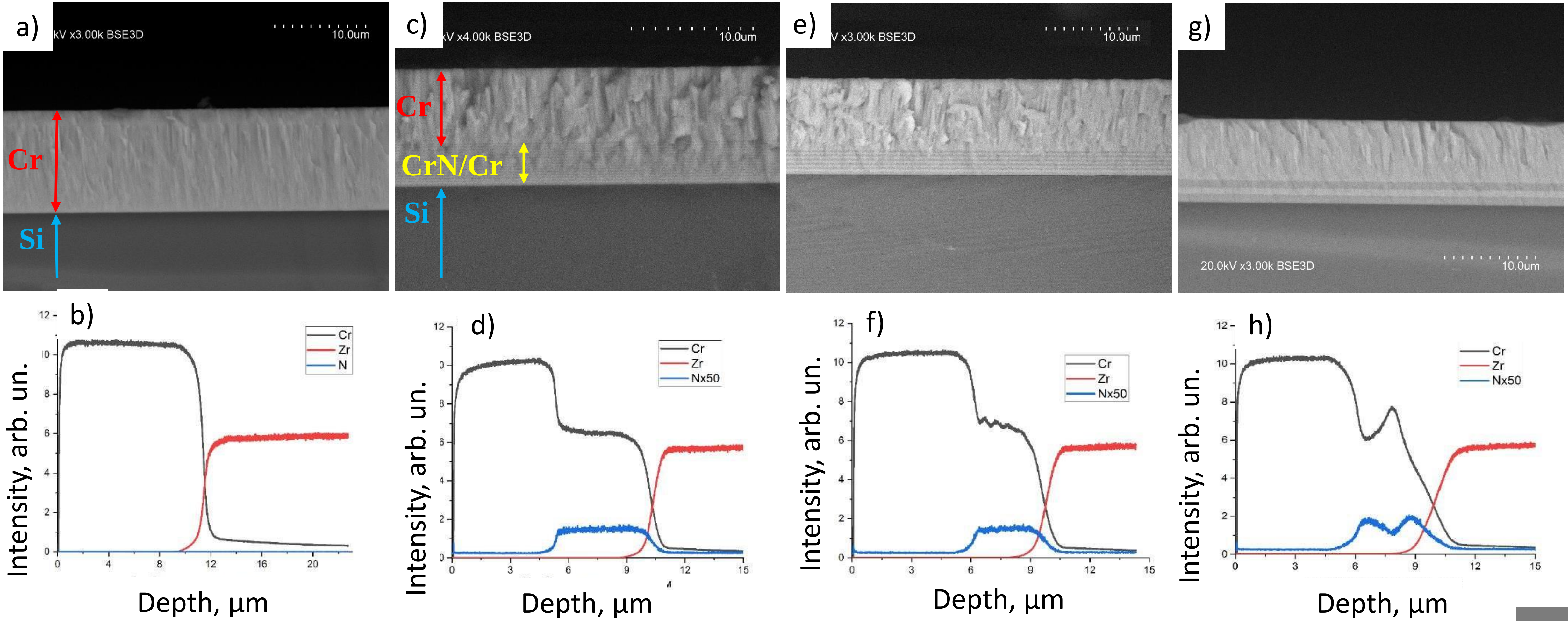

Fig. 3. The cross-section microstructure and depth distributions of Cr, Zr and N in the (a, b) Cr, (c, d) CrN/Cr-100, (e, f) CrN/Cr-250 and (g, h) CrN/Cr-750 coatings obtained by SEM and GDOES.

Adhesion and wear rate of Cr-based coatings

Fig. 4. Optical images of scratch grooves after testing up to 50 N.

Table 1 – Wear rate of the samples

Sample	Wear rate, 10^{-5} $mm^3/(m \cdot N)$
Uncoated E110	190.00
Cr	4.17
CrN/Cr-100	3.83
CrN/Cr-250	4.33
CrN/Cr-750	5.33

- Cracking of single-layer Cr coatings started **at 15 N.**
- Increase in resistance of cracking resistance of the CrN/Cr coatings:
  - CrN/Cr-100 – **at 24 N;**
  - CrN/Cr-250 – **no cracking;**
  - CrN/Cr-750 – **no cracking.**
- Increase in wear resistance of Cr-coated Zr alloy **by two orders**.

Thermal cycling: 4-100 cycles

Goal of this experiment – to estimate a resistance to cracking under thermal cycling.

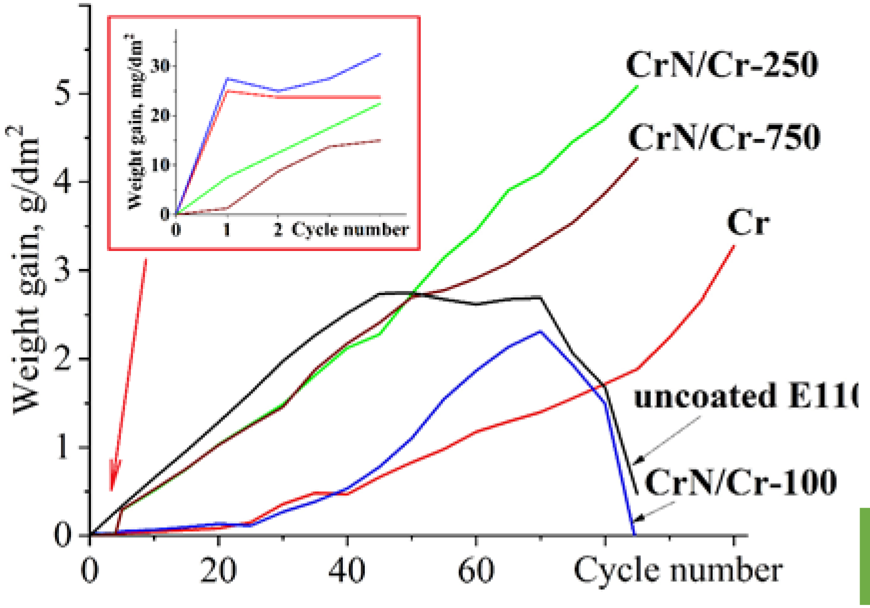

Fig. 5. Mass gain of the samples.

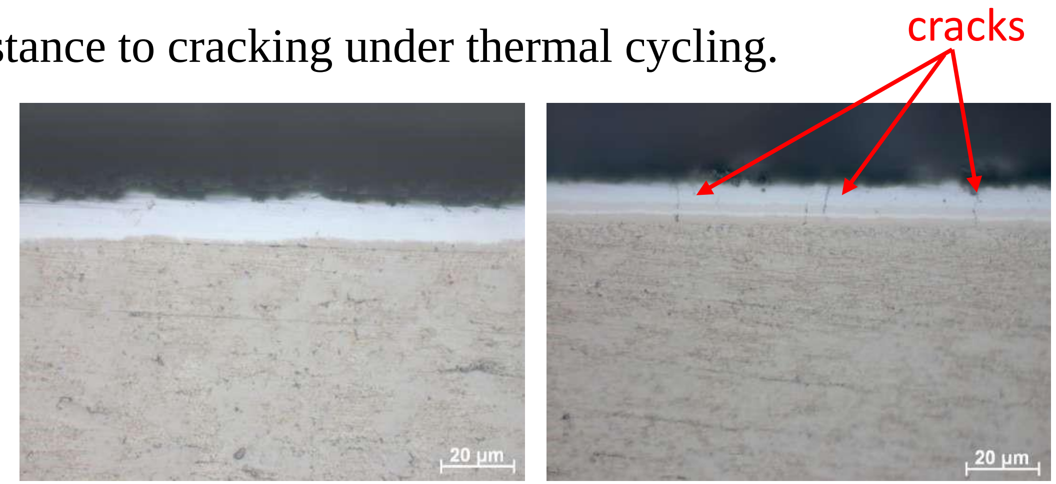

Fig. 6. Optical images of cross-section microstructure of Cr (**left**) and CrN/Cr-100 (**right**) after 4 thermal cycles.

Conditions of thermal cycling:
- atmosphere – ambient air;
- temperature – 1000 ^oC;
- oxidation time – 2 min.

sample	Cr	CrN/Cr-100	CrN/Cr-250	CrN/Cr-750
Linear density of cracks (L), mm^{-1}	4.6	8.5	23.0	19.3

- The coated samples have the similar dependence of the weight gain during **4** thermal cycles.
- The linear density of cracks is depended on the coating type:
  - the single-layer Cr coating had lower ***L*** than that of the multilayer CrN/Cr coatings;
  - the CrN/Cr-100 coating had the lowest value of *L* (**8.5 mm^{-1}**) among other CrN/Cr coatings.

- Up to ~40 thermal cycles, these samples had the same weight gains **(~0.5 mg/dm^2**) that are less than **1 wt.%**.

High-temperature steam oxidation at 1200 °C: pure Cr

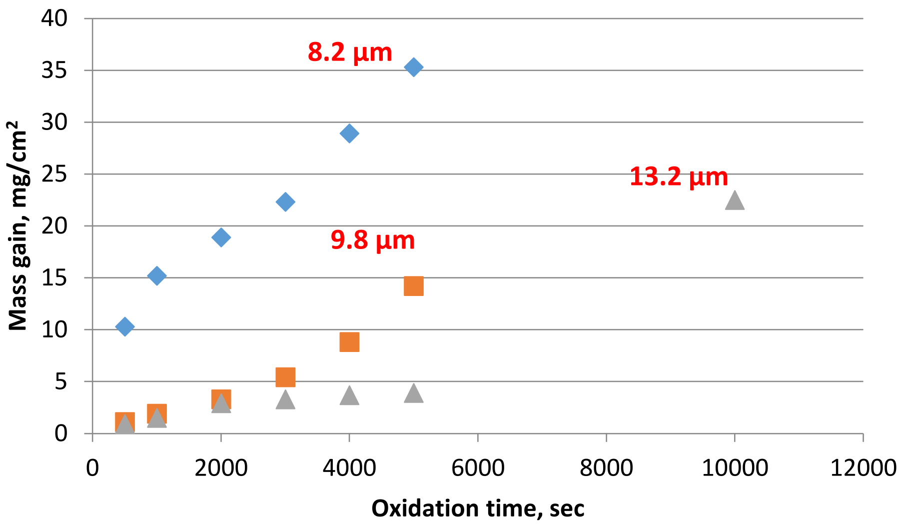

Fig. 9. Mass gain of the Zr alloy with 8.2, 9.8 and 13.2 µm-thick Cr coatings.

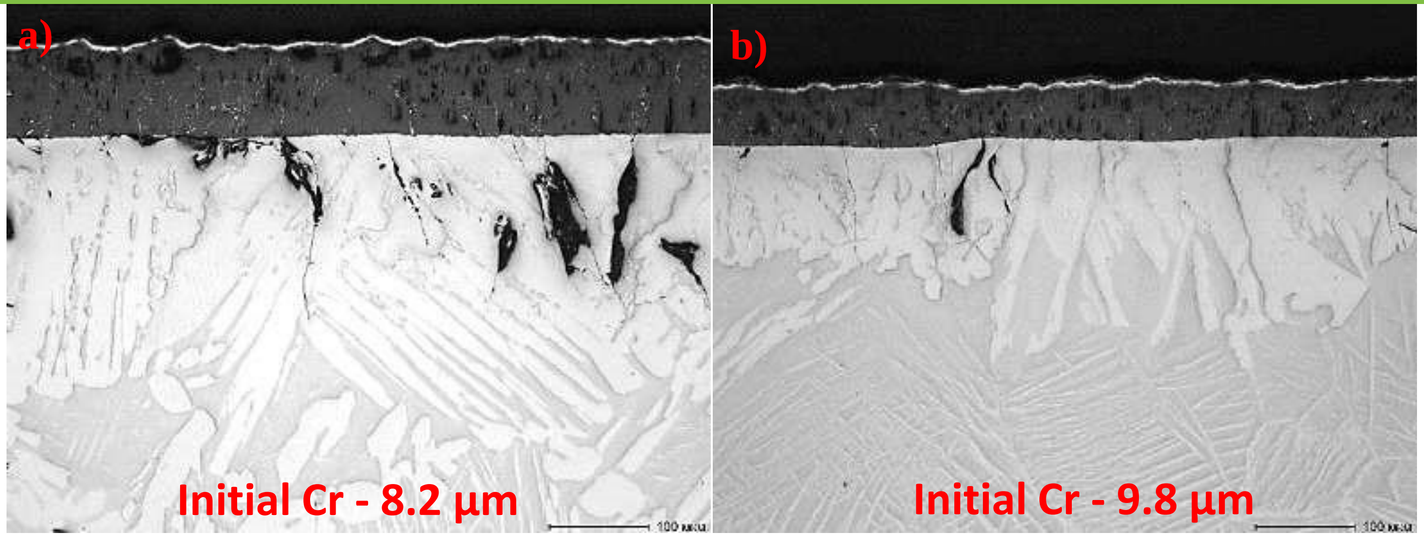

Fig. 11. The cross-section microstructure of the Zr alloy with pure Cr coatings with (a) 8.2 and (b) 9.8 µm after 5000 s oxidation test.

- **Thicker Cr coatings have less mass gain and higher protective time than that of the Cr coating with lower thickness.**

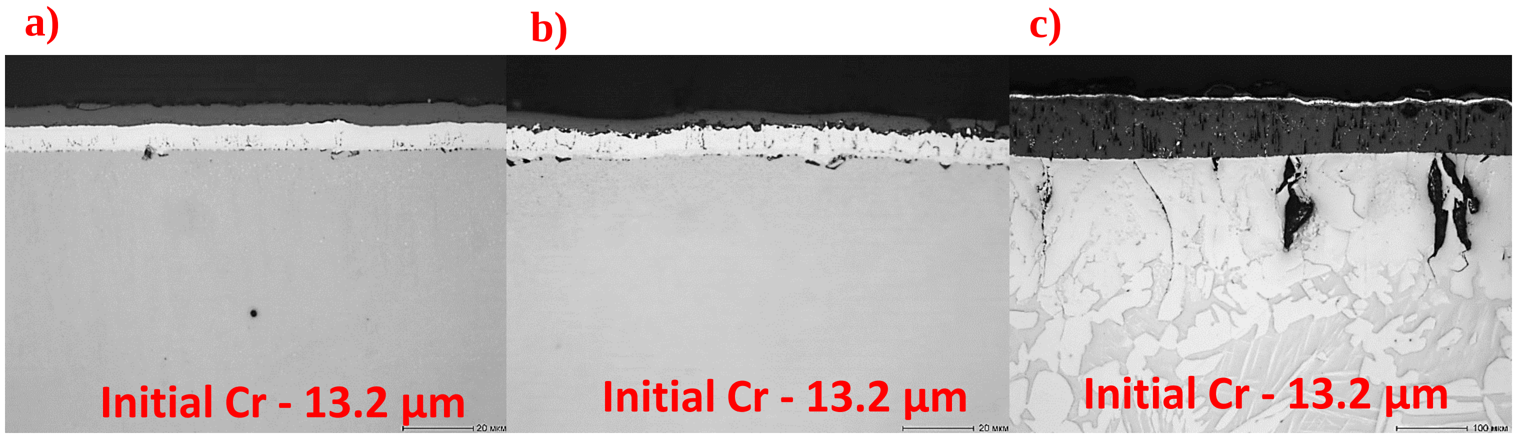

Fig. 12. The cross-section microstructure of the Zr alloy with pure 13.2 µm-thick Cr coating after (a) 1000, (b) 5000 and (c) 10 000 s.

High-temperature steam oxidation at 1330 °C (2 min): Cr and CrN/Cr

E110 alloy

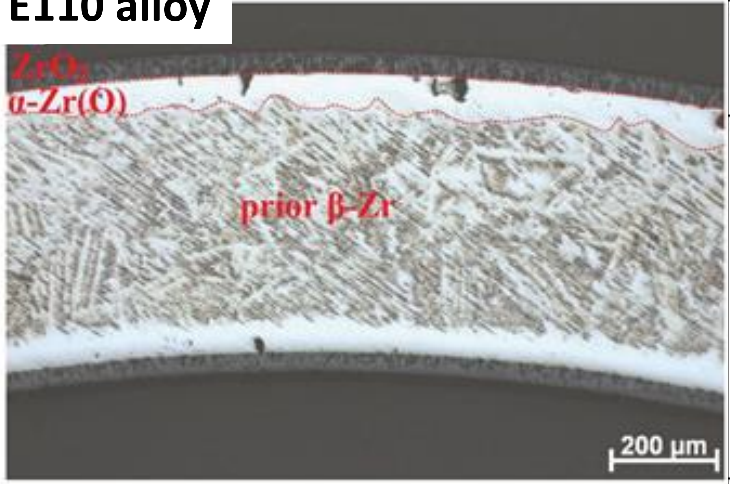

uncoated E110 alloy	Cr	CrN/Cr-100	CrN/Cr-250	CrN/Cr-750
			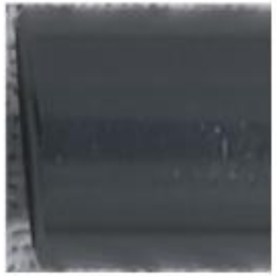	
8.5 mg/cm^2	3.2 mg/cm^2	3.8 mg/cm^2	3.1 mg/cm^2	3.2 mg/cm^2

Fig. 15. Appearance and mass gain of the samples after oxidation.

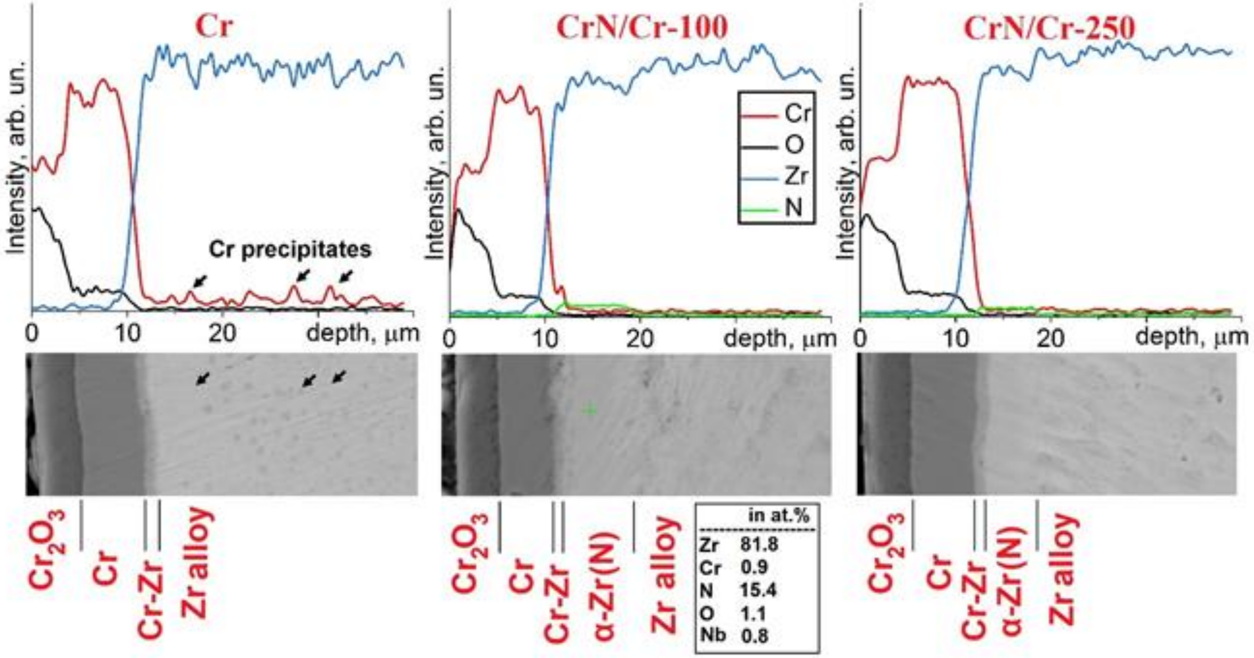

- All coatings were protective during the short period.
-
- The Cr precipitates were found at high depths (>20 μm) in the sample coated by the single-layer Cr coating.
- Since the α-Zr(N) layer formed at the coating/alloy interface, which can slow down the interdiffusion because less diffusion rates and solubility of Cr in α-Zr in comparison with the β-Zr.

High-temperature steam oxidation at 1400 °C (2 min): Cr and CrN/Cr

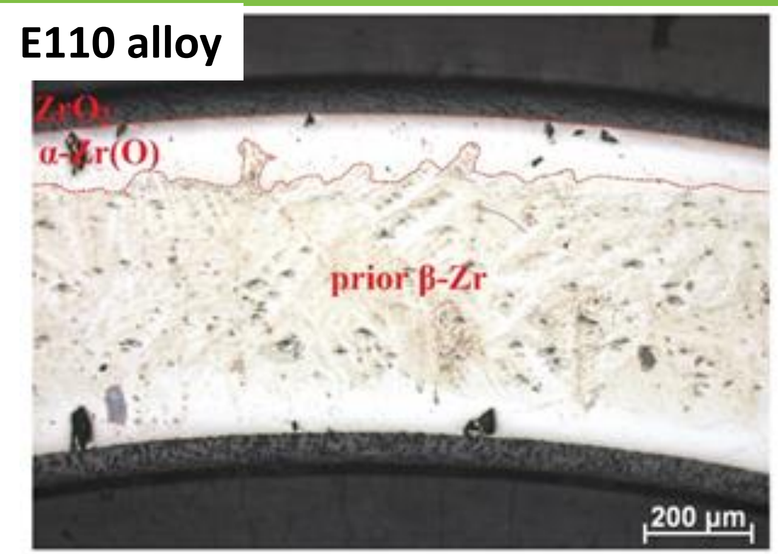

uncoated E110 alloy	Cr	CrN/Cr-100	CrN/Cr-250	CrN/Cr-750
				
12.5 mg/cm²	10.1 mg/cm²	12.7 mg/cm²	14.3 mg/cm²	10.8 mg/cm²

Fig. 16. Appearance and mass gain of the samples after oxidation.

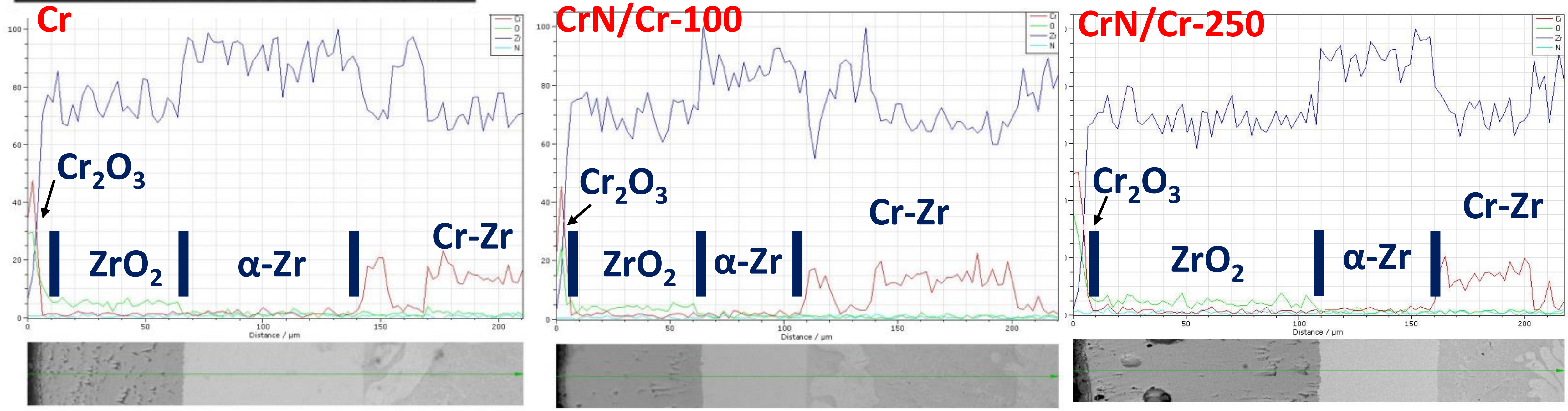

Fig. 17. Cross-section microstructure of the (**left**) Cr-, (**center**) CrN/Cr-100- and (**right**) CrN/Cr-250-coated E110 alloy after the oxidation test.

High-temperature steam oxidation at 1400 °C (2 min): Cr and CrN/Cr

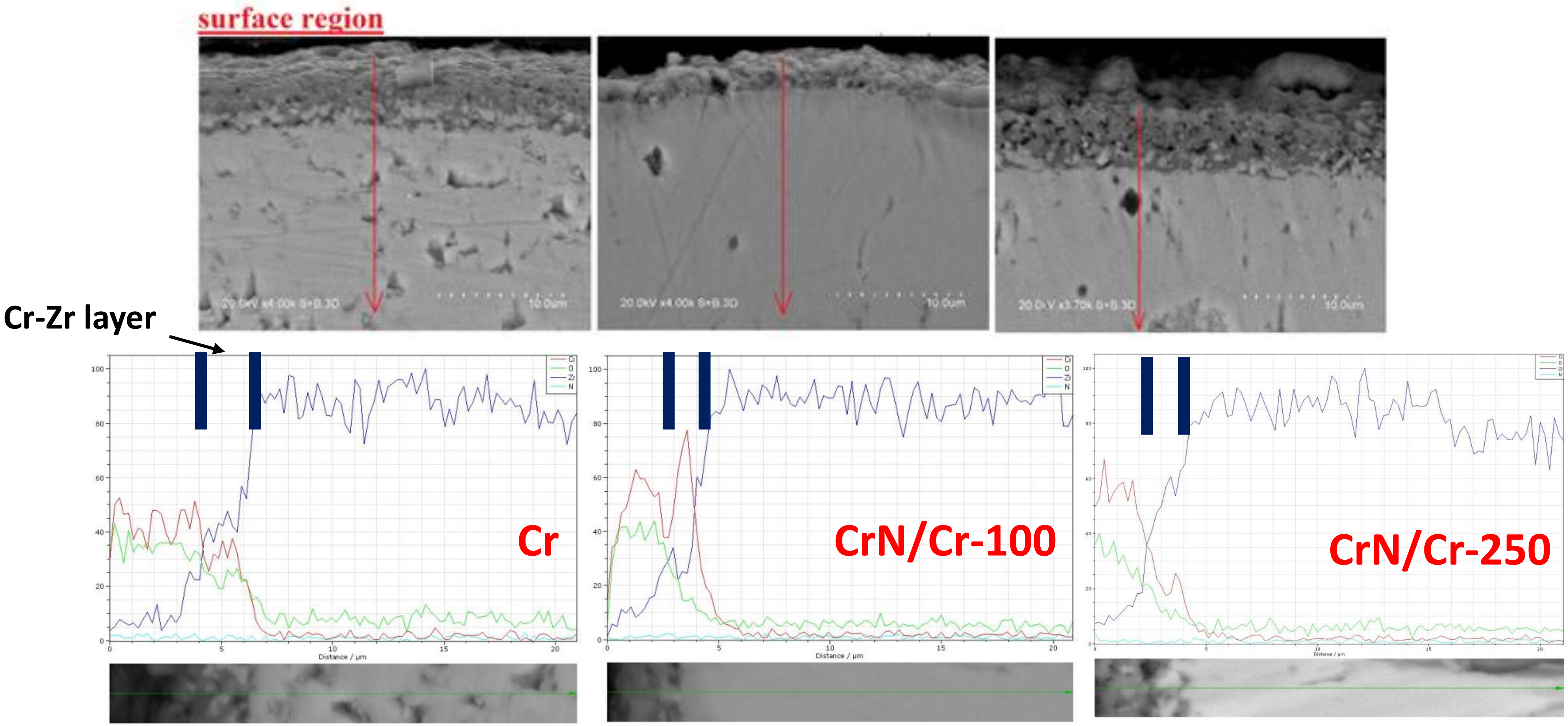

Fig 18. Cross-section microstructure of the (**left**) Cr-, (**center**) CrN/Cr-100- and (**right**) CrN/Cr-250-coated E110 alloy after the oxidation test in surface region.

- Barrier CrN/Cr layer can slow down a Cr-Zr interdiffusion due to the forming of α-Zr(N) underneath the coating.

Conclusion

1. Increase in the wear resistance of E110 alloy by two orders of magnitude.

2. Cracking resistance of Cr coatings with CrN/Cr multilayers is higher than that of the single-layer Cr coating under scratch testing.

3. Multilayer design of Cr-based coatings affects the cracking resistance of the coatings under thermal cycling. The decrease of the thickness of Cr and CrN layers leads to reduce the linear density of cracks from 23.0 to 8.5 mm^{-1} and increase in oxidation resistance of the coated alloy in air. The lowest linear density of cracks was found for pure Cr coating.

4. The barrier layer consisted of CrN/Cr multilayers can slow down interdiffusion between Cr coating and E110 alloy at high temperatures due to the formation of N-stabilized α-Zr phase underneath the Cr-based coating. This effect can work only for the short time for oxidation at 1330 °C and does not matter for oxidation test at 1400 °C.

Motivation for future studies - modification of commercially used Zr alloys to stabilize α-Zr phase at high temperatures can improve the oxidation behavior of Cr-coated Zr alloys in a steam.

TOMSK POLYTECHNIC UNIVERSITY
ТОМСКИЙ ПОЛИТЕХНИЧЕСКИЙ УНИВЕРСИТЕТ

Karlsruhe Institute of Technology

26th International QUENCH Workshop

Multilayer protective CrN/Cr coatings on E110 zirconium alloy[1]

D.V. Sidelev[a,*], S.E. Ruchkin[a], M.S. Syrtanov[a], E.B. Kashkarov[a]

[a] Tomsk Polytechnic University, 30 Lenina av., Tomsk, 634050, Russian Federation

*Tel.: +7-3822-70-17-77-1-2518#; e-mail: sidelevdv@tpu.ru

[1]**The reported study was funded by RFBR and ROSATOM, project number 20-21-00037.**

K. Vizelkova, J. Stuckert, U. Stegmaier

KIT

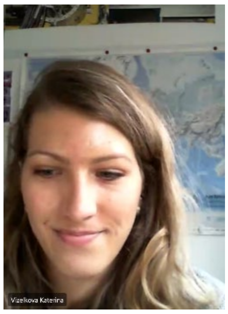

The results of high temperature single rod tests with chromium coated cladding

Accident Tolerant Fuel materials have been widely studied since the Fukushima accident in 2011. Deposition of protective coatings on nuclear fuel claddings has been considered as a near-term concept that will reduce the high-temperature oxidation rate of zirconium-based alloys and enhance accident tolerance of reactor cores by providing additional coping time.

This study is focused on high-temperature oxidation experimental behavior of Zr cladding alloys coated with Cr layers by PVD technique. Coated and reference uncoated samples of Zr alloy were tested in several experiments. The presented results include high-temperature steam oxidation under transient conditions with maximum temperatures reached between 1200 and 1400°C. Coated and reference samples were characterized pre- and post-testing using optical microscopy, scanning electron microscopy and other techniques including X-ray diffraction.

The redistribution of Cr between cladding layers was determined including diffusion of Cr up to boundary between α-Zr(O) and β-Zr layers. A significant decrease in the hydrogen release for coated claddings in comparison with uncoated claddings was shown in experiments with fast transients from 600 to 1250 °C.

Karlsruhe Institute of Technology

Institute for Applied Materials

The results of high temperature single rod tests with chromium coated cladding

K. Vizelkova, J. Stuckert, U. Stegmaier

QWS 26

Institute for Applied Materials; Program NUSAFE

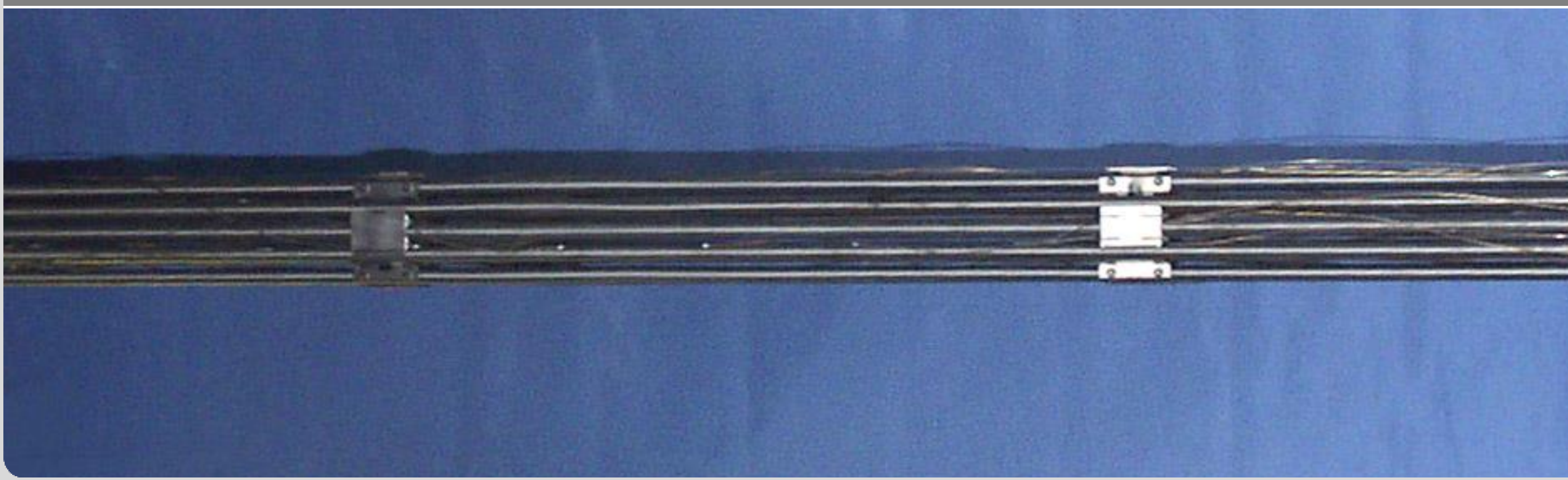

Why chromium coating?

- \+ High corrosion resistance at operation temperatures
- \+ Reduced hydrogen release and absorption
- \+ Acts as a diffusion barrier
- \+ Similar thermal expansion coefficient (4.9 µm/(m·K) at 25°C) compared to Zr (5.7 µm/(m·K) at 25°C)
- \+ Resistance to ballooning and rupture

- – Cr-Zr eutectic formation at the temperature above 1350 °C and melting
- – Enhanced embrittlement of Zr-based substrate due to Cr-diffusion into the substrate

Zr-alloy sample with PVD Cr coating

- Coating performed at OERLIKON BALZERS GmbH
- Zr-alloy:
  - M5^{TM} (Zr-1Nb)
  - ZIRLO^{TM} (Zr-1.0Sn-1.0Nb-0.1Fe)

Zr-alloy tube before coating by Cr

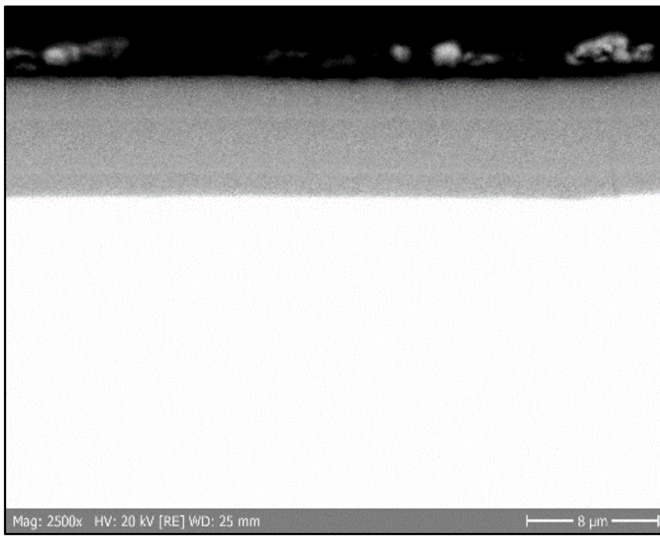

Cr layer (7µm)

Zr based substrate

SEM image of PVD Cr layers

capillary Zr tube (sample holder and pressure normalizer)

Zr plug

Zr alloy cladding coated by Cr

Zr plug

Coated empty sample welded at KIT and prepared for SETs

Samples for IAEA round robin tests at T=1200…1400 °C

SET 1

Long term oxidation tests

Tube furnace with heat insulation

Transient + constant T

t > 500 s

SET 2

Oxidation tests under LOCA conditions

Inductive furnace with radiative heat loss

t < 500 s

SET 1: Long term oxidation tests in the tube furnace LORA

tube furnace

sample withdrawn from the furnace

Matrix of long term oxidation tests with M5 and ZIRLO claddings

Sample	Atmosphere	Transient [min]	Maximal temperature [°C]	Duration of oxidation [min]	Cooldown	Comment
MC-1	O_2+Ar	-	setup 1345 escalation to 1787	-	-	performed; sample significantly melted
MC-2	O_2+Ar	30	1100	30	in air at RT	performed
MC-3	O_2+Ar	37.5	1200	10	in air at RT	performed
MCs-1	O_2+Ar	41.25	1200	5	in air at RT	performed
Zos-1	O_2+Ar	41.25	1350 (escalation to 1500)	5	in air at RT	performed; sample partially melted

MC tubes: OD=10.75 mm, wall 725 µm;

MCs and Zos tubes: OD=9.5 mm, wall 570 µm

Appearance of coated cladding samples oxidized in tube furnace

MC-2:
1100 °C
during 1800 s

MC-3:
1200 °C
during 600 s

MCs-1:
1200 °C
during 300 s

Outer layers after long term oxidation

Karlsruhe Institute of Technology

MC-2: 1100 °C during 1800 s

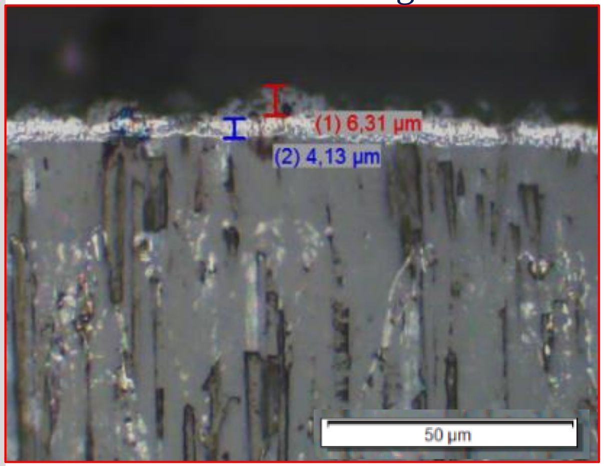

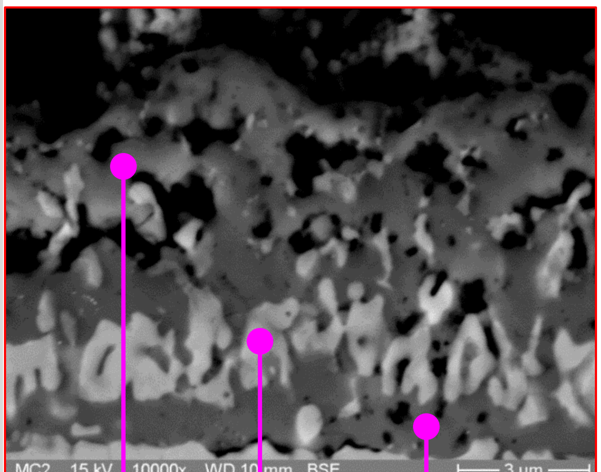

Cr_2O_3 α-Zr(O) +Cr Cr_2O_3

MC-3: 1200 °C during 600 s

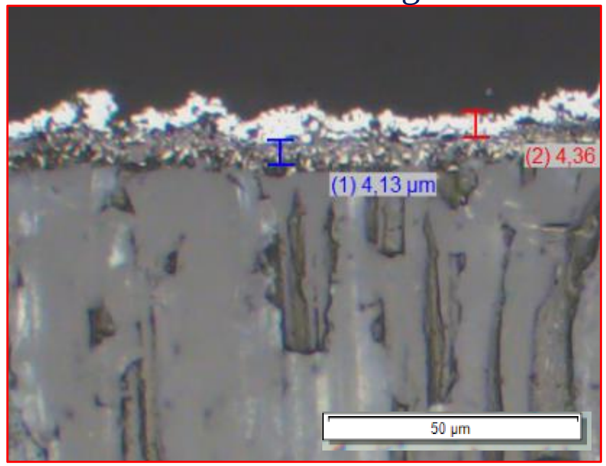

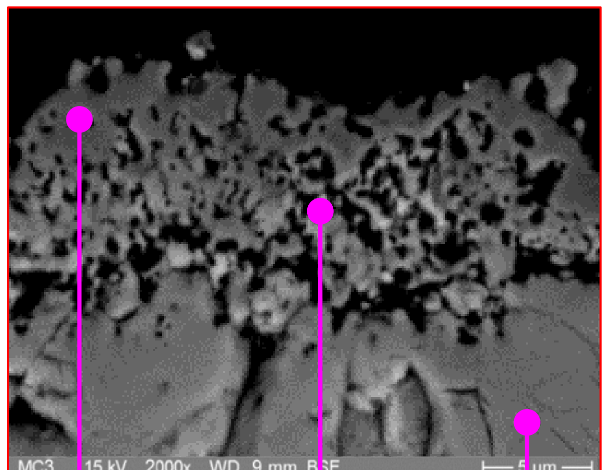

Cr $+Cr_2O_3$ Cr_2O_3 $+ZrO_2$ ZrO_2

MCs-1: 1200 °C during 300 s

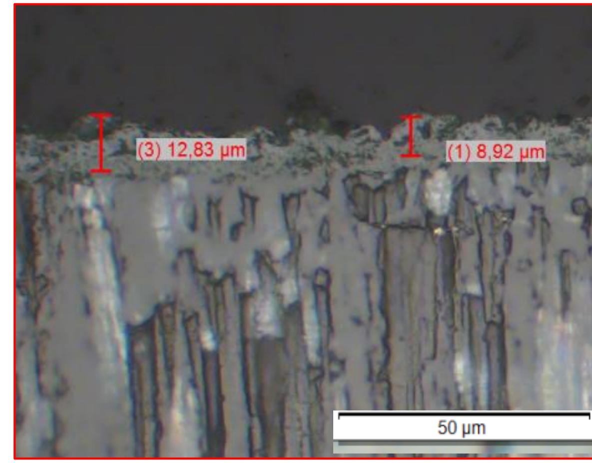

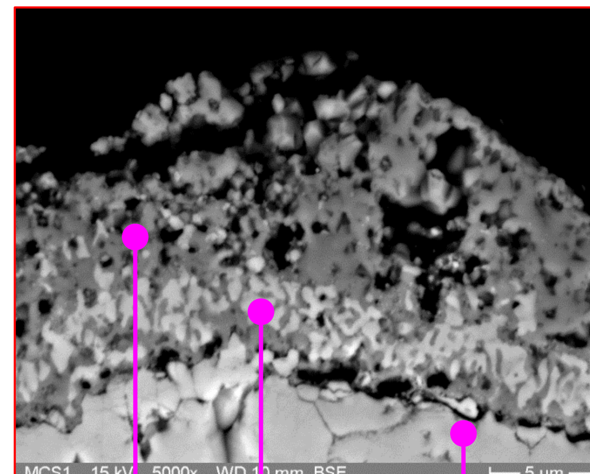

Cr_2O_3 α-Zr(O) +Cr ZrO_2

Cr diffusion into the cladding bulk during long term oxidation

Karlsruhe Institute of Technology

MC-2: 1200 °C during 30 min

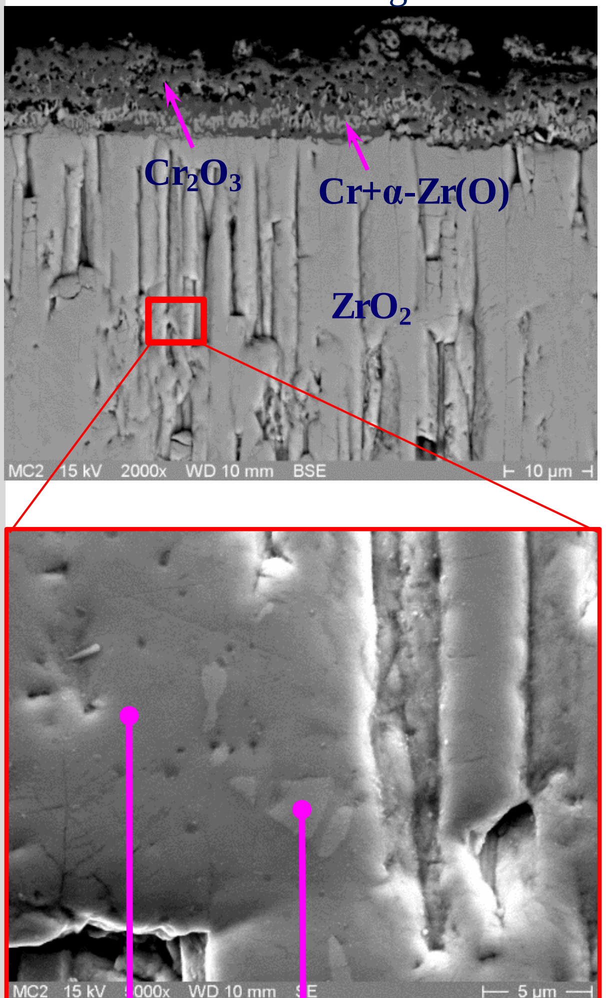

ZrO_2

Cr +α-Zr(O)

MC-3: 1300 °C during 10 min

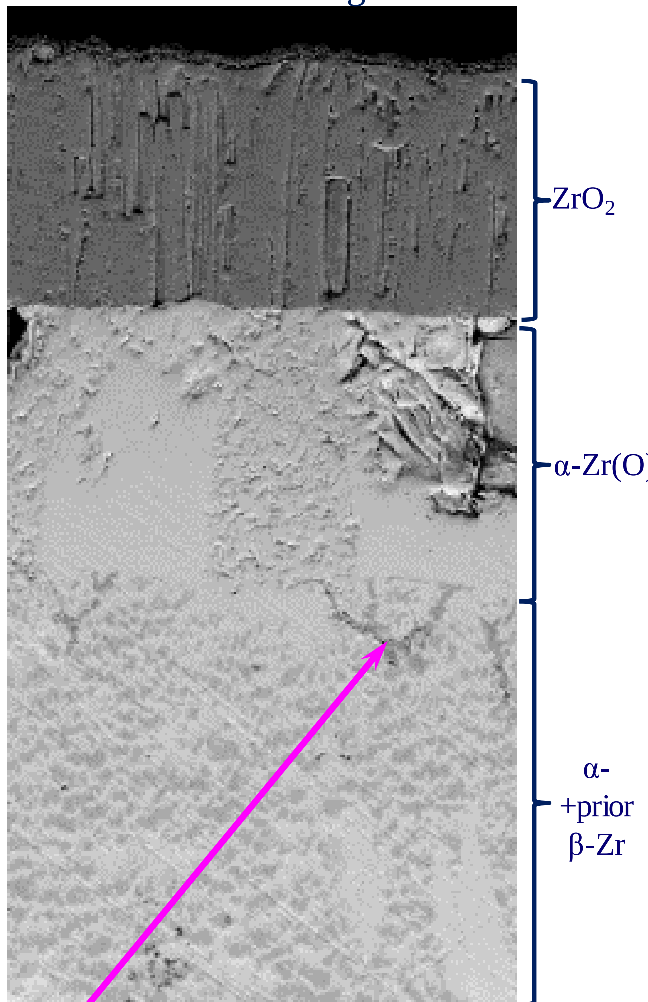

Cr at the boundary between α-Zr(O) and β-Zr

MCs-1: 1350 °C during 5 min

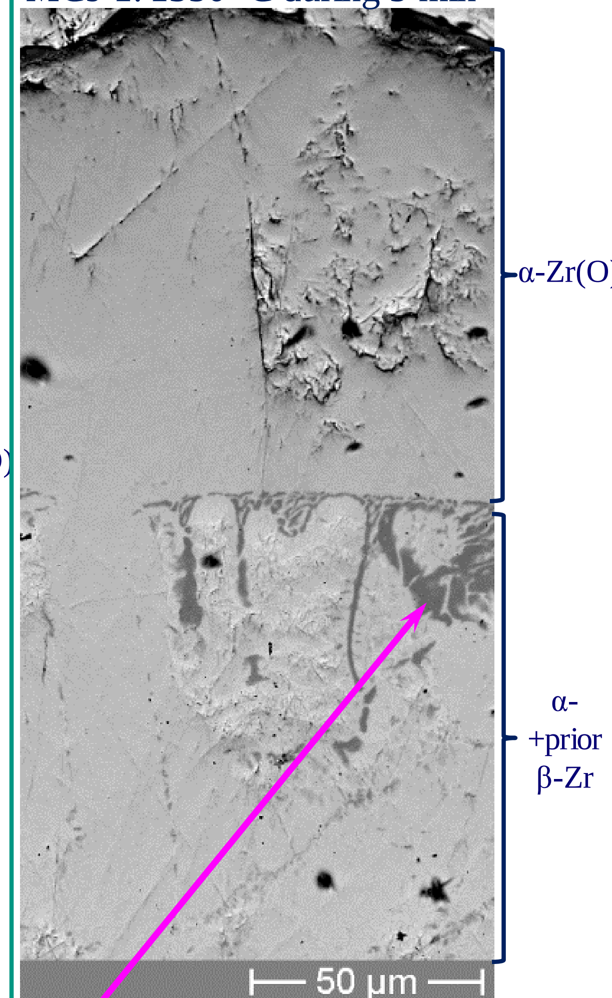

Cr at the boundary between α-Zr(O) and β-Zr

Catastrophic oxidation and temperature escalation at T>1300 °C in tube furnace (without radiation heat loss)

Karlsruhe Institute of Technology

sample MC-1: injection of oxygen at 1350°C

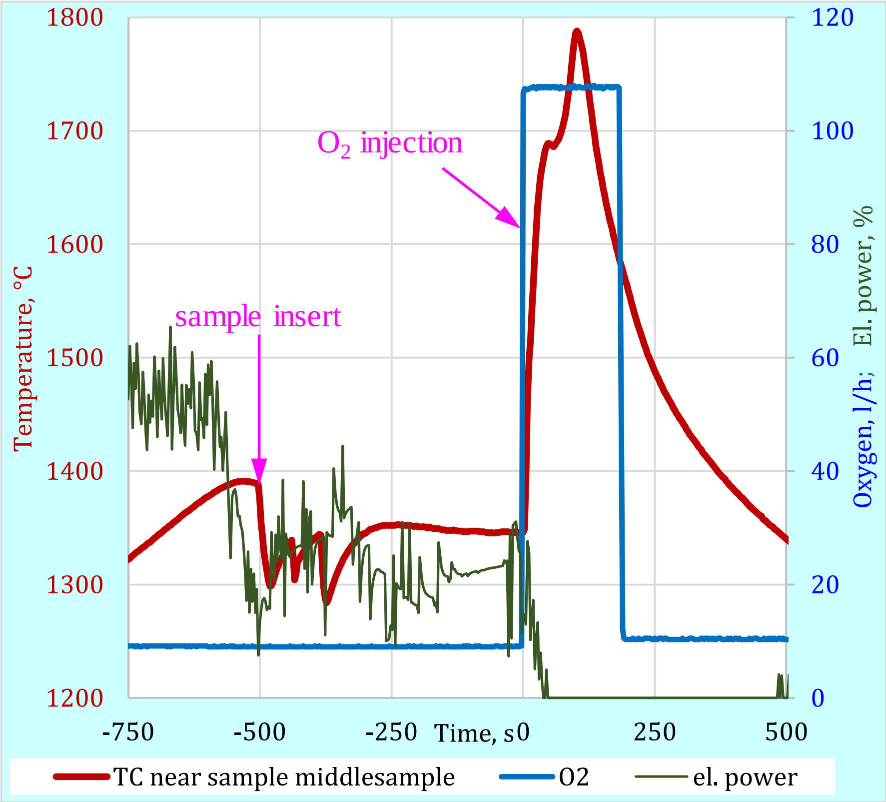

sample ZOs-1: temperature escalation in oxygen during slow transient

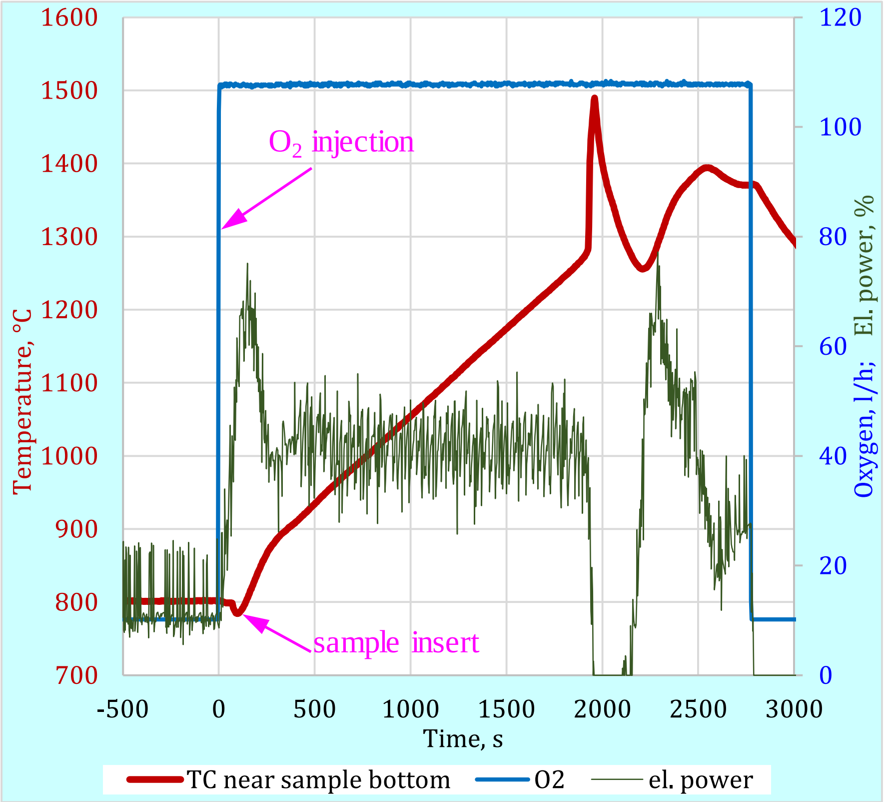

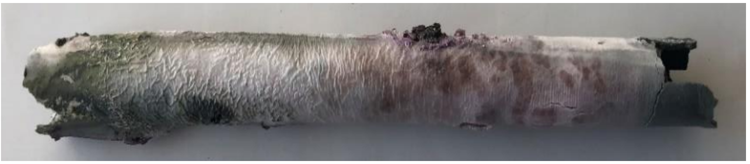

sample completely destroyed

SET 2: Simulation of LOCA heating rates in inductive furnace: cladding oxidation in steam

H_2+Ar + steam

Ar + steam

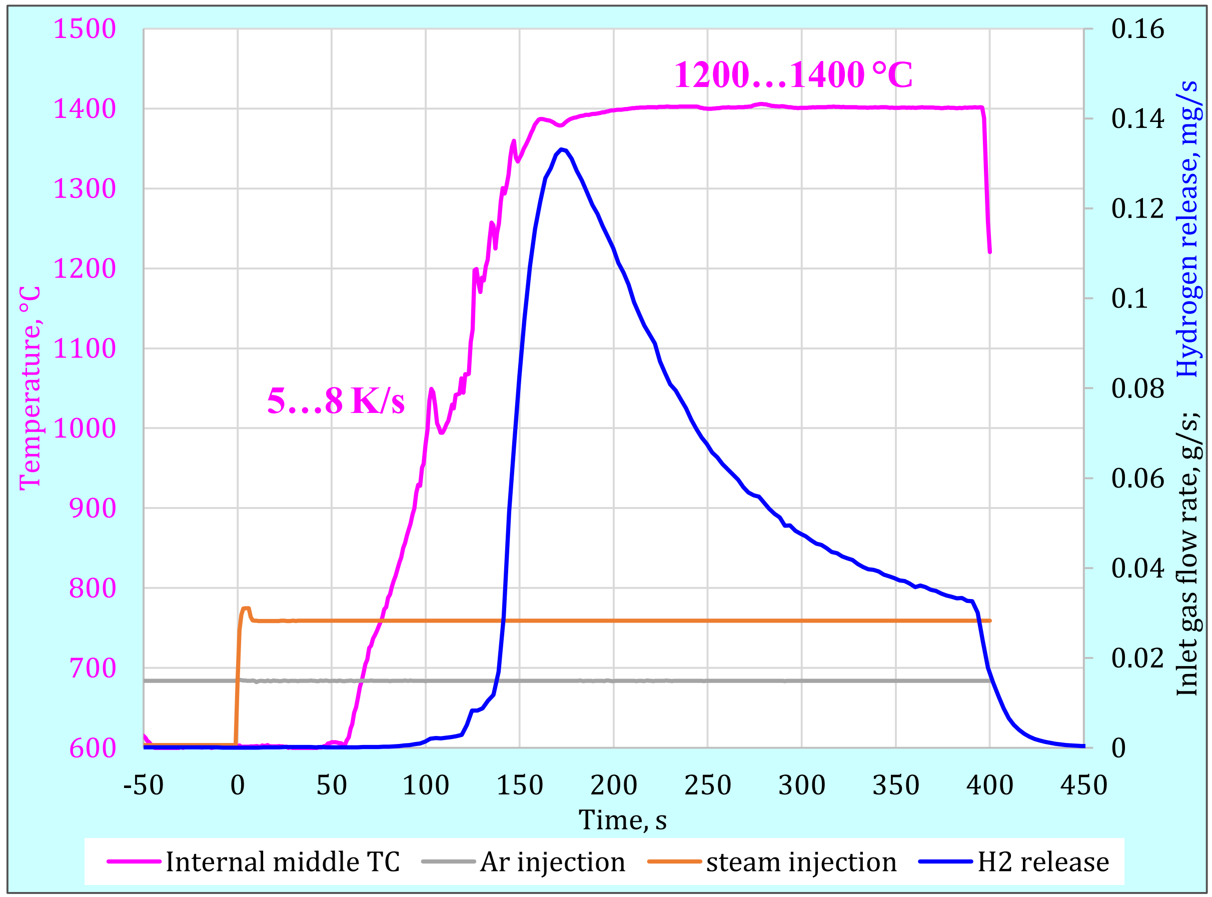

Matrix of single rod tests to perform under LOCA conditions

MC tubes: OD=10.75 mm, wall 725 µm; MCs and Zos tubes: OD=9.5 mm, wall 570 µm

Karlsruhe Institute of Technology

Sample	Heating rate [K/s]	Maximal clad temperature T_{max} [°C]	Duration of oxidation at T_{max} [min]	Cooldown	Comment
MC-4	7	1200	10	steam + Ar	performed
MC-5	7	1200	15	steam + Ar	performed
MC-6	8	1300	5	steam + Ar	performed
MC-7	6	1250	10	steam + Ar	performed
MCs-2	8	1360	6	steam + Ar	performed
MCs-3	8	1360	0	steam + Ar	performed
MCs-4	5	1250	6 (1250°→900°)	water	performed
MCs-5	5	1250	0	steam + Ar	performed
ZOs-2	5	1200	4	steam + Ar	performed
ZOs-3	5	1380	0	steam + Ar	performed
ZOs-4	5	1200	4	steam + Ar	performed
ZOs-5	5	1400	4	steam + Ar	performed

Appearance of coated cladding samples oxidized in inductive furnace

MC-4: 1200 °C
during 10 min

MC-5: 1200 °C
during 15 min

MC-7: 1250 °C
during 10 min

MC-6: 1350 °C
during 5 min

LOCA heating rate: cladding microstructure after oxidation at 1200 °C

MC-4: 1200 °C during 10 min

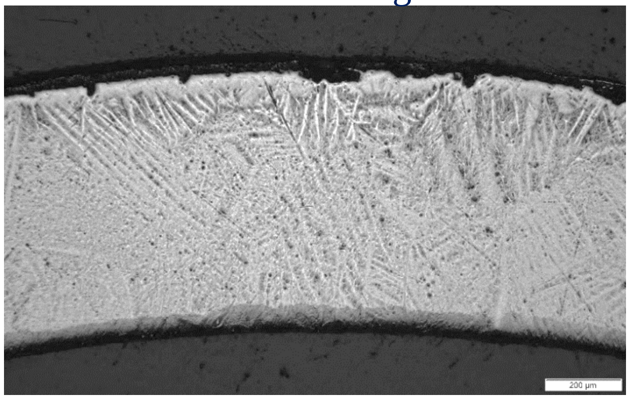

MC-5: 1200 °C during 15 min

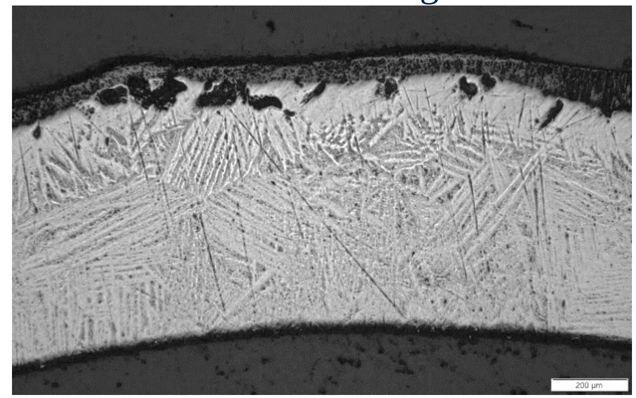

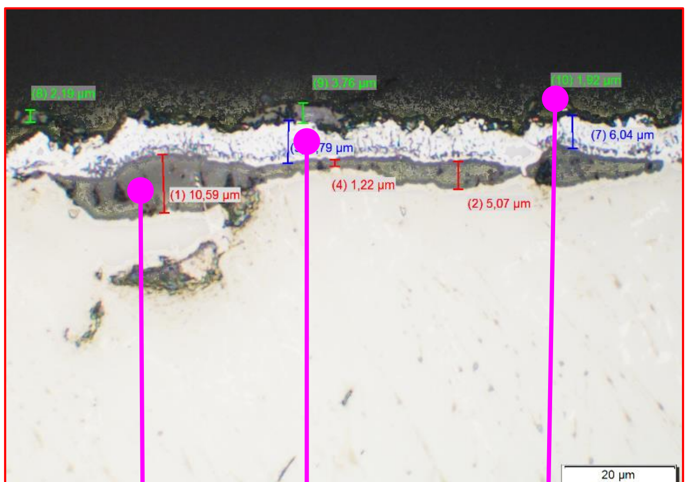

ZrO_2: 2…25 µm

Cr: 5µm

Cr_2O_3: 5µm

ZrO_2: 75 µm

Cr_2O_3: 3…7 µm

Cr: 0…7 µm

LOCA heating rate: diffusion of Cr through the cladding layers

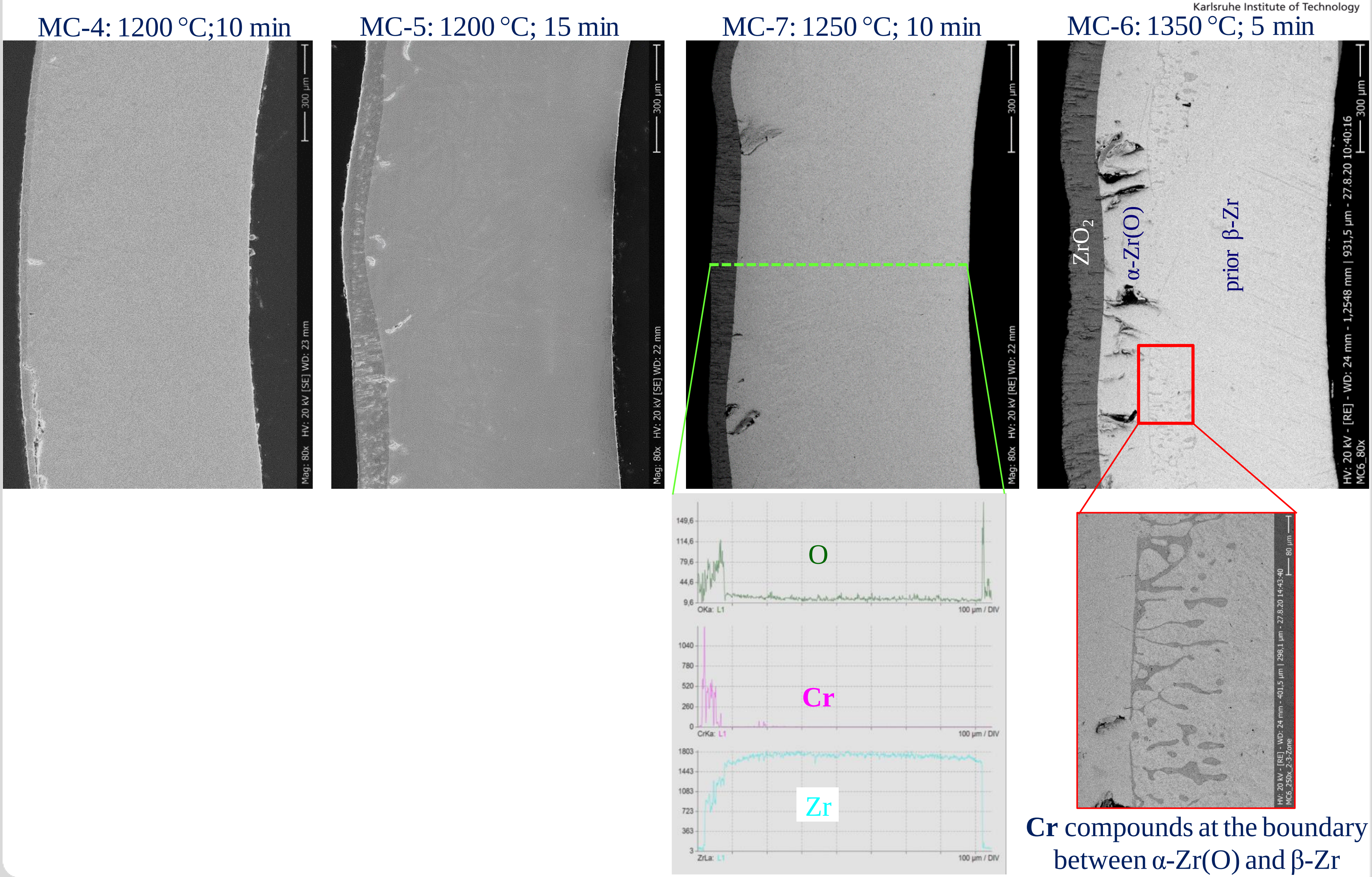

Cr compounds at the boundary between α-Zr(O) and β-Zr

LOCA heating rate:
comparison of uncoated sample with coated sample

Non-coated sample (Z-3) **vs. Cr-coated sample** (MC-7)

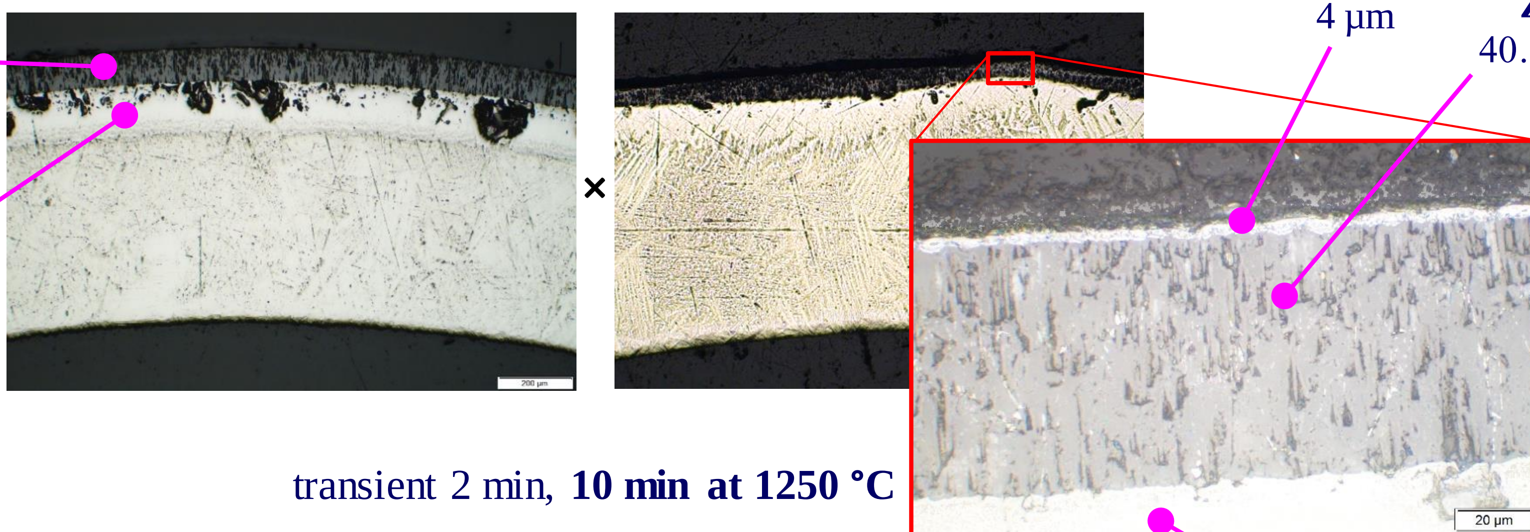

transient 2 min, **10 min at 1250 °C**

Influence of duration of oxidation in steam

LOCA transient followed by a constant temperature of 1400 °C

sample MCs-3: transient with 8 K/s, then 1400 °C during 3 s

sample MCs-2: transient with 8 K/s, then 1400 °C during 240 s

Cladding microstructure immediately after LOCA transient from 600 °C to 1400 °C

- formation of surface blisters containing Laves phase $ZrCr_2$

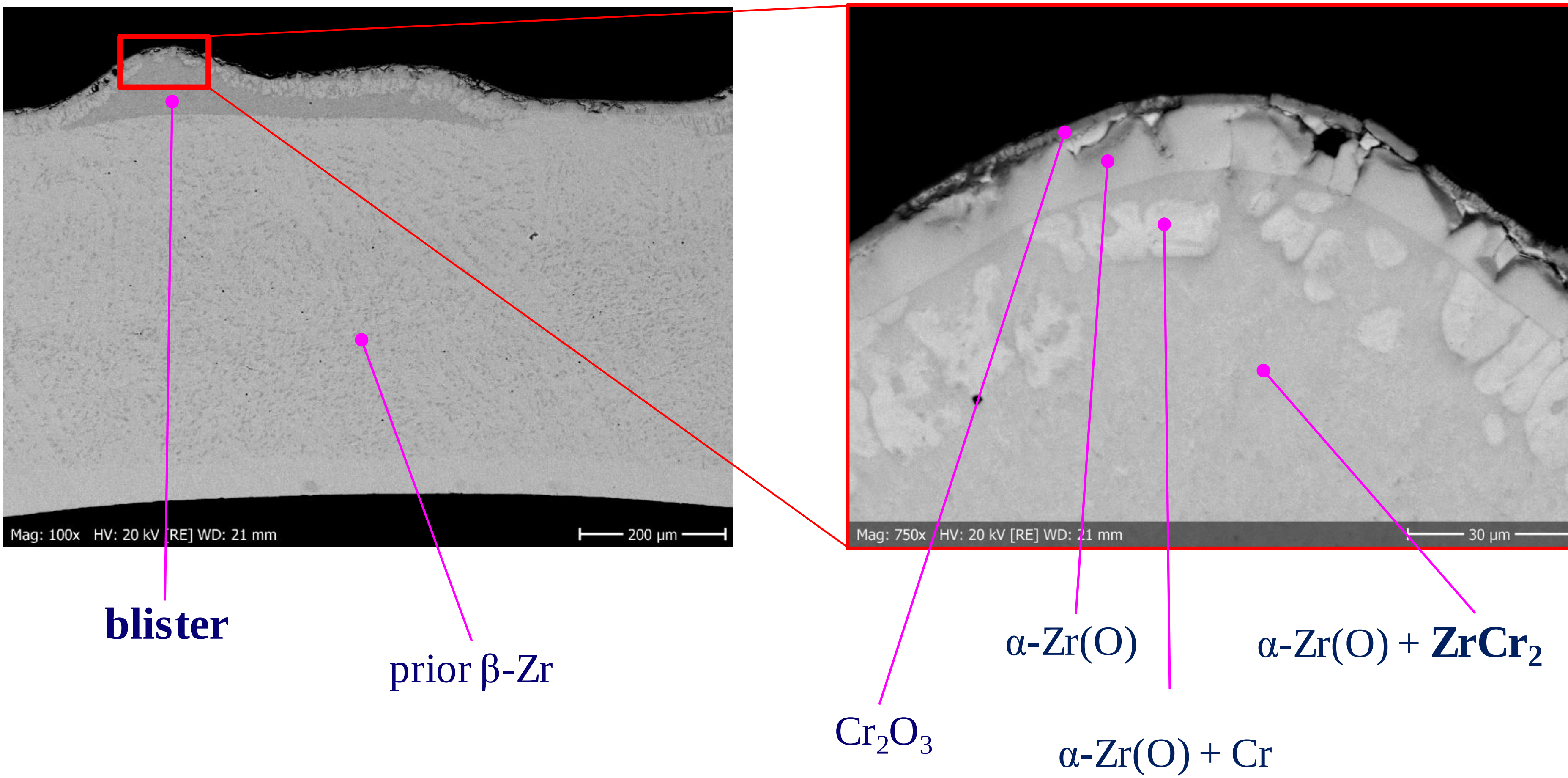

Cladding microstructure after LOCA transient and following holding at 1400 °C during 240 s

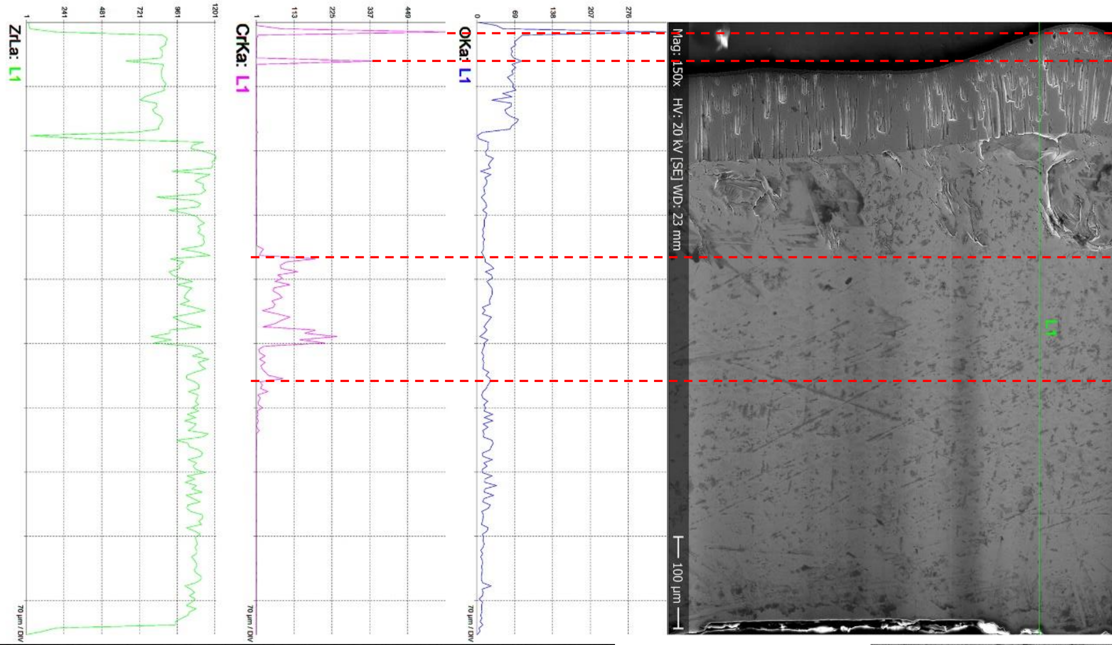

Cr_2O_3

Cr inside ZrO_2 especially inside blisters

Cr at transition α-Zr(O)→β-Zr

Cr_2O_3

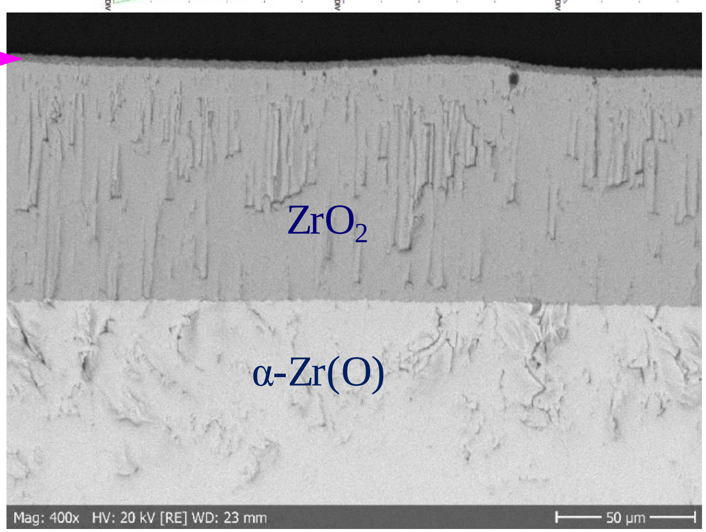

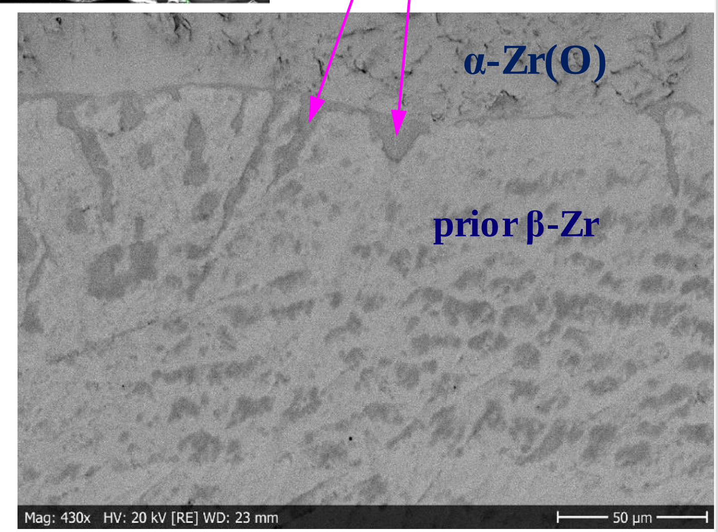

Influence of coating on hydrogen release
(LOCA transient 5 K/s from 600 to1250 °C, then cooldown to 900 °C and quenching)

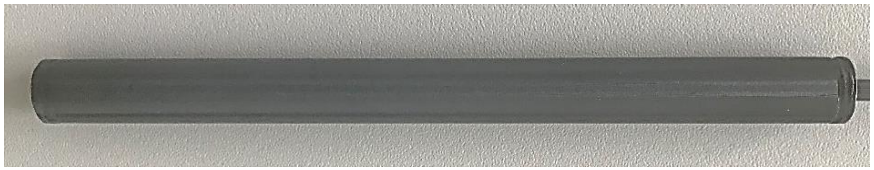

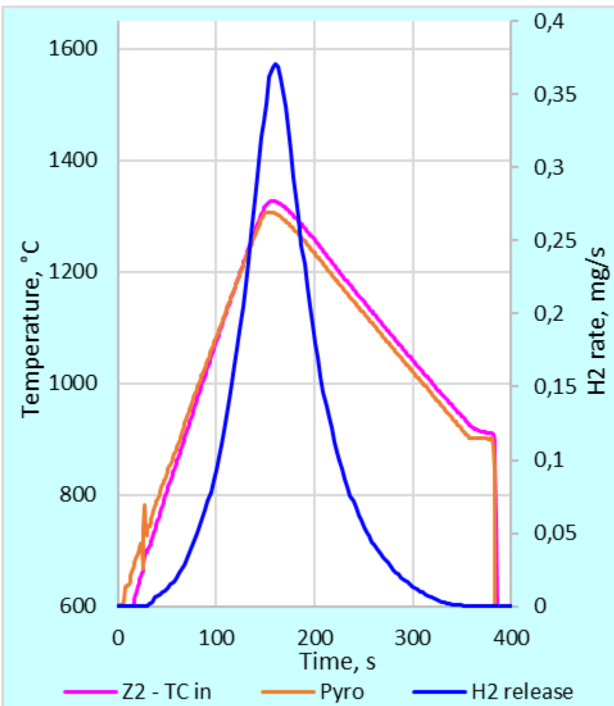

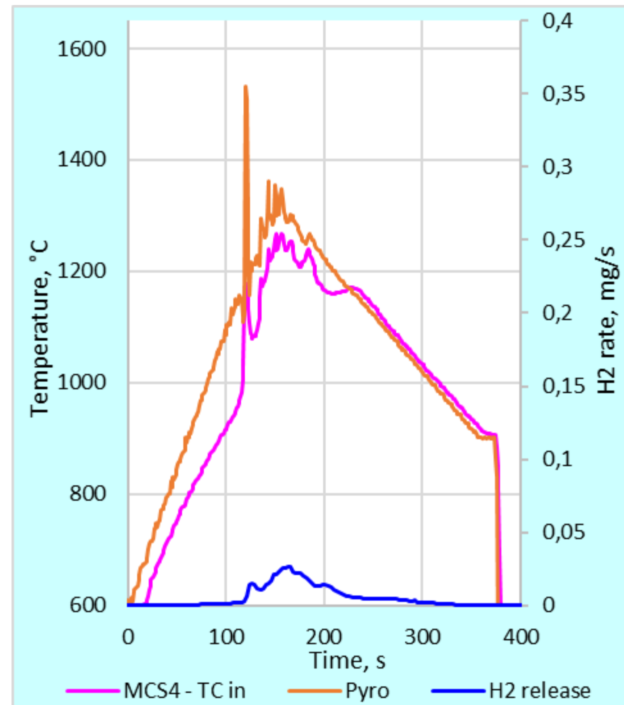

not coated sample Z2 (Zry-4)

coated sample MCs-4 (M5)

Negligible influence of Zr alloy (as substrate) on hydrogen release
for coated samples tested under similar high temperature conditions

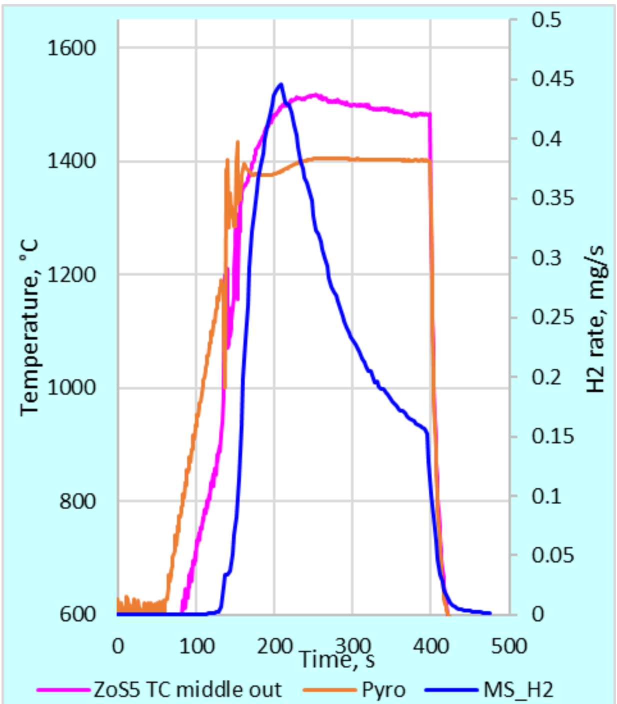

ZIRLO™ (sample Zos5)

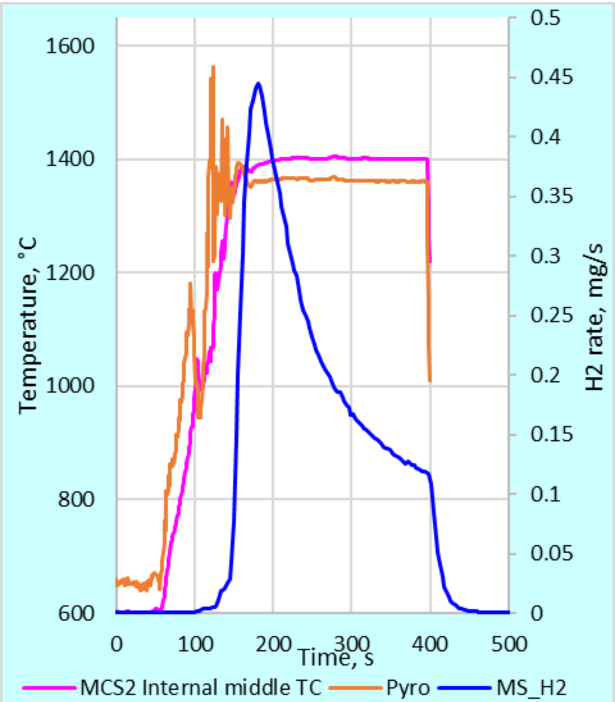

M5™ (sample MCs2)

Summary

➢ <u>Low heat-up rate</u>:

- ➢ Catastrophic oxidation at T>1300 °C in the absence of radiation heat loss.
- ➢ Diffusion of Cr through ZrO_2 and α-Zr(O) layer and Cr compounds at the boundary between α-Zr(O) and prior β-Zr layers.

➢ <u>Fast (LOCA) transient</u>:

- ➢ Decrease of cladding surface oxidation for Cr coated samples in comparison to not coated samples; moderate decrease of ZrO_2 growth, significant decrease of α-Zr(O) growth.
- ➢ Numerous blisters (local swellings) at the outer cladding surface. Zr-Cr eutectic at 1350 °C and formation of Laves phase $ZrCr_2$.
- ➢ The influence of direct heating on blister formation should be clarified: the electrical conductivity of Cr is higher in comparison to Zr (factor 3).

Thank you for your attention

http://www.iam.kit.edu/awp/163.php
http://quench.forschung.kit.edu/

C. Tang, M. Steinbrück, M. Grosse, S. Ulrich,
H.J. Seifert, M. Stüber

KIT

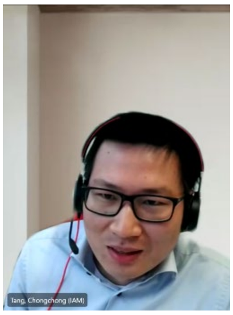

Magnetron-sputtered Cr-C-Al based coatings for enhanced accident tolerant fuel (ATF) zirconium-based alloy cladding

Surface modification of zirconium-based alloy cladding via deposition of oxidation-resistant coatings comprises one near-term evolutionary strategy of ATF claddings, which preserves favorable neutronic and irradiation properties of the zirconium alloy cladding as substrate. Coatings in the Cr-C-Al system represent one attractive and promising concept since they offer the ability to form passivation Cr_2O_3 scale under nominal conditions (hydrothermal corrosion) and protective Al2O3 scale during accidental scenarios (high-temperature steam oxidation), respectively.

The carbon-containing ternary system potentially avoids the eutectic reaction between the coating and the substrate at relatively low temperatures. In addition, in this system one ternary-layered carbide exists, i.e. Cr_2AlC MAX phase, which possesses unique physical and mechanical properties and excellent high-temperature oxidation resistance.

In this study, magnetron-sputtered Cr/C/Al elemental multilayers with chemical composition corresponding to the Cr_2AlC stoichiometry have been synthesized on Zircaloy-4 substrate. Different thermal processing conditions have been explored to examine the effect of annealing parameters on their microstructure formation, mechanical properties, and corrosion and oxidation performance. Annealing of the multilayers at 400°C led to the formation of nanocrystalline structure consisting of intermetallic and binary carbide phases. Single-phase and basal-plane textured Cr_2AlC coatings were synthesized after thermal annealing at 550°C. However, micro-cracking appeared on the 550°C annealed coatings owing to thermal expansion discrepancy between the Cr_2AlC MAX phase and the Zr alloy substrate. All coatings demonstrated excellent, combined oxidation and corrosion resistance via growth of an adherent and dense α-Al_2O_3 scale during high-temperature oxidation in steam and of a thin passivation Cr_2O_3 layer during hydrothermal corrosion in an autoclave. Via adjusting the multilayer design and annealing parameters, Cr-C-Al based coatings are attractive candidates as one type of coated ATF claddings.

Magnetron-sputtered Cr-C-Al based coatings for enhanced accident tolerant fuel (ATF) zirconium-based alloy cladding

Chongchong Tang, Martin Steinbrück, Mirco Grosse, Sven Ulrich, Hans Jürgen Seifert, Michael Stüber

Institute for Applied Materials (IAM-AWP), Karlsruhe Institute of Technology (KIT),76344 Eggenstein-Leopoldshafen, Germany

chongchong.tang@kit.edu

Institute for Applied Materials IAM-AWP & Program NUSAFE

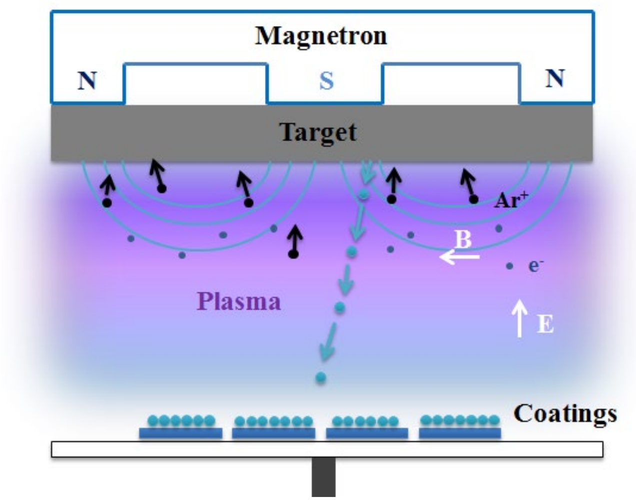

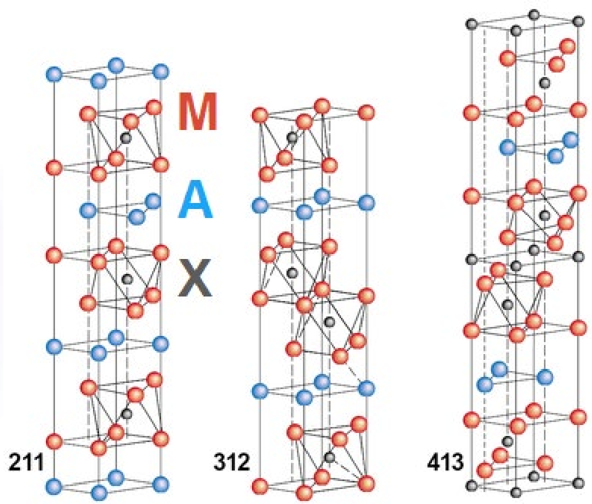

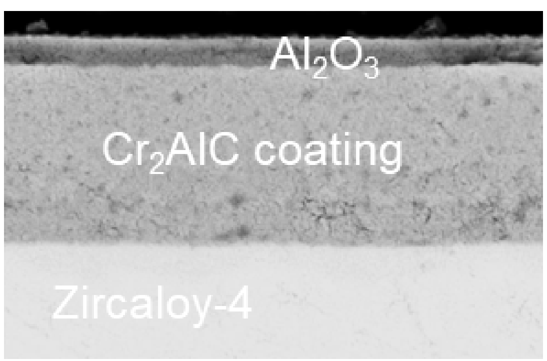

Accident tolerant fuels (ATF) cladding

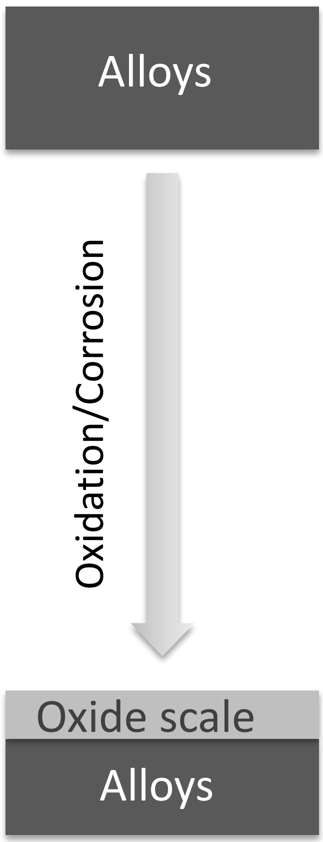

➢ Accident scenarios – HT steam oxidation

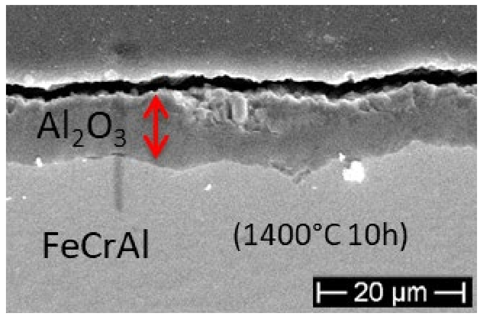

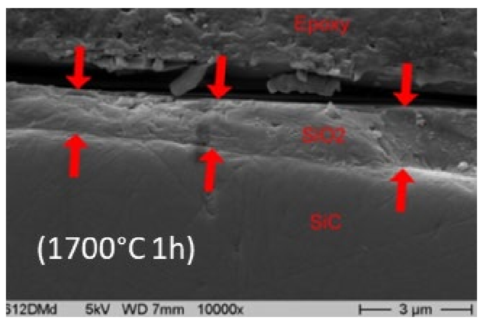

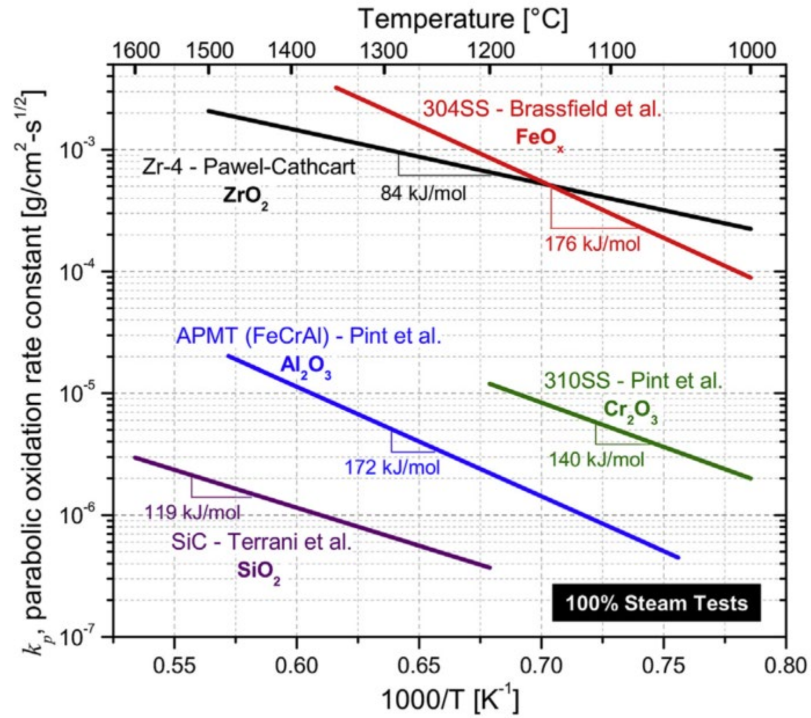

$M + H_2O = MO + H_2$

$\Delta G < 0$, spontaneous reaction

$$\left(\frac{\Delta m}{A}\right)^2 = kt \qquad k = Ae^{-E_a/RT}$$

Accident tolerant fuels (ATF) cladding

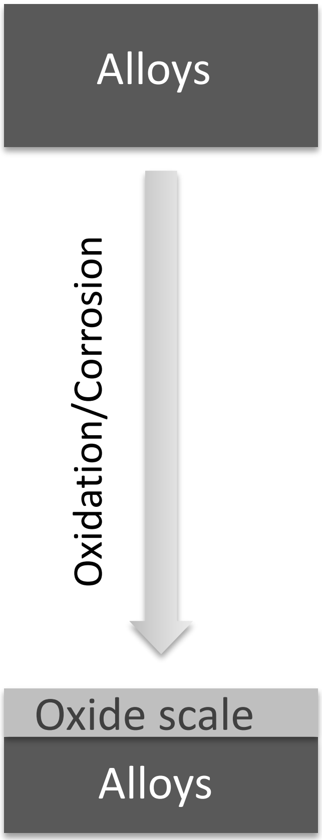

$M + H_2O = MO + H_2$

$\Delta G < 0$, spontaneous reaction

- **Normal operation – Hydrothermal corrosion**

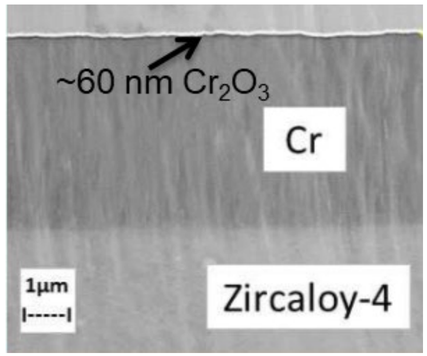

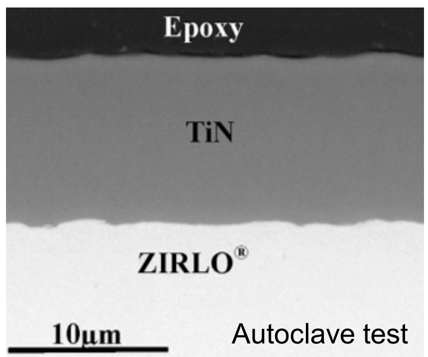

TiO_2, ZrO_2, Cr_2O_3 stable

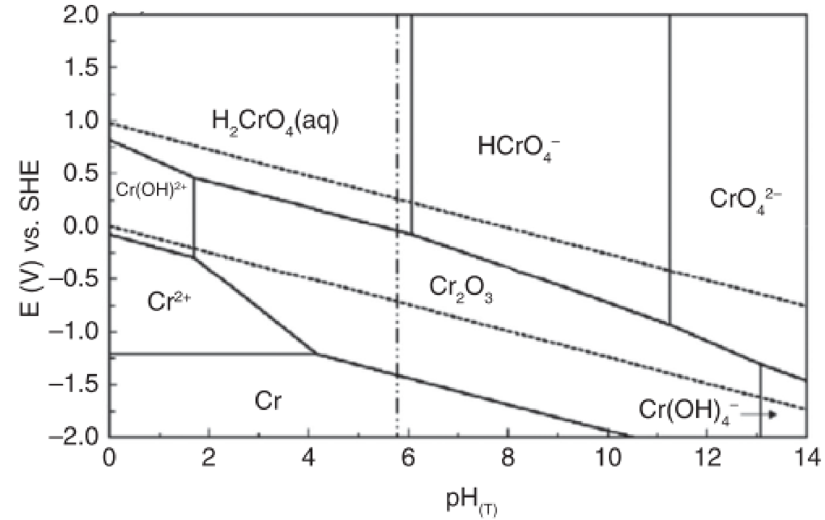

$$\left(\frac{\Delta m}{A}\right)^2 = kt \qquad k = Ae^{-E_a/RT}$$

Al-based MAX phases: Potential for combined excellent oxidation + corrosion resistance

MAX phase

- Ternary carbide and nitride compounds described by the general formula $M_{n+1}AX_n$ (MAX), where n typical is 1, 2, 3
- Layered crystal structures: $M_{n+1}X_n$ layers interleaved with A layer

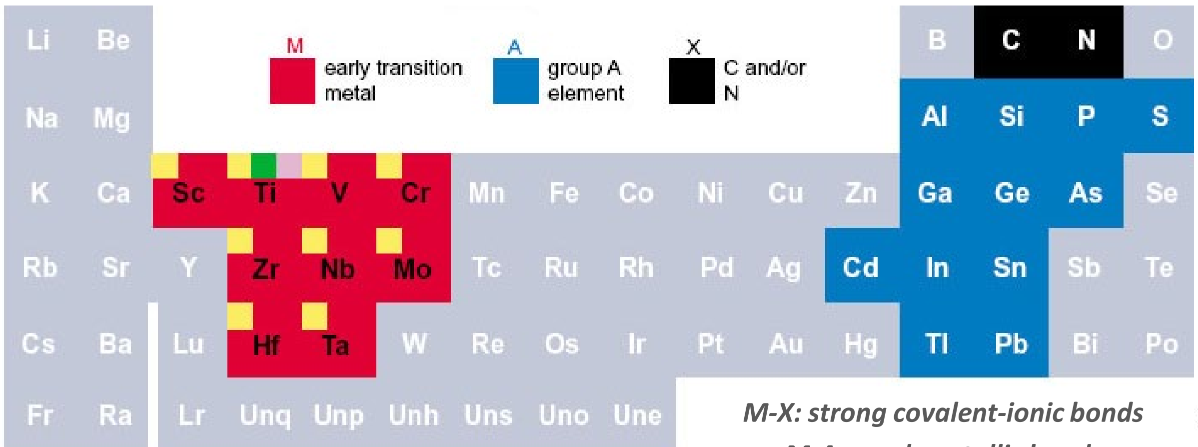

M-X: strong covalent-ionic bonds
M-A: weak metallic bonds

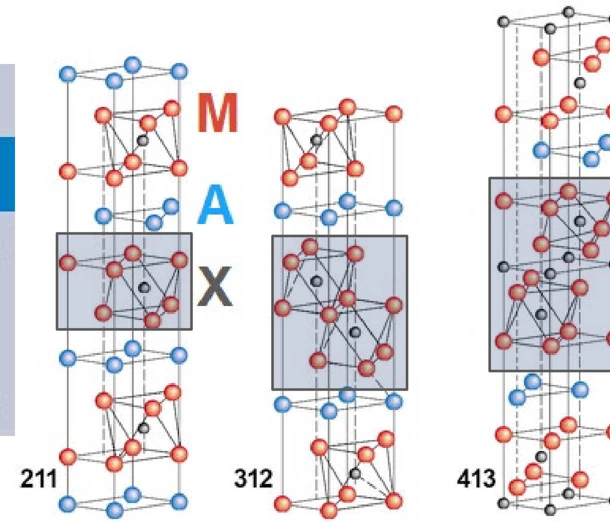

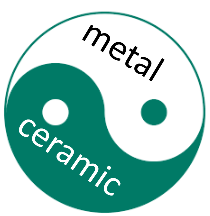

Unique combination of physical, chemical, mechanical properties of both metals and ceramics

Machinability | *Low density* | *Damage tolerance*

High melting/decomposition temperature | *Thermal conductivity*

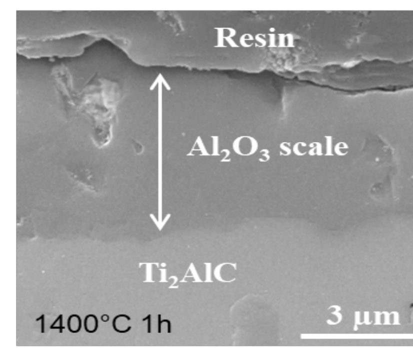

M.W. Barsoum, MAX phases: properties of machinable ternary carbides and nitrides, John Wiley & Sons, 2013.

MAX phase coatings

- Spraying
  - High-velocity oxy-fuel spray
  - Cold spraying
- Physical vapor deposition (PVD)
  - Cathodic arc evaporation
  - Pulsed laser deposition
  - Magnetron sputtering
    sputtering with 3 element sources
    sputtering with compound targets
    reactive sputtering
    sputtering-solid state reactions
- Chemical vapor deposition

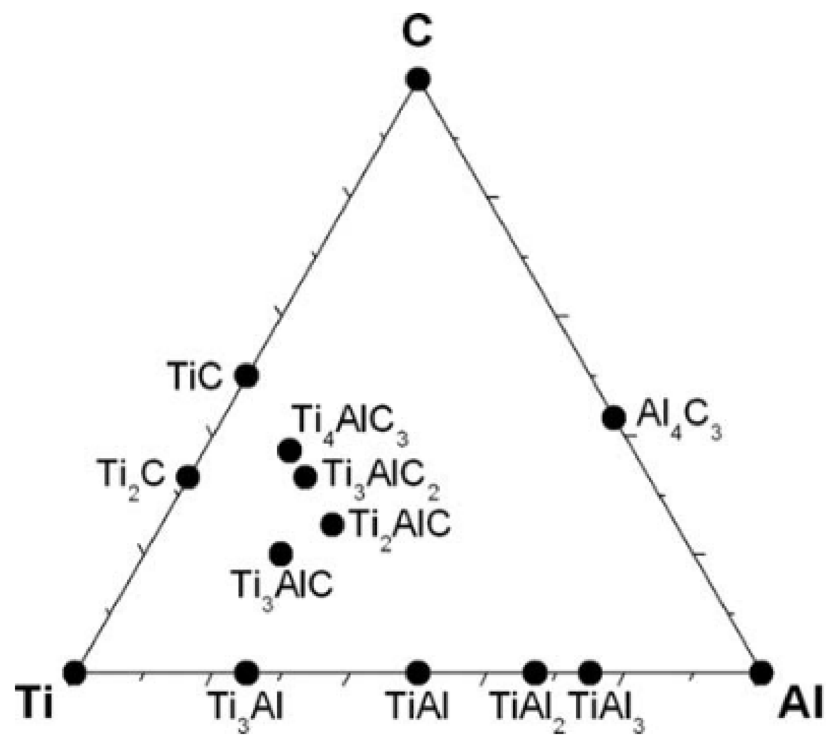

Challenges

Phase Pure → Low-tem. Synthesis → Textured Microstructure

Dahlqvist et al. Physical Review B 81 (2010) 024111.

Coating design & synthesis

A two-step approach

Nanoscale multilayers

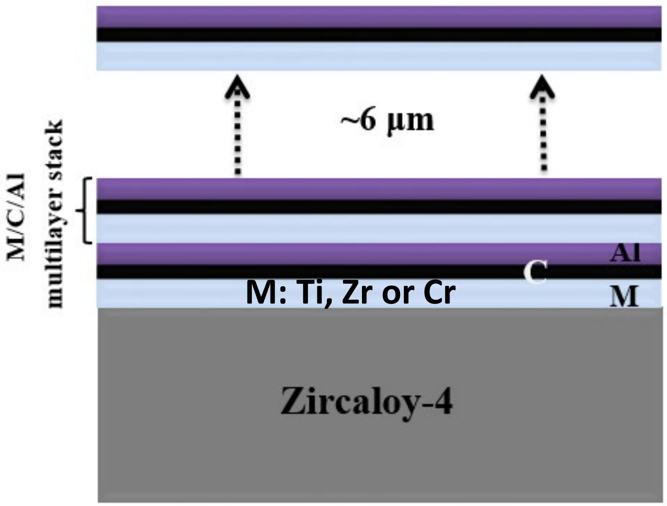

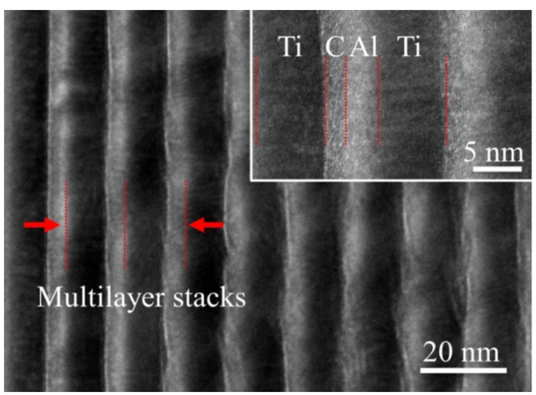

Ex-situ annealing

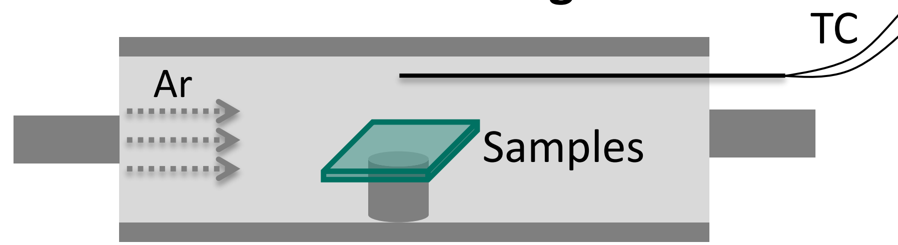

- ❖ Precise stoichiometry control
- ❖ Phase pure coatings with basal-plane textured structure
- ❖ Relatively low annealing temperature

Coating design & synthesis

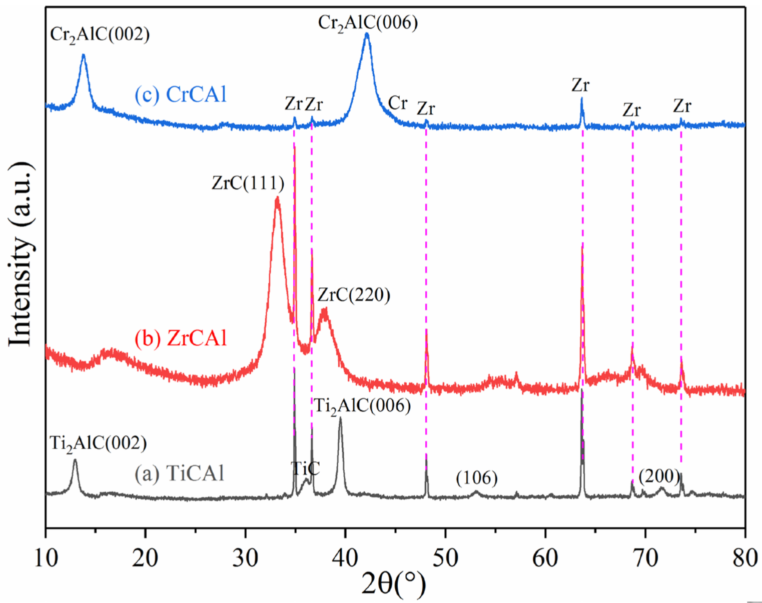

- Annealing : 800°C for Ti_2AlC, 550°C for Cr_2AlC, 600°C for Zr(Al)C), 10 min, Ar
- No MAX phase formation in Zr-C-Al system
- Nanocrystalline coatings, free of columnar growth
- Micro-cracking on Cr_2AlC coatings
- Low oxidation resistance of Ti and Zr based coatings

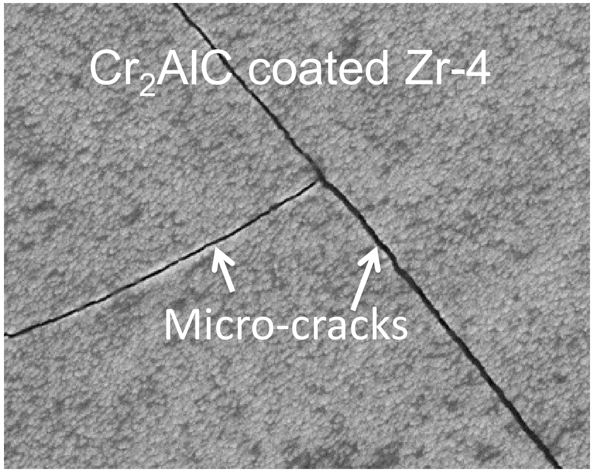

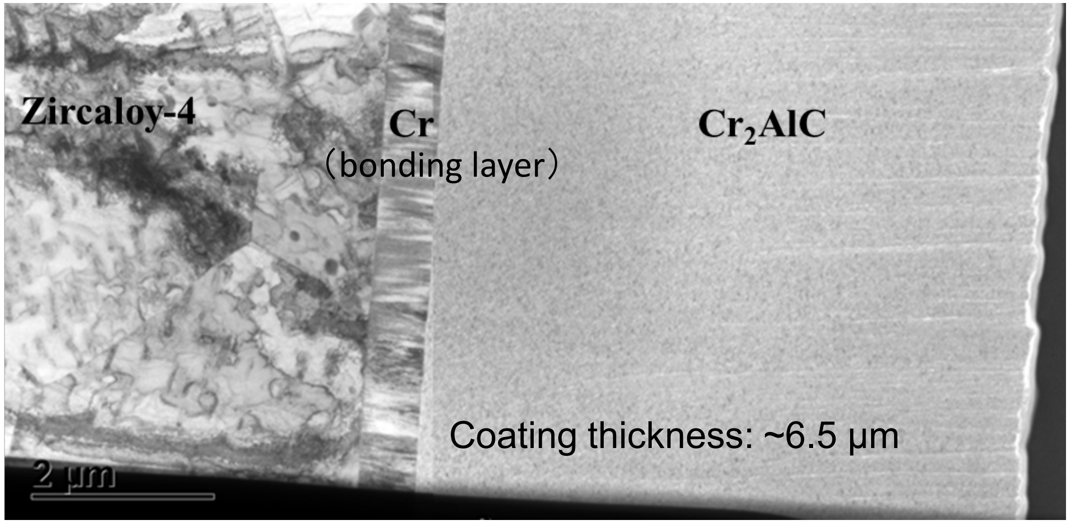

Coating design & synthesis

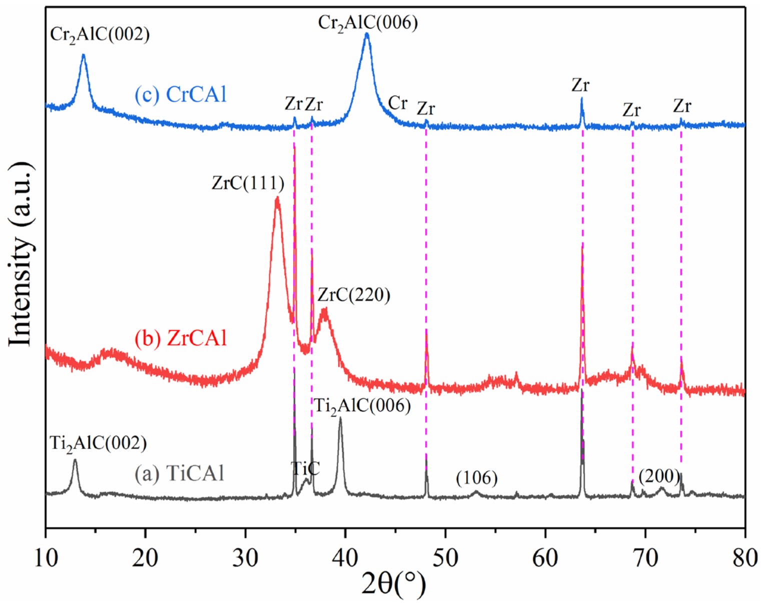

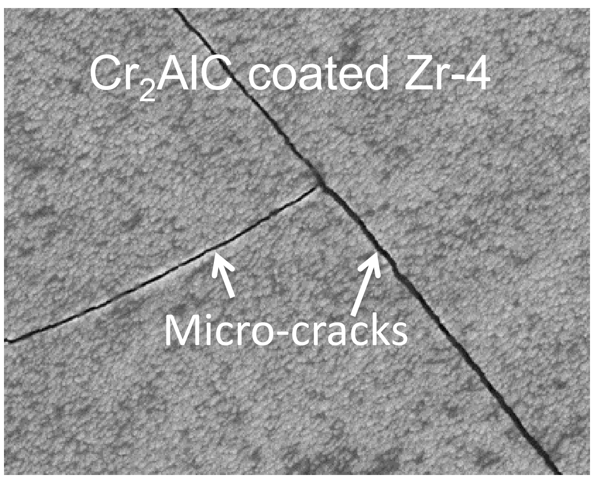

- Annealing : 800°C for Ti_2AlC, 550°C for Cr_2AlC, 600°C for Zr(Al)C), 10 min, Ar
- No MAX phase formation in Zr-C-Al system
- Nanocrystalline coatings, free of columnar growth
- Micro-cracking on Cr_2AlC coatings
- Low oxidation resistance of Ti and Zr based coatings

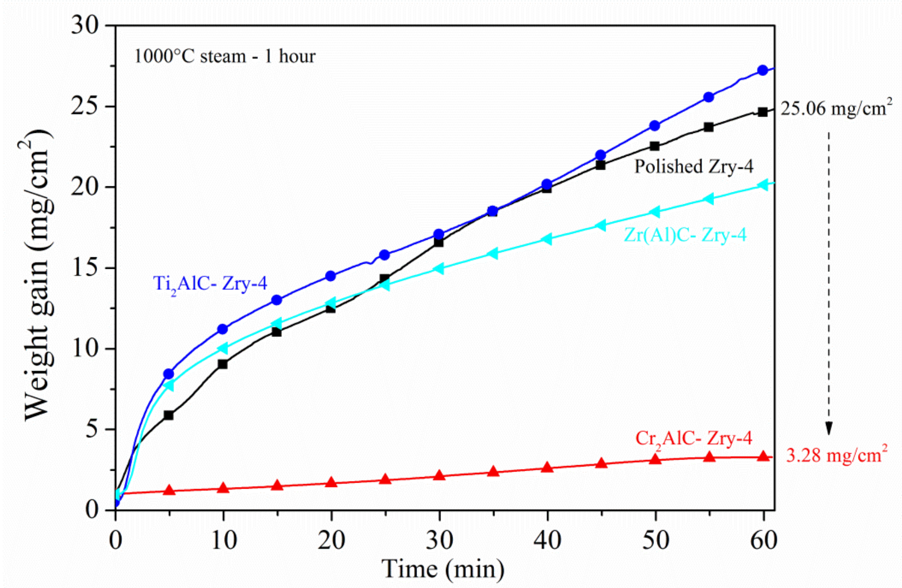

Steam oxidation & hydrothermal corrosion

- Static autoclave (Westinghouse test T949)
- 360°C pure water + ~ 18.8 MPa, Duration: 3 days

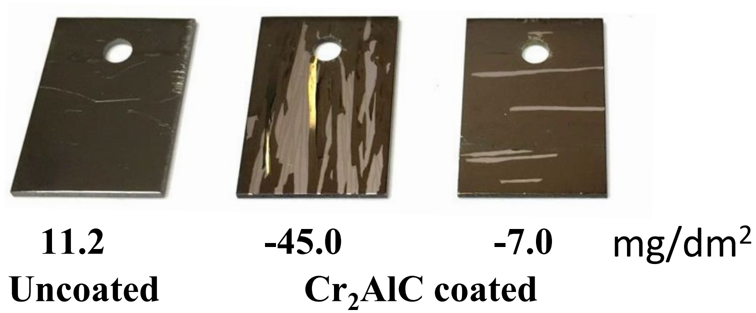

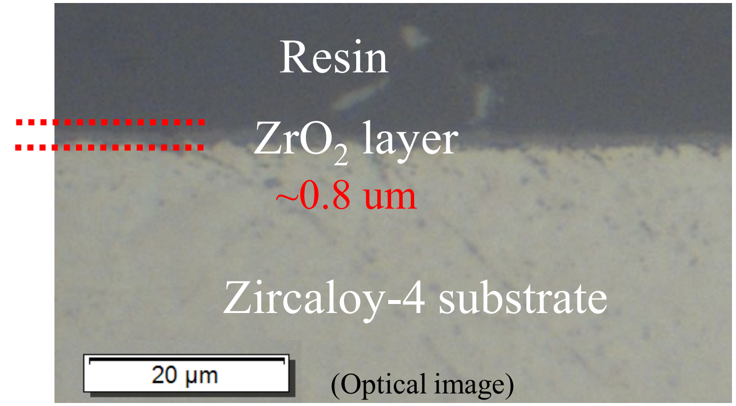

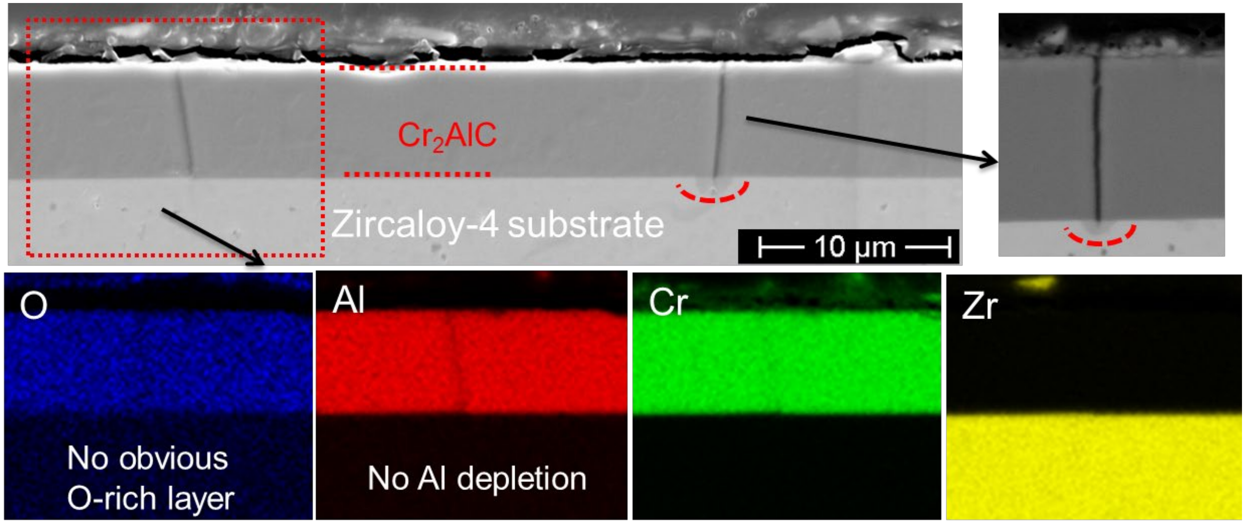

- Partial delamination after autoclave test
- Excellent corrosion resistance with undetectable oxide layer (passivation Cr_2O_3 layer)

Development of Cr-C-Al based coating

- Two designs

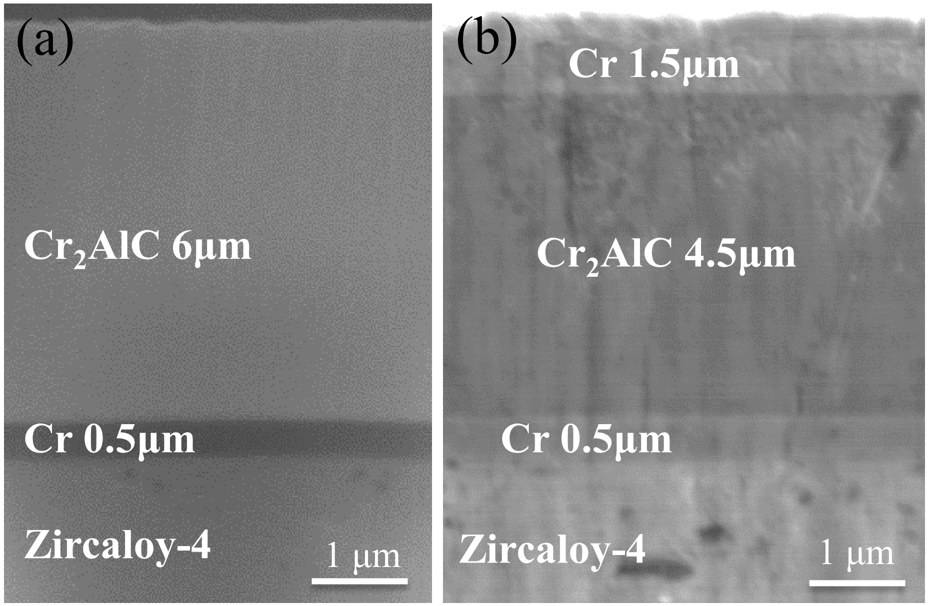

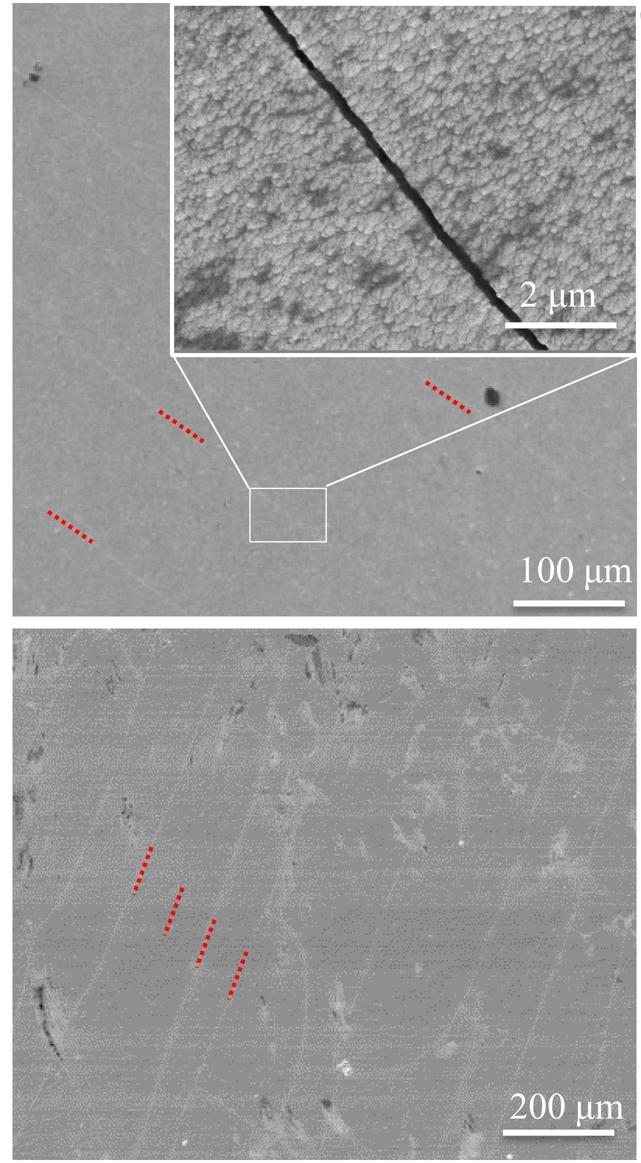

- Cr overlayer avoids potential hydrothermal dissolution of Al (long-term normal operation)
- Enhanced mechanical properties typical for multilayer design
- Micro-cracking after 550°C annealing

IAM Institute for Applied Materials

Development of Cr-C-Al based coating

- **Transient oxidation**

300-1200°C 10 K/min + 1200°C 10min, steam

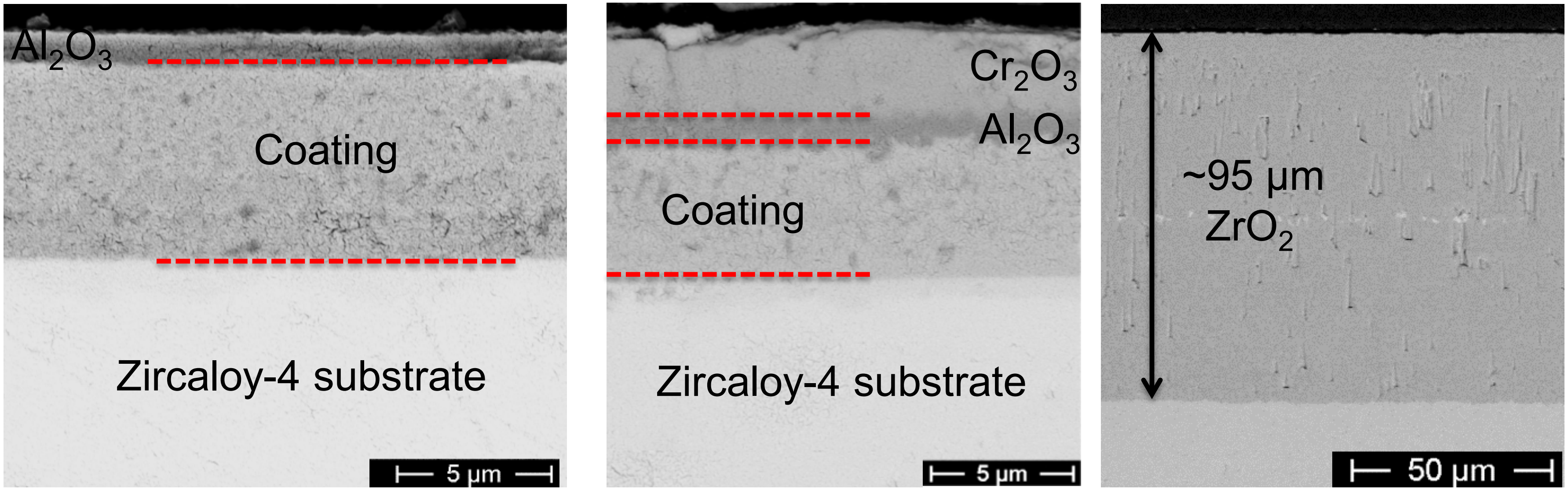

Cr_2AlC coating | Cr/ Cr_2AlC coating | Uncoated Zircaloy-4

Development of Cr-C-Al based coating

➢ **Effect of annealing conditions**

High tensile stress during cooling leading to cracking

$$\sigma_c^T = \frac{E_c(\alpha_s - \alpha_c)\Delta T}{(1 - v_c) + \left(2t_c E_c / t_s E_s\right)(1 - v_s)}$$

$$\sigma = \frac{250 \times (6 - 13) \times 10^{-6} \times 550}{(1 - 0.24) + (2 \times 6.5 \times \frac{250}{575 \times 99.3})(1 - 0.37)}$$

$= \sim 1.2$ GPa

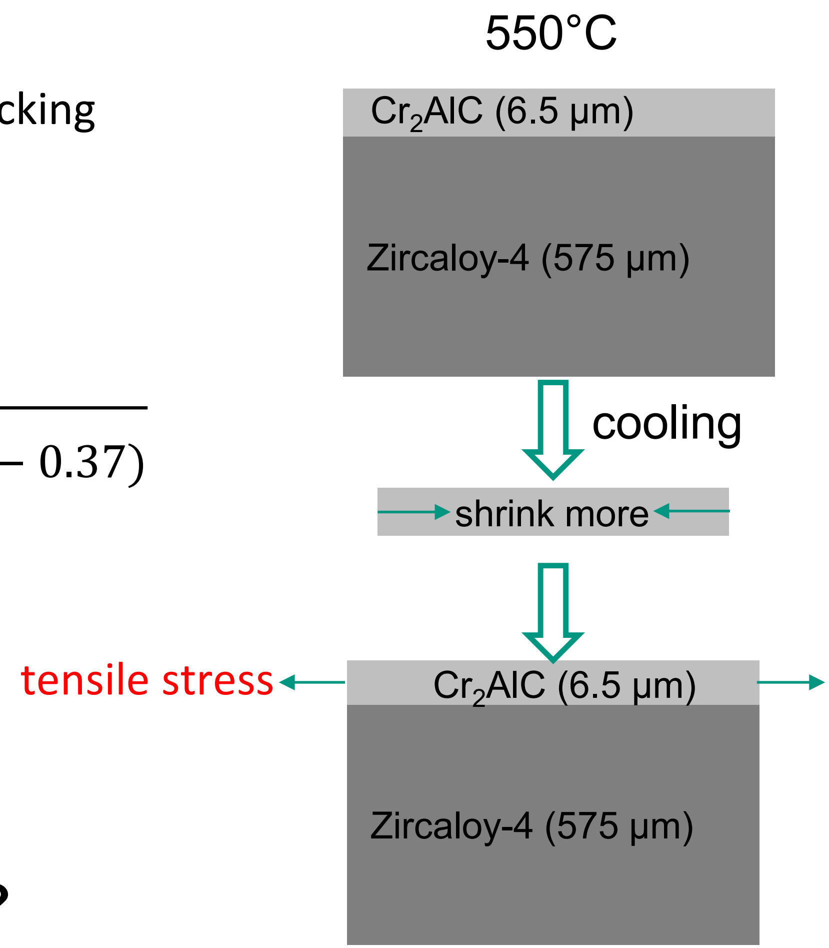

Annealing temperature

550°C $\Rightarrow$ **400°C ?**

Typical stress-relieved annealed (SRA) temperature of Zircaloy cladding tubes

Development of Cr-C-Al based coating

- **Effect of annealing conditions**

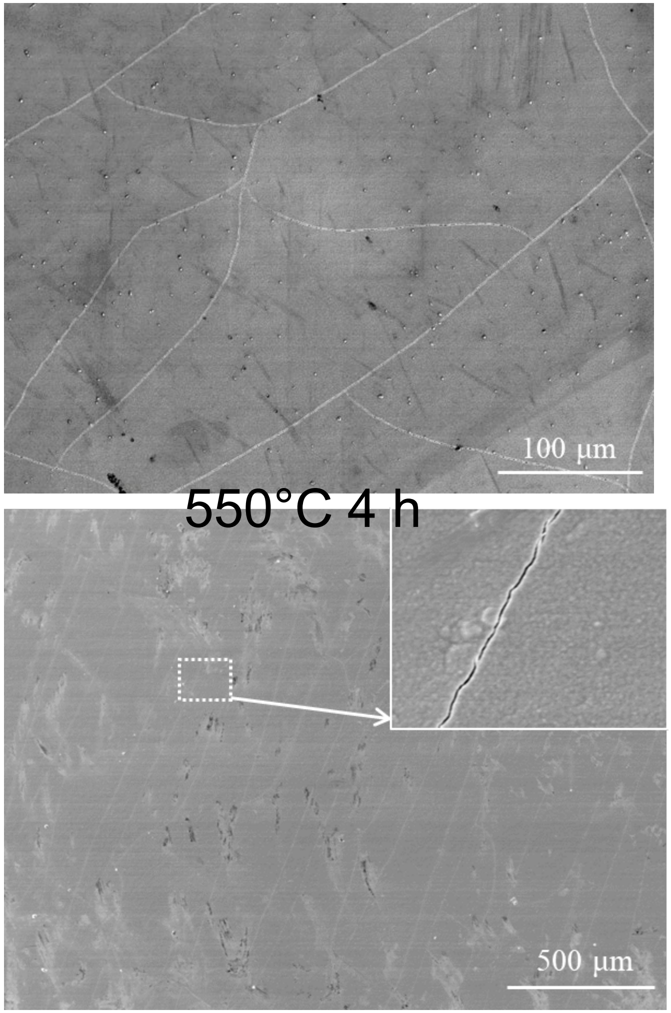

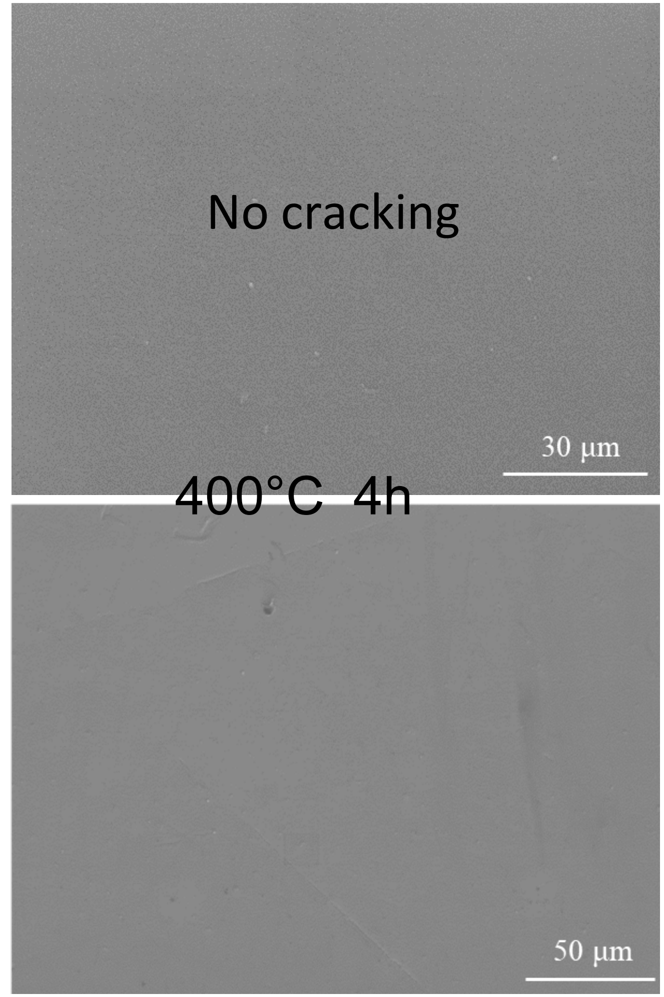

Development of Cr-C-Al based coating

Karlsruhe Institute of Technology

➢ Effect of annealing conditions

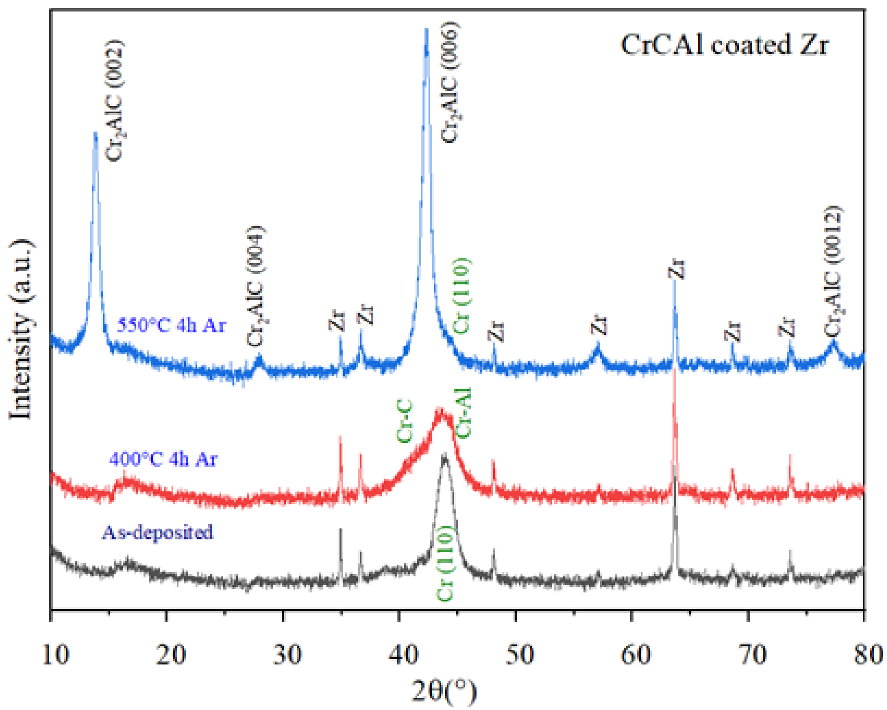

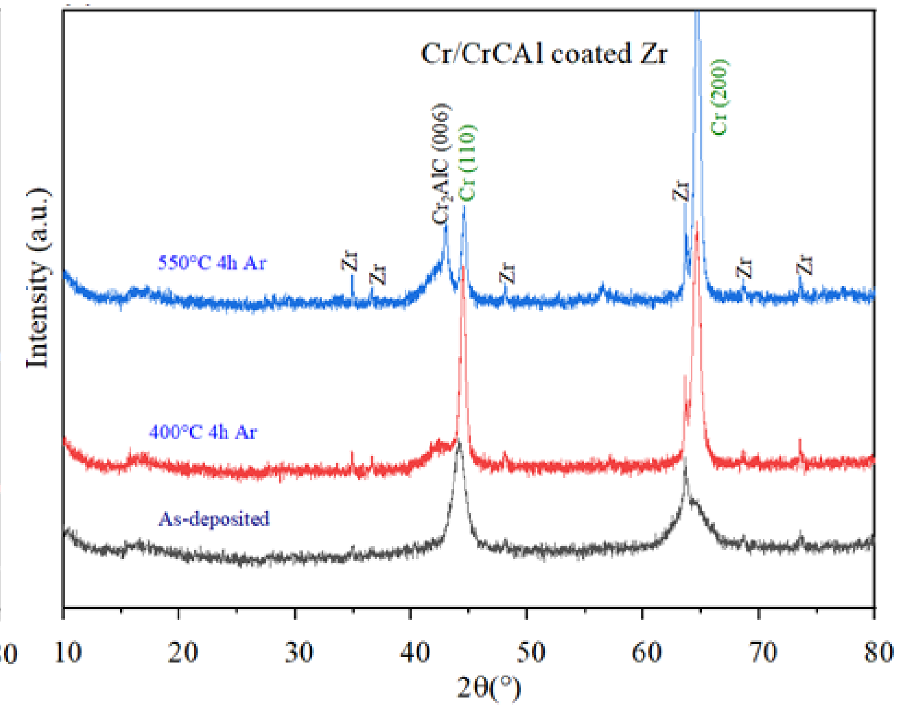

- ❖ Formation of Cr-C and Cr-Al nanocrystalline composites after annealing at 400°C for 4 h
- ❖ The absence of Cr_2AlC makes the coating cracking-free

IAM Institute for Applied Materials

Development of Cr-C-Al based coating

- **Effect of annealing conditions**

Indentation

ID.	Hardness (H, GPa)	Young's modulus (E*, GPa)	H/E*
CrCAl 400°C 4h	11.3 ± 0.3	179.4 ± 4.0	0.063
CrCAl 550°C 4h	14.1 ± 0.5	212.0 ± 8.1	0.067
Cr/CrCAl 400°C 4h	12.2 ± 0.4	189.2 ± 8.3	0.064
Cr/CrCAl 550°C 4h	13.7 ± 0.3	219.6 ± 10.3	0.063

Scratch test (0-30 N)

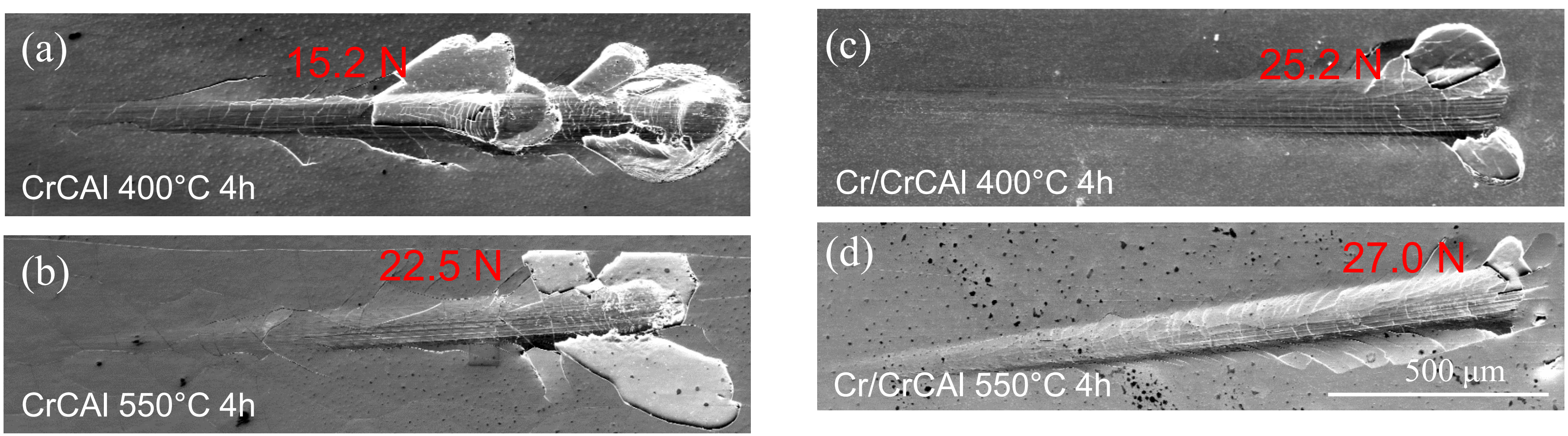

Development of Cr-C-Al based coating

➢ **Effect of annealing conditions**

❖ Excellent corrosion resistance with growth of thin Cr_2O_3 layer for the CrCAl composite coatings

❖ No spallation was observed for the CrCAl coatings after the relatively long-term autoclave test

❖ Tiny spallation around the suspension hole for Cr/CrCAl coatings

❖ 400°C annealing temperature is acceptable for nuclear industry

Weight change: uncoated Zr 0.3 mg,
CrCAl coated Zr: 0.3 mg
Cr/CrCAl coated Zr: -0.5 mg

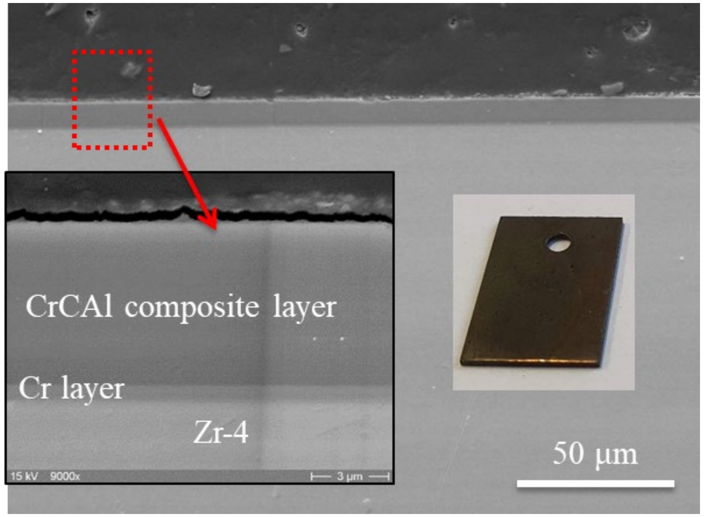

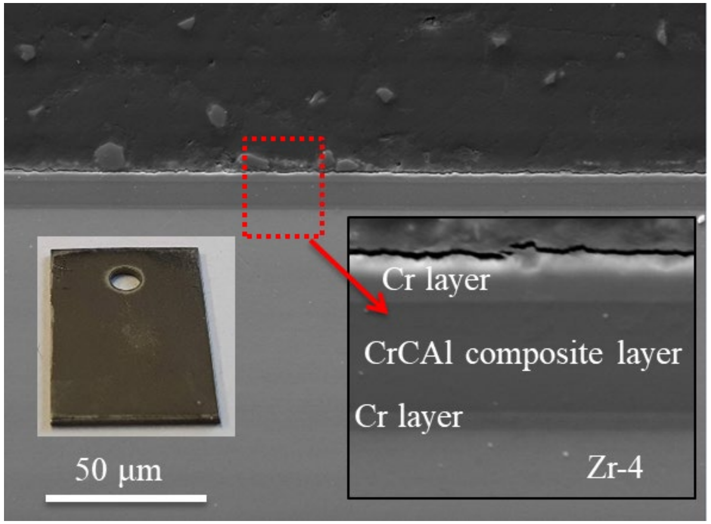

Static autoclave with 1000 ppm B, 2 ppm Li at 330°C and 18 Mpa, 30 days (KU LEUVEN)

Summary

- MAX phase coatings synthesis and steam oxidation
  - Low oxidation performance of Ti_2AlC and Zr(Al)C coatings
  - Excellent oxidation resistance with self-healing capability of Cr_2AlC coatings
- Cr-C-Al based coatings
  - Micro-cracking on Cr_2AlC coatings due to thermal expansion coefficient mismatch
  - Formation of Cr-C and Cr-Al nanocrystalline composites after annealing at 400°C for 4 h without cracking
  - Excellent corrosion and oxidation resistance for composite coating
  - Nanocrystalline Cr-C-Al based composite coatings show promising for ATF application with acceptable annealing T
  - *Mechanical properties, irradiation behavior, long-term in-pile corrosion*

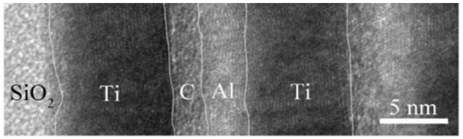

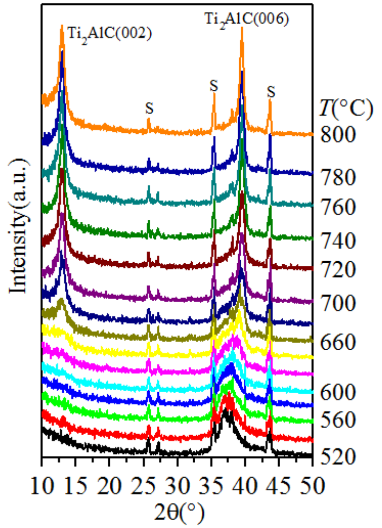

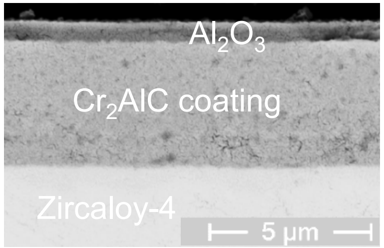

Acknowledgements

The QUENCH team at KIT and the KIT program NUSAFE

Thin film group at IAM-AWP

International cooperation partners: IL TROVATORE, Westinghouse, IAEA ACTOF,   etc

Thank you for your attention!

M. Steinbrück, M. Grosse, U. Stegmaier (KIT)

J. Braun, C. Lorrette (CEA)

High-temperature oxidation of silicon carbide composites for nuclear applications

Silicon carbide composites are among the promising ATF (accident tolerant fuel) materials for substitution of zirconium alloys as cladding for nuclear fuel. This class of materials combines good mechanical properties and high thermal conductivity with excellent resistance against irradiation and oxidation/corrosion up to very high temperatures.

This paper presents a brief overview on high-temperature (HT) oxidation of silicon carbide in various atmospheres as well as results of high-temperature oxidation experiments with SiC_f/SiC composite materials in steam simulating severe accident conditions in Light Water Reactors (LWR). Nuclear grade tubular samples were fabricated at CEA, and the experiments were conducted within the frameworks of the European IL TROVATORE program and KIT's ATF cladding research projects. Post-test examinations were performed at KIT (metallography & X-ray tomography) and CEA (mechanical testing).

Experiments in steam up to 1900°C were conducted in the inductively heated QUENCH-SR (Single Rod) facility coupled with mass spectrometry for off-gas analyses. Very limited oxidation of the SiC_f/SiC cladding was observed up to 1700°C due to the formation of a protective silica scale on the SiC protective "sealcoat". Cladding tubes failure accompanied by strong gas release and volatilization occurred beyond 1800°C when the SiC_f/SiC composite itself was attacked. Additionally, the mechanical performance of such quenched clad segments after oxidation for one hour in steam at 1700°C was not significantly affected. The non-linear elastic damageable behavior of the composite was maintained, as well as its geometry was fully preserved confirming high potential in terms of safety benefit.

Generally, the SiC composite material investigated offers very promising HT oxidation/corrosion and mechanical properties for application in LWRs.

Karlsruhe Institute of Technology

High-temperature oxidation of silicon carbide composites for nuclear applications

M. Steinbrück, M. Grosse, U. Stegmaier (KIT)
J. Braun, C. Lorrette (CEA)

26th International QUENCH Workshop, MS Teams, 6-9 December 2021

Institute for Applied Materials IAM-AWP & Program NUSAFE

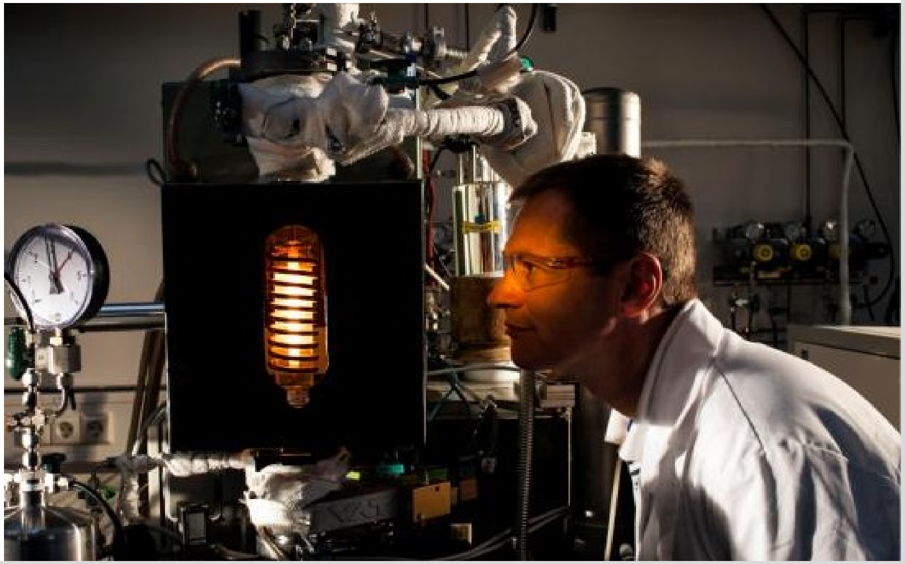

Outline

- Introduction and motivation
- Brief summary on high-temperature oxidation SiC
- Samples and experimental conditions
- Steam oxidation of SiC_f/SiC ceramic matrix composites
  - Transient test 1400 $\rightarrow$ 1850°C
  - Isothermal tests 1 hour at 1700°C
- Mechanical testing
- Conclusions

SiC_{fiber}/SiC ceramic matrix composites

- Silicon carbide ceramic-matrix-composites (CMC) are considered as promising candidates for accident tolerant fuel (ATF) cladding tubes in GFRs and LWRs
- They provide excellent oxidation resistance, good neutronic properties, high melting (decomposition) temperature, and good mechanical properties

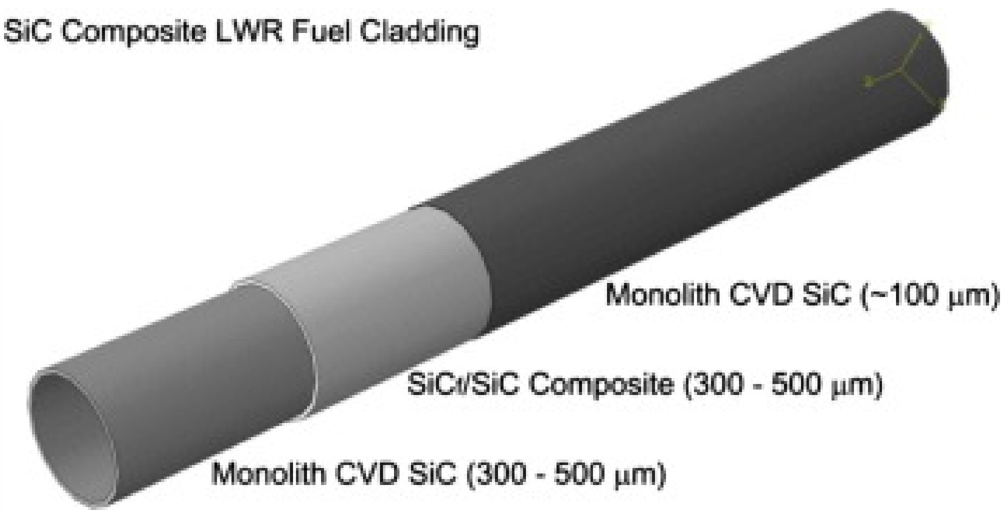

SiC triplex tube

SiC-SiC cladding tubes

Kim, JNM 458 (2015) 29-36
Image by ORNL

Reaction of SiC with oxygen

- Either passive oxidation
  - Mass gain
  - Formation of a protective oxide scale

$$SiC + \frac{3}{2}O_2 \rightarrow SiO_2 + CO$$

$$SiC + 2O_2 \rightarrow SiO_2 + CO_2$$

- Or active oxidation
  - Mass loss
  - Degradation of the material

$$SiC + O_2 \rightarrow SiO(g) + CO$$

➢ The mechanism is dependent on temperature and oxygen partial pressure

➢ Active oxidation is strongly affected by thermal hydraulic boundary conditions

Reaction of SiC with steam

$$SiC + 3H_2O \rightarrow SiO_2 + CO + 3H_2$$

Parabolic oxidation → SiO_2 layer growth

and simultaneously

$$SiO_2 + 2H_2O \rightarrow Si(OH)_4$$

Linear volatilization → SiO_2 layer loss

$$\frac{dx}{dt} = \frac{k_p}{2x} - k_l$$

Paralinear kinetics

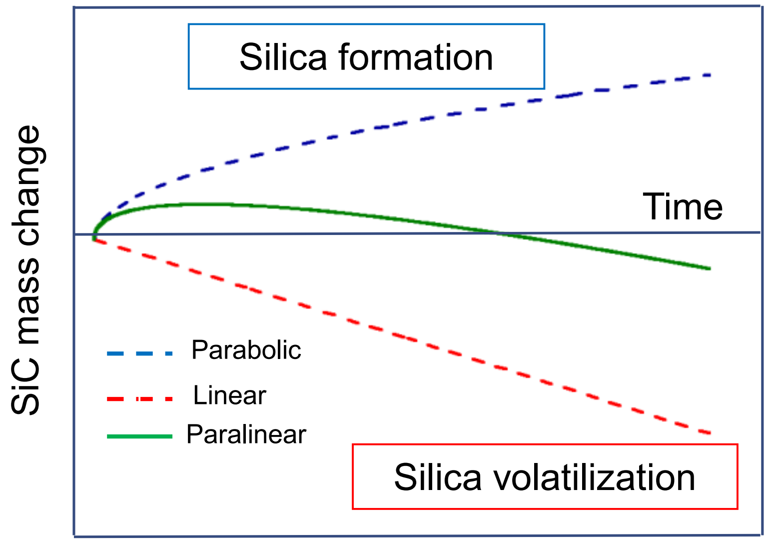

$T_{melt}(SiO_2) \approx 1725°C$

SiC_f/SiC cladding tube samples

- Samples were manufactured at the CEA Saclay
- Fiber: 3rd generation Hi-Nicalon Type S with excellent mechanical properties
- Texture: 2 layers of +/- 45° filament winding
- Matrix: Chemical vapor infiltration (CVI) with high purity and β-SiC microstructure
- Interphase: ≈100 nm of Pyrocarbon (PyC)
- Superficial bond coat: 50-100 µm monolithic CVI SiC
- Grinding of the inner and outer surfaces to reach final dimensions

HT oxidation in steam of SiC_f-SiC cladding

- Three samples provided by CEA with graphite core
  - 1 transient test
  - 2 identical isothermal tests at 1700°C with final quenching by water

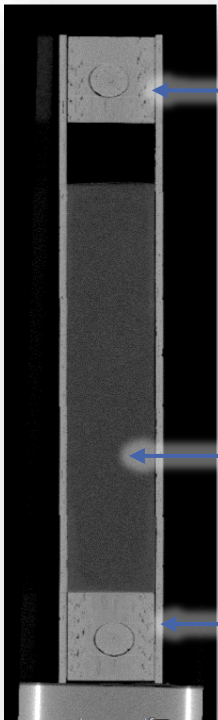

X-ray tomography image of sample

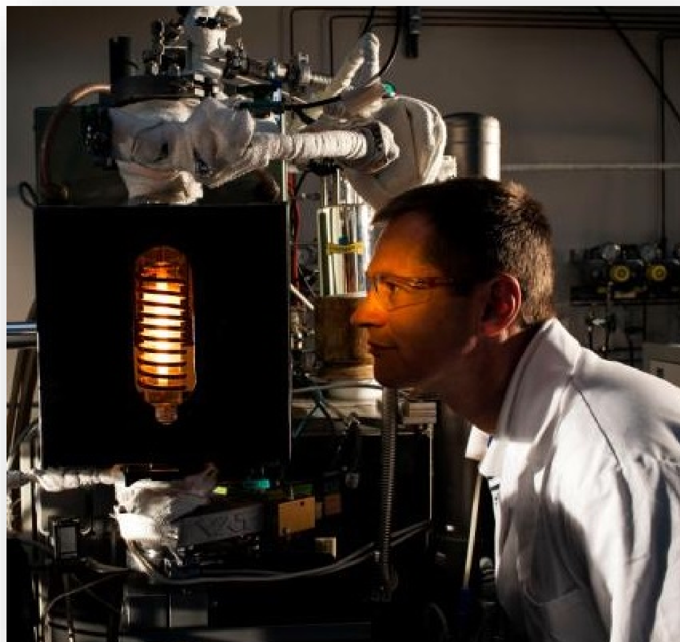

QUENCH-SR with inductive heating

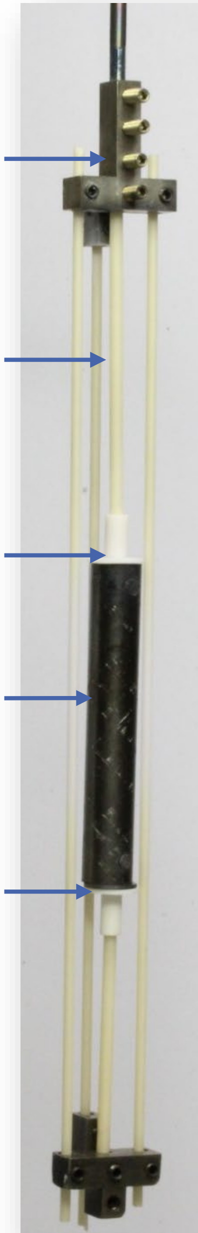

Modified sample holder

Transient test: Conduct and MS results

T_{ox} = 1400 → 1850°C, 10 K/min

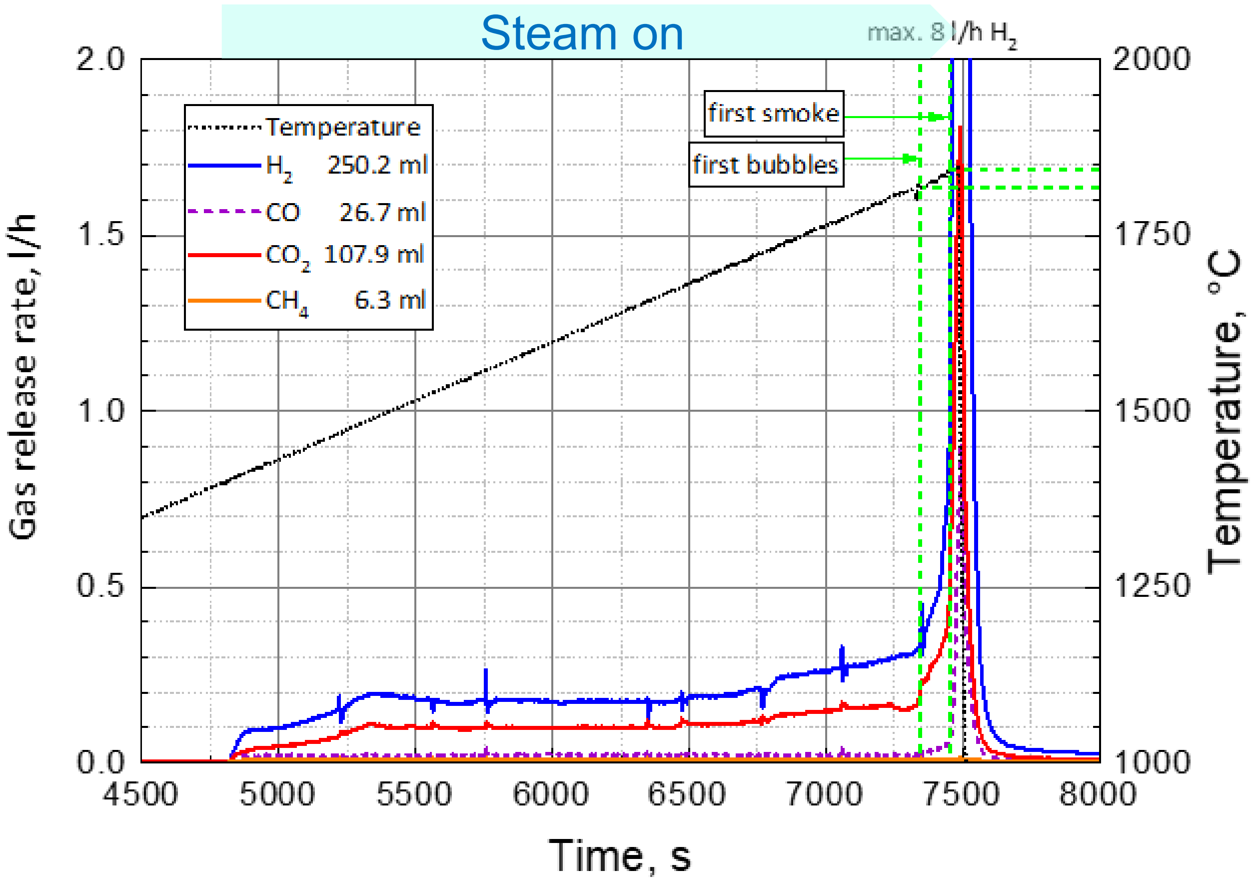

Video snapshot at 1845°C

- Low oxidation kinetics up to ca. 1750°C
- Bubble formation, strong gas release, SiO_x volatilization above ~1750°C

IAM Institute for Applied Materials

Transient test: Post-test appearance

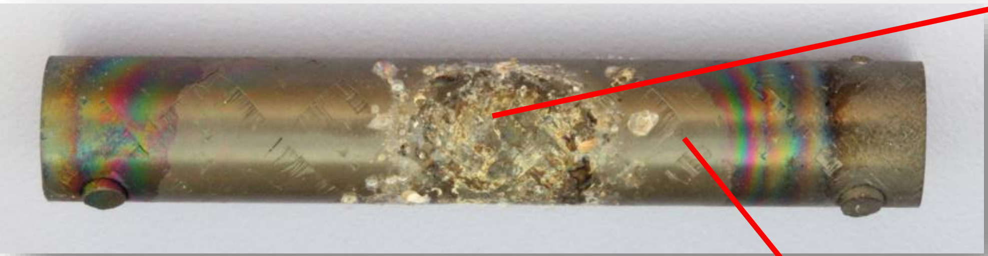

Sample after the transient test up to 1845°C

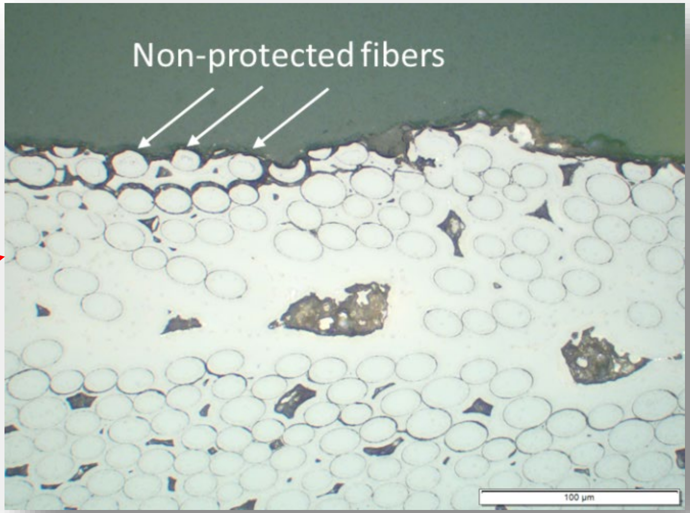

OM from the failure region

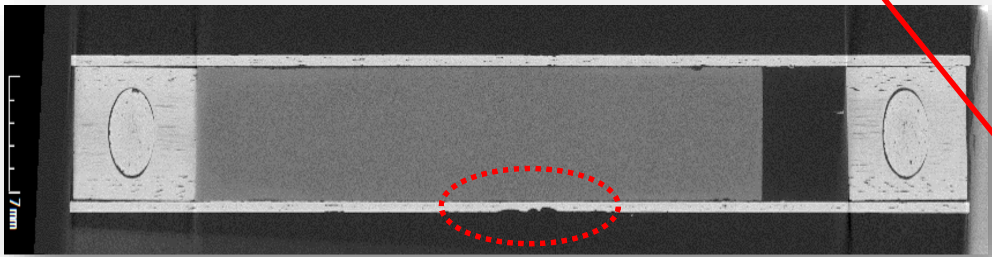

X-ray tomography, longitudinal cut

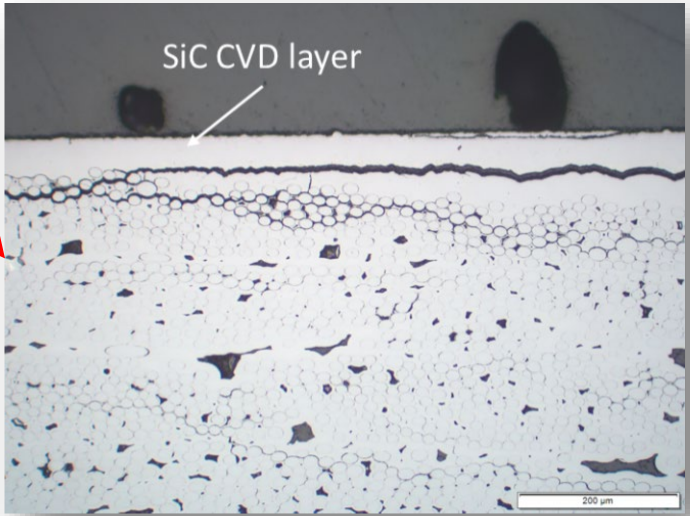

OM from the non-failure region

- Local failure of the CVI seal-coat above 1750°C and attack of SiC fibers

Isothermal test at 1700°C:
Gas release and post-test appearance

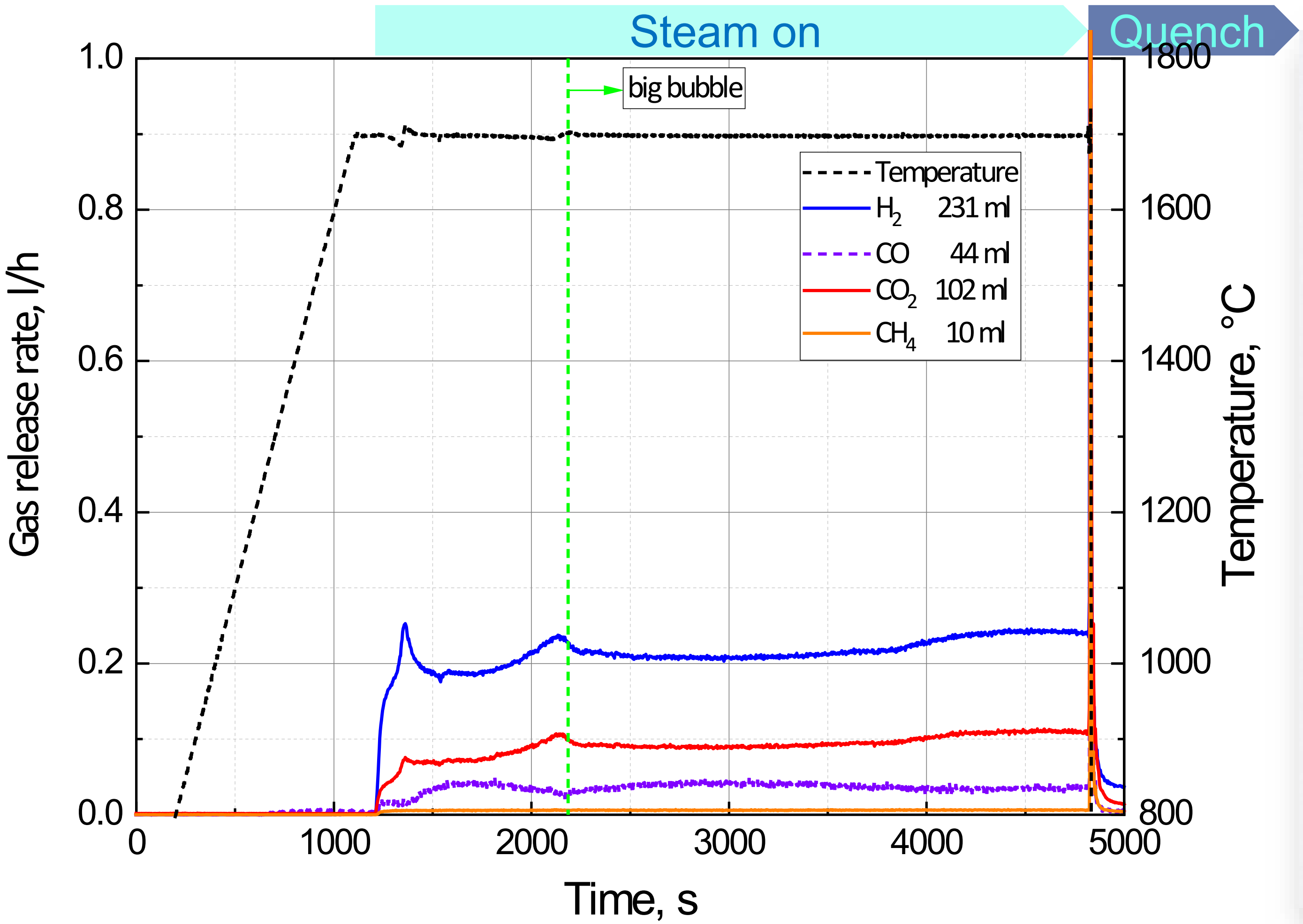

- Very limited oxidation of the SiC_f/SiC cladding at 1700°C

Quenching of SiC-02 by 95°C water after 1-hour isothermal oxidation in steam

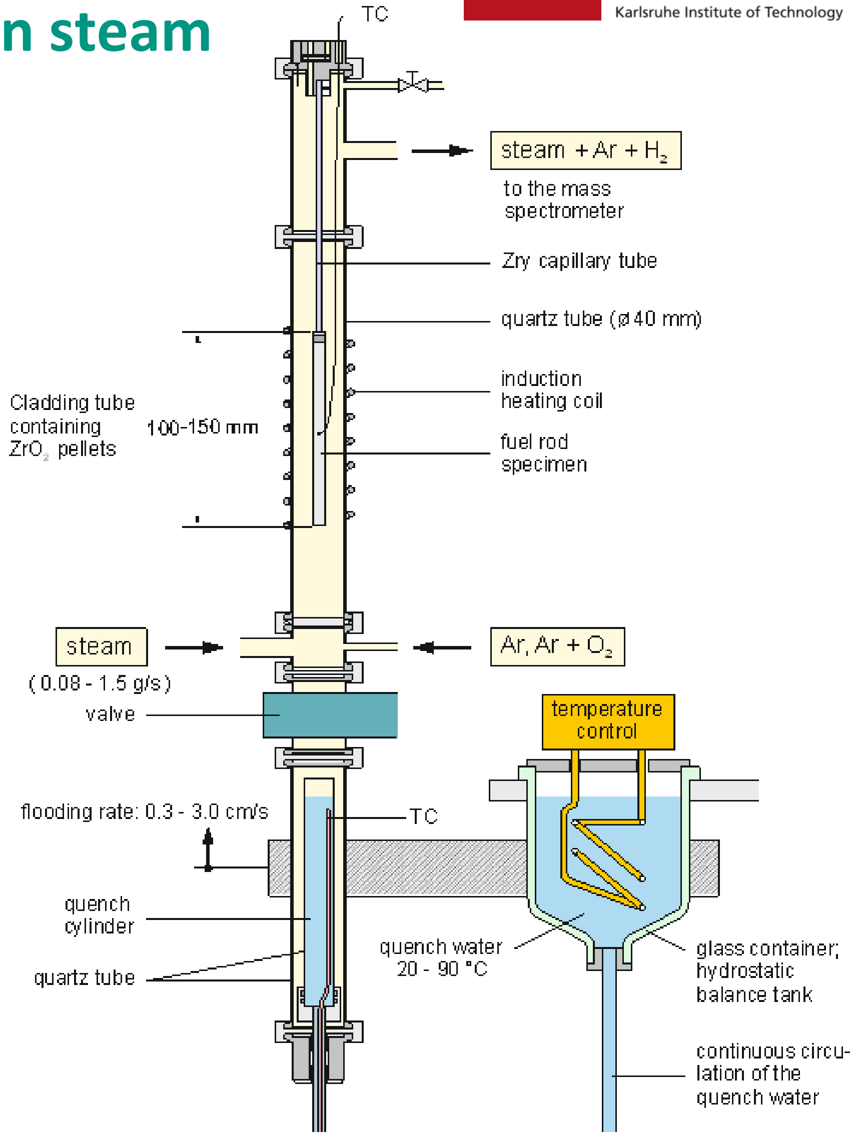

Isothermal test at 1700°C: OM of longitudinal cross section

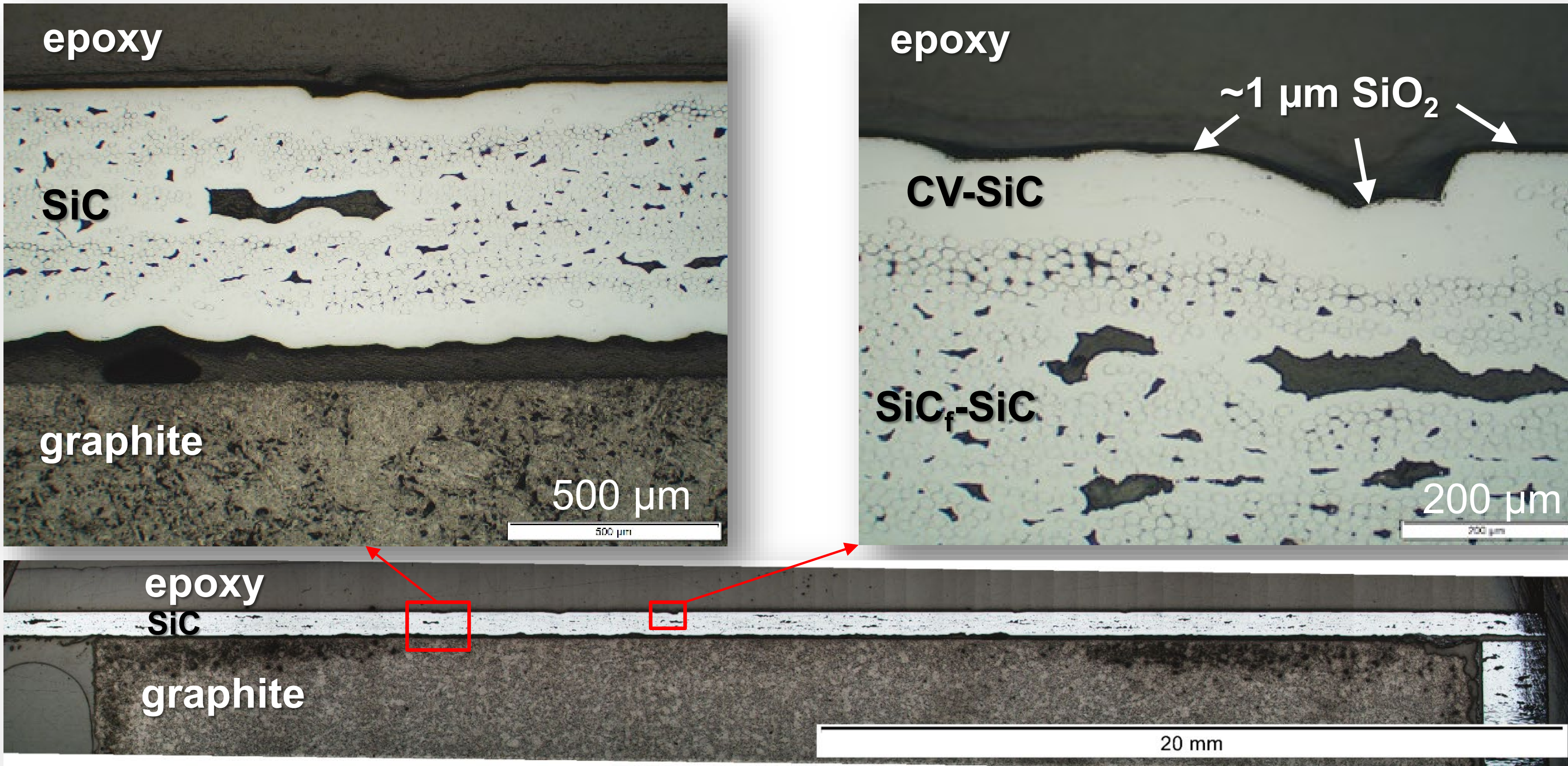

➡ External CVI seal-coat of SiC_f/SiC cladding kept intact

Isothermal test at 1700°C: Surface images by SEM

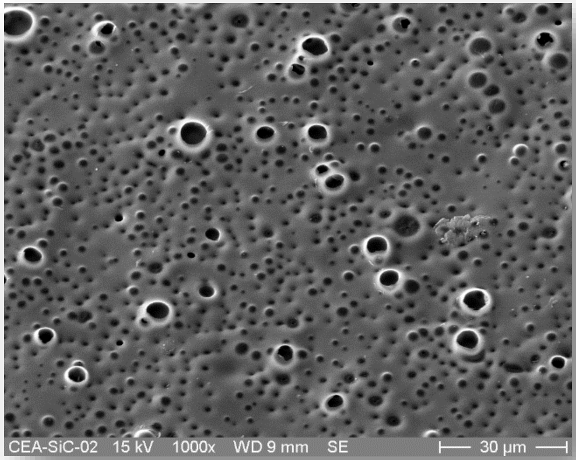

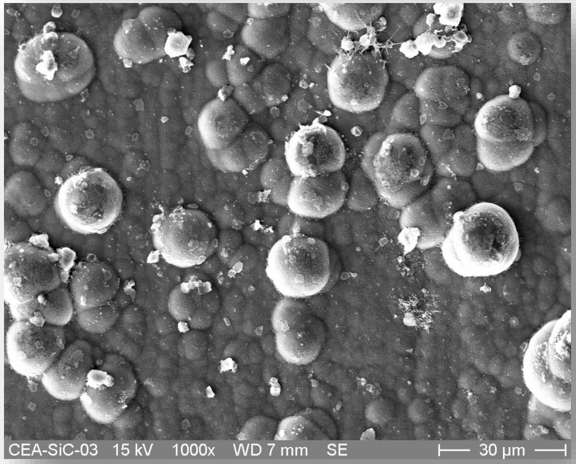

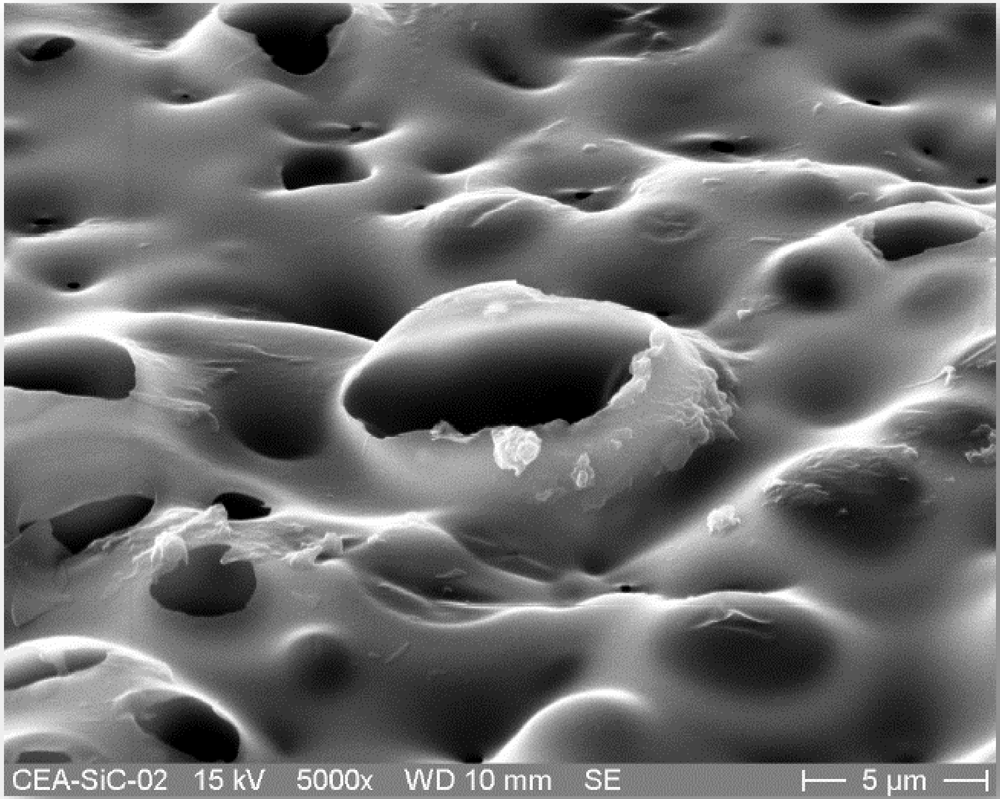

- Closed and burst small bubbles were locally observed

Residual tensile stress-strain behavior after 1-h oxidation at 1700°C and quench by 95°C water

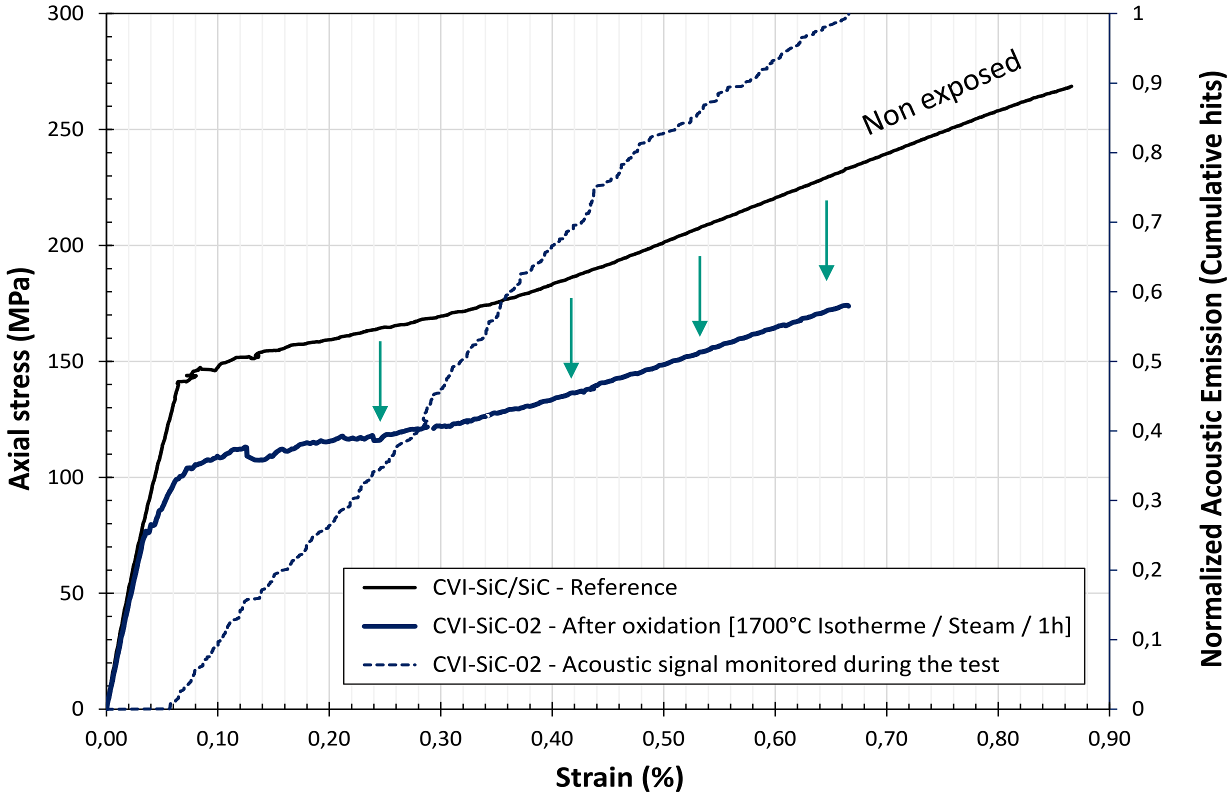

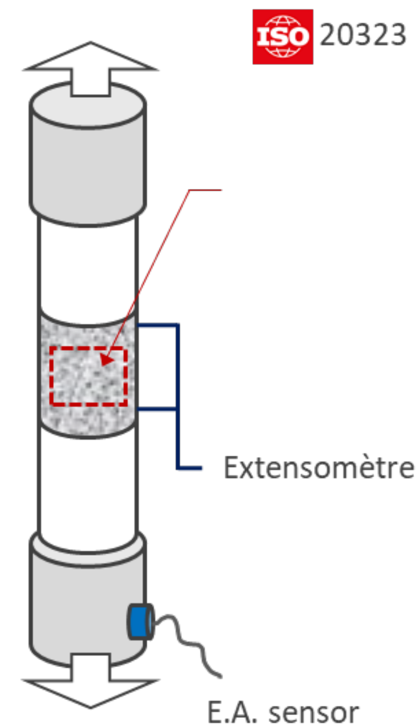

- Retention of mechanical strength with slight decrease in modulus
- Tensile strength reduction due to thermal degradation of SiC fibers at >1600°C
- No matrix micro-cracking saturation as seen in the acoustic emission curve

Fracture surface after tensile test

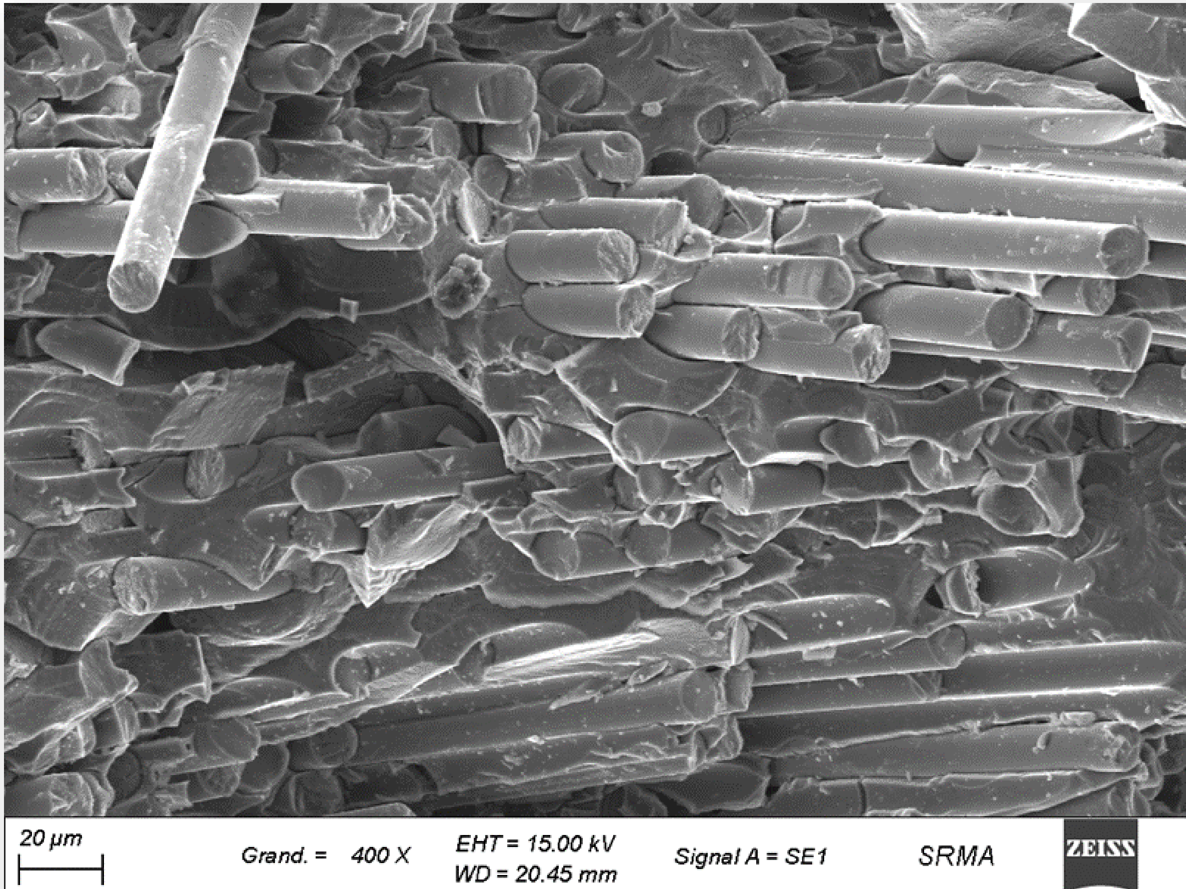

- Pull-out of non-oxidized fibers with high lengths
- Fiber-matrix composite with low interfacial shear strength remained intact after exposure to hard conditions

Conclusion

- Advanced nuclear grade SiC_f/SiC CMC cladding tube segments withstood exposure in steam and only slightly degraded at 1700°C and beyond.
- As long as the superficial CVI SiC bond-coat remains intact, the fiber-matrix composite retains its damage-tolerant behavior.
- Slight degradation of the mechanical properties due to the degradation of the fibers' strength beyond 1600°C.
- Strong degradation of the CMC cladding tube occurred only after failure of the superficial CVI SiC bond coat at T > 1750°C with strong oxidation of the PyC-coated fibers.

➔ This study confirms the excellent accident tolerance of SiC_f/SiC CMC cladding.

Acknowledgements

- This research has received funding from the Euratom Research and Training Programme 2014–2018 under grant agreement No. 740415 (H2020 IL TROVATORE).
- KIT: P. Severloh (ceramographic PTE) and A. Meier (X-ray tomography)
- CEA: E. Rouesne (SEM examinations) and S. Le Bras (mechanical tests)

- You for kind attention

Institute for Applied Materials

P. Červenka[a,b], J. Krejci[b], A. Chalupova[b], L. Cvrcek[a], P. Gávelová[c], M. Ševecek[b]

[a] UJP Prague

[b] CTU Prague

[c] RC Rez

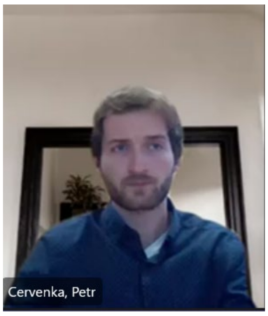

Mechanical properties degradation of Cr-coated cladding under the loss-of-coolant accident conditions

Development of nuclear fuels with enhanced accident tolerance is one of the main current objectives of researchers around the world. The contribution focuses on Cr-coated cladding concept developed in cooperation of UJP Praha a.s. and CTU in Prague. Presented results show highly protective behavior of thin Cr-layers against high temperature steam oxidation and improved mechanical ductility of samples after transients. A more complex approach to simulate LOCA transient is applied in presented study. A set of experiments was performed to understand with the behavior of Cr-coated claddings during the whole phenomena. The presented results show the influence of coatings on high-temperature creep, ballooning size, time to burst, cracking of coating, high temperature oxidation through cracked and intact coating. Secondary oxidation and hydriding from inner uncoated surface after cladding failure is discussed as well. Microhardness and microstructure analysis of the material after testing revealed local cladding damage. The mechanical properties of cladding after LOCA can locally deteriorate due to cracks in coating, but the influence on the bulk mechanical behavior of the whole fuel cladding needs to be further investigated.

Mechanical properties degradation of Cr-coated cladding under the loss-of-coolant accident conditions

Petr ČERVENKA [a, b], Jakub KREJČÍ [b], Adéla CHALUPOVÁ [b], Ladislav CVRČEK [a], Petra GÁVELOVÁ [c], Martin ŠEVEČEK [d]

[a] UJP Praha a.s., Nad Kamínkou 1345, 156 10, Prague - Zbraslav, Czech Republic

[b] Czech Technical University in Prague, Faculty of Mechanical Engineering, Department of Material Engineering, Karlovo náměstí 293/13, 120 00, Prague 2, Czech Republic

[c] Research Centre Řež s.r.o., Hlavní 130, Husinec - Řež, 250 68 Husinec, Czech Republic

[d] Czech Technical University in Prague, Faculty of Nuclear Sciences and Physical Engineering, Department of Nuclear Reactors, V Holešovickách 2, 180 00, Prague 8, Czech Republic

26th International QUENCH Workshop 08/12/2021

Outline

1. **Introduction – approaches to enhance the nuclear safety**
2. **Tested specimens**
3. **Experiments & results**
    1. HT steam oxidation -> WDS profiles
    2. Secondary hydriding after burst test
4. **Summary & future research work**

Introduction – approaches to enhance the nuclear safety

Context of the research

- 2011: Fukushima Daiichi nuclear disaster
- Development and testing of various **A**ccident **T**olerant **F**uels (**ATF**s)
- Most promising concept: Chromium coating of current cladding

Complication

- Coatings are brittle, can not withstand high plastic strain

What will be analyzed

- Material properties after simulated LB-LOCA accident with coating defects
- Separate effect experiments

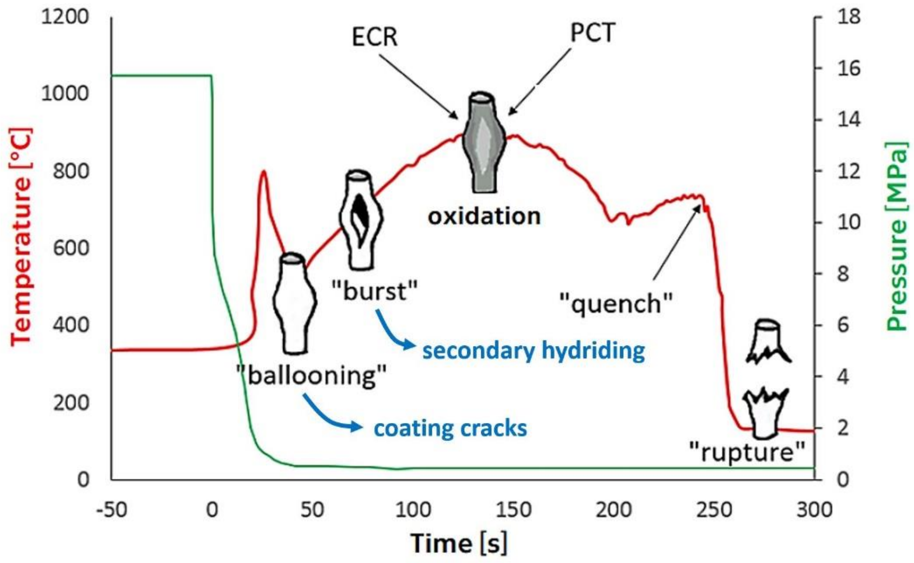

Already presented positive impact of the coating on:

- Hydrogen absorption
- Corrosion rate under normal operating conditions
- Balloning size
- Time to burst
- HT oxidation → reduced weight gain, mechanical properties (ductility, hardness etc…)

Tested specimens

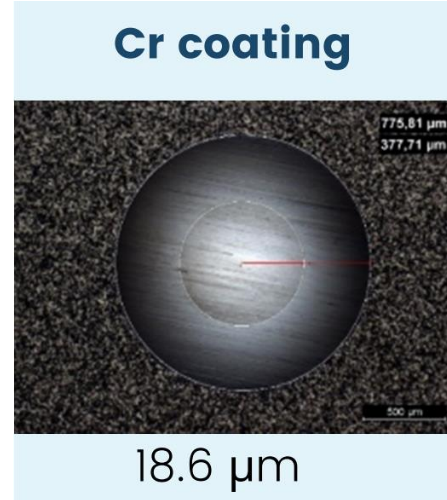

- Standard Zr-alloy, length 45 – 90 mm
- Cr coating, PVD method (Hauzer Flexicoat 850)
- Thickness 18,6 µm, Calotest method (CSM Instrument)

- **Two approaches to damage the protective Cr scale, followed by HT oxidation:**
  - ➢ **Scratch test** – single scratches made on the scratch test device (Revetest Xpress)
  - ➢ **Burst test** – ballooning process terminated after cladding failure

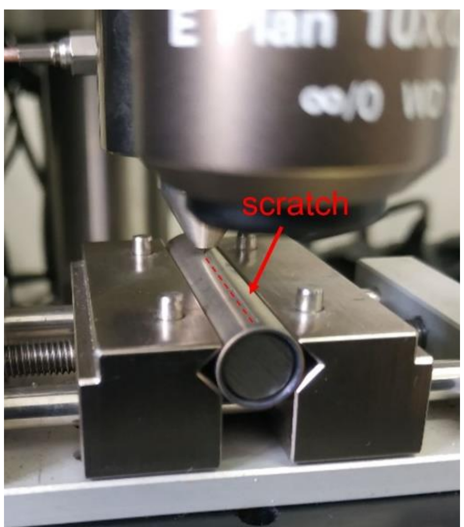

High-temperature steam oxidation

- **Testing device:** Electric resistant furnace
- **Parameters:** Temperature 1200 °C, atmospheric pressure, atmosphere Ar + steam mixture, quenching into iced water

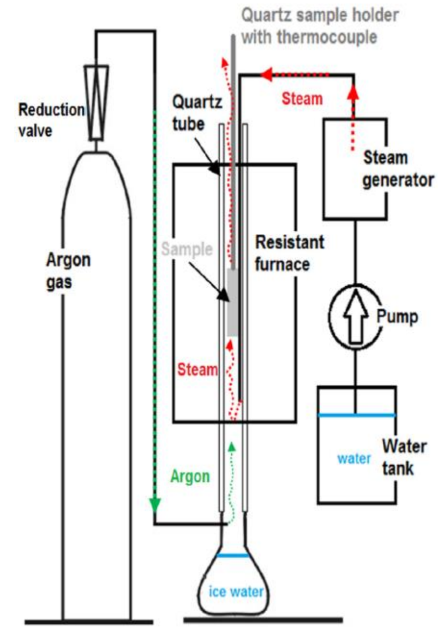

EXPERIMENT: HT steam oxidation (1200 °C; 4,5 – 9 min), specimens **after scratch test** (with damaged coating layer)

SCRATCH TEST

Detailed study of diffusive processes through the coating cracks → WDS profiles

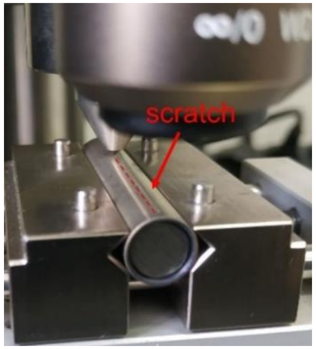

Results – scratch test WDS profiles

- No diffusion of Cr in the area directly below the coating crack
- WDS profile similar to the uncoated specimens

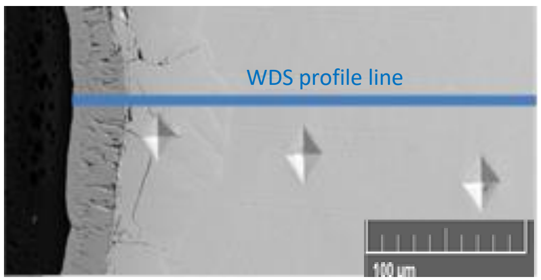

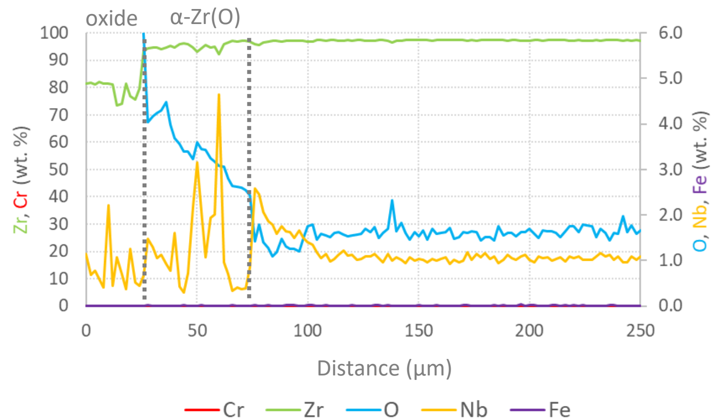

Cr-coated specimen
4,5 min oxidation

WDS line perpendicular to the coating in the area of the defect

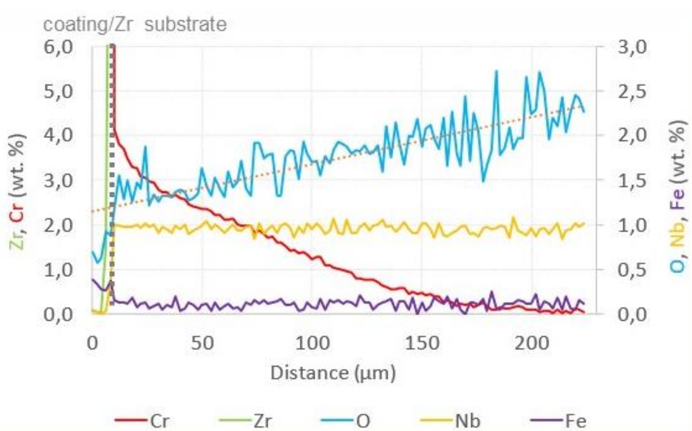

Cr-coated specimen
9 min oxidation

WDS line perpendicular to the coating

Existing studies on protectivity of chromium coating

- Positive impact of integral Cr scale even in case of longer oxidation times (9 min)
- Impermeable O diffusion barrier

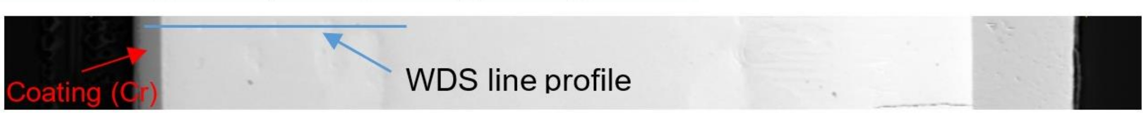

Results – scratch test WDS profiles

- Diffusion of Cr into Zr matrix -> Cr enriched, hence stabilized ß-Zr phase -> **accelerated diffusion kinetics of O (higher diffusion coefficient of O in ß-Zr)**
- The concentration of O is increased with any non-zero amount of Cr diffused, rapidly drops when the Cr concentration reaches zero

Stable concentration of O (increased)

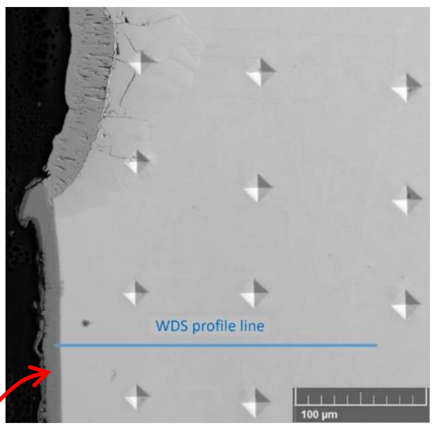

coating

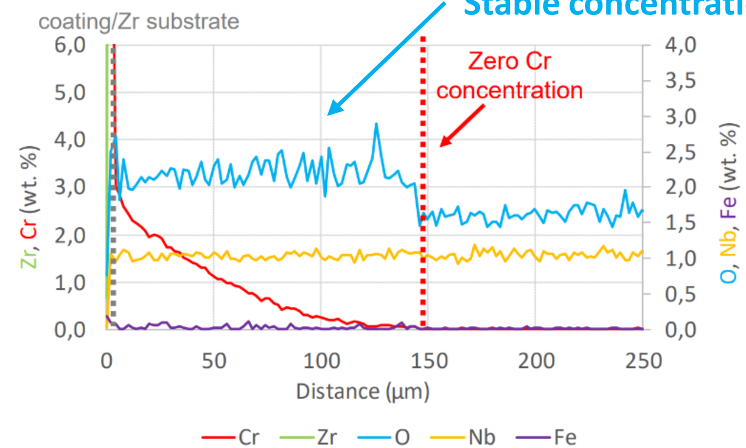

Cr-coated specimen
4,5 min oxidation
WDS line perpendicular to the coating

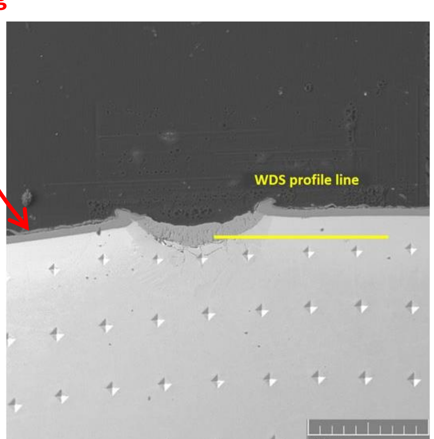

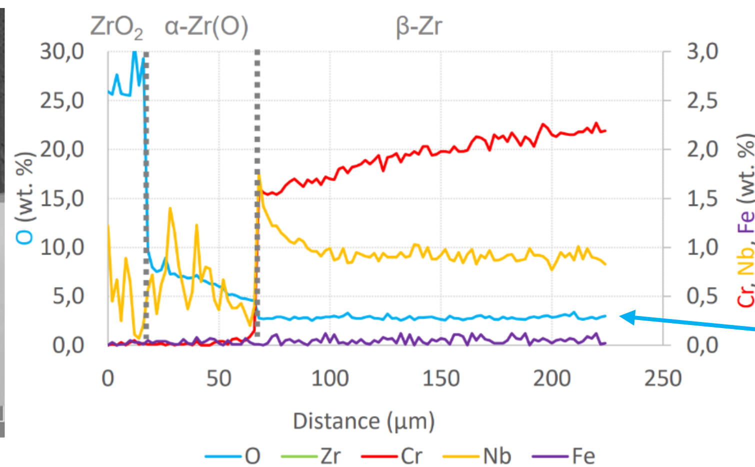

Cr-coated specimen
4,5 min oxidation
WDS line parallel to the coating

accelerated O diffusion observed

Stable concentration of O (increased)

Ballooning & burst test

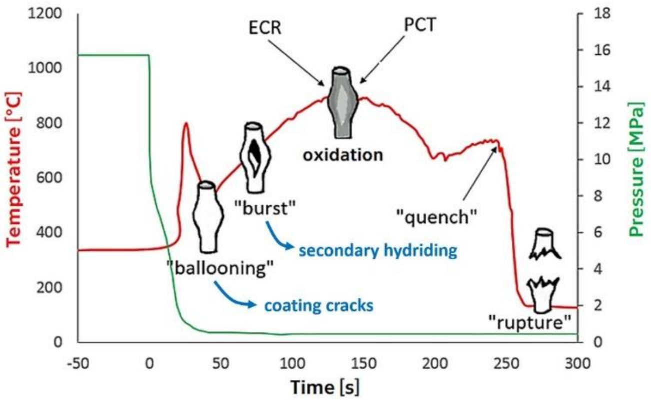

- **Testing device:** Resistance furnace
- **Parameters:** cladding failure temperature 899 °C, argon atmosphere, inner pressure 4 MPa, ramp speed 7 °C/s (from 360 °C), temperature recorded by K thermocouples

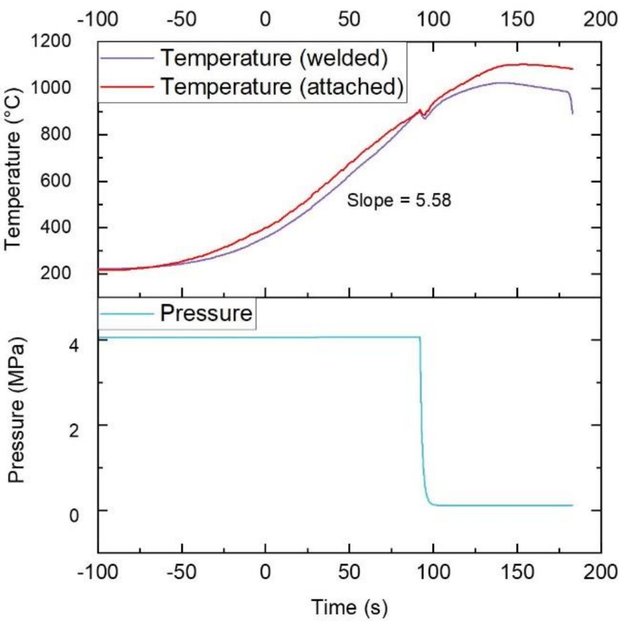

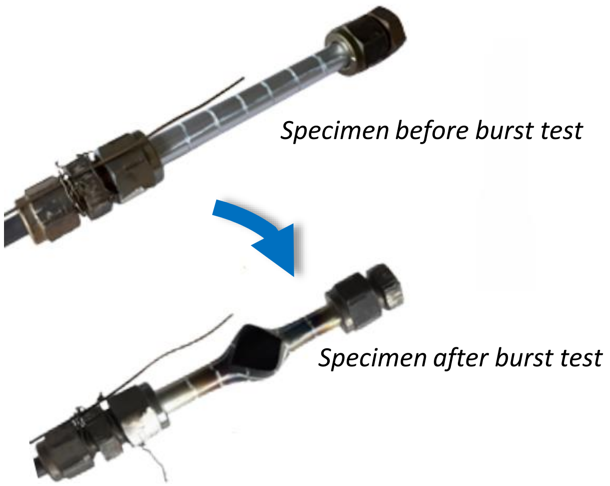

Secondary hydriding after burst test

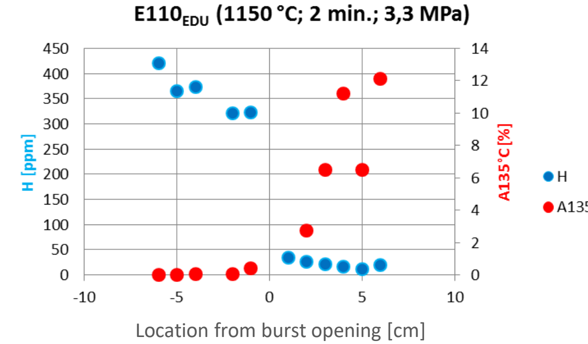

- High hydrogen content may cause cladding embrittlement
- Schematic illustrations of secondary hydriding upon HT steam oxidation after burst:

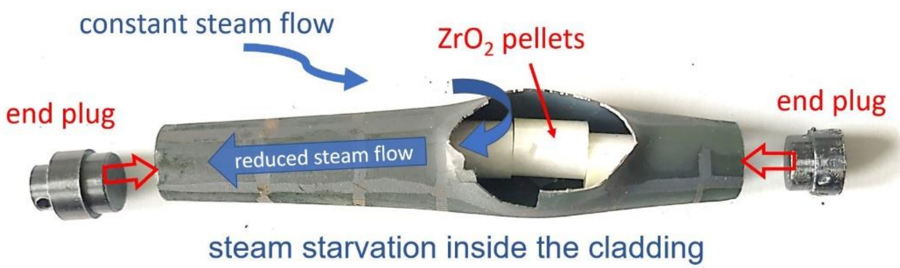

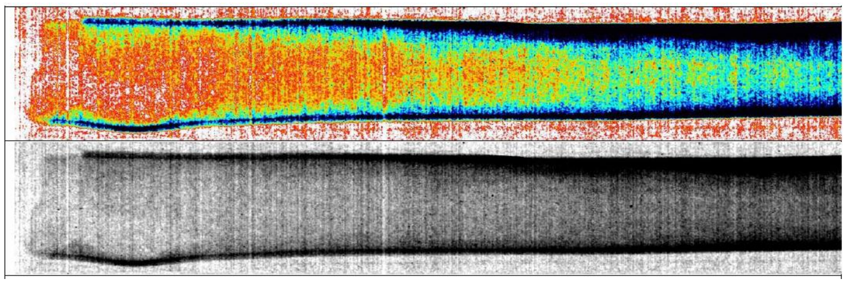

EXPERIMENT: HT steam oxidation (1200 °C, 5 min) after burst, cladding filled with ZrO_2 pellets impeding the steam flow inside the cladding

Results – secondary hydriding
Metallography, H content

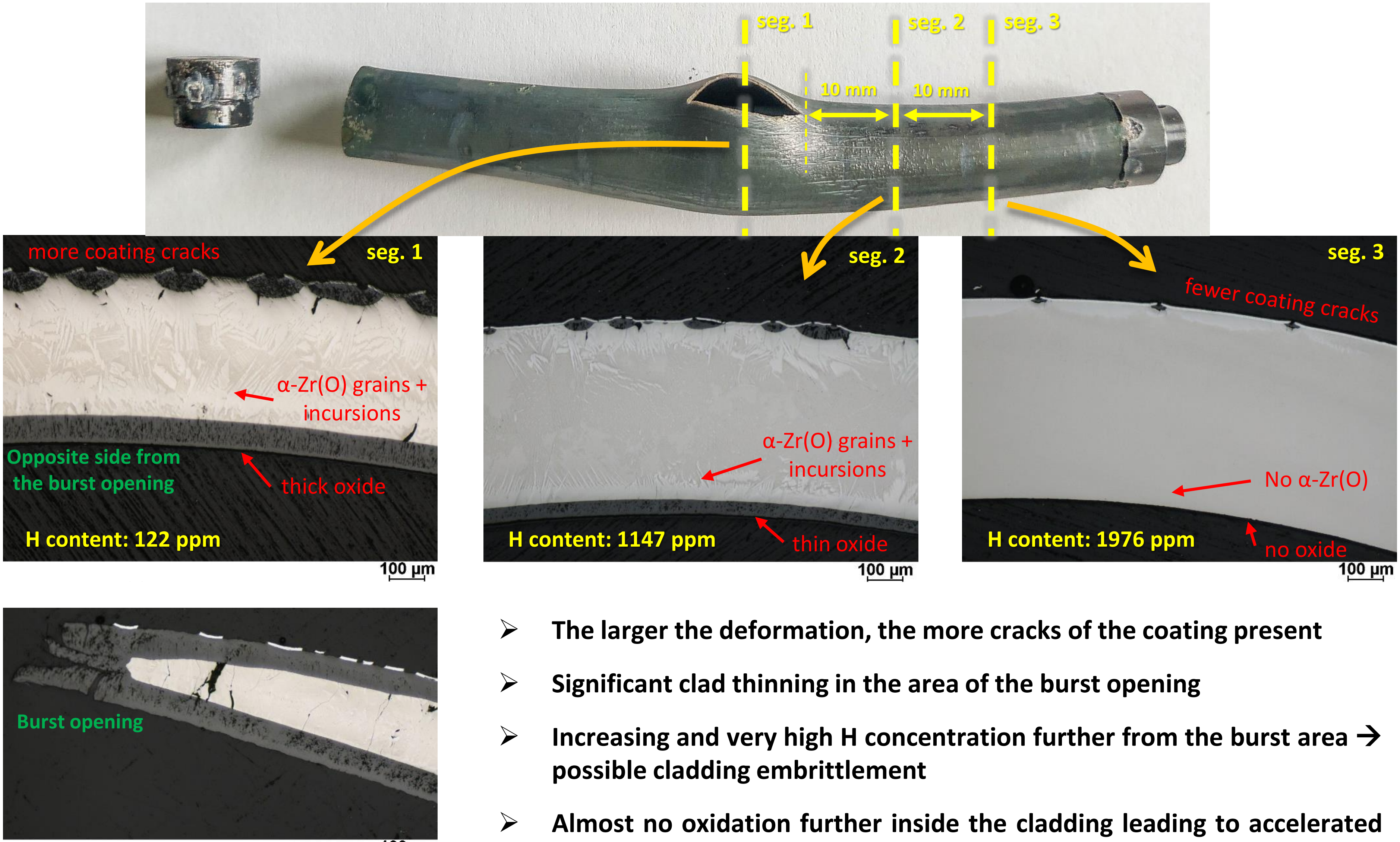

- The larger the deformation, the more cracks of the coating present
- Significant clad thinning in the area of the burst opening
- Increasing and very high H concentration further from the burst area → possible cladding embrittlement
- Almost no oxidation further inside the cladding leading to accelerated hydrogen pickup

Summary & conclusion

Separate effect experiments were performed:

- ✓ **HT steam oxidation after scratch test** – diffusion of Cr into Zr matrix → Cr stabilizing β-Zr phase, accelerated diffusion kinetics of O
- ✓ **Ballooning + burst test** → the larger the deformation, the more cracks in the Cr scale
- ✓ **Secondary hydriding** → hydrided zone in the inner cladding (H content ~2000 wppm)

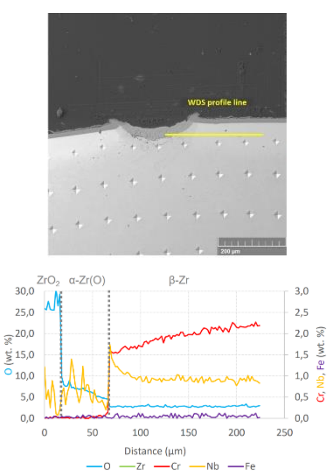

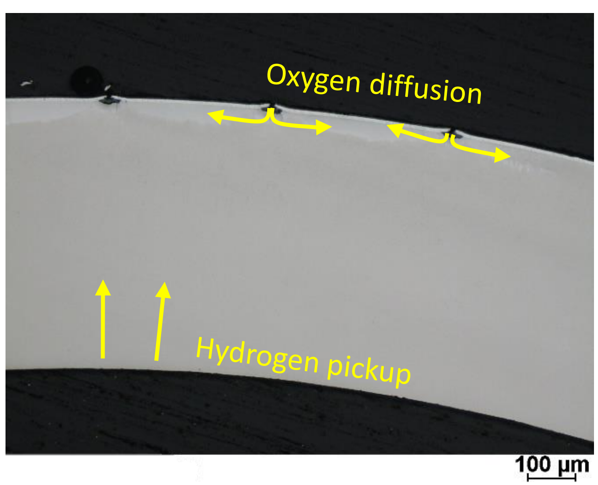

- ➢ **Increased O content even in areas so far believed to be protected by Cr coating**
- ➢ **All these phenomena must be taken into account → new methodology suitable for coated cladding**

Future work

Semi-integral test – the complex evaluation of all possible causes of cladding failure in one experiment:

- ❑ Ballooning + burst
- ❑ High-temperature steam oxidation + secondary hydriding
- ❑ Axial load

Acknowledgements

The authors wish to thank the whole Zirconium Alloys Team at UJP PRAHA a.s. for sample preparation and post-experimental analyses.

Special thanks to P. Halodová and P. Gávelová (Research Centre Řež s.r.o.) for performing the SEM analysis, Martin Ševeček (CTU in Prague) for neutron radiography images and Ladislav Cvrček (CTU in Prague) for chromium coating deposition.

Financial support of this research through ČEZ a.s. company is gratefully acknowledged. Also, this work was supported by the Institutional Support by Ministry of Industry and Trade, Technology Agency of the Czech Republic grant No. TK03020169.

QUESTIONS & DISCUSSION

Petr Červenka

p.cervenka@fs.cvut.cz

Czech Technical University in Prague, Faculty of Mechanical Engineering, Department of Material Engineering, Karlovo náměstí 293/13, 120 00, Prague, Czech Republic

UJP Praha a.s., Nad Kamínkou 1345, 156 10, Prague - Zbraslav, Czech Republic

P. Doyle, J. Harp, A. Nelson

ORNL

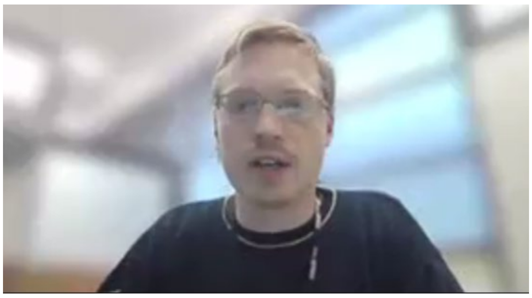

Microstructural Analysis of Iron-Chromium-Aluminum Samples Exposed to LOCA-Type Conditions Followed by Quench

The QUENCH-19 experiment was performed to examine the behavior of FeCrAl-alloy B136Y3 as a potential nuclear fuel cladding under accident conditions. The test involved heating a rod bundle in Ar/steam followed by a rapid liquid water quench. The rod bundle, consisting of W-heaters surrounded by zirconia cylinders and then sheathed with cladding, achieved a peak temperature of just over 1,400°C at the hottest locations.

Post-test characterization revealed that the exterior of the FeCrAl formed a thin layer of aluminum oxide that protected most of the underlying cladding and surrogate fuel rods. However, a few rods were heavily corroded with a few rods being entirely destroyed at a few elevations. This behavior was attributed to deleterious interactions between the FeCrAl and the thermocouple sheaths, followed by extensive interaction, and to FeCrAl/ZrO2 interactions. Absent these effects, it is suggested that FeCrAl's performance may be acceptable under these conditions.

Microstructural Analysis of Iron-Chromium-Aluminum Samples Exposed to LOCA-Type Conditions Followed by Quench

Peter Doyle
Jason Harp
Andrew Nelson

26th International QUENCH Workshop

Acknowledgements:
- Juri Stuckert
- Martin Steinbrueck
- Mirco Grosse
- Kurt Terrani

Introduction

- Since 1998, QUENCH tests have been performed at KIT in Germany to determine the effects of rapid quenching on surrogate fuel rods during a simulated LOCA quench test (M. Steinbrück, et al., Synopsis and outcome of the QUENCH experimental program, Nucl. Eng. Des. 240 (2010) 1714–1727)
- Typical setup involves heating to temperature, pre-oxidizing the rods, rapidly heating the system to simulate an accident, and then rapidly quenching with water.
- These tests investigated behavior of Zr-based rods determining:
  - Hydrogen generation
  - Impact of control rods (B_4C or AgInCd)
  - Effect of air ingress during quench
  - Effect of changing composition of rods

State-of-the art FeCrAl alloys show excellent oxidation behavior up to 1400℃

K. Lipkina, et al., A study of the oxidation behaviour of FeCrAl-ODS in air and steam environments up to 1400 °C, J. Nucl. Mater. 541 (2020) 152305.

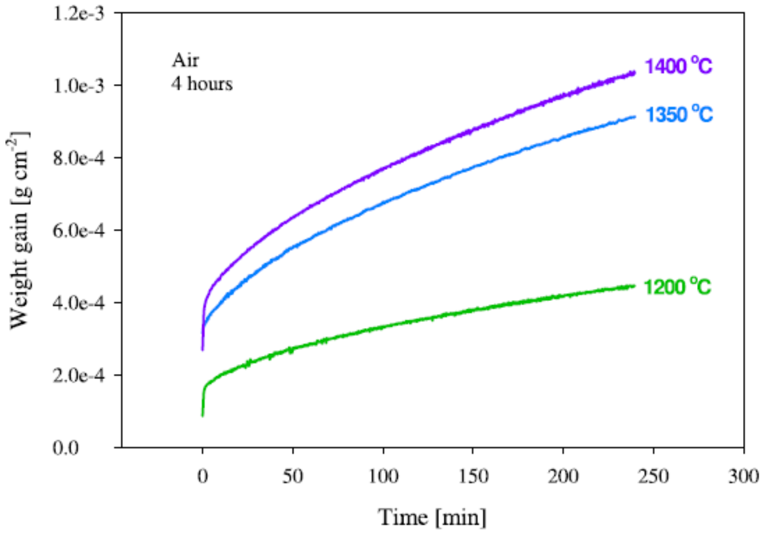

(a) Oxidation in air

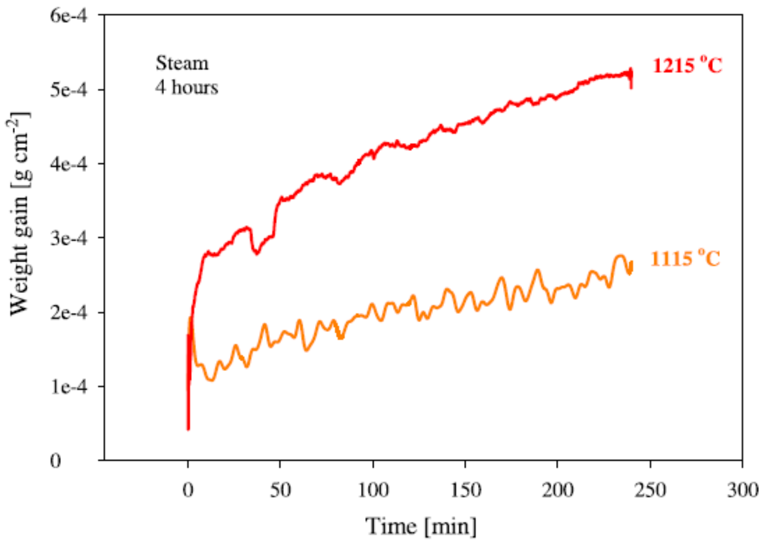

(b) Oxidation in steam

S. Dryepondt, et al., Development of low-Cr ODS FeCrAl alloys for accident-tolerant fuel cladding, J. Nucl. Mater. 501 (2018) 59–71.

Weight Gain After Exposure (mg/cm^2)

	Air	Steam	
Alloy	1400°C, 4hr	1400°C, 4hr	1450°C, 5min
125YT	0. 3	>100	>100
125YZ	0. 69	0. 71	>100
125YF	3. 24	1. 51	>100
PM2KP	NA	1. 02	>100
PM2K_SG	1.66	1. 23, >100	NA
PM2K_LG	NA	1. 19	4h, 3.14

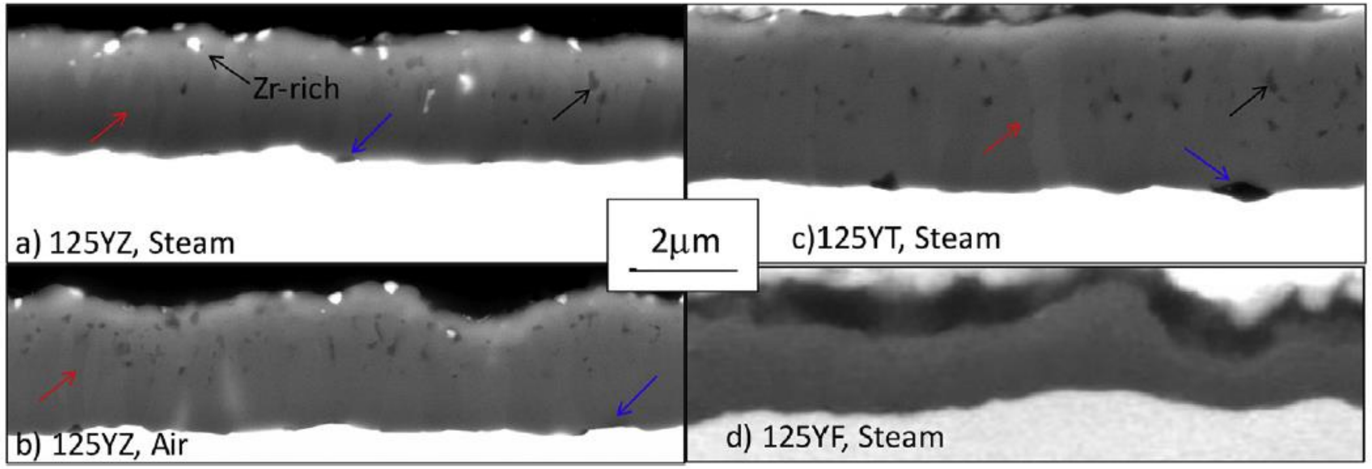

Under both normal operation and accident conditions, FeCrAl alloys demonstrate excellent corrosion behavior

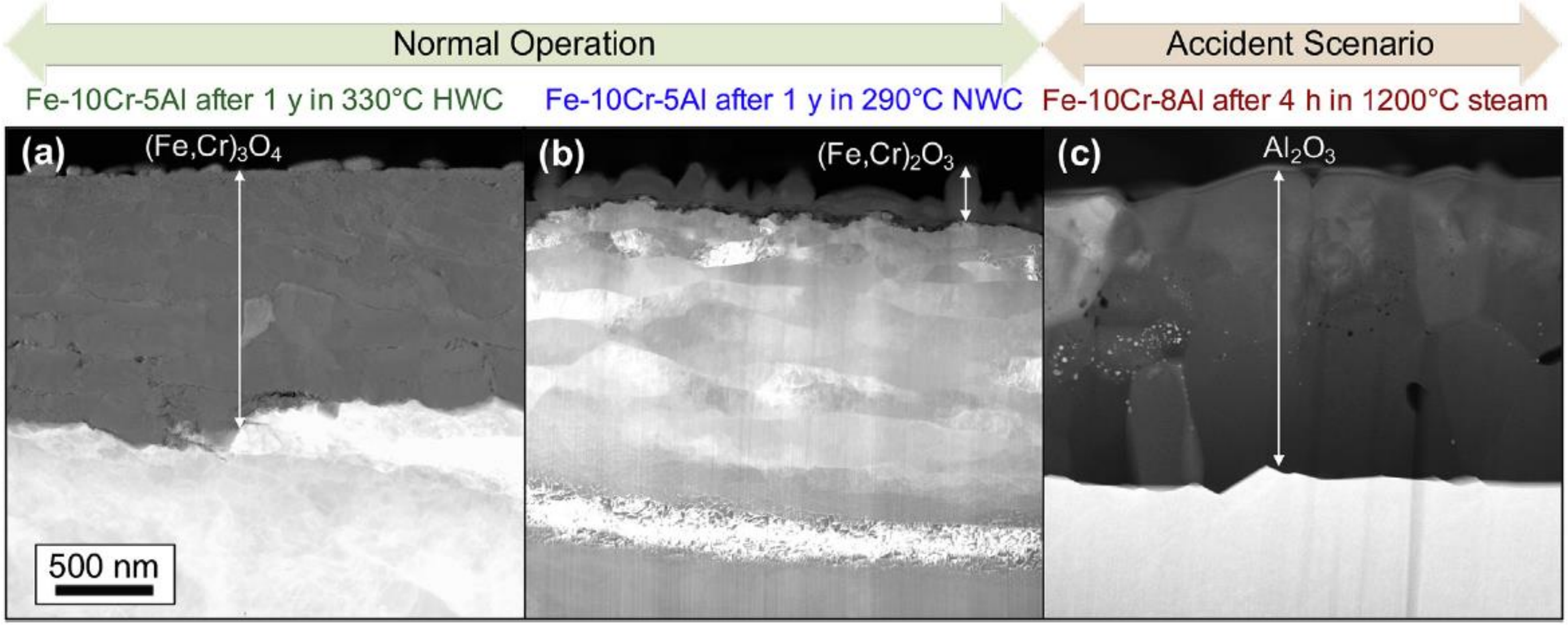

K.A. Terrani, Accident tolerant fuel cladding development: Promise, status, and challenges, J. Nucl. Mater. 501 (2018) 13–30.

Previous QUENCH tests have shown significant QUENCH-induced zircaloy failures

- Objective: determine the impact of LOCA followed by rapid quench on FeCrAl rods (B136Y3)

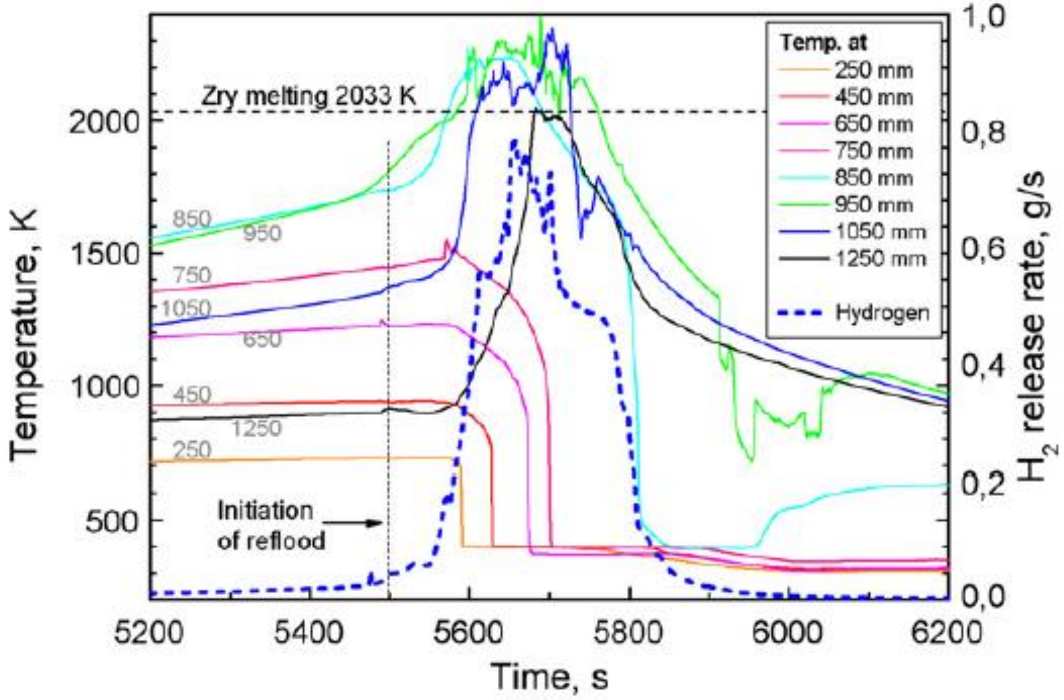

M. Steinbrück, et al., Synopsis and outcome of the QUENCH experimental program, Nucl. Eng. Des. 240 (2010) 1714–1727

Setup of the QUENCH Test

- Designed to be similar to QUENCH-15
  - Flowing steam/Ar mix through bundle of 24 surrogate fuel rods, followed by rapid water quench
  - Rods composed of W heater core, ZrO_2 ring, FeCrAl (B136Y) outer tube
  - 7 FeCrAl (Kanthal) rods were inserted on the outside of the bundle for instrumentation
  - Shroud also made of Kanthal
  - Thermocouples attached at different elevations (Attachments shown on the right. Elevations values are distance from the start of the W-heated section)
- Heating conducted in three stages:
  - 6000s pre-oxidation
  - 1130s rapid transient
  - 2000s hold (not present in Q15)

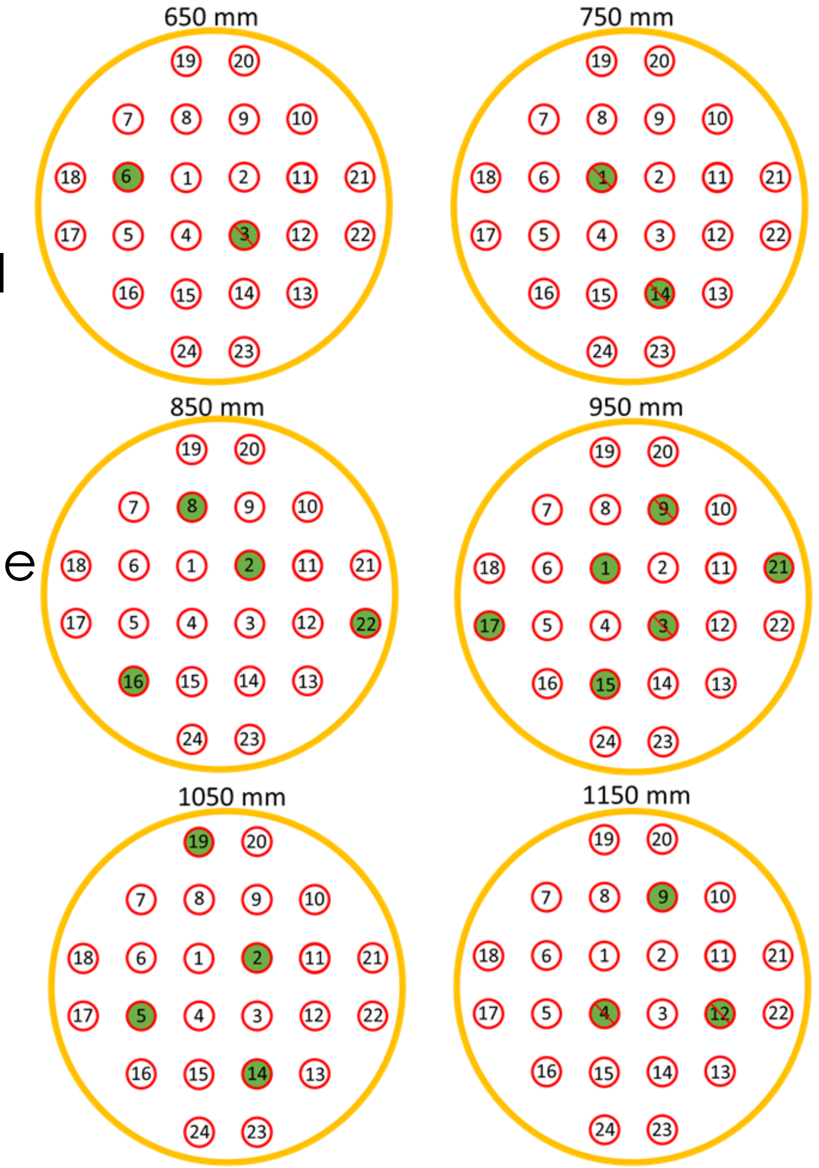

FeCrAl Material Compositions	
Kanthal	$Fe_{bal}Cr_{22}Al_{5.8}Si_{0.7}Mn_{0.4}C_{0.08}$
B136Y3	$Fe_{bal}Cr_{13}Al_{6.2}Y_{0.03}C_{0.01}$

Temperature Profiles Show a maximum temperature of ~1450 ℃

- Rods 17-24 are external (E)
- Rods 5-15 are middle (M)
- Rods 1-4 are internal (I)

- Maximum temperature is on the internal rod section at 850 mm
- Several thermocouples failed before the end of the test, especially at higher elevation
- Rods in similar radial locations at the same elevation did not necessarily have similar temperatures

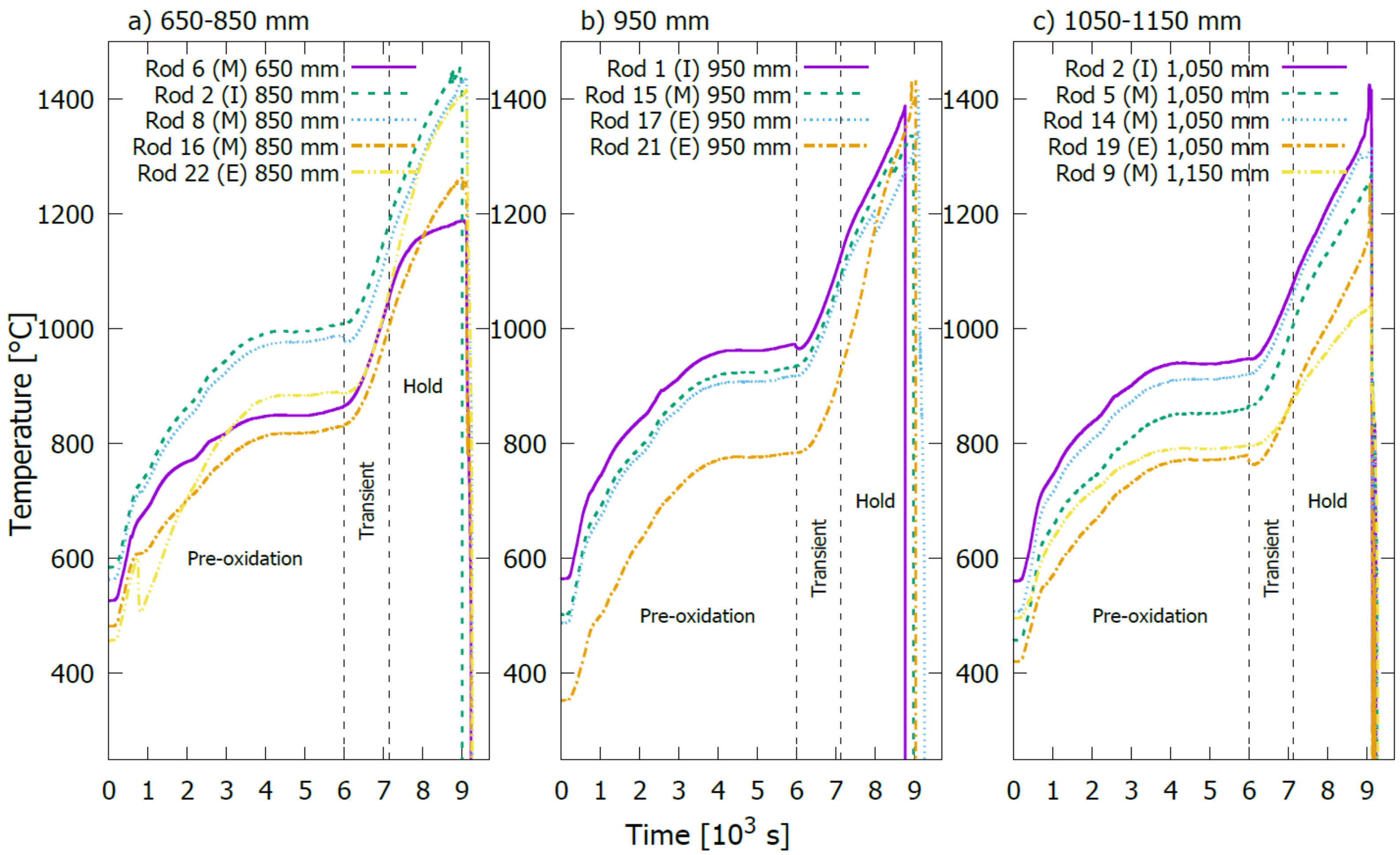

Microscopy of internal rods shows significant elevation dependence

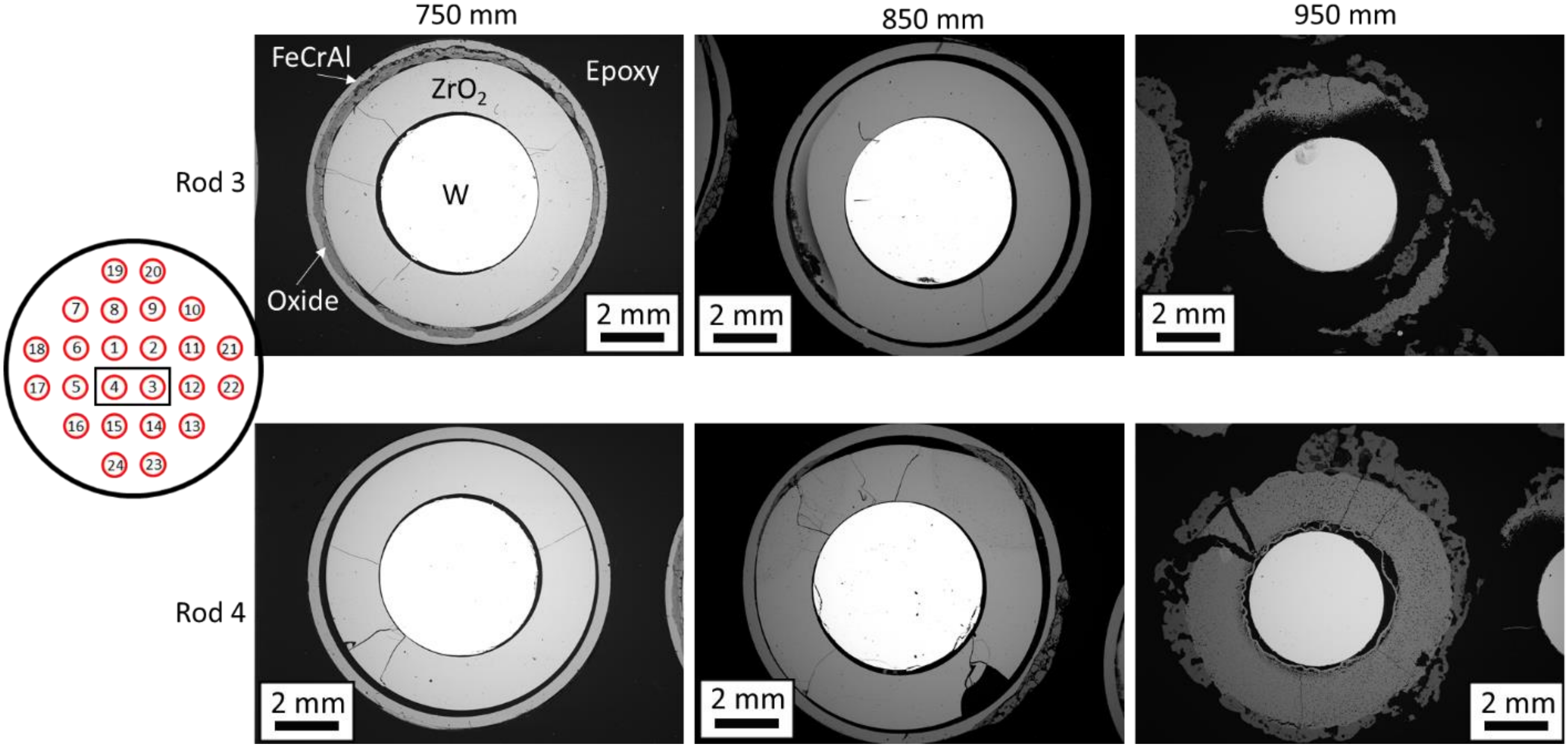

Internal oxidation was accompanied by diffusion of FeCrAl components into ZrO_2

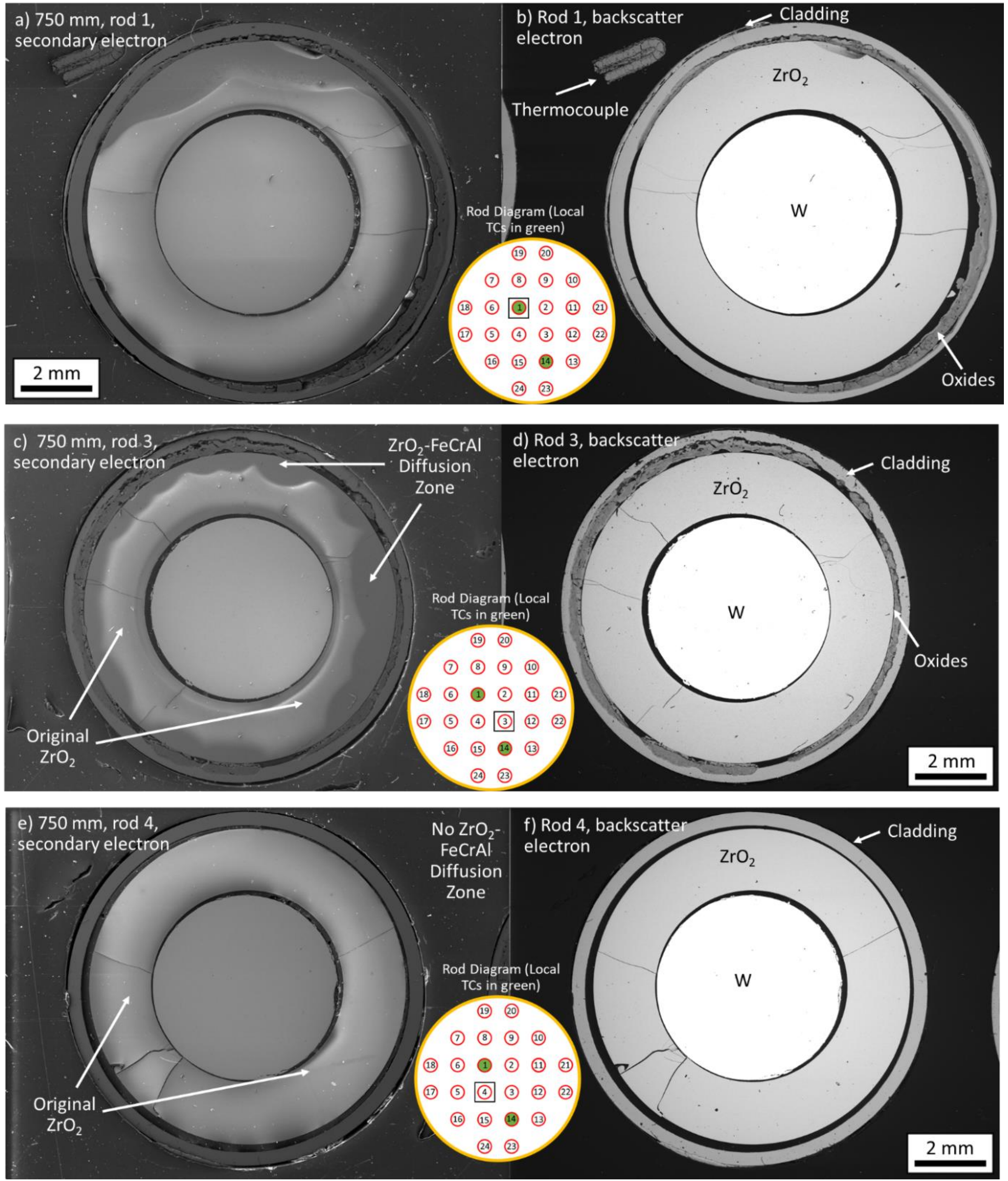

OAK RIDGE National Laboratory

Internal oxidation was accompanied by diffusion of FeCrAl components into ZrO_2; thin external oxide formed

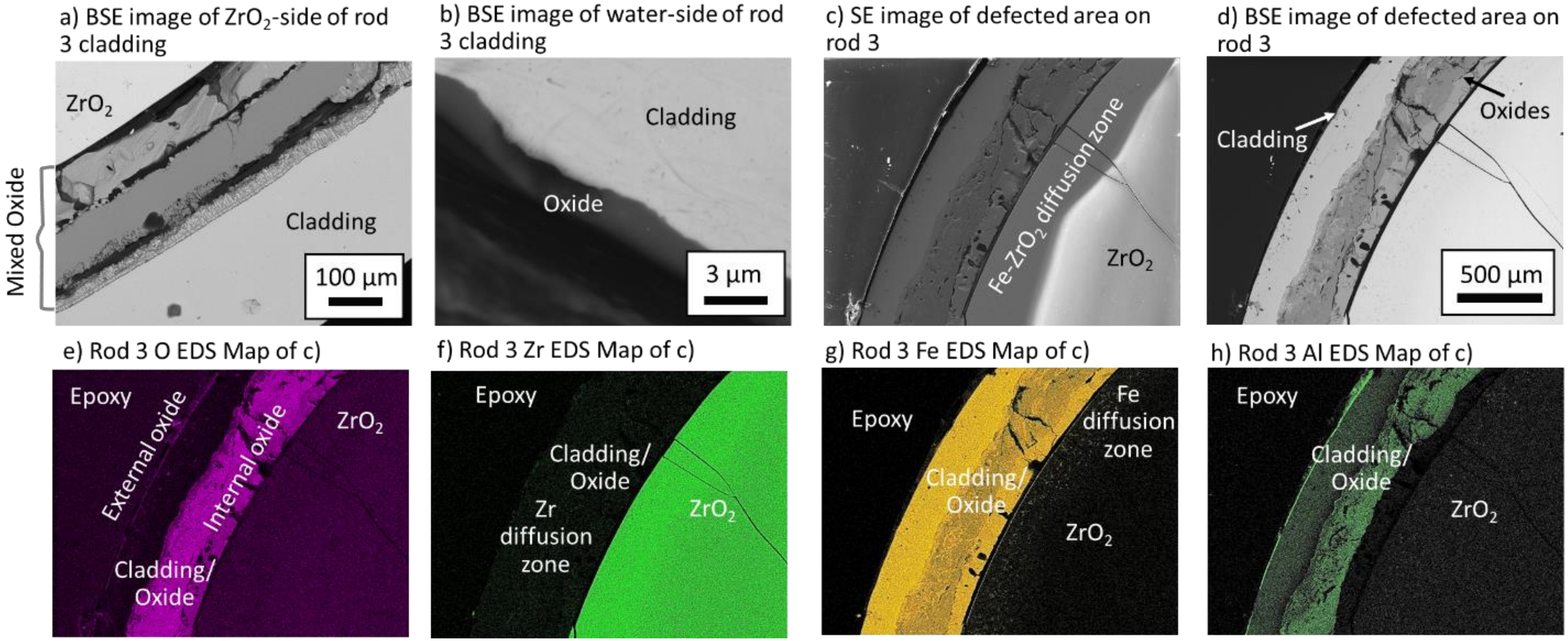

Internal rods were inconsistently damaged at 850mm, based on thermocouple location

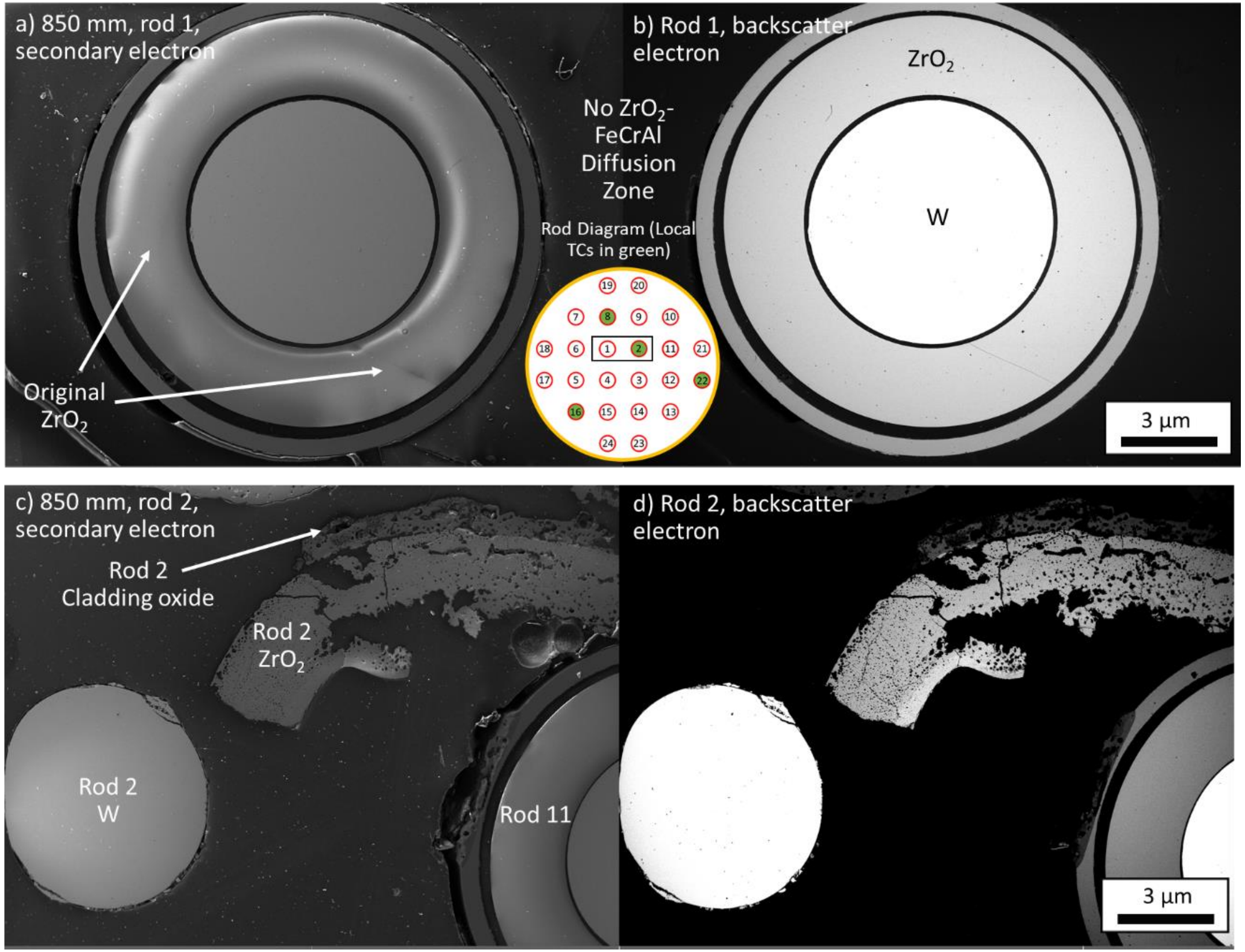

OAK RIDGE National Laboratory

On internal pins at 950mm, significant diffusion was observed at 950mm between cladding and ZrO_2

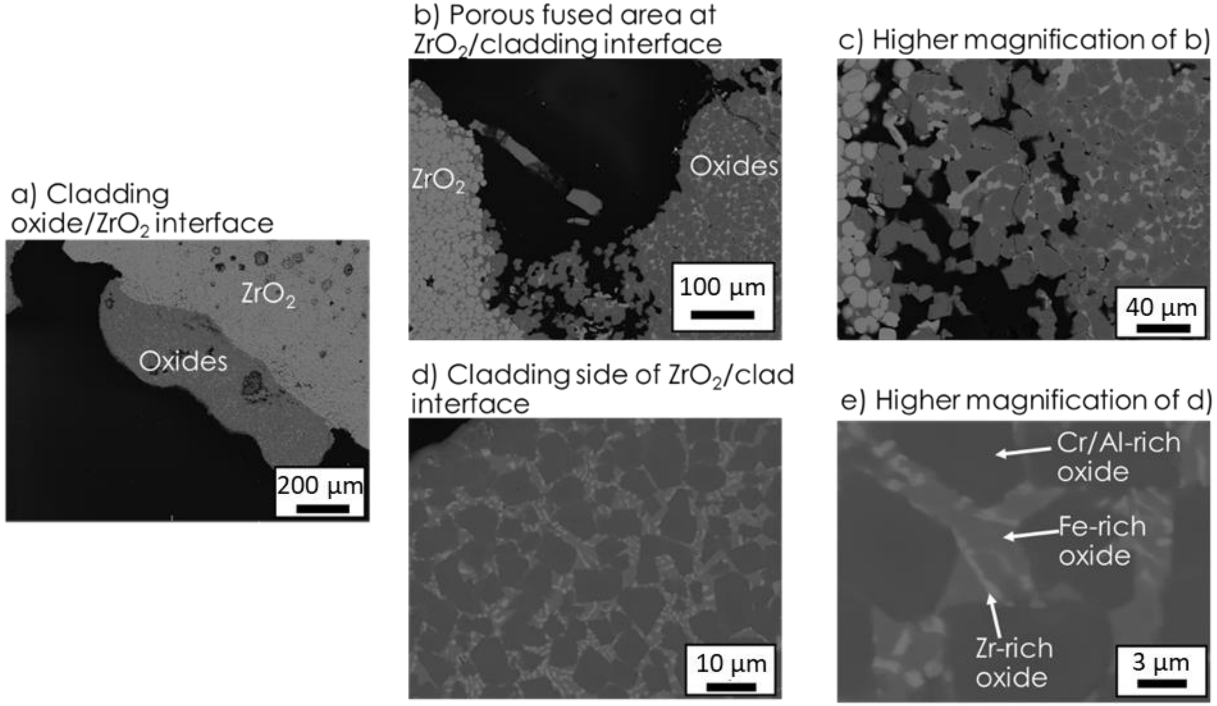

BSE Images of ZrO_2/FeCrAl interface on rod 1 at 950mm elevation. Oxides are mixed together in both ZrO_2 and FeCrAl oxide

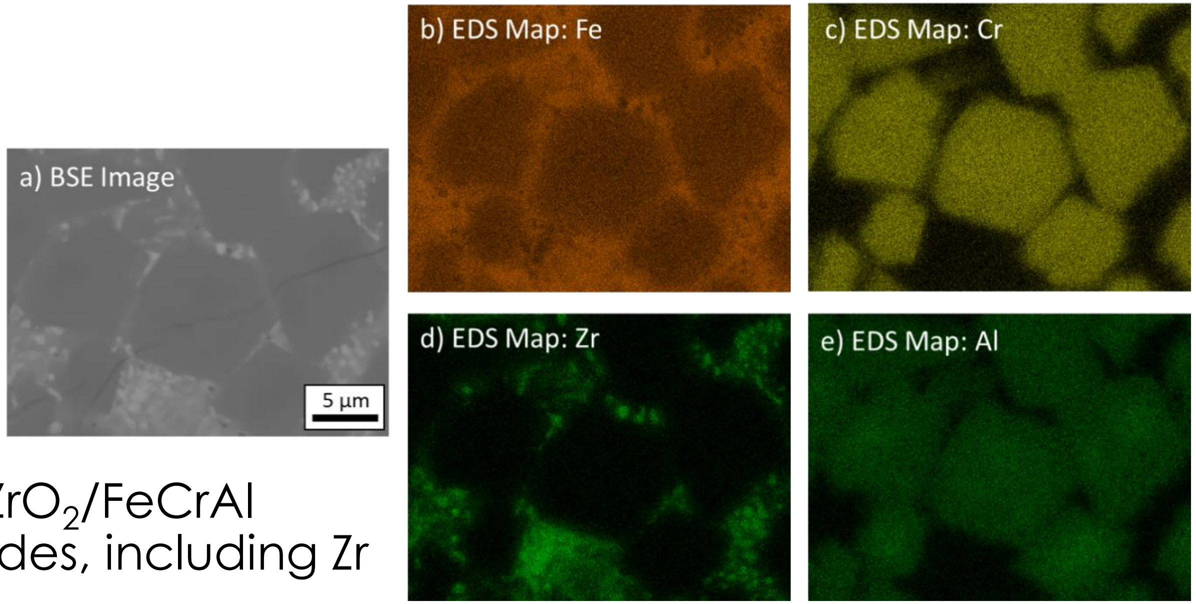

EDS maps of FeCrAl-side of ZrO_2/FeCrAl interface showing mixed oxides, including Zr

Middle rods showed strong correlation between thermocouple sheaths and cladding attack. Away from thermocouples, cladding remained intact.

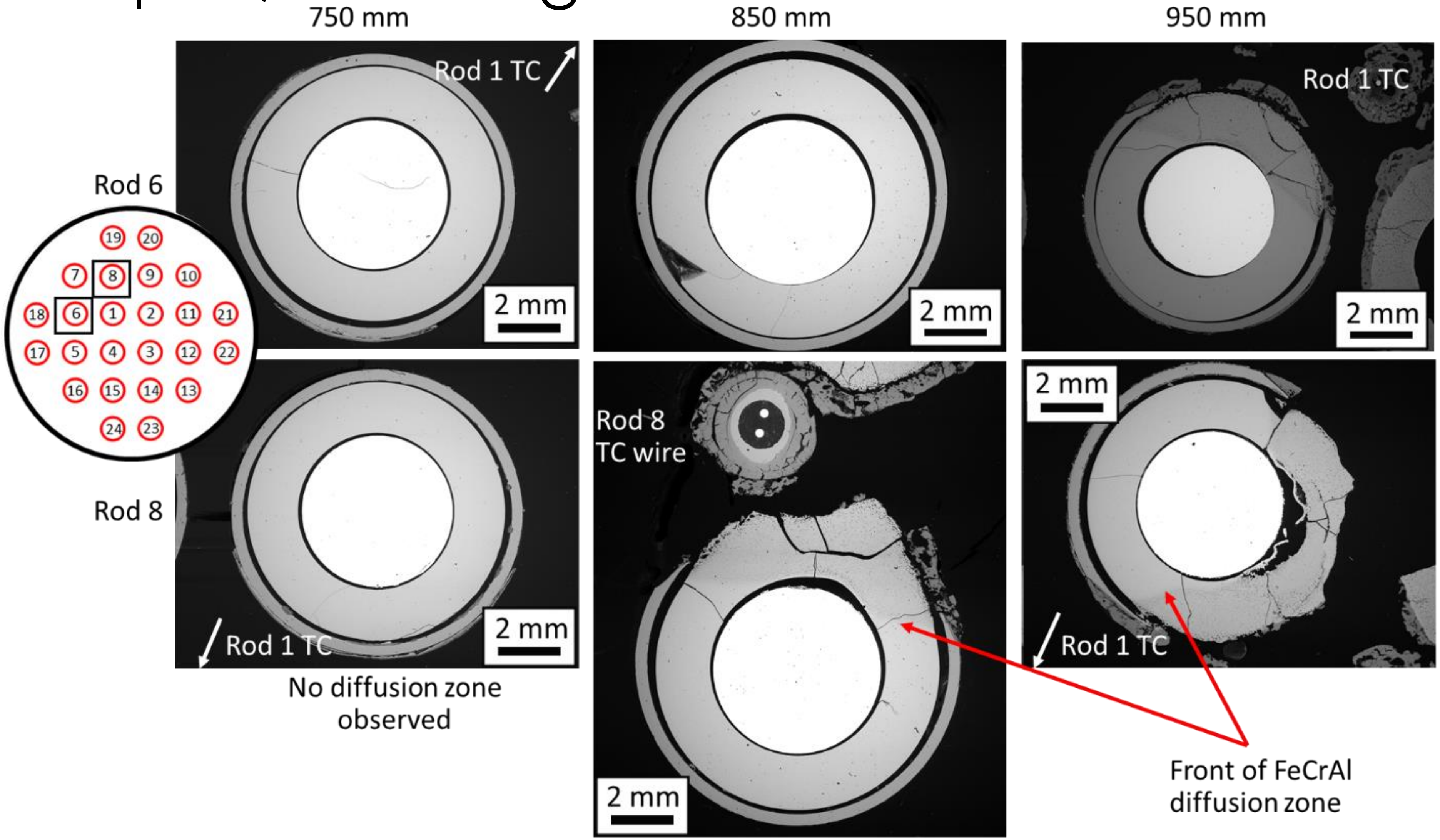

At 750 mm, all external rods were fully intact

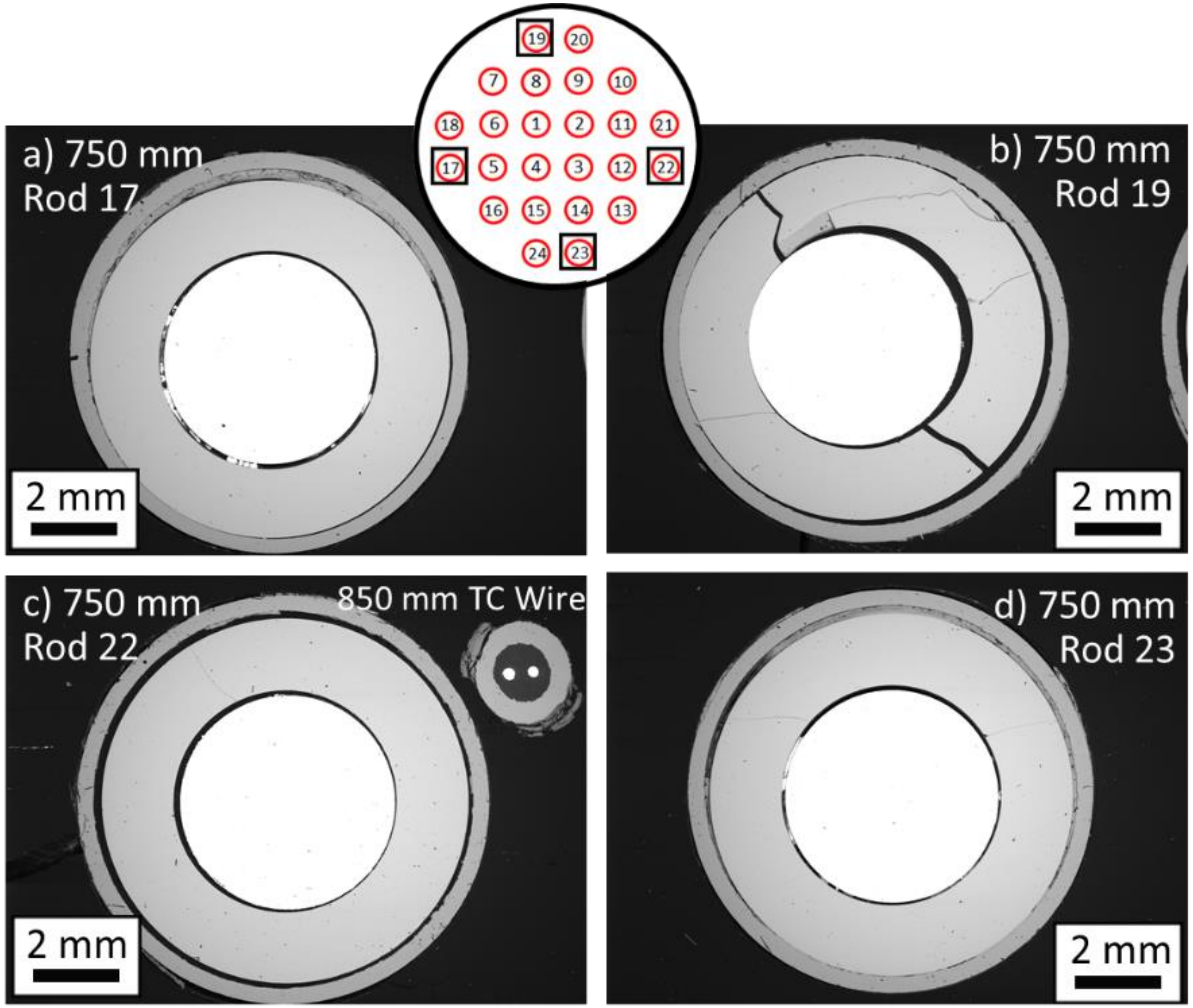

Oak Ridge National Laboratory

External rods showed strong correlation between thermocouple sheaths and cladding attack. Away from thermocouples, cladding remained intact.

850 mm

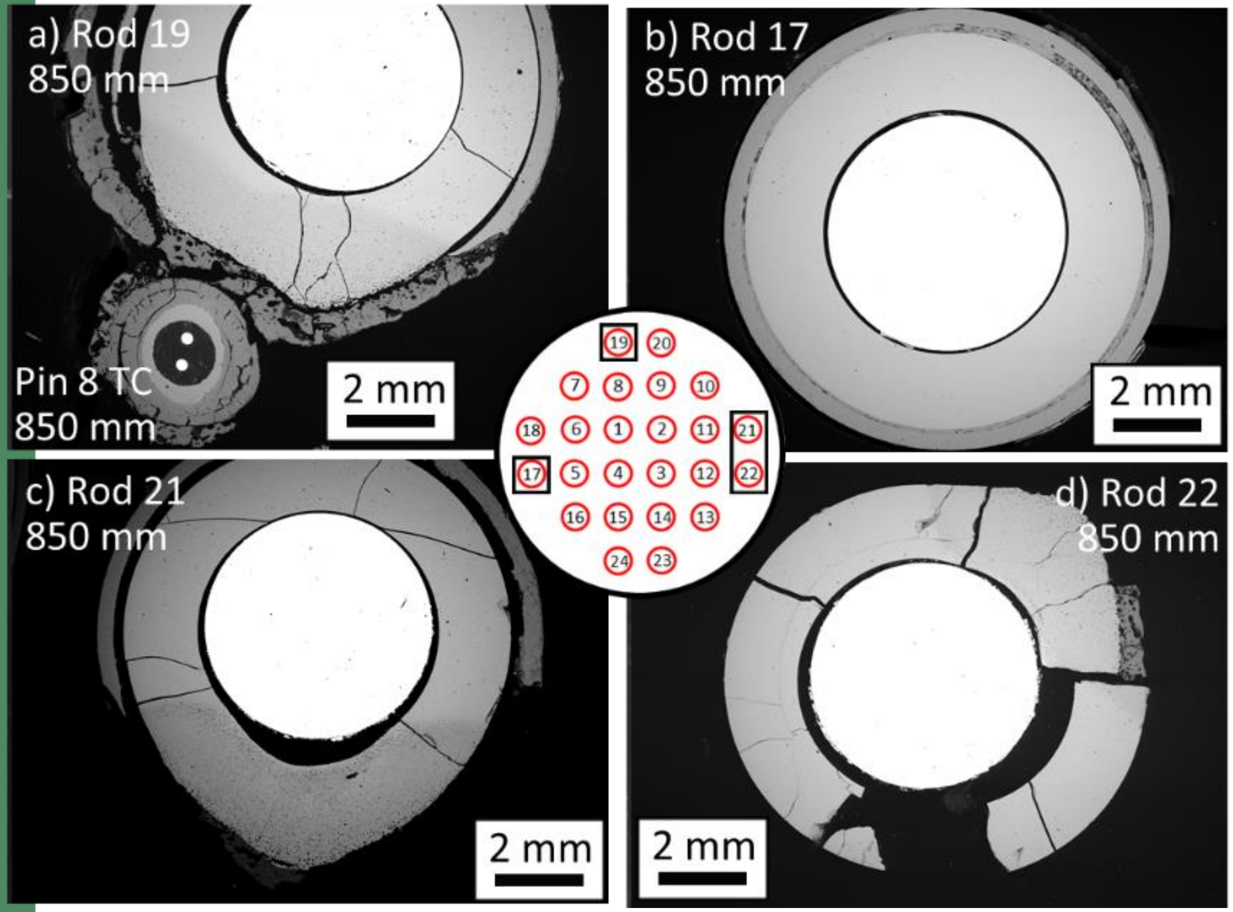

950 mm

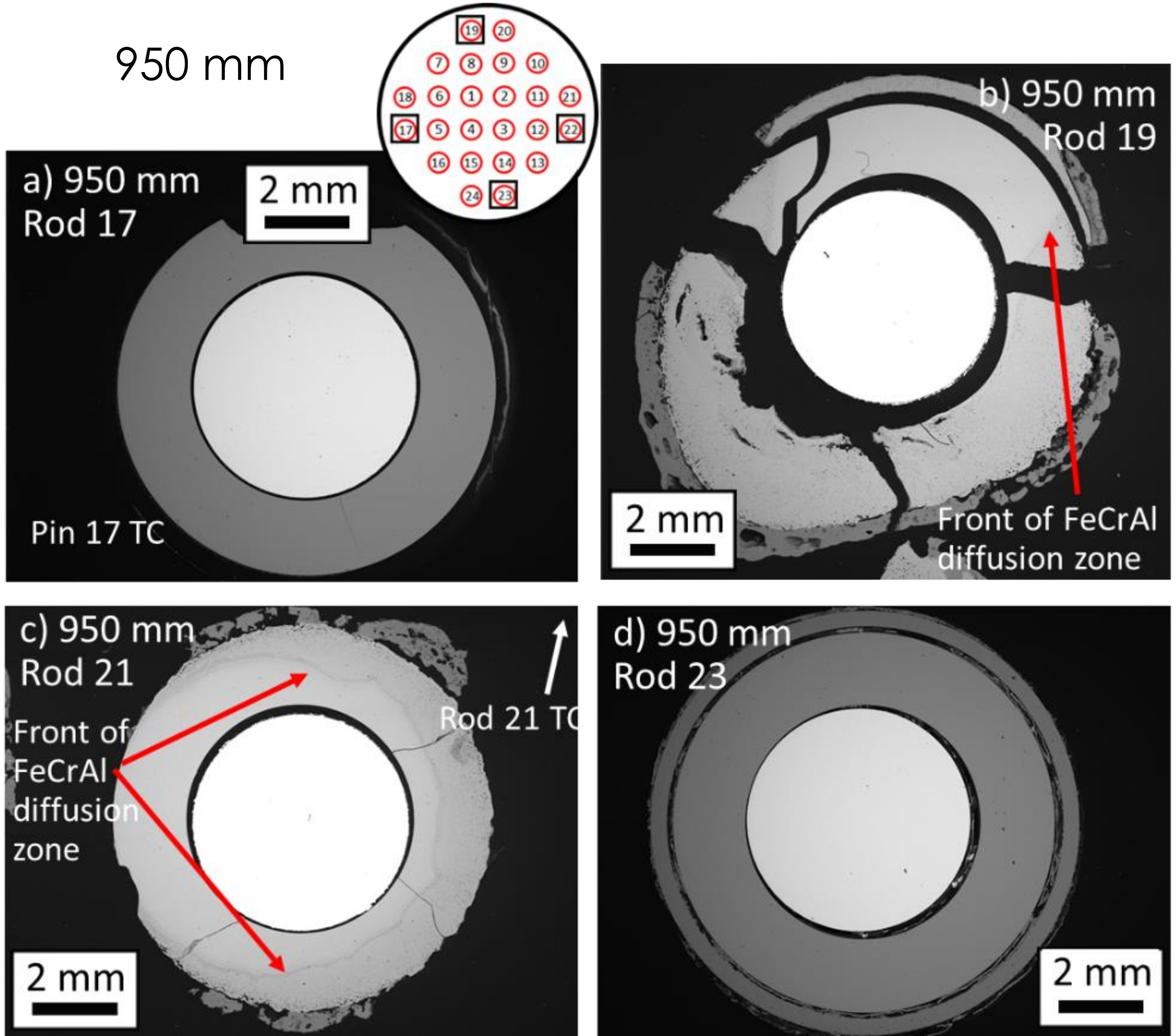

OAK RIDGE
National Laboratory

Conclusion

- A QUENCH test was performed at KIT to determine the accident-response characteristics of B136Y3 FeCrAl rods
- The maximum temperature of ~1450℃ was achieved at 850 mm after a hold period of 2000 seconds following a 1130 second heating
- In the absence of thermocouple sheaths, cladding remained intact with a resilient oxide film
- Near thermocouples and above 750 mm (>1200-1300℃), significant chemical attack of thermocouple sheaths and cladding was observed
- Internal FeCrAl/ZrO_2 interactions occurred, possibly due to leakage of steam to the rod interior and/or due to thermocouple interactions
- Insignificant oxidation of Kanthal rods was observed

F. Boldt, D. Nahm

GRS Munich

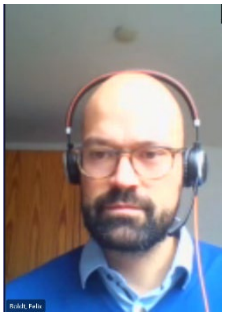

The SPIZWURZ Project – Bundle Experiment and Benchmark on Axial Hydrogen Diffusion

The SPIZWURZ project is performed in cooperation of GRS and KIT including the BGZ as observer. The aim of the planned work is the experimental and theoretical determination of the solubility and diffusion of hydrogen in cladding tube materials under mechanical stress. Investigation of the influence of stress and material specific terms on the hydrogen flow in common cladding tube materials as well as the influence of irradiation and the stress state. KIT's QUENCH facility will be applied for a long-term bundle experiment on the axial hydrogen diffusion in cladding tubes. 21 electrically heated fuel rod simulators create a temperature distribution profile over the rod length. Each individual rod thus offers areas with the same temperature above and below the maximum temperature. Prehydrided claddings will be subject of cooling rates of approximately 1 K/d over a period of eight months covering temperature ranges of dry-storage conditions between 400 °C and 150 °C. Due to the axial temperature gradient in the QUENCH bundle, all temperatures relevant for interim storage are simulated. At the end of the experiment, the hydrogen and hydride content, distribution as well as the hydride orientation will be analysed at several axial levels.

As a preliminary calculation the GRS code ATHLET-CD will be used estimating the thermal boundary conditions for the bundle test. GRS organizes a “blind benchmark” as complementary approach open for all participants using fuel rod simulation codes to predict the thermo-mechanical and hydrogen behaviour within the bundle. The results of the benchmark and of the bundle experiment will be analysed for the further validation and development of hydrogen diffusion models in fuel rod codes.

The SPIZWURZ Project – Bundle Experiment and Benchmark on Axial Hydrogen Diffusion

Felix Boldt[1),2)], Daniel Nahm[1)]

[1)]Gesellschaft für Anlagen- und Reaktorsicherheit (GRS) gGmbH
[2)]Technical University of Munich, Chair of Nuclear Technology

26th QUENCH Workshop, KIT Karlsruhe

9th December 2021

Content

Introduction

SPIZWURZ project
Hydrogen behaviour
Bundle experiment

Benchmark proposal

Boundary conditions
Expected results
Organisation

Outlook and Timeline

Spannungs**i**ndu**z**ierte **W**asserstoff**u**mlagerung in Brennstabhüllrohren während längerfristige**r** **Z**wischenlagerung (SPIZWURZ)

Purple gentian
(Ger. Spitzwurz)

Stress-induced hydrogen rearrangement in fuel rod claddings during long-term dry storage (SPIZWURZ)

Introduction *SPIZWURZ project*

- Joint project of GRS global research for safety and KIT Karlsruher Institut für Technologie and as observer BGZ Gesellschaft für Zwischenlagerung mbH
- Experimental determination and theoretical description of the solubility and diffusion of hydrogen in cladding tube materials under long-term dry storage conditions.
- Qualitative and quantitative description of hydrogen diffusion on a macroscopic and microscopic level for improved prediction of the formation of hydride structures in zirconium-based cladding tube materials and the resulting material embrittlement.
- Improvement of the data on the pellet-cladding interaction during dry storage.
- Consolidation of all results into a consistent description of real cladding tube materials under conditions of longer-term interim storage with reference to irradiation and slow cooling rates.

SPIZWURZ Benchmark

Introduction *Hydrogen behaviour*

- Evaluation of the fuel rod integrity requires knowledge of the local H concentration in the cladding tube.
- Dissolved hydrogen changes its distribution under the influence of temperature, concentration and stress gradients by diffusion.
- No complete description of the hydrogen flow $\overrightarrow{J_\mathrm{H}}$ in the literature.

$$\overrightarrow{J_\mathrm{H}} = \vec{J}(c_\mathrm{H}, \mu_H, T, \sigma, MT)$$

c_H : *hydrogen concentration,*
μ_H: *chemical potential,*
T: *temperature,*
σ: *stress,*
MT: material texture.

- SPIZWURZ Project investigates the hydrogen flow in fuel rod claddings in parameter ranges typical for dry storage conditions.

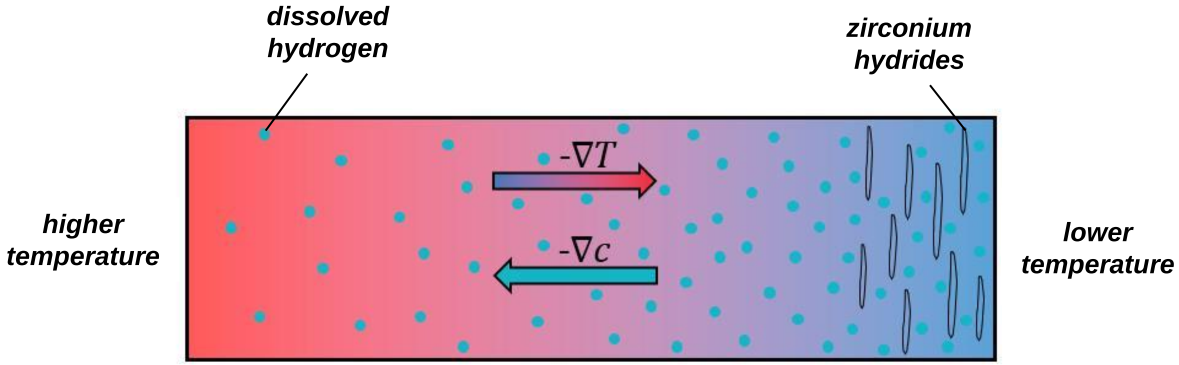

Hydrogen migrates according to concentration (∇c), temperature (∇T) and stress gradients (not displayed)

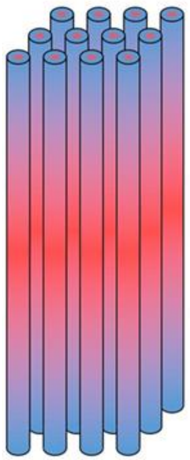

At dry storage conditions, slow cooling rates cause a hydrogen diffusion in close-to-equilibrium conditions

Introduction *Bundle experiment*

KIT's QUENCH facility will be used for an eight months lasting experiment

Cladding pre-treatment

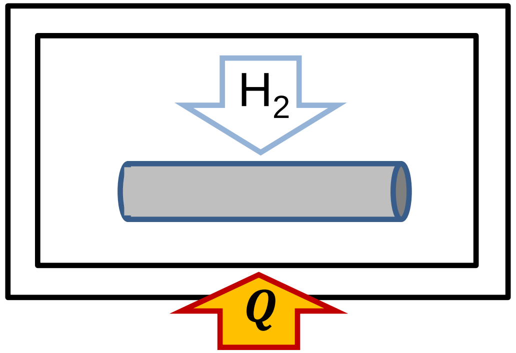

- Hydrogen loading at KIT furnace

Power development

- Boundary condition for QUENCH facility (Simulation with ATHLET-CD code)

Long-term bundle test

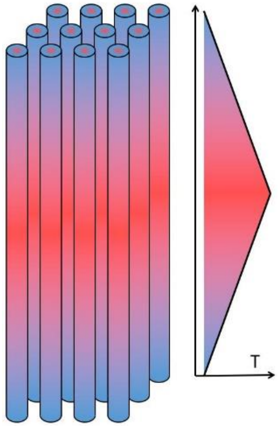

- Hydrogen diffusion under long-term cool-down

Analysis of the hydrogen distribution

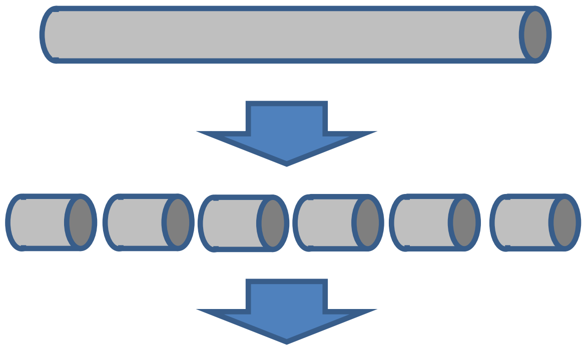

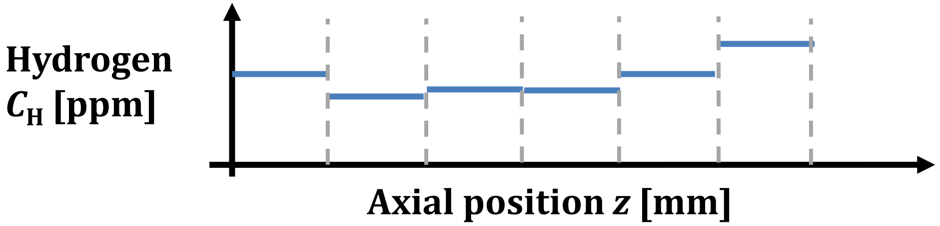

- Neutron radiography
- Metallographic analysis
- Hot vacuum extraction of hydrogen

Introduction *Bundle experiment*

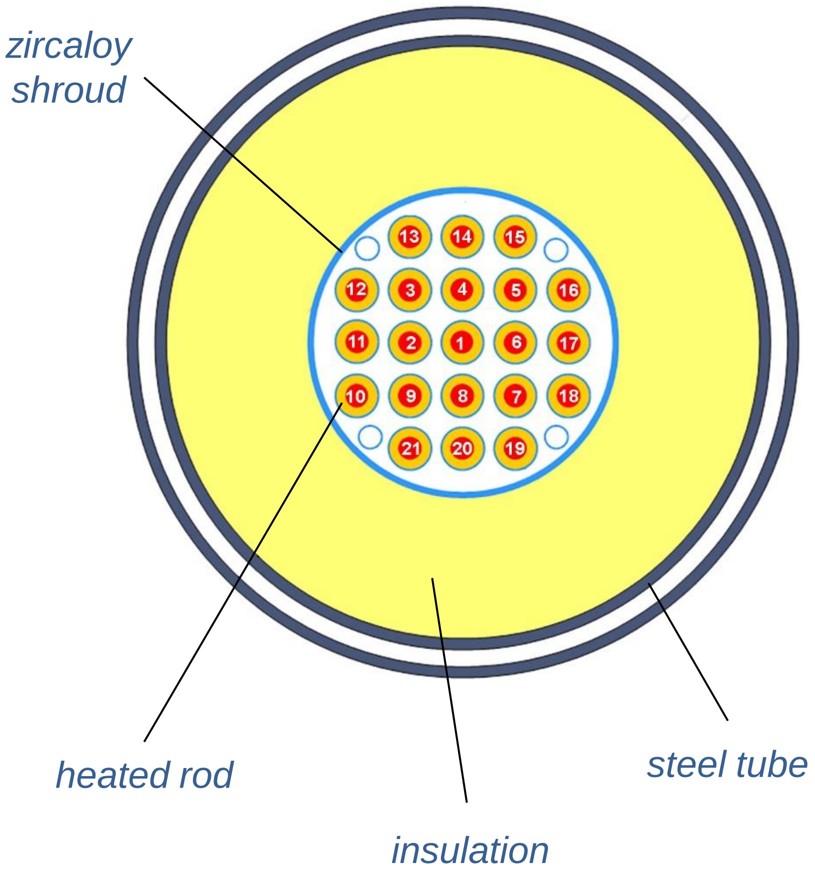

The SPIZWURZ bundle

- 21 electrically heated fuel rod simulators
- Pressure and heating power control for every rod
- Test matrix involving 3 materials, 2 pressures (70 and 100 bar), 2 hydrogen concentrations (100 and 300 wppm)

Material	p_{max}, $C_{H,max}$	p_{max}, $C_{H,min}$	p_{min}, $C_{H,min}$	p_{min}, $C_{H,max}$
Zry-4	2x	2x	2x	2x
Optimized Zirlo	2x	2x	2x	2x
Duplex DX-D4	2x	1x	1x	1x

- Start temperature of $T_{\max} = 400\ °\text{C}$
- Cooling rate of $\frac{\Delta T}{\Delta t} = 1{,}0\,\frac{\text{K}}{\text{d}}$
- Bell-shaped temperature profile provides temperature decrease two both ends
  - Two samples per rod with same temperature

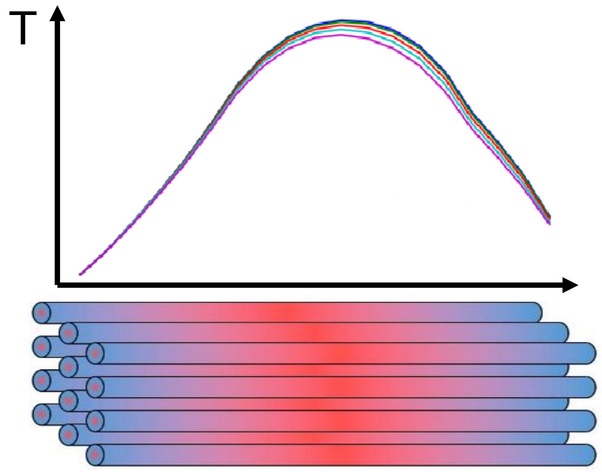

Introduction *Bundle experiment*

Specification calculations performed with AC^2/ATHLET-CD

- Five groups of rods
  - ROD1: 1
  - ROD2: 2, 4, 6, 8
  - ROD3: 3, 5, 7, 9
  - ROD4: 11, 14, 17, 20
  - ROD5: 10, 12, 13, 15, 16, 18, 19, 21
- Constant environment temperature
- Targets:
  - 400 °C central temperature at the beginning of the transient
  - Decrease of maximum temperature 1,0 K/d

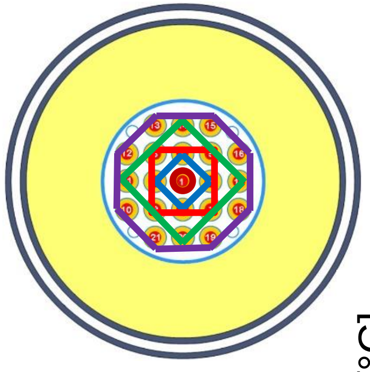

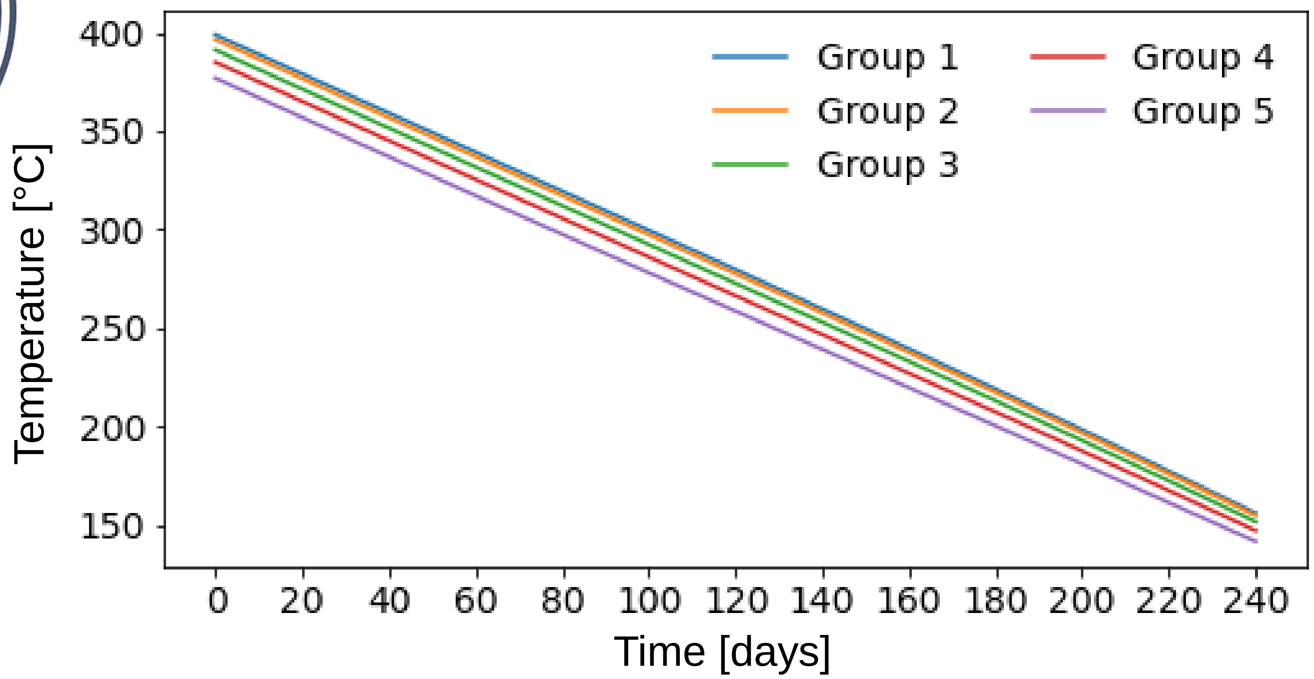

➢ Constant power decrease of 19.5 W/month starting with 485 W during heat-up until beginning of transient

- Final set-up of BIC in cooperation with KIT before and during experiment conduct

Benchmark *Boundary conditions*

Results for the hydrogen distribution and the hydride characterization will be available at the end of the project

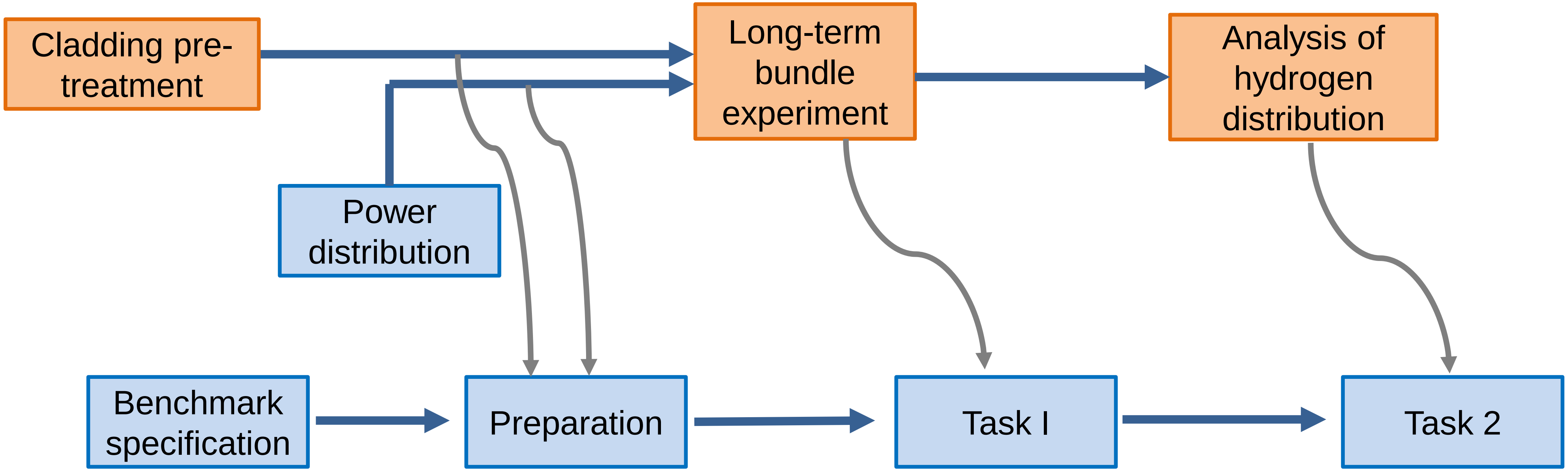

- Test calculation for code users
- Thermal boundary conditions from ATHLET-CD
- Test case for hydrogen distribution model

- Blind Benchmark
- Thermal boundary conditions from QUENCH facility
- Prediction of hydrogen distribution

- Open Task Benchmark
- All results known
- Optimization of hydrogen models

Benchmark *Expected results*

Expected Benchmark output
- Axial distribution of hydrogen
- Amount and location of hydride precipitates
- Orientation of precipitated hydrides (radial/circumferential)
- Effect of diffusion type

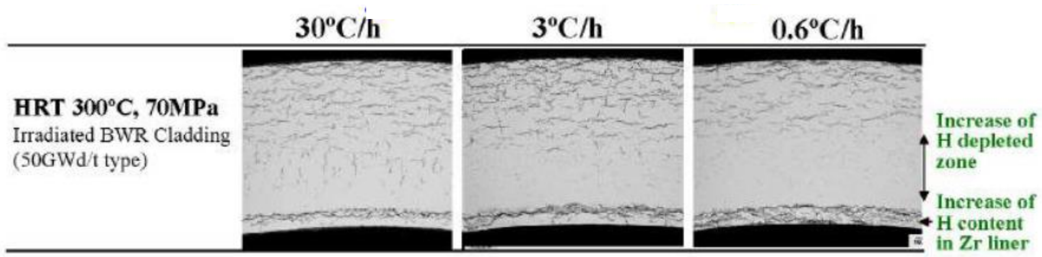

UNF Dispositon Campaign, SRNL-STI-2015-00256

Benefits for the experiment
- Measurements available at the end of the bundle test
- Transient evolution of hydrogen concentration via calculation

Questions to answer:
- *Diffusion type?*
- *Material influence?*
- *Hydride reorientation*

Model optimization perspectives
- Boundary conditions well known
- Spatial resolution of hydrogen distribution available
- Cladding material variation
- Realistic temperature ranges

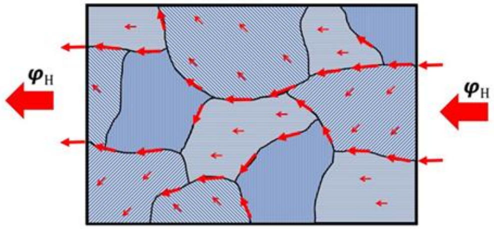

Texture dependency on diffusion?

Benchmark *Outlook and Timeline*

Results for the hydrogen distribution and the hydride characterization are available at the end of the project

Benchmark specification → Preparation phase → Task I → Task II

Fall 2021 | *1st half 2022* | *2nd half 2022 Preliminary results* | *1st half 2023 Final results*

Benchmark participation

- Open for everyone
- Published as report
- Participation via email to
  felix.boldt@grs.de and
  daniel.nahm@grs.de

SPIZWURZ project contacts

- Project coordinator: Felix Boldt (GRS)
- Hydrogen experiments and QUENCH-facility:
  Mirco Grosse (KIT IAM) *mirco.grosse@kit.edu*
- Fuel-pellet interaction:
  Michel Herm (KIT INE) *michel.herm@kit.edu*

The SPIZWURZ Project – Bundle Experiment and Benchmark on Axial Hydrogen Diffusion

Thank you for your kind attention!


source: BGZ

This work is part of a project funded by the Federal Ministry for Economic Affairs and Energy

M. Marchetti, M. Herm, T. König,
A. Walschburger, V. Metz

KIT

Experimental work performed at the shielded box line of the KIT-INE in the framework of the SpizWurZ project

After removal from the nuclear reactor core, the spent nuclear fuel (SNF) is subjected to a series of physical-chemical phenomena, which might impact its safety in interim dry storage.

SNF pellets with high average burnup present larger fuel volumes at the end of the useful life due to the accumulation of insoluble solid fission products and noble gases and this leads to the disappearance of the as-fabricated pellet-clad-gap. Further swelling is expected as a consequence of the actinides decays and the accumulation of helium. This leads to larger cladding hoop stress. The goal of the present work is to study the variation of the diameter of an irradiated Zircaloy-4 cladding after the chemical digestion of the UO_x pellet.

Experimental work performed at the shielded box line of the KIT-INE in the framework of the SpizWurZ project

M. Marchetti, ***M. Herm, T. König, A. Walschburger and V. Metz***

Karlsruhe Institute of Technology, Institute for Nuclear Waste Disposal, P.O. Box 3640, 76021, Karlsruhe, Germany

26th International QUENCH Workshop

6 - 10 December 2021
online

Karlsruhe Institute of Technology, Germany

Outline

- SpizWurZ project – rationale of work package II
- Material object of study
- Experimental
- Conclusions / Outlook

Rationale of work package II: structural integrity of the Spent Nuclear Fuel (SNF)

The cladding integrity in Interim Dry Storage is influenced among other factors, by the SNF irradiation history and the average burnup at discharge.

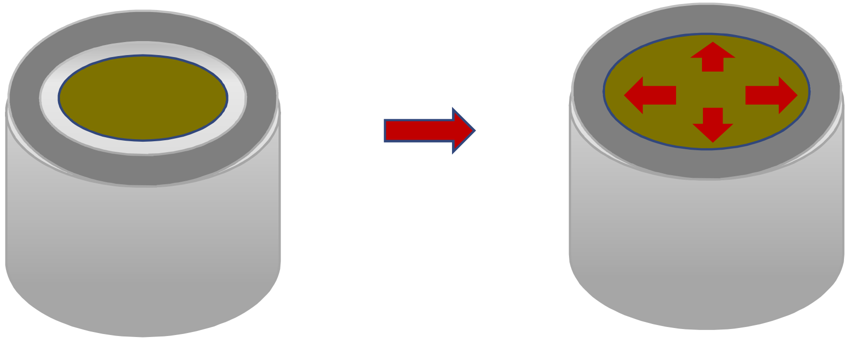

At high-burnup

- The swelling of the fuel (solid FPs and noble gases precipitation) causes the pellet to enter in contact with the cladding with PCI (mechanical and chemical). The hoop stress increases.

- Further swelling caused by the He precipitation in the fuel matrix and increase of the lattice parameter might increase the hoop stress in the cladding.

Goal

Variation of the diameter for an irradiated Zircaloy-4 cladding after 30 years of storage and following the removal of the nuclear fuel pellet.

⬇

Calculate the hoop stress on the cladding caused by the fuel pellet swelling.

Material object of study

Fuel rod segment irradiated in the PWR Gösgen (Switzerland):

- Fuel type: UO_2 with initial enrichment of ^{235}U: 3.8%.
- Irradiation: four cycles / 1226 effective full power days.
- Average linear power: 260 W·cm^{-1}.
- Average burn-up of: 50.4 GWd·t_{HM}^{-1}.
- Cooling time: ~ 31.6 y.
- Cladding material: Zircaloy-4

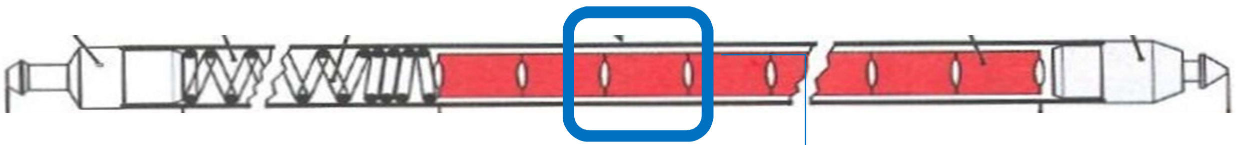

Pellet in contact with fuel

Material object of study

Fuel rod 5810 irradiated in the PWR Obrigheim (Germany):

- Fuel type: MOX with 3.2% Pu_{fiss} (optimised co-milling process, OCOM).
- Cycles: 4.
- Effective full power: 1157 days.
- Average linear power: 200 W/cm.
- Average burn-up: 38.0 GWd/t_{HM}.
- Cooling time: 32 years.
- Cladding material: Zircaloy-4

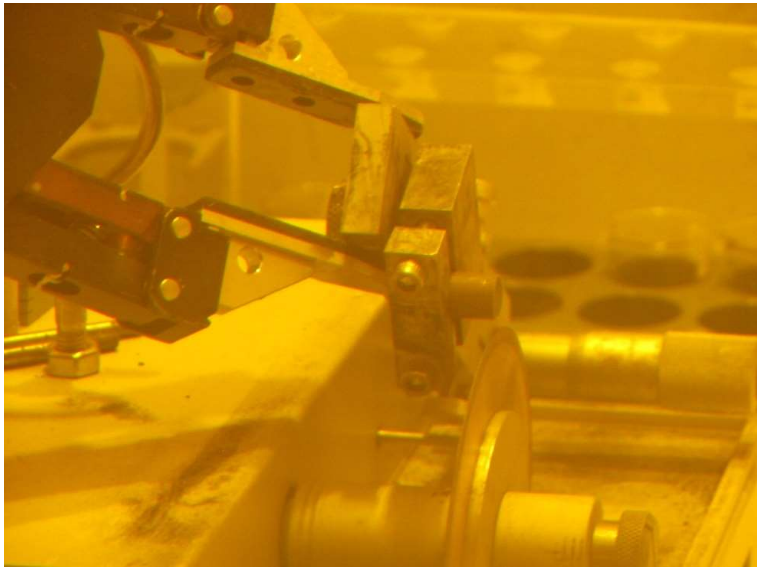

Diameter variation measurement UO2 fuel rod segment

Cross section of the UO_2 pellet segment chosen for diameter variation measurement. Axial length ~ 8 mm

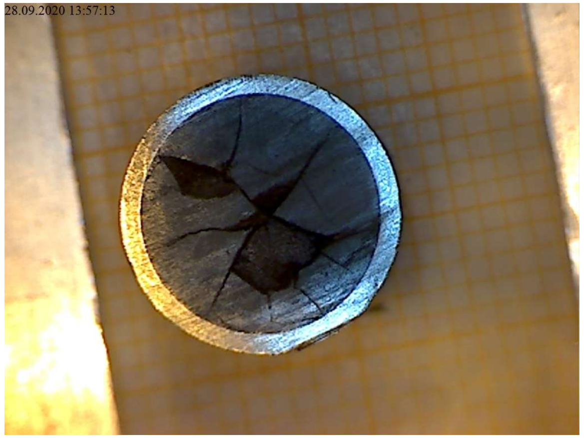

Diameter measurement by means of a laser scan micrometre installed in a shielded box.

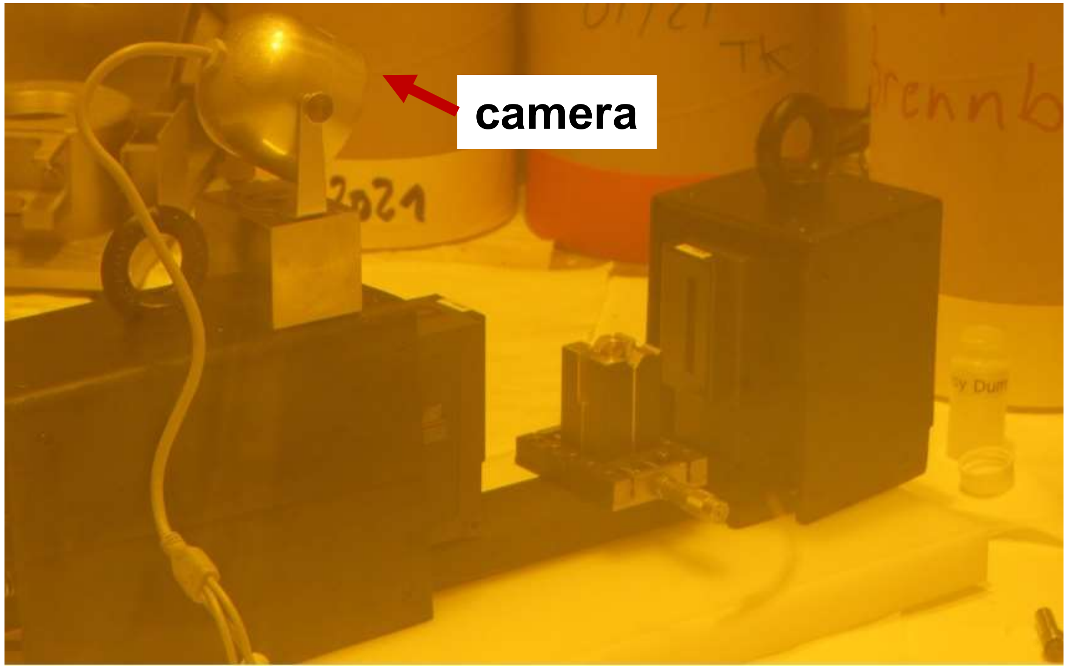

- **High accuracy with a linearity of ±1.0 µm**
- **Repeatability of ±0.1 µm**

Diameter variation measurement UO_2 fuel rod segment

The laser beam scans at high and known speed. The interruption represented by the segment enables the detector to provide the measurement of the diameter (D).

- **The segment is rotated and moved along the axial direction.**
- **The measurements reveal an oval cross-section**

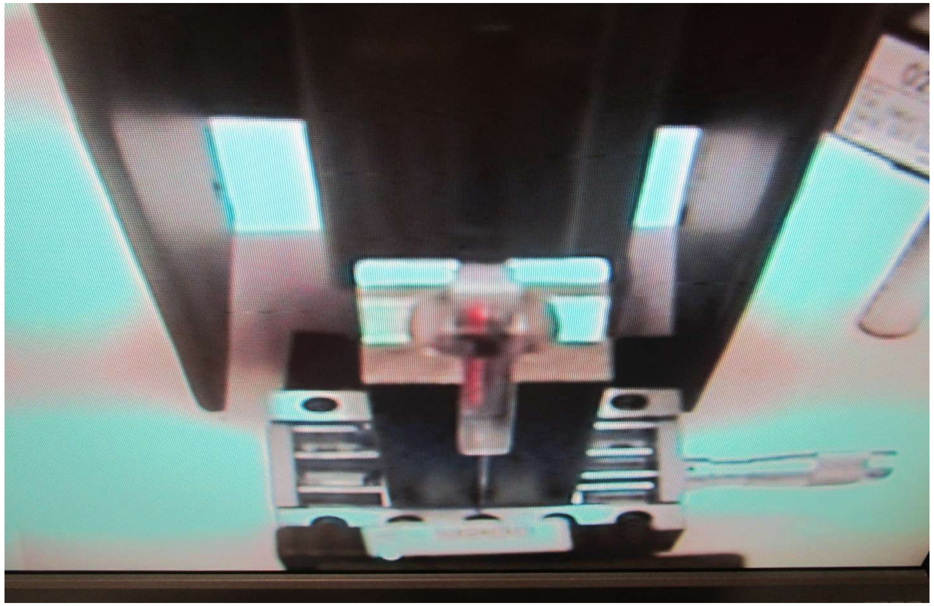

View from the camera

Diameter variation measurement UO_2 fuel

Karlsruhe Institute of Technology

At the pellet - pellet interface

D_{MAX} ~ 10.713 mm

Pellet-
Pellet
interface

D_{MIN} ~ 10.679 mm

About **34** µm difference between maximum and minimum measured diameters

Diameter variation measurement UO_2 fuel

D_{MAX} ~ 10.720 mm

In the central axial position:

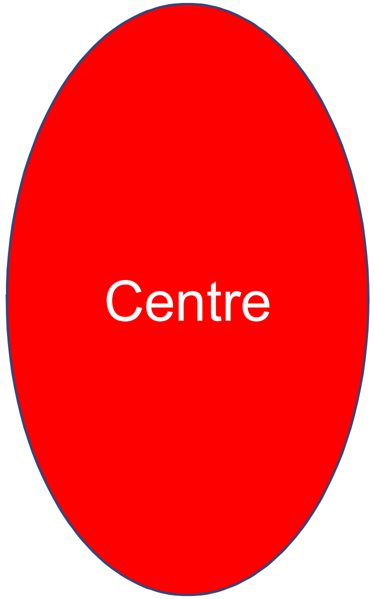

D_{MIN} ~ 10.667 mm

About **53** µm difference between maximum and minimum measured diameters

Diameter variation measurement

Karlsruhe Institute of Technology

From preliminary modelling performed by **GRS** the variation induced by the fuel removal **is ≤ 20 μm.**

The external diameter differences due to the sample position are larger than the predict diameter decrease.

Diameter variation measurement

Specimen – cladding (fueled or defueled)

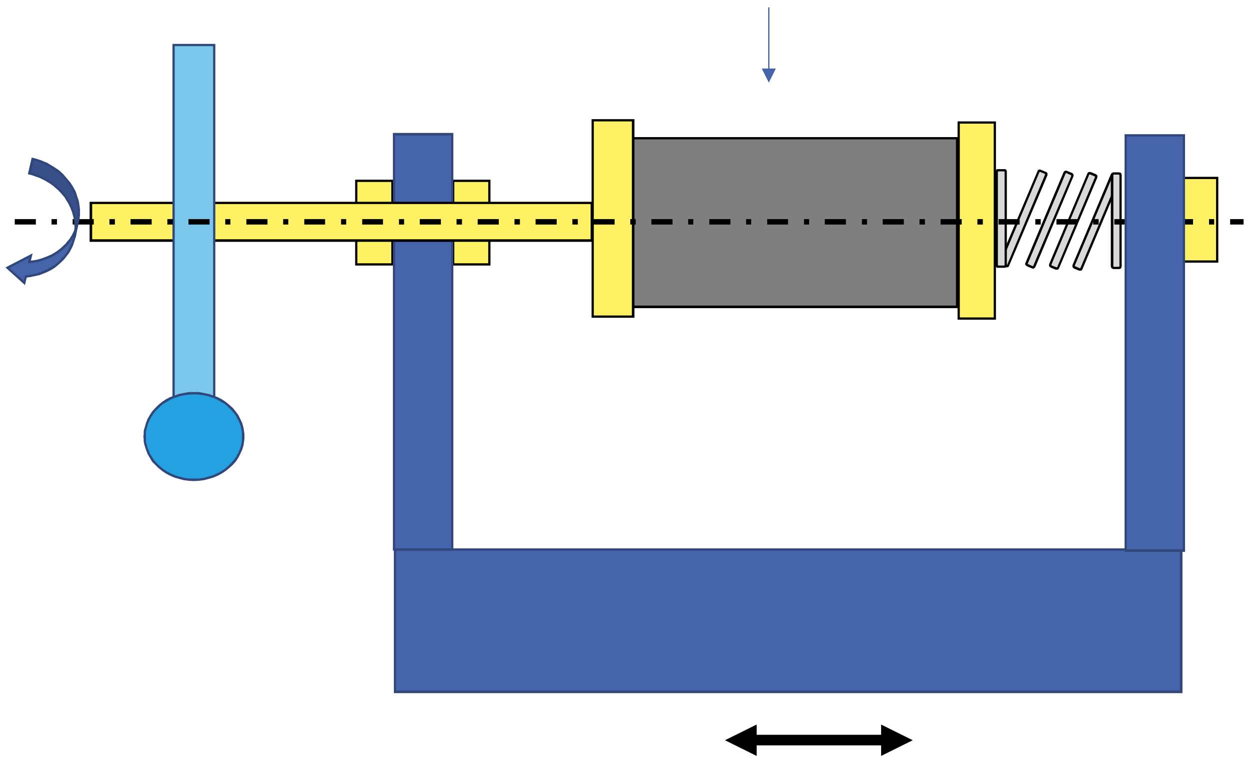

Apparatus movement

Designed by Felix Boldt (GRS)

Diameter variation measurement

- **Chemical decladding** of SNF in hot cell with Ti-lined autoclave:

  Alkaline digestion in **$(NH_4)_2CO_3$ / H_2O_2** at room temperature for 5 days.

Autoclave

Outlook

- Study the variation of the cladding diameter by using precise positions before and after defueling.

- Repeat the experimental campaign using a sample with inter-pellet-gap to better observe “hour glassing” effect.

- Determine the hoop stress borne by the cladding and caused by the pellet volume expansion

Acknowledgment

- Felix Boldt (GRS, gGmbH)

S. Weick, M. Große, M. Steinbrück, H.J. Seifert

KIT

Neutron investigations of the hydrogen diffusion dynamics in different cladding tube materials

Materials can be investigated non-destructive with respect to their structure and dynamic properties by neutron scattering of slow neutrons. Thus, neutron radiography and tomography investigations are used to determine dynamic processes like the diffusion in condensed matter. For Zirconium alloy cladding tubes, the hydrogen distribution and thus the hydrogen diffusion dynamics can be visualised ex situ and in situ. Because of the very low neutron cross section of Zirconium, the metal is nearly invisible for neutrons and the contrarily behaving hydrogen that scatters neutrons strongly, appears as dark contrast in neutron images. Contrarily to the destructive hot gas extraction where the average hydrogen concentration is referred to a specific area, this method is non-destructive and allows the detection of even small amounts of hydrogen with regard to the precise sample location.

This paper focuses on investigations of hydrogen diffusion dynamics in cladding tubes via neutron radiography and hot gas extraction. The hot gas extractions were conducted at the laboratory of the chemical analytic at the KIT Karlsruhe, Germany. The neutron radiography measurements were conducted with polychromatic neutron beams in the cold energy range at the ICON facility at SINQ, Paul Scherrer Institute Villigen, Switzerland. Therefore, different cladding tube samples were hydrogenated with variations in loading time and temperature by using either hydrogen gas or ZrH2-powder. The Zr claddings Zircaloy-4 and DUPLEX were investigated mutually at the same conditions and can be directly compared regarding the hydrogen diffusion process.

Neutron investigations of the hydrogen diffusion dynamics in different cladding tube materials

Sarah Weick, Mirco Große, Martin Steinbrück, Hans Jürgen Seifert

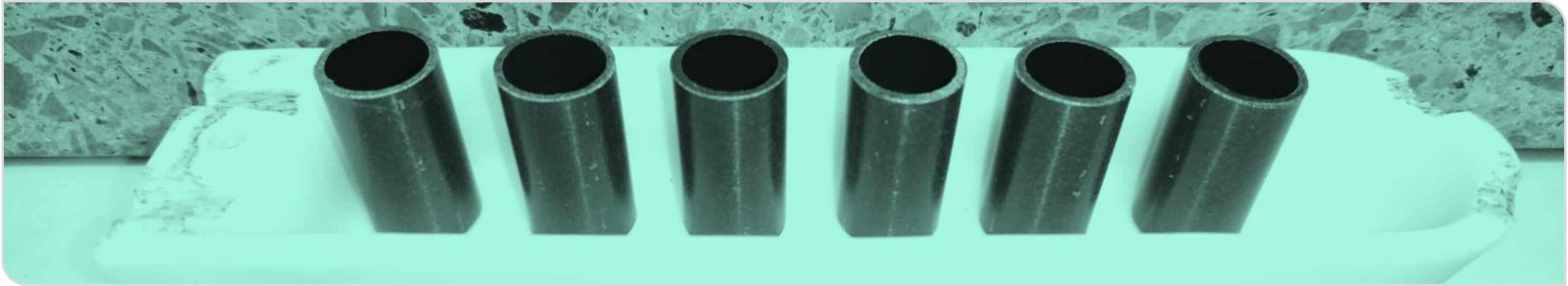

Project SPIZWURZ

- **SPIZWURZ** = Spannungsinduzierte Wasserstoffumlagerung in Brennstabhüllrohren während längerfristiger Zwischenlagerung
  (Strain induced hydrogen redistribution in fuel cladding tubes during longterm interim storage)

→ cladding tube stability under dry longterm conditions (transport & storage casks)

- H uptake by Zr alloy cladding tubes

- H influence on mechanical properties (diffusion, hydride precipication)

- different cladding tube materials (Zircaloy-4, Dx/D4-Duplex, ZIRLO™)

Introduction – Hydrogen embrittlement

- H in cladding tubes
  - H uptake favoured by foreign atoms, additives & textures
  - mechanical strain & chemical activity → influence H diffusion

- Zr Hydrides
  - circumferential or radially orientated
  - reduce strength & ductility
  - delayed hydride cracking (DHC)

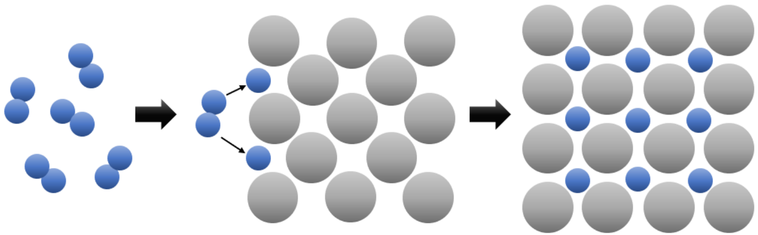

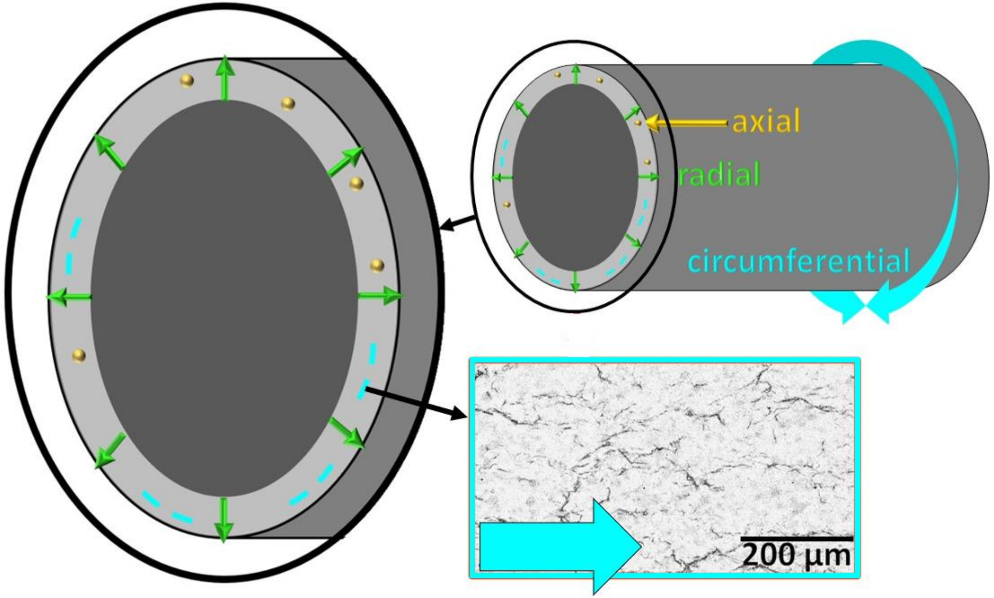

Introduction - Zr-H System

- Zr-H phases
  - which phases exist?
  - which stability areas?

→ **<550°C**:
no phase transition
α→β expected

Grosse-et-al., 2020 after Steinbrück, 2004

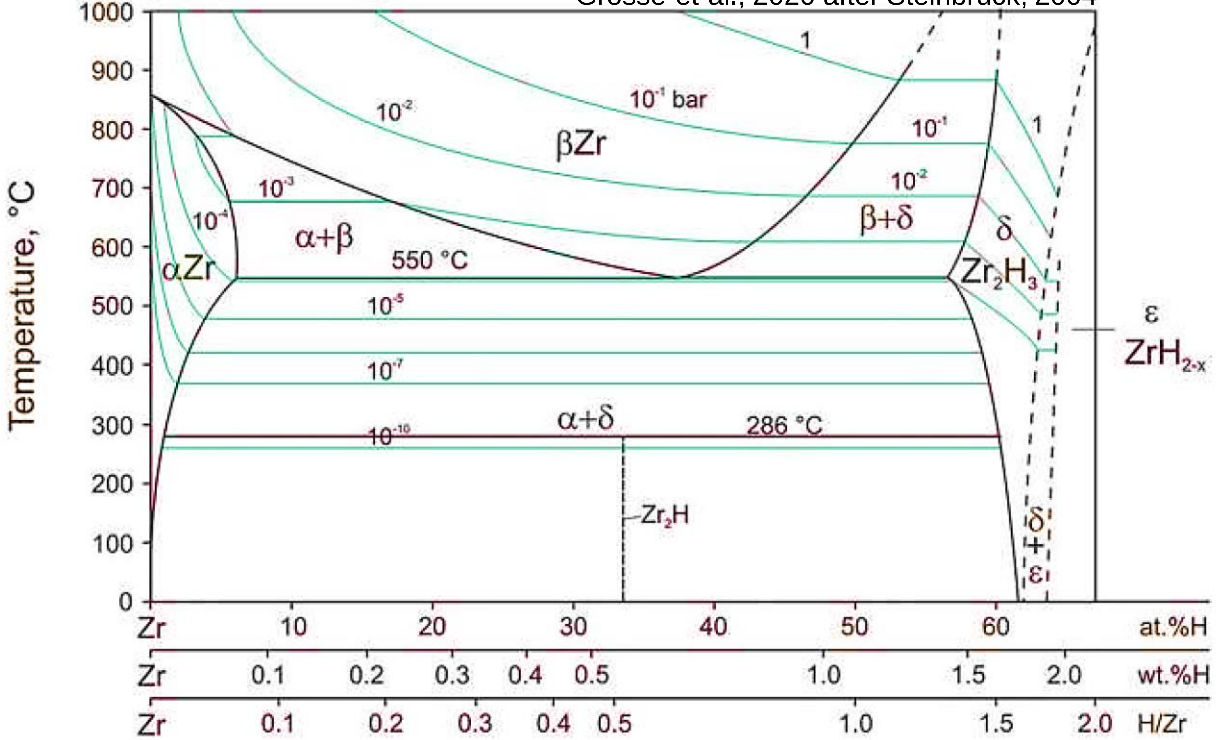

Samples

- original cladding tubes
- different zirconium alloys: Zry-4 & DX/D4
- different oxide layer thicknesses (pre-ox.)
- annealing from gas phase & ZrH_2 powder

→ diffusion in axial & circumferential direction

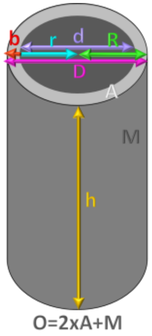

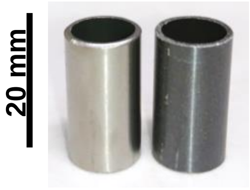

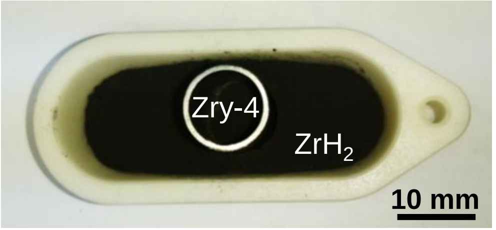

Alloy	Sn [wt.%]	Fe [wt.%]	Cr [wt.%]	O [wt.%]
α-Zr	-	-	-	-
Zry-4	1,3	0,2	0,1	0,13
D4	0,5	0,5	0,2	0,14

	h	b	O	A
Zry-4	20 mm	0,725 mm	1305,45 mm²	22,83 mm²
DUPLEX	20 mm	0,725 mm	1305,45 mm²	22,83 mm²

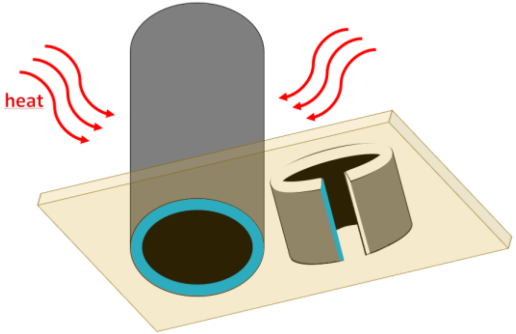

Neutron radiography

$$I = I_0 \cdot e^{-\sigma N d}$$

$$T = \frac{I}{I_0} = \exp(-\Sigma_{total} \cdot s)$$

I: intensity
T: transmission
σ: neutron crosssection
N: neutron flux intensity
d: sample thickness
S: path length of the neutron beam
Σ: total neutron crosssection

ICON facility at the PSI

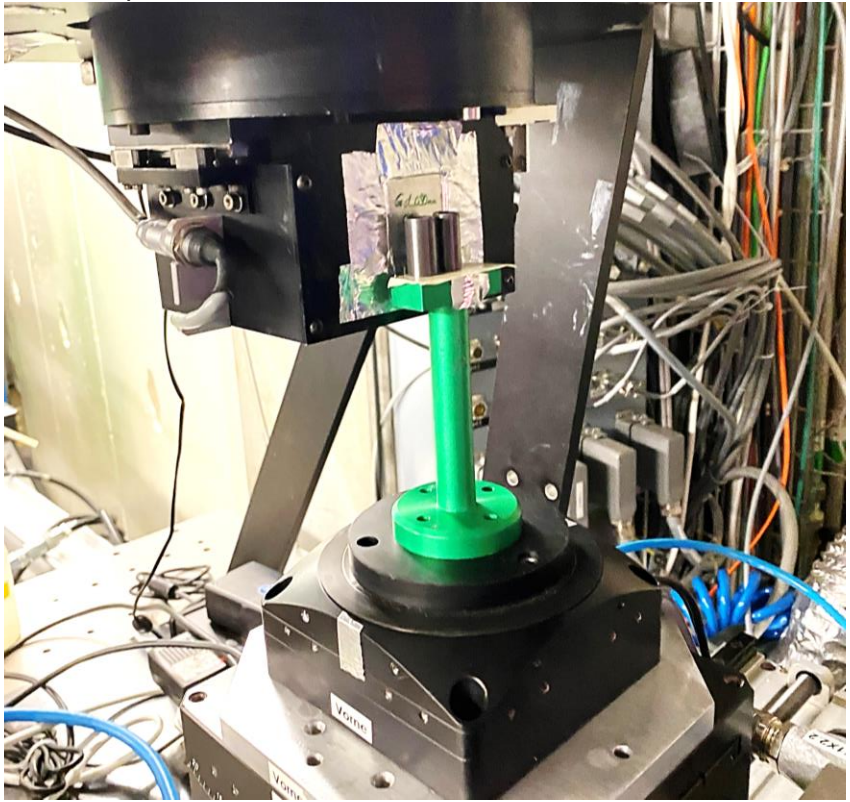

Carrier Gas Hot Extraction

- sample segmentation
- statistical prove
- standards (Zr, Ti)

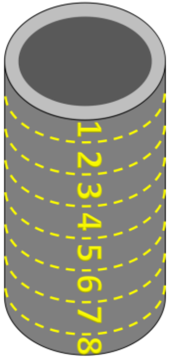

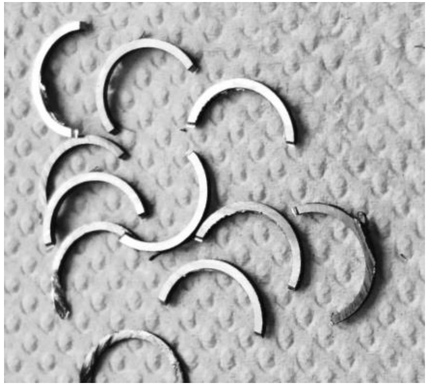

Neutron Radiography - calibration

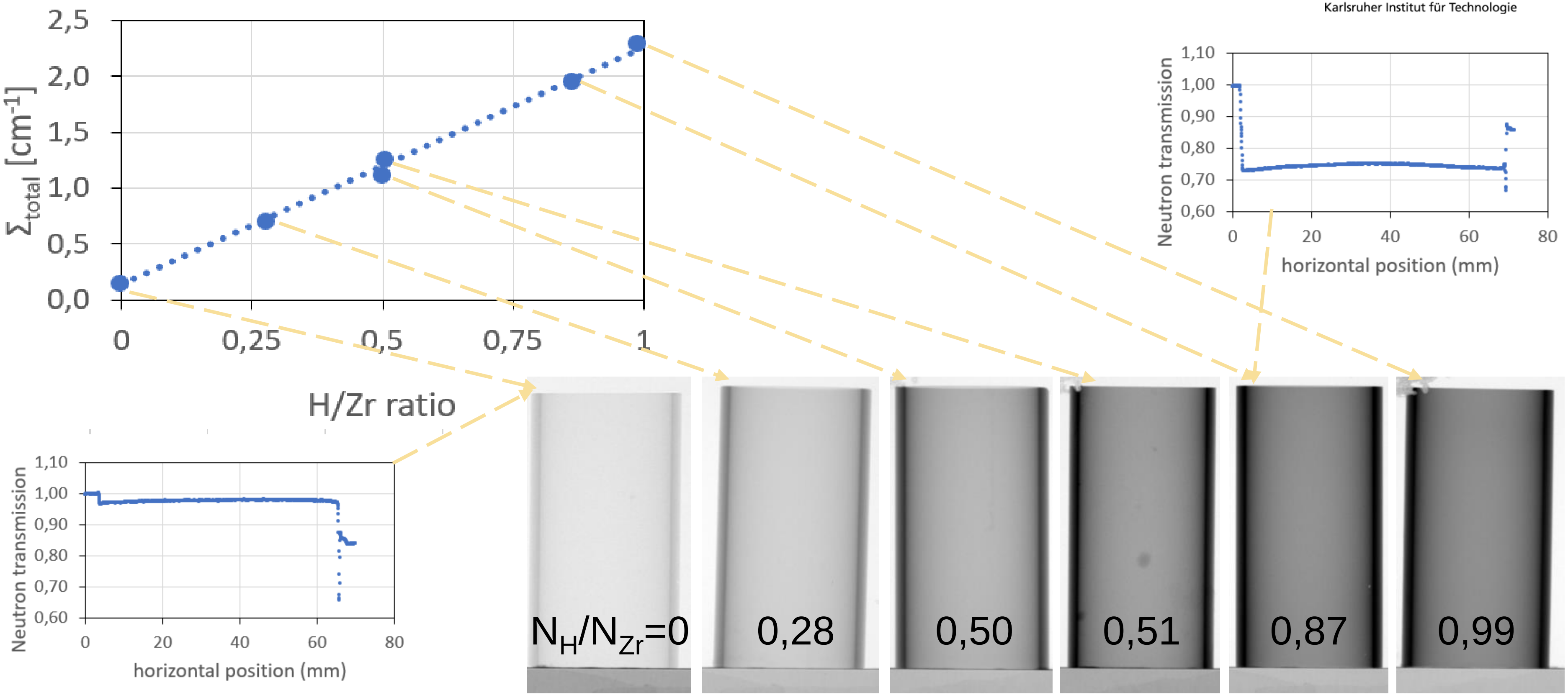

Results – Diff. in axial direction

- ZrH_2 powder, Ar
- pre- & non-oxidized

→ T influence?
→ t influence?

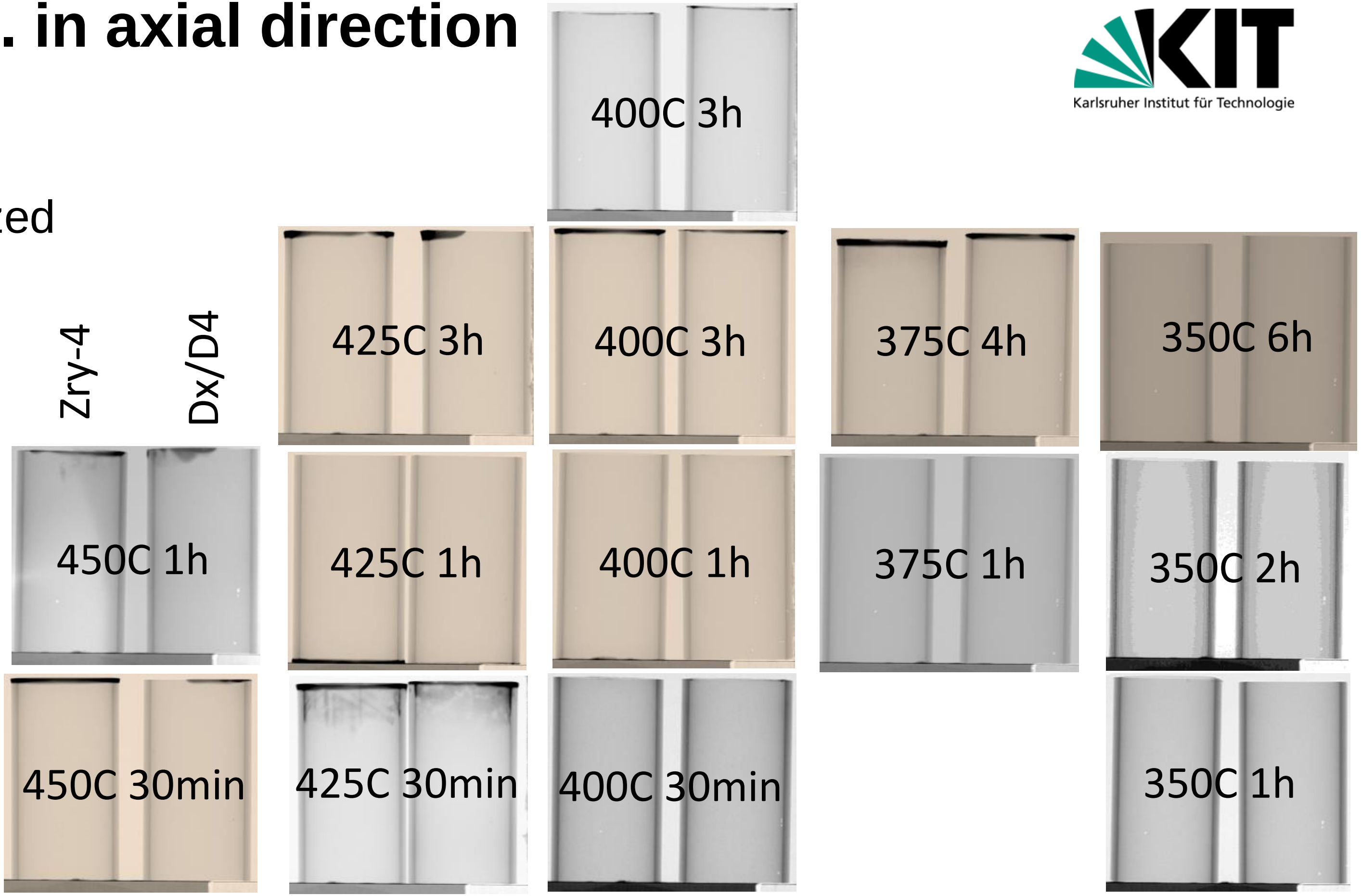

Results – Diff. in axial direction

- ZrH_2 powder, Ar

→ 450-375°C
→ 3h loading

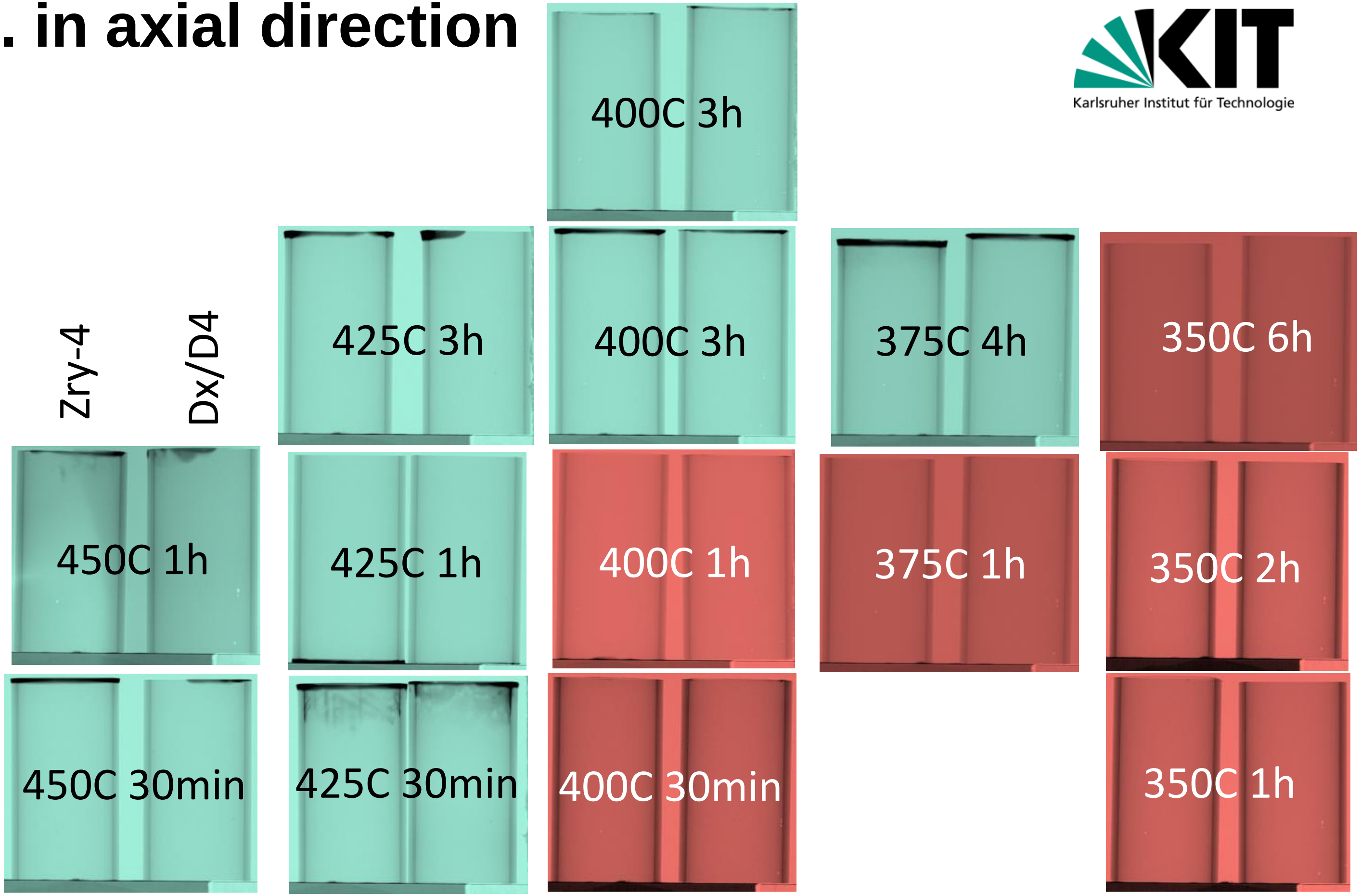

Results – Diff. in axial direction

- ZrH_2 powder, Ar, 400°C, 3h

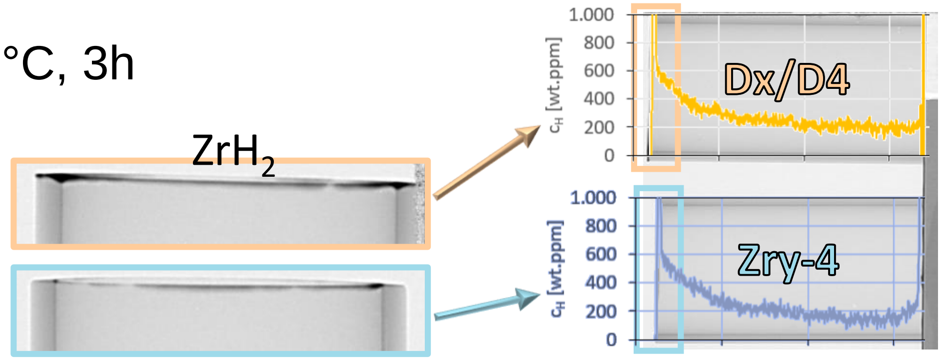

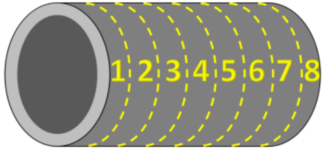

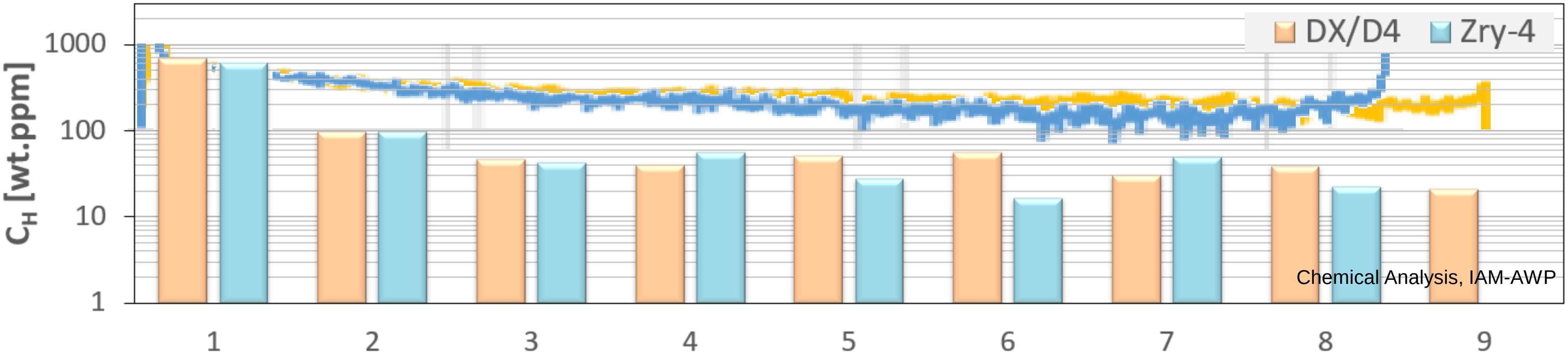

Results – Diff. in axial direction

- ZrH_2 powder, Ar, 400°C, 3h, pre-ox.

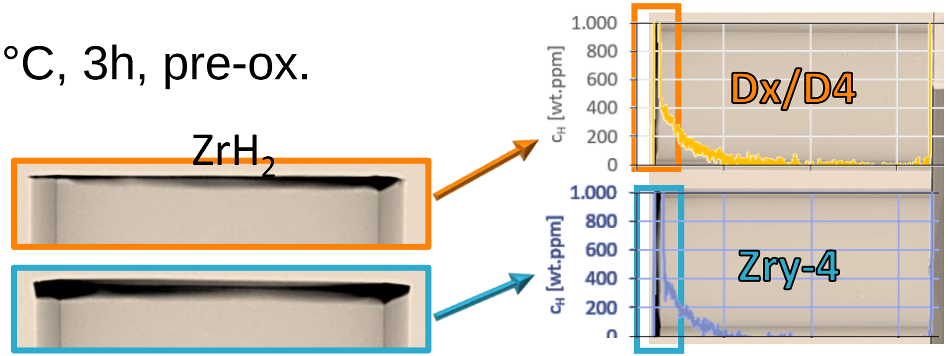

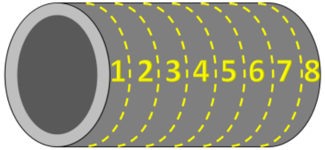

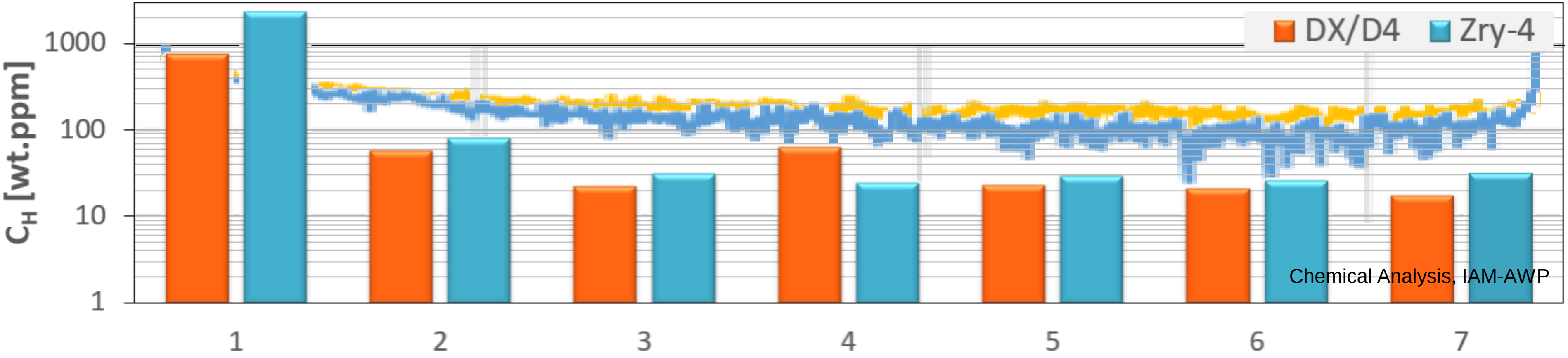

Results – Diff. in axial/circumferential direction

- ZrH_2 powder, Ar → DX/D4: 400°C, 3h, pre-ox.
  → Zry-4: 450°C, 1h

↓

Zry-4: 425°C, 1h, pre-ox.

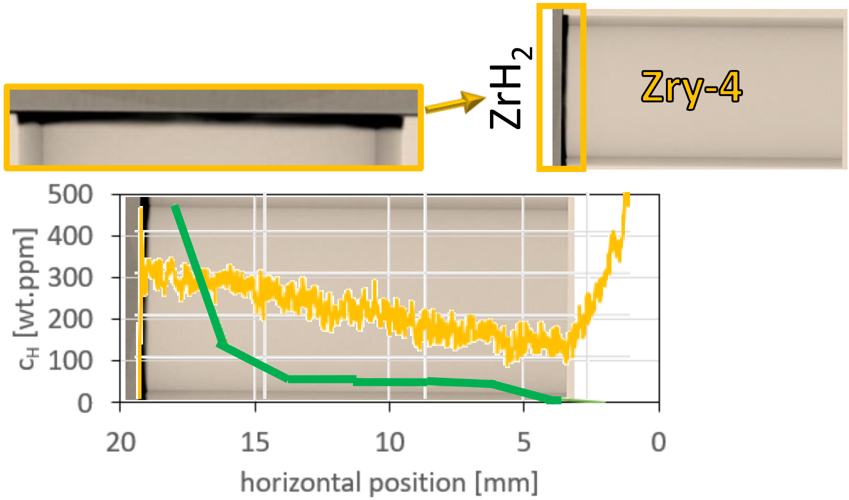

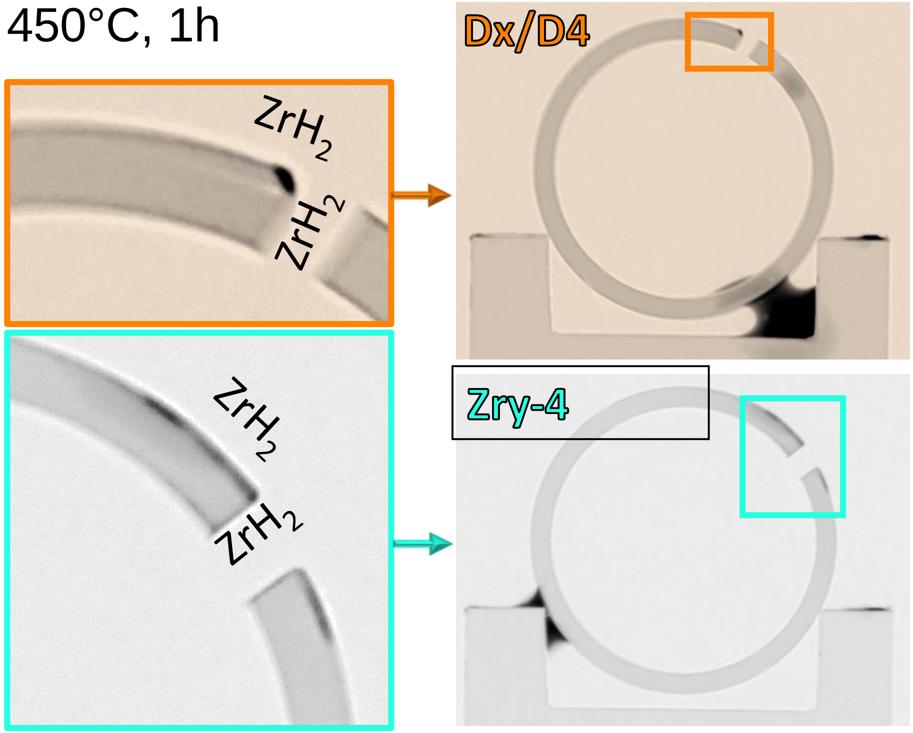

Summary & Outlook

- successfull hydrogen loading with ZrH_2 powder from 450-375°C (t=3h)
- loading: T influence > t influence
- loading differs between pre- & non-oxidized samples -> more defined with pre-ozidized samples; H pick-up of non-oxidized samples at all surfaces

→ diffusion successful, but only investigated in its final state

- experiments will be repeated for sufficient T- & t- conditions in-situ
- experiments will be expanded with an applied stress field (in-situ)

→ differentiating each diffusion step

Acknowledgements

- The SPIZWURZ project is funded by the Federal Ministry for Economic Affairs and Energy (FKZ 1501609B)
- The authors thank Anders Kaestner & David Mannes for providing beamtime at the ICON facility at SINQ, PSI & for their assistance during the measurements /analysis
- QUENCH group & colleagues at KIT

F. Fagnoni[1,2], L.I. Duarte[1,2], J.M. Wheeler[2], J. Bertsch[1]

[1] PSI
[2] ETH

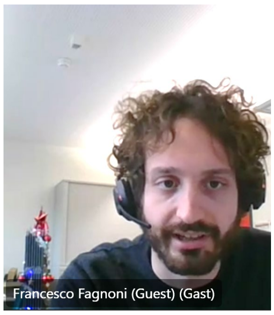

Elevated temperature hardness measurements of Zry-4 in the presence of hydrogen in solid solution

During the operation in the reactor, corrosion of the zirconium-based fuel cladding generates hydrogen, which partially diffuses into the metal. Hydrogen, both in solid solution and in its precipitated form, i.e. as hydrides, affects the mechanical performance of the cladding. Depending on the amount of hydrogen, temperature and deformation rate, different embrittlement mechanisms can be activated. While most current research on spent fuel cladding focuses on embrittlement from hydrides, this work concentrates on hydrogen in solid solution. Hydrogen tends to diffuse towards dislocations, forming Cottrell atmospheres around them.

The presence of a hydrogen atmosphere reduces both the energy barrier required to generate new dislocations and the Peierls stress needed to move a dislocation, causing an overall increased ductility of the metal. This phenomenon, known as Hydrogen-Enhanced Localized Plasticity (HELP), has been extensively studied in FCC and BCC metals, but a complete understanding and description of this phenomenon in Zr based alloys and HCP metals in general is lacking. The HELP effect is source of concern as the conditions of temperature and hydrogen concentration required to activate HELP might be locally present during handling and transportation of spent fuel between the various waste storage phases.

In the presented work, the effect of hydrogen in solid solution has been evaluated by elevated temperature nano-hardness testing of recrystallized Zircaloy-4 sheet material. Results show indications of hydrogen-induced softening at temperatures above 100°C at the tested hydrogen concentration of 230 wppm.

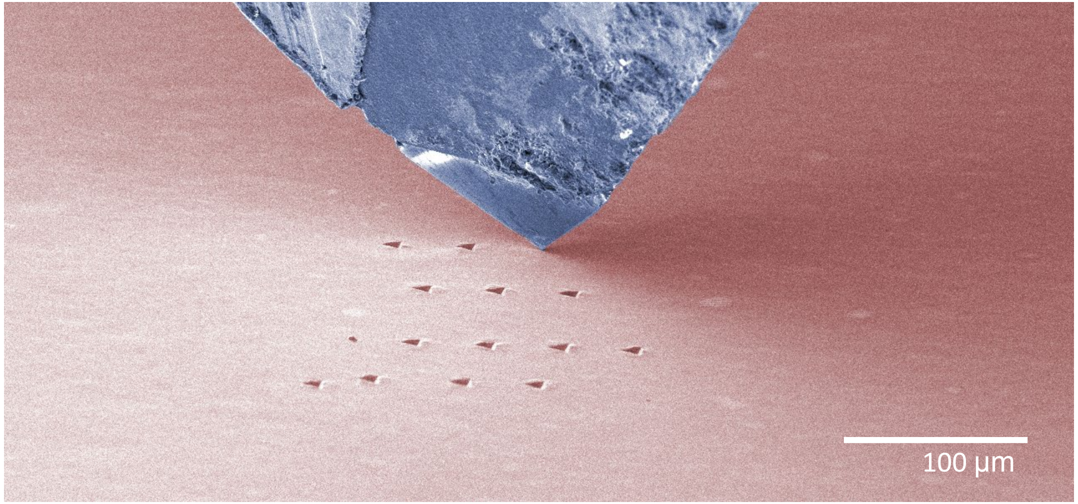

Fagnoni Francesco[1,2], Liliana I. Duarte[1,2], Jeffrey M. Wheeler[2], Johannes Bertsch[1]
[1] PSI :: Laboratory for Nuclear Materials :: Nuclear Fuels Group; [2] ETH :: Laboratory for Nanometallurgy :: Department of Materials.

Elevated Temperature Hardness Test of Zry-4 in the Presence of Hydrogen in Solid Solution

QUENCH workshop 2021 :: 6 - 10 December 2021

H embrittlement in Zr

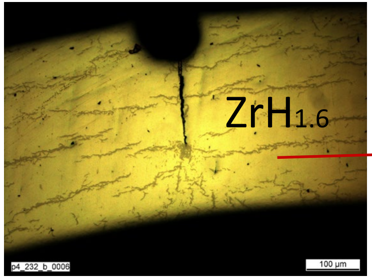

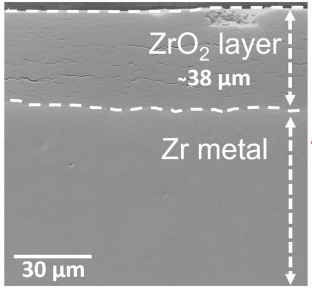

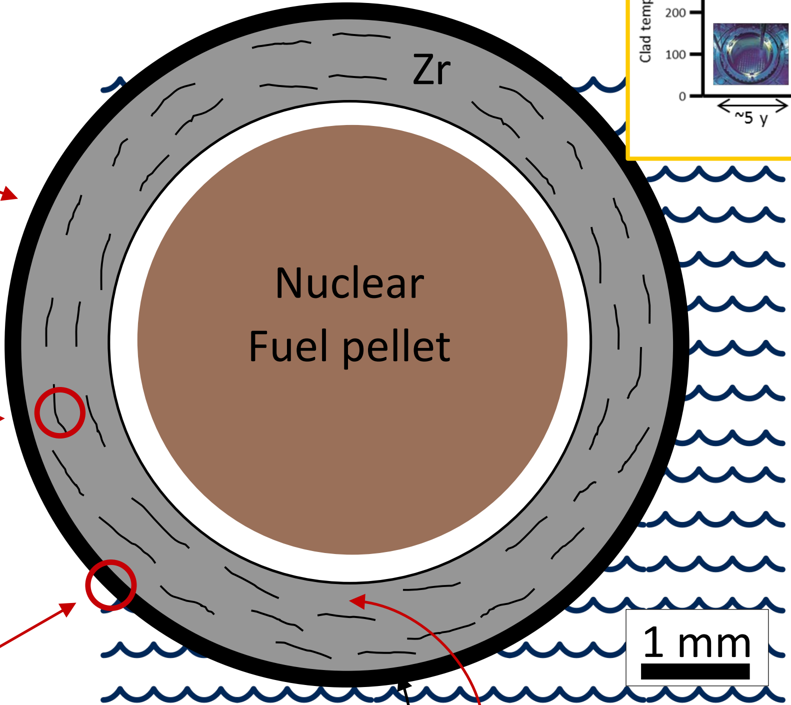

SNF lifetime:

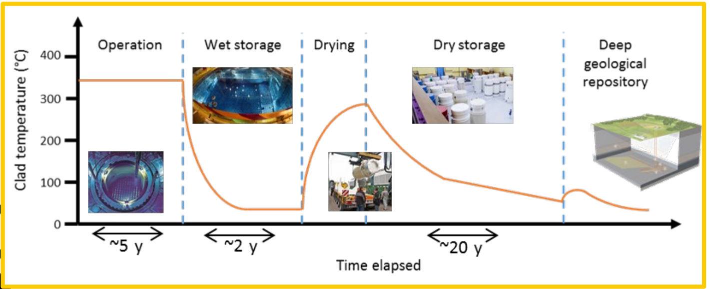

Area of main interest

During operation

$Zr + 2\,H_2O \rightarrow ZrO_2 + 2\,H_2$

■ → ZrO_2 - Oxide layer

Image credits: Axpo – Beznau reactor core; Zwilag – intermediate storage; A. Codewith – DHC; O. Yetik – Zr oxide

Mechanisms of H embrittlement

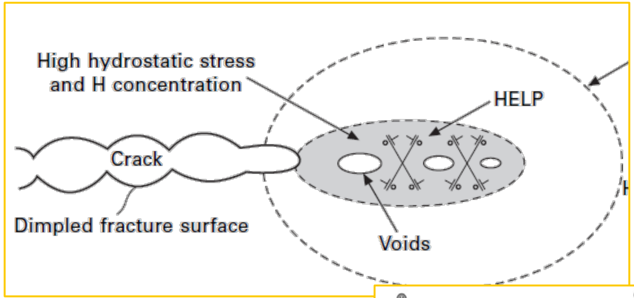

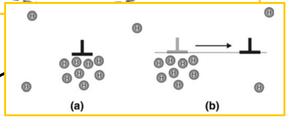

H in solid solution

HEDE
decohesion

Defactant concept

HELP
localized plastic flow

Dislocation pinning

HESIV
Hydrogen-enhanced strain induced vacancy

AIDE
Absorption-induced dislocation emission

Dislocation enhanced mobility

DHC

Cleavage

Hydrides precipitates

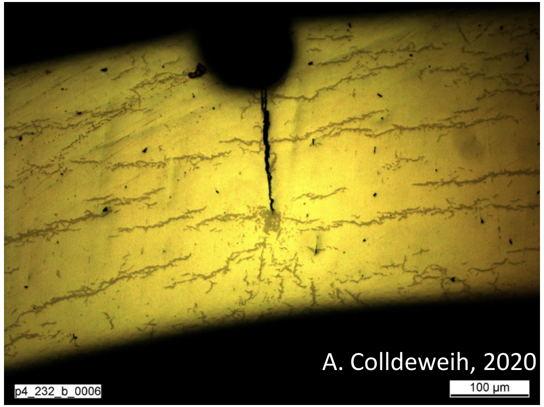

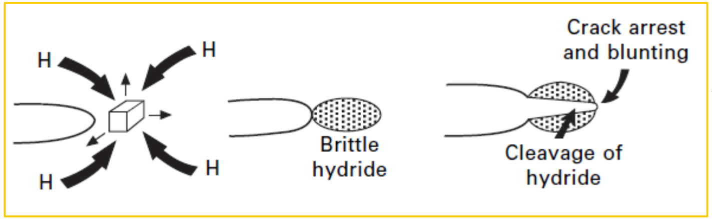

DOI: 10.1016/S0022-5096(03)00052-8

Increased temperature hardness test

High temperature hardness testing has been selected as first experiment to define the boundary conditions necessary to observe the HELP effect vs competitive hydreogen embrittlement phenomena

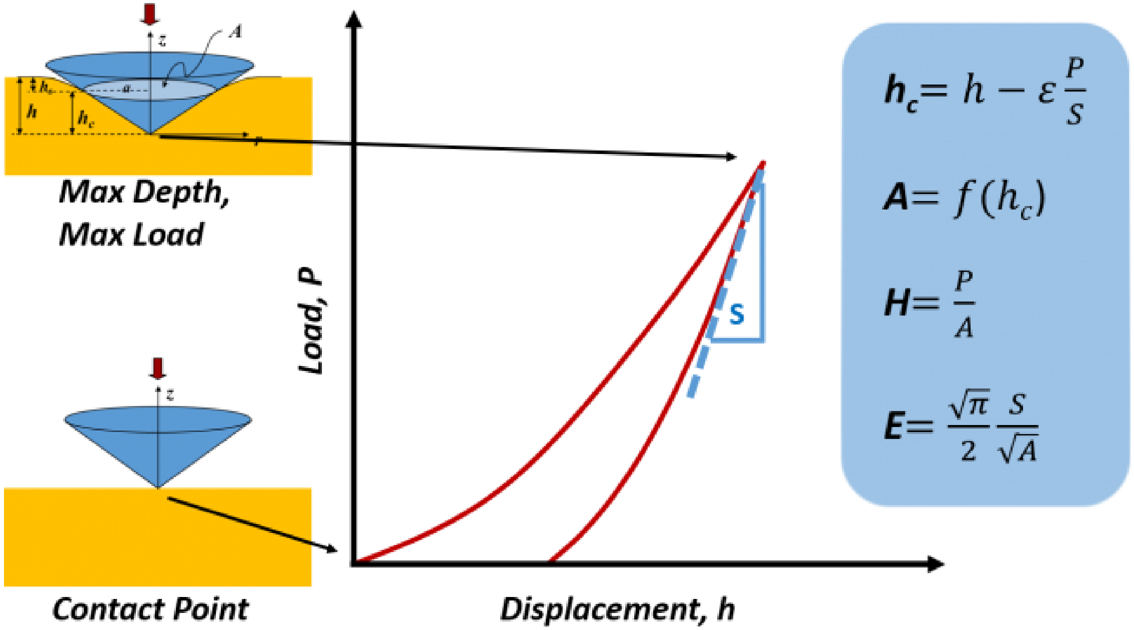

https://www.nanoscience.com/techniques/nanoindentation/

High temperature nano indentation – experiment setup

- Tescan Vega3 SEM with an Alemnis *In Situ* Indenter - heated tip;
- Berkovich diamond indenter;
- help from Jeffrey M. Wheeler and Ralph Spolenak LNM group;
- First test AR and 230 wppm -
  T= 25-100-200-300-400 °C;
- Hardness and elastic modulus measurements.

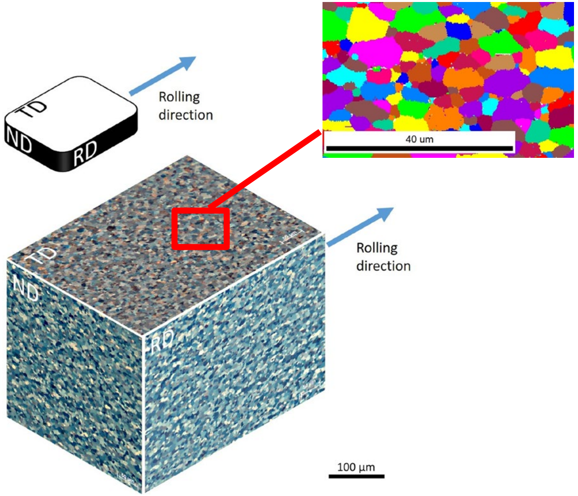

1) H charging

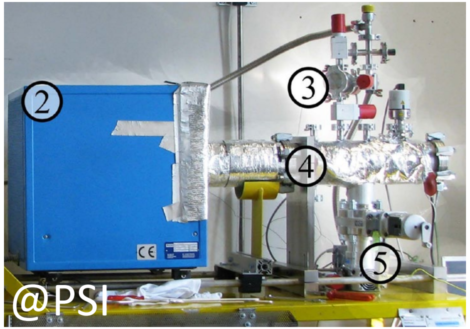

2) H measuring

3) indentation

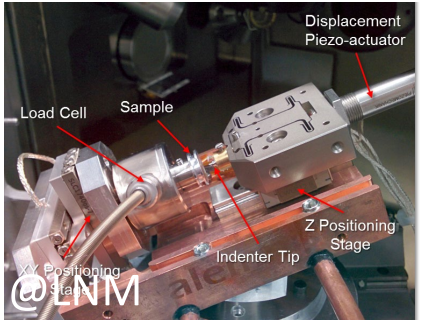

4) evaluation

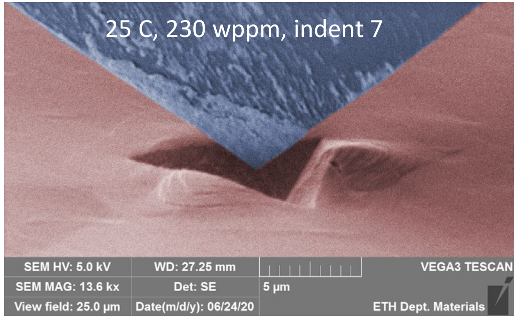

Results presented at:

Hot nano indentation results 1/2

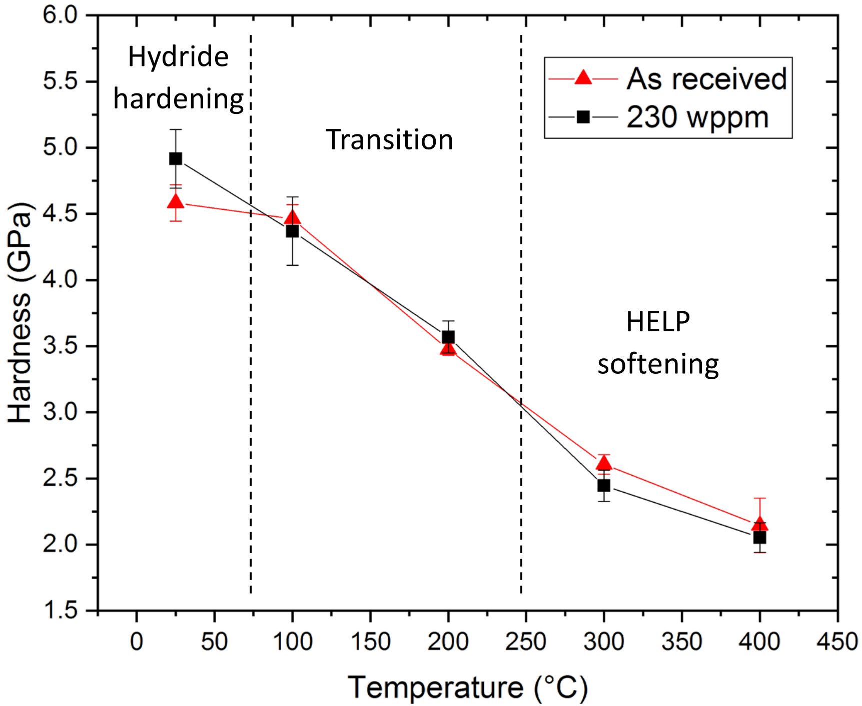

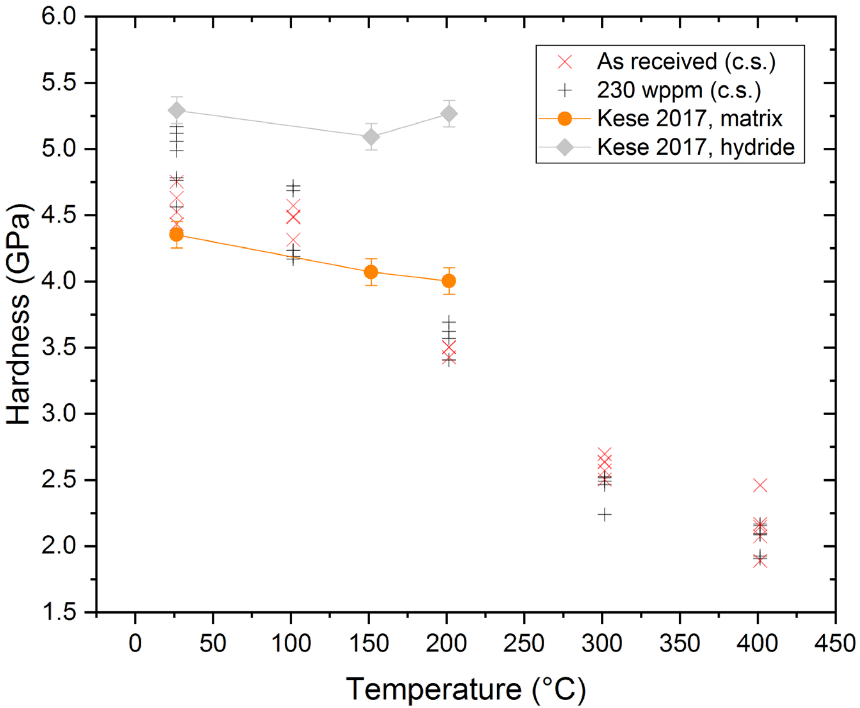

25 °C

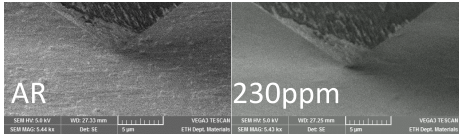

200 °C

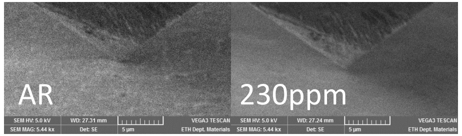

300 °C

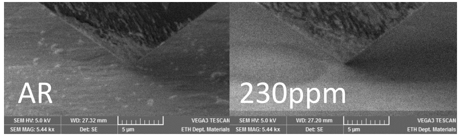

400 °C

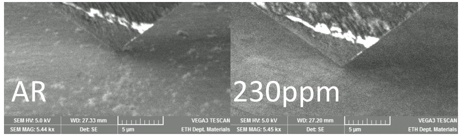

Results presented at: TopFuel SANTANDER SPAIN 2021

PAUL SCHERRER INSTITUT PSI

Hot nano indentation results 2/2

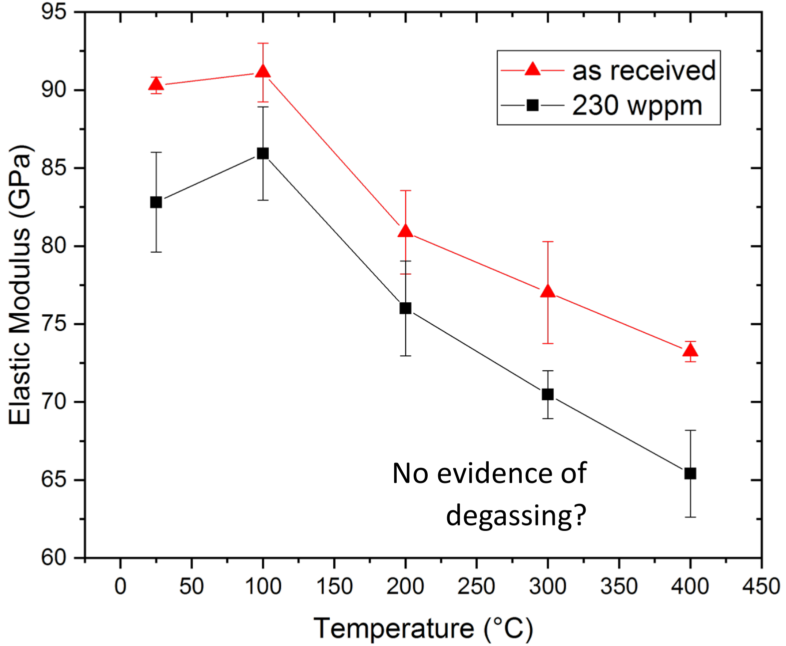

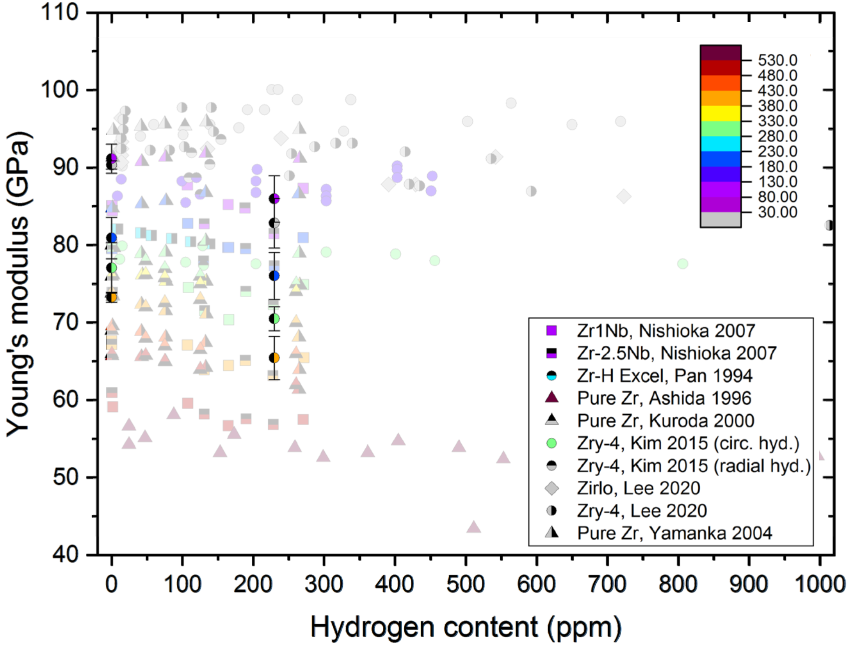

25 °C

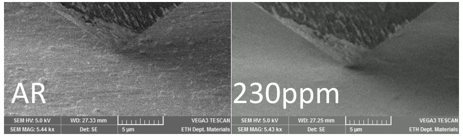

200 °C

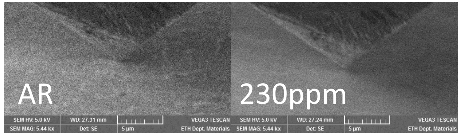

300 °C

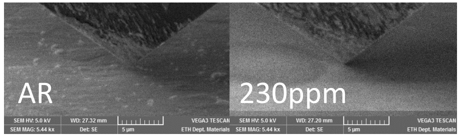

400 °C

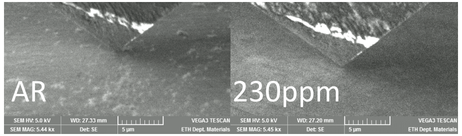

Microindentation

- To overcome the limitations of nanoindentation, a new set of mesurements has been performed with a newly restored Nikon High Temperature Microhardness Tester at ETH LNM;
- Test matrix consisting in Zry-4 material in as-received conditions and charged at **50, 90, 120, 230 and 700 wppm**;
- Indentations performed at room temperature **(25 °C), 100 °C, 200 °C, 300 °C, 400 °C** , in both **heating and cooling**

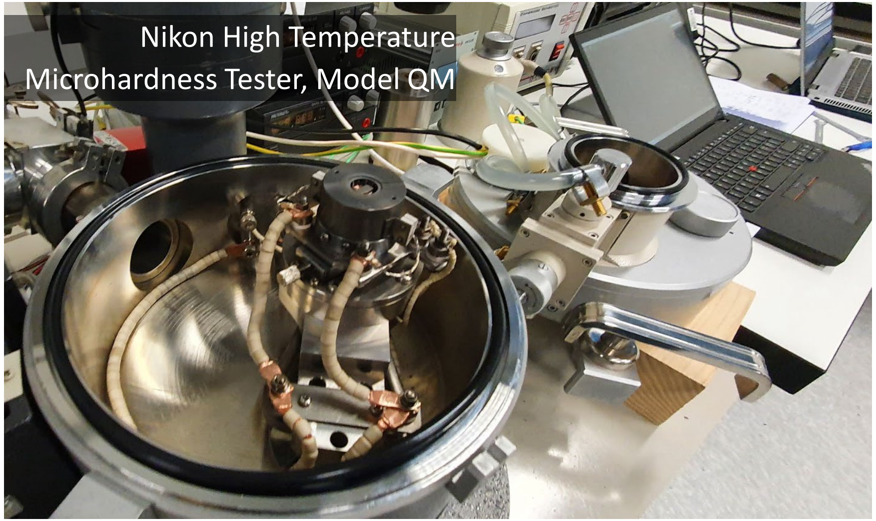

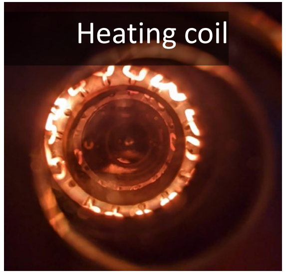

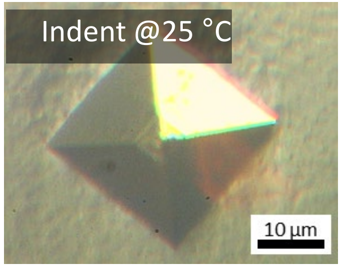

Hot micro-indentation results 1/2

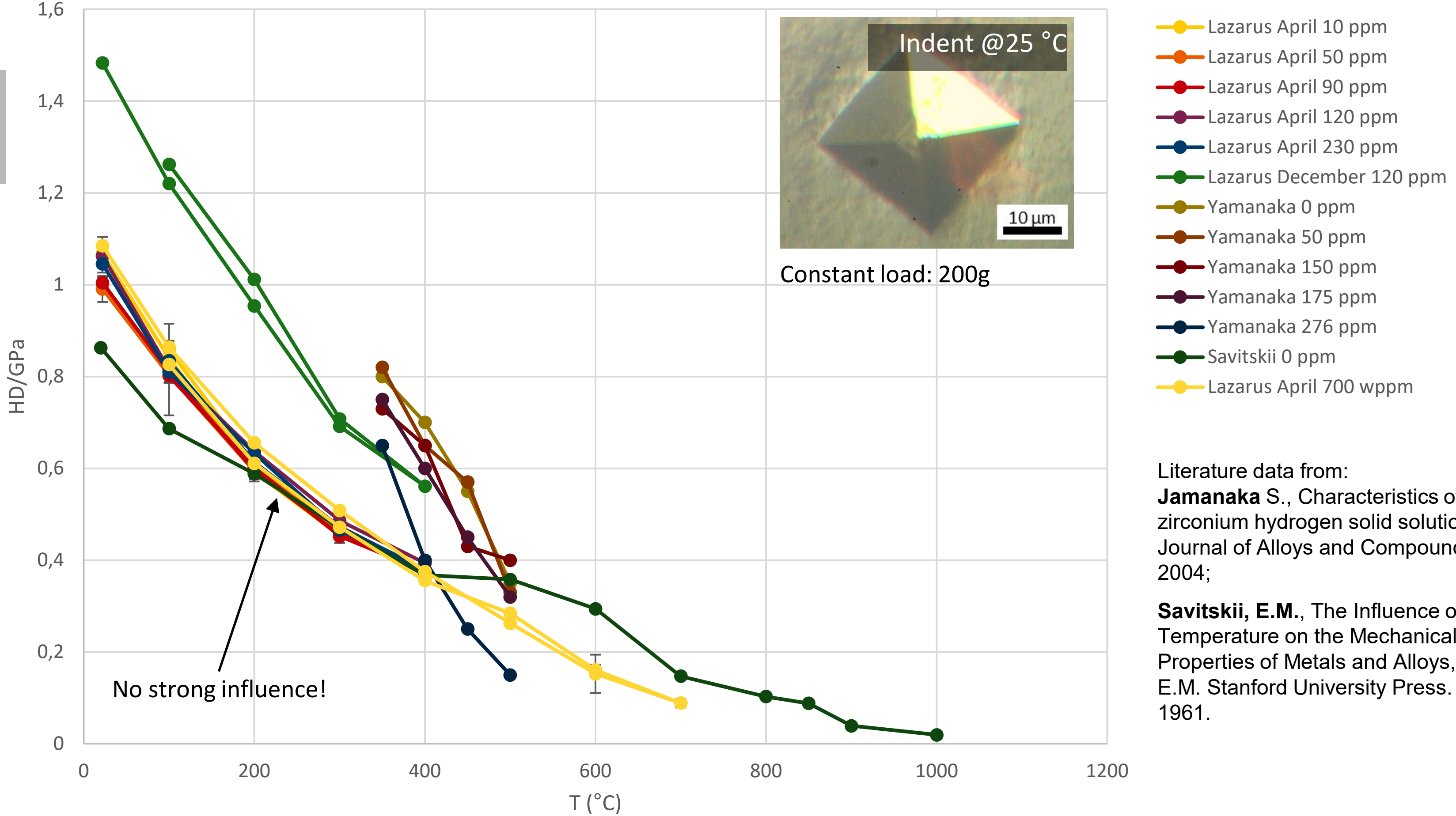

Literature data from:
Jamanaka S., Characteristics of zirconium hydrogen solid solution, Journal of Alloys and Compounds, 2004;

Savitskii, E.M., The Influence of Temperature on the Mechanical Properties of Metals and Alloys, E.M. Stanford University Press. 1961.

Hot micro-indentation results, in reference to AR

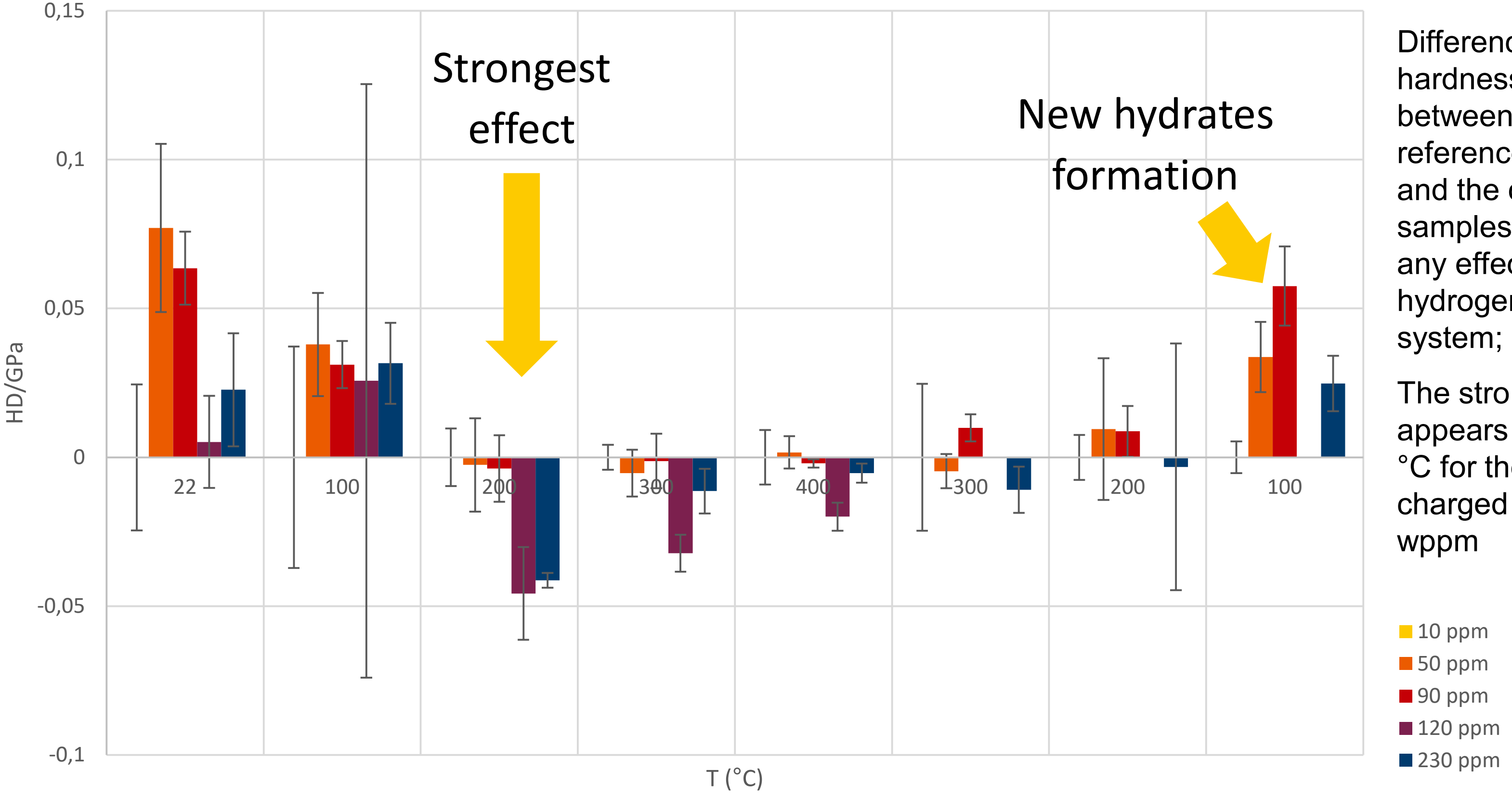

Difference in hardness values between the reference material and the charged samples highlight any effect due to the hydrogen in the system;

The stronger effect appears to be at 200 °C for the sample charged a 120 wppm

Effect of TSSD/TSSP?

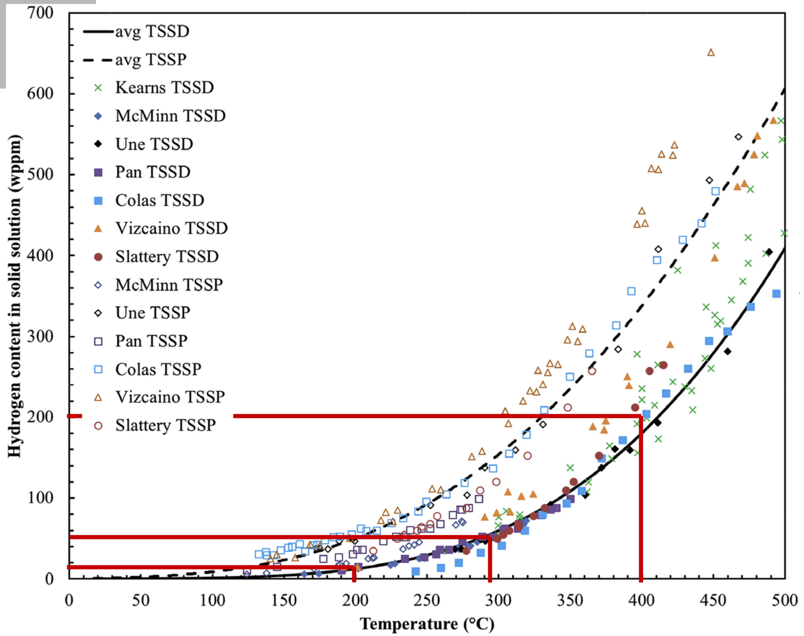

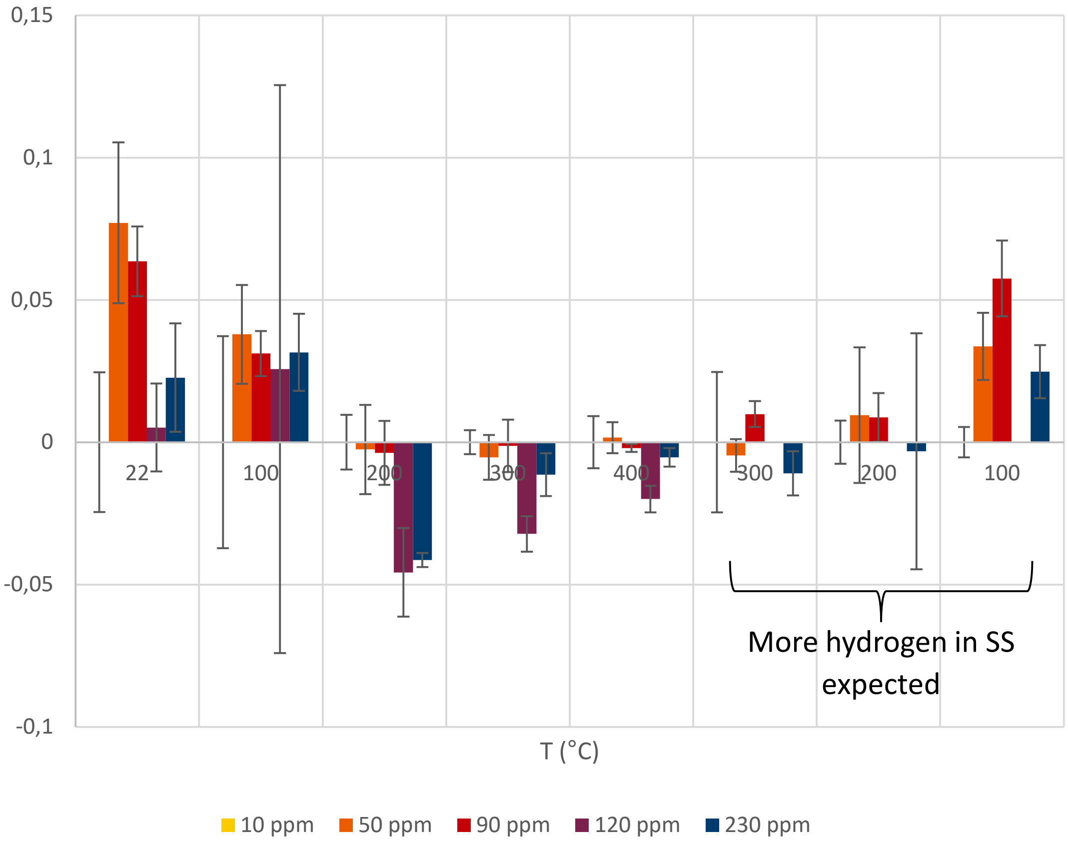

Is H escaping in high vacuum at increased temperatures?

Experimental setup

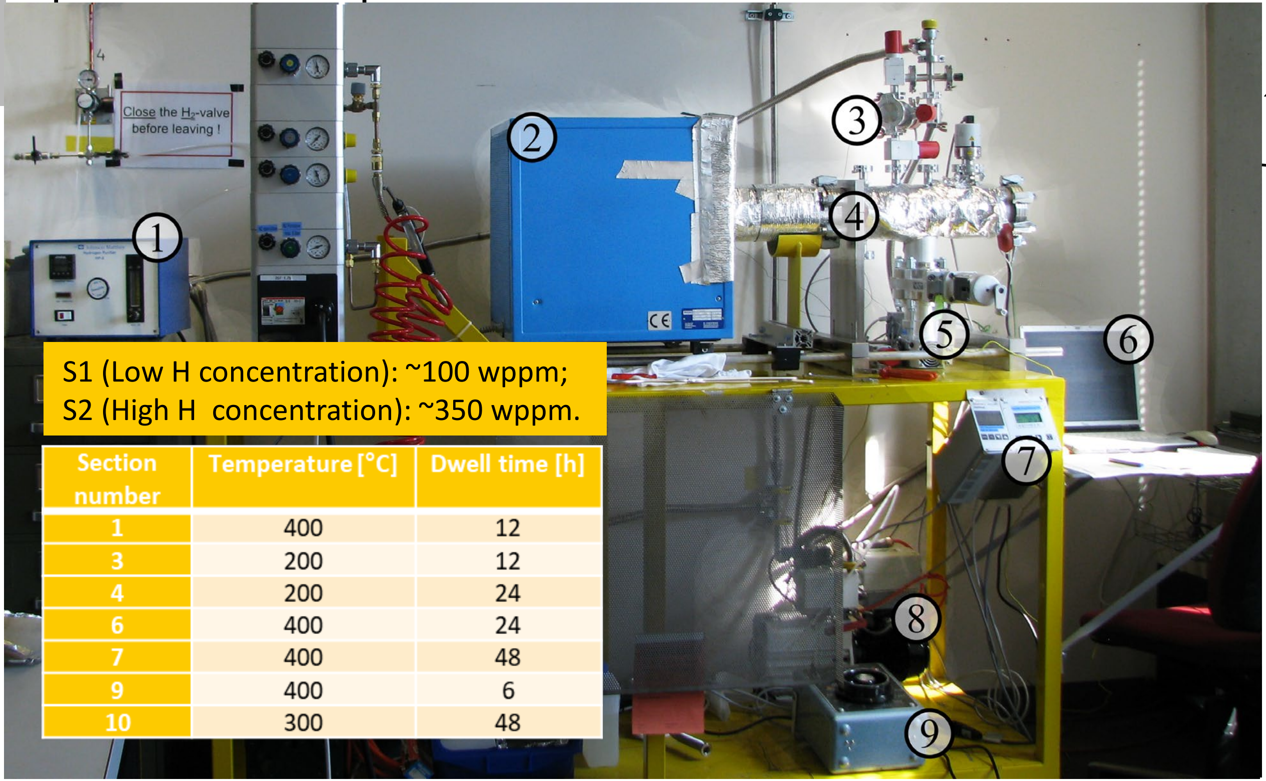

S1 (Low H concentration): ~100 wppm;
S2 (High H concentration): ~350 wppm.

Section number	Temperature [°C]	Dwell time [h]
1	400	12
3	200	12
4	200	24
6	400	24
7	400	48
9	400	6
10	300	48

Zr tube

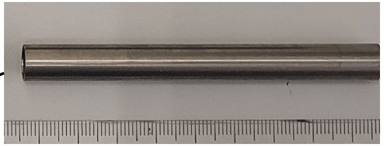

H-charging

Sectioning

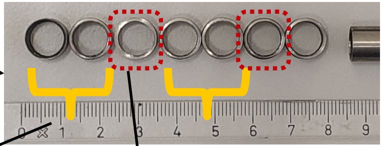

Vacuum degassing

Hydrogen measurement

Hydrogen measurement

PAUL SCHERRER INSTITUT

Hydrogen desorption results and modeling

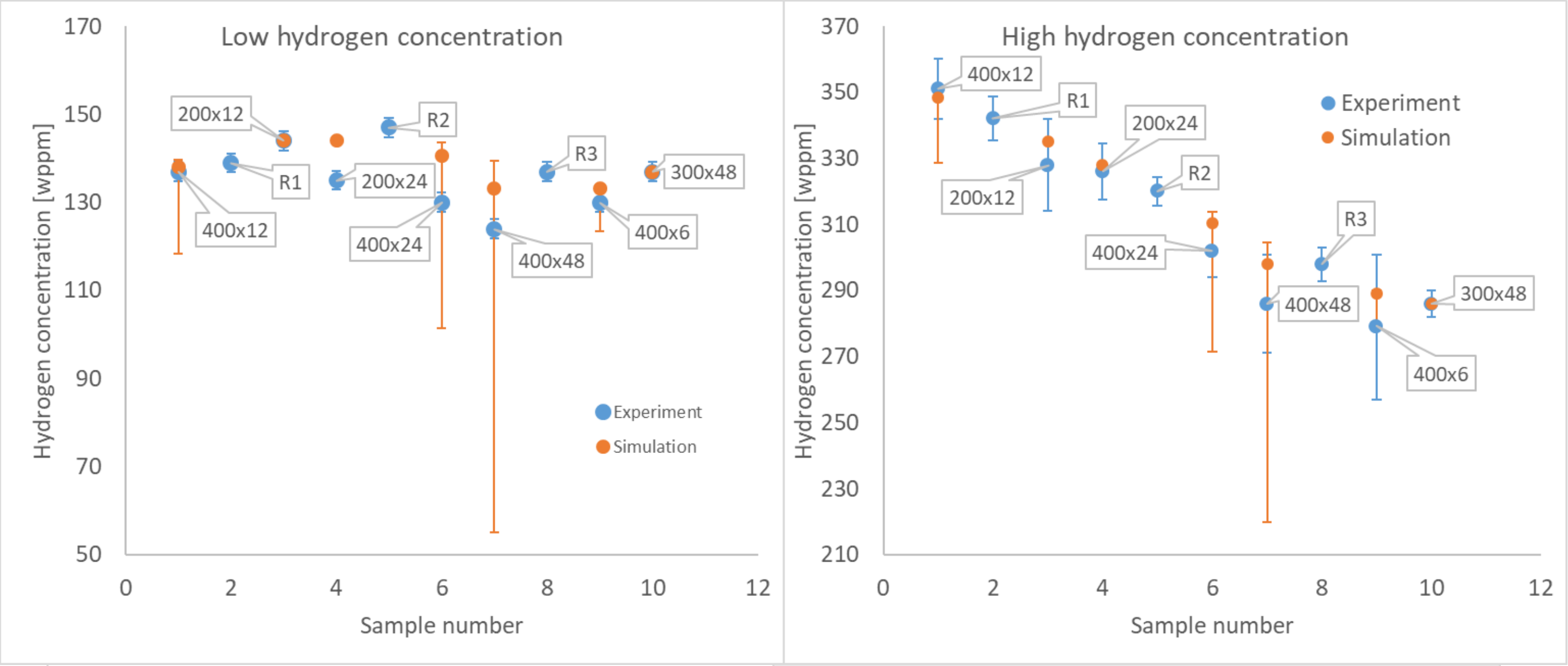

Micro-mechanical experiments in conditions of high vacuum/high temperature environment **can** be used as a tool to study the effect of hydrogen on the mechanical properties of zirconium alloys in the range of temperatures and hydrogen content relevant for the study of cladding mechanical behaviour in dry storage conditions (T<300 °C; H<350 wppm).

Conclusions

- As expected, the transition between hydrates-induced hardening and hydrogen-induced softening has been observed around TSS;
- In the micro-indentation experiment, the strongest softening effect is recorded around 200°C at hydrogen concentration between 100 and 200 wppm; The softening effect seems to be les pronounced at higher temperatures;
- Degassing of the samples due to the exposure to high-temperature/high vacuum has been excluded as possible explanation of the converging effect recorded at 400°C in both nanoindentation and microintentation experiments;

Many thanks at LNM/PSI and D-MATL/ETH for the support and lab usage, at MIDAS for the scientific discussion, and ENSI for the financial support.

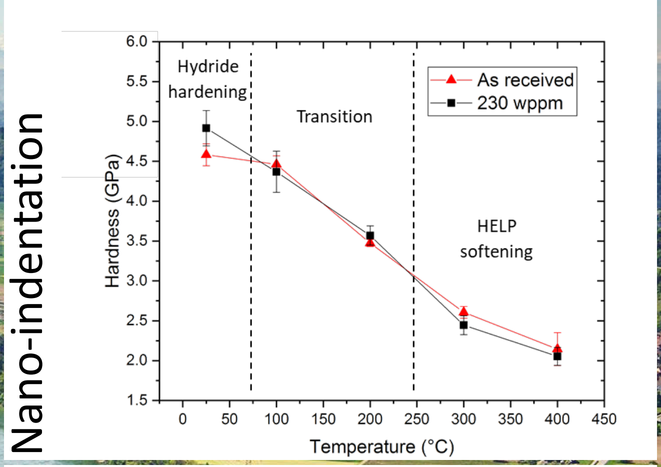

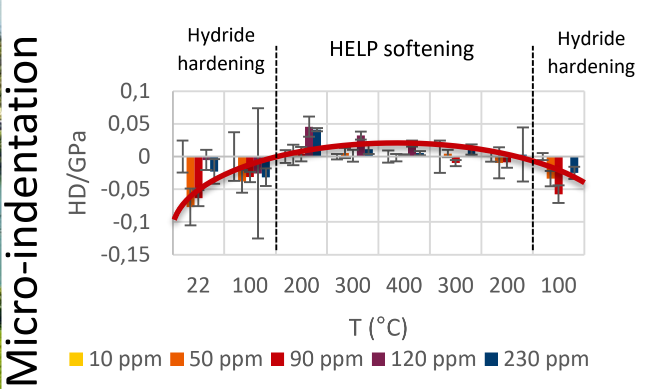

HELP effect in iron – still an open topic

- The HELP effect has been extensively studied in iron, but a complete understanding is still missing;
- H.K.Birnbaum, MSE 1994: Hydrogen-enhanced localized plasticity—a mechanism for hydrogen-related fracture
  https://doi.org/10.1016/0921-5093(94)90975-X
- Jinwoo Kim, JHE 2019: Microstructural and micro-mechanical characterization during hydrogen charging: An in situ scanning electron microscopy study
  https://doi.org/10.1016/j.ijhydene.2018.10.128
- Peng Gong, natureresearch 2020: kinetic model for which the hydrogen trapped locally in the cores of dislocations is responsible for the enhanced plasticity by TEM observations
  https://doi.org/10.1038/s41598-020-66965-z

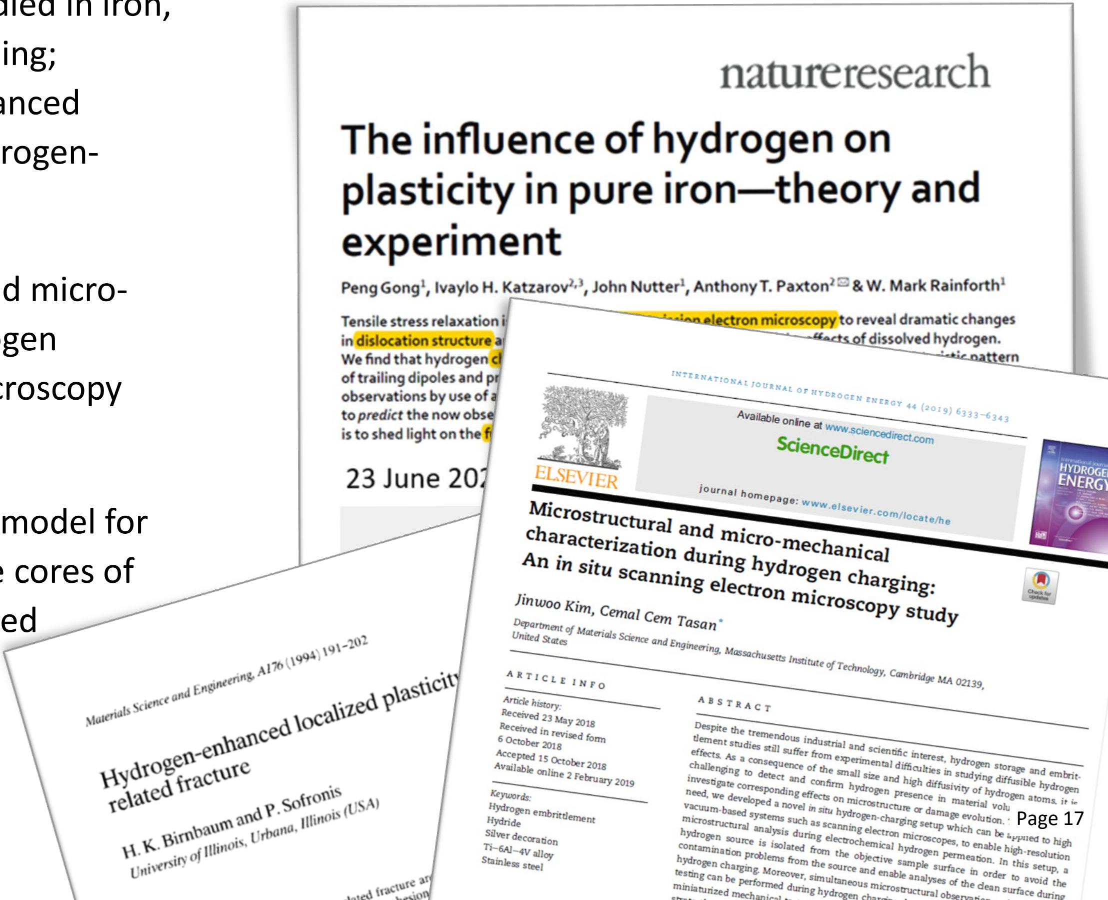

PAUL SCHERRER INSTITUT

Strain-rate jump analysis

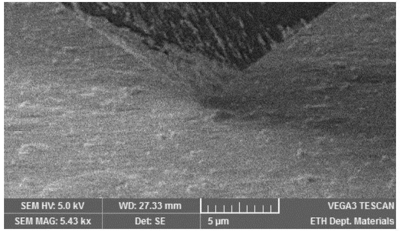

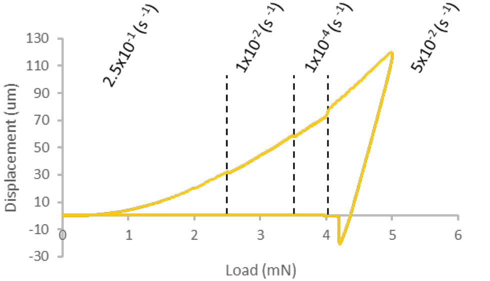

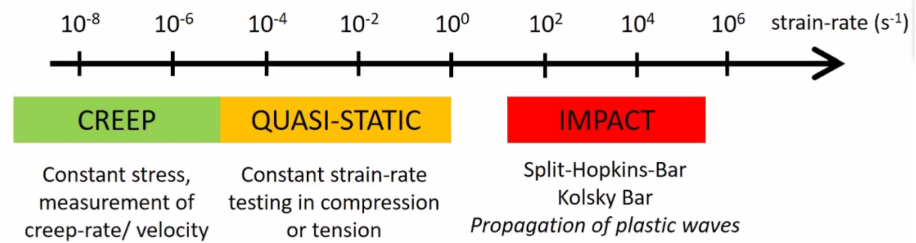

Determination of strain rate sensitivity, activation volume and activated dislocations

By strain rate jump analysis is possible to check the influence of the deformation rate on the dislocation motion activation.

By measuring the strain rate sensibility and activation volume is possible to model the response of the material from impact testing to creep;

As the HELP effect is dependent on the relative speed of dislocations and diffusion of hydrogen atmospheres, a strong influence of the deformation rate is expected.

4 indents for each temperature and condition have been performed with variable strain rate;

By interpolating the flow stress at different stain rates is possible to obtain the strain rate sensitivity, activation volume and activation energy;

Flow rate stress at different strain rates and temperatures has also been recorded.

Strain rate jumps analysis - results

STRAIN-RATE SENSITIVITY *m*

$$m = \frac{\partial \ln \sigma}{\partial \ln \dot{\varepsilon}} \sim \frac{\partial \ln H}{\partial \ln \dot{\varepsilon}} = \frac{\ln H_2 - \ln H_1}{\ln \dot{\varepsilon}_2 - \ln \dot{\varepsilon}_1}$$

ACTIVATION VOLUME *v**

$$v^* = C^* \cdot \sqrt{3} \cdot kT \cdot \frac{\partial \ln \dot{\varepsilon}}{\partial H} \sim C^* \cdot \sqrt{3} \cdot \frac{kT}{m \cdot H}$$

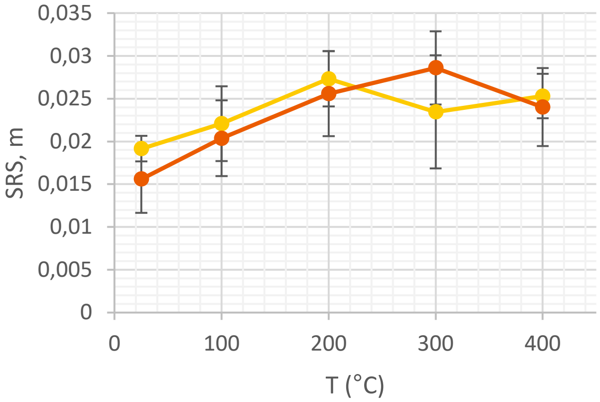

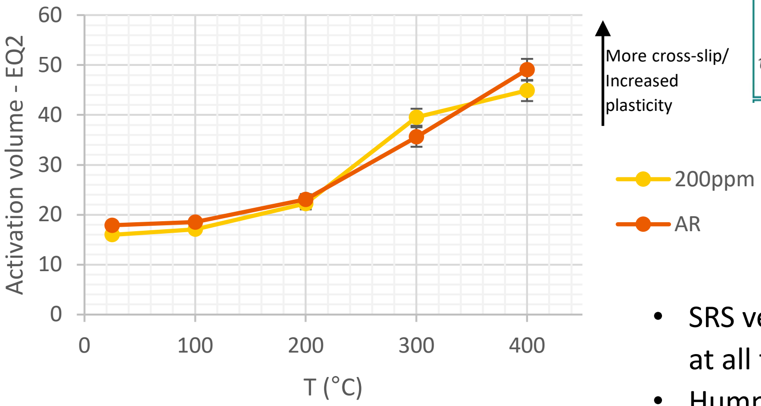

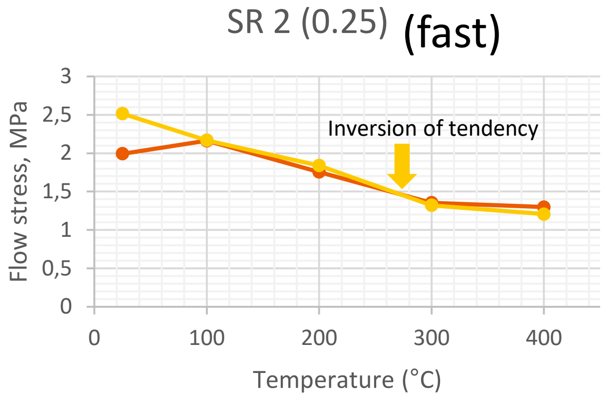

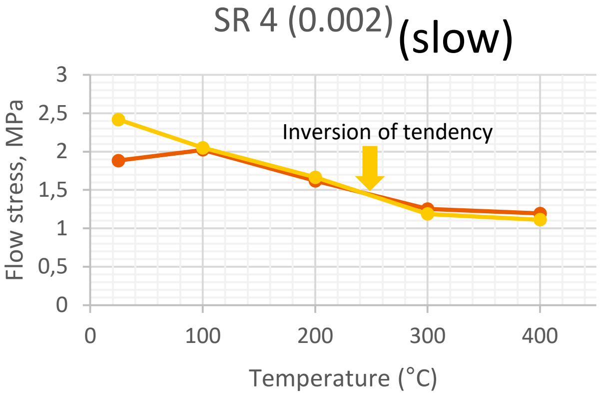

- SRS very low (solute drag forming) at all the temperatures;
- Hump in activation volume/SRS at 300°C.
- Higher flow stress of hydrated sample at room temperature;
- Slightly reduced flow stress for hydrated sample at 400°C
- Reduced flow stress at lower strain rates

Next steps (1/3): H Outgassing in high temperature/high vacuum conditions

- Even if we lose only 10% of hydrogen, this loss might be localized in the sampled area (close to the surface;
- To help solve this question, experiments and modeling collaboration with simulations **Piotr Konarski** took place during summer 2021
- Results will be presented at ETSON awards, Paris, Nov. 2021, but show indications of very limited H degassing in high-vacuum at T<400°C and uniform composition in the sample thickness

“[...] Understanding the degassing rate as a function of the temperature and hydrogen content at pressures typical for SEM analysis would therefore constitute a stepping-stone to enable the use of state-of-the-art micromechanical techniques to the study of the effect of hydrogen in zirconium at elevated temperatures.

In the presented study, the desorption of hydrogen has been studied in Zry-4 plate material charged between 100 and 700 wppm and at temperatures between 100 °C and 500 °C at a constant pressure of 10^{-5} mbar. Similar studies have been conducted in the past, but none in the range of temperatures and hydrogen concentration relevant for spent nuclear fuel storage. The results are fitted to a diffusion model and can be used to enable the study of hydrogen effect in zirconium alloys by elevated temperature in-situ micromechanical techniques in high vacuum conditions.”

Next steps (3/3): macro-mechanic experiments

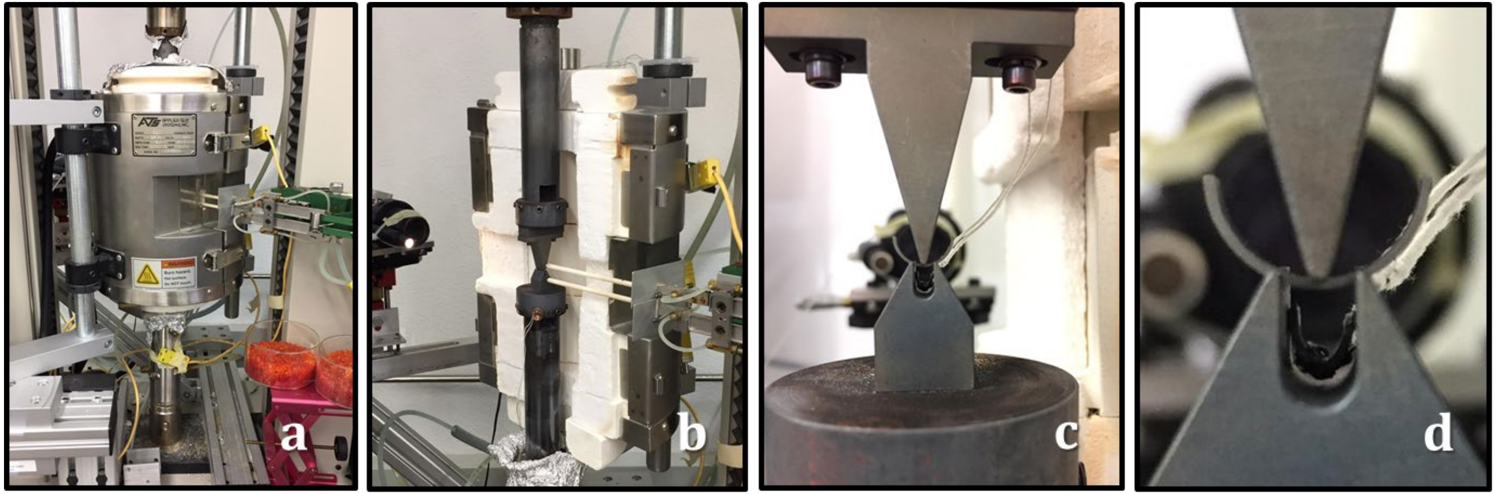

3-point bendibend testing of cladding specimens hydrogenatedand at elevated temperature is ongoing at PSI

HELP in Zr – Effect on mechanical properties

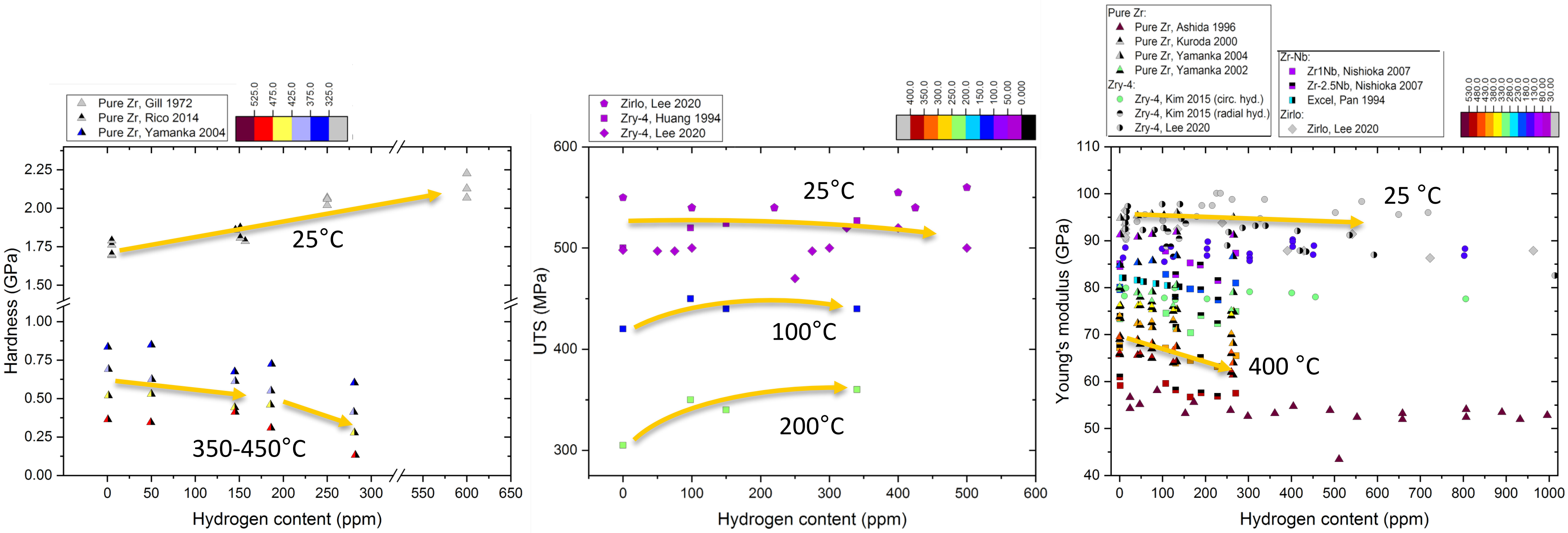

HELP effect has not been studied directly in Zr; however, indication of help effect can be found in the results from high temperature experiments in presence of hydrogen:

e.g. elastic moduli decrease with increased H in Solid Solution (SS), hardness decrease with increased H in SS, relative ultimate tensile strength increase with increase in H in SS.

Why HELP effect in Zr is relevant for nuclear waste safety?

- From literature, evidence of softening effect active in zirconium alloys at H concentration between 300 wppm and few wppm and temperatures between 100 °C and 400 °C;
- Conditions for HELP effect might be present during the transport phase of Spent Nuclear Fuel (SNF);
- HELP effect on mechanical performances on zirconium alloys is unclear.

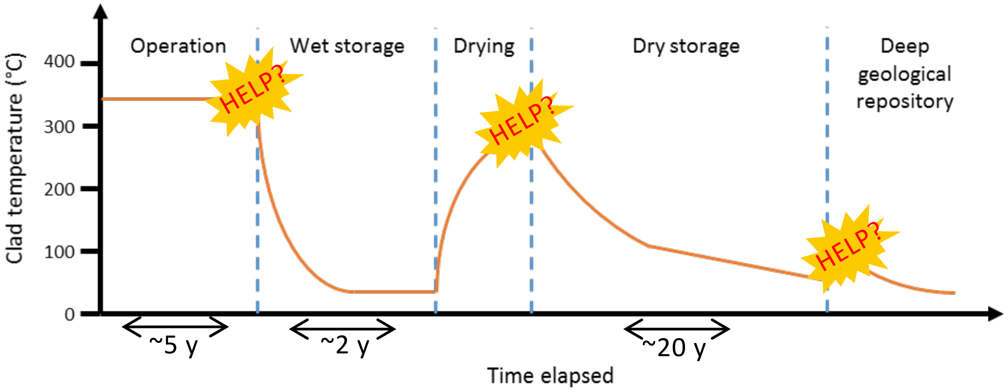

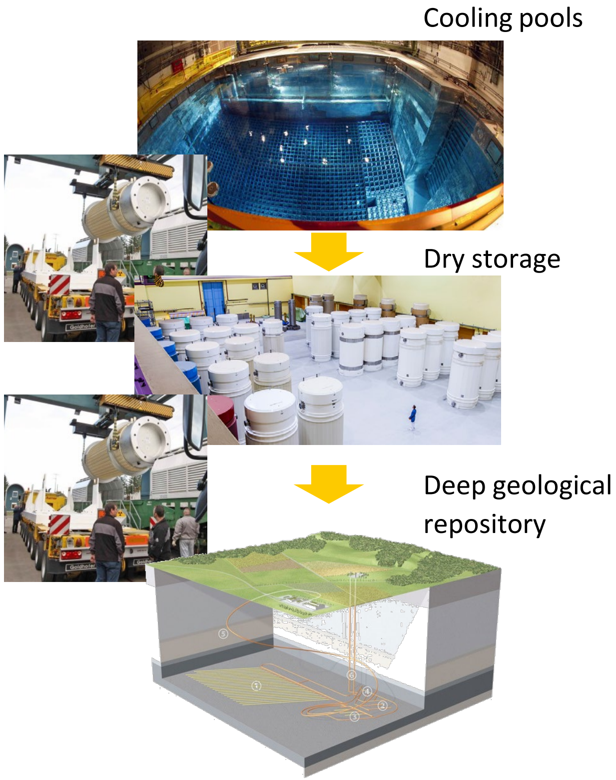

PAUL SCHERRER INSTITUT

HELP in Zr – Effects on creep behaviour

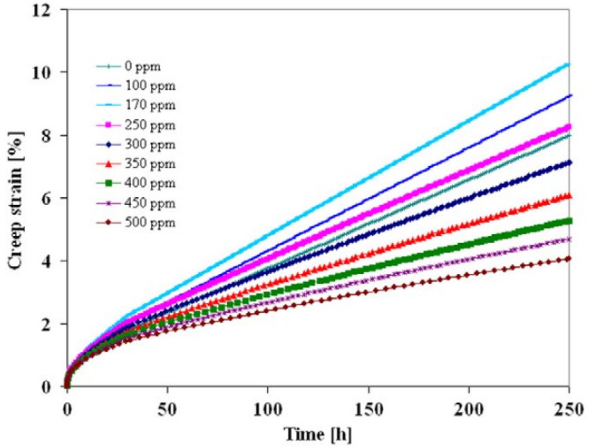

Fig. 8. Creep strain versus time curves at 400 °C under an applied stress of 120 MPa for different hydrogen contents.

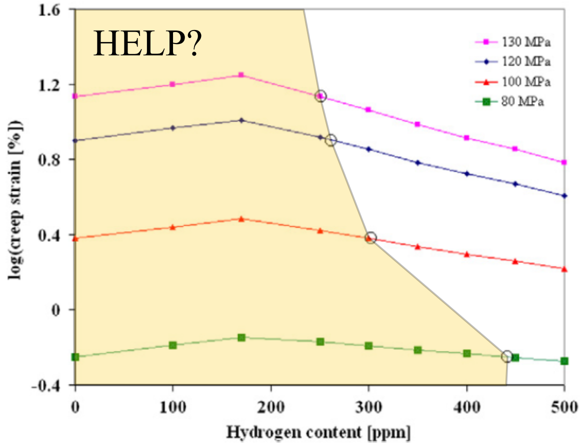

Fig. 10. Creep strain (on log scale) at 250 h as a function of hydrogen content for different applied stresses; the circles indicate the hydrogen contents for the same creep strain as without hydrogen.

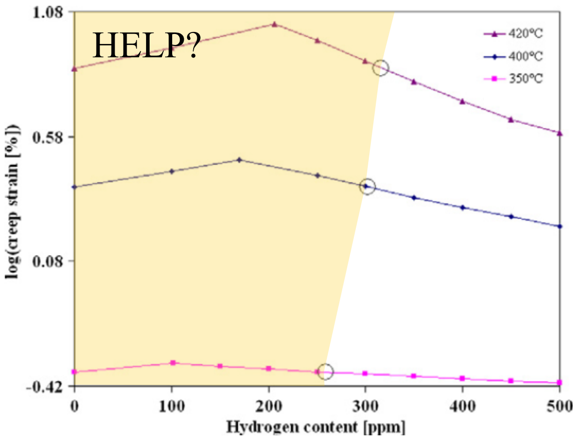

Fig. 12. Creep strain after 250 h as a function of hydrogen content at different temperatures under an applied stress of 100 MPa; the circles indicate the hydrogen contents for the same creep strain as without hydrogen.

Hydrogen in solid solution accelerates creep via HELP whereas hydrides cause a compressive stress around themselves due to their elastic behaviour; Evidence of this phenomena can be found in in the work V. Mallipudi et al., where creep strain increases with increase of the hydrogen content up to TSS, and decreases for a further increase of the hydrogen content.

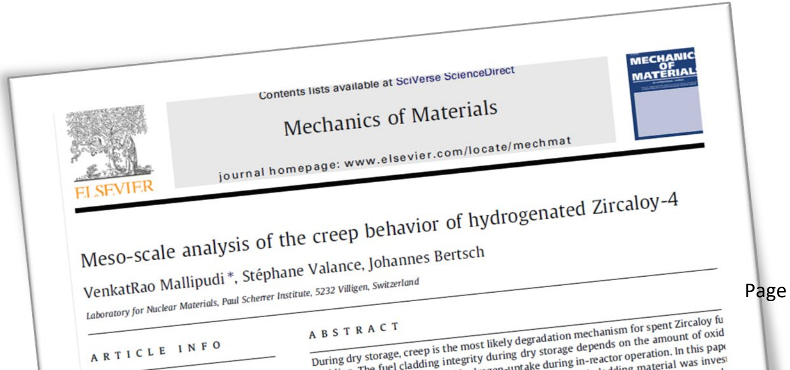
Contents lists available at SciVerse ScienceDirect

Mechanics of Materials

journal homepage: www.elsevier.com/locate/mechmat

ELSEVIER

MECHANICS OF MATERIALS

Meso-scale analysis of the creep behavior of hydrogenated Zircaloy-4

VenkatRao Mallipudi *, Stéphane Valance, Johannes Bertsch

Laboratory for Nuclear Materials, Paul Scherrer Institute, 5232 Villigen, Switzerland

ARTICLE INFO

ABSTRACT

During dry storage, creep is the most likely degradation mechanism for spent Zircaloy fu... during dry storage depends on the amount of oxid... during in-reactor operation. In this pape...

L.I. Duarte

PSI & ETH

Hydrogen quantification in zirconium cladding materials using high-resolution neutron radiography imaging

Zirconium alloys are used as fuel cladding in nuclear reactors due to their excellent combination of mechanical and chemical properties, and their low neutron absorption. It is of high importance that these components maintain integrity during their lifetime in the reactor and in dry-storage conditions.

During their operation in the reactor, the claddings are subject to aging mechanisms, driven by thermal- and pressure-changes, radiation and corrosion in contact with the cooling water. From the latter mechanism results hydrogen. While a fraction of it is released into the reactor environment, the other part is absorbed and diffuses into the cladding. The hydrogen has very limited solubility in zirconium alloys, and when the solid solubility is exceeded hydrides precipitation occurs, so-called hydrides are formed. These hydrides, which are less ductile than the surrounding metal matrix, can have detrimental effects on the mechanical properties of the fuel cladding, as, for example, the deterioration of fracture toughness or creep behavior of the material.

The hydrides morphology including the hydrides orientation with respect to mechanical loading plays an important role for the spent fuel integrity after unloading, for handling, intermediate dry storage and transportation. In this context, the hydrogen distribution in the cladding and the quantification is of high importance.

High-resolution neutron imaging with PSI's neutron microscope has become an excellent non-destructive tool providing a hydrogen quantification in un- and irradiated nuclear fuel claddings, with a sub-5 µm resolution and sub-10 wppm sensitivity to hydrogen. As hydrogen (hydrides) can often have a non-uniform distribution due to the high mobility of hydrogen interstitial atoms, the risk to the nuclear fuel rod integrity can significantly be raised. The application of the neutron microscopy on irradiated fuel cladding sections is unique. In this presentation, hydrogen distribution of un- and irradiated cladding rods samples from the Swiss nuclear power plants using the neutron microscope will be presented.

PAUL SCHERRER INSTITUT

Liliana Duarte, PhD ETH Zürich
Nuclear Fuels Group :: Laboratory for Nuclear Materials :: Paul Scherrer Institut

Hydrogen quantification in zirconium cladding materials using high-resolution neutron radiography

26th International Quench Workshop, 9th of December 2021, online

Nuclear Energy in Switzerland

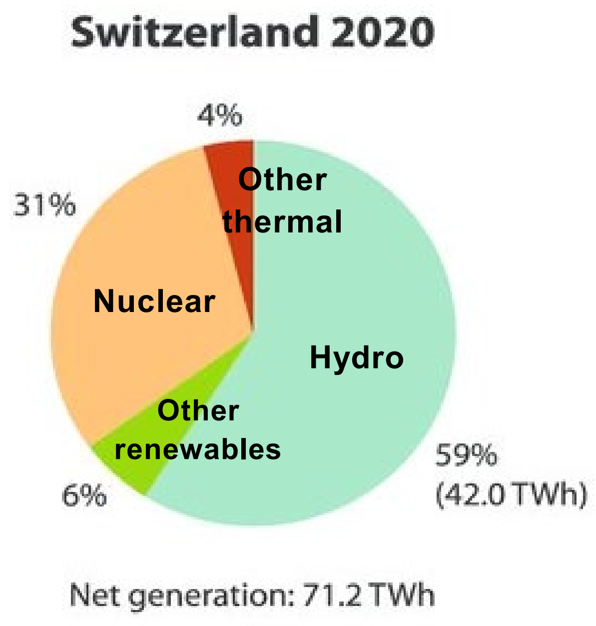

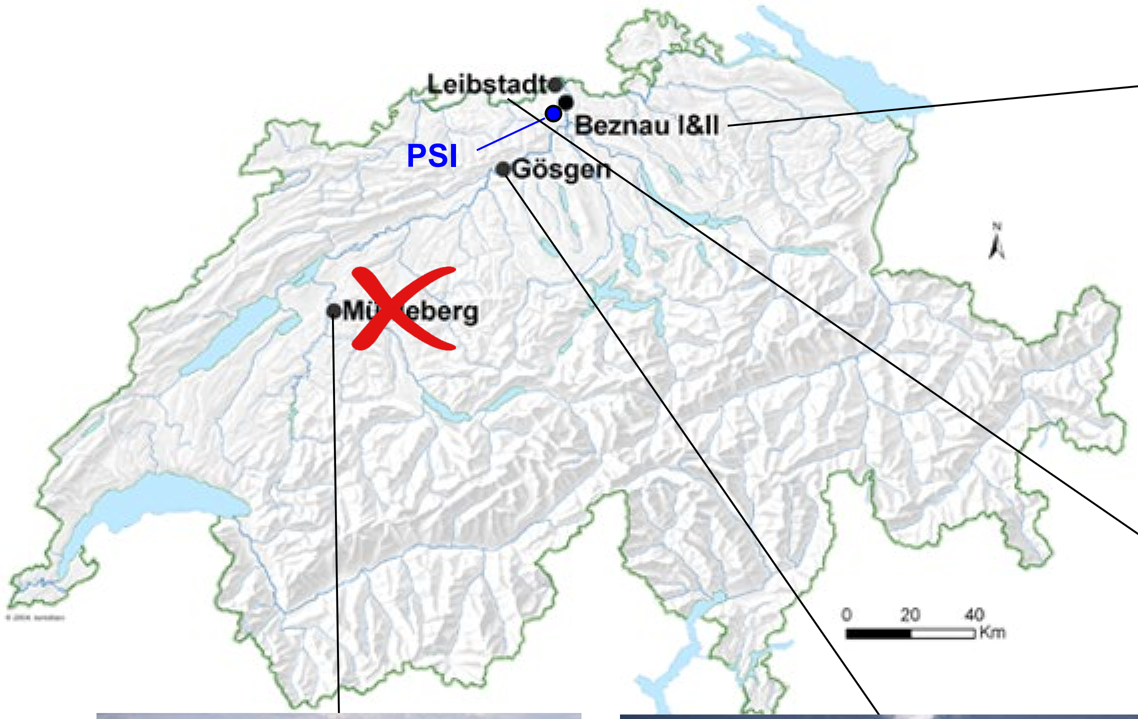

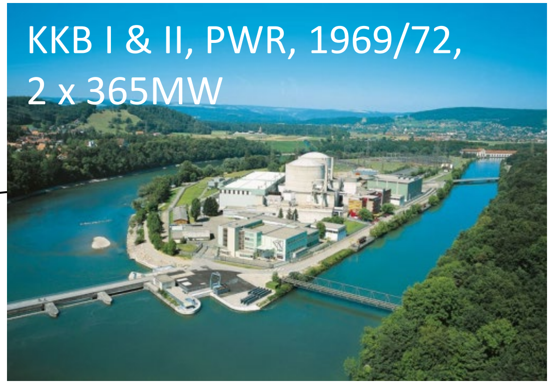

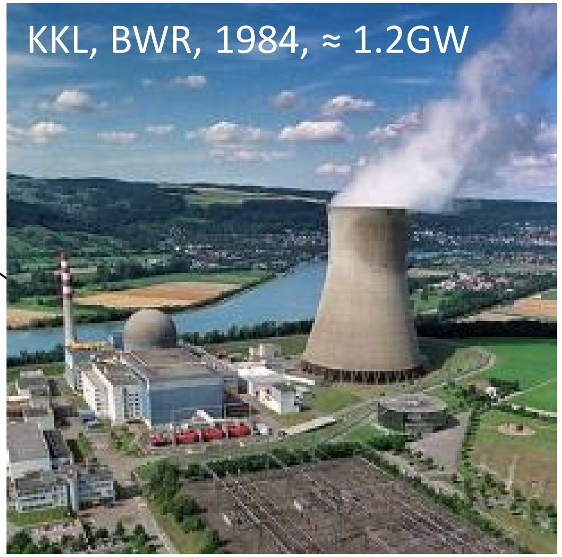

https://www.foronuclear.org/en/resources/infographics/nuclear-fuel/
Source of map: University of Bern, Canupis study

Nuclear Waste Management in Switzerland

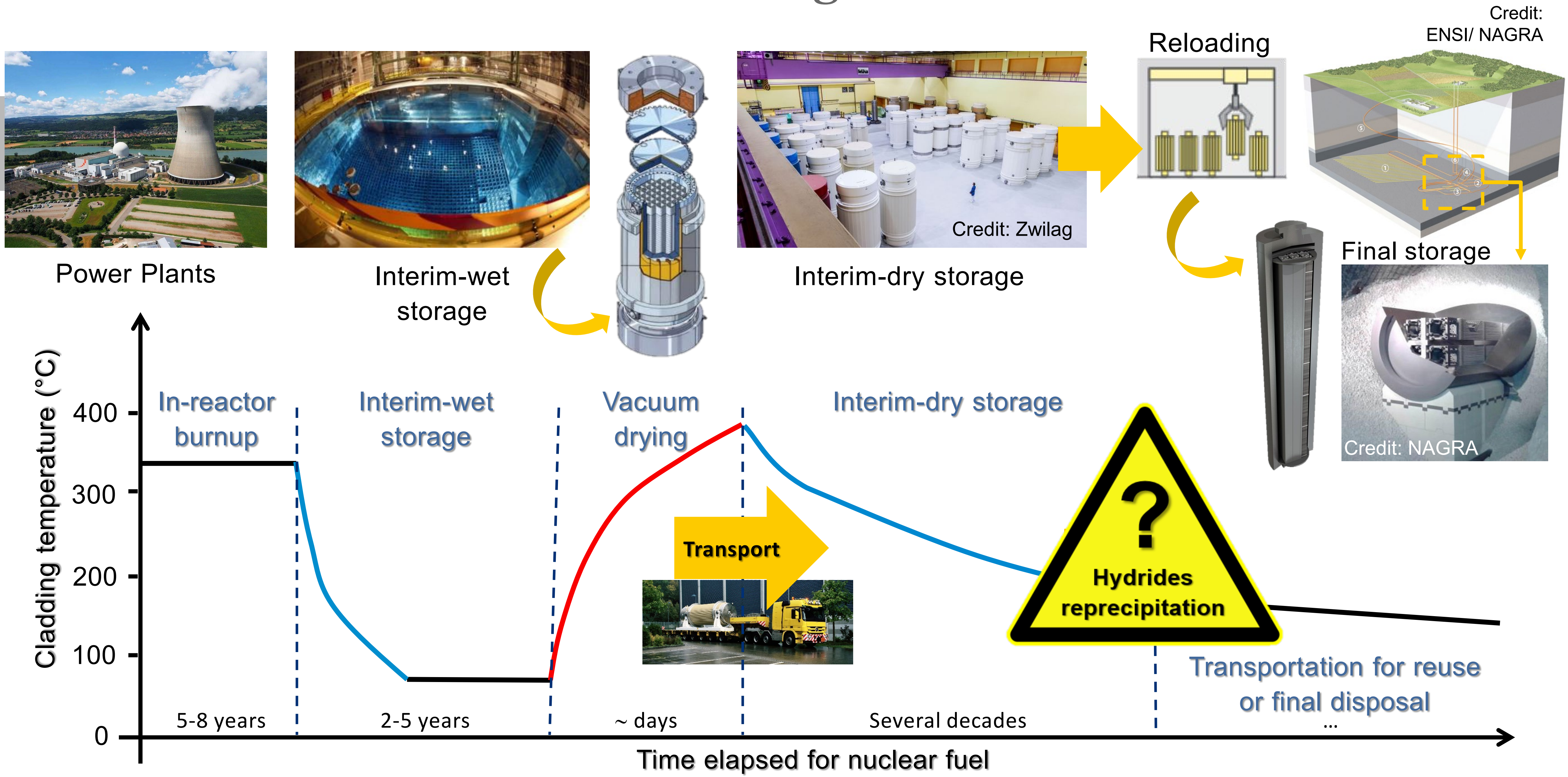

https://doi.org/10.1016/j.net.2017.08.012

PAUL SCHERRER INSTITUT PSI

Zirconium Cladding Materials and Hydrides

During reactor operation, hydrogen is created at the hot cladding surface:

- Hydrides Precipitation **(solubility and concentration)**
- Zirconium Hydrides → Embrittlement of cladding **(fracture toughness)**
- **Reorientation** of Hydrides **(Hoop stress, cooling rates)**

$$Zr + 2\,H_2O \rightarrow ZrO_2 + 2\,H_2$$

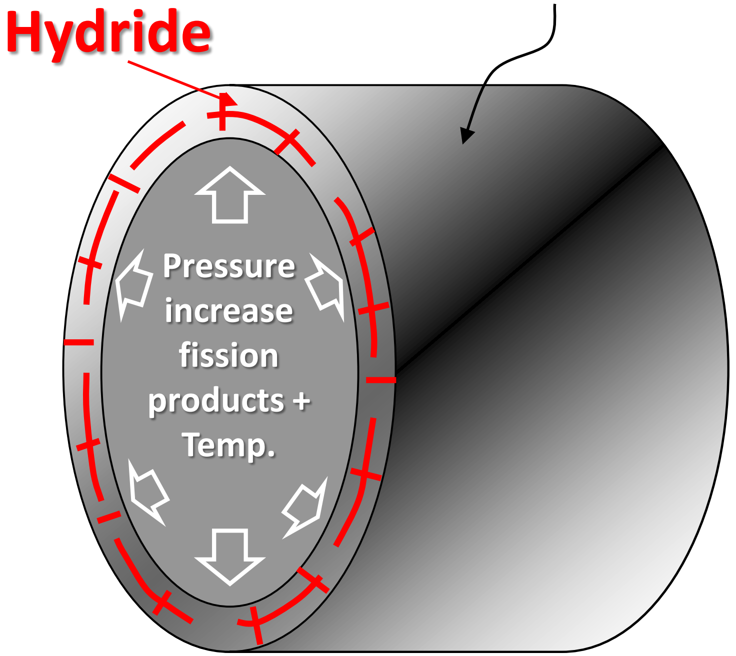

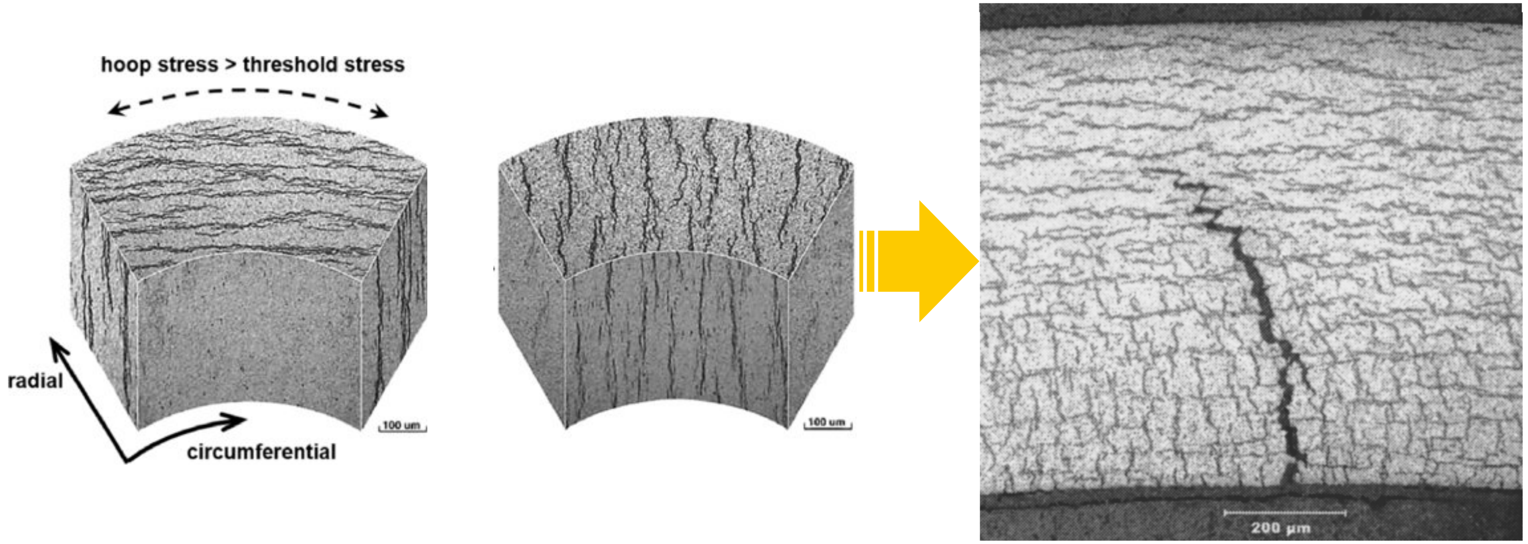

With increasing burn-up these effects can affect the mechanical stability of fuel claddings.

Safety and integrity of the NF claddings

R. S. Daum et al.; Journal of Nuclear Science and Technology, 43:9, 1054-1067(2012)

Zirconium cladding alloys: the role of liner

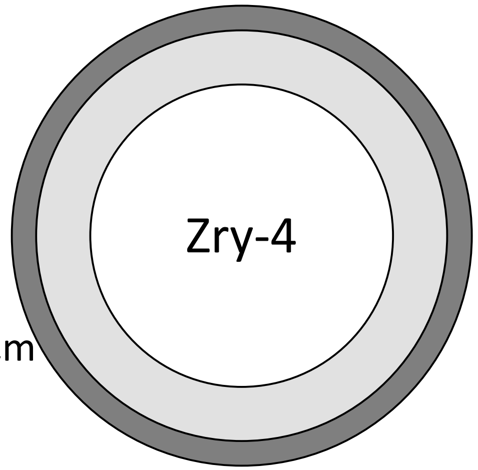

Outer Liner ~ 100µm
KKG/PWR

↑ Corrosion resistance
↑ Reduces the formation of radial hydrides leading to incipient cracks

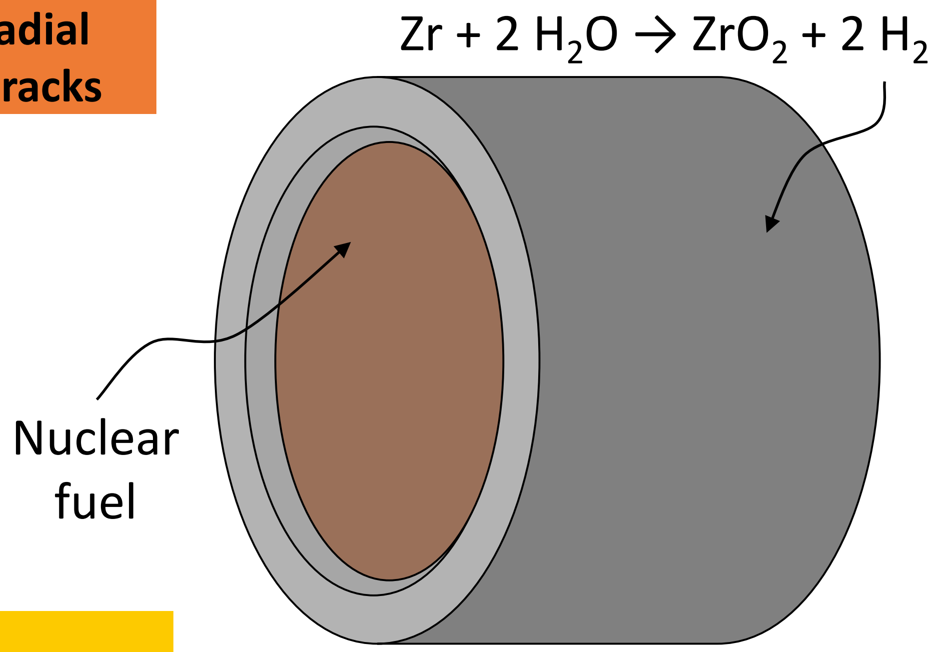

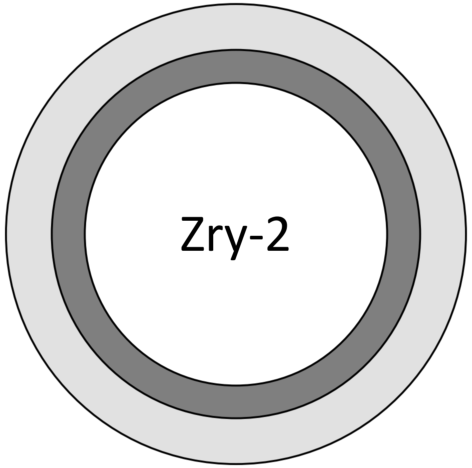

↑ Improves the PCI

Inner Liner ~70µm
KKL/BWR

Zirconium cladding alloys: the role of liner

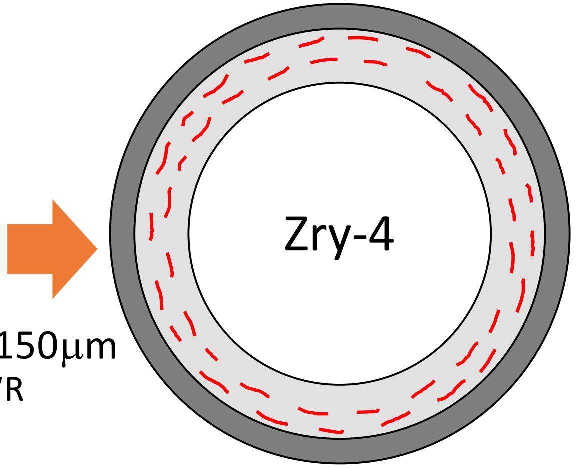

Outer Liner 150µm
KKG/PWR

↑ Corrosion resistance
↑ Reduces the formation of radial hydrides leading to incipient cracks

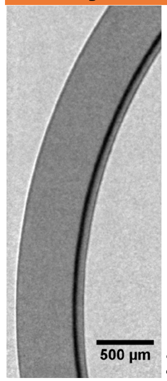

Outer liner
Zry-4 (DX-D4)

$Zr + 2\,H_2O \rightarrow ZrO_2 + 2\,H_2$

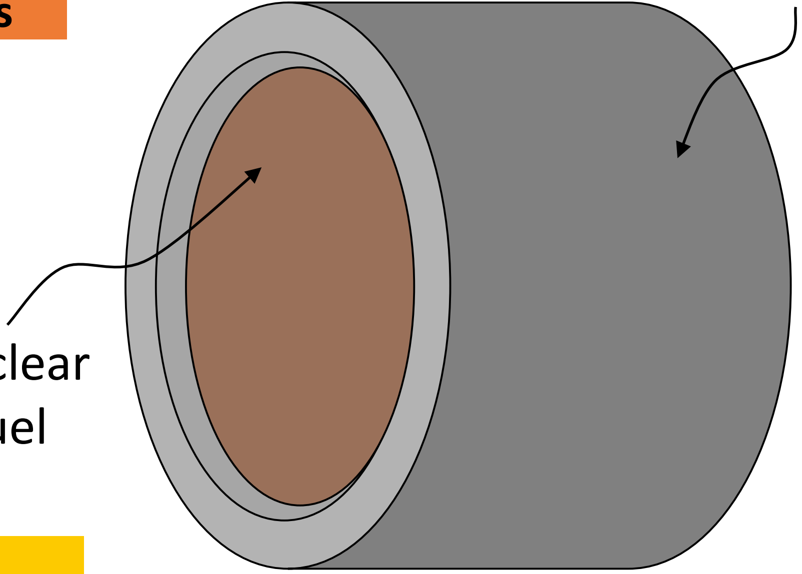

Nuclear fuel

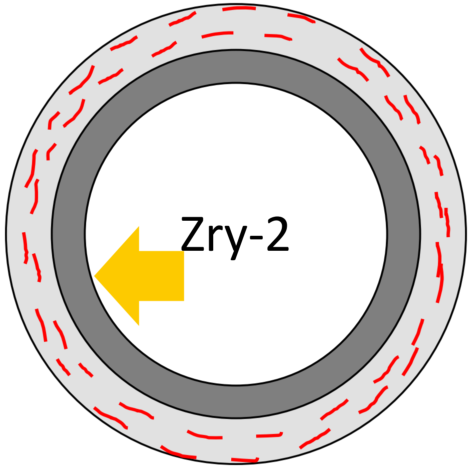

Inner Liner ~70µm
KKL/BWR

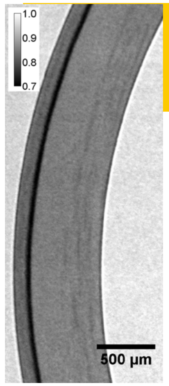

↑ Improves the PCI

Inner liner
Zry-2 (LTP)

Zirconium cladding alloys: the role of liner

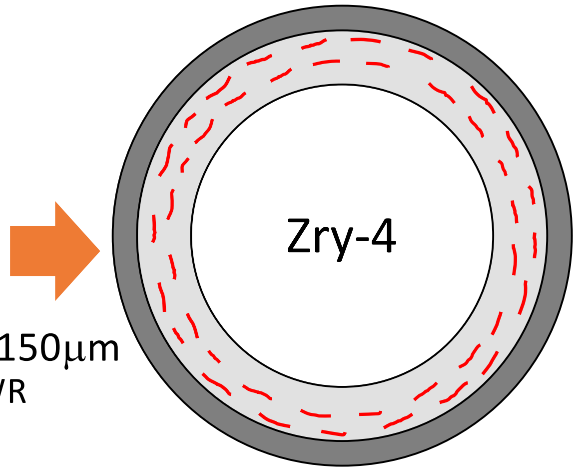

Outer Liner 150µm
KKG/PWR

↑ Corrosion resistance
↑ Reduces the formation of radial hydrides leading to incipient cracks

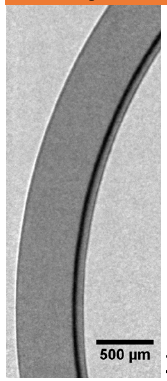

Outer liner
Zry-4 (DX-D4)

$Zr + 2\,H_2O \rightarrow ZrO_2 + 2\,H_2$

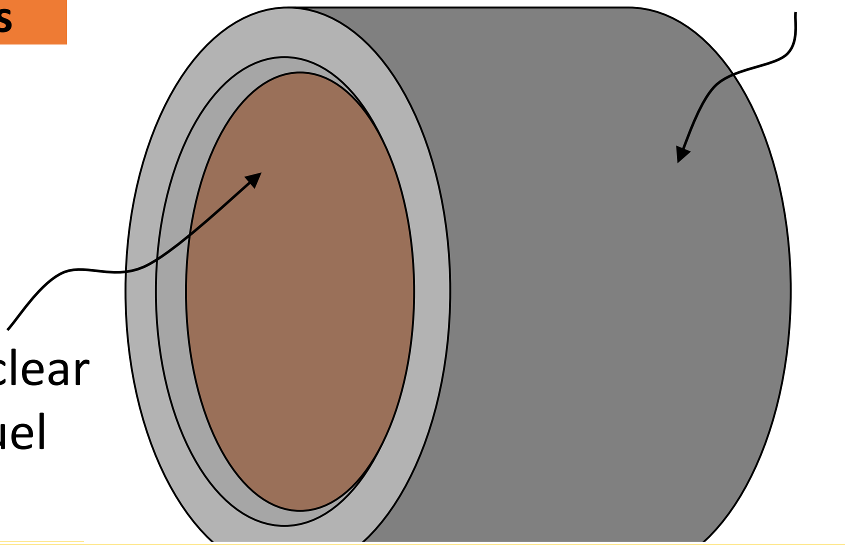

Nuclear fuel

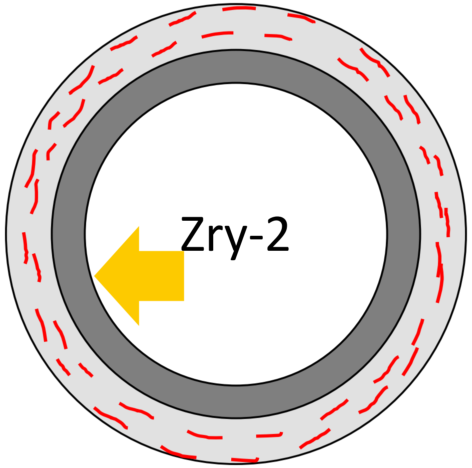

Inner Liner ~70µm
KKL/BWR

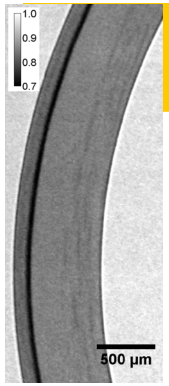

↑ Improves the PCI

Inner liner
Zry-2 (LTP)

QUESTIONS

- Role of the liner composition?
- Diffusion of Hydrogen into the liner?
- Influence of **Temperature and Stress** gradient in the hydrides migration?

Outline

- ✓ Motivation
- ✓ **Hydrogen Quantification by Neutron Radiography**
  - Characterization and quantification techniques Liner/temperature/stress
  - Hydrides evaluation in zirconium irradiated cladding
- ✓ **Summary**
- ✓ **Outlook**

PAUL SCHERRER INSTITUT PSI

Neutron radiography imaging (SINQ)

SINQ spallation neutron source (PSI,Switzerland)

Neutron microscope at POLDI/ICON thermal neutron beam line

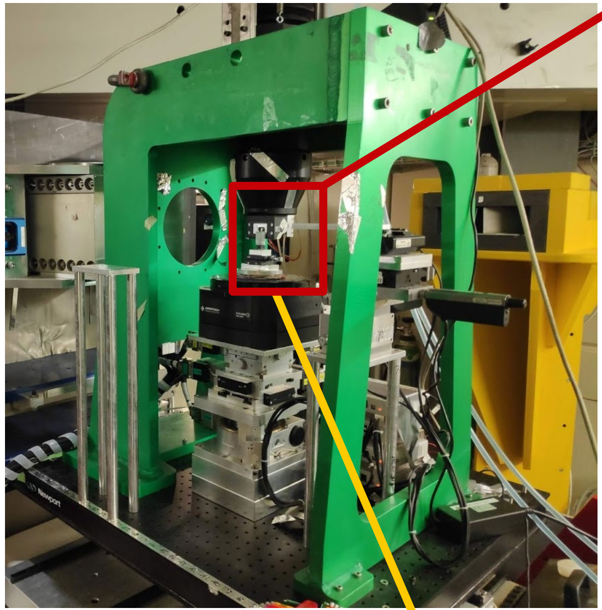

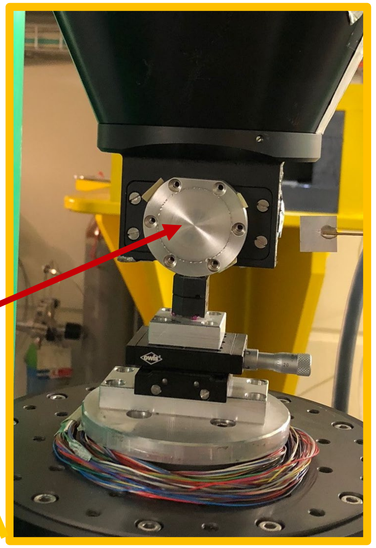

Comparison of mass attenuation coefficients for X-rays, γ-rays, thermal and fast neutrons.

T. Buecherl, and C. L. von Gostomski, 16th WCNDT, Montreal Canada, (20

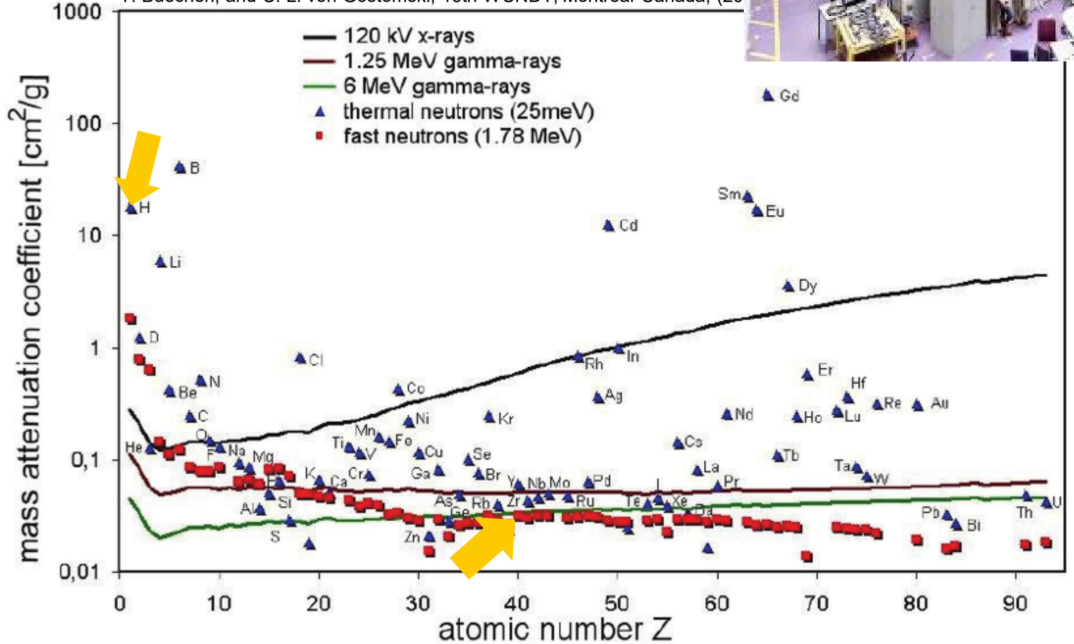

Active box container with irradiated sample inside

P. Trtik, R. Zubler, W. Gong, J. Bertsch, Liliana I. Duarte; (2020) Review of Scientific Instruments, 91(5), 056103

PAUL SCHERRER INSTITUT PSI

Neutron attenuation imaging

Neutron imaging principle

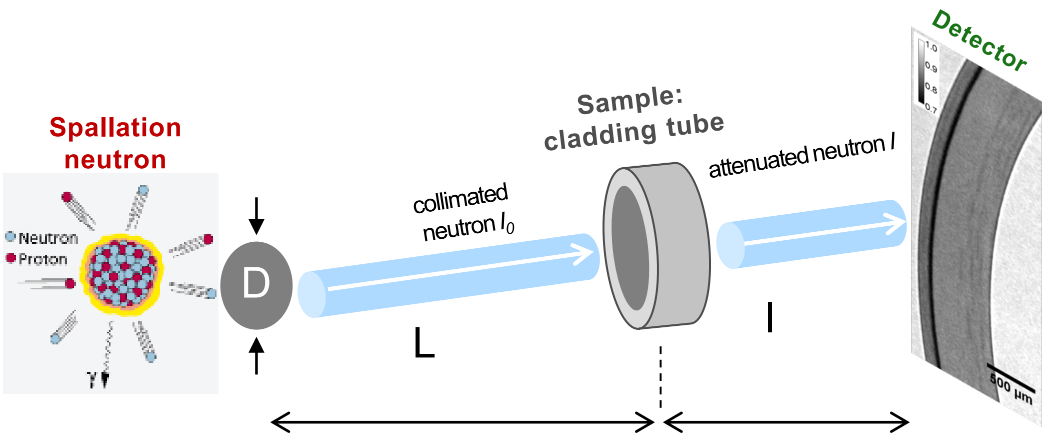

Beer-Lambert Law

$$\boldsymbol{T(x,y) = \frac{I(x,y)}{I_0(x,y)} = \exp(-\Sigma_{total}(x,y)\cdot s)}$$

$$\Sigma_{total}(x,y) = \Sigma_{composition}(x,y) + \Sigma_{microstructure}(x,y) + \boxed{c_H(x,y)\sigma_H}$$

absorption
incoherent scattering

diffuse scattering
(crystal defects)

H effect

Imaging Setup NRI

$^{157}Gd_2O_2S$:Tb scintillator, 3.5 µm thickness.

CCD camera, 2048 × 2048 pixels, pixel size of 2.7 µm.

L/D ratio ~220, exposure 3min×5, 1min×30

Tube segments 4.5mm // neutron beam

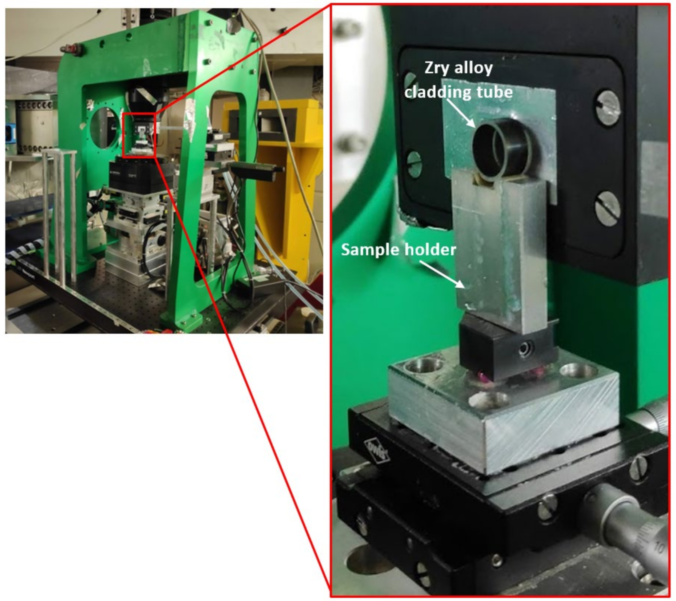

Hydrogen quantification in Zr alloys with liner DX-D4 cladding Experimental vs. Simulation

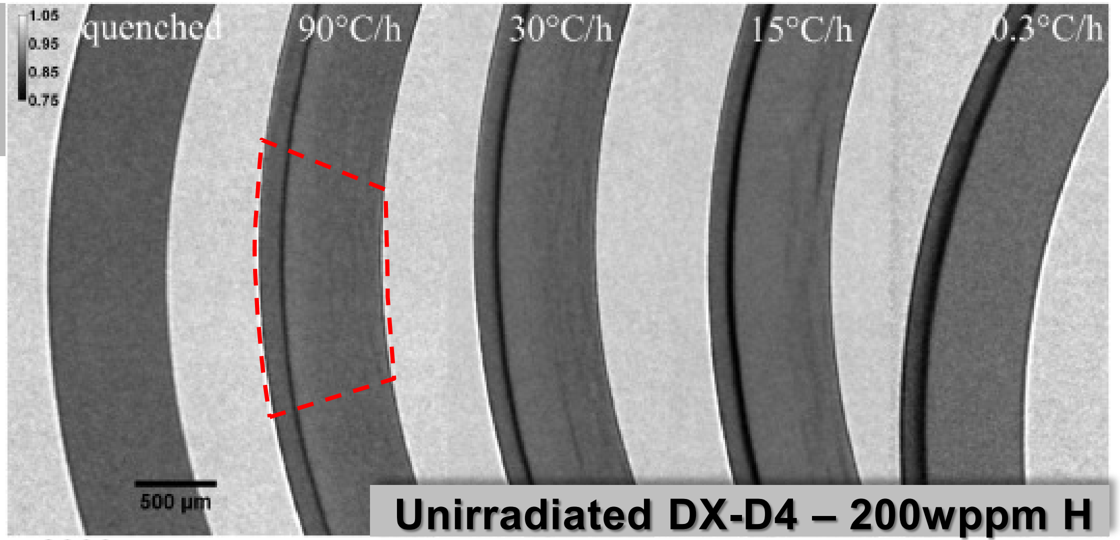

W. Gong, P. Trtik, A.W. Colldeweih, L.I. Duarte, M. Grosse, E. Lehmann, J. Bertsch; JNM, 526 (2019) 151757

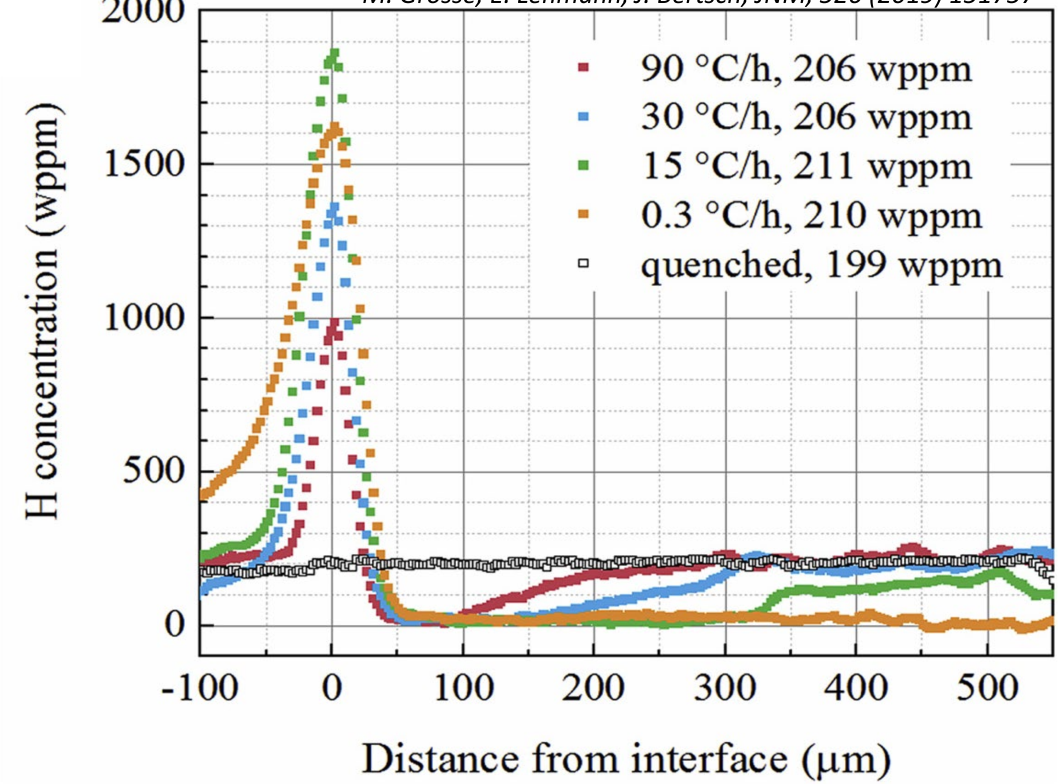

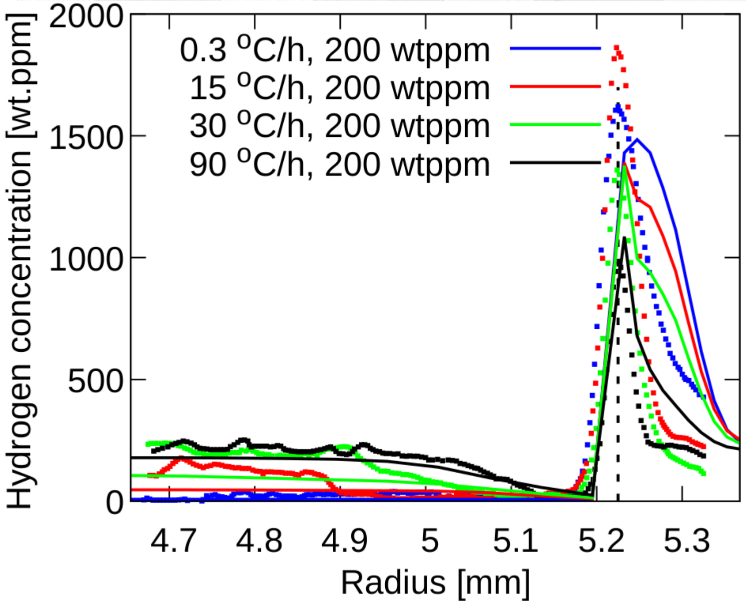

***Simulation of hydrogen distribution in the NF cladding with liner and experimental validation, P. Konarski, C. Cozzo, G. Khvostov, H. Ferroukhi (LRT/NES)**

*P. Konarski, C. Cozzo, G. Khvostov, H. Ferroukhi; TopFuel 2021 Conference, Santander, October 2021

Hydrogen redistribution in the liner

LTP2, No Liner, ~200wppm Hydrogen

AR | Q | 30 °C/h | 3 °C/h

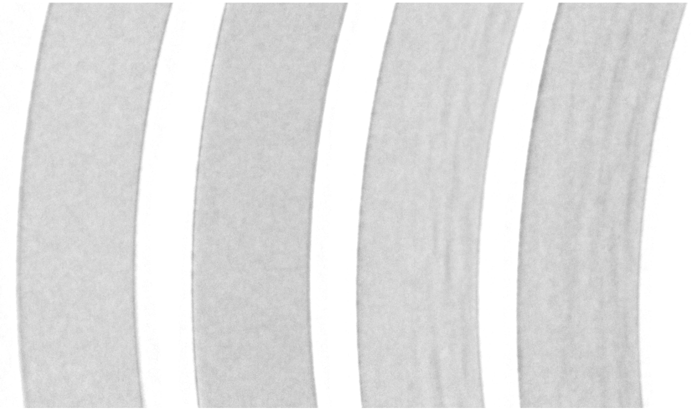

LTP, Fe-liner, ~200wppm Hydrogen

AR | Q | 30 °C/h | 3 °C/h

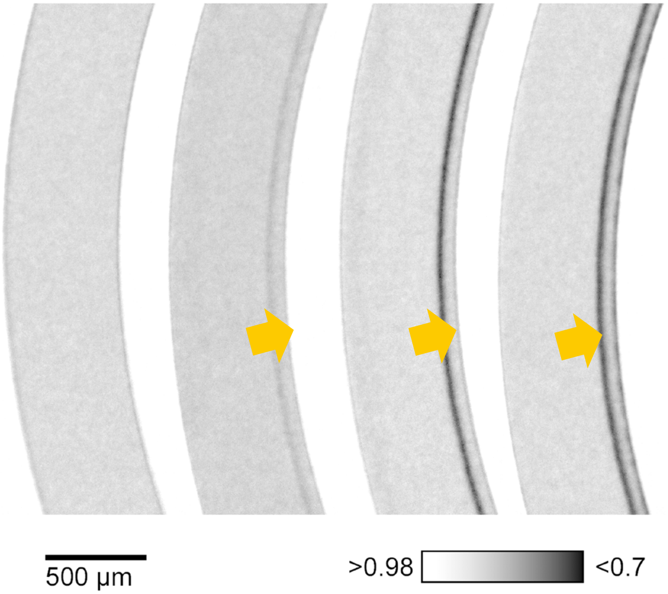

DIC, 200ppm, 30 C/h

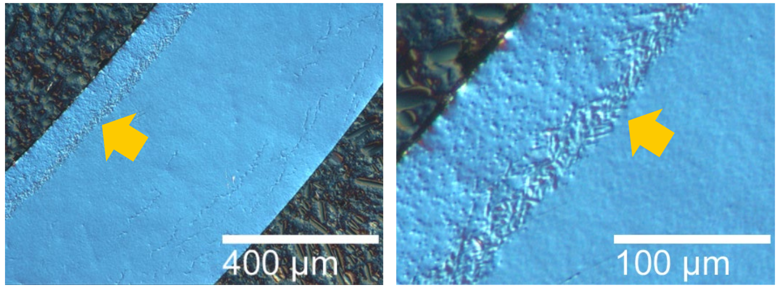

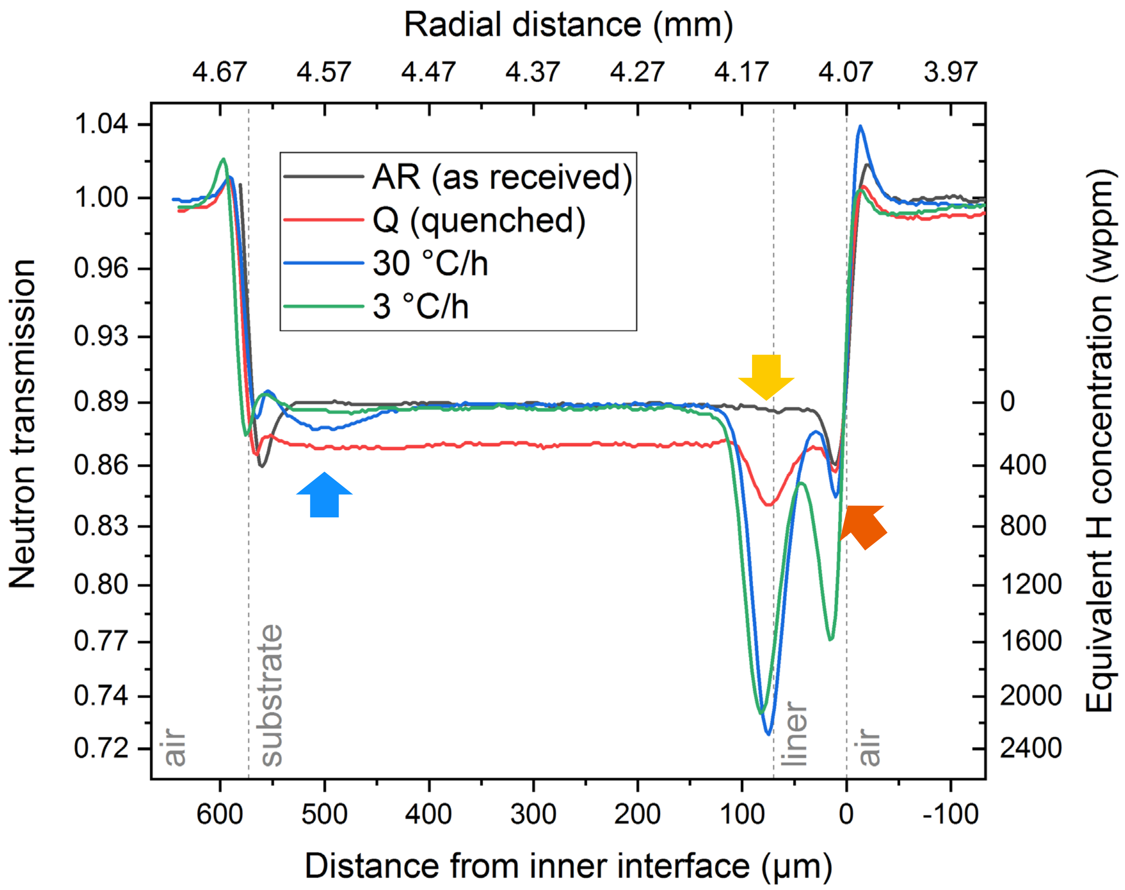

Hydrogen redistribution in the liner induced by temperature

LK3/L, Sn-liner, ~200wppm Hydrogen

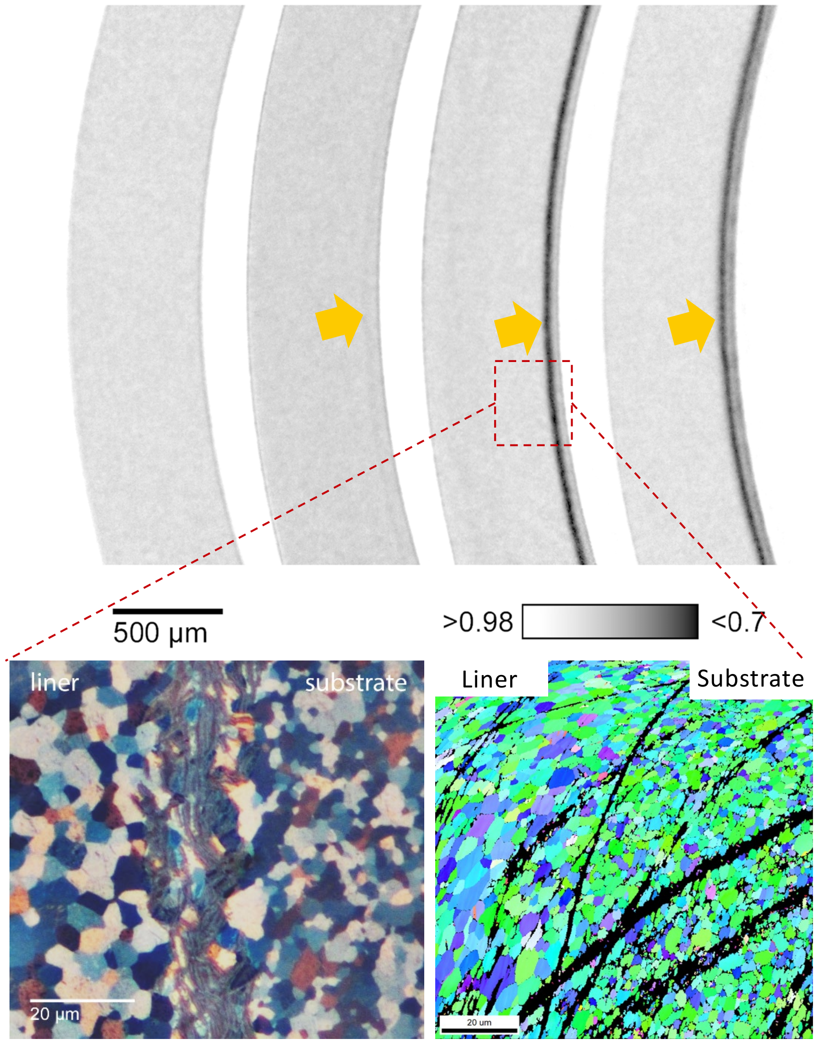

OM - Pol. light

SEM - EBSD

DIC, 200ppm, 30 C/h

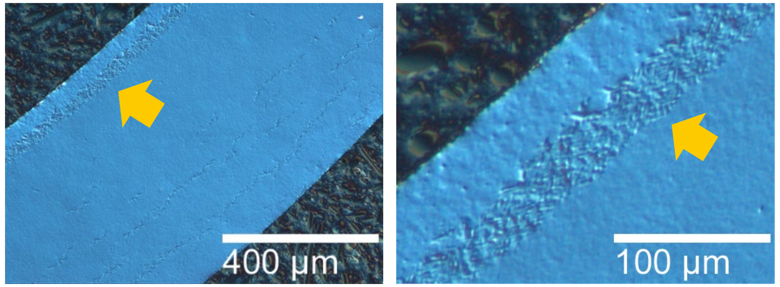

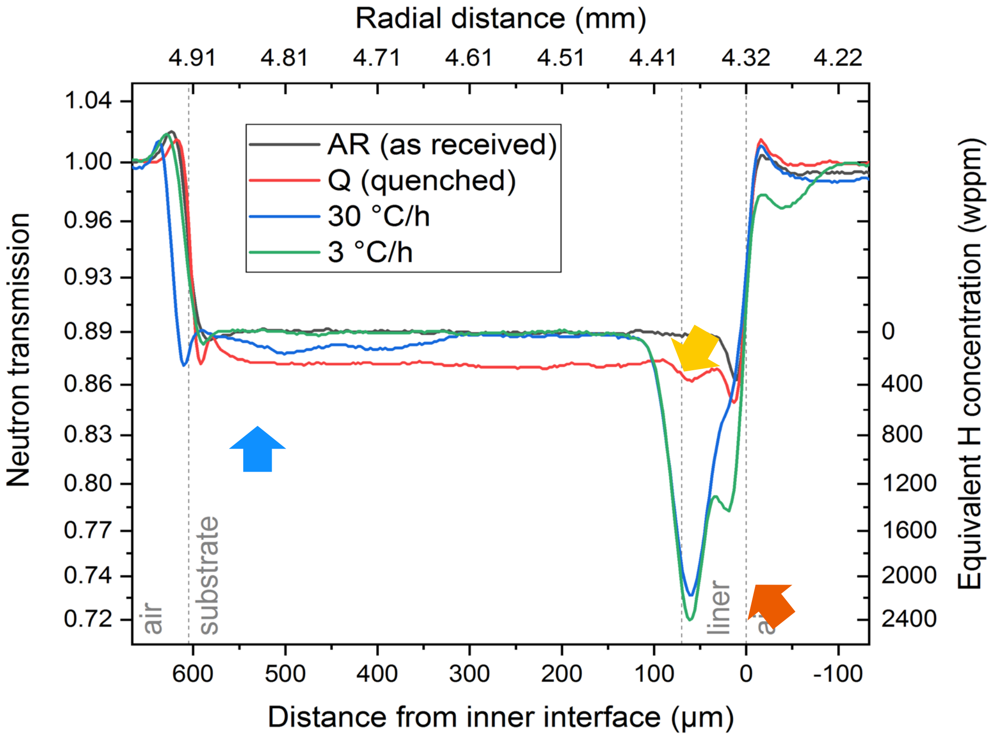

Neutron Radiography Imaging of Irradiated cladding samples – Results

Hydrogen evaluation after operation and redistribution induced by liner/temperature/stress

2.5mSv/h
@ 5 cm

Burnup of 70 MWd/kgU
Hydrogen 441wppm

POLDI Nov. 2018

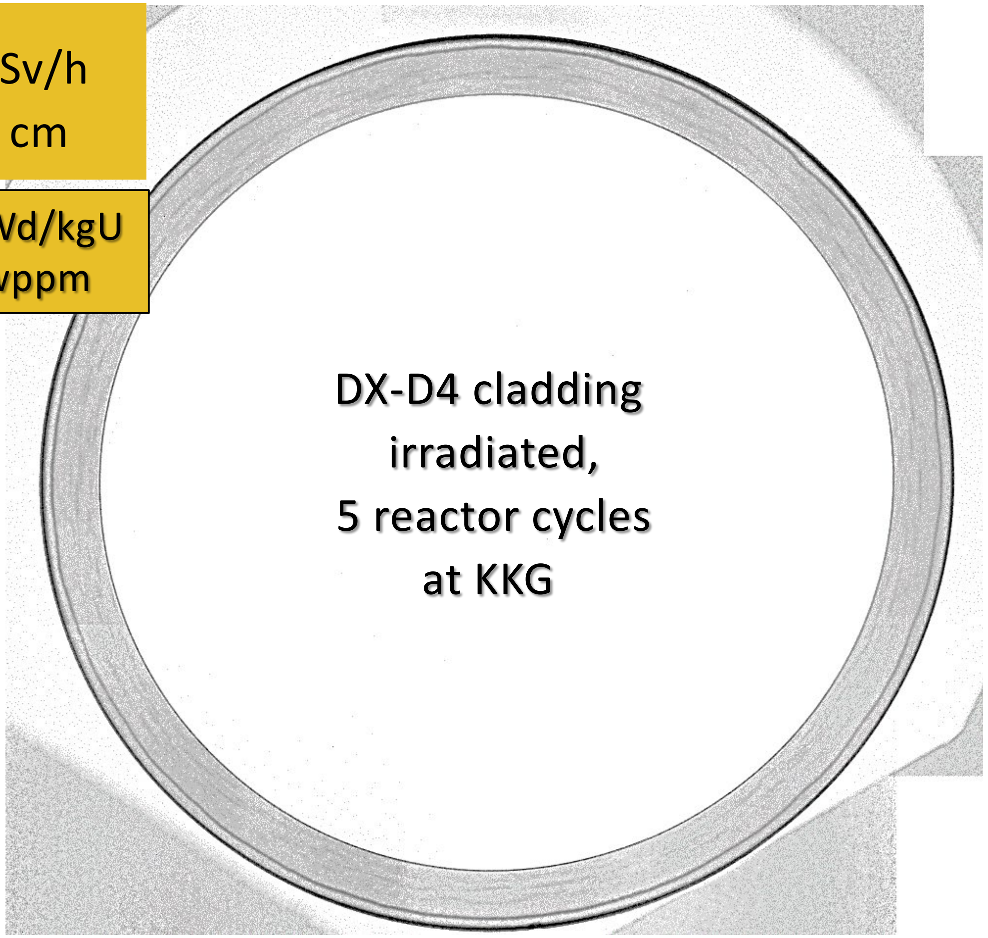

L.I. Duarte, et al,
TopFuel 2019,
September 2019
Seattle, USA

ICON Nov. 2020

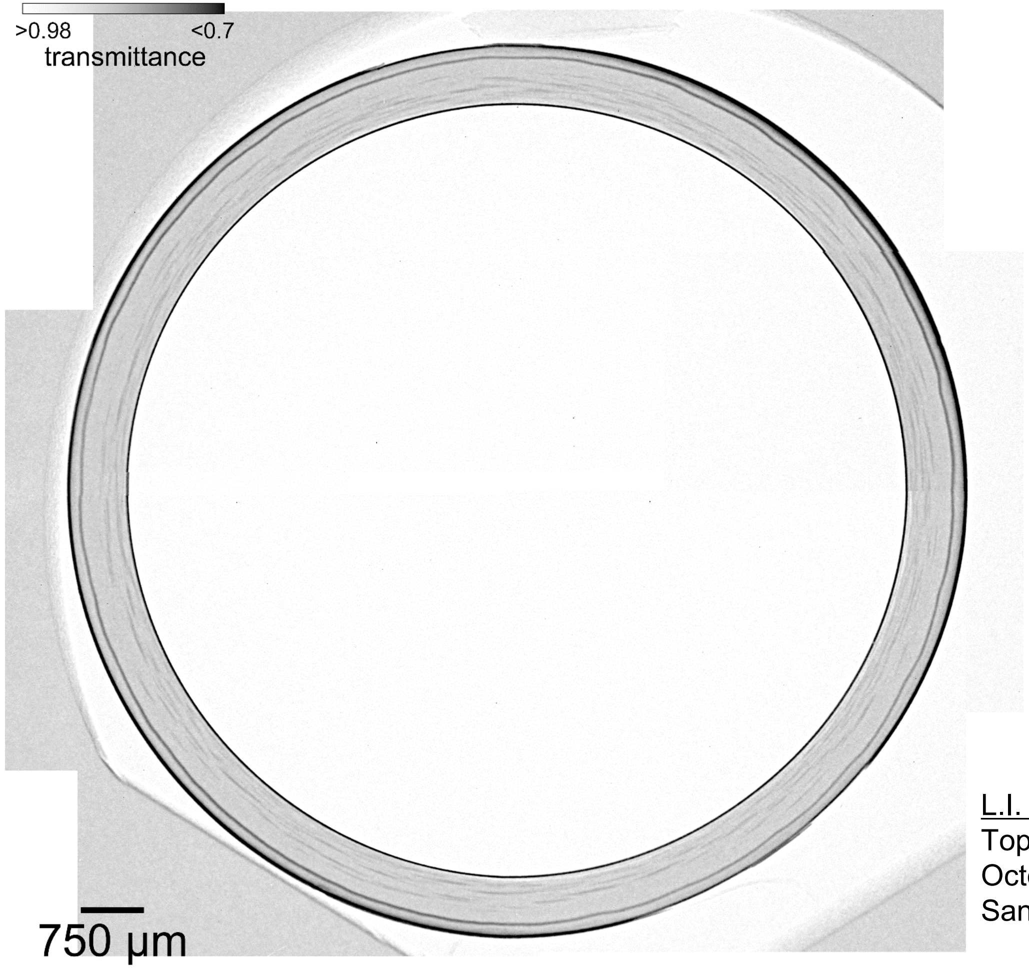

L.I. Duarte, et al,
TopFuel 2021,
October 2021,
Santander, Spain

Neutron Radiography Imaging of Irradiated cladding samples – Results (2)

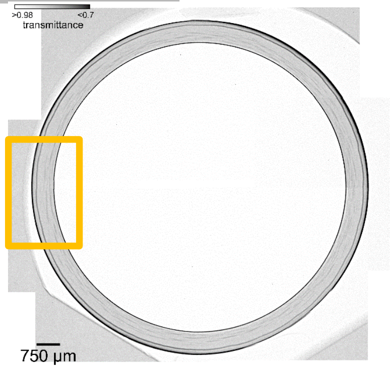

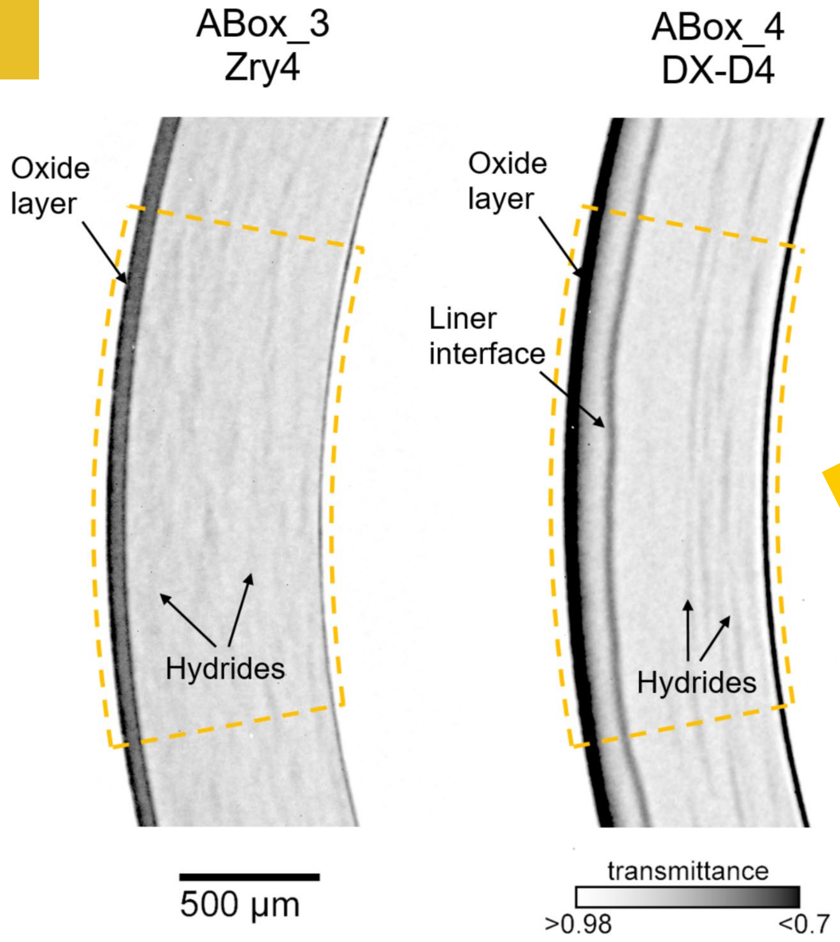

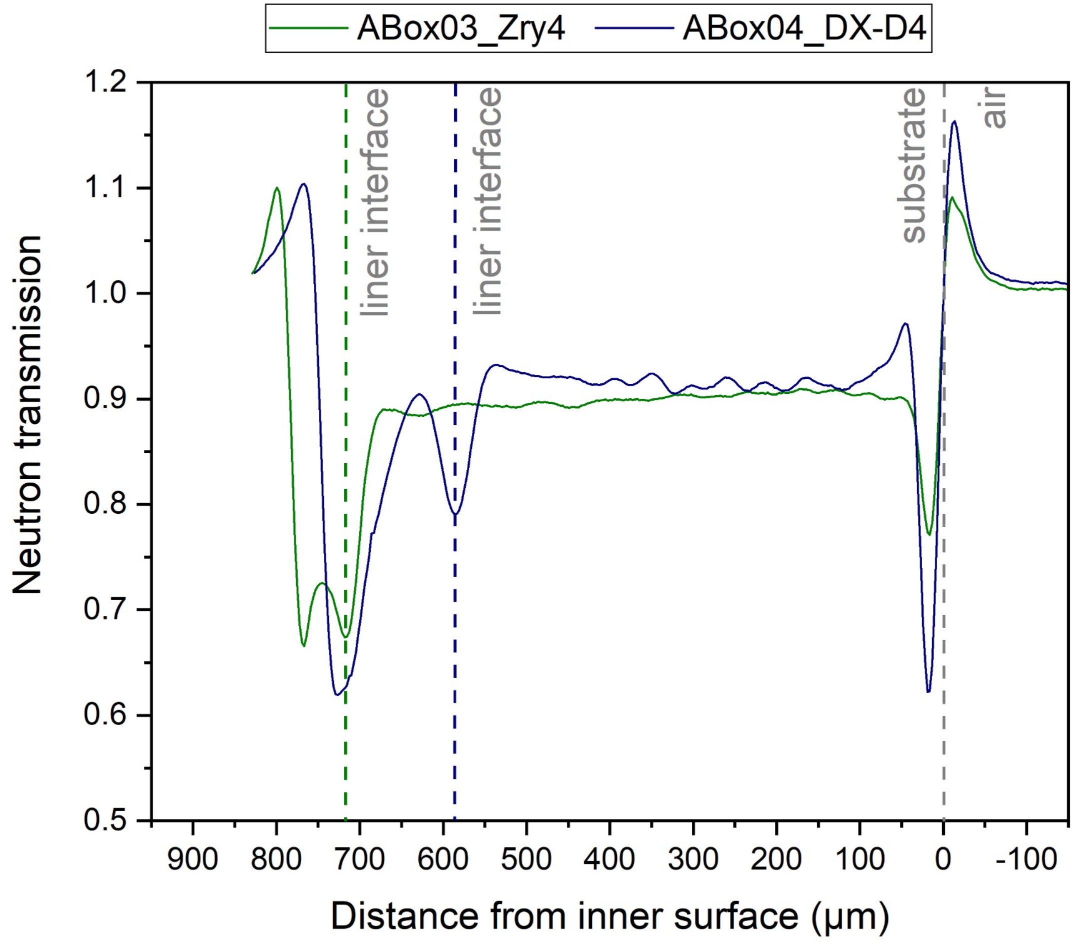

L.I. Duarte, O. Yetik, F. Fagnoni, A. Colldeweih, R. Zubler, P. Trtik, J. Bertsch, TopFuel 2021, Santander, Spain

O. Yetik, L.I. Duarte, F. Fagnoni, A. Colldeweih, R. Zubler, M.A. Pouchon, P. Trtik, J. Bertsch, TopFuel 2021, Santander, Spain

Neutron imaging of hydrogen redistribution induced by liner/temperature/stress

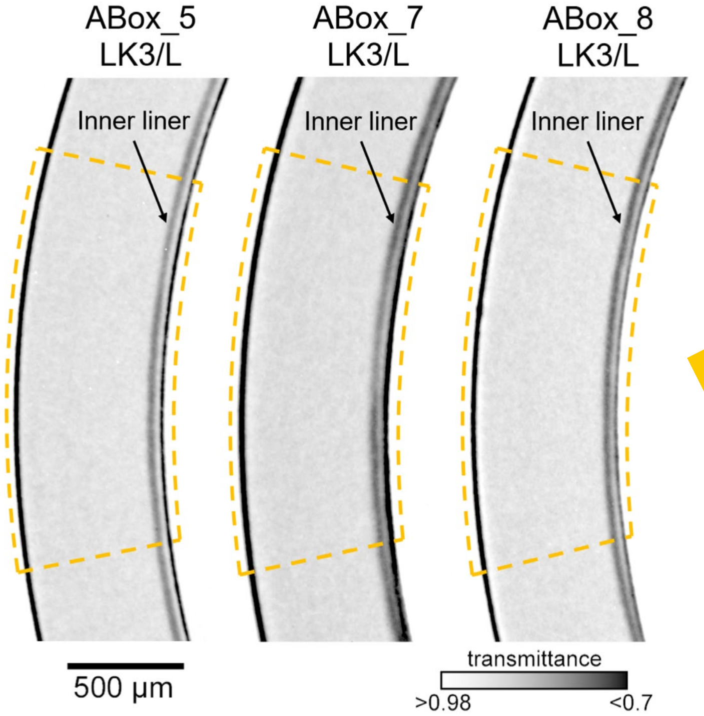

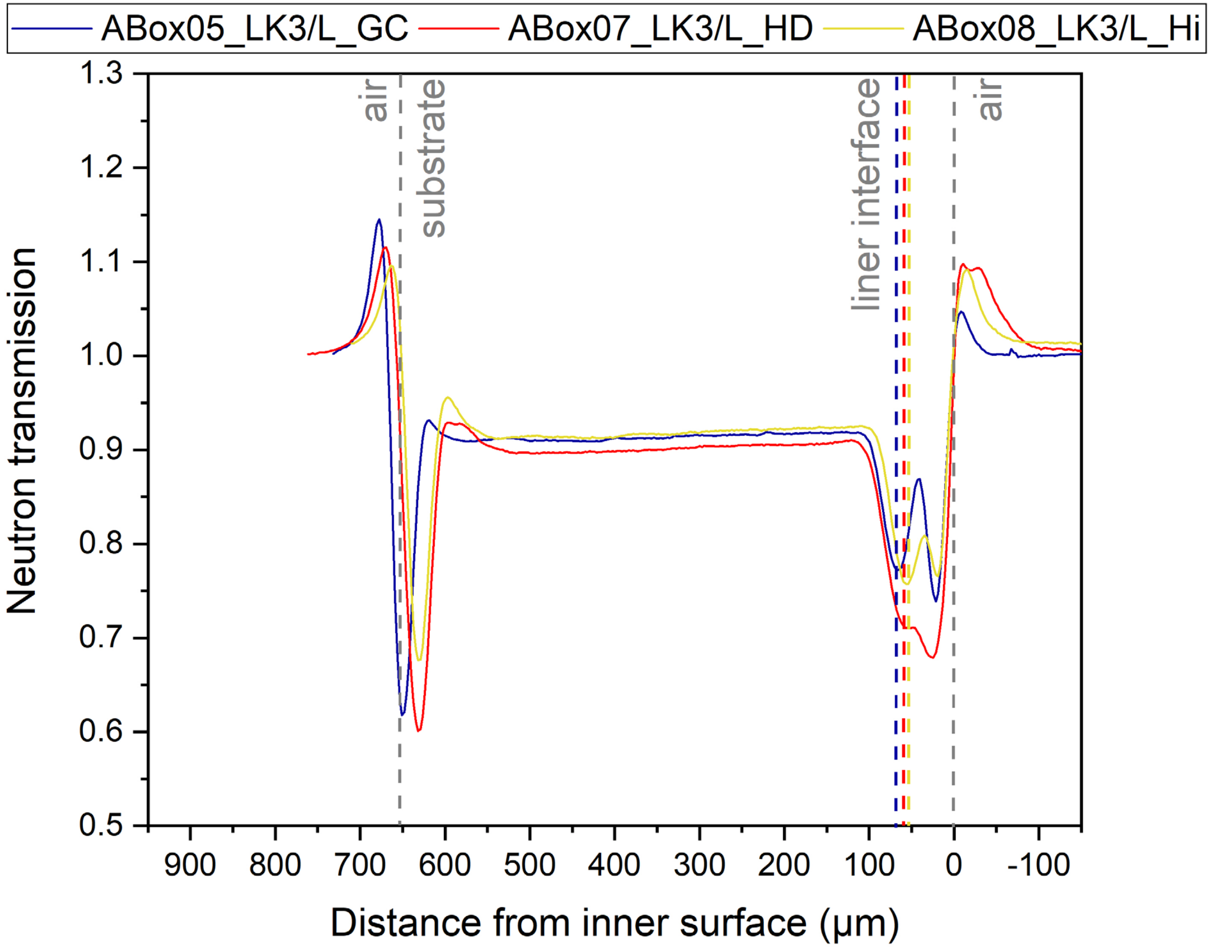

L.I. Duarte et. al, TopFuel 2021, Santander, Spain (submitted for a conference paper)

Hydrides re-orientation in Zr cladding with C-shape

- Mechanical experiment with C-shape sample:
  C-ring, as generally used, is a constant-strain specimen with tensile stress produced on the exterior of the ring by tightening a bolt centered on the diameter of the ring.

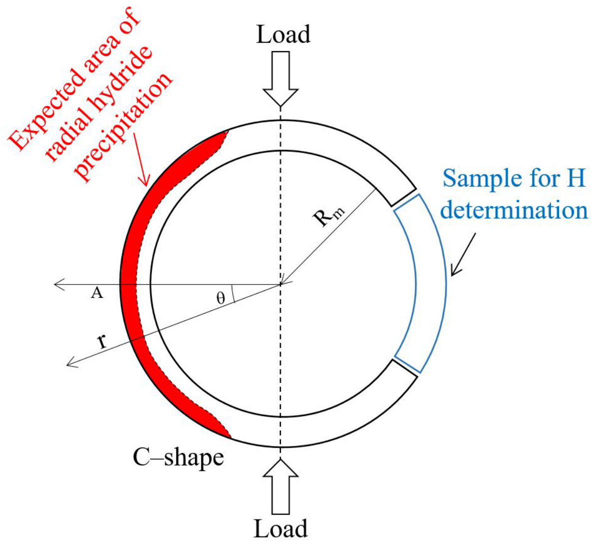

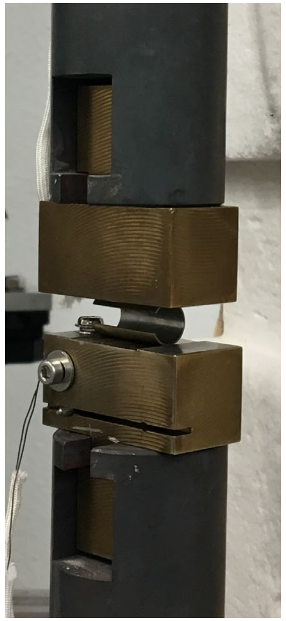

- Constant Force of 20N with different hydrogen content (0, 100, 200 wppm) and with thermo-cycling;
- Collaboration with IRSN (France);
- Model produced with ABAQUS software Stress analyses and comparing with the experimental results
- Support by **Diego Mora Mendez (LNM)**

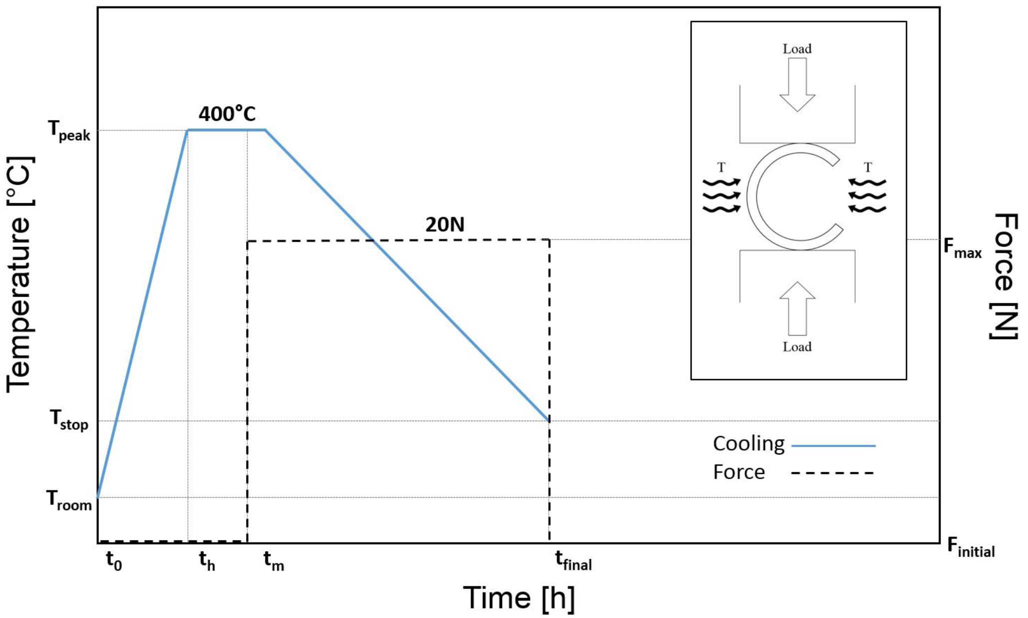

C-shape samples evaluation by NRI and OM

✓ Neutron radiography image (NRI)

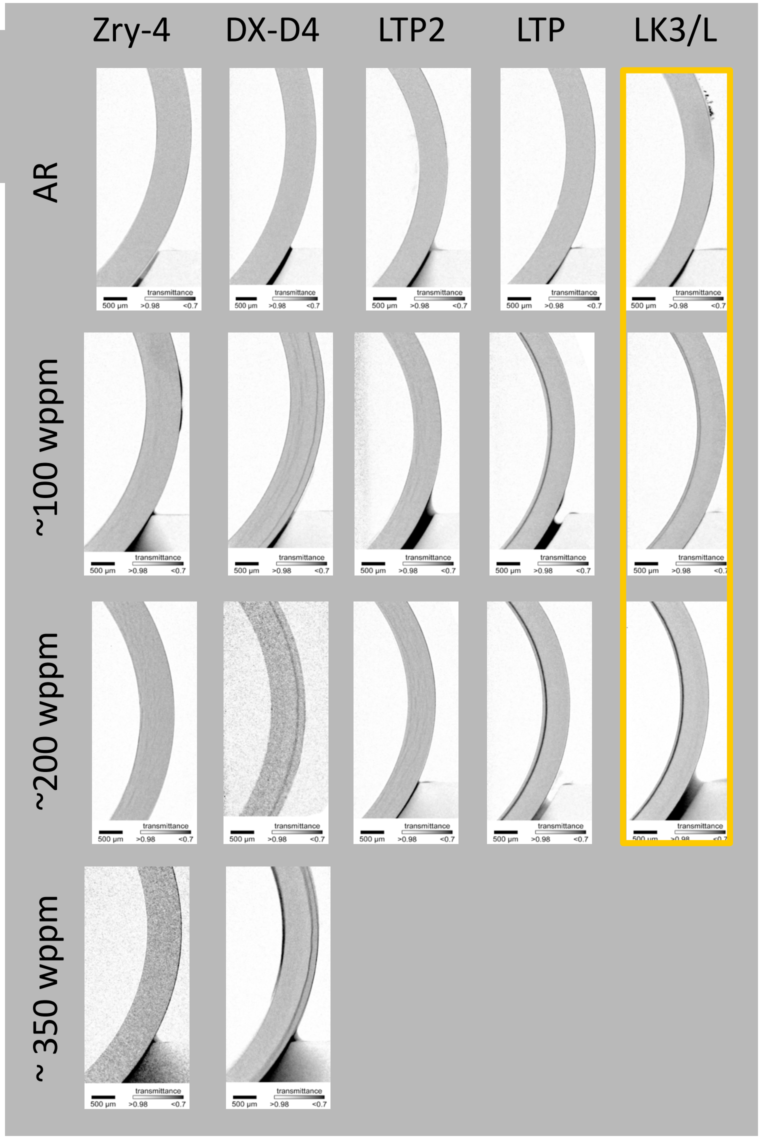

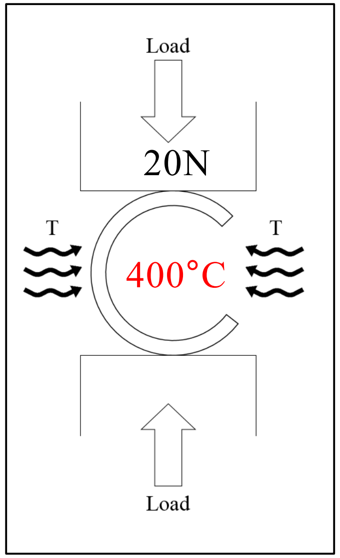

✓ Optical micrographs (OM)

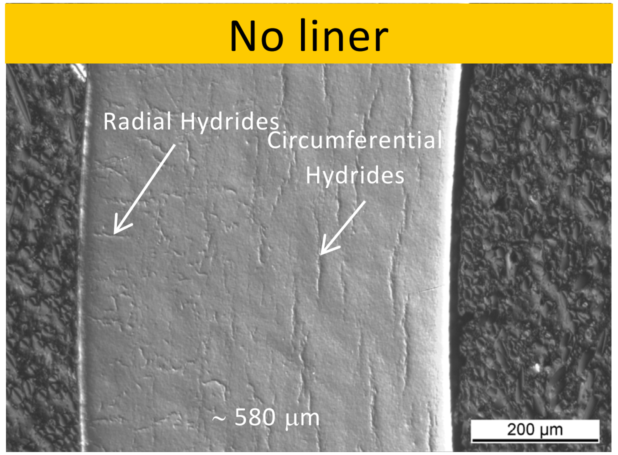

LTP2 – 200 ppm

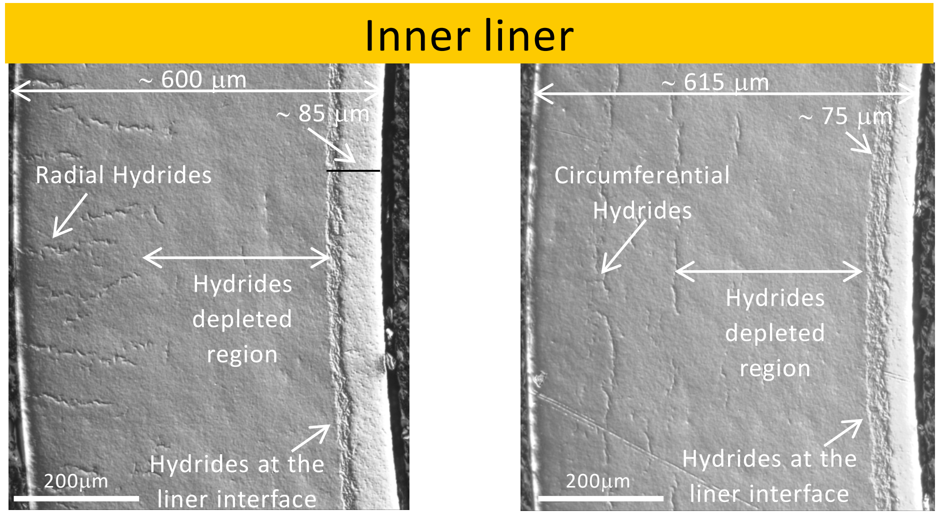

LTP - 200 ppm

LK3/L – 200 ppm

PAUL SCHERRER INSTITUT

Summary

- Neutron radiography imaging proved to be a useful technique for hydrogen qualitative and quantitative measurements for non- and irradiated zirconium cladding materials
- Mechanical testing with C-shape samples
    - Correlating the mechanical properties of the zirconium cladding materials with different stresses and hydrogen contents.
    - Validation of simulations models with the experimental results.
- Understanding the mechanisms of hydrides reorientation/diffusion towards the liner.

Wir schaffen Wissen – heute für morgen

- Financial supported by ENSI, *swissnuclear* and Swiss Expert Group Fuels (ESB), Nagra.
- Scientific discussion with AHL, LNM, LRT, LNS, EMF, ETHZ, EPFL and EMPA.
- SINQ
- Swiss Nuclear Power Plants KKG, KKL
- Westinghouse and Framatome for the cladding material

Thank you for your attention

M. Ayanoglu, J. Harp, R. Montgomery, B. Bevard,
P. Cantonwine

ORNL

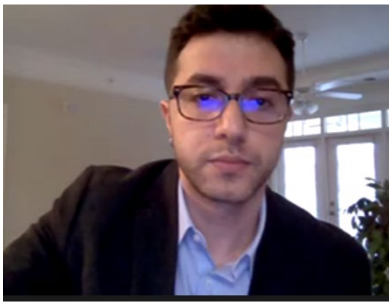

Hydrogen measurements and metallographic examination of high-burnup nuclear spent fuel claddings

During light water reactor operation, hydrogen is produced as a byproduct of waterside cladding corrosion. Some of the hydrogen is picked up by the zirconium alloy cladding, and if the hydrogen concentration exceeds the solubility limit, picked-up hydrogen precipitates as zirconium hydride platelets. Depending on the density and orientation of the hydride platelets and the loading scenario, the platelets can significantly affect the fuel-cladding performance. Therefore, investigating the hydride morphology and their spatial distributions in high-burnup (HBU) spent nuclear fuel (SNF) claddings is key to understand and predict the behavior of the HBU SNF rods during the long-term dry storage.

Metallographic (MET) examinations and hydrogen measurements were performed on various as-received and heat-treated (HT) HBU fuel claddings at Oak Ridge National Laboratory to investigate the effect of dry storage vacuum drying temperature on hydrogen behavior and resulting hydride morphology as a part of DOE NE High-Burnup Spent Fuel Data project. Three as-received fuel rods were heat-treated at 400oC at their as-discharged rod internal pressure followed by slow cool to room temperature. The as-received rods and the heat-treated rods were examined using optical microscopy and LECO 836 series OHN analyzer.

All baseline (i.e., as-received) rods had mainly circumferential hydrides. After the heat-treatment, MET examinations revealed the formation of long hydrides in M5 fuel cladding near the clad inner diameter. For ZIRLO and Zircaloy-4, the radial hydrides were short, and their lengths are limited by the circumferential hydrides that did not dissolve during the heat treatment.

Cladding hydrogen measurements showed similar total H contents in the baseline and HT fuel claddings. The baseline HBU M5 cladding has the lowest hydride concentration, following by the baseline-ZIRLO and the baseline Low-tin Zircaloy-4. Similarly, the HT M5 cladding has the lowest hydride concentration, following by HT ZIRLO and HT Zircaloy-4. MET examinations of the baseline specimens showed uniformly distributed circumferential hydrides in the M5 cladding, whereas hydrides in ZIRLO cladding were preferentially precipitated near clad inner and outer diameters. For the case of the Low-tin Zircaloy-4 and the Zircaloy-4 samples, a hydride rim was observed near the cladding outer diameter, in addition to the very high density of hydride platelets.

U.S. DEPARTMENT OF ENERGY | Office of NUCLEAR ENERGY

Clean. Reliable. Nuclear.

QUENCH 2021

Hydrogen Measurements and Metallographic Examination of High-Burnup Nuclear Spent Fuel Claddings

Muhammet Ayanoglu, Jason Harp, Rose Montgomery, Bruce Bevard, Paul Cantonwine

Used Fuel and Nuclear Material Disposition Group, Oak Ridge National Laboratory

Background

Project goal: Understanding the effect of long-term storage and transportation on high-burnup Light Water Reactor (LWR) fuels

North Anna Nuclear Power Plant

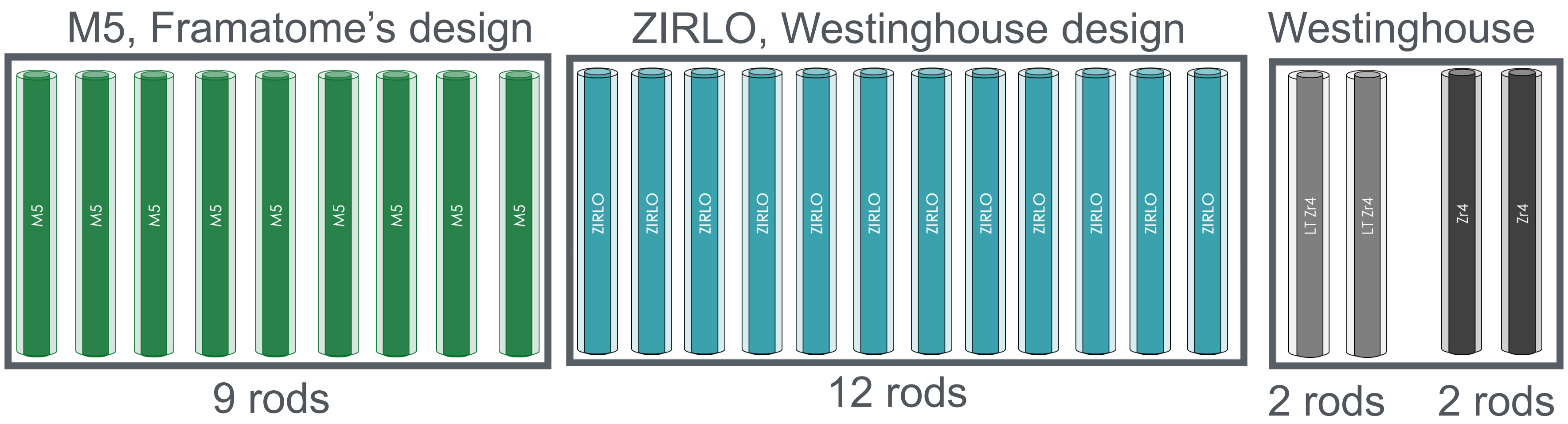

- 25 high-burnup (HBU) spent nuclear fuel rods (48–59 GWd/MTU)
- Different types of fuel cladding: M5, ZIRLO, low-tin (LT) Zr-4, Zr-4
- Nondestructive examination was completed at Oak Ridge National Laboratory's (ORNL's) Irradiated Fuels Examination Laboratory (IFEL)
- Destructive examination of seven rods is ongoing: three ZIRLO, two M5, one LT Zr-4, and one Zr-4 clad rod

R. Montgomery et al., Key Results from Detailed Nondestructive Examinations of 25 Pressurized Water Reactor High Burnup Spent Nuclear Fuel Rods, Nucl. Sci. and Eng., 193, 885-902, 2019.

During light water reactor operation, Zircaloy nuclear fuel cladding undergoes waterside corrosion and produces H as a byproduct…

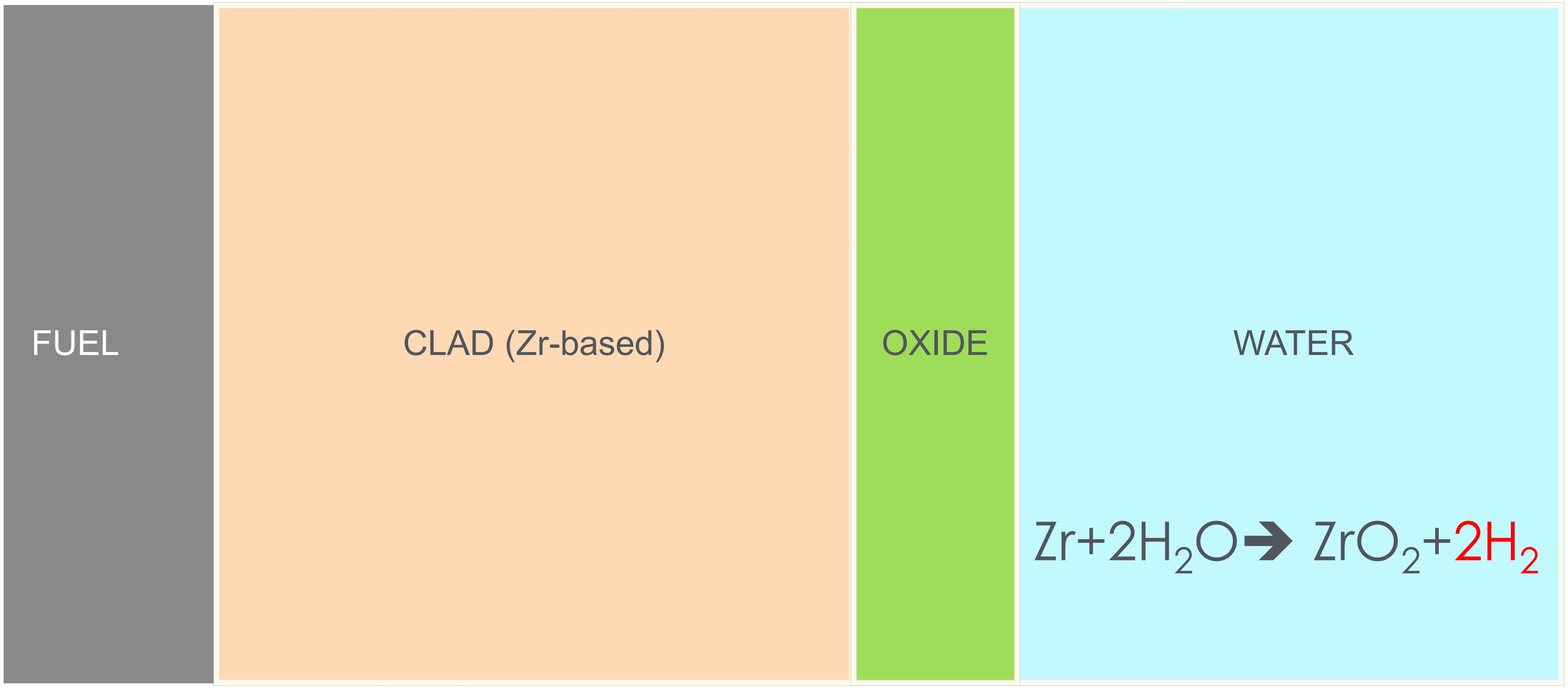

A fraction of H is picked up by the fuel cladding and precipitated as zirconium hydride when the H solubility limit is exceeded

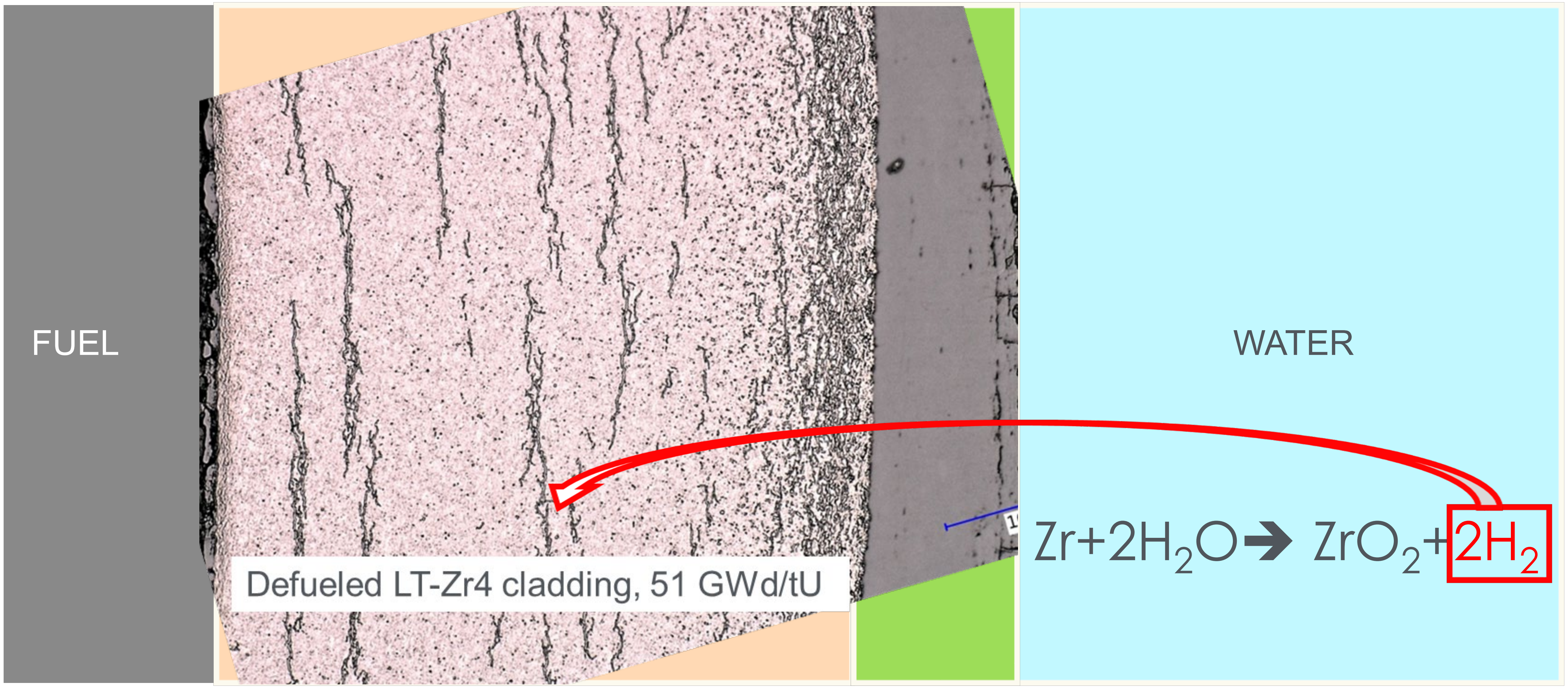

For dry-storage, fuel rods undergo a series of heating/cooling steps to remove any residual water, which prevents further corrosion that could cause hydride reorientation

Heating ➔ hydride dissolution

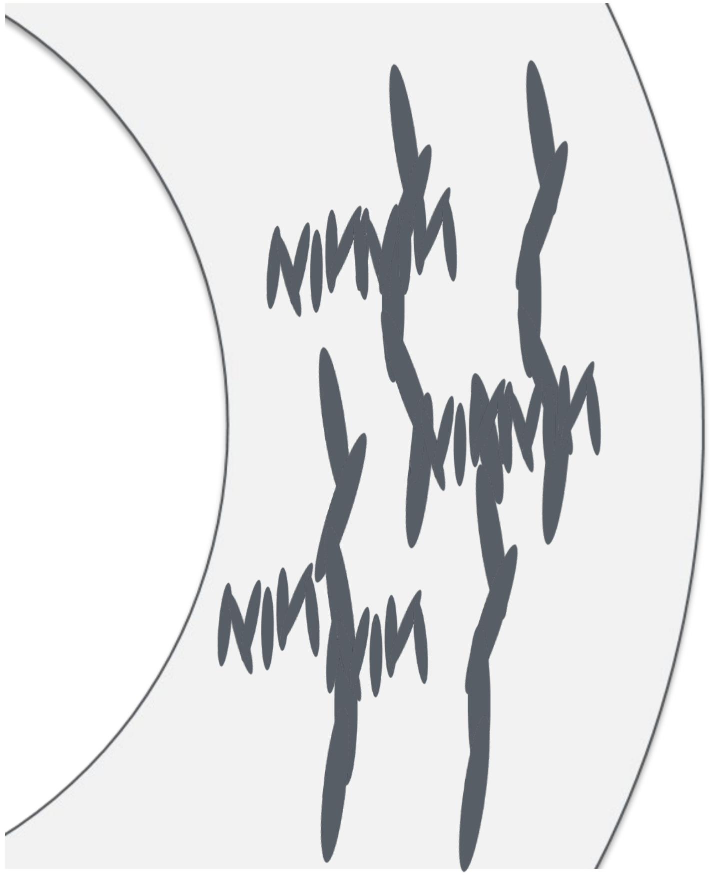

Cooling ➔ hydride reprecipitation/reorientation

Baseline fuel cladding

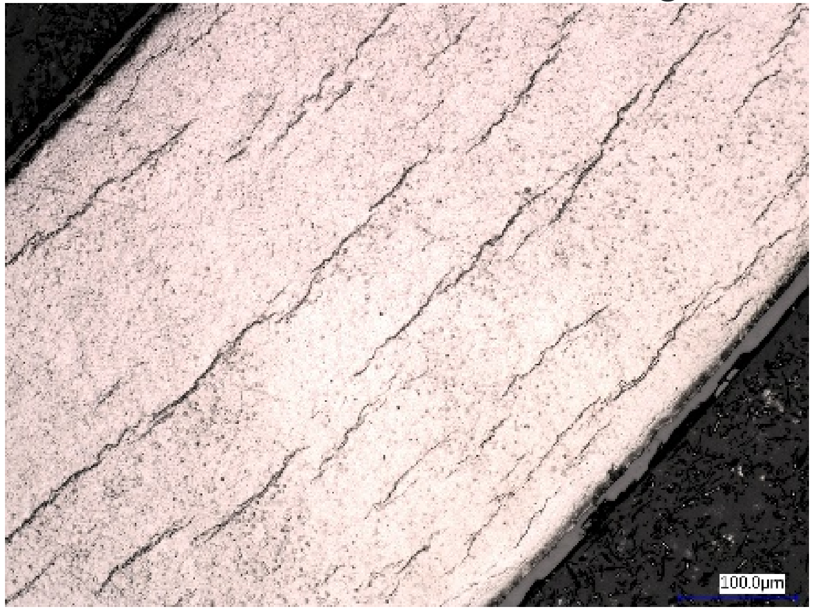

Heat-treated (HT) fuel cladding

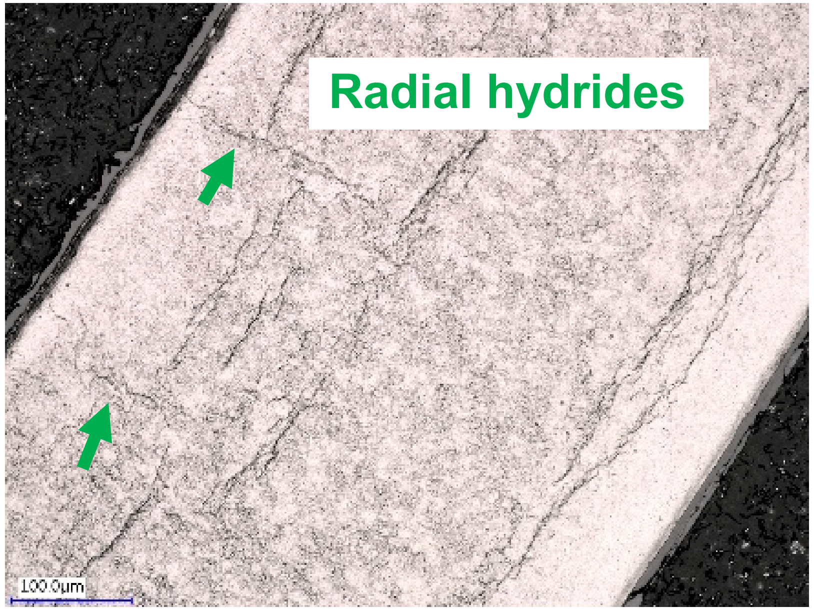

Defueled M5 fuel cladding, 52 GWd/tU

Motivation

- Spatial distribution of hydrides and their reorientation can influence the performance of fuel cladding during dry storage
- Hydride is more brittle than the fuel cladding, which accelerates crack propagation

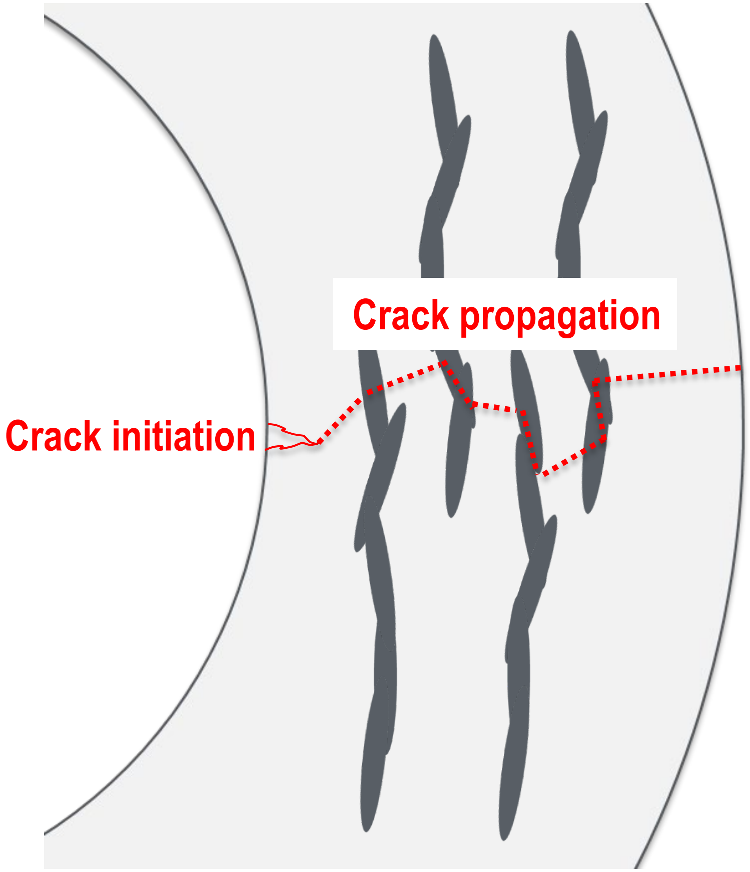

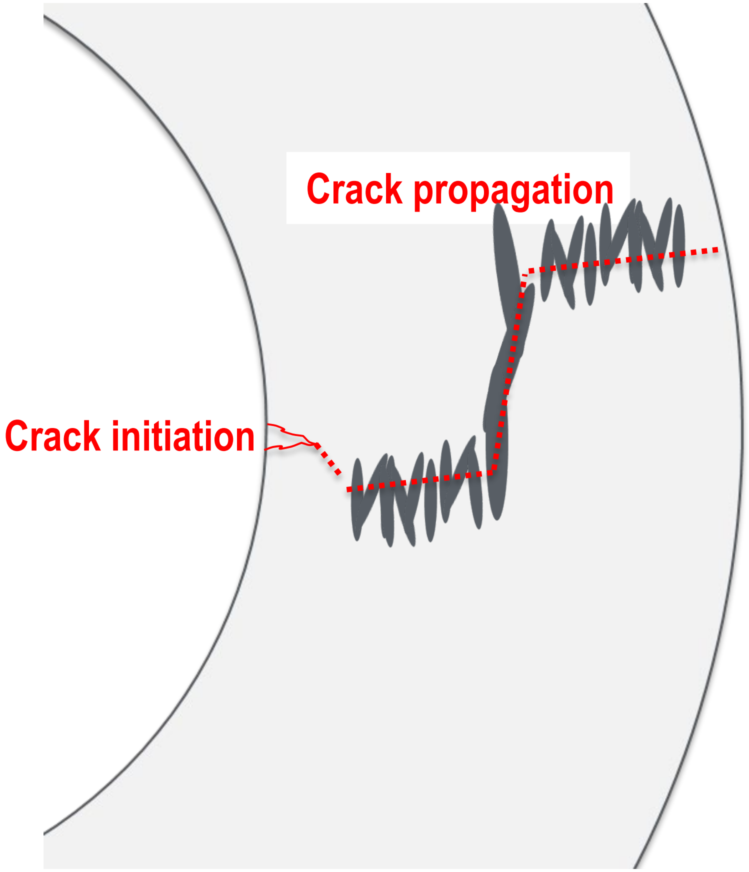

Hydrogen measurement at ORNL’s IFEL

- The H content was measured from 14 of the 20 samples using Laboratory Equipment Corporation (LECO).
- Samples were cut/defueled from high-burnup (HBU) spent fuel rods and quartered before the LECO measurements

Cutting LECO sample

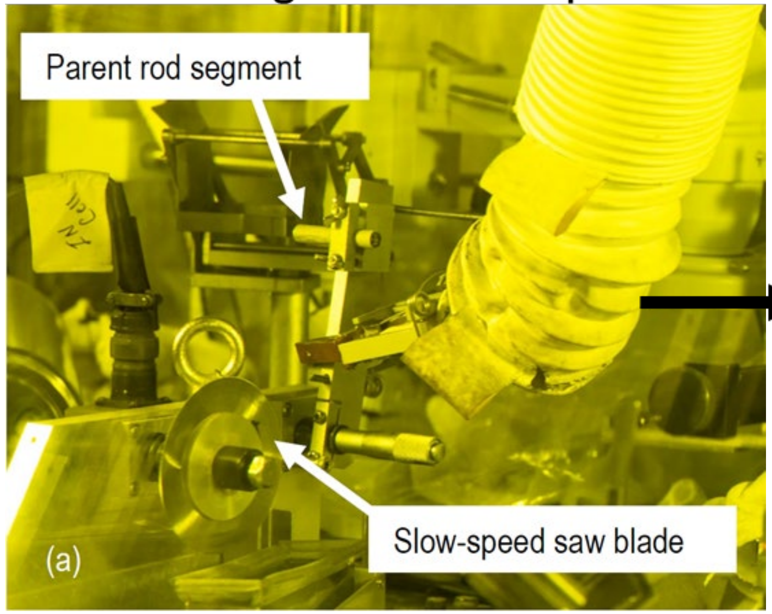

Defueled cladding

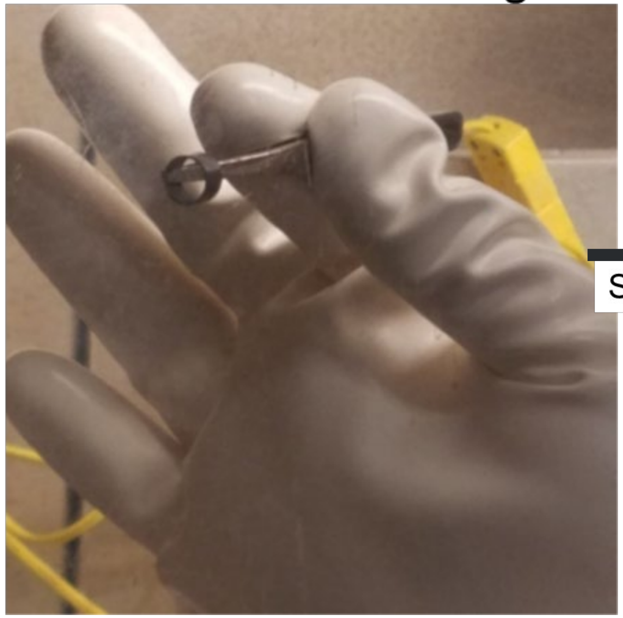

Stage used for quartering

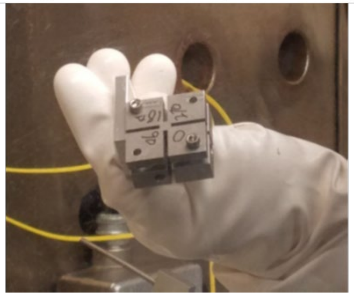

After quartering

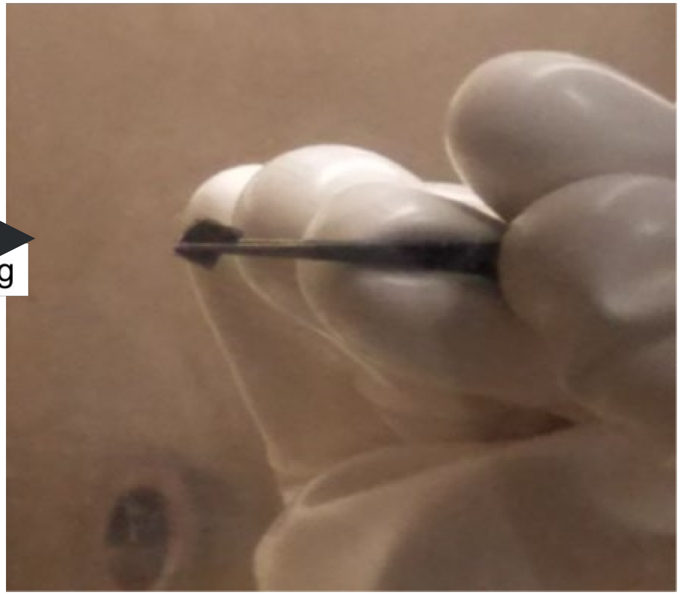

- H was measured as total H content in weight parts per million (i.e., cladding+oxide)

Measured H content vs. oxide thickness

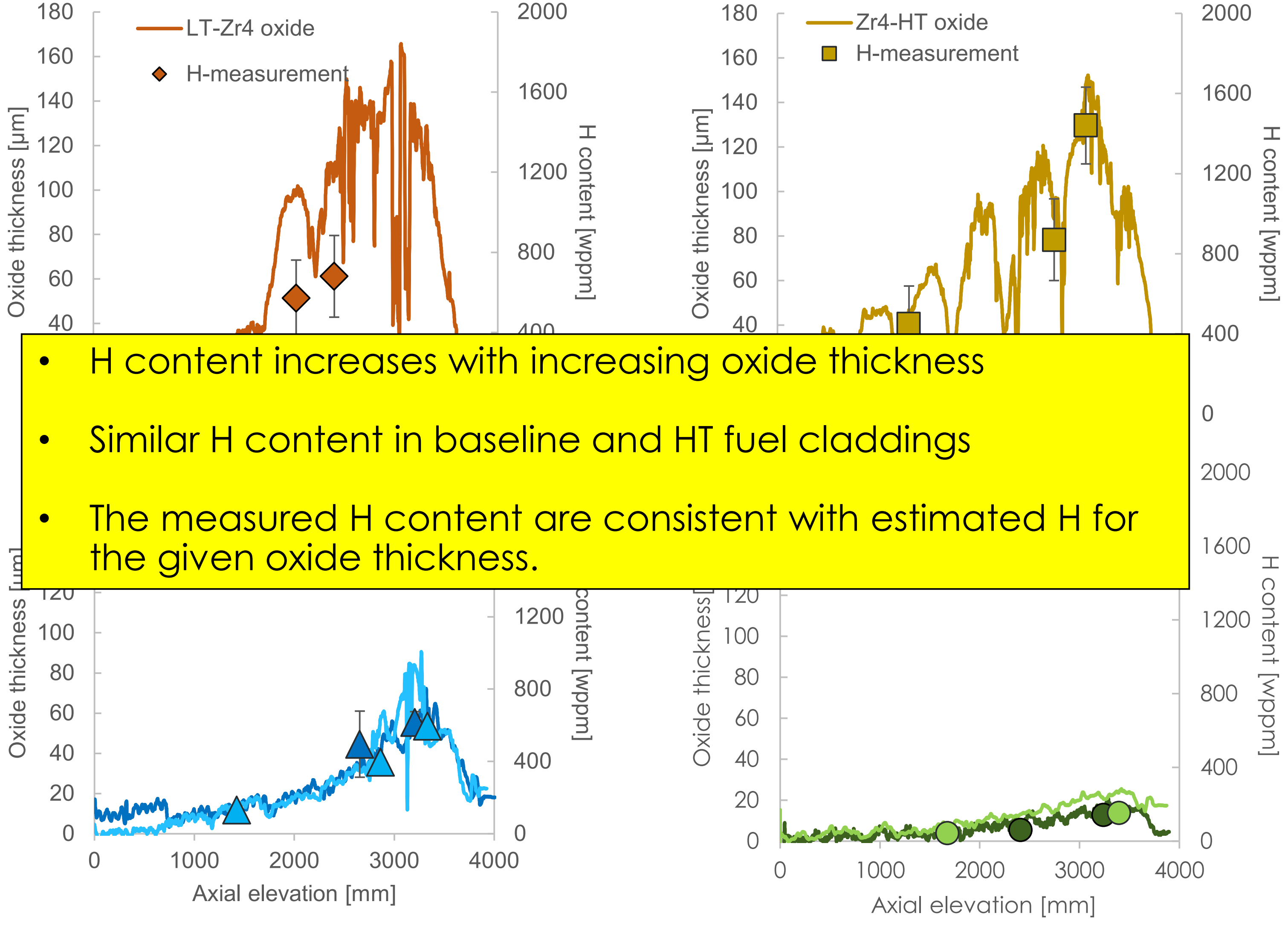

- H content increases with increasing oxide thickness
- Similar H content in baseline and HT fuel claddings
- The measured H content are consistent with estimated H for the given oxide thickness.

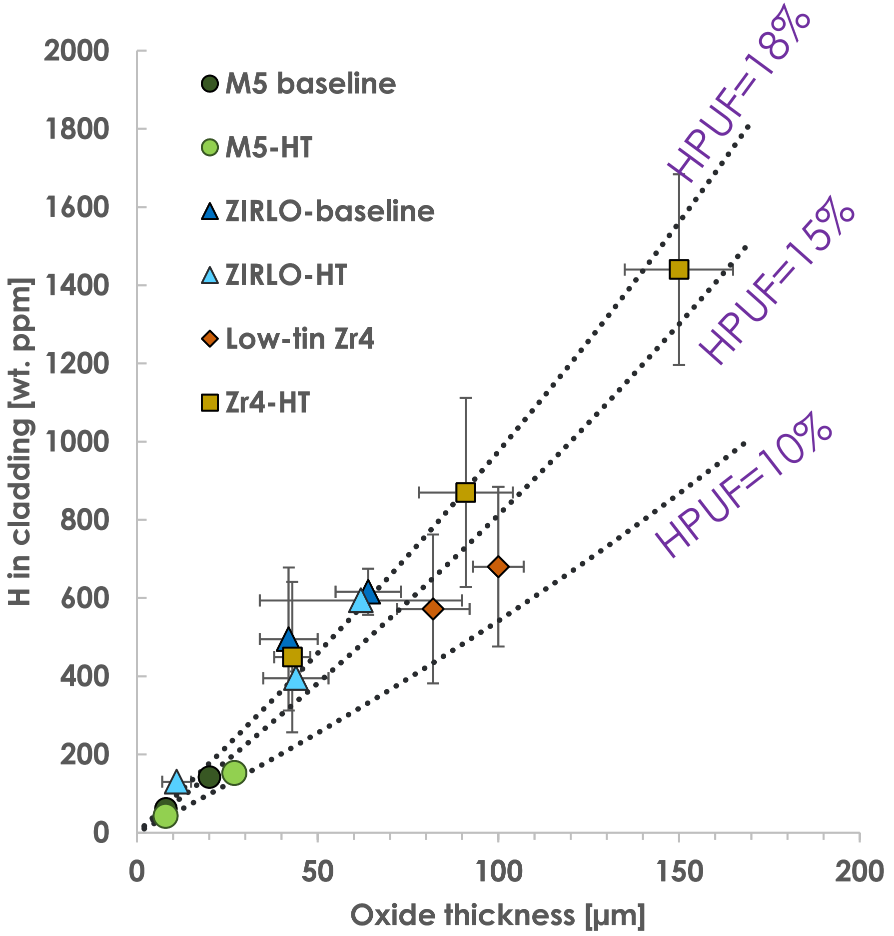

Preliminary metallography (MET) examination of selected high-burnup (HBU) defueled cladding

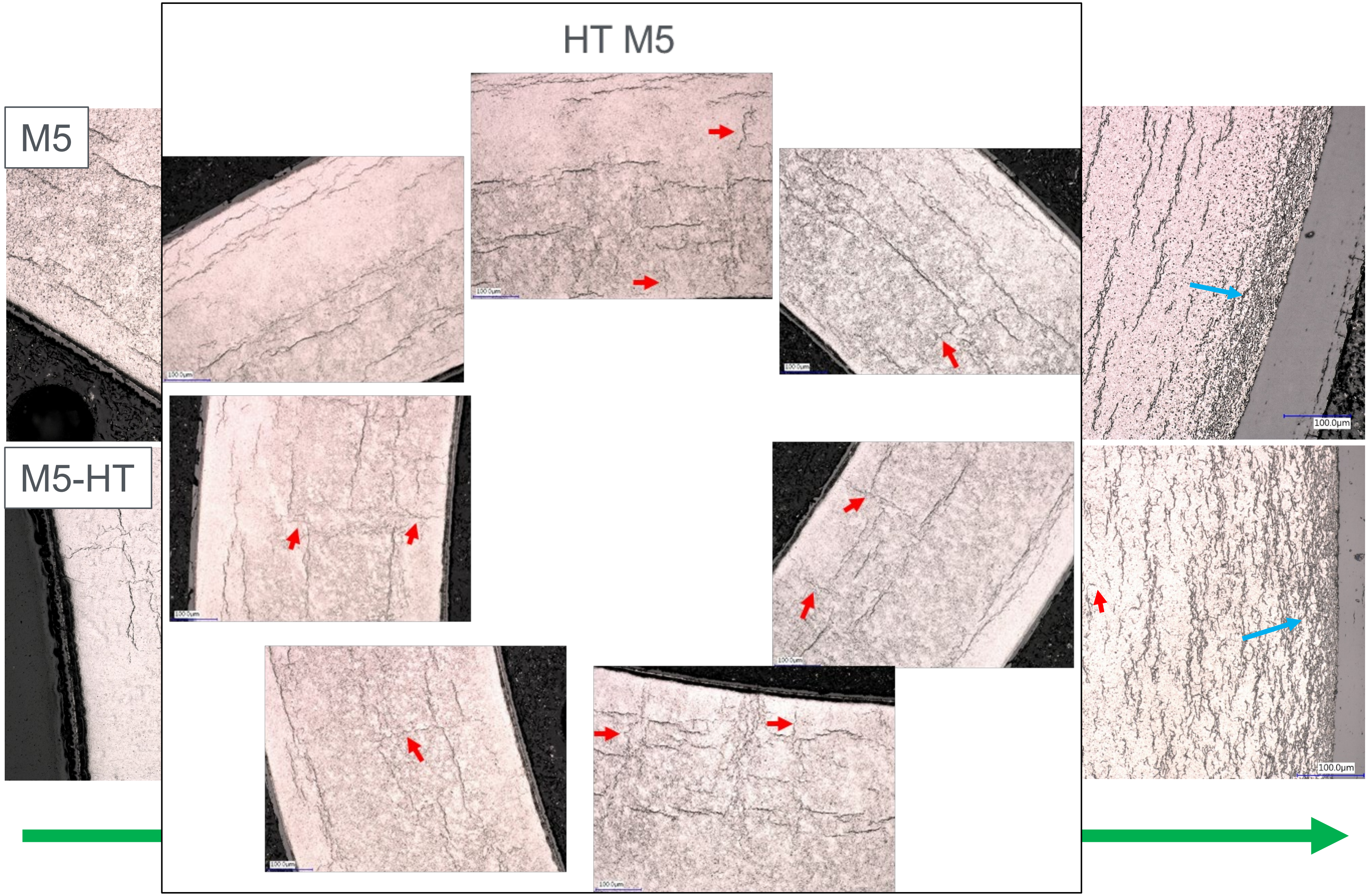

- Highest hydride density in Zr-4 fuel claddings followed by ZIRLO and M5
- Hydride rim observed in Zr-4 and ZIRLO but not in M5 fuel cladding
- Hydride reorientation, especially in HT M5 fuel cladding (mainly inner cladding regions)

Summary and future work

- The cladding H content was measured for 14 defueled HBU fuel cladding samples
  - The H content increased with increasing oxide thickness
  - The lowest H was found in M5 fuel cladding, which has the lowest oxidation
- Metallographic images of as-received and HT cladding provided information about the H density and spatial distribution
  - Long radial hydrides were observed in HT-M5 fuel cladding, especially near clad inner diameter
  - For ZIRLO and Zr-4, there were a few small radial hydrides
- Further MET examination and H measurement is recommended
- Microhardness and fatigue tests could investigate the mechanical response of different HBU fuel cladding during dry storage and transportation

THANK YOU

P. Cantonwine, H.Wang, M. Ayanoglu, B. Bevard,
R. Montgomery, ,

ORNL

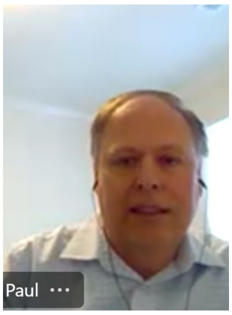

Fatigue Testing of High Burnup PWR Fuel Rods with Zircaloy-4 cladding with and without Heat Treatment to Simulate a Drying Cycle

To reach a geological repository, LWR fuel first goes into dry storage at the plant site or in a off-site dry storage facility. After some time, the fuel will be transported to a geological repository (potentially after repackaging). It is well known that the largest post operation SNF temperatures are reached during an initial vacuum drying evolution, and it is this evolution that potentially can result in reorientation of hydrides in the radial direction.

The effect of a simulated drying heat treatment on the subsequent fatigue life of high-burnup Zircaloy-4 fuel rods has been evaluated at Oak Ridge National Laboratory (ORNL) under bending conditions to understand the limiting transportation conditions. A full-length rod with a rod average burnup of 60 GWd/MTU was heat treated by ramping the temperature to 400 oC at ~10 oC/hr, holding for 10 hr. and decreasing the temperature at ~4 °C/hr. Fatigue samples were then cut and tested from elevations in the upper half of the fuel rod. Metallography and LECO measurements indicate a hydrogen content from 600-800 ppm to greater than 1000 ppm. The fuel rod that wasn't heat treated had a rod average burnup of 51 GWd/MTU and the cladding was a low-tin version of Zircaloy-4. Fatigue samples were cut and tested from similar elevations compared to the heat-treated fuel rod.

Metallography and LECO measurements indicate hydrogen in the 550 to 700 ppm range at the elevations around 2000 mm, which is comparable to that observed in the higher burnup Zircaloy-4 rod. The fatigue testing was performed in the ORNL hotcells using a unique Cyclic Integrated Reversible-Bending Fatigue Testing (CIRFT) system that is able to load the sample in pure bending. Results of these fatigue tests and the potential role of corrosion and hydrogen pickup will be discussed.

Fatigue Testing of High Burnup PWR Fuel Rods with Zircaloy-4 cladding with and without Heat Treatment to Simulate a Drying Cycle

Paul Cantonwine, Hong Wang, Muhammet Ayanoglu, Bruce Bevard, and Rose Montgomery

ORNL is managed by UT-Battelle LLC for the US Department of Energy

ORNL/SPR-2020/1780, "Sister Rod Destructive Examinations (FY20) Appendix F: Cyclic Integrated Reversible-Bending Fatigue Tests,"
ORNL/SPR-2020/1745, "Sister Rod Destructive Examinations (FY20) Appendix A: Full-Length Rod Heat Treatments"
ORNL/SPR-2018/801, "Sister RodNondestructive Examination Final Report"

Outline

- Motivation
- Experimental Procedure
  - Simulated Vacuum Drying Heat Treatment
  - Cyclic Integrated Reversible Bending Fatigue Testing (CIRFT) System
- Fatigue Test Results
- Summary/Conclusions

Dispositioning Used Nuclear Fuel Involves High Temperatures in Vacuum Drying and Vibrations during Transportation

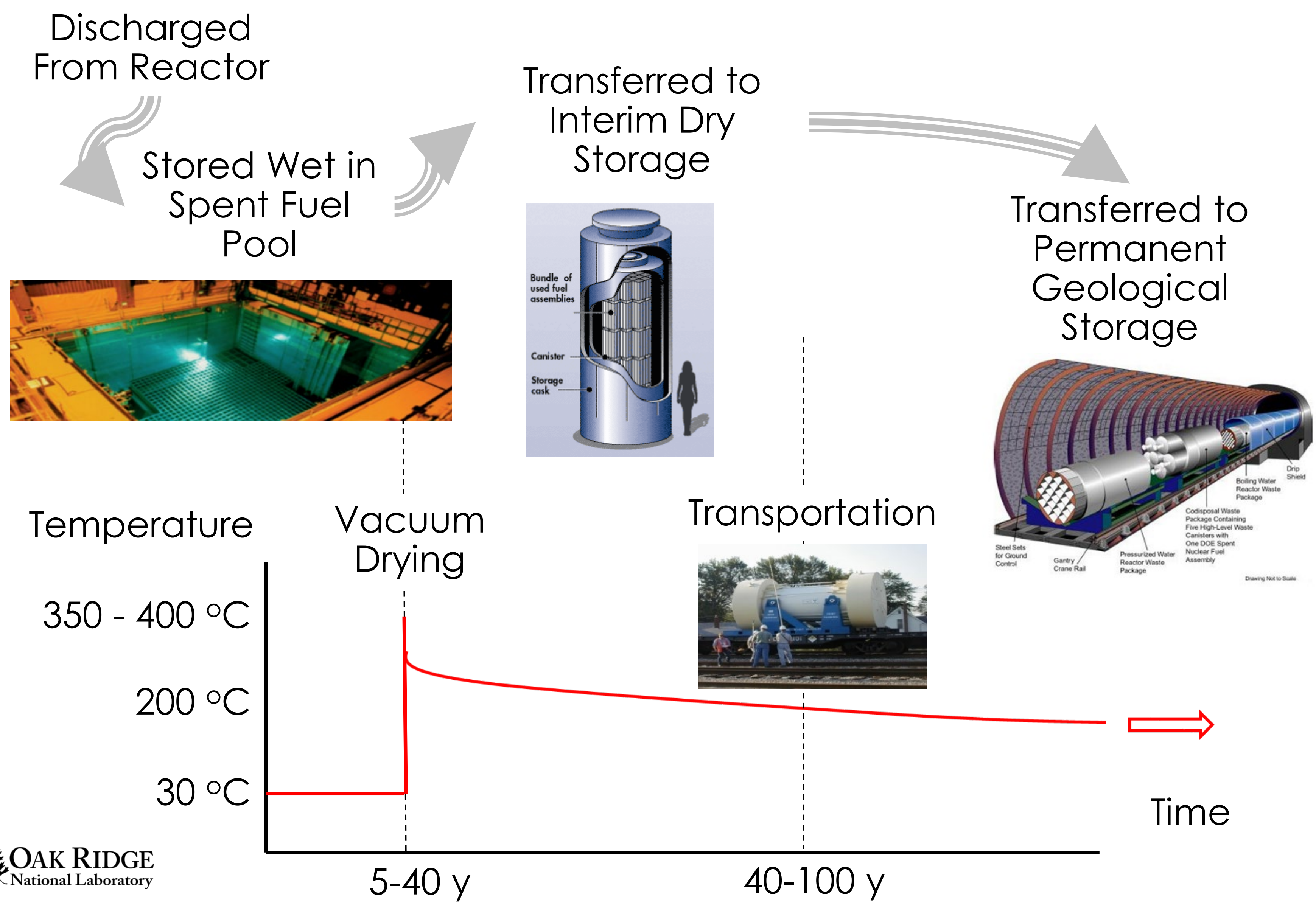

During transportation of SNF, fuel rod bending will occur under different vibration loads depending on the cask and conditions

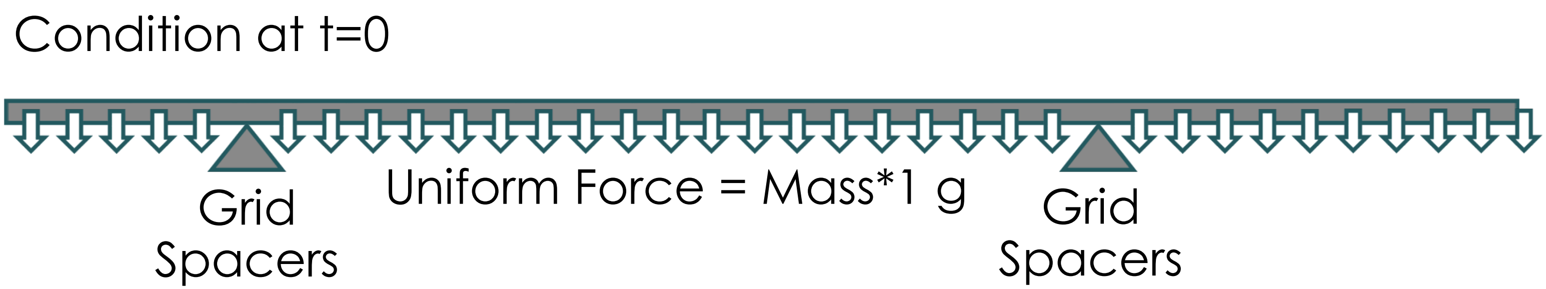

- Transportation vibrations will cause fuel rod motion resulting in fatigue cycling
- Two important questions are
  - What is the magnitude (and frequency) of the fatigue cycles?
  - What is the fatigue life of the SNF?

Maximum accelerations under normal transportations are less than 1.5 g

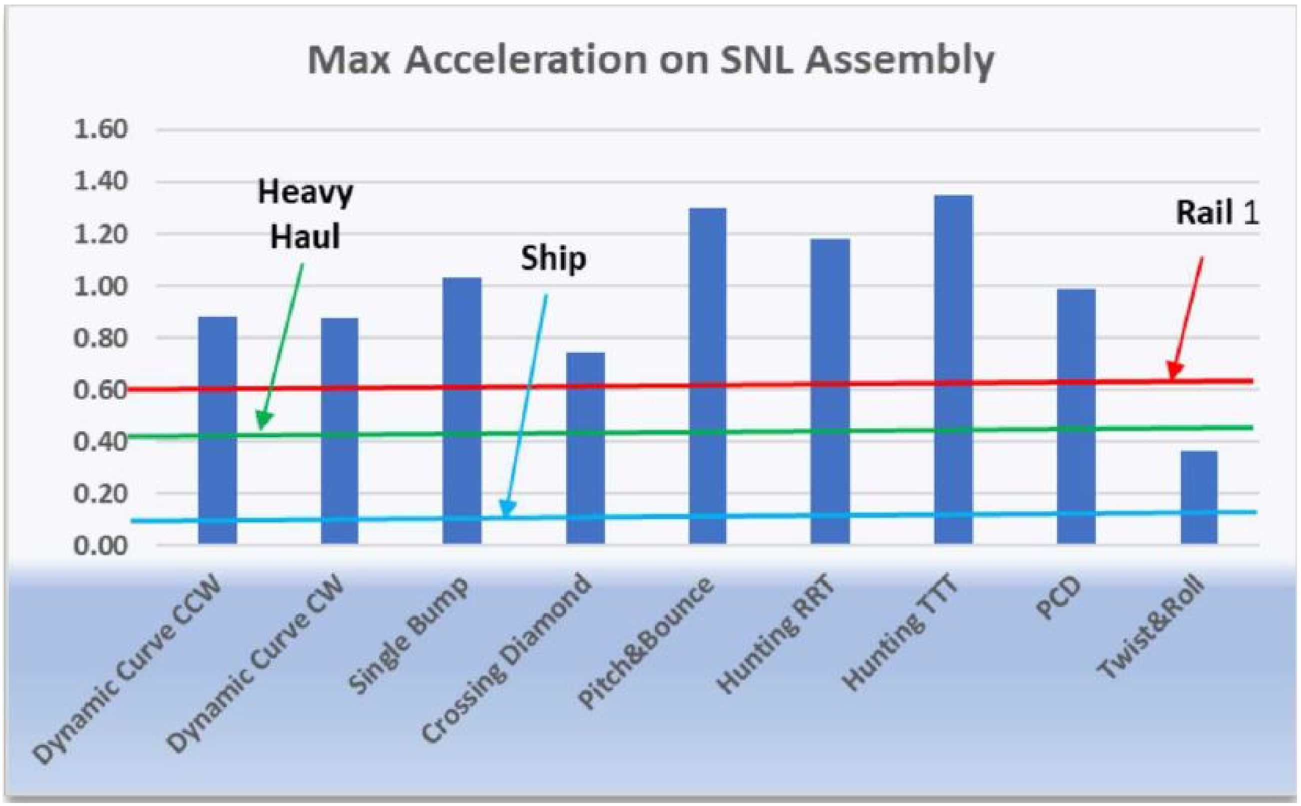

Accelerations measured under extreme test conditions at the Transportation Technology Center, Inc. (TTCI) compared to maximum accelerations observed during Ship, Rail and Heavy Haul Truck transportation

Figure 11-11, SAND2018-13258R, November 19, 2018

Does O'Donnell/Langer Represent Fatigue of a Fuel Rod?

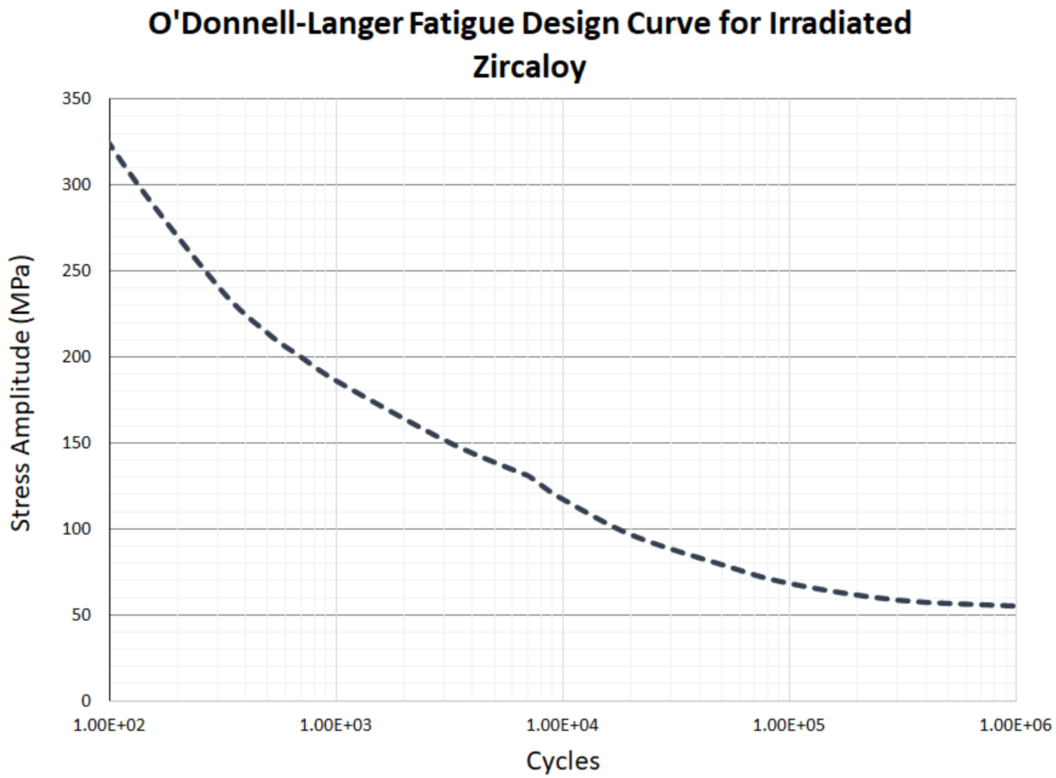

Objective

Characterize the fatigue life of used nuclear fuel

- At high burnup
- With and without simulated vacuum drying

ORNL has Heat Treatment and Fatigue Testing Capabilities in Hot Cells

- Spent Fuel Rod Heat Treatment Oven (T ≤ 530 °C)
  - Simulates temperature in vacuum drying
- Cyclic Integrated Reversible Fatigue Testing (CIRFT) System
  - Tests fuel rods in pure bending
  - Can apply both positive and negative curvatures

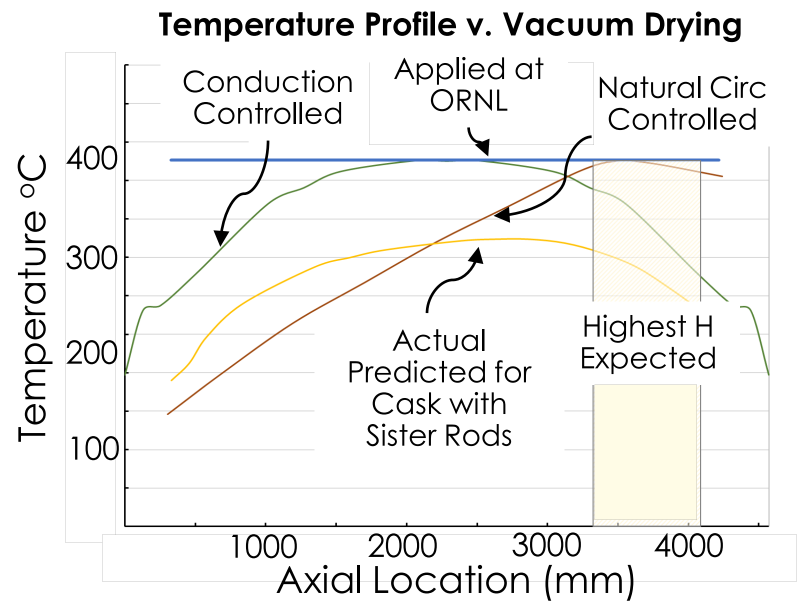

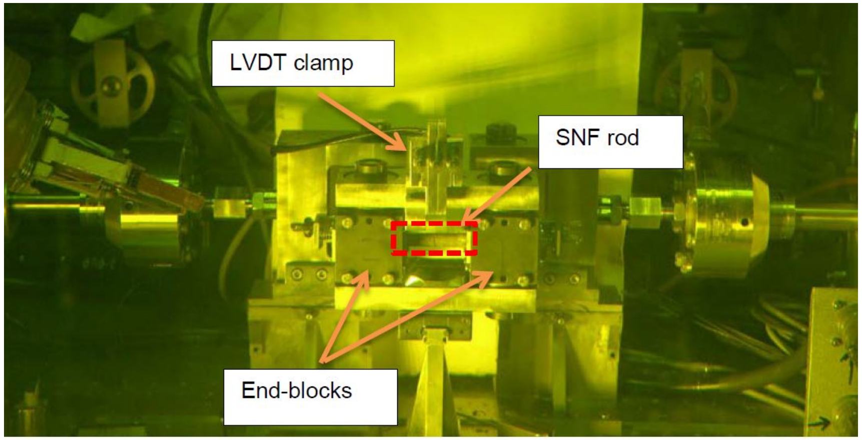

OAK RIDGE National Laboratory

Reversible Loading in CIRFT Created by Linear Displacement of U-Frame Fixture

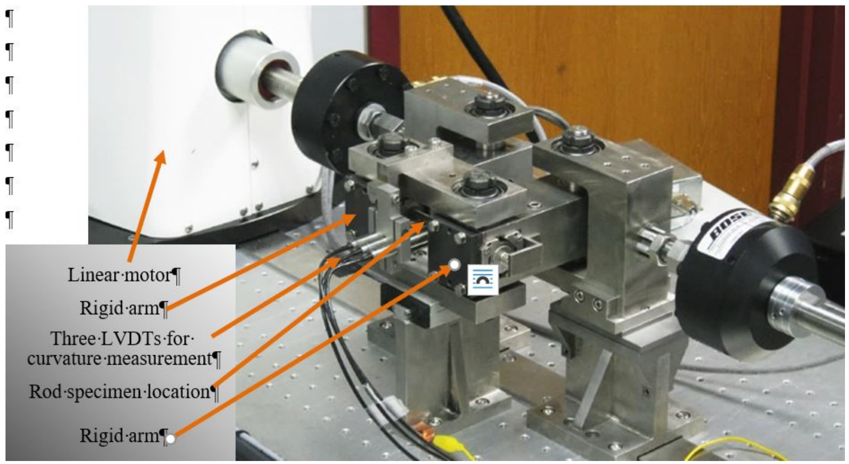

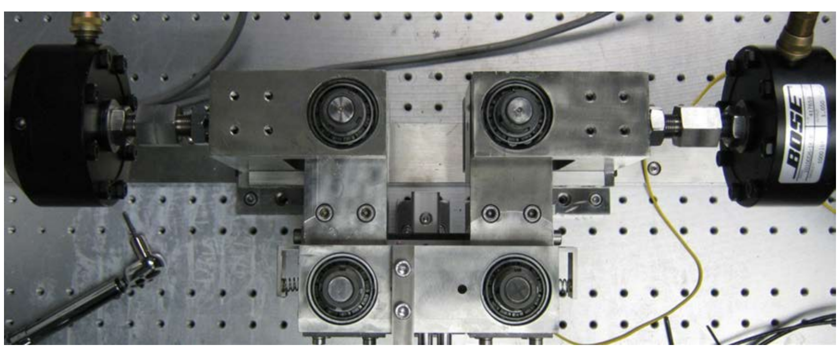

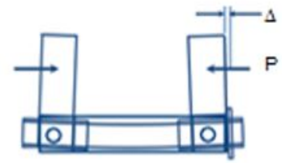

(a) Rigid arms are closing. The curvature is concave outward and designated with a negative sign.

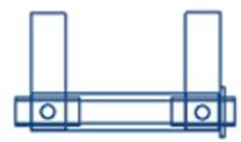

(b) Rigid arms are in neutral position.

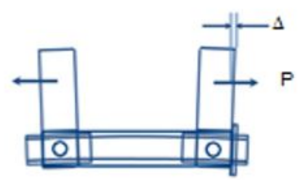

(c) Rigid arms are opening. The curvature concave inward and designated with a positive sign.

OAK RIDGE National Laboratory

Fuel Rod Fatigue Test Results Compare Well to Zircaloy Cladding Design Curve

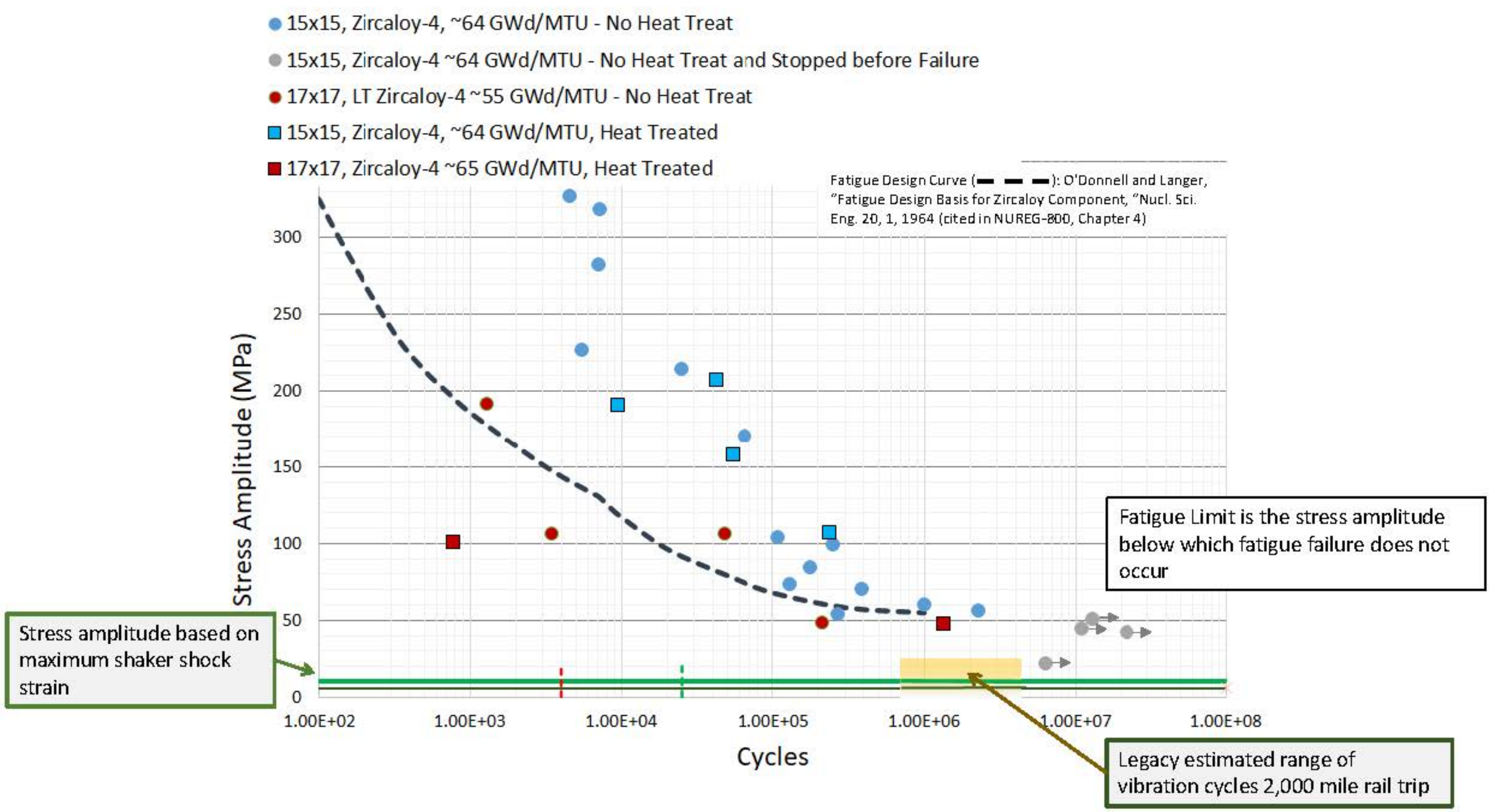

Observations
- No obvious affect of a heat treatment that simulates vacuum drying
- O'Donnell-Langer is a reasonable estimate of the fatigue limit
- The fatigue limit is well above estimated stress from measured transportation accelerations
- More data needed to understand low-cycle fatigue response
  - 17x17 data for M5 and ZIRLO is more like the 15x15 Zircaloy-4 data

Oxide Spalling Correlates with Decreased Low-Cycle Fatigue Life

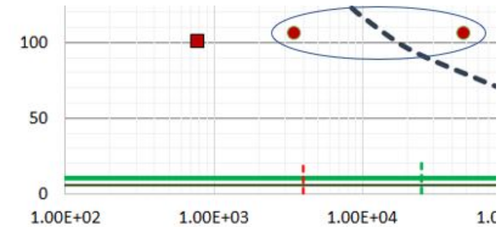

Below O'Donnell-Langer

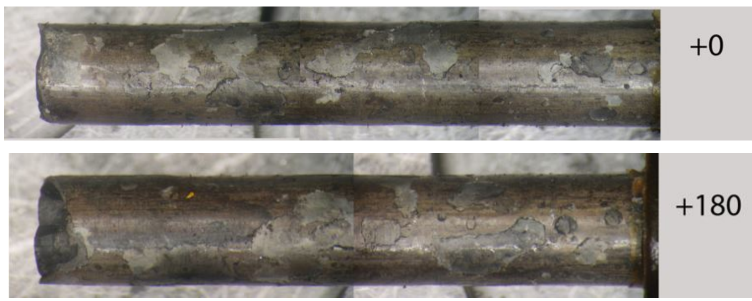

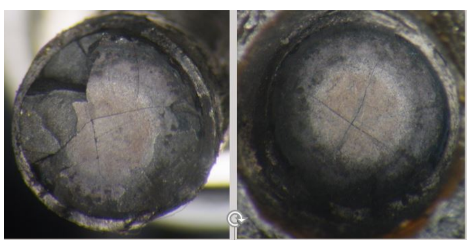

Fatigue Test Conditions
17x17 LT Zircaloy-4 Cladding
No Heat Treat
48 GWd/MTU
Applied Stress = ~100 MPa
3450 cycles to failure
3A1F05-3214-3367

Above O'Donnell-Langer

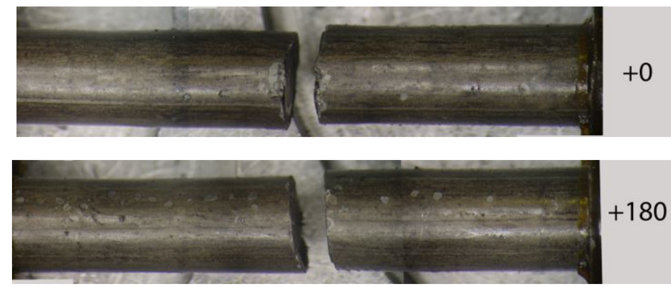

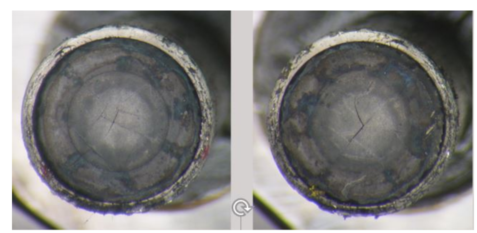

Fatigue Test Conditions
17x17 LT Zircaloy-4 Cladding
No Heat Treat
56 GWd/MTU
Applied Stress = ~100 MPa
48200 cycles to failure
3A1F05-2025-2178

Observations
- Failures occurred at pellet-pellet interface
- Significant oxide spalling observed on rod prior to testing that failed below O'Donnell-Langer

No Correlation between Oxide Spalling and High-Cycle Fatigue Performance

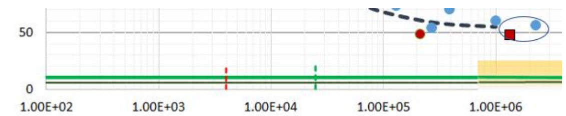

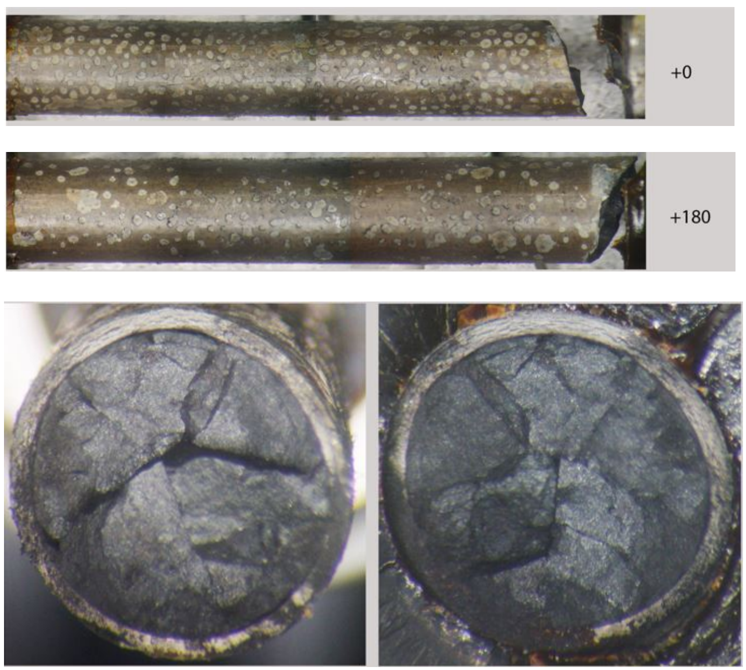

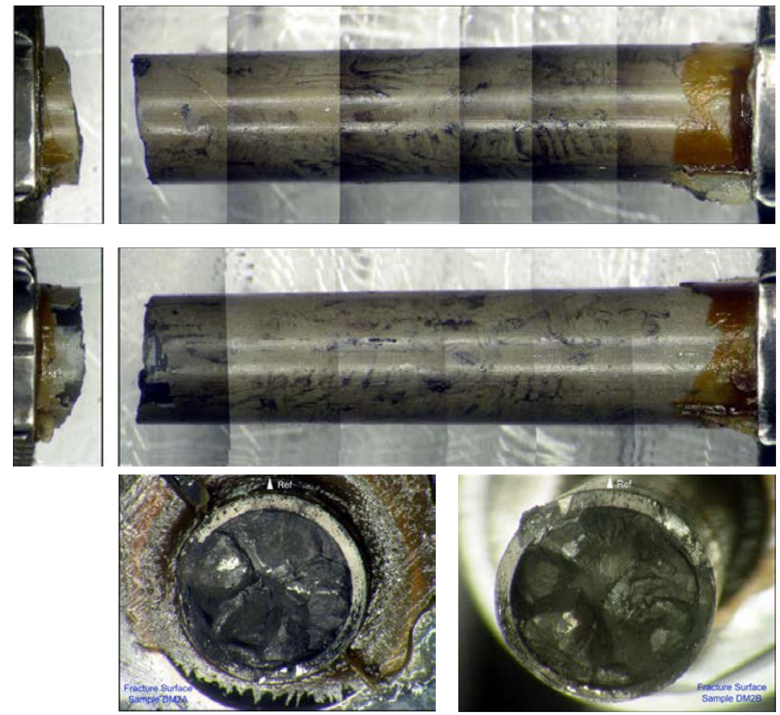

<u>Fatigue Test Conditions</u>
17x17 Zircaloy-4 Cladding
Heat Treated
66 GWd/MTU
Applied Stress = ~50 MPa
1.34E6 cycles to failure
F35P17-2027-2180

Observations
- Failures occurred within pellet
    - Failure at pellet-pellet interface also observed at low stress but less often
- No correlation of oxide spalling with performance

<u>Fatigue Test Conditions</u>
15x15 Zircaloy-4 Cladding
No Heat Treat
66 GWd/MTU
Applied Stress = ~50 MPa
2.3E6 cycles to failure
HBR-DM2

Potential Stress Concentration Mechanisms – Pellet-Pellet Crack Opening and Oxide Spalling

From Mechanics of Bending

$$\sigma = E\varepsilon = E\kappa r_{rod}$$

Radius of Fuel Rod

Cladding Modulus

Curvature

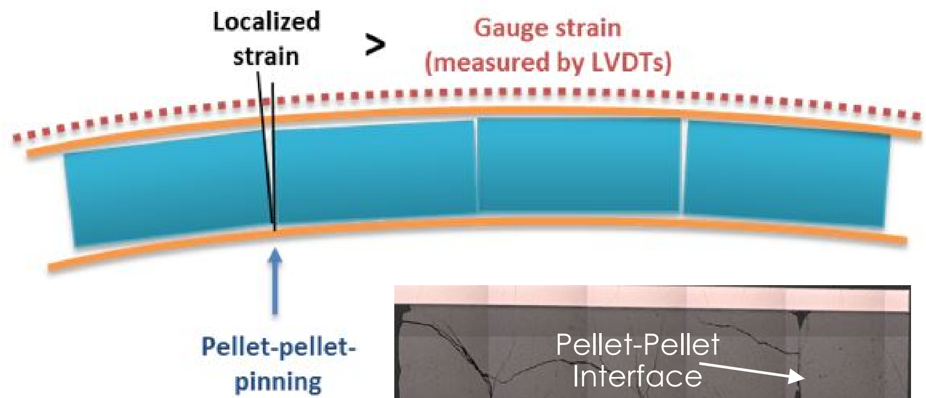

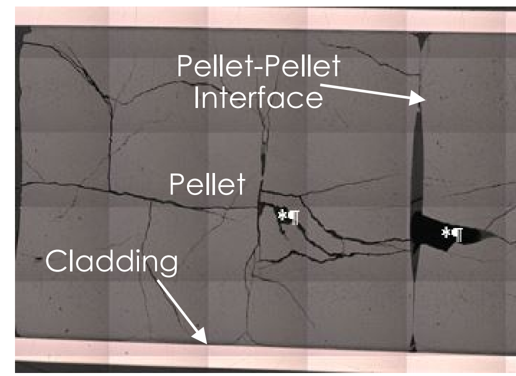

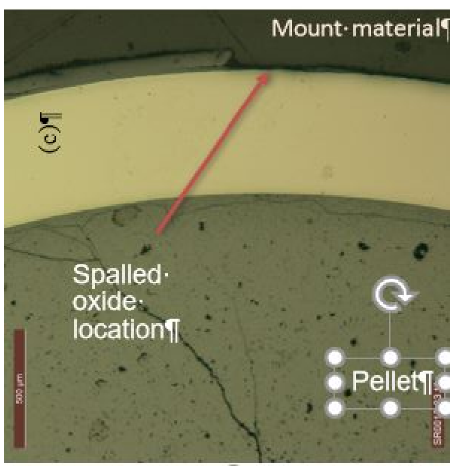

- Where oxide spalling occurs, load carried by oxide would be transferred to cladding

- Pellets deform in bending by cracks and pellet-pellet interfaces opening
- When pellet-cladding bonding occurs, localized strain (and stress) expected where cracks/interfaces open during bending

OAK RIDGE National Laboratory

Summary and Conclusions

- In terms of stress and cycle to failure, there is no obvious affect of simulated vacuum drying on fatigue life
- O'Donnell-Langer is a reasonable estimate of the fatigue limit for both 15x15 and 17x17 irradiated fuel rods with Zircaloy-4 cladding
- Suspect that pellet-pellet interface, pellet cracks and oxide spalling (if present) could be stress concentration mechanisms
  - Appears to have a greater effect under low-cycle fatigue conditions
- Additional work needed to better understand the potential role pellet deformation via crack/interface opening has on stress concentrations in the cladding

Questions or Comments

QWS26 - List of participants

Family Name	First Name	Institution	Country
Allison	Chris	INNOVATIVE SYSTEMS SOFTWARE	USA
Ayanoglu	Muhammet	Oak Ridge National Laboratory	USA
Befeno	Ignace	EDF	France
Bertsch	Johannes	Paul Scherrer Institut	Germany
Bevard	Bruce	Oak Ridge National Laboratory	USA
Birchley	Jonathan	none	UK
Brachet	Jean-Christophe	CEA, Paris-Saclay University	France
Campbell	Shawn	U.S. NRC	USA
Cantonwine	Paul	Oak Ridge National Laboratory	USA
Cervenka	Petr	CTU, UJP	Czech Republic
Chen	Minghui	University of New Mexico	USA
Colldeweih	Aaron	Paul Scherrer Institut	Switzerland
Czerniak	Luke	Westinghouse Electric Company	USA
Doyle	Peter	Oak Ridge National Laboratory	USA
Duarte	Liliana	PSI	Switzerland
Duriez	Christian	IRSN	France
Elsalamouny	Noura	Lithuania Energy Institute	Lithuania
Esmaili	Hossein	U.S. NRC	USA
Esmaili	Hossein	U.S. Nuclear Regulatory Commission	USA
Fagnoni	Francesco	Paul Scherrer Institut (PSI)	Switzerland
Farkas	Róbert	Centre for Energy Research	Hungary
Fernandez-Cosials	Kevin	UPM	Spain
Gabrielli	Fabrizio	Karlsruhe Institute of Technology	Germany
Grosse	Mirco	Karlsruhe Institute of Technology	Germany
Haste	Timothy	Imperial College, London	UK
Herm	Michel	KIT	Germany
Hollands	Thorsten	GRS	Germany
Hózer	Zoltán	Centre for Energy Research (EK)	Hungary
Ioka	Ikuo	Japan Atomic Energy Agency	Japan
Jaeckel	Bernd	Paul-Scherrer-Institut	Switzerland
Kaliatka	Tadas	Lithuania Energy Institute	Lithuania

Khalil	Sarah	Alexandria University	Egypt
Kim	Jae Joon	Korea Advanced Institute of Science and Technology	Republic of Korea
König	Tobias	Karlsruhe Institute of Technology	Germany
Krejci	Jakub	UJP PRAHA a.s.	Czech Republic
Lecomte	Marylène	Framatome	France
Lind	Terttaliisa	Paul Scherrer Institut	Switzerland
Liu	Tong	ShangHai Jiao Tong University	China
Liu	Junkai	Institute for Applied Materials, Karlsruhe Institute of Technology	Germany
Marchetti	Mara	KIT-INE	Germany
Marková	Tereza	Czech Technical University Prague	Czech Republic
Martin	Julie-Jiona	OECD NEA	France / International organisation
Mohamad	Afiqa	Japan Atomic Energy Agency	Japan
Montgomery	Rose	Oak Ridge National Laboratory	USA
Murat	Onur	Karlsruhe Institute of Technology	Germany
Muscher	Heinrich	KIT	Germany
Nahm	Daniel	Gesellschaft für Anlagen- und Reaktorsicherheit	Germany
Nakamura	Kinya	Central Research Institute of Electric Power Industry (CRIEPI)	Japan
Nemoto	Yoshiyuki	JAEA	Japan
Nukatsuka	Shigehiro	MHI NS Enginnering	Japan
Nyvlt	Sebastian	CTU in Prague	Czech Republic
Peng	Xu	Idaho National Laboratory	USA
Pshenichnikov	Anton	Japan Atomic Energy Agency	Japan
Rouge	Emmanuel	IRSN	France
Sagan	Michael	Framatome	France
Salay	Michael	USNRC	USA
sanchez espinoza	Victor Hugo	KIT/INR	Germany
Sappl	Jonathan	GRS	Germany
Sartowska	Bożena	Institute of Nuclear Chemistry and Technology	Poland

Sasahara	Akihiro	Central research institute of electric power industry	Japan
Ševeček	Martin	Czech Technical University in Prague	Czech Republic
Shawn	Campbell	U.S. NRC	USA
Sidelev	Dmitrii	Tomsk Polytechnic University	Russia
Sim	Ki Seob	IAEA	Austria
Stegmaier	Ulrike	KIT IAM-AWP	Germany
Steinbrück	Martin	KIT-IAM-AWP	Germany
Stuckert	Juri	Karlsruhe Institute of Technology (KIT)	Germany
Suckow	Detlef	Paul Scherrer Institut	Switzerland
Tang	Chongchong	Karlsruhe Institute of Technology	Germany
Tromm	Thomas-Walter	KIT	Germany
Van Uffelen	Paul	European Commission, Joint Research Centre	Germany
Vasiliev	Alexander	Nuclear Safety Institute	Russia
Veshchunov	Mikhail	CTU, Prague	Czech Republic
Vileiniškis	Virginijus	Lithuanian Energy Institute	Lithuania
Vizelkova	Katerina	KIT	Germany
Wang	Beiqi	Shanghai Jiao Tong University	China
Weick	Sarah	KIT	Germany
Wolff	Marc	ENSI - Eidgenössisches Nuklearsicherheitsinspektorat	Switzerland
Xu	Peng	Idaho National Laboratory	US